UNIVERSITY OF NEWCASTLE UPON TYNE
DEPARTMENT OF CIVIL ENGINEERING

# ARTIFICIAL GROUNDWATER RECHARGE IN KUWAIT: PLANNING AND MANAGEMENT

by
MESHAN MOHAMMAD AL-OTAIBI

NEWCASTLE UNIVERSITY LIBRARY
097 51104 X
Thesis L5997

THESIS SUBMITTED IN FULFILMENT OF THE REQUIREMENTS
FOR THE DEGREE OF DOCTOR OF PHILOSOPHY

AUGUST 1997

# ABSTRACT

Storing freshwater in brackish aquifers using artificial recharge has been predicted (using a rigorous numerical modelling technique) to be a very beneficial water management alternative for Kuwait. Two possible practices of freshwater injection and recovery have been identified. First, through a seasonal cycle, desalination plants can operate at their optimum capacity all over the year irrespective of seasonal fluctuations in water demand, and also the aquifer yield can be increased at the same time. The optimum location for this storage is suggested to be the Shigaya-B wellfield, mainly because of the high specific injection rates of the injection wells, and its location in a highly depleted area. The other benefit of artificial recharge to Kuwait is using the aquifer as a long-term strategic reserve for freshwater to be used later during the emergency conditions. The Shigaya-A wellfield is suggested to be the optimum site for this storage, mainly because of the high freshwater recovery efficiency, and the sufficient depth of aquifer head allowing additional build-up inside the injection wells due to well face clogging.

Using a sub-regional numerical model, the optimum management variables required to inject and recover freshwater at the two types of storages have been identified, including; number and geometry of injection/recovery wells, their injection/recovery rates, and the duration of injection necessary to recover the intended quantity and quality of freshwater. Also, the recovery efficiency of freshwater storage and recovery practice has been estimated.

From an analysis of freshwater injection-withdrawals field experimental data (for a single well, SU-10), using a single-well numerical model, it was possible to quantify the clogging factor, and differentiate between its different causes. It has been found that most of the clogging occurred due to air entrapment, and not due to the formation or recharge water properties. This means that clogging during this experiment is due to a fault in the injection system, and that well injection capacity is likely to be higher if this avoided.

Further modelling was implemented to devise methods for minimising displacement and quality deterioration of the artificially-recharged freshwater mound, by the regional groundwater flow, if it is stored for a long time. The preferred methods involve operation of "hydraulic gradient-control" pumping wells outside the storage area to create a zone of zero hydraulic gradient (stagnation zone) around the stored water mound. A management model using the response matrix approach was implemented to determine the optimum pumping rates of these wells necessary to produce the intended hydraulic gradient. By the time all the usable stored water is irrecoverable without these controls (after 4 years), it was possible using this technique to recover about 55 % of this water.

*Thanks To God,,*

# ACKNOWLEDGEMENTS

I want to take this opportunity to thank Dr. Paul L. Younger for his superior guidance and continuous encouragement during the preparation of this thesis. I want to thank all other staff of the Department of Civil Engineering, University of Newcastle upon Tyne who have helped me during the years of study here.

I would like to acknowledge the financial support of the Kuwait Government through the Kuwait Institute for Scientific Research. I would also thank all the staff of the Water Resources Division in the Institute for their support and their valuable suggestions during the years of my study.

I would like to thank the Ministry of Electricity and Water for providing me with the essential hydrological data which they hold.

Also, my acknowledgement to Dr. H. Yazicigil from the Middle East University (Turkey) for his great assistance in formulating, desgining, and running the optimization model which is used in this study.

My special thanks to my dearest friends in the Saturday group (Al-Helekah) especially Fahhad Al-Harbi and Khaled Al-Berakk and their families who made both my and my family stay in Newcastle enjoyable and meaningful.

Lastly, the warmest thanks to my dearest wife and my lovely children Mohammed, Saad, Sarah, and Nouf who have been very supportive during the preparation of this thesis.

# TABLE OF CONTENT

**1. INTRODUCTION** ..... **1**
1.1 BRIEF DESCRIPTION OF THE STUDY AREA ..... 1
1.2 STATEMENT OF THE PROBLEM ..... 1
1.3 OBJECTIVES OF THE STUDY ..... 2
1.3.1 INTRODUCTION ..... 2
1.3.2 OBJECTIVES OF THE STUDY ..... 3
1.4 RESEARCH CONCEPTUAL FRAMEWORK ..... 4
1.4.1 HYDROGEOLOGICAL ASSESSMENT ..... 4
1.4.2 FRESHWATER INJECTION-WITHDRAWAL FIELD EXPERIMENT ..... 5
1.4.3 NUMERICAL GROUNDWATER HYDRAULIC AND TRANSPORT SIMULATION MODELS ..... 5
1.4.4 MANAGEMENT MODELS ..... 7
1.5 LAYOUT OF THE THESIS ..... 8
1.6 PREVIOUS STUDIES ON ARTIFICIAL RECHARGE IN KUWAIT ..... 9

**2. LITERATURE REVIEW: ARTIFICIAL GROUNDWATER RECHARGE** ..... **12**
2.1 INTRODUCTION ..... 12
2.2 METHODS OF ARTIFICIAL RECHARGE ..... 13
2.3 GENERAL PURPOSES OF ARTIFICIAL RECHARGE ..... 15
2.4 SITE SELECTION ..... 22
2.5 CLOGGING ..... 23
2.5.1 INTRODUCTION ..... 23
2.5.2 CLOGGING RELATION TO FORMATION TYPE ..... 24
2.5.3 GENERAL CAUSES OF CLOGGING ..... 25
2.5.4 GENERAL PREVENTION AND REMEDIES OF CLOGGING ..... 25
2.5.5 EXAMPLES OF CLOGGING CAUSES AND REMEDIES ..... 27
2.5.5.1 SUSPENDED MATERIAL ..... 27
2.5.5.2 CHEMICAL REACTIONS ..... 31
2.5.5.3 AIR ANTRAINMANT ..... 34
2.5.5.4 BACTERIAL CONTAMINATION ..... 35
2.6 RECOVERY EFFICIENCY ..... 37
2.7 DISPERSIVITY ESTIMATION USING TRACER TESTS ..... 42
2.7.1 INTRODUCTION ..... 42
2.7.2 TRACER TESTS ..... 43
2.7.3 MODELLING OF DISPERSION TESTS ..... 49
2.8 MANAGEMENT MODELS ..... 54
2.8.1 INTRODUCTION ..... 54
2.8.2 GROUNDWATER HYDRAULIC MANAGEMENT MODELS ..... 55
2.8.3 RESPONSE MATRIX APPROACH ..... 56

**3. GEOLOGICAL AND HYDROLOGICAL SITUATION OF KUWAIT** ..... **62**
3.1 GEOLOGICAL SETTING ..... 62
3.1.1 GENERAL TOPOGRAPHIC AND CLIMATOLOGICAL CONDITIONS ..... 62
3.1.2 LITHOSTRATIGRAPHY ..... 64
3.1.3 GENERAL STRUCTURE ..... 67
3.2 GROUNDWATER HYDROLOGY ..... 69
3.2.1 AQUIFER AND AQUITARD BOUNDARIES ..... 69
3.2.2 HYDRAULIC PROPERTIES OF AQUIFERS AND AQUITARDS ..... 74
3.2.3 POTENTIOMETRIC WATER LEVELS OF THE AQUIFERS ..... 82
3.2.4 GROUNDWATER UTILISATION IN KUWAIT ..... 93
3.2.5 WATER QUALITY ..... 99

**4. REGIONAL NUMERICAL GROUNDWATER MODEL ..... 103**
4.1 INTRODUCTION ..... 103
4.2 GROUNDWATER FLOW MODEL ..... 104
4.2.1 MODELLING APPLICATION PROCEDURES ..... 104
4.2.2 CONCEPTUAL MODEL ..... 106
4.2.3 GRID DESIGN ..... 109
4.2.4 PARAMETER INITIALISATION ..... 111
4.2.5 NUMERICAL MODEL CALIBRATION ..... 117
4.2.5.1 STEADY STATE CALIBRATION ..... 120
4.2.5.2 TRANSIENT CALIBRATION ..... 129
4.2.6 MODEL VERIFICATION ..... 147
4.2.7 PREDICTIVE SIMULATION ..... 149
4.3 SOLUTE TRANSPORT MODEL ..... 155
4.3.1 INTRODUCTION ..... 155
4.3.2 MODEL PARAMETERS ..... 156
4.3.3 SOLUTION PARAMETERS ..... 158

**5. SINGLE-WELL INJECTION-RECOVERY TEST ..... 161**
5.1 INTRODUCTION ..... 161
5.2 TEST SITE ..... 163
5.3 INJECTION-RECOVERY EXPERIMENT ..... 165
5.4 METHODS OF INTERPRETING THE EXPERIMENTAL DATA ..... 171
5.4.1 NUMERICAL MODEL ..... 171
5.4.1.1 INTERMEDIATE MODEL ..... 172
5.4.1.2 SINGLE-WELL MODEL ..... 174
5.4.2 PUMPING TEST DATA INTERPRETATION ..... 183
5.5 EVALUATION OF INJECTION-WITHDRAWAL EXPERIMENTAL DATA ..... 195
5.5.1 HYDRAULIC RESULTS ..... 195
5.5.2 WELL FACE CLOGGING ..... 196
5.5.2.1 CLOGGING EVALUATION ..... 198
5.5.2.2 DIFFERENTIATION BETWEEN CLOGGING CAUSES ..... 201
5.5.3 TRANSPORT SIMULATION ..... 206

**6. OPTIONS FOR AQUIFER STORAGE AND RECOVERY ..... 216**
6.1 INTRODUCTION ..... 216
6.2 SELECTION OF THE TARGET AQUIFER FOR ARTIFICIAL RECHARGE ..... 217
6.3 CLASSIFICATION OF AVAILABLE SITES FOR ARTIFICIAL RECHARGE ..... 220
6.3.1 TRANSMISSIVITY ..... 221
6.3.2 SPECIFIC INJECTION RATE (SIR) ..... 221
6.3.3 RECOVERY EFFICIENCY ..... 229
6.4 SITE SELECTION CRITERIA ..... 233
6.4.1 GENERAL CRITERIA ..... 234
6.4.2 CRITERIA FOR SELECTING THE LONG-TERM STORAGE SITE ..... 235
6.4.3 CRITERIA FOR SELECTING THE SHORT-TERM (SEASONAL) STORAGE SITE ..... 236
6.5 SITE SELECTION ..... 236
6.5.1 LONG-TERM STRATEGIC RESERVE SITE ..... 237
6.5.2 SHORT-TERM STORAGE SITE ..... 238

**7. MANAGEMENT OPTIONS FOR AQUIFER STORAGE AND RECOVERY ..... 239**
7.1 INTRODUCTION ..... 239
7.2 AVAILABILITY OF WATER FOR RECHARGE ..... 241
7.2.1 SOURCES OF WATER FOR RECHARGE ..... 241
7.2.2 RANKING OF WATER SOURCES FOR RECHARGE ..... 245
7.3 NUMERICAL MODEL (SUB-REGIONAL) ..... 246
7.4 SEASONAL CYCLES OF STORAGE AND RECOVERY ..... 254
7.4.1 INJECTION VOLUME ..... 256
7.4.2 RECOVERY EFFICIENCY ..... 257
7.4.3 ROLE OF CYCLIC INJECTION/RECOVERY IN THE OPTIMUM OPERATION OF DESALINATION PLANTS ..... 261
7.4.4 ROLE OF CYCLIC INJECTION/RECOVERY IN INCREASING THE AQUIFER YIELD ..... 271
7.5 LONG-TERM STRATEGIC RESERVE ..... 278
7.5.1 FORECASTED FRESHWATER DEMAND ..... 278
7.5.2 SOURCES OF FRESHWATER DURING EMERGENCY ..... 279
7.5.3 SCENARIOS OF FRESHWATER CRISIS ..... 282

**8. OPTIMAL OPERATION TO MAINTAIN FRESHWATER STORAGE ..... 293**
8.1 INTRODUCTION ..... 293
8.2 PROBLEM DESCRIPTION ..... 294
8.3 SOLUTION BASIS ..... 296
8.4 SIMULATION MODEL ..... 302
8.5 RESPONSE FUNCTIONS ..... 302
8.6 OPTIMISATION MODEL ..... 303
8.6.1 LINEAR PROGRAMMING FORMULATION ..... 303
8.6.2 OPTIMISATION ALGORITHM (MINOS) ..... 308
8.6.2.1 INTRODUCTION ..... 308
8.6.2.2 DATA INPUT FORMAT ..... 309
8.7 OPTIMAL SOLUTION VALIDITY ..... 312
8.8 MANAGEMENT MODEL RESULTS ..... 312
8.8.1 HYDRAULIC RESULTS ..... 314
8.8.2 TRANSPORT RESULTS ..... 317

**9. MAIN FINDINGS, CONCLUSION, AND RECOMMENDATIONS ..... 324**
9.1 INTRODUCTION ..... 324
9.2 GROUNDWATER MODELLING ..... 324
9.2.1 FLOW MODELS ..... 325
9.2.2 TRANSPORT MODEL ..... 325
9.2.3 RECOMMENDATIONS ..... 326
9.3 GROUNDWATER ABSTRACTION ..... 327
9.3.1 PRESENT DEVELOPMENT ..... 327
9.3.2 FUTURE DEVELOPMENT ..... 327
9.3.3 RECOMMENDATIONS ..... 328
9.4 WATER INJECTION-WITHDRAWAL EXPERIMENT ..... 328
9.4.1 WELL FACE CLOGGING ..... 329
9.4.2 AQUIFER DISPERSIVITY ..... 330
9.4.3 RECOVERY EFFICIENCY ..... 330
9.4.4 RECOMMENDATIONS ..... 330
9.5 ARTIFICIAL GROUNDWATER RECHARGE ..... 331
9.5.1 SEASONAL CYCLIC OF WATER INJECTION AND RECOVERY ..... 332
9.5.2 LONG-TERM STRATEGIC RESERVE FOR EMERGENCY CONDITIONS ..... 334
9.5.3 RECOMMENDATIONS ..... 335
9.6 HYDRAULIC-GRADIENT CONTROL TO MAINTAIN STORED FRESHWATER LENS ..... 336

**REFERENCES ..... 338**
**APPENDIX-I (MODFLOW GROUNDWATER FLOW MODEL) ..... 347**
**APPENDIX-II (MT3D SOLUTE TRANSPORT MODEL) ..... 353**
**APPENDIX-III (MANAGEMENT MODEL HYDRAULIC OUTPUTS) ..... 364**

# LIST OF FIGURES

Figure 3.1: Topographic map for the Kuwait (m amsl) ..... 63
Figure 3.2: Major anticlinal structures shown on the top of Dammam Formation, m amsl. ..... 68
Figure 3.3: Lithological and hydrogeologic logs for the main aquifers and aquitards in Kuwait..... 70
Figure 3.4: Cross section showing the main aquifer and aquitard units ..... 71
Figure 3.5: Pre-development saturated thickness of the Kuwait Group aquifer, m. ..... 73
Figure 3.6: Isopach map of the basal clay and cherty limestone capping the top of the Dammam aquifer (aquitard layer), m. ..... 75
Figure 3.7: Bottom of the Dammam Formation aquifer, m amsl. ..... 76
Figure 3.8: Kriged Kuwait Group aquifer transmissivity values ($m^2/d$), and locations of their measurement. ..... 79
Figure 3.9: Kriged Dammam aquifer transmissivity values ($m^2/d$), and their measurement. ..... 80
Figure 3.10: Schematic cross section showing the pattern of natural groundwater flow in Kuwait aquifer system ..... 84
Figure 3.11: Regional initial potentiometric head of the Dammam aquifer, m amsl. ..... 85
Figure 3.12: Observed initial potentiometric head of the Kuwait Group aquifer, m amsl ..... 86
Figure 3.13: Observed water level for the Kuwait Group aquifer at 1988, m amsl. ..... 88
Figure 3.14: Observed potentiometric head of the Dammam aquifer at 1990, m amsl. ..... 89
Figure 3.15: Observed potentiometric head of the Dammam aquifer at 1995, m amsl. ..... 90
Figure 3.16: Observed total drawdown in potentiometric head of the Dammam aquifer to 1990..... 91
Figure 3.17: Observed total drawdown in potentiometric head of the Dammam aquifer to 1995..... 92
Figure 3.18: Location of the existing water wellfields in Kuwait. ..... 95
Figure 3.19: Seasonal fluctuation in groundwater abstraction from water wellfields in Kuwait. ..... 98
Figure 3.20: Observed pre-development salinity (mg/l) of the Dammam aquifer ..... 101
Figure 3.21: Observed salinity of the Dammam aquifer (mg/l) in 1990 ..... 102

Figure 4.1: Conceptual model of Kuwait aquifer systems used in numerical simulation. ..... 107
Figure 4.2: Irregular finite-difference grids used in the regional numerical model. ..... 110
Figure 4.3: Kuwait Group aquifer grid design and boundary conditions used in the regional model. ..... 112
Figure 4.4: Dammam Formation aquifer grid design and boundary conditions used in the regional model. ..... 113
Figure 4.5: Kriged hydraulic conductivity map for the Kuwait Group aquifer (m/d). ..... 115
Figure 4.6: Kriged hydraulic conductivity map for the Dammam Formation aquifer (m/d). ..... 116
Figure 4.7: Matching between the simulated and observed water levels of the Kuwait Group aquifer obtained during the stead-state calibration of the regional model, m amsl. ..... 122
Figure 4.8: Matching between the simulated and observed potentiometric heads of the Dammam aquifer obtained during the steady-state calibration of the regional model, m amsl. ... 123
Figure 4.9: Calibrated hydraulic conductivity of the Kuwait Group aquifer, m/d. ..... 125
Figure 4.10: Calibrated hydraulic conductivity of the Dammam Formation aquifer, m/d. ..... 126
Figure 4.11: Calibrated aquitard vertical leakance (1/day). ..... 127
Figure 4.12: Sketch diagram showing simulated volume of the aquifer system mass balance at ..... different points located in the direction of flow, in $m^3/d$. ..... 129
Figure 4.13: Simulated total drawdown in potentiometric head of the Dammam aquifer (DM) to 1990, m. ..... 136
Figure 4.14: Simulated Vs observed water level maps for the Kuwait Group (KG) aquifer at 1988, m amsl. ..... 137

Figure 4.15: Simulated Vs observed water level hydrographs at selected observation wells tapping the Dammam aquifer (DM), m amsl. ..... 139
Figure 4.16: Simulated water level of the Kuwait Group (KG) aquifer at the end of selected stress periods (7 years interval) of the transient condition. ..... 140
Figure 4.17: Simulated potentiometric head of the Dammam (DM) aquifer at the end of selected stress periods (7 years interval) of the transient calibration. ..... 141
Figures 4.18: Simulated total drawdown in the Kuwait Group aquifer water level to the end of 1995. ..... 142
Figure 4.19: Simulated total drawdown in the Dammam aquifer potentiometric head to1995 ... 143
Figure 4.20: Simulated Vs observed potentiometric head of the Dammam aquifer at 1995. ..... 148
Figure 4.21: Simulated potentiometric head for the KG and DM aquifers by 2010 during Scenario 1 (present development), m amsl. ..... 152
Figure 4.22: Simulated potentiometric head for the KG and DM aquifers by 2010 during Scenario 2 (controlled development), m amsl. ..... 153
Figure 4.23: Simulated potentiometric head for the KG and DM aquifers by 2010 during Scenario 3 (intensive development), m amsl. ..... 154

Figure 5.1: Location of injection-recovery test wells. ..... 162
Figure 5.2: Lithological log and construction details for Well SU-10. ..... 164
Figure 5.3: Observed water level changes during the injection/recovery experiment. ..... 168
Figure 5.4: Schematic diagram showing the down-hole pipe assembly used for injection test ..... 169
Figure 5.5: Schematic diagram showing the down-hole pipe assembly used for recovery test ..... 170
Figure 5.6: Embedded grids of the intermediate model, and the nested area of the single-well model. ..... 173
Figure 5.7: Simulated total drawdown in the DM potentiometric head when the test well was pumped during the long-term recovery test showing the maximum radius of influence179
Figure 5.8: Obtained match between the observed and the simulated aquifer potentiometric head during the pre-injection constant-rate and recovery tests, which were used for the transient calibration. ..... 182
Figure 5.9: Simulated and observed change in the DM potentiometric head during the long-term recovery test. ..... 183
Figure 5.10 : Curve matching between the observed drawdown in aquifer head during the pre-injection constant-rate pumping test with type curve obtained using the Hantush-Jacob (1955) method ..... 187
Figure 5.11: Curve matching between the observed drawdown in aquifer head during the post-injection constant-rate pumping test with type curve obtained using the Hantush-Jacob (1955) method ..... 187
Figure 5.12: Fitted straight line through the observed residuals drawdown recorded after the pre-injection constant-rate pumping test using Theis Recovery (1935) method. ..... 189
Figure 5.13: Fitted straight line through the observed residuals drawdown recorded after the post-injection constant-rate pumping test using Theis Recovery (1935) method. ..... 189
Figure 5.14: Fitted straight line through the observed residuals drawdown recorded after the first injection phase using Theis Recovery (1935) method. ..... 190
Figure 5.15: Plotted drawdown observed at the four steps during the pre-injection step-drawdown test. ..... 192
Figure 5.16: Determination of head loss coefficients (B and C) for the pre-injection and post-injection step-drawdown tests using Hantush-Bierschenk's method. ..... 193
Figure 5.17: Difference between the simulated and the observed build-up inside the recharge well as obtained during the injection test, which may related to the effect of well face clogging. ..... 195
Figure 5.18: Development of well face clogging during the injection test, and the variation in SIR of the injection well as a result of this clogging. ..... 200

Figure 5.19: Development of well face clogging during the water injection resulting from the possible two causes, suspended solids and air entrapment. ..... 204
Figure 5.20: Simulated versus observed breakthrough curve of recovered water relative concentration. ..... 212
Figure 5.21: Simulated relative concentration ($C/C_0$) around the test well after the freshwater injection was completed. ..... 213
Figure 5.22: Simulated recovery efficiency using the calibrated aquifer parameters, and recovery efficiency resulting from reducing the aquifer porosity to half of its original calibrated value. ..... 215

Figure 6.1: (A, B, and C): Simulated change in the Dammam potentiometric head after six months of water injection at the injection fields Shigaya-A, B, and C. ..... 226
Figure 6.2 (A, B, C, and D): Simulated change in the Dammam potentiometric head after six months of water injection at the injection fields Shigaya-D and E, Sulaibiya, and Umm Gudair. ..... 227

Figure 7.1: Seasonal fluctuation in the urban freshwater demand. ..... 241
Figure 7.2 (A and B) : (A) location of the sub-regional model relative to the regional model. (B) Domain discretization and boundary conditions of the sub-regional model. 247
Figure 7.3: Matching between the simulated and observed water level of the Kuwait Group aquifer obtained during the steady-state calibration of the sub-regional model. ..... 250
Figure 7.4: Matching between the simulated and observed initial potentiometric head of the Dammam aquifer during the steady-state calibration of the sub-regional mode. ..... 251
Figure 7.5: Simulated total drawdown in the Dammam aquifer potentiometric head to 1995 using the sub-regional model. ..... 252
Figure 7.6: Concentration profile of the aquifer water during injection half-cycles, and for the recovered water during recovery half-cycles, simulated during the seasonal cyclic injection/recovery in the Shigaya-B wellfield. ..... 259
Figure 7.7: Forecasted urban freshwater demand and the desalination plants production rate. ..... 262
Figure 7.8: Achieved operational rate of desalination plants if cyclic injection-recovery of freshwater is applied, with a comparison to the optimum capacity of the plants and the actual seasonal fluctuation in desalination plants operation. ..... 269
Figure 7.9: Simulated head of DM aquifer during the cyclic injection/recovery option at a selected well node in the injected site Shigaya-B. ..... 270
Figure 7.10: Simulated drawdown in the Dammam aquifer potentiometric head from 1995- 2005 under Scenario 1 due to the groundwater abstraction from the existing wellfields using the regional model ..... 272
Figure 7.11(A and B): Simulated changes in the Dammam aquifer potentiometric head during the seasonal freshwater injection-recovery at Shigaya-B wellfield using the regional model, A: at the last injection half-cycle (winter 2005). B: at the last recovery half-cycle (summer 2005). ..... 273
Figure 7.12 (A and B): Simulated changes in the Dammam aquifer potentiometric head during the seasonal freshwater injection-recovery at the Shigaya-D using the regional model. A: at the last injection half-cycle (winter 2005). B: at the last recovery half-cycle (summer 2005). ..... 276
Figure 7.13: Time-head plot at a selected node showing the simulated changes in the DM aquifer potentiometric head (using the sub-regional model) during the freshwater injection and recovery stages at the strategic reserve (Shigaya-A wellfield) under scenario B. ..... 284
Figure 7.14: Simulated isosalinity map for the recommended strategic reserve after the freshwater injection was completed in 4.16 year (as Scenario B assumes) using 20 wells. ..... 285

Figure 7.15: Concentration profile simulated at two selected wells (central and corner) during the freshwater injection-recovery at the strategic reserve (Shigaya-A wellfield) simulated using the sub-regional model (as Scenario B assumes). ..... 286
Figure 7.16: Simulated changes in the Dammam aquifer potentiometric head a after water injection was completed in 5.26 years (as Scenario C of emergency conditions assumes).. ..... 289
Figure 7.17: Simulated isosalinity map for the recommended strategic reserve after the freshwater injection was completed in 5.26 (as Scenario C of the emergency conditions assumes) ..... 290

Figure 8.1: Displacement of the stored freshwater lens at Shigaya-A wellfield after a residence time of 6 years resulting from the existing regional groundwater flow. ... 295
Figure 8.2: (A and B): (A) components and (B) location of the problem domain to be solved using the management model. ..... 297
Figure 8.3: Conceptual diagram for the present groundwater flow pattern which needs to be changed by creating a zero hydraulic gradient between the nodes A and B using the gradient-control wells. ..... 299
Figure 8.4: Flow chart for the steps of the used management model. ..... 301
Figure 8.5 : Simulated potentiometric head of the DM aquifer at year 2000 used as initial heads for the management model. ..... 306
Figure 8.6: Simulated potentiometric head of the DM aquifer after 6 years of storing freshwater at Shigaya-A wellfield if groundwater abstraction proceeds without any control. ..... 315
Figure 8.7: Simulated potentiometric head of the DM aquifer after 6 years of storing freshwater at the Shigaya-A wellfield using optimum pumping rates of the gradient-control and supply wells as determined by the management model. ..... 316
Figure 8.8: Displacement of the stored freshwater lens after 6 years of residence if gradient -control wells are used to maintain it. ..... 318
Figure 8.9 (A and B): Comparison between the change in simulated TDS for the stored water (after freshwater recharge completed) during 6 years of storage, and 1 year of recovery with and without using gradient-control wells at an internal and border wells. 322

# LIST OF TABLES

Table 3.1 :Lithostratigraphic characteristics of geologic deposits in Kuwait ..... 65
Table 3.2: Summary statistics for the DM and KG aquifers transmissivity..... 77
Table 3.3: Reported Storativity values for the KG and DM aquifers ..... 81
Table 3.4: Reported leakage factor values obtained from pumping tests ..... 82
Table 3.5: Existing groundwater wellfields in Kuwait..... 94
Table 3.6: Total wellfields groundwater abstraction in Kuwait, in $Mm^3$ ..... 97

Table 4.1: Simulated groundwater balance for the aquifer system under steady state conditions... 124
Table 4.2: Calculation time steps within one stress period..... 131
Table 4.3: The average transmissivities of the aquifers at the wellfields having dual-wells, and the percentage of groundwater contribution for each aquifer to the pumping of these wells. 132
Table 4.4: Mass balance results for Kuwait aquifer system, in $m^3$/day ..... 145
Table 4.5: Wellfield operation schedule for different development scenarios..... 150

Table 5.1: Injection-recovery experiment procedure at Well SU-10..... 166
Table 5.2: Initial aquifers parameters as entered to the single-well model using the steady- state calibrated parameters of the intermediate model..... 174
Table 5.3: More reliable DM aquifer parameters for the single-well model, as calibrated through iterative procedure between the steady-state and transient calibration..... 182
Table 5.4: Determined specific drawdown, and the estimated head loss coefficients with the Hantush-Bierschenk method for the pre-injection and post-injection step-drawdown tests..... 192
Table 5.5: Obtained Dammam aquifer parameters by pumping and recovery tests for Well SU-10..... 194
Table 5.6: Measured and recovered water level rise during injection and the equivalent c logging factor for Well SU-10..... 199
Table 5.7: Measured and corrected drawdown during the long-term recovery test..... 201
Table 5.8: Simulated recovery efficiency using the calibrated aquifer parameters, and increase in the recovery efficiency which can result if the effective porosity or dispersivity of the aquifer are reduced to half of their original values..... 214
Table 5.9: Percentage of improvement in recovery efficiency with the TDS of recovered water TDS..... 215

Table 6.1: Classification of the sites available for artificial groundwater recharge according to the transmissivity of DM aquifer..... 221
Table 6.2: Quantification of the clogging effects on injection rate and water level rise inside the injection wells at the available sites for artificial recharge..... 224
Table 6.3: Classification of the available sites for artificial groundwater recharge according to their wells Specific Injection Rate (SIR)..... 228
Table 6.4: Classification of the available sites for artificial groundwater recharge according to the estimated percentage of recovery efficiency using the regional transport model..... 233
Table 6.5: Simulated deficit in the rate of latera! groundwater inflow when the DM aquifer was injected with water at Shigaya-C, and Umm Gudair fields..... 237

Table 7.1: Computed water budget by the sub-regional model for the aquifer system under steady state conditions. ..... 249
Table 7.2: Recovery efficiency for the recovered water simulated during recovery half-cycles at the Shigaya-B field, (TDS in mg/l). ..... 259
Table 7.3: Percentage of improvement in recovery efficiency from cycle to cycle ..... 260
Table 7.4: Difference between the optimum capacity of desalination plants and the desalinated water consumption. ..... 261
Table 7.5: Simulated TDS of the recovered water during the recovery half-cycles (summer) ..... 265
Table 7.6: Contribution of different sources in supplying the urban freshwater demand during summer seasons. ..... 267
Table 7.7: Expected rise in the DM aquifer head if the seasonal cycles of injection/recovery are implemented at the Shigaya-B wellfield. ..... 274
Table 7.8: The required withdrawal rate of the stored water to meet the freshwater demand during the emergency conditions (as scenario B assumes) ..... 287
Table 7.9: Summary of the optimum injection and withdrawal schedules during the creation of the strategic freshwater reserve to face the freshwater emergency as Scenario B assumes. 287
Table 7.10: Summary of the optimum injection and withdrawal schedules during the creation of the strategic freshwater reserve to face the freshwater emergency as Scenario C assumes. 291
Table 7.11: Summary of the portion that the different sources of freshwater can supply during the two assumed scenarios of freshwater emergency. ..... 292

Table 8.1: Optimal discharge rates for the supply and gradient-control wells during the 7 planning periods as obtained by the optimisation algorithm (MINOS). ..... 313
Table 8.2: Comparison between the simulated recovery efficiency of the stored water with a TDS < 1500 mg/l after a successive years of storage ..... 320

# 1. INTRODUCTION

## 1.1 BRIEF DESCRIPTION OF THE STUDY AREA

The state of Kuwait is located on the western side of the Arabian Gulf between 3150 to 3330 UTM N and 650 to 840 UTM E. It occupies about 18,000 $Km^2$ of desert and off-shore islands. The population of Kuwait is about two million (Ministry of planning, 1996).

Kuwait, as in most of the Arabian Peninsula, has an arid climate. The mean monthly temperatures over Kuwait ranges from $45^{o}$ C in July to $12^{o}$ C in January. The relative humidity is generally low because of the prevailing hot and dry westerly winds, and monthly relative humidity varies between 19% in June and 64% in January (Amer et al., 1990).

Rainfall is low and irregular in occurrence. The annual average is about 115 mm, which occurs essentially in the form of thunder showers mainly between November and April. On the other hand, annual potential evapotranspiration is high, averaging about 2,266 mm/year (Amer et al., 1990), leading to a high negative deficit in the water budget, creating impossible conditions for perennial surface water systems to exist. Therefore, water demands in Kuwait are met mainly by brackish groundwater abstraction and seawater desalination.

Aquifers containing usable groundwater are restricted in Kuwait to the geological units of the unconfined Kuwait Group, and the underlying confined Dammam Formation aquifers. Due to its high TDS (3000-5000 mg/l) in Kuwait, groundwater is used mainly for non-domestic purposes (i.e. irrigation and industrial uses); in addition it is blended with desalinated water for drinking purposes.

## 1.2 STATEMENT OF THE PROBLEM

Based on the water system operation, hydrological conditions, and water demand in Kuwait, three main issues were identified as follows:

1. Sole dependency on desalination plants for potable water supply. The only source for potable water in Kuwait is sea water desalination. There is a danger that the desalination

plants will lost part or total of their capacity in event of emergency conditions resulting for example from; sea water pollution (e.g. with crude oil), mechanical failure of desalination plants, or vandalism or terrorist activities against the desalination plants.

2. Operating desalination plants at poor efficiency. All of the urban potable water comes from sea water desalination plants. These plants have fixed optimal operational capacities. Operation of desalination plants at other outputs results in sub-optimal efficiencies. Water demand, however, varies significantly on a seasonal basis, high in summer and low in winter. Hence, most of the year, desalination plants are operating at poor or low efficiency.
3. Subjecting the aquifers to overpumping is creating a massive decline in their potentiometric heads. This decline is inducing sea water intrusion and upward leakage of the deep saline water leading to a deterioration of the groundwater quality.

Artificial groundwater recharge is proposed to be implemented in this study to solve the above problems. However, one of the limitations, is the potential for deterioration of the artificially recharged stored water recovery efficiency. That could be caused by the displacement by, and mixing with, regional groundwater flow as the delay in recovering the stored water from aquifers proceeds.

## *1.3 OBJECTIVES OF THE STUDY*

### 1.3.1 INTRODUCTION

Prior to this study the only motive for investigating artificial groundwater recharge in Kuwait is simply to store freshwater in the aquifers for emergency use. The present study is the first in Kuwait to investigate the feasibility of implementing the artificial recharge to improve overall water system efficiency through a conjunctive use between aquifers and desalinated water production. Moreover, all previous studies concerning artificial groundwater recharge in Kuwait (see section 1.6) were site-specific studies, to investigate the technical feasibility of recharging the aquifers in Kuwait. By contrast, the present study is the first in Kuwait to examine the feasibility of artificial groundwater recharge on a regional scale covering the whole of Kuwait.

Furthermore, in this study the influence of regional groundwater flow in shifting the artificially recharged stored water mound away from its position and deteriorating the quality of its water was solved. Through a new technique using management models, installation of hydraulic "gradient-control" pumping wells outside the stored water mound has been simulated. The optimum pumping rates for these wells to develop the zero hydraulic gradient was determined using the management models.

### 1.3.2 OBJECTIVES OF THE STUDY

Seasonal water demand fluctuations could be overcome through short-term storage, in which the excess desalinated water during winter is stored to be used later during the water peak demand in summer. Also, part of the surplus of desalinated water could be placed in long-term storage to meet the shortage in potable water demand under emergency conditions.

However, since Kuwait is an arid country, with no rivers, canals or lakes to be used as natural storages, aquifers could provide the promised storages. The underground storage of freshwater in brackish aquifers by artificial recharge may be used as an alternative to a surface reservoir. Such a process would typically involve injection of freshwater, storage until needed and subsequent abstraction from the same well. Storing water underground has the advantages of; (i) being economically more feasible than surface storages, because of the low cost of construction and maintenance, (ii) minimising evapo-transpiration losses, and (iii) being relatively safe from pollution threats.

Based on the above benefits of using artificial groundwater recharge in Kuwait, the objectives of this study were defined as follows:

1. Model the study area to obtain the following:
   a) Achieve a representative set of aquifer and aquitard parameters that can be relied on in the evaluation of the aquifer system.
   b) Determine the pre-development water budget of the aquifer system and use it to explain the present behaviour of the aquifer system.
   c) Predict the hydraulic and transport response of the aquifers to groundwater abstraction and/or artificial groundwater recharge.

2. Evaluate the aquifer response to artificial water recharge, and investigate the practical difficulties resulting from the well injection using a pilot freshwater injection-withdrawal experiment.
3. Evaluate the feasibility of using the artificial groundwater recharge in Kuwait to develop; (1) a long term freshwater underground storage for emergency use, and (2) a freshwater seasonal storage to facilitate operating the desalination plants with their optimum capacity all over the year irrespective of the seasonal fluctuation in water demand. This is the main objective of using the seasonal storage, however, a secondary benefit could be obtained through increasing the depleted aquifer yield.
4. Rank the possible sites for artificial groundwater recharge, and select the optimum sites, (one for a long term strategic reserve and one for seasonal, short term storage).
5. Determine the optimum management variables which must be satisfied to establish the long term strategic and the seasonal storages, including; the number and geometry of the injection wells, their injection/recovery rates, duration of water injection required to create the intended quantity and quality of freshwater.
6. Develop techniques to maintain artificially-recharged stored freshwater for a long time.

## 1.4 RESEARCH CONCEPTUAL FRAMEWORK

This research will be carried out using the following combination of approaches:

1. Hydrogeological assessment;
2. Freshwater injection-withdrawal field experiment;
3. Numerical groundwater flow and transport simulation models; and
4. Management models.

### 1.4.1 HYDROGEOLOGICAL ASSESSMENT

An assessment was carried out in order to understand the varied of hydrogeological characteristics of the study area. The assessment was based on previously available data. Parameters such as hydraulic conductivity, storativity, aquifer thickness, boundary conditions, etc. were assessed as these parameters are very important for the progress of the research. This allowed identification of the geological and hydrogeological conditions influencing the aquifer system response to artificial groundwater recharge, and the recovery efficiency of the recharged water.

### 1.4.2 FRESHWATER INJECTION-WITHDRAWAL FIELD EXPERIMENT

Since Kuwait is located in an arid region, its climatic and hydrogeological conditions make the use of water-spreading techniques to recharge aquifers are impractical process. This is due to the extremely high evaporation rate, and to the dryness and relatively large thickness of the unsaturated zone. Therefore, the well injection could be the only possible method to recharge the aquifers in Kuwait.

A freshwater injection-recovery field experiment was carried out using a single-well (SU-10) in the Sulaibiya wellfield completed in the Dammam aquifer. The recharge water was potable; hence the TDS was used as a natural tracer since there was a contrast in its concentration between the recharge water and the brackish aquifer water. Subsequent to injection which was conducted for about 30 days, the injected water was withdrawn from the same well for about 90 days until the quality of pumped water reached the background level. Water level and tracer concentrations were measured at the test well during injection and withdrawal periods.

The experimental data from this test were analysed using a single-well numerical model (explained subsequently in section 1.4.3) to achieve the following objectives:

1. Evaluate the development of well face clogging, and differentiate between its possible causes;
2. Assess the quantity of water which could be injected successfully using a single-well;
3. Estimate the aquifer dispersivity and its relationship with other aquifer parameters; and
4. Estimate the recovery efficiency of the test.

### 1.4.3 NUMERICAL GROUNDWATER HYDRAULIC AND TRANSPORT SIMULATION MODELS

Three three-dimensional numerical groundwater flow and transport models were used to carry out this research. These were; regional, sub-regional, and single-well models. All these models are multi-layered consisting of the KG and DM aquifers. The MODFLOW groundwater flow modelling package (McDonald and Harbaugh, 1988), and the three-dimensional transport code MT3D (Zheng, 1990) were used to solve these models.

MT3D was chosen because it uses particle-tracking techniques to solve the advection term in the transport governing equation. Hence, the resultant solution will be free of numerical dispersion and artificial oscillation. This advantage is not provided by the other published solute transport codes. Also, it is very efficient with respect to computer memory and execution time, which is particularly desirable for the three-dimensional modelling (Zheng, 1990). MODFLOW is the most widely used groundwater flow package, and is thus well-tested, and well-documented (Fetter, 1994). Due to these reasons, in addition to its compatibility with MT3D, it was accordingly selected for the present study. Detail descriptions for the MODFLOW and MT3D codes are presented in Appendix I and Appendix II, respectively.

**I-Regional Groundwater Hydraulic and Transport Model**

This model is constructed to model the aquifer system on a regional scale, covering Kuwait and adjoining areas of Saudi Arabia. The model domain is discretized into 73x70 cells having irregular nodal spacing (ranging from 2000 to 5000 m), where $\Delta x = \Delta y$. This model will be used to complete the following activities:

1. Finding the more reliable aquifers parameters, determine the pre-development water budget, and to predict the aquifer response to the present and future groundwater abstraction (objective no. 1)
2. Ranking the sites available for artificial groundwater recharge (objective no. 4) through:
   a) Simulating the aquifer hydraulic response to artificial groundwater recharge, and hence to determine the volume of water which can be injected at each site, taking into consideration the effect of well clogging in reducing the well injection capacity, and creating an additional build-up inside the injection wells.
   b) Simulating changes in the native groundwater TDS during freshwater injection, and variations in the recovered water TDS during the recovery periods; hence the freshwater recovery efficiency at each site can be estimated.

**II- Sub-regional Groundwater Hydraulic and Transport Model**

In order to obtain more reliable results and simulate the freshwater injection and recovery at the optimum sites (as selected using the regional model) in greater detail, it is necessary to construct a model with smaller grid spacing. A sub-regional model was designed to cover

most of the existing wellfields and particularly the two recommended sites for artificial groundwater recharge. The selected area to be modelled was nested on the regional model coarse grids. Then this sub-regional model was modelled separately. The modelled domain was discretized using a rectangular mesh consisting of 80x176 cells with uniform spacing (where $\Delta x = \Delta y = 500$ m).

This model will be used to examine the management options available for storing-recovering freshwater in and from the aquifer for the long-term and the seasonal storages. Thus, the optimum management variables can be determined for each motivation of artificial recharge; storing freshwater for emergency use, and the seasonal cyclic injection-recovery of desalinated water, required to operate the desalination plants with their optimum capacities (objective no. 5).

**III- Single-well Groundwater Hydraulic and Transport Model**

This model is needed to analyse the freshwater injection-withdrawal experimental data to identify and investigate the well face clogging characteristics, estimate the aquifer dispersivity, and to determine the recovery efficiency of the test (objective no. 2).

In order to represent the freshwater injection-withdrawals experiment in reasonable detail and to define the modelled area within meaningful boundaries, the technique of Telescopic Mesh Refinement (Ward et al., 1987) was used to construct the single-well model. This was achieved through defining sub-regional boundaries within the regional flow model, which then define a new smaller problem domain. For more accuracy in defining the boundary conditions, the telescopic refinement done on two steps, until the model grids became small enough. The final design for the single-well model consists of 55x55 cells with irregular grid spacing. A very fine grid spacing (0.5 x 0.5 m) was used at the centre of the model, to represent the location of the well. Away from this node, the grid spacing was gradually increased to reach 67.8 m for the boundary nodes.

## 1.4.4 MANAGEMENT MODELS

The effect of regional groundwater flow in depleting the artificially recharged stored water after ceasing the injection process was investigated. In order to overcome such an effect

and maintain the stored freshwater for a longer time a new technique is proposed in this study. This involves installation of hydraulic "gradient-control" pumping wells outside the storage area which would be used to create a zone of zero hydraulic gradient around the area. A management model (which is a combination of the groundwater simulation and the optimisation models) based on linear systems theory was used to find the optimal pumping schedules of these gradient-control wells required to create the intended zero hydraulic gradient. Also, the optimal pumping rates from the groundwater supply wells which surround the stored water mound were determined.

Such a technique is a valuable contribution which could be applied in maintaining a stored freshwater mound after stopping the water injection in other areas (especially in the areas where such effects are very strong), and it is not restricted to the hydrogeological situation in Kuwait.

## 1.5 LAYOUT OF THE THESIS

The thesis is organised into 9 chapters giving detailed accounts of every aspect of the study, with this chapter as the introductory to the whole study. A literature review which was carried out on various topics related to the study is presented in Chapter 2. In Chapter 3, insights into the geology and hydrology of the area are presented, which were gained in order to understand the physical nature of the study system. Development of the regional model, and the simulated hydraulic response of the aquifer to the present and future groundwater abstraction are presented in Chapter 4. The study then progresses (Chapter 5) to analyse the injection-withdrawals field experiment using a single-well model. In Chapter 6, all the available sites were ranked and the optimum ones were recommended, based on the injected aquifer transmissivity, specific injection rates for the site wells, and the recovery efficiency of the artificial recharge practice. Chapter 7 includes an assessment of the availability of the various sources of water for artificial recharge, ranking these sources, and selecting the most suitable one. Also, in Chapter 7, a sub-regional model is presented which was used to evaluate the feasibility of applying the seasonal cyclic of water injection and recovery. In addition the development of a long-term strategic reserve is assessed in Chapter 7, including the management variables required to establish this storage. In Chapter 8, application of hydraulic "gradient-control" wells to maintain the stored freshwater

mound is assessed with the help of the management models. It is the purpose of Chapter 9 to summarise the main findings of the research, draw out the conclusion and recommend future works that might enhance the results obtained in the current study.

## 1.6 PREVIOUS STUDIES ON ARTIFICIAL RECHARGE IN KUWAIT

Recharge Pits : Artificial recharge in Kuwait was first tried by Parsons Corporation in 1964, when a recharge pit was constructed in the Raudhatain region to collect surface run-off during occasional rainstorms. The results of this study were reported by Senay (1977). During the test, recharged water reached the aquifer within 80-90 h after the occurrence of the rainstorm and raised the water level by about 0.9 m in the nearby observation well. From preliminary infiltration tests, Parsons concluded that:

1. Average infiltration capacity of recharge pits to be 9.1 m/d.
2. The amount of chlorine required to counteract the clogging effect of bacterial and algal growth was 4-8 mg/l.

Further conclusions were drawn by Senay (1977) and these were:

1. The average vertical permeability between the bottom of the recharge pit and the aquifer is reasonably high, which encourages the consideration of recharging throughout it.
2. During artificial recharge using recharge pits, water accumulates in the aquifer in the form of a floating lens. The thickness of the lens is not thick enough to facilitate the recovery of a reasonable quantity of the recharged water. This factor is particularly important in an area where there is no impermeable layer to prevent upward leakage of the underlying brackish or saline water, which is the case in Raudhatain.

Senay (1977) stated that the main drawback of using the recharge pits in Kuwait is the high evaporation rate (with an average value of 3.6 mm/d in winter and much higher values in summer) will cause loss of recharge water.

Hamdan et al. (1986) recommend that artificial groundwater recharge experiments be carried out to determine whether run-off water could be used for recharge in the depressions of the Umm Ar-Rimmam and Al-Aujah basins in the Jal Az-Zor region.

Injection Wells: The Ministry of Water and Electricity (MEW) conducted preliminary studies to evaluate the feasibility of artificially recharging the Kuwait Group aquifer using injection well, in the Raudhatain freshwater field (Jones, 1976). These tests showed that significant clogging can be induced by injection if untreated water is used for recharge.

Injection and pumping tests were undertaken by the Ministry of Electricity and Water (MEW) (Senay, 1977) at the Raudhatain water field (Fig. 3.18) to study the degree of clogging induced by injection and the quality change of injected water during the recovery period. One of these tests was carried out at Well R-53 between 12 October 1972 and 6 January 1973. The injection rate was 1309 $m^3/d$ and it was undertaken over a period of 27 days. Senay (1977) observed that the specific capacity of the well was reduced as a result of clogging from the predicted value of 159 $m^2/d$ to 86 $m^2/d$ at the end of the test. A step discharge test was undertaken at the end of injection. During this test, the well condition steadily improved, and towards the end of the step discharge test, the specific capacity of the well reached the initial estimated value.

Another injection test was undertaken by MEW during 1977 in the Raudhatain area (Fig. 3.18) to study the water quality changes in the recovered water. Water from well R-58 with a TDS value of 400 mg/l was used for recharge in well R-63 with a TDS value of 2500 mg/l. Water was recharged at a constant rate of 655 $m^3/d$ over a period of 29 days, pumped back over a period of 40 days. A significant aspect of this test was that no clogging was noticed during injection. Since the recharge water came from the same aquifer, and since water was injected directly resulting for non-existence of air entrapment. Senay (1977) estimated that about 10% of the injected water was recovered without undergoing any quality changes, and a total of about 52% was recovered with a quality of less than 1000 mg/l TDS.

Pyne (1989) emphasised that artificial recharge of aquifers in Kuwait is possible from the technical and hydrogeological points of view. He underlined that the Kuwait Group and Dammam Formation aquifers are prospective targets for the application of ASR (aquifer storage and recovery) technology in Kuwait.

Mukhopadhyay et al (1994) carried out Injection-withdrawal experiments at three wells (SU-10, C-105 and SU-135A) located in the Sulaibiya and Shigaya-C wellfields. The followings are some of the major conclusions/observations drawn from their experiments:

1. Suspended Solids. One of the major sources of clogging was suspended solids. Solids injected per unit open area of screens in Well SU-135A approximated 40 $mg/cm^2$ at an injection rate of 655 $m^3/d$. Suspended solids increased to around 200 $mg/cm^2$ at a flow rate of 1178-2095 $m^3/d$. periodic back-flushing clears clogging caused by suspended solids. Pre-treating injected water with slow sand filtration or membrane filtration helps reduce clogging.
2. Air Entrainment is a frequent cause of clogging. Air entrainment clogging could be reduced by improving injection pipeline design. Improvements usually include, making the injection pipeline system airtight and maintaining positive pressure in the system.
3. Injection Zones. Recharge wells need to be designed so that most of the injection water enters a particular zone of a given aquifer, especially when a vertical hydraulic gradient exists between aquifer zones.
4. Clogging in the Kuwait Group Aquifer (Well SU-135), simple back-pumping did not clear clogging in the Kuwait Group aquifer. Acidization and surging were required to clear clogging. In this case, clogging might have been caused by bacterial growth on the well screen and gravel pack. Most frequently encountered bacteria are iron oxidizing bacteria like Gallionella ferruginea and certain species of sulphate-reducing bacteria. Groundwater analysis at the injection site shows iron levels in formation water less than 0.05 mg/l. Growth of iron-oxidizing bacteria requires higher iron levels. But corrosion of the pipeline by dissolved oxygen may provide required $Fe^{2+}$ for the growth of iron-oxidising bacteria.
5. One way to suppress growth of iron-oxidising bacteria is to minimise the dissolved oxygen level in the injected water or to use PVC pipes for injection. Sulphates are high in the formation water at SU-135A (1050 mg/l). It is likely that sulphate-reducing bacteria might be growing on well screens and causing clogging. Further studies are required in this area to identify the nature and control of bacteria causing clogging.
6. Tracers. Selection of tracers and uniform mixing of tracers is essential for successfully monitoring the movement of injected water.

# 2. LITERATURE REVIEW: ARTIFICIAL GROUNDWATER RECHARGE

## 2.1 INTRODUCTION

Selected literature related to the present study were critically reviewed during the earlier part of the research. These include:

1. Possible applications for artificial recharge technique in groundwater systems;
2. The clogging of recharge wells; causes and cures;
3. Factors affecting recovery efficiency;
4. Estimating aquifer dispersivity using tracer tests; and
5. Applications of management models in managing groundwater resources.

The underground storage of fresh water in saline aquifers by the artificial recharge process may be used as an alternative to the surface reservoir. Such a process would typically involve injection of fresh water, storage until needed and subsequent production from the same well. Storing water underground has the advantages of minimising evapo-transpiration losses, equalising water temperatures, providing natural filtration and ensuring a protected local water supply during times of emergency. Also, the artificial recharge can be used to increase the depleted aquifer water levels in order to halt undesirable effects resulting from overpumping (such as salt water intrusion). Two main techniques are used for artificial groundwater recharge; water spreading and well-injection.

The use of well injection is limited by a particular difficulty resulting from a clogging of the well face (or well screen if present), and the formation pores around the injection well. This is considered to be the most serious difficulty caused by using well injection in artificial recharge. Most changes in hydraulic characteristics of the injection zone relate to air entrainment, geochemical precipitation of dissolved solids, or to deposition from bacteria, or suspended solids, that are introduced by injected water. The result is decreased permeability due to clogging of the well bore or screen and the injection zone.

The recovery efficiency is a prime indicator used to evaluate the success of the artificial groundwater recharge practice. That is the ratio of volume of usable water that can be recovered to total volume of recharged water. The recovery efficiency is affected by several factors, such as dispersion and mixing at the fresh-saline water interface, reshaping of the interface because of density differences between the fluids, and groundwater movement in the native aquifer system.

Using the solute transport models in the simulating of injected water behaviour and its concentration profile at any radius and time needs preliminary studies to determine the transport and hydraulic parameters. Tracer tests are the most reliable field method for obtaining information describing advection and dispersion in aquifers.

Management models (i.e. an integration of both simulation and optimisation models) can be used as a beneficial tool for groundwater planning and management. In the last section of this chapter the role of such models in managing groundwater resources will be presented.

## 2.2 METHODS OF ARTIFICIAL RECHARGE

Artificial groundwater recharge is defined by Sniegocki and Brown (1970) as the increasing of the rate of water flow into an aquifer, directly or indirectly, by some activity of man, either by plan or accident.

Artificial groundwater recharge is a well established technique in use around the world for the augmentation of water supplies and the reclamation of wastewater.

The methods of artificial recharge are grouped into two main categories :

1. Water spreading : releasing water over the ground surface in order to increase the quantity of water infiltrating into the ground and then percolating to the water table. Spreading techniques include basin, stream channel, ditch and flooding, and spray irrigating.
2. Well injection : the direct introduction of the recharge water to the aquifer by the use of injection wells.

Each of the two types of techniques has advantages and disadvantages that must be considered in terms of local conditions prior to selecting a technique for use. The followings factors should be considered in selecting the technique that best fits a particular set of local conditions (Kimrey, 1989):

**Water spreading requires:**

- Extensive land areas
- Permeable surface materials, hydraulic connection between the surface materials and the aquifer, and downward head gradient
- Relatively little construction or use of specialised equipment to implement and operate
- Little or no water pretreatment
- Some periodic maintenance
- Relatively little monitoring

**Well injection requires:**

- Little land area
- Specialised well construction
- Expensive construction and specialised equipment to implement and operate
- Water pretreatment
- Periodic to frequent maintenance
- Frequent to continuous monitoring.

Successful use of artificial recharge requires a thorough knowledge of the physical and chemical characteristics of the aquifer system, and extensive on-site experimentation and tailoring of the artificial recharge technique to fit the local or areal conditions. In general, water spreading techniques are less expensive than well injection and large quantities of water can be handled, particularly if suitable and relatively inexpensive land is available. Water spreading can also result in significant improvement in the quality of recharge waters during infiltration and movement through the unsaturated zone and the receiving aquifer. In comparison, well injection techniques are often used for emplacement of fresh recharge water into saline aquifer zones to form a manageable lens of freshwater, which may later be partially withdrawn for use or continue to be maintained as a barrier against salt-water encroachment (Kimrey, 1989).

## 2.3 GENERAL PURPOSES OF ARTIFICIAL RECHARGE

Artificial groundwater recharge has been practiced for scores of years throughout the world. The purpose of artificial recharge is to increase the rate at which water enters aquifers in order to supplement the quantity of groundwater storage. Artificial groundwater recharge can be an important element of a fully developed water management system, in which aquifers can be used as underground storages. As surface storage of water becomes less available and as over-consumption of groundwater resources leads to saline water intrusion and land subsidence, the need for techniques that enhance and supplement the natural recharge, and increase the utilisation of aquifer for storage, will become more vital. Generally, artificial recharge has many advantages and potential uses and is used basically to increase the groundwater storage in the aquifer. Artificial recharge can also be used a barrier to prevent or reduce saline water encroachment

The purposes of artificial recharge vary in general from one place to another, and from one period to another. A number of artificial recharge purposes were identified from literature, including :

1. Making use of aquifer storage and increasing the yield of a resource system;
2. Seasonal storage adjustment aimed at increasing the supply capacity during the summer months of peak demand;
3. The build-up of hydrological barriers and replenishment of depleted aquifers for the prevention of sea water intrusion, and to avoid quality deterioration due to upward leakage or upconing of saline waters;
4. Improving the quality of wastewater during infiltration through the soil and/or the zone of aeration;
5. Disposing of chemically or thermally polluted liquids;
6. Storing warm or hot water for energy conservation; and
7. Conserving peak flood discharges in rivers.

The following are some examples of the uses of artificial groundwater recharge in three selected countries:

**Britain**

In Britain, the artificial groundwater recharge is practiced mainly in three areas on an experimental basis; the London Basin, the Bunter Sandstone outcrop in Nottinghamshire, and the Lower Greensand near Hardham (Edworthy and Downing, 1979).

Joseph (1981) stated the following uses of artificial groundwater recharge in Britain:

1. Effluent disposal: This practice has the dual function of providing additional treatment (reclamation) and of disposal.
2. Storage augmentation: In the Lee Valley, artificial recharge was used to augment the storage for a complete water resources development, the usual sequence of water resource development at this site is as follows :
   a) Annual demand met entirely by abstraction from the local river
   b) Demand exceeds supply capacity of river occasionally, if minimum flow constraints are to be met; groundwater abstraction required at times of minimum river flow
   c) Demand and groundwater abstraction increases until the combined local groundwater and surfaces water resources are exceeded at times of low flow
   d) Water is drawn from the river during periods of excess flow in the winter and is stored in the aquifer for use during a period of low river flow.

In the London Basin, artificial recharge has been practiced by infiltrating water through basins or by injecting water into wells in the confined areas. This practice has been adopted to achieve the following objectives (Water Resources Board, 1972) :

- To conserve surplus surface water by utilising the storage available in the Chalk and lower London Tertiaries
- To increase the total yield of water resources by operating in conjunction surface and groundwater reservoirs in the Thames Basin
- To raise groundwater levels, thereby increasing the yield from existing wells, reducing operating costs and reducing saline intrusion.

Recent publications about artificial groundwater recharge in United Kingdom have focused on groundwater quality changes, either the improvement of recharge treated sewage effluent using

surface basins, or for the chemical reactions taken place between the recharged and the native waters (e.g. ; Montgomery, 1988; Rae and Parker, 1992; and Kinniburgh et al., 1994).

Montgomery (1988) studied the effects of groundwater recharge at nine sites at chalk, Triassic sandstones and alluvial gravel sites. He noticed that artificial recharge is a remarkably effective method of removing organic, ammonia, bacteria and viruses. However, he mentioned that, due to the tendency of calcium, magnesium. sodium, chloride and sulphate to be conserved during artificial recharge, this could restrict the use of recharged effluent for irrigation in arid climates. Thus, he recommended that the method of applying the effluent to the recharge area needs to be selected based on the effluent type, climate, and soil conditions. Also, the site should be investigated geologically.

Rae and Parker (1992) identified the mineralogical and geochemical factors influencing the quality of the recharge water in the London Basin aquifer system (Tertiary sands and Cretaceous chalk). These authors established phase associations for the Fe (pyrite, glauconite, and smectite), Mn (carbonates, gypsum, and clays) and S (gypsum, pyrite, and organic matter). They found that concentration of these elements vary considerably on a local scale, making basin-wide predictions difficult. Also, they noticed that the oxidation of pyrite is a process of major significance, and controlled to a certain extent by stratigrahpic factors, particularly the thickness of clay cover to the aquifer elements that control access of air and surface water.

Kinniburgh et al. (1994) investigated the effect of artificial groundwater recharge on the Basal sands and Chalk aquifers in the Lee Valley. They studied the drawbacks of artificial groundwater recharge at this location. One of these drawbacks is the potential for developing poor-quality groundwater as a result of pyrite oxidation. From obtaining porewater chemistry profiles from fresh cores through the basal aquifer at four sites, they found that the sites with highest $SO_4$ concentration (up to 33.000 mg/l) had a porewater pH of 3.45. Whereas, they found that water pumped from chalk showed little evidence of these extreme conditions. These authors noticed that there is no overall correlation between the bulk pyrite content of the sediment and the porewater $SO_4$ concentration within the sediment. They also mentioned that the principal mechanism governing the generation of $SO_4$ is the oxidation of pyrite which is

present in small amounts through the basal sands. The acid released during this oxidation reacts with smectite, illite, glauconite, feldspar and calcite, leading to high concentrations of Mg, K, Ca and other solutes in the porewater. They found that the high concentrations of $SO_4$ in the porewaters indicate that the extent of oxidation is controlled by the entry of air rather than the input of dissolved oxygen or nitrate in the groundwater or recharge water.

**United States**

Recharge wells are found through the USA. In 1988, 558 of the 719 injection wells surveyed in 14 states were recharging aquifers. The others were being used for saltwater intrusion barriers, drainage and subsidence control (Bouwer et al 1990). The following benefits are obtained by artificial recharge in US :

1. Seasonal storage: this includes the use of aquifers for underground storage, where surplus freshwater is stored in aquifers during winter and retrieved back during the summer months, when peak water demands and low water levels in reservoirs place strains on the water system. This practice is applied in Virginia (Brown and Silvey, 1985), Nevada (Brothers and Katzer, 1990) and Florida (Kwiatkowski et al., 1990).
2. Reducing the groundwater overdraft and replenishment of depleted aquifers: in Texas, the depleted water table of the Ogallala aquifer, which is pumped for irrigation use, is recharged with the surface water available from playa lakes (Brown and Keys, 1985). Also, in El Paso, Texas, a recharge project involving 38,000 $m^3/d$ was applied in order to reduce the mining of the underground reserve and to provide a secure water supply over the long term (Knorr and Cliett, 1985). In Eastern Arkansas, the declines in alluvial aquifer potentiometric head and potential groundwater shortages were augmented by means of artificial recharge (Masciopinto et al., 1991).
3. To prevent saline water intrusion of the local aquifers: this scheme of artificial recharge is utilised extensively in San Francisco Bay, which provides a practical example of this application (Todd, 1970; Hamlin, 1987; and Bouwer, 1990). This practice has also been used for more than 35 years in Los Angeles to prevent saline intrusion in the local aquifers; between 200 and 300 Mliters/d is injected through 180 wells (Joseph, 1981). In Atlantic

City, recharging the sand aquifer was used to increase the water in storage and reduce the potential for saltwater intrusion (May, 1985).

4. The disposal of urban drainage water and flood control: artificial recharge is used in smoothing out stream variations, which means pumping the flood runoff into the aquifer and releasing the water back in areas of low runoff. On Long Island, New York, more than 2200 lagoons are used for this purpose. Also, effluent recharge schemes are operated at Phoenix (Arizona), Pinellas Peninsula (Florida), and Leaky Acres (California) (Joseph, 1981). In Arizona, dry wells are used extensively for on site disposal of stormwater, and in certain industrial areas as a conduit to groundwater for contaminated runoff and other wastes (Haney et al., 1988).
5. Water quality and modification: in the Atlantic Coastal Plain, about 8 million gallons of treated drinking water have been injected into an aquifer of poor water quality. Later, the water has been successfully recovered through a dual-well (Castro, 1994).

**Aquifer Storage and Recovery (ASR)** technology is a relatively new concept in management of both potable and non-potable water systems. The basic concept of ASR is to treat water to potable standards during periods of low demand and inject the water into an underground aquifer. During periods of high demand, the water is recovered for use from the same injection wells. In ASR the groundwater system is used as a natural, giant storage tank. This technique is widely practised in the USA (e.g. : Amens and Jones, 1989; Kwiatkowski et al., 1990; Pyne, 1989; Dwarkanath and Ibison, 1991; Aiken and Pyne, 1992; Missimer et al., 1992; Buros and Pyne, 1993; Castro, 1994; and Bloetscher et al., 1996)

Amens and Jones (1989) found that at least 50% of the cost associated with treatment plant or transmission main enlargements can be saved at the sites which have good potential for ASR in Texas. They found that other benefits can be obtained if ASR is used, including: more effective use of water treatment plant and/or pipeline capacity; a large reservoir of treated water is readily available; improving the management of river water resources; and prevention of saltwater intrusion. They mentioned the conditions that are necessary to determine whether ASR is feasible in a particular setting, these are: (1) A seasonal variation in water supply, demand, or both. They maximum day demand should be at least 1.3 times the average daily demand; (2) A

useful ASR recovery capacity exceeding 1 mgd; and (3) A suitable ASR storage zone, as determined by engineering, hydrologeologic, water quality, economic, geochemical and other criteria. Also, they recommended that the ASR test program requires about three years to confirm feasibility and to complete one fully permitted, operational ASR well. Additional ASR wells can then be added easily as the need arises.

Kwiatkowski et al. (1990) described the use of a numerical model constructed for Marathon, Florida, which showed that use of ASR in a saline aquifer is feasible. They conducted a preliminary evaluation using a 16 inch diameter ASR well and two observation wells. These authors mentioned that cycles testing should provide the final data necessary to evaluate full-scale implementation of ASR in the Florida keys.

Pyne (1989) explained the concept of ASR, areas in USA which are practising such a technique, and its benefits to groundwater management. He stated that because the ASR is typically reducing the capital cost for water facilities expansion, it is increasly being accepted by water utility managers as desirable component of utility expansion plans. He also, explained the ability of ASR to improve system reliability in areas subject to emergency loss or contamination. Also, the role of ASR in preventing salt water intrusion, raising groundwater level to control land subsidence were presented by this author. By shifting the impact of surface water withdrawals from dry periods to wet periods, ASR is a positive and environmentally desirable water management tool, whether the period is seasonal or long-term.

Dwarkanath and Ibison (1991) found that an ASR system is benefiting Chesapeake, Virginia in three ways: (1) surface water sources are being used for efficient recharge during periods of low demand and high availability, (2) the facility allows the city to operate the existing river water treatment plant at full capacity throughout the year, and (3) water is now available when the chloride level in the river exceeds 250 mg/l and at any other times when the demand is greater than the available capacity.

Aiken and Pyne (1992) stated that the most recent application of ASR includes adding 131 l/s of ASR recovery capacity to 110 l/s of treatment plant expansion. With ASR, they found that the

utility could postpone the first treatment plant expansion by 10 years and the required expansion would be smaller (110 l/s versus 220 l/s). They mentioned three principal criteria governing the site-specific feasibility of ASR: (1) a seasonal demand in water supply or demand, (2) a reasonable scale of water facilities capacity, and (3) and/or a suitable storage zone. They stated that the feasibility must be determined for each site and typically investigated in phases. In the first phase, a conceptual plan is developed and significant technical and regulatory issues and addressed. In the second phase, prototype facilities are constructed, tested and permitted. During the third phase, ASR facilities are expanded as required to meet project needs.

**Israel**

Artificial recharge has been extensively practiced in Israel (as stated by Harpaz, 1970) for more than ten years, using more than a hundred wells. Harpaz (1970) outlined the main purposes of artificial recharge in Israel as;

1. Storing excess water to be used during dry periods and seasons of high demands;
2. The reduction of groundwater overdraft and replenishment of depleted aquifers in order to:
   a) Avoid salinization that may develop at the aquifer boundaries,
   b) Allow abandoned shallow wells to operate again;
3. The formation of pressure barriers against saline water intrusion; and
4. Improving the quality of water supplied to consumers by mixing the groundwater with the imported recharge water.

## 2.4 SITE SELECTION

Site selection and water evaluation includes the consideration of physical site criteria, the availability, and quality of the source water, and the quality and quantity of recovered water. The selection of the artificial recharge method (or methods) depends basically on such physical criteria as climate, topography, surface and subsurface geology, water quality and quantity involved. It also depends on other factors such as costs, technology and land use.

Wood (1980) stated that the following questions must be quantified if viable site selection criteria are to be developed:

1. How much source water is available, when and at what rate ?
2. What is the quality of the source water; dissolved solids content, temperature, organic content, ionic ratios, suspended solids, trace metals, bacterial and virus content ?
3. How much underground storage space is available, and at what depth ?
4. How readily will the aquifer accept the recharge water, and how readily can it be recovered?
5. How will the quality of water change after recharge ?
6. How quickly will the aquifer plug due to chemical, physical or bacterial processes?

Kimrey (1989) considered that in planning for injection, a good knowledge of the aquifer's coefficients of storage and transmissivity and its degree of hydraulic connection to adjacent zones is required. Thus, site selection should be started with a thorough hydrogeological survey, which should investigate the receiving aquifer, or injection zone, as well as the materials that underlie and overlie the injection zone. Also, the rate at which an aquifer will accept injection water has to be quantified. He assumed that this rate is dependent only upon the aquifer's capability to transmit and store water, if there are no attendant physical processes or geochemical reactions that may change the aquifer/s hydraulic characteristics. He stated that the drilling and testing of overlying and underlying materials should include determination of lithology and the quality of formation water, and evaluation of the degree to which they confine the injection zone. Drilling and initial testing of the injection zone should include determination of lithology, water quality, transmissivity, and storage properties. These data should be used for the design and construction of a test-injection well, or wells, for experimental work to further explore the feasibility of artificial recharge at the site.

## 2.5 CLOGGING

### 2.5.1 INTRODUCTION

The clogging of the well face (or well screen, if present), and formation pores around the injection well is considered to be the greatest difficulty introduced by using well injection. It is essential that any clogging characteristics be identified and investigated during injection-recovery tests, so that remedial steps may be planned and taken. Ideally, prevention of clogging problems may be achieved by higher pretreatment of recharge water. In order to determine the least treatment that can be given to recharge water and still permit injecting the water with a minimum of technical difficulties, it is desirable to isolate each cause of clogging and quantitatively evaluate its effect. In addition, the first cause of clogging to be isolated and obviated should be the one that plugs the well or aquifer most rapidly and severely (Sniegocki and Brown, 1970).

Baffa et al. (1965) used the term "clogging rate" to describe the rate of change of injection head to quantify the clogging mechanisms in an injection well. He found this term which is the additional rise in water head above the predicted to be about 0.03 m/day as an average for 11 injection wells in Los Angeles, USA.

Harpaz (1971) used the specific injection rate (SIR) as an indicator of the well's injection capacity (that is the injection rate divided by the rise of water table inside the well). He employed this indicator in addition to the analysing of the backwashed material in the laboratory to determine and evaluate the effect of clogging on the hydraulic characteristics of the dual wells used for injection/abstraction purposes. From an artificial recharge project carried out for a hundred deep wells completed in different formations (sandstone, dolomite, limestone, and basalt) in Israel, he determined and evaluated the effects of clogging on the hydraulic characteristics of the injected wells through observation of the changes in the injection rates. Harpaz (1970) concluded that initial recharge rates decline generally along with the cumulative injected amounts and the duration of recharge due to well clogging.

### 2.5.2 CLOGGING RELATION TO FORMATION TYPE

Rebhun and Schwarz (1968) conducted a field survey and a laboratory test to examine any possible clogging which may result from the artificially recharging of production wells by lake water in Israel. They observed during the test that the water will enter the fractures and holes in the limestone aquifer that are large compared with the pores of sandy granular or sandstone consolidated formations. The filtering out of suspended materials in limestone is less effective than in sandstone, and the accumulation of organic solids in the close vicinity of the well is smaller. Thus, they concluded that the clogging and contamination processes in limestone are much less pronounced and detectable than in sandstone.

The same observation was also reported by Harpaz (1970), who observed that the limestone wells have much larger capacities than other wells (completed in sandstone, basalt, and dolomite aquifers) even without redevelopment. The injection rates for limestone wells vary between 300 $m^3/h$ to 2350 $m^3/h$ without any noticeable decline over time. These rates are far greater than the installed pumping capacities in the same wells, and are often limited by the equipment installations at the wells and not by the intake capacity of the aquifer. He found that even though if the injection capacities of the limestone wells declined during the recharge, they remained high enough to sustain the full injection rates throughout a long recharge period. He further concluded that the quality of the recharge water (whether of lake or ground origin) has a significant effect on the capacity of the wells.

In contrast, sandstone wells are more prone to clogging. For instance, Vecchioli (1972) found that if reclaimed water was to be recharged into a sand aquifer using an injection well (at Bay Park, Long Island, USA), stringent quality requirements would have to be maintained on the injected water to minimise well clogging. For example, the turbidity, iron, aluminum, and phosphate content of the injected water would have to be kept at near-zero levels, and the water would have to be chlorinated; otherwise, the rate of clogging would require frequent redevelopment of the well.

Joseph (1981) stated that, based on his experience of artificial recharge, clogging is a particularly difficult problem in boreholes in granular aquifers and it is difficult to clean the well face properly. Thus, he recommended the necessity for using a potable water for the wells in such aquifers to minimise the clogging development.

### 2.5.3 GENERAL CAUSES OF CLOGGING

Most of the factors causing well clogging have been found from experience of artificial groundwater recharge all over the world. These have been documented by many authors (such as; Sniegocki, 1963; Baffa et al., 1965; Sniegocki and Brown, 1970; Krone, 1970; Harpaz, 1970; Brown and Singor, 1972; Bichara, 1974; Huisman, 1983; Bichara, 1988). The following causes have been identified:

1. Gas binding or air entrainment in the aquifer;
2. Suspended particles in the recharge water;
3. Bacterial contamination of the aquifer by the recharge water and subsequent clogging by bacterial growths;
4. Chemical reactions between the groundwater and recharge water causing precipitation of insoluble products;
5. The swelling of clay colloids in the aquifer;
6. Ion exchange reactions that could result in clay particles dispersal;
7. The precipitation of iron in the recharge water and groundwater involving iron reducing bacteria or sulphates splitting organisms; and
8. The mechanical jamming of the aquifer, caused by particle rearrangement when the direction of water movement through the aquifer is reversed or excessive injection pressure is applied.

### 2.5.4 GENERAL PREVENTION AND REMEDIES OF CLOGGING

Kimrey (1989) stated that the experience in the south-eastern United States and other areas indicates that reactions, or processes, which result in clogging are reduced if recharge water is free of suspended solids, bacteria and entrained air, and is similar in its chemical characteristics to the formation water. He also mentioned that injection into fissured formations, with fractures or solution cavities comes less clogging compared to injection in intergranular formations.

The building up of the water head with time as a result of clogging can be reduced by three methods :

1. High pre-treatment of the recharge water which may lower the content of suspended matter.

2. Increasing the number of the injection wells which will lower the injection rate and the velocity of recharged water.
3. Enlarging the well dimensions to lower the value of recharge water velocity.

The general requirements for water to be recharged through wells (Sniegocki and Brown, 1970; Krone, 1970; Vecchioli, 1972; Flavin, 1979, and Huisman, 1983) are as follows:

1. In general, chemical reactions between the injected water, native groundwater water, and the aquifer that cause clogging can be avoided by recharging with water that is chemically and physically compatible with the aquifer environment.
2. The dissolved solids concentration should be such that a sodium adsorption ratio less than 3 and as low as is feasible be maintained, and the concentrations of dissolved substances should be suitable for most sensitive use at the discharge sites. Precipitation of compounds resulting from combination of recharge water and aquifer water should be avoided.
3. The dissolved gas concentration should be less than the saturation concentrations at temperatures and pressures that will occur in the aquifer. Also, the aeration has to be avoided and the recharge water temperature showed be the same or greater than that of the aquifer.
4. The introduction of air can be prevented by lowering the injection pipe below the water table in the recharge well, also the air entrainment during recharge can be eliminated by installing a valve at the bottom of the injection pipe inside the recharge well to maintain at least atmospheric pressure in the pipe. In addition, air-tightening the injection pipeline system should be considered to prevent air entrainment
5. The suspended solids concentration should be as low as is attainable.
6. The recharged water should be chlorinated, and the nutrient concentrations should be maintained at the lowest possible level to minimise biological growths.

It is unreliable to generalise about the above mentioned factors responsible for clogging development, because local specification of the injection site (such as well construction, formation characteristics), and the quality of the recharge water and the native groundwater all have a significant effect on the factors that may cause well clogging. Thus, with respect to clogging, the local characteristics of these factors are more important than the more general characteristics (Baffa et al., 1965). The examples in the following section describe the effect of

such clogging factors at different conditions including various formations and waters, as observed during well-recharge field experiments.

## 2.5.5 EXAMPLES OF CLOGGING CAUSES AND REMEDIES

### 2.5.5.1 SUSPENDED MATERIAL

Brown and Signor (1972) described clogging of well bore by particulate matter consisting dominantly of silt and clay particles as the most critical problem in injection water into wells. The silt and clay plate-out on the inside of the well bore and also move with the water out into the aquifer, finally preventing the water from entering the aquifer. Because of the relatively small area inside the screened part of the well bore, particulate matter may greatly reduce the permeability of the aquifer near the well bore. Theoretically, he explained that the permeability could be maintained by reducing the amount of suspended material injected to zero or near zero.

Baffa et al. (1965) described the source of the fine-grained clogging material introduced by injected water into the formation pores, to the eroded particles from residual layers of drilling fluids on the sides of the drilled hole or within the formation itself. There may be orientation of the formation particles into a denser, less permeable pattern. He related the clogging mechanism to the size of the particles, the gradation of the formation, and the flow velocity, particles may filter out within a fraction of an inch of the face of the well or may be carried on into the formation.

Rahman et al. (1969) constructed a laboratory model to simulate the recharge into a well in a fine sand aquifer, and to investigate the effect of sediment concentration on the well recharge. They used a uniform fine sand, and two types of recharge water; clear tap water, and a sediment laden water which is obtaining by mixing of 50% bentonite and 50% kaolinite with tap water. Generally, the following conclusions were drawn from their study:

1. Suspended sediments sealed the interspaces of the fine sand and reduced the hydraulic conductivity by about 45% after about 8 hours of recharge for tests with 500 ppm sediment in the recharge water. The hydraulic conductivity was reduced by about 20% and 30% for the tests with 100 and 200 ppm water, respectively.

2. 80 - 90 % of the sediments was the maximum that could travel through the aquifer to the outlet of the model. Most of the larger sediment particles remained in the sand near the well screen. The tests did not run long enough for the well to be sealed completely. But if the tests had run longer, the percentage of sediments moving through the aquifer would be expected to decrease, and the aquifer would eventually become completely sealed.
3. Sediment concentrations in the range 100-500 ppm reduced the recharge rate. It appeared that any amount of clay in the recharge water would affect the recharge rates in the aquifer consisting of such fine sand, since 10-20 % of the clay was always filtered by the model aquifer sand during these tests.

Harpaz (1971) pointed that when large quantities of lake-water (even if potable), containing minute quantities of silt (less than 2 mg/l) and organic matter (150-800 A.S.U.) are introduced into a well, these particles are filtered out, by the gravel pack or the porous aquifers material, and form an impermeable mat, mainly organic, at the borehole face, which will develop resistance to water flow, both inwards and outwards.

Sniegocki and Brown (1970) found from well injection tests, that if all other recharge factors are considered equal, the recharge rate for a given concentration of suspended material or doubling the concentration of suspended materials for a given recharge rate will result in approximately doubling the clogging rate. With water having significantly different concentrations of turbidity, they found that the water having the highest turbidity caused a 40 % loss of specific capacity of the recharge well, and injection of water having the lowest turbidity caused only a 3 % loss in specific capacity. The distance that plugging occurred was found by these authors to be on the well screen and in the aquifer less than 1.5 m from the recharge well. They believed that the removing of these sediments is unlikely to be achieved with any of the common methods of well redevelopment.

Bichara (1988) reproduced field conditions in the laboratory in order to investigate redevelopment techniques of a clogged well. He recharged segmental perspex models with water of controlled quality and temperature containing different types of suspended solids of known size, using both gravel and non-gravel-packed wells. He found that the most efficient

method of redeveloping a clogged recharge well was by multiple reversals of flow direction (pumping and recharging the aquifer). He also concluded that either increasing the driving head under which the reversal flow is carried out nor increasing the duration of the reversal of flow has a marked beneficial effect. In addition, he found that the non-gravel-packed wells were easier to redevelop than gravel-packed ones, and the use of backwashing tubes in the gravel pack was not very successful in restoring the well efficiency.

When the injection head in an injection well reaches the maximum desirable level or limit of available injection water pressure, some type of redevelopment is necessary, so that the well will remain in service at the desired injection rate. Well development may be achieved by one of several methods, some of which are as follows (Baffa et al., 1965):

1. Bailing and surging with a cable tool rig;
2. Jet pumping and surging with an air lift; and
3. Pumping and surging with a deep-well turbine pump.

Baffa et al. (1965) considered the third method to be the more effective than the other two. He related the selection of redevelopment method used at each well to the method of its construction and its operating experience, in terms of known tendencies to yield fine sands and silts and historical evidence of caving around the well casing. He recommended for gravel-packed wells, the addition of gravel to the top of the gravel column as redevelopment proceeds to avoid the formation of voids underground.

Harpaz (1970) found that short intermissions in injection often restored the recharging rates, but only in the first part of the recharging period before severe clogging had already occurred. He recommended several short repumpings during the recharging stages to be carried out for an immediate and considerable improvement in the recharge capacity of the wells. The frequency of redevelopment should be determined, for each well, on the basis of its performance during the recharge season. For dual wells (used for recharge and abstraction), he considered that the long-term pumping of recharged wells for supply purpose was an effective practice in removing the clogging from well face if it is not severly occured.

Because the filtration process to remove the suspended solids from recharge water is costly, especially for water for agricultural use, some authors believe (e.g. Harpaz, 1971; Brown and Singer, 1972) that the ideal recharge well would be one in which particulate matter from injected water would deposit and from which the particles could subsequently be removed by redevelopment. Because a single well can be used both for recharge and for discharge, it may be feasible to remove some of the particulate matter from recharge water by filtration at the well-bore face, and remove these particles from the well bore by pumping. If such a practice is successful, they recommended using a built-in facility for redevelopment of the recharge system as being more economical.

Some rate of clogging may be economically tolerable when costs of additional pretreatment are compared with costs of periodic rehabilitation of the injection wells by hydraulic surging, chemical flushing, or other redevelopment methods. However, in some cases, remediation of clogging problems (particularly with screened wells) may prove too expensive and thus will negate the use of artificial recharge by well injection on a regular basis (Kimrey, 1989).

Huisman (1983) stated that well clogging is primarily caused by the high entrance rates of the recharged water into aquifers, which is one to two orders of magnitude higher than that with spreading ditches. He mentioned that even the best quality drinking water may contain some clogging substances, which after deposition at the interface between the well screen (or gravel pack, when present) and the surrounding formation increases the injection head. After some time, this injection head becomes too high, requiring a cleaning of the well screen and the surrounding formation to restore its capacity. This cleaning is seldom completely successful; some clogging will remain, requiring cleaning at ever shorter intervals or at ever increasing injection heads. These intervals will finally become so short or the head (after cleaning) so high that building a new well will be a more economic solution. Huisman (1983) related the development of clogging to the pore sizes of the aquifer. With consolidated or unconsolidated sandy formations, the pores are small, and an intensive pre-treatment, up to drinking-water quality is necessary to maintain the intervals between two successive cleanings at acceptable values. With gravel aquifers and much larger pore sizes, a limited pre-treatment may be satisfactory, while with fissured-rock aquifers and openings varying from a few centimetres to

some meters wide, no treatment at all may be required. In the latter case, however, the purification accompanying underground flow is also small, meaning that pre-treatment may be necessary to prevent contamination of the aquifer over large areas by impurities present in the recharge water.

Knorr and Cliett (1985) related some of the build-up in the aquifer head during well-injection (in El Paso, Texas, USA) to the initial build-up of the mound around the injection well and some to well clogging. They attributed the resultant clogging to the movement of silt and clay within the injection interval. Based on the decline in well injection specific capacity, they found that the well should be developed frequently (about every 6 months).

In south Australia urban stormwater is injected into a brackish aquifer using injection wells. Pavelic and Dillon (1996) observed during the water injection using such water that the main cause of clogging is the accumulation of suspended sediments at the well face. They used airlifting to redevelop the clogged wells on an annual basis. They noticed during monitoring of the suspended sediments load, along with the particle size distribution of the sediments extracted during airlifting, that a very small portion (about 1 %) are derived from the stormwater, and most extracted sediments are derived from the sands of the aquifer matrix, which are mobilised as calcite dissolves.

#### 2.5.5.2 CHEMICAL REACTIONS

The chemical aspects of clogging of injection wells primarily involves a chemical reaction. Chemical clogging may occur at the casing perforations, at the formation face, or in the aquifer itself. Baffa et al. (1965) mentioned some of the conditions responsible for causing chemical clogging, as follows :

1. precipitated metabolic products of autotrophic bacteria including hydroxide of iron, ferrous bicarbonate and metal sulfides of sulfur, or calcium carbonate, particularly in the presence of high concentrations of dissolved oxygen or chlorine;
2. chemicals in the injected water and in the formation itself;
3. the contact of injected water and native underground water of different chemical characteristics yielding precipitation;

4. the solution and redeposition of gypsum; and
5. the reaction of high-sodium water with soil particles causing deflocculation of the formation.

Baffa et al. (1965) found that water prepared for municipal and industrial purposes and having a relatively balanced calcium carbonate content will create problems when it moves through the gravel packing aquifer immediately adjacent to the well casing. He attributed this to the nature of calcium carbonate deposition where the tendency to deposit is increased in the presence of greater surface area for such deposition. Thus, by the nature of the travel of water in underground formations, a maximum opportunity is presented for the deposition of calcium carbonate. He reported that some success has been experienced with regulation of calcium carbonate deposition by lowering the pH with acid injection.

Theoretical analysis by Warner and Doty (1967) suggests that calcium carbonate could be precipitated from mixtures of two waters both initially stable with respect to dissolved calcium carbonate. They also found during a well-recharge experiment, that the dissolved ferrous iron in native ground water could be precipitated as ferric oxide or hydroxide as a result of mixing with oxygen-bearing recharge water, which is a time-dependent reaction. They suggested the injection of non-reactive water between the aquifer water and the main body of the injected liquid as a buffer zone to prevent chemical reactions out to a point where any clogging that does occur will have little influence on the intake rate of the injection well.

Sniegocki and Brown (1970) attributed the change in the kind and the amount of adsorbed ions to the unbalanced equilibrium caused by rapidly introducing water that differs in composition from that of the native groundwater. They explained the chemical clogging of a recharge well and aquifer to be commonly slow and not hydraulically obvious for a considerable period of time. Long term recharge would be place-injected water at a great distance from the recharge well. Consequently, chemical plugging would be occur through a relatively large part of the aquifer. They found that such plugging is in contrast to mechanical plugging by suspended solids, air entrainment, and microorganisms which generally would be localised to within a few meters of the recharge well. They stated that the redevelopment of the recharge well after chemical plugging may be difficult or nearly impossible, because the plugging may occur through a large volume of the aquifer. Many of the chemical reactions between injected water,

the native groundwater, and the aquifer are reversible. Therefore, they believed that one of the best means of redeveloping a recharge well after clogging caused by chemical reactions is to use the recharge well as a production well. Furthermore, such practice would help maintain intake capacities of a recharge well that may be clogged from other causes of clogging. They focused on the importance of polishing the injected water to match the groundwater. This ensures that the aquifers, which comprise distribution and storage systems that cannot be replaced by engineering works, are preserved for future use.

Brown and Singer (1972) found that at some cases (such as on some recharge wells at the Southern High Plains, USA), the use of pumping and surging is not a conspicuously successful way to remove particulate matter that deposited by chemical reactions.

Vecchioli (1972) considered the clogging that remained after swabbing operation to material bonded tightly to the aquifer grains, such as cementing of sand grains by a chemical compound. He observed during an injection test that the first water pumped from the injection well after injection ended had concentrations of iron and phosphate (largely in solid or particulate state) that were many times greater than those of the water injected. He found from acid treatment applied next to the injection well to restore its capacity, that the acid solution pumped from the well had very high concentrations of iron, aluminum, and phosphate, which sustained the role of these constituents in clogging.

Vecchioli (1972) applied hydrochloric acid treatment to remove the deposited constituents, where it was pumped into the well and left standing in the well overnight until the following day when the well was pumped. The pumped acid solution had very high concentrations of iron, aluminum, and phosphate, which reflect the role of these constituents in clogging. He found that the specific capacity of the well was improved by about 50 % after such a treatment.

Joseph (1981) mentioned that the injection of treated water into a saline aquifer (as at an injection site in USA) will cause severe clogging very rapidly because the change in ionic balance leads to deflocculation and mobilisation of clay particles. Clay minerals are particularly

affected by ion exchange reactions and, as a result, many of these clay minerals will swell or be dispersed in a semi-colloidal suspension, either effect may change the permeability of an aquifer.

Brothers and Katzer (1990) found during an artificial recharge process at Las Vegas Valley, Nevada, USA, where treated Colorado River water was injected into a sandy gravel aquifer, that the first problem is the potential for clay particles in the aquifer sediments to swell or disperse. He referred this process to the higher concentration of sodium that recharge water had than the native groundwater.

On the other hand, some chemical reactions may improve the aquifer's permeability. For example, Hamlin (1987) observed from an injection test in Palo Alto Baylands along the San Francisco Bay, where reclaimed water is injected into alluvial aquifer, an apparent increase of 2 % in well specific capacity during injection. He attributed this to the possible dissolution of calcite in the aquifer as a result of dilution of native water by injected freshwater.

Bouwer (1996) stated that wastewater treated to very pure quality with reverse osmosis (RO) will have a low TDS concentration, which makes it corrosive and aggressive. Thus he suggested that the interaction between this water and the receiving aquifer must then be well understood to make sure that this corrosive water does not mobilise chemicals from minerals and other solid phases of the aquifer.

#### 2.5.5.3 AIR ANTRAINMANT

Johnes (1982) attributed the formation of gas bubbles in the pores of an aquifer to:

- chemical or biochemical action (e.g. the reduction of nitrate to ammonia and nitrogen gas)
- supersaturated gases coming out of solution
- gas bubbles being carried in the water in a recharge borehole to the face of the aquifer.

Sniegocki (1963) found during an artificial recharge test using a recharge well screened in alluvium aquifer in the Grand Prairies region of Arkansas, USA, that the air entrainment was the most serious cause of plugging. Clogging was developed very rapidly at that test, where the reduction in permeability around the recharge well was at least 50 % within 5 hours when air

was permitted to enter the well with the recharge water. He concluded that even if free air is not permitted to enter an injection well with the recharge water, gas binding can still occur, and that the gases may be liberated from solution if the injected water is warmed by contact with the native water groundwater and aquifer. This form of gas binding may be more difficult to control than that caused by free air injected with the recharge water. He also attributed the generation of heat and release of gases to the possibility of biological decomposition of suspended organic matter exists in the injected water.

In order to eliminate air entrainment during well recharge, Sniegocki and Reed (1963) recommended the installation of a valve at the bottom of the injection pipe inside the recharge well to maintain at least atmospheric pressure in the pipe.

Sniegocki and Brown (1970) used sodium hexametaphosphate to develop a recharged well clogged by air entrainment, which was mixed with water and placed in the recharge well. Then freshwater was injected to move the mixture out into the aquifer. After a contact period of 24 hours the well was surged by turning a pump installed in the well off and on for short periods of time. The well was then pumped and surged until all the sodium hexametaphosphate had been removed. They attributed the effect of hexametaphosphate to its action in reducing the surface tension of water in the aquifer, permitting removal of air bubbles from interstitial spaces by pumping.

O'Shea (1984) used a down-hole valve during borehole recharge of the Folkestone beds at Hardham, Sussex, to control recharge rates and prevent air entry into the aquifer. He designed the test well to have the pump and motor at the bottom of a rising main, followed in turn by a non-return valve and recharge valve, thereby enabling it to be used as a dual-purpose recharge/abstraction rising main.

### 2.5.5.4 BACTERIAL CONTAMINATION

Bacterial action has been reported by many authors (e.g. Baffa et al., 1965; Krone, 1970; Vecchioli, 1972), to be a significant factor in causing the clogging of the injection wells,

especially during a long-term recharge operation. They have agreed that the main reason for biological growth is the presence of oxygen and organic nutrients in natural waters which will encourage the growth of micro-organic in and around the recharge well. This growth may occur inside or outside the casing and perforations, at the aquifer face, or in pores of aquifers some distance from the well. If the well is idle for a time, nuisance level tastes and odorous can result from these organisms decomposition. They believed that the most effective way to prevent the growth of bacteria is the chlorination of the recharge water. They suggested using high chlorination rates (8-12 mg/l) at the initial stages of injection, and after a long period, the chlorination rate (1.5 mg/l) can be reduced. In addition to chlorination, they recommended eliminating the nutrients source from the recharge water as far as possible.

Baffa et al. (1965) considered the growth caused from either new organisms introduced by injection or stimulation of previously dormant microorganisms within the formation. They reported that the most troublesome is the slime-forming type, which may be due to the slime growths themselves or to chemical products, including sulphate reduction or the precipitation of iron salts.

Harpaz (1970) observed during injection experiments in Israel that in wells clogged by bacterial actions, the initially repumped water is usually contaminated by high turbidity by decaying organic matter and with high coliform bacteria. This contamination was removed by means of short but rigorous repumping after recharge. He found that clearing the pumped water of the suspended matter may take some 15 minutes in limestone wells, and up to several hours in sandstone wells.

Vecchioli (1972) found that the injection of unchlorinated water for a 10-day period, will cause more severe clogging than the injection of water having a total chlorine residual of at least 2 mg/l. During one of the many injection tests he conducted, where the recharge water was less turbid and contained approximately the same or less amounts of iron and phosphate than the water in other tests. He noticed that the clogging during that test is higher, which attributed to bacteria levels. He also observed at the end of that particular test, that the head in the injection well was about 12 feet higher than that in the observation well, which suggests that much of the clogging occurred due to the growth of bateria at the screen of the injection well.

## *2.6 RECOVERY EFFICIENCY*

Artificial recharge usually involves injection and recovery of higher quality water than the lower quality formation water, and then at a later stage, the cycle is reversed and part of the injected water is withdrawn for use. Injections are generally made when recharge water is available to be stored, and recovery is applied when the stored water is needed.

The injection of water of low density (freshwater) into an aquifer that contains water of higher density (brackish or saline water) results in the formation of a lens or bubble, of the lower density water. The waters of different density will tend to mix in a transitional zone at the outer limits of the lens, so that the total amount of freshwater that is injected cannot be fully recovered. If water is withdrawn from the storage lens until its quality declines to some arbitrary limit, the ratio of volume recovered to volume injected is an index of the efficiency of the recharge-recovery operation. The ratio, expressed in a percentage, is known as the "recovery efficiency". This parameter, which must be determined experimentally, is the most useful and practical indicator of the feasibility of an artificial-recharge operation (Kimrey, 1989).

Esmail and Kimbler (1967) identified two principal physical processes which will take place during the storage process and can affect the recovery of fresh water :

1. mixing by diffusion and dispersion; and
2. gravity segregation.

As Fried and Combarnous (1971) explained, "dispersion" is the general term that describes all the physical phenomena governing the evolution of a transition zone created between two miscible fluids brought into contact.

Gravity segregation occurs when two fluids of different densities are in contact; as time passes, the denser fluid sinks and spreads along the bottom, whereas the lighter fluid rises (Esmail and Kimbler, 1967).

The long residence time (i.e. the delay between the completion of storing freshwater and the time of recovering this stored water) is a third factor in reducing the recovery efficiency caused

by the existing movement of regional water flow (Esmail and Kimbler, 1967; Moulder, 1970; Kimbler, 1975; Merritt, 1985).

Harpaz and Bear (1964) have reported the effects of flow fields, diffusion and mixing in both laboratory models and field experiments in Israel. Their work and other investigations have provided a mathematical basis for predicting recovery of freshwater stored in saline aquifers. They carried out two field tests at the Lod 20 site in Israel which showed very poor recovery results. The tests also illustrate the adverse effects of strong natural flow fields and of the time that water remains in storage. The poor recovery was largely due to down-gradient movement of the injected water in the natural flow field and to the difference in idle time between injection and recovery pumping for the two tests. Also some of the adverse effects must be attributed to the character of the rock. These authors found that the mixing at the interface between the freshwater and salt water might be greater in dolomite than in sandstone.

Esmail and Kimbler (1967) reported two cases of gravity segregation, One is the so-called static case where there is no bulk flow except that arising from convective currents attributable to gravity. The second is called dynamic gravity segregation, since it occurs in the presence of bulk flow. An example of the latter would be the segregation that occurs during the displacement of a fluid by an injected fluid of different density. They tested their models with a pilot storage experiment in Plague Mines in Louisiana, USA, and calculated the mixing and gravity segregation that results from the mixing of the injected freshwater with the native saline water to estimate the recoverable fresh water. As the leading edge of the mixed zone approaches the well bore, the effect of radial geometry on the inclination of the interface becomes important and an additional correction must be made. The main conclusions obtained from their investigations are:

1. Mixing between miscible fluids retards gravity segregation; and
2. Storage of freshwater in saline aquifers appears feasible from a recovery point of view under moderately favorable conditions (i.e. low permeabilities, high flow rates, and reasonably short storage times). Small density differences would also achieve a similar result.

Kumar and Kimbler (1970) used a three dimensional laboratory flow model in which both mixing and gravitational segregation occur simultaneously to predict the efficiency with which freshwater stored in saline aquifers might be recovered for later use. They found an agreement between the experimental results and the calculation procedure by existing analytical and empirical relationships. They suggested that even for unfavourable conditions the artificial recharge process might become feasible on a long term basis because the recovery efficiency improves with the number of injection-production cycles. Furthermore, they draw the following conclusions on the basis of computer calculations for hypothetical aquifer and operating conditions :

1. The storage of freshwater in saline aquifers appears technically feasible, and the most favourable parameters are low aquifer water salinities, low permeabilities, and thin formations.
2. The larger the density difference between the injected freshwater and saline aquifer water, the less efficient the process is.
3. For hypothetical conditions, effective porosity does not significantly alter recovery efficiency for porosity values greater than 0.15. Porosity may alter recovery efficiency through changes in permeability and dispersion coefficient.
4. Stratification or layering improves the recovery efficiency where individual layers have identical rock properties and where there is no cross flow between them.

Mualem and Bear (1974) studied the shape of the interface in a coastal aquifer in which a thin horizontal semi-pervious layer is present. They conducted laboratory experiments which showed that under these conditions a discontinuity in the shape of the interface occurs such that a freshwater region exists under the semi-pervious layer, while immediately above it saline or mixed water is present in the aquifer. They presented in their work an approximate solution for the shape of the interface below the semi-pervious layer and for the extent of the freshwater region above it under steady-state flow. Their solution is based on the Dupuit assumptions and on a linearization of part of the flow equations. Using laboratory experiments on a Hele-Shaw model, they found an agreement between the forecast interface profiles and those actually observed in the model. From the results of the experiments it follows that the separation of the interface into two parts, below and above the semipervious layer, decreases as the length of

landward seawater intrusion increases. They proposed a solution which can be readily applied to the case of a phreatic surface under an artificial recharge basin when the aquifer is separated into sub-aquifers by a series of semi-pervious layers.

Kimbler (1975) found that the cyclic storage of fresh water in a horizontal aquifer that possesses primary permeability and porosity is technically feasible. He also found that the deterious effect of pre-existing groundwater movement can be counteracted by creating an isopotential zone, or zone of stagnation, within the volume of the aquifer selected for storage of freshwater. Moreover, the following conclusions were obtained from his work:

1. The recovery efficiency in cyclic operation of injection and recovery improves cycle by cycle even if the initial efficiency is low.
2. The larger the density difference between aquifer water and injected water, the poorer the recovery efficiency during the first cycle.
3. The density of the aquifer must be determined in situ. However, the principal effect of a different dispersivity is to change the recovery efficiency, and thus the cyclic water loss. If the density difference is small, the value of the dispersivity can range over three orders of magnitude without substantially changing the recovery efficiency.
4. To determine the size of the land area needed for the well field and, if needed, the isopotential zone, it is essential to make an in-situ determination of aquifer porosity.

Singh and Murty (1980) conducted an experiment to determine the functional form of the diffusion coefficient by assuming that the movement of solutes from saline water into a recharged layer of freshwater in aquifers is by diffusion. They found the diffusion coefficient to be dependent on concentration and related to a constant depending upon the aquifer material. In addition, they developed an implicit finite difference solution to the non-linear diffusion equation using the preceding functional form of the diffusion coefficient. This numerical solution was used to determine the salinity profile with respect to time in a freshwater layer stored over a saline layer in groundwater aquifers. The salinity profiles are useful in predicting the water quality of the recharged freshwater layer.

Investigations have been made of the injection, and recovery, of surplus freshwater in Central and South Florida, USA (Merritt, 1983; Merritt 1985; and Tibbals and Frazee, 1976) which permit the following conclusions to be made about the factors which affect recovery efficiency:

1. Physical processes which limit the recoverability of injected freshwater are hydrodynamic dispersion, buoyancy stratification, and down gradient displacement by the local background flow system.
2. For a given volume of injected freshwater, the rate at which freshwater is injected or recovered does not appear to affect recovery efficiency. Generally, recovery efficiency will improve with increased volumes.
3. The length of time in storage does not affect recovery efficiency if the gradient does not significantly move the stored water, and if buoyancy stratification cannot occur under prevailing hydrogeologic conditions.
4. Partial penetration for the injection well does not appreciably affect recovery efficiency.
5. Recovery efficiency improves with repeated cycles, rapidly during initial cycles and then more slowly as a limit is approached.
6. Aquifers with water just saline enough to be unsuitable for consumptive use are optimum for freshwater injection and recovery, whereas very saline aquifers are least suitable.
7. Verification of the feasibility of cyclic injection, storage, and recovery of freshwater at specific sites can be determined only by performing actual tests. The amount of injected water that can be recovered before the withdrawn water exceeds the specified concentrations is the prime indicator of the engineering success of the practice.

## *2.7 DISPERSIVITY ESTIMATION USING TRACER TESTS*

### 2.7.1 INTRODUCTION

Solute transport through porous media is of practical importance in many applications, such as injection of freshwater into saline aquifers, salt water intrusion of coastal aquifers, and contaminant migration. Solute movement can be described in terms of only the process of advection by which solutes move at the same speed as the average linear velocity of groundwater, but complete a description of the transport of a solute requires consideration of two other processes: dispersion and chemical reactions. In saturated flow through porous media, velocities vary widely across any single pore, just as in a capillary tube where the velocity distribution in laminar flow is parabolic. In addition, the pores posses different sizes, shapes, and orientations. As a result, when a labelled miscible liquid (referred to as a tracer) is introduced into a flow system, it spreads gradually to occupy an increasing portion of the flow region. This means that there is a deviation in solute movement from the average linear velocity due to the local heterogenities. This phenomenon is known as dispersion and constitutes a non-steady, irreversible mixing process by which the tracer disperses within the surrounding water (Freeze and Cherry, 1979).

According to Freeze and Cherry (1979), dispersivity is the most elusive of the solute transport parameters. They mentioned that the laboratory column tests for longitudinal dispersivity performed with disturbed or undisturbed samples of unconsolidated geological materials yield values in the range of 0.1 - 2 cm. However, field measured values for dispersivity or model-calibrated values range up to 100 m or larger.

It is confirmed by many authors (e.g. Anderson, 1979; Pickens and Grisak, 1981; Gelhar et al., 1992) that the field-scale dispersivities are several orders of magnitude greater than lab-scale values for the same material. It is generally agreed that this difference is a reflection of the influence of nature heterogeneities which produce irregular flow pattern at the field scale. Consequently, laboratory measurements of dispersivity cannot be used to predict field values of dispersivity. Another complicating factor in quantifying dispersion is the so-called scale effect,

whereby dispersivity seems to increase with the scale of the solute movement in other words dispersivity seemingly increases as the solutes moves down-gradient (Anderson and Woessner, 1992).

Gelhar et al. (1985), having examined the literature concerning dispersion, found that there was currently a debate in the literatures regarding dispersion terms. They claimed that the dispersivity values in the governing transport equation are in a sense correction factors to account for the fact that it is not practical, and perhaps even impossible, to delineate the velocity distribution in detail. They believed that some investigators advocate better resolution of the velocity distribution in order to minimise errors associated with estimating dispersivity values. Others propose that theoretically derived formulas involving parameters that describe the statistics of the hydraulic conductivity distribution be used to calculate dispersivities. They stated that the dispersivities are traditionally estimated from trial-and-error model calibration and from tracer tests.

### 2.7.2 TRACER TESTS

In the tracer tests, a non-reactive tracer is introduced into the groundwater system, where the duration and quantity of tracer input are known. This will be through step (continuous input of mass), or pulse (instantaneous or slug input). During the test, the concentration distribution is recorded to produce a breakthrough curve. Gelhar et al. (1992) presented a classification for the tracer test as follows:

1. Natural gradient tests, that is conducted under ambient groundwater flow conditions.
2. Tests under flow configuration induced by pumping or recharge, including the following tests:
   a) Radial flow tracer tests, where a radial flow configuration is created by the test, of divided into two types:
      i) Diverging radial flow test, where a pulse or step input of tracers is injected at a recharge well and the time distribution of tracer is recorded at an observation well.
      ii) Converging radial flow tests, where the tracer is injected at an observation well and the time distribution is recorded at a distant pumping well.

b) Two-well tests, where both a recharge well and pumping well are operating. Tracer is injected at the recharge well and tracer breakthrough is observed at the pumping well. Recirculation of the water (containing tracer) from the pumping well to the recharge well is often employed.

c) Single-well, injection-withdrawal tests, where tracer is injected for a certain period and then recovered from the same well, and the time distribution of tracer is recorded at the well itself during the production stage.

Among the published studies illustrating the various types of tracer tests are the followings :

Hoopes and Harlemen (1967) presented some measured tracer distributions in a laboratory model to verify the theoretical predictions and to show the relative importance of convection, dispersion and diffusion on the displacement process in laboratory model and a field situation.

Sauty (1980) studied the non-reactive transport of solute materials in groundwater, or hydrodispersive transfer. He considered in his work several types of flow fields: linear flow, with one and two dimensional dispersion; and radial flow under diverging and converging conditions. His analysis included the two main possibilities for introduction of solutes into an aquifer: continuous, and instantaneous (or slug) injection.

Pickens et al. (1981) evaluated the dispersive and adsorptive properties of a sandy aquifer using a radial injection dual-tracer test with non-reactive $^{131}I$ and reactive $^{82}Br$ tracers. They monitored the tracer migration by using multilevel point-sampling devices located at various radial distances and depths. The resulting effective dispersivity values for $^{82}Br$ were typically a factor of 2-5 larger than those obtained for $^{131}I$. The distribution coefficient values obtained from analysis of the breakthrough curves at three depths and two radial distances ranged from 2.6 to 5.6 ml/g. They also made a correlation of adsorbed $^{82}Br$ radioactivity with grain size fractions and demonstrated preferential adsorption to the finest fraction. They determined the relative amounts of electostatics and specifically adsorbed $^{82}Br$ on the aquifer sediments with desorption experiments on core sediments using selective chemical extractions. The withdrawal phase breakthrough curves for the well, obtained immediately following the injection phases

showed essentially full tracer recoveries for both $^{131}I$ and $^{82}Br$. Relatively slow desorption of $^{82}Br$, indicated by extreme tailing of the return breakthrough curve and analysis of residual radio-activity on sediments cores, provided a further indication of the non-equilibrium nature of the adsorption-desorption phenomena.

Pickens and Grisak (1981) investigated the magnitude of longitudinal dispersivity in a sandy, stratified aquifer using laboratory column and field tracer tests. Their field investigations included two single-well injection-withdrawal tracer tests and a two-well, recirculating withdrawal injection tracer test. The tracer movement within the aquifer was monitored with multilevel point-sampling instrumentation. They found that the value of dispersivity is constant at 0.7 cm to be representative at the scale of an individual level within the aquifer. They also established the dispersivity from laboratory column tracer tests as a representative laboratory-scale value for sand from the field site which is 0.035 cm. They attributed the scale effect observed between the laboratory dispersivity and the dispersivity from individual levels in the aquifer to the greater inhomogeneity of the aquifer and the averaging caused by the groundwater sampling system. They derived the scale-dependent full aquifer dispersivity expressions, relating dispersivity to the statistical properties of a stratified geologic system where hydraulic conductivity distribution is normal, log normal or arbitrary, and found that the dispersivity is a linear function of the mean travel distance.

Hoehn and Roberts (1982) interpreted data from field tracer experiments to evaluate the adequacy of an advection-dispersion model for simulating field conditions. They applied a stimulus-response approach based on chemical reactor theory. Two different pulse stimuli at an injection well resulted in responses in two observation wells. It is clear in their work that the breakthrough response curves revealed extended trailing edges, especially at the nearer well. They employed a two-domain model to extend the simple advection-dispersion equation to account for the observed tailing, and the response curves of concentrations were fitted with finite-difference simulations which agreed with the field observations. On the other hand the response at more distant wells were characterised by values of dispersivity equal to or slightly smaller than those at the nearer well.

Guven et al. (1985) deal with the definition and measurement of the dispersive properties of a stratified aquifer based on the single-well tracer test. In this type of test, tracer is pumped into the formation for a period of time and then pumped out; sampling-observation wells which are multilevel were also used during the test. Their analysis of such a test was based on a Lagrangian-Eulerian numerical model which considers the depth of dependent advection in the radial direction and local hydrodynamic dispersion in the vertical and radial directions. The full-aquifer breakthrough curves measured in the observation wells in a single-well test in a stratified aquifer were determined by the hydraulic conductivity profile in the region between the injection-withdrawal well and the observation well, if the travel distance between these wells is typical of most test geometries. They found that the amount of mixing will depend on both the hydraulic conductivity distribution in the aquifer and the size of the experiment, and as the experiment scale increases, the effects of local vertical dispersion will become larger compared to the effect of local radial dispersion. They concluded that in the initial design of tracer test an understanding of the type of non-homogeneity and more information of a broad nature concerning the types or classification of non-homogenates that exist in natural aquifers would be very useful.

Molz et al. (1985) described the design and performance of single-well tracer tests utilising multilevel observation wells at a field site nearer Mobile, Alabama, USA During the test, each sampling zone contained an electrical conductivity probe and was connected to the surface with two lengths of vacuum tubing. Results showed that the sampling zones were well isolated and that sampling zone mixing was necessary to achieve results that were independent of probe placement within a given zone. They concluded that the permeability values based on tracer travel times from the injection-recovery well to the multilevel observation well varied by factor of 4 over the aquifer thickness. They described the experimental results as reasonably consistent with permeability trends inferred during thermal energy storage experiments performed earlier at the same site.

Molz et. al. (1986) conducted a two-well tracer test in non circulating mode in which the water from the withdrawal well is wasted at a safe distance from the test area. The objectives for their study were to describe the performance and results of a two-well test using the single well

hydraulic conductivity distribution reported by Molz et al. (1985). Two types of simulations were included in the study, one based on a horizontal, stratified, three-dimensional velocity field with fully three-dimensional local hydrodynamic dispersion; and the other based on the stratified velocity field alone with zero local distribution. The reported experiment implied that over the distances applicable to the two-well test the spreading of the tracer slug in the studied aquifer was dependent largely on macroscopic velocity variations that were quantifiable in terms of the inferred permeability distributions. A comparison between the measured and predicted concentration breakthrough curves at the individual levels was included in the study, which indicates that the aquifer stratification is not perfect between the injection and withdrawal wells. However, they noted that a normalised hydraulic conductivity trend appears to be dominating in the general flow region in the vicinity of the line connecting the two pumping wells. This rough knowledge of distribution was then used to predict the variations in the concentration level with time in the withdrawal well throughout the two-well test.

Bachmat and Bugayevski (1988) presented the theoretical basis of a field technique for evaluating longitudinal dispersivity and effective porosity by a single-well test, releasing a measured quantity of an ideal tracer instantaneously into the well at rest, allowing it and move with the natural flow velocity, and pumping it back after a certain delay time. They used the observed data for estimating the dispersivity and effective porosity; their interpretation of the data was based on an approximate analytical solution of the direct problem by means of the method of small perturbations and super position and on an iterative procedure for solving the inverse problem.

Novakowski and Lapcevic (1988) described the results and interpretation of five induced-gradient tracer tests performed at five different average inter-borehole fluid velocities in a single fracture in monzonitic gneiss. They used radioactive $^{82}Br$ and fluorescent dye as conservative tracers where the tracers, were pulse injected into radial convergent and injection-withdrawal flow fields. The flow fields were established between straddle packers isolating the fracture in three boreholes. They established the tracer breakthrough curves from samples of the withdrawn groundwater and have been interpreted using residence time distribution (RTD) theory and two deterministic simulation models. The model parameters were determined for each tracer test by

fitting the model simulations to the field RTD. The observation of the fits between the two simulation models and the field RTD suggest the existence of an initial advective dominated period of solute transport progressing to Fickian-type behaviour with increasing tracer residence time or decreasing fluid viscosity. They concluded that the dispersion of a conservative solute within single fracture under natural flow conditions can be described by a simple advection-dispersion model, provided that the flow field is not channelled and non-hydrodynamic transport processes such as matrix diffusion are appropriately considered.

Gelhar et al. (1992) reviewed dispersivity observations from 59 field test in order to evaluate their reliability, based on delineated criteria including: flow configuration, tracer and input, method of interpretation, and scale of the test. Accordingly, they classified these data into two categories of dispersivity value:

1. High reliability: where each of the following criteria have to be met:
   a) Tracer test was either ambient flow, radial diverging flow, or two-well instantaneous;
   b) Tracer input was well defined;
   c) Tracer was conservative;
   d) Spatial dimensionality of the tracer concentration measurements was appropriate; and
   e) Analysis of the tracer concentration data was appropriate.
2. Low reliability: where one of the following criteria was met:
   a) Two-well recirculating test with step input was used;
   b) Single-well injection-withdrawal test with tracer monitoring at the single well was used;
   c) Tracer input was not clearly defined;
   d) Measurement of tracer concentration in space was inadequate; and
   e) The equation used to obtain dispersivity was not appropriate for the data collected.

The main observations from the review undertaken Gelhar et al. (1992), are as follows :

1. Field-estimated longitudinal dispersivity has systematic increase trends with the observation scale. The longitudinal dispersivities ranged from 10-2 to 104 m, with their scale ranging from 10-1 to 105 m.
2. If dispersivity data is evaluated in terms of reliability, the trend towards increase dispersivity with scale of test cannot be extrapolated with confidence to all scales. The largest high-

reliability dispersivity value they reported is 4 m (Mobile Alabama, USA) and the largest scale of high reliability values is 250 m (Cape Cod, Massachusetts, USA). It is uncertain whether dispersivity increases indefinitely with scale or whether the relationship becomes constant for very large scales.

3. When reliability of the data is considered, the apparent difference between fractured and porous media at small scales is regarded as less significant because none of the fractured media data are of high reliability.
4. Dispersivities at small displacements will be underestimated if based on breakthrough curves measured in localised samplers in individual layers.
5. In a few cases, appropriate observations and/or interpretations would most likely lead to larger dispersivities.
6. For horizontal transverse dispersivities, there appears to be a trend towards increasing dispersivity with scale, but this appearance results from low-reliability data.
7. The vertical transverse dispersivity is much smaller than the horizontal transverse dispersivity, apparently reflecting the roughly horizontal stratification of hydraulic conductivity.
8. It is common practice to select constant values of the ratio of longitudinal to transverse dispersivities. The practice has popular of using, in numerical simulations, a horizontal transverse dispersivity which is about one third of the longitudinal dispersivity. There does not appear to be any real justification for using this ratio.
9. The horizontal transverse dispersivity is 1-2 orders of magnitude smaller than the vertical transverse dispersivity.

### 2.7.3 MODELLING OF DISPERSION TESTS

Dispersivity can be determined by fitting one-, two- or three-dimensional solute transport analytical or numerical solutions with the experimental data obtained by the tracer test. The methods of spatial moment can also be used in dispersivity estimation.

The governing equation for solute transport, known as the advection-dispersion equation, (Bear and Verruijt, 1987) is given below:

$$\frac{\partial C}{\partial t} = -V\frac{\partial C}{\partial x} + D\frac{\partial^2 C}{\partial x^2} \tag{2.1}$$

where

D : dispersion coefficient.

C : solute concentration.

V : average velocity.

Thus, the first term in the right-hand side is the change of the concentration due to advective transport, while the second term expresses the influence of dispersion on the concentration distribution. This equation should be solved, subject to certain initial and boundary conditions.

The coefficient of dispersion can be connected with velocity as:

$$D = \alpha V \tag{2.2}$$

where $\alpha$ is the dispersivity of the porous medium (L).

The analytical solution expressing the concentration distribution at a column of homogeneous porous medium was obtained by Ogata and Banks (1961) in the following form:

$$\frac{C}{C_0} = \frac{1}{2}\left[\operatorname{erfc}\left(\frac{x - V_t}{\sqrt{4Dt}}\right) + \exp\left(\frac{xV}{D}\right)\operatorname{erfc}\left(\frac{x + Vt}{\sqrt{4Dt}}\right)\right] \tag{2.3}$$

where erfc (C) is the complementary error function.

The determination of dispersivity requires a recorded concentration at a fixed point as a function of time, yielding a breakthrough curve which can be done through laboratory or field tracer tests. Dispersivities can be estimated from trail-and error model calibration using the observed concentration distribution (breakthrough curve) as a calibration target (Anderson and Woessner, 1992). A review of some of the published articles concerning the estimation of dispersivity using analytical or numerical modelling is set out below:

Hoopes and Harleman (1967) developed the mass conservation equation for a dissolved substance in two - dimensional groundwater flow. In the case of radial flow from a well, a simple approximate expression for the radial and temporal distribution of a dissolved substances introduced at the well was obtained. A comparison of the approximate expression with a numerical solution to the differential equation was given for defining the region in which the approximate solution is valid.

Krizek et al. (1973) developed a mathematical model to describe the hydrodynamic dispersion of a contaminant within the joint network of horizontally oriented, fractured rock aquifer confined at the top and bottom by two aquiclude. The contaminant is introduced into the joint system along a vertical line which simulated a well, and the time-dependent propagation of equiconcentration contours was determined. The independent variables included are: flow regime; degree of mixing that occurs at a node; joint orientations; and injection well pressure.

Zuber (1986) emphasised that the dispersivity value obtained from a given field experiment depends, sometimes to a high degree, on the mathematical model used in the analysis, and on the scale of the experiment. He pointed out that the aquifers are commonly stratified, which makes the tracers travel at different rates through the different layers. He also noted that the differences in hydraulic conductivity in the stratified aquifers are a dominant influence on the dispersivity values computed from concentration response data. He concluded that the tests in which monitoring wells with large screened intervals are used can yield large apparent dispersivities because of mixing in the well screen.

Moraniville et al. (1976) discussed the effect of non-uniformity on dispersion and the effect of anisotropy on dispersion using a stochastic model based on a random ensemble of idealised pores distributed according to some joint probability density function. They also calculated the dispersion tensor for a homogeneous medium in terms of single step averages and then considered this for particular probability density distributions. They compared their modelled results with laboratory measurements in unconsolidated media.

Chen (1985) developed analytical and approximate solutions for radial dispersion in aquifers with simultaneous diffusion into adjacent strata. He assumed that the contaminants were transported from the injection well by advection and mechanical dispersion with steady state and radially diverging groundwater flow field. He used a mathematical model consisting of two coupled differential equations to investigate concentration distributions in the main aquifer as well as in the adjacent aquitards and by using Laplace transforms. Firstly, he obtained analytical solutions valid for small time periods. Secondly, to determine the concentration distributions for intermediate and long intervals, he numerically inverted the appropriate transformed solution in the Laplace domain with stehfest algorithm. He found an agreement between the analytical solutions and the approximate solutions for small time intervals. Another conclusion be obtained from his study is the delay movement of contaminant due to the diffusive leakage. Finally, he recommended that the resultant solutions can be applied to study radial dispersion in granular aquifers bounded by relatively low permeability aquitards or in planer fractures.

Huyakorn et al. (1986) presented a simulation study of two-well, injection-withdrawal tracer tests in stratified granular aquifers at two separated sites. The first site was located near the Chalk River in Canada and the second site was in Mobile, Alabama, USA. These two sites are different in terms of vertical distribution of hydraulic conductivity, well spacing, flow rates, test durations, and tracer travel distances. Furthermore, the conducting test at the Chalk River site is in a recirculating mode, whereas the test at the Mobile site is conducted in a noncirculating mode. They performed their test simulations in three dimensions using the curvilinear finite element model, they concluding that the breakthrough curves at individual levels in the same observation well are influenced by hydraulic conductivity stratification, which can be detected by a comparison predicted breakthrough curves and measured data from the same observation well. If the areal variation of the aquifer is neglected in the simulation, agreement between the model predictions and field data will be good for some levels and poor for others. In addition, they found that the spatial distributions of concentration are influenced by the presence of hydraulic conductivity stratification and by the boundary condition at the injection well.

Huang (1991) discussed ways of using the analytical solutions for various one-dimensional tracer models and the tracer breakthrough curve to estimate average interstical velocity of the

flow. He demonstrated some empirical methods, such as dividing the distance by the time of peak concentration occurrence or the first breakthrough time, and argued that the accuracy of the empirical method is influenced by the dispersion degree of the tracer. He also discussed a modified one-dimensional instantaneous injection model. He concluded that the effective initial concentration which has been calculated from the tracer breakthrough must be less than the initial injection concentration, and the difference between the initial injection concentration and the calculated effective initial concentration might be used to evaluate the degree of tracer loss resulting from a combined effect of multi-directional dispersion, adsorption and decomposition.

Guven et al. (1992) developed a three-dimensional, advection-based numerical model for simulating two-well injection withdrawal tracer tests in heterogeneous granular aquifers. Their model has been applied to perform various simulations of actual two-well tracer test conducted in a confined aquifer at field site near Mobile, Alabama, USA. The developed numerical model is based on a simplified Lagrangian approach, in which the transport of the tracer between the injection and withdrawal wells is modelled, taking into account advection only, and neglected such processes as dispersion, sorption, and chemical or biological reactions. The results of this work indicate that it is possible to construct realistic, predictive models of contaminant transport in heterogeneous granular aquifers, if the necessary field measurements of the 3-D spatial distribution of hydraulic conductivity is obtained.

## 2.8 MANAGEMENT MODELS

### 2.8.1 INTRODUCTION

The management of groundwater resources involves the allocation of groundwater supplies and water quality to competing water demands and uses. The resources allocation problem is characterised by conflicting objectives and complex hydrologic, environmental and economic constraints. Groundwater simulation models are predictive management tools which provide the groundwater planner with quantitative techniques for analysing alternative groundwater pumping or recharge schedules. However, the simulation models do not identify automatically the optimal groundwater development, design or operational policies for an aquifer system (Willis and Yeh, 1987). Determining the proper objective function in a groundwater management model is often difficult but is an essential aspect of management modelling which should not be ignored. The difficulty can be solved by using a combined groundwater management model consisting of simulation and optimisation models. The combined management model considers the particular behaviour of a given groundwater system and determines the best operating policy under the objectives and restrictions dictated by the water manager (Gorelick, 1983).

Groundwater management models can be classified into two main types (Gorelick, 1983):

- Groundwater hydraulic and water quality management models; and
- Groundwater policy evaluation and allocation models.

The categories distinguish between models in which management decisions are primarily concerned with groundwater hydraulics, groundwater quality, and those inspecting policy evaluation as well as the economics of water allocation. The groundwater hydraulic and water quality management models are aimed at managing groundwater stresses such as pumping and recharge. These models treat the stresses and hydraulic heads directly as management model decision variables. The groundwater policy evaluation and allocation models can be used to inspect complex economic interactions, such as the influence of institutions upon the behaviour of an agricultural economy or complex groundwater-surface water allocation problems.

Although these models do not explicitly determine regional groundwater policy, they can be used in policy evaluation. These models are generally characterised by multiple optimisations, one for each subarea in a region, and have a strong economic management component (Gorelick, 1983).

In both categories the models employ the optimisation techniques of linear or quadratic programming. Such techniques attempt to optimise an objective, such as minimisation of costs or maximisation of well production, and are subject to a set of linear algebraic constraints which limit or specify the values of decision variables such as drawdown, hydraulic gradients, or pumping rates. In both categories the simulation model component of the management models is based upon the equation of groundwater flow in saturated media (Willis and Yeh, 1987).

This review concerns the joint use of groundwater simulation models and optimisation models. Only models which simulate groundwater hydraulics or groundwater solute behaviour by solving the governing partial differential flow and transport equations are considered. Of particular interest is the use of linear programming along with numerical simulation.

### 2.8.2 GROUNDWATER HYDRAULIC MANAGEMENT MODELS

Groundwater hydraulic management models incorporate a simulation model of a particular groundwater system as constraints in the management model. Management decisions as well as simulation of groundwater behaviour are accomplished simultaneously. Two techniques are used: the embedding method: and the response matrix approach.

In the embedding method the finite difference or finite element approximations of the governing flow equations are treated as part of the constraint set of a linear programming model. Decision variables are hydraulic heads at each node as well as local stresses such as pumping rates and boundary conditions (Aguado and Remson, 1974). In the response matrix approach, an external groundwater simulation model is used to develop unit responses. Each unit response describes the influence of pulse stimulus (such as pumping for a brief period) upon hydraulic heads at points of interest throughout a system. An assemblage of unit responses, a response matrix, is included in the management model. The decision variables in a linear, mixed integer (or

quadratic program) include the local stresses such as pumping or injection rates and may include hydraulic heads or drawdown at the discretion of the modeler (Heidari, 1982).

The embedded simulation model yields a great deal of information regarding aquifer behaviour. However, management rarely involves all hydraulic heads over space and time. Therefore, there is a risk that many of the decision variables and constraints will be contained unnecessarily in the linear programming model. For computational economy and the avoidance of numerical difficulties, many authors have recommended that the application of the embedding approach (e.g. Gorelick, 1983; Willis and Yeh, 1987: and Yazicigil, 1990) should be restricted to small, steady state problems.

On the other hand, in the response matrix approach constraints are included only for specified locations and times: unnecessary constraints or decision variables are not incorporated into the linear programming management model. Therefore, it can handle large transient systems in an efficient manner (Gorelick, 1983). Only the response matrix approach will be carried in this review, because it is proposed to use this method to find the optimal pumping rates by gradient control wells to maintain a zero hydraulic gradient around a stored freshwater lens created through artificial recharge.

### 2.8.3 RESPONSE MATRIX APPROACH

This method was mainly used by many authors to achieve the following objective functions:

1. Optimal planning policies for the regional groundwater system (e.g. to determine the potential yield, and to minimise the potential impacts, of salt-water intrusion. ( Heidari, 1982; Willis, 1983; Willis and Philip, 1984; Yazicigil et al., 1987: Yazicigil, 1990).
2. Optimal wells location (Rosenwald and Green, 1974; Maddock, 1972).
3. Optimal capacity-expansion of water wellfields (Basagaoglu and Yazicigil, 1995).
4. Optimal conjunctive use of groundwater and surface water (Danskin and Gorelick, 1985).
5. Optimal groundwater management strategy in contaminated aquifers (Colarullo et al., 1984).
6. Optimal remediation design for contaminated aquifers (Ahlfeld et al., 1988).

Some of these examples of applying this method are presented below:

Maddock (1972) developed a mixed integer quadratic programming model to find the optimal well selection that minimised pumping costs plus fixed costs for well and pipeline construction. The quadratic portion or the objective (pumping times lift) was made separately by a transformation that enabled solution by a combination of mixed integer and separable programming. This study illustrated sensitivity and error analysis to evaluate the effects on planning activities of uncertainty in economic and hydrologic factors.

Rosenwald and Green (1974) identified the best location for a specified number of wells so that the production-demand curve is met as closely as possible. An external finite difference model was used to generate a transient response matrix which described pressure changes caused by pumping.

Molz and Bell (1977) applied the embedded method to control the hydraulic gradient in a hypothetical aquifer used for fluid storage. They combined the steady state finite-difference equation with the gradient conditions in the storage region to develop a linear programming problem solved to find the optimum initial design of a wellfield that will create a finite gradient in a given region.

Heidari (1982) applied the response matrix approach to groundwater hydraulic management in Kansas, USA, where the unconfined system was treated as a confined aquifer as an approximation. The response matrix was utilised in a linear program which maximised pumping rates over time. Total pumping during each time period was forced to meet demands. Each pumping rate was limited by water rights. Drawdown at any time was constrained to a fraction of the total saturated thickness. Different solutions were obtained under maximum drawdown fractions which ranged from 0.1 to 0.25. To reduce the number of decision variables, wells were clustered into 61 well fields. Separate models were run for a 5-year a and 10-year planning horizons. In each case the time horizon was broken down into five equal management time units of 1 and 2 years, respectively. The models consisted of 610 decision variables (pumping rates and drawdowns) and were subject to 615 constraints. The linear programming models were

solved using MINOS [Saunders, 1977]. Heidari (1982) has demonstrated that the response matrix approach is applicable to a real world system and is a valuable tool for evaluating groundwater management strategies.

Willis (1983) applied the response matrix approach to the agricultural Yun Lin basin, Taiwan. The linear programming problem was to determine the optimal pumping scheme for three consecutive periods in order to meet agricultural water demands. The objectives were to maximise the sum of hydraulic heads and minimise the total water deficit. Constraints were placed on local groundwater demands, hydraulic heads, and well capacity. The simulation model used a finite element network containing 101 nodes. Each iteration of the linear programming problem, which had 225 constraints and 438 decision variables.

Willis and Philip (1984) presented a planning model for the optimal management of groundwater systems. The model, formulated as a bi-objective optimisation problem allocates over a series of planning periods. The optimal policies were planned to determine the potential yield from the water system, to minimise the potential impacts of salt water intrusion, and to allocate groundwater to competing water demands within the river basin. The objectives of the planning model were: (1) To minimise the sum of the hydraulic heads in the basin, a linear surrogate for minimising groundwater extraction costs; and (2) to minimise the total water deficit for the entire basin. The planning model was applied to the Yun Lin groundwater basin, Taiwan. A series of computer programs were designed to generate the coefficient matrix of the linear programming model. The resulting mathematical optimisation problem has 146 decision variables and constraints (not including slack, surplus, artificial variables or upper and lower bounds on the head and pumping rates). The optimisation model was solved with the APEX-III optimisation package developed by the Control Data Corporation.

Colarullo et al. (1984) used the response matrix approach to develop a groundwater management model to be used in identifying the optimal strategy for allocating limited freshwater supplies and containing wastes in a hypothetical aquifer affected by brine contamination from surface disposal ponds. Hydraulic constraints were formulated using linear systems theory to describe drawdown and velocity variables as linear functions of supply and

interception well discharge decision variables. The MINOS algorithm was used to identify the optimal combination of pumping well discharges. After suitable scaling of the problem, the minimum cost was obtained after 118 iterations.

Atwood and Gorleick (1985) used as a realistic setting for a hypothetical test to develop a hydraulic stabilisation to remove of groundwater contaminant plume. A two-stage planning procedure was used to select the best wells and their optimal pumping/recharge schedules to contain the plume while a well or system of wells within the plume removes the contaminated water. In the first stage, they combined groundwater flow and solute transport model to simulate contaminant removal under an assumed velocity field. The result is approximated plume boundary location as a function of time. In the second stage, a linear program, which includes a groundwater flow model as part of the set of constraints, they determined the optimum well selection and their optimal pumping/recharge rates.

Danskin and Gorelick (1985) developed a management model for the optimal allocation of water resources for a multiaquifer groundwater and surface water system near Livermore, California, USA. The groundwater system was analysed using a transient, quasi-three-dimensional model that considers the nonlinear behaviour of the unconfined aquifer. The surface water system consists of a reservoir that discharges water to three streams, which in turn recharge the upper aquifer. The management model constrained 255 constraints which fall into four categories:

1. Constraints related to well pumpages which guarantee that water targets are satisfied;
2. Constraints that ensure the maintenance of high quality groundwater by recharging stream water of good quality which dilutes poorer quality underflow to the basin;
3. Constraints that relate to the surface water system; and
4. Constraints that define the interaction of the surface water and groundwater system.

The management model was solved using the mathematical programming system extended and mixed-integer programming package (MPSX-MIP).

Yazicigil et al. (1987) applied a groundwater hydraulic management model to determine the optimal development and operating policies of a regional aquifer in the Eastern Province of Saudi Arabia. The hydraulic response of the aquifer system is represented by a simulation model that is linked to an optimisation management model using response functions. The resulting linear optimisation model had 315 constraints and 300 decision variables (not including the upper and lower bounds on pumping rates). Yearly optimal groundwater extraction rates over a planning horizon of 15 years were determined for four scenarios, each reflecting alternative groundwater development policies. The results were presented in the form of tradeoff curves, relating drawdowns to optimal pumpage to enhance the decision-maker's ability to select the best development policy from a set of alternatives. The results illustrate how various optimal management schemes can be devised to increase the total withdrawal from aquifer while preventing excessive dewatering.

Cijun Li et al. (1987) used a simulation model in conjunction with linear and nonlinear programming to examine the effects of various management choices on the optimal allocation of imported water from artificial groundwater recharge through surface basin in the San Juan Valley of Central California, USA. The objective function is the minimising of net drawdown below reference levels at the end of the management period. Two sets of decision variables were used: the first set consists of recharge rates in the recharge sites; and the second set of value of drawdown in each of the active cells in the basin which depend on the recharge rates. The study has demonstrated that decision regarding objective functions and their reference levels can be made only after careful consideration of basin characteristics and management goals.

Ahelfeld et al. (1988) used an optimisation approach to design contaminated groundwater aquifer remediation strategies. The methodology combines two-dimensional, convective-dispersive transport simulation, nonlinear optimisation, and sensitivity theory. The design variables are the location of the pumping wells and their pumping rates. Remediation strategies were generated based on different design criteria as represented by two alternative optimisation formulations. The first assumed that the analyst was seeking to remove all of the plume as quickly as possible within specified economic and physical limitations. The second was to reduce the contaminant concentration levels in the aquifer to satisfy regulatory standards. The

study demonstrated that the field scale simulation models can be incorporated into a nonlinear optimisation framework to solve important design problems.

Yazicigil (1990) developed three groundwater management models to determine the optimal planning and operating policies of a multiaquifer system in Eastern Saudi Arabia for an eight-year planning period. The model system was represented by a three-dimensional simulation model included in linear optimisation models using response functions. Yearly optimal pumping policies were determined for 52 well fields under three management objectives that maximised agricultural water withdrawals and minimised total drawdowns and pumping costs, subject to constraints related to the system's response equations, demand requirements, drawdown limitations, and discharge bounds. The objective function and the constraints were included in a linear programming problem that was solved using the MINOS [Murtagh and Saunders 1983] algorithm.

Suryanarayana and Akan (1996) used a simulation-optimisation model to maximise the wastewater recharge into an aquifer while satisfying the water quantity and quality requirements of the pumping wells. Their model is based on the two-dimensional unsteady groundwater flow and solute equations. They employed the response matrix approach for both flow and solute transport components of the model to allow time varying pumping and recharge rates.

# 3. GEOLOGICAL AND HYDROLOGICAL SITUATION OF KUWAIT

## *3.1 GEOLOGICAL SETTING*

### 3.1.1 GENERAL TOPOGRAPHIC AND CLIMATOLOGICAL CONDITIONS

The territory of Kuwait extends over an area of desert and low-lying lands. The terrain is part of a vast sedimentary basin that was formed during the Pleistocene. The topographic relief is generally flat, but depressions and ridges do reflect the structure of the underlying geological formations. The land surface generally slopes towards the north east with an average inclination of 1 in 500. The highest area in Kuwait occurs in the south west at an elevation of 275m amsl (Fig 3.1).

The climate of Kuwait is characterised by hot summers with occasional periods of extreme humidity, and mild to cold winters. The mean annual precipitation is about 115mm and the maximum and minimum annual precipitation recorded are 360 and 20mm respectively (Ministry of Planning, 1996). There is no conspicuous pattern of periodicity in high and low precipitation. Rainfall is strictly confined to the period from November to April, within which January and April are the most rainy months. Average annual evaporation rate is 2,266 mm (Amer et al., 1990). This high evaporation results in the concentration of salts near the land surface, thus enriching the upper zones of the soil with gypsum, common salt and calcium carbonate. The intensity of the rain storms has led to the formation of a conspicuous and dense surface drainage network of deep and long wadis that extend from the inland mountains in Saudi Arabia. They drain seasonal basins (such as Wadi Al-Rimmah, Wadi Al-Batin, Wadi Al-Mussanah, Wadi Al-Atki and Wadi Al-Sahba) which debouch into the Arabian Gulf. Substantial flows of water are caused for short durations by severe storms, leading to the accumulation of water in numerous playas. Thus, lenses of fresh water are formed over the phreatic water table. In case of sufficient replenishment, these lenses flatten with time because of their flow towards the sea. The mineral content of the flowing water increases with time because of the contact with sediment salts along its journey.

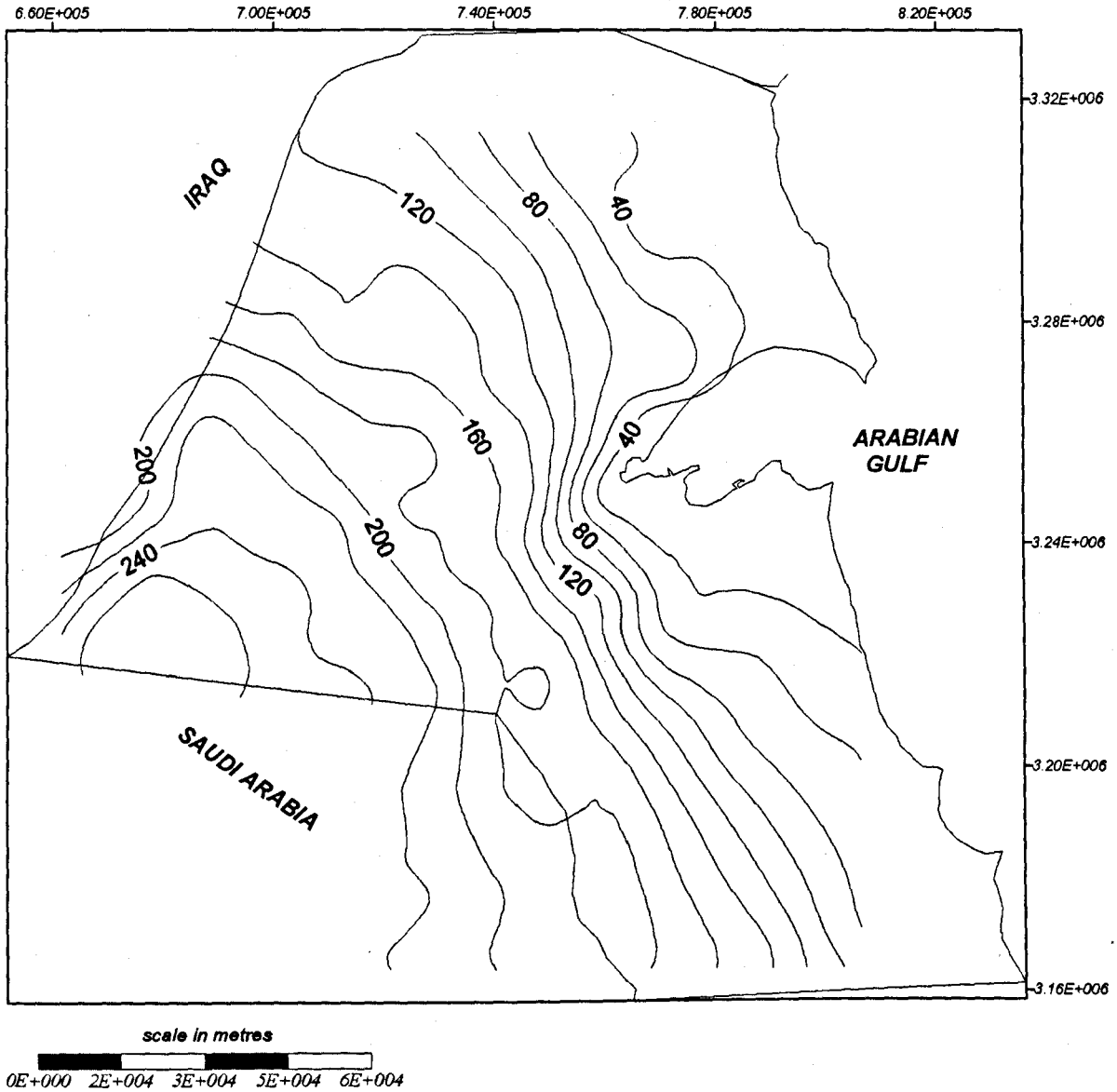


Figure 3.1: Topographic map for the Kuwait (m amsl)

### 3.1.2 LITHOSTRATIGRAPHY

Aquifers containing usable groundwater are restricted in Kuwait to the geological units of the Kuwait Group, and the Dammam Formation of the Hassa Group (Table 3.1). The lithostratigraphy and lithological description of the relevant geological units are as follows:

**I) Holocene deposits**

These deposits overlie the Kuwait Group in many areas of Kuwait, and consist of a surficial cover of aeolian sands, playa deposits (inland sabkhas), desert floor deposits, coastal sabkhas and beach deposits along the Gulf coast.

**II) Kuwait Group**

The Kuwait Group can generally be subdivided into three formations in descending order; Dibdibbah Formation (Pleistocene), Lower Fars Formation (Lower-Middle Miocene), and Ghar Formation (Oligocene-lower Miocene). In the southern part of Kuwait, where the fossiliferous beds of Lower Fars Formation are absent, due to similarity in lithology it is not possible to subdivide the consolidated sands overlying the Dammam Formation and the term Kuwait Group is applied to the whole section.

**1) Dibdibbah Formation**: This consists of a fluvial sequence of well-sorted, often cross-bedded sands and gravel with subordinate intercalations or lenticular bodies of sandy clays, sandstone, conglomerate, and siltstone. The sediments are locally cemented by lime or gypsum. The maximum thickness of the Dibdibbah Formation occurs in the northern of Kuwait where it reaches about 180 m, whereas disappears in the southern part of Kuwait.

**2) Lower Fars Formation**: This consists of alternating beds of red and yellow sandstones with red and green clays and various intermediate clayey sandstones and silty clays. Its thickness ranges from about 60 m in west Kuwait to about 180 m in the north of Kuwait.

**3) Ghar Formation** : This is recognisable in the northern and north-eastern part of Kuwait where it unconformably rests on the Dammam Formation and is overlain by the Lower Fars Formation. It consists mainly of marine and terrestrial unconsolidated sand, silt, and gravel. Some, limestone, clay, and anhydrite beds also occur in this Formation.

**III) Hassa Group**

The Hassa Group consists of three formations: the Dammam Formation (Middle Eocene), the Rus Formation (Upper Paleocene-Early Eocene), and Umm Er Radhuma Formation (Paleocene-Lower Eocene).

| Geochronology (Time) | | | | Lithostratigraphy | | | Lithology | |
|---|---|---|---|---|---|---|---|---|
| Era | Period | | Epoch | Group | Formation | Member | | |
| Cenozoic | Quaternary | | Holocene | | | | Inland Deposits: Sand, gravel | Coastal Deposits: Sand, mud, calcareous sandstone |
| | | | Pleistocene | Kuwait Group | Dibdibba Formation | Upper Member | Coarse-grained pebbly sand with thin intercalations of clayey sand and clay; pebble and cobble gravel and conglomerate. | |
| | Tertiary | Neogene | Pliocene | | | Lower Member | Coarse-grained, poorly sorted sandstone with carbonate cement and scattered pebbles. | |
| | | | Miocene | | Fars and Ghar Formations | Upper Member of Fars Formation | Northern Kuwait: Interbedded well sorted sand and sandstone, silty sand and sandstone with clay and clayey sand, and minor thin-bedded fossiliferous limestone in the east, prominent soft white calcareous sandstone in the west. | Southern Kuwait: Undifferentiated; interbedded sand and clayey sand with subordinate clay, sandstone and soft white nodular limestone. |
| | | | | | | Lower Member of Fars Formation and Ghar Formation | Interbedded well sorted sand and clayey sand with subordinate clay; prominent fawn cross-bedded sandstone layers with gypsum and carbonate cement. | |
| | | | Oligocene | | | | Sediments missing due to nondeposition or erosion | |
| | | | | | | | Unconformity | |
| | | Paleogene | Eocene | Hasa Group | Dammam Formation | | Dolomitic limestone with silicified limestone at top and nummulitic shale at base. | |
| | | | Paleocene | | Rus Formation | | Anhydritic evaporites, limestone and some marl. | |
| | | | | | Umm Er Radhuma Formation | | Marly limestone, dolomite, and some anhydrite. | |

Table 3.1 :Lithostratigraphic characteristics of geologic deposits in Kuwait (after Hunting, 1981)

**1) Dammam Formation** : The Dammam Formation rocks are the oldest rocks actually exposed in Kuwait. Locally, the formation is subdivided into three members (A, B, and C) from top to bottom, on the basis of stratigraphic characteristics (Al-Awadi, 1988).

**Member A** : This is the topmost member of the Dammam Formation and is distinctly different from the other two members. It consists of white, very friable, porous dolomite with thin chert lenses and nodules. There are occasional thin, dense fossiliferous zones. The top of the unit is marked by a karstified and cherty zone below the unconformity.

**Member B** : This member is the most complex member of the Dammam Formation. It is subdivided into six submembers. At the bottom, it originates with banded, bituminous algal limestone and grades upwards into fossiliferous, dolomitized and silicified limestone, occasionally silty. Further upwards, a highly silicified and dolomitized fossiliferous limestone grades into silty lignite with dolomite interlayers. Finally, it ends at the top with dolomitized fossiliferous limestone containing large shell fragments. This member is of Early to Middle Eocene age.

**Member C**: This consists of nummulitic limestone with shale interlayers at the base, grading into fossiliferous limestone at the top. The transition to the overlying member B is accompanied by a decrease of fossil frequency and an increase of dark clastic laminates, with enrichment of some organic matter.

The Dammam Formation is recognised by the occurrence of karstification and fracturing produced and controlled by dissolution and migration of calcium carbonate in water. So the resulting karst features depend on the intensity of dissolution processes. If dissolution prevails then the karst will be porous and if precipitation prevails then the resultant karst will be cemented and almost all pores and cavities will be cemented by the precipitated carbonate. The Dammam Formation occurs at depths ranging from near the surface at the Ahmadi ridge where it outcrops, to about 550 m depth in the north-east part of Kuwait. Its thickness ranges from about 120 m in the south-west of Kuwait to about 300 m in the north-east at Bubiyan Island.

**2) Rus Formation**: In Kuwait the Rus Formation is solely a subsurface unit composed of hard, dense, massive anhydrite and unfossiliferous limestone with few blue shale and marl beds. The formation in general has low porosity. This formation is of Lower Eocene age, it thickness ranges between 75 m and 200 m, and is underlain by the Umm Er Radhuma Formation.

**3) Umm Er Radhuma Formation**: This consists mostly of anhydrite, and dolomitic, marly limestone interbbeded with infrequent fossiliferous horizons. It ranges in thickness between 425 m in the north to about 610 m south-west of Khubbar Island (Omar et al., 1981). The age of this Formation is Lower Eocene- Palaeocene.

### 3.1.3 GENERAL STRUCTURE

According to Mitchell (1957), Kuwait is situated on the unstable shelf of the Arabian Shield. Within the Shield itself, epienogenic vertical movement and also tensional and shearing movement took place. There was a gradual facies change from continental through mixed-continental-marine to a marine continental lagoonal facies outward from the Shield. Increasing subsidence in the direction of the basin axis is indicated by the general thickening of the sedimentary beds in this direction. The subsidence in the basin and the deposition of sediments on a gently sloping sea floor, cause a gently dipping of the sedimentary beds towards the east and north east in Kuwait. This regular dip is interrupted by the Ahmadi ridge and by other major elongated anticline structures which are present at Rawdhatain, Umm Gudair, Wafra and Minagish. The general trend of these elongated anticline and syncline structures is north west-south east. These structures are associated with major faulting and fracturing. Kassler (1973) suggested these structures are growth structures and are also affected by salt diapiric movement. One exception of these structures is the Ahmadi structure which appears to be the result of horizontal compression in Post-Eocene times and is probably related to the Zagros orogeny (Mitton, 1967). Many faults or shear zones are found on top of the Dammam Formation in the south western and north western parts of Kuwait, with most of these structures running in the north-north east direction (Al-Sarawi, 1980). The major structure features were shown on top of Dammam Formation (Fig. 3.2). A geophysical survey has been carried out on 1968 by the Compagnie General de Geophysique (CGG) using the seismic reflection method and the electric resistivity method over an area of 1100 $km^2$ in western Kuwait. The results obtained from their study indicate, in addition to the anticlines and synclines, several tectonized zones that may be faults (in areas where there are throws) and zones of shearing (where such throws are lacking).

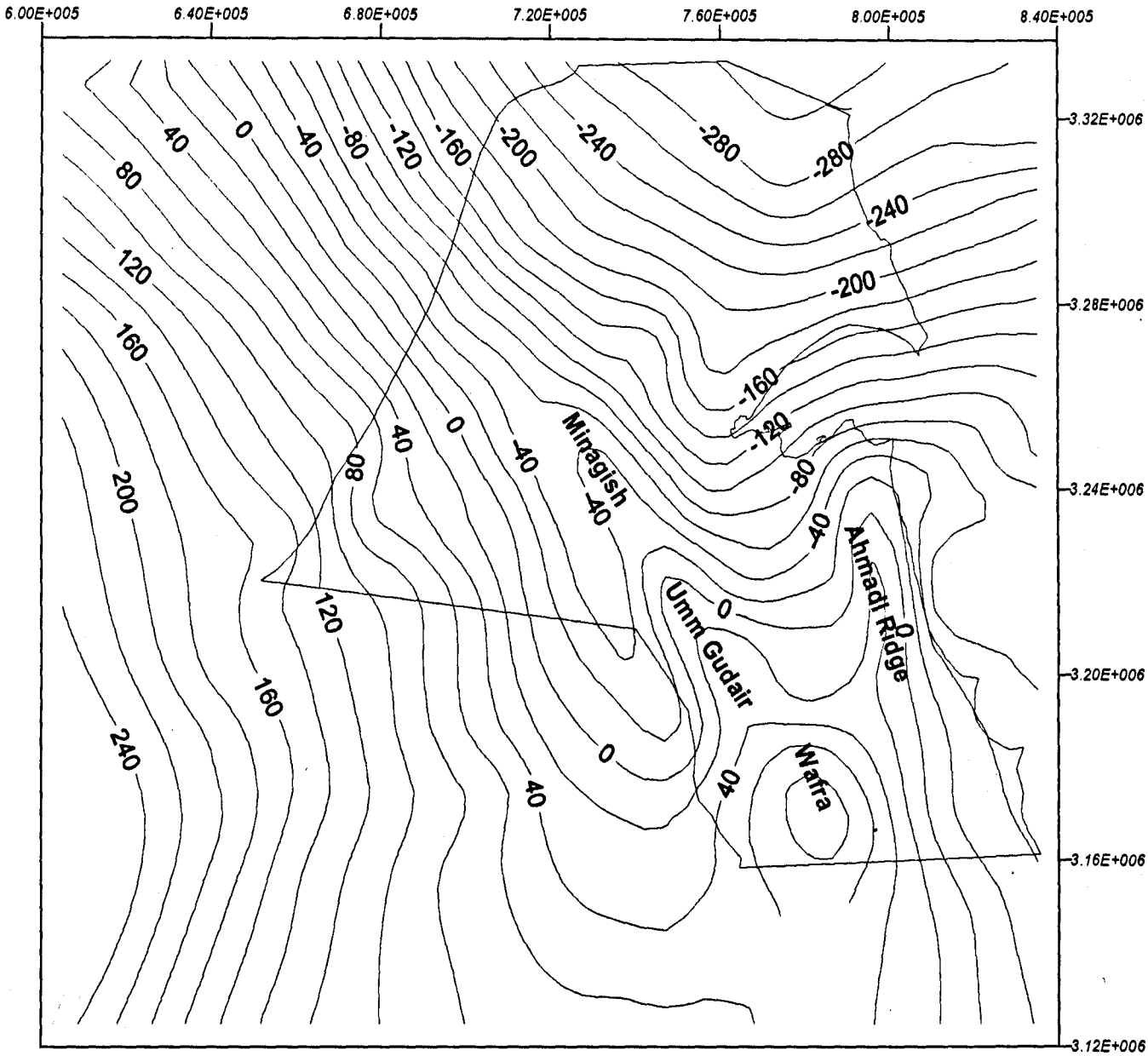


Figure 3.2: Major anticlines structures shown on the top of Dammam Formation, m amsl.

If the anti-clinal axes correspond to the decompression in Dammam Formation, their location may be of interest from a hydrogeological point of view. On the other hand, the synclines and shear zones should be avoided because they represent zones of compression in which the ground water movement can be anticipated to be slow. However, such zones may possibly contain small karstic conduits or minor fractures. The effective secondary porosity value is relatively high in the upper Dammam members, but it decreases gradually in the direction of groundwater flow towards the north-east (Omar et al., 1981).

## *3.2 GROUNDWATER HYDROLOGY*

### 3.2.1 AQUIFER AND AQUITARD BOUNDARIES

The Neogene-Quaternary (Kuwait Group) and Eocene (Dammam Formation) aquifer systems are the only developed aquifers in Kuwait because they contain usable water, whereas the other deep aquifers have connate water.

These aquifer systems in Kuwait consist mainly of saturated sediments of the Kuwait Group and the underlying Dammam Formation. The upper limit of the system is the water table and its lower boundary is the nummulitic limestone interbedded with shale at the base of the Dammam Formation. The system is separated from the deeper hydrostratigraphic units by the Rus Formation, which is a dense impervious anhydrite. Figure 3.3 shows the lithological and hydrological units of the aquifer system in Kuwait. In addition Figure 3.4 illustrates a cross-section showing the vertical and horizontal extent of these units.

**Kuwait Group (KG) Aquifer**

The Kuwait Group aquifer comprises of the saturated part of the unconsolidated to semi-consolidated clastic sediments of the Kuwait Group. In the Kuwait region, the Kuwait Group aquifer is classified as a multi-aquifer system divided into three water-bearing zones, except in the southern part of Kuwait, where it is classified as one aquifer and cannot be differentiated. The uppermost water bearing zone occurs only locally in depressions of the northern part of Kuwait, in the form of shallow elongated fresh water lenses formed by the

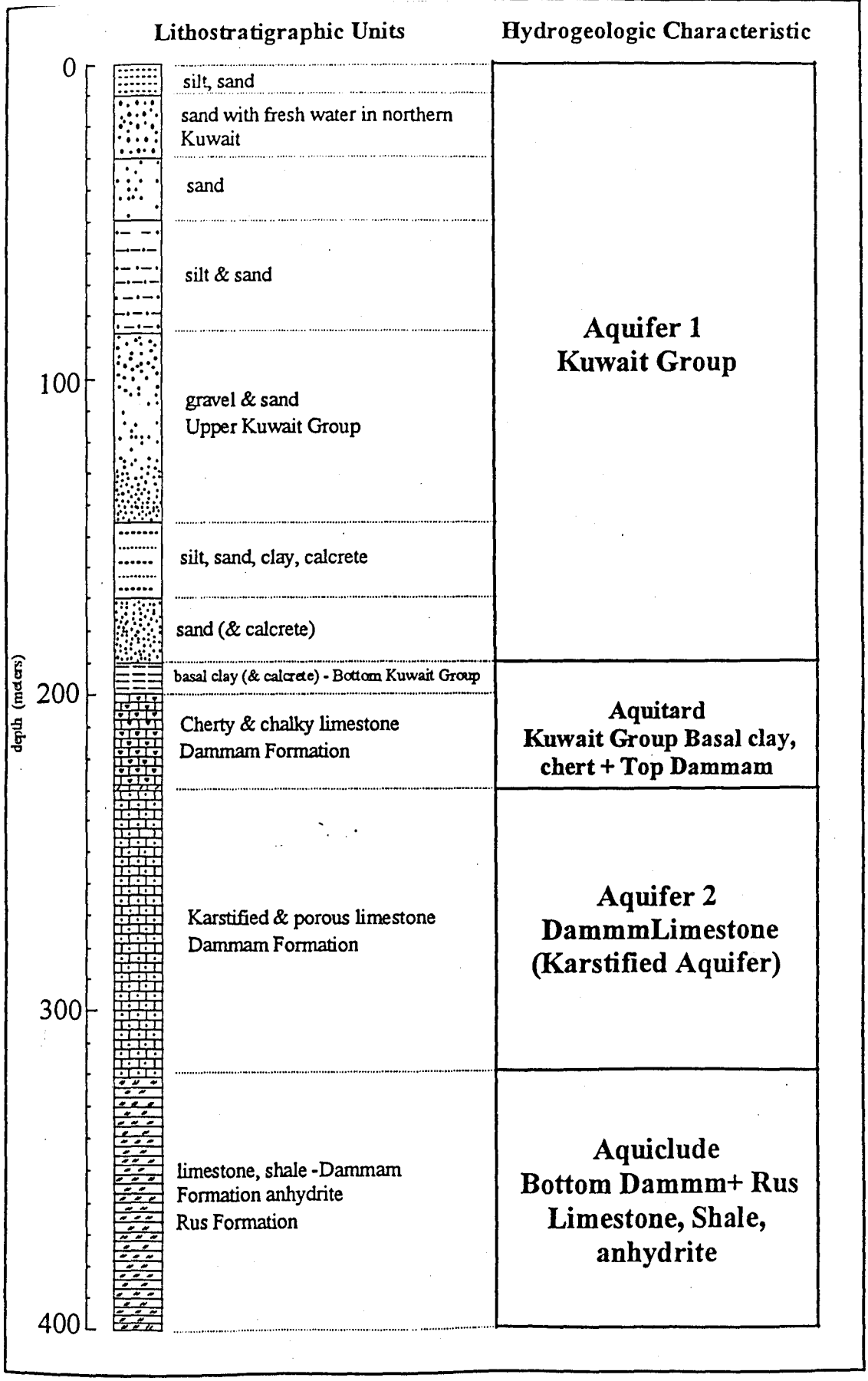


Figure 3.3: Lithological and hydrogeologic logs for the main aquifers and aquitards in Kuwait (after Amer, 1990)

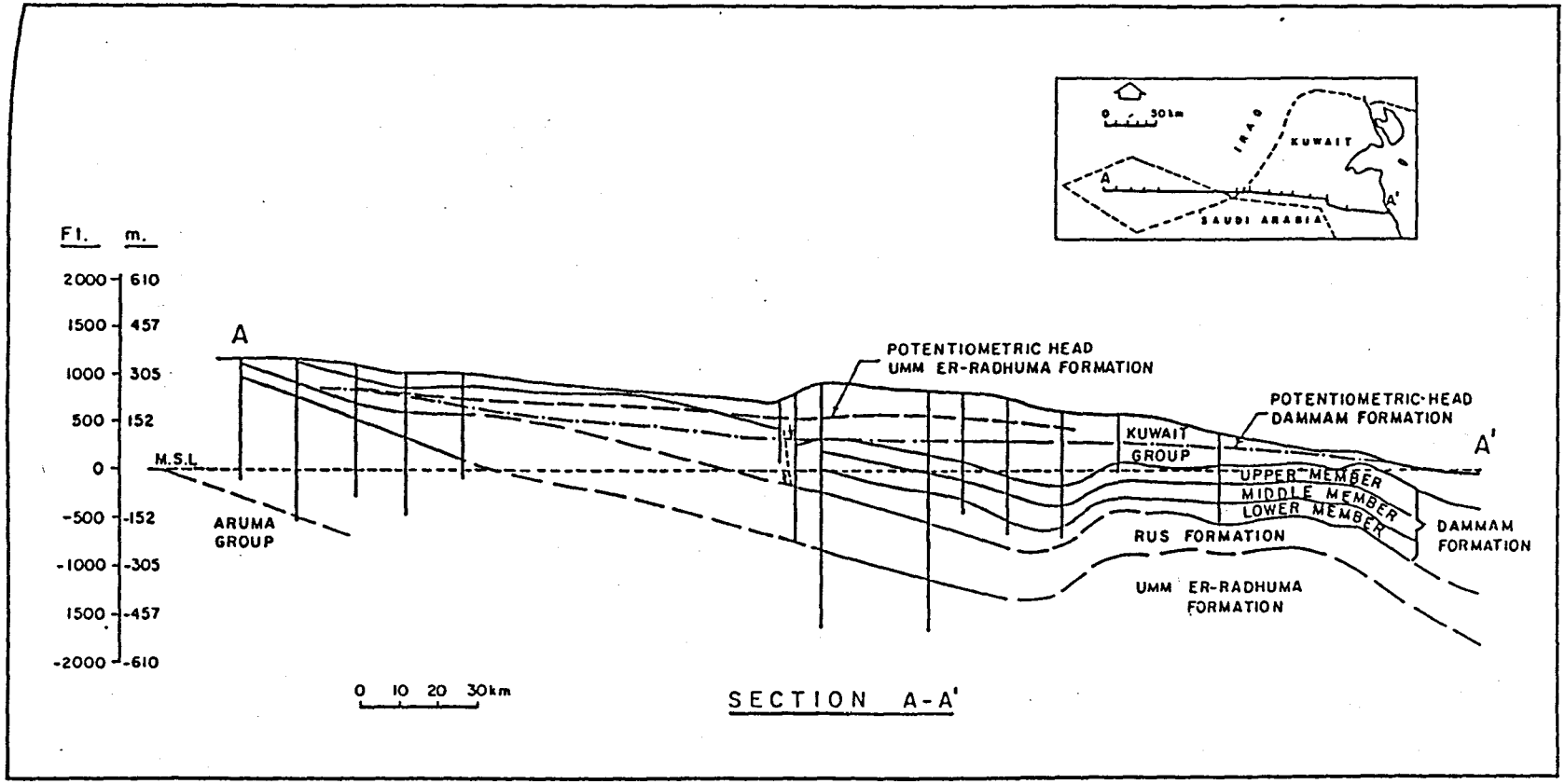


Figure 3.4: Cross section showing the main aquifer and aquitard units (after Senay, 1977)

infiltration of occasionally accumulated rain water. These include the Rawdhatain and Umm Al-Aish water fields, which represent the only source of fresh ground water in Kuwait. The sediments in these areas consist mainly of sand and gravel of Recent age exposed at the surface. These merge below with the sand and gravels of the Dibdiba formation of Pleistocene Age. Its saturated thickness ranges from 10-30m thick. The other two water-bearing units are; the upper Kuwait Group (UKG) and the lower Kuwait Group (LKG) aquifers. The latter is a sandy facies overlain by a silt bed which alternates to calcrete or clay at some locations, forming an aquitard layer separating between the UKG and LKG aquifers. The LKG aquifer generally has a uniform thickness (where it exists) of about 30-40m. The upper Kuwait Group (UKG) aquifer is composed of interbedded layers of silt and sandstone representing the majority of the Kuwait Group (KG) aquifer.

For the purpose of production, all the completed wells in the Kuwait Group (KG) aquifer were screened against every productive zone within aquifer. No distinction between upper and lower Kuwait Group aquifers was considered. This led to a lack of available hydrological information for each aquifer separately. As a result, the Kuwait Group aquifer was treated as one aquifer in this study. Furthermore, due to their limited areal extent and locality, fresh water lenses in northern Kuwait were not included. The Kuwait Group aquifer is considered as an unconfined aquifer, where its upper boundary is taken at the water table, and its lower boundary is taken at the basal clay, belonging to the base of the Kuwait Group aquifer. Figure 3.5 is an "isopach" map showing the pre-development saturated thickness of the Kuwait Group aquifer. Laterally, the limits of the aquifer cannot be identified within the study area, because it extends regionally beyond the Kuwaiti political borders towards Iraq and Saudi Arabia. However, the aquifer boundaries can be identified at the east with the Gulf shoreline, and in the south-west where the aquifer becomes unsaturated. Additionally, this aquifer does not exist in the Al-Ahmadi anticline where the Dammam Formation is exposed at the surface. The saturated thickness of KG aquifer increases from about 50m in the south to about 250m in the north (Fig. 3.5).

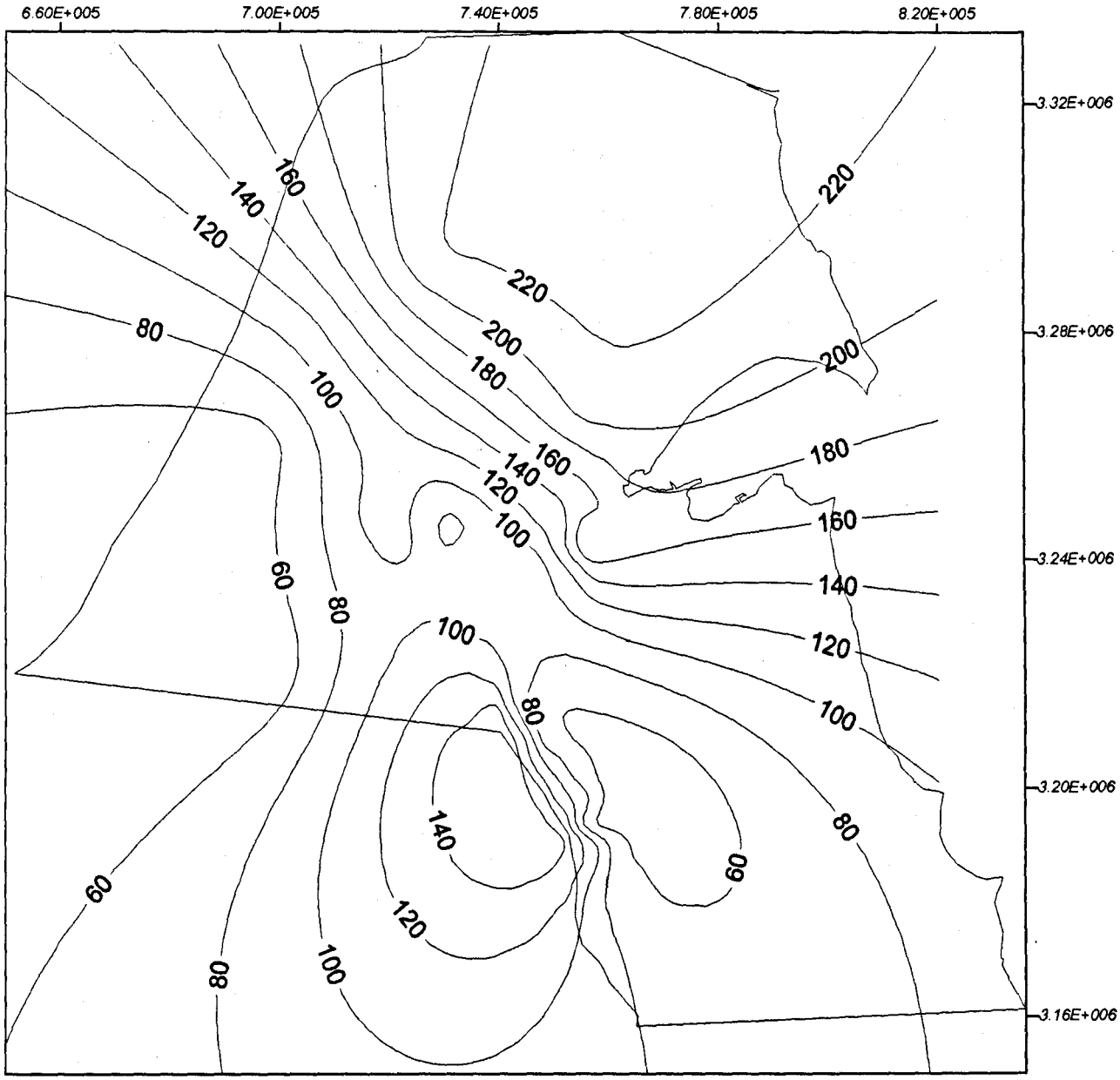


Figure 3.5: Pre-development saturated thickness of the Kuwait Group aquifer, m.

**Dammam Formation (DM) Aquifer**

The Dammam Formation aquifer consists mainly of the chalky and karstified limestone of the upper and middle Dammam Formation. The basal clay and calcrete layers of the Kuwait Group and the hard cherty chalky limestone unit of the upper Dammam Formation forming together an aquitard layer which represents the upper limit of Dammam aquifer. An isopach map showing the thickness of the aquitard which separates the Dammam and Kuwait Group aquifers was prepared, using the thickness data obtained from the lithological logs (Fig. 3.6). This aquitard has a discontinuous lateral extent, and no obvious trend was observed, although, its thickness ranges from 5m to 25m. A combination of the lower member of Dammam Formation (Member C) which is a low porosity layer of limestone inter-bedded with shales, with the anydrites of the Rus Formation, denote the lower limit of the aquifer.

No precise information about the bottom of DM aquifer are available, so its bottom was determined from the data of total drilled depth for the constructed wells in this aquifer because all the completed wells in DM aquifer did not penetrate the lower shaley member of DM. Subsequently, the kriging method was used to interpolate the bottom of DM aquifer in the rest of study area (Fig. 3.7). Its total thickness ranges from about 120m in the south west to about 250m in the north of Kuwait. Laterally, the DM aquifer presents over the whole study area. The eastern limit of the aquifer defined by the saline/brackish water front, located approximately parallel to the Arabian Gulf coastline. Generally, this aquifer occurs under a confined condition, except at the western part of Kuwait where it alternates to unconfined condition.

### 3.2.2 HYDRAULIC PROPERTIES OF AQUIFERS AND AQUITARDS

The hydraulic parameters of the KG and DM aquifers were obtained from the Kuwaiti Ministry of Electricity and Water (MEW) records of pumping tests conducted in the water wellfields and in a number of exploratory and private wells. There is some deficiency in the conducted pumping test data in Kuwait, which led to a lack of obtained parameters. The majority of the available pumping test data was collected from single-well tests in which drawdown changes during pumping were measured in the production well itself, without the use of piezometers.

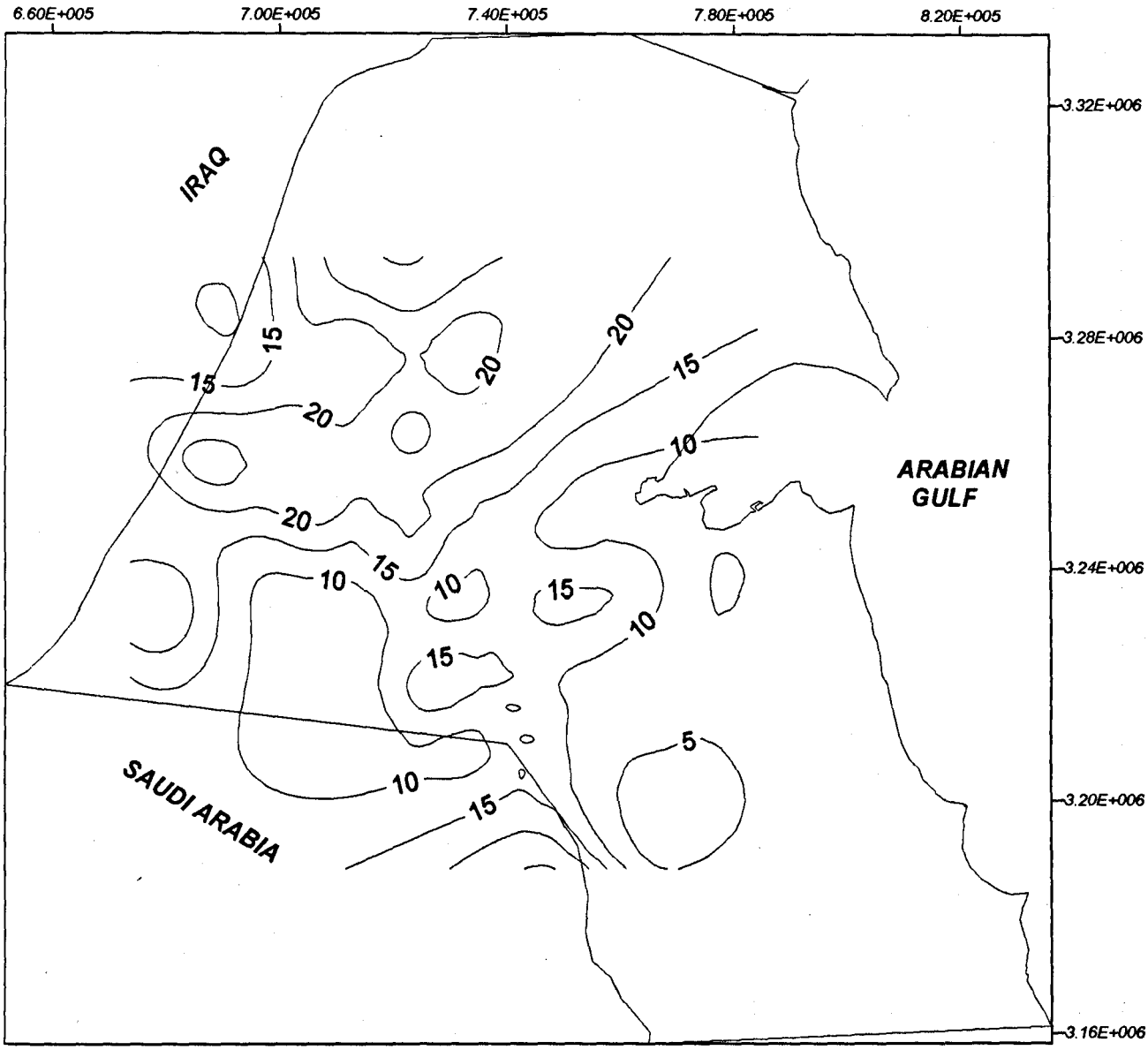


Figure 3.6: Isopach map of the basal clay and cherty limestone capping the top of the Dammam aquifer (aquitard layer), m.

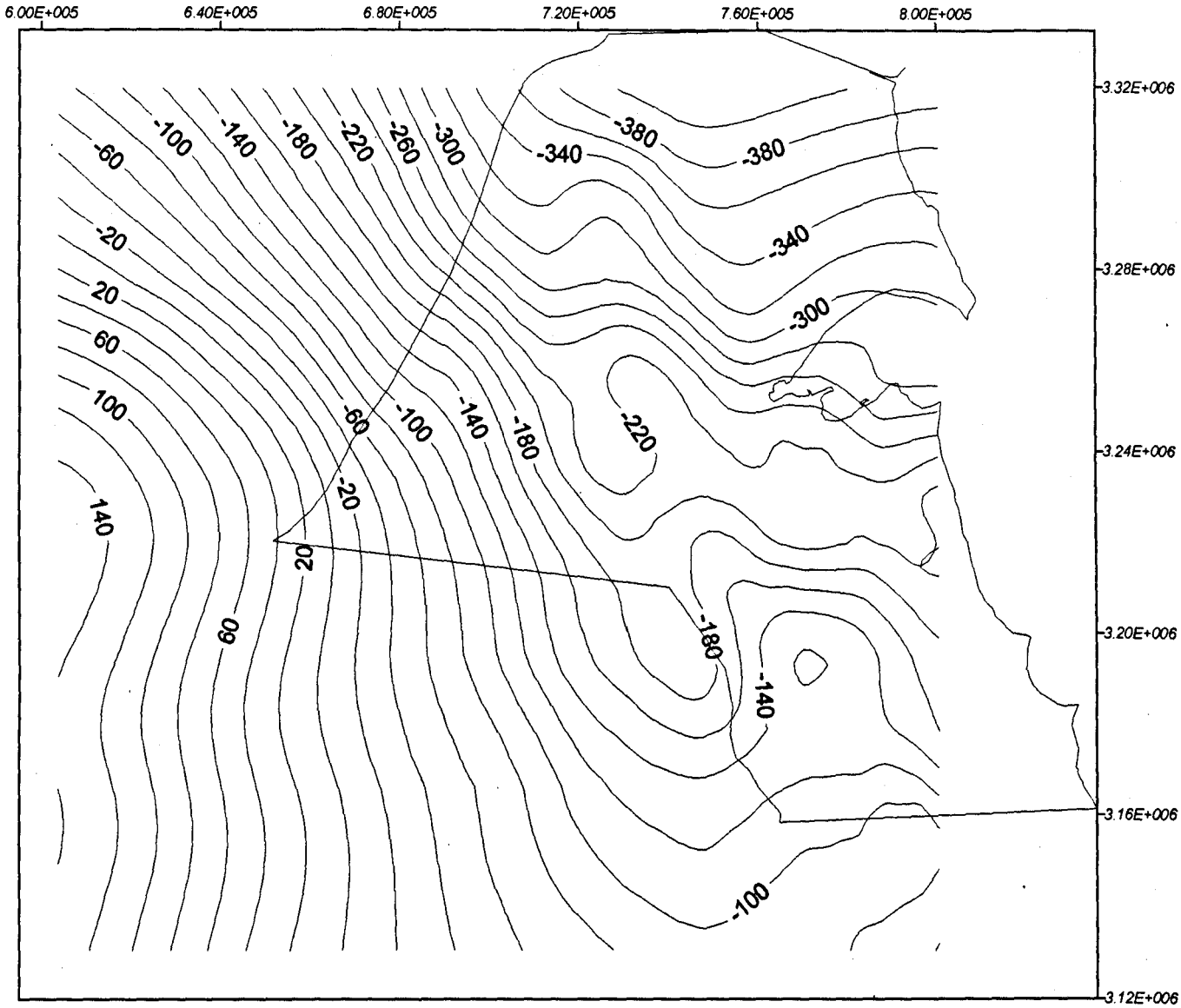


Figure 3.7: Bottom of the Dammam Formation aquifer, m amsl.

Consequently, some hydraulic properties for the aquifer system cannot be identified using these type of tests. These include the storage coefficient, vertical hydraulic conductivity for the aquifers and aquitards, and the leakage factor.

## Aquifer Transmissivity

The Kuwait Group (KG) and Dammam Formation (DM) aquifers have contrasting hydraulic properties, due to the contrast in their depositional environments. The transmissivity of the KG aquifer depends on the aquifer saturated thickness and its hydraulic conductivity. This is related to grain size distribution and the degree of cementation. The transmissivity of the aquifer is high in well sorted sand and gravel; and significantly decreases where the degree of cementation or clay percentage increases (Senay, 1986). On the other hand, the transmissivity of the Dammam aquifer is highly variable due to differential karstification, fracturing, dolomitization, and faulting in the limestone layers (Burdon and Al-Sharhan, 1968). The accepted transmissivity values in this study are those which have been obtained from pumping tests conducted for each aquifer separately. Values obtained from pumping tests carried out using a dual-well completion, where both aquifers are pumped at the same time, were disregarded. The data set consists of 102 transmissivity measurements for the KG aquifer and 184 measurements for the DM aquifer (Table 3.2). The statistical analysis which was performed for the transmissivity readings for both aquifers, shows large variations between the maximum and the minimum values for each aquifer. particularly evident for the DM aquifer, which has the higher mean and variance, indicating its karstic and fractured nature.

| **Parameter** | **KG aquifer** | **DM aquifer** |
|---|---|---|
| Number of readings | 102 | 184 |
| Mean ($m^2/d$) | 373 | 678 |
| St. Deviation | 211 | 1,558 |
| Minimum value ($m^2/d$) | 35 | 13 |
| Maximum value ($m^2/d$) | 864 | 17,280 |

Table 3.2: Summary statistics for the DM and KG aquifres transmissivity.

The transmissivity of the DM aquifer ranges between about 13 $m^2/d$, recorded in the Sulaibiya area, and 17,280 $m^2/d$, recorded at Shigaya-C wellfield. The KG aquifer has a transmissivity range between 35 and 864 $m^2/d$, not related to a particular location.

The majority of obtainable transmissivity values are restricted to the water wellfield locations where the production wells exist. Therefore, the kriging method using SURFER software was utilised to interpolate the transmissivity at other locations where values are sparse. Figures 3.8 and 3.9 show the transmissivity values and the locations at which the transmissivity measurements of the KG and DM aquifers were taken, respectively.

## Aquifer Storage Coefficients

Piezometer readings during pumping tests are essential to obtain the storage coefficient of the tested aquifer. However, these readings are very rarely available for the pumping tests conducted in Kuwait leading to a lack in the reported storage coefficient values for the DM and KG aquifers. Table 3.3 presents the available storativity values for the DM aquifer as provided by the MEW, and the specific yield values for the KG aquifer as obtained by Al-otaibi (1993) for selected areas in Kuwait, where observation wells were used during the pumping tests. The reported storage coefficient values for the DM aquifer show a wide range of variation, from $1 \times 10^{-5}$ to 0.325. On the other hand, the specific yield for the KG aquifer have less variation range, from $1 \times 10^{-3}$ to $1 \times 10^{-1}$ (dimensionless).

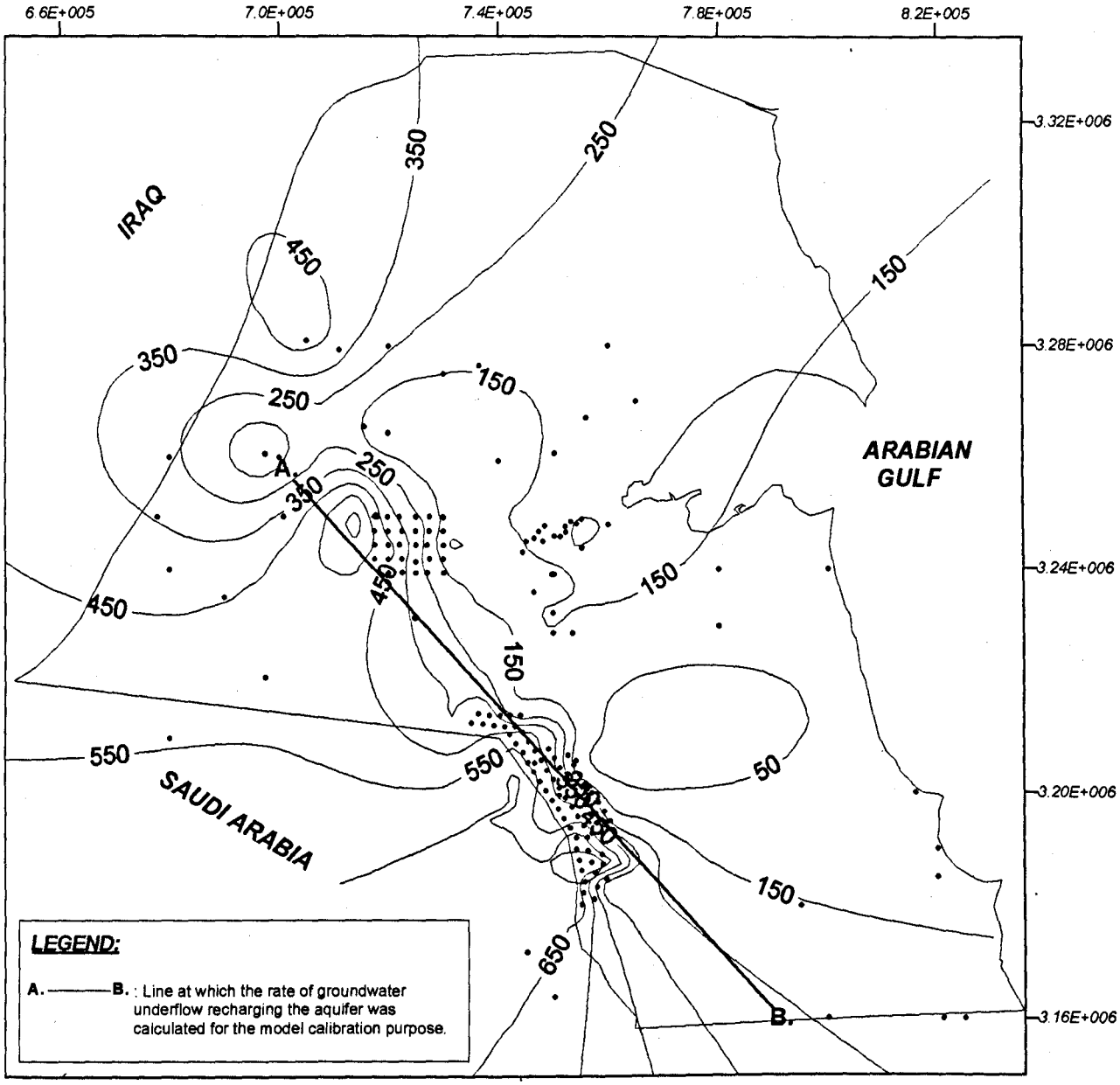


Figure 3.8: Kriged Kuwait Group aquifer transmissivity values ($m^2/d$), and locations of their measurement.

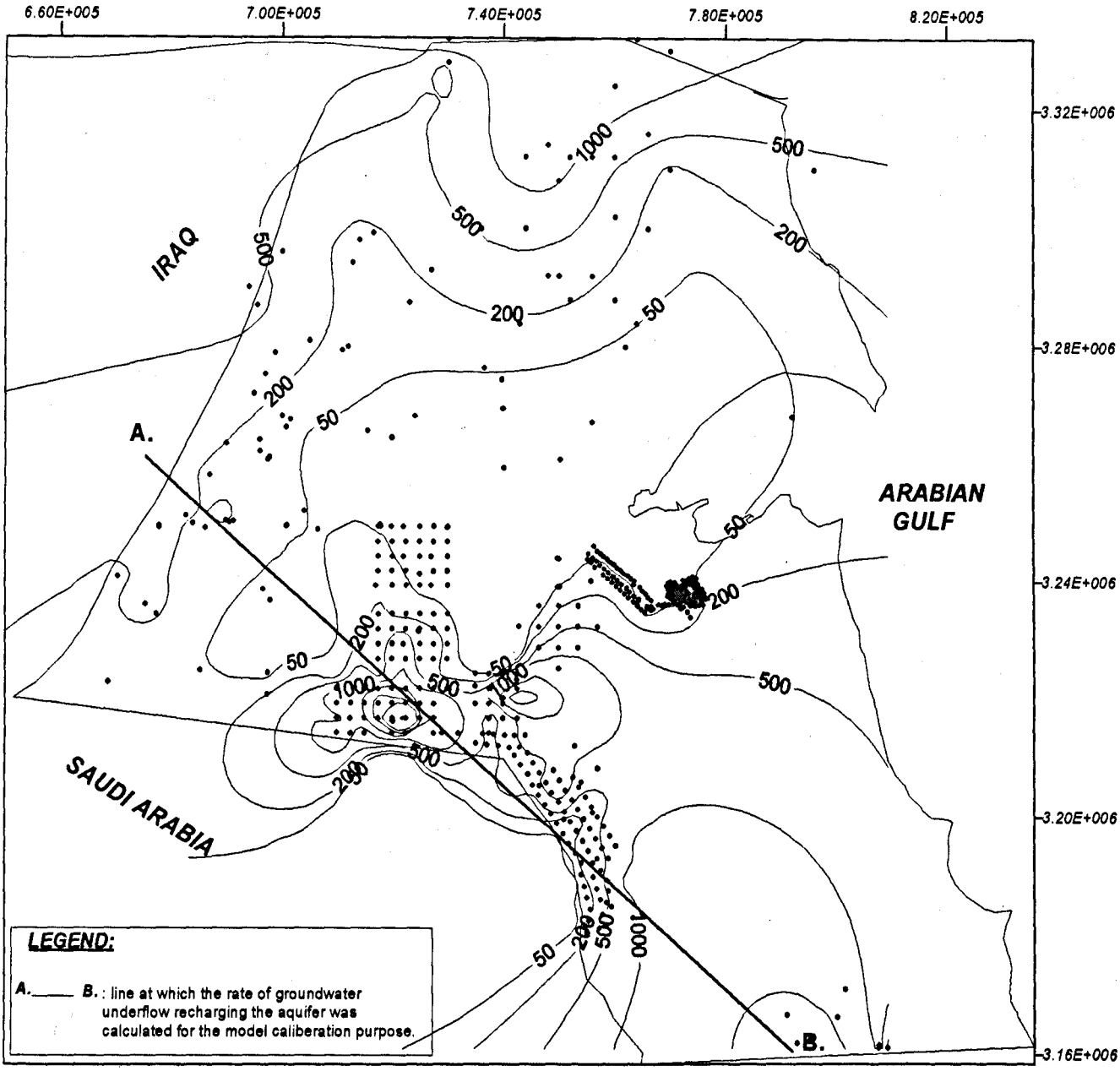


Figure 3.9: Kriged Dammam aquifer transmissivity values ($m^2/d$), and their measurement.

| Dammam Formation Aquifer | | | | Kuwait Group Aquifer | |
|---|---|---|---|---|---|
| Well | S | Well | S | Well | S |
| SW PW1 | 0.0006 | SW24 PW3 | 0.325 | M13 | 0.0156 |
| SW1 OW2 | 0.00025 | SW25 OW1 | 0.00068 | AB-4 (KISR) | 0.001 |
| SW4 OW2 | 0.0005 | SW26 | 0.000006 | WA-1 KISR) | 0.05 |
| SW4 OW1 | 0.0016 | SW26 OW1 | 0.00044 | AQ-2 (KISR) | 0.1 |
| SW5 PW1 | 0.00089 | SW33 | 0.000015 | | |
| SW5 OW1 | 0.00034 | UG OW3L | 0.00016 | | |
| SW6 PW1 | 0.00024 | NEUG EXP3 | 0.00019 | | |
| SW6 OW1 | 0.0003 | Abdaliya field | 0.0005 | | |
| SW8 PW1 | 0.00022 | SU112 | 0.00015 | | |
| SW8 OW1 | 0.000001 | SU80 | 0.0004 | | |
| SW9 PW1 | 0.0043 | SUOW4 | 0.0002 | | |
| SW10 PW1 | 0.0028 | KOC 40,42 | 0.00036 | | |
| SW15 PW | 0.00023 | W4 | 0.0003 | | |
| SW19 OW1 | 0.006 | SB6 | 0.0003 | | |
| SW20 PW1 | 0.024 | | | | |

Table 1.3: Reported storage coefficient values for the DM aquifer, and specific yield values for the KG aquifer (dimensionless).

## Aquitard Hydraulic Properties

The leakage factor (L), which determines the distribution of the leakage into a semi-confined aquifer, is defined as (Kruseman and Ridder, 1990):

$$L = \sqrt{K.b.C} \quad \text{or} \quad L = \sqrt{T\frac{b'}{K'}} \qquad (3.1)$$

where $k$ is the hydraulic conductivity of the semi-confined aquifer, $b$, is its saturated thickness, $c$ is the hydraulic resistance ($\frac{b'}{K'}$), and $K'$ and $b'$ are the hydraulic conductivity and the saturated thickness of the semi-pervious layer, respectively. The leakage factor has the dimension of length, and as higher the value of $L$ indicates.

The main aquitard in the aquifer system in Kuwait is the cherty limestone separating the leaky DM aquifer from the unconfined KG aquifer. The thickness of this aquitard ranges from 5 to 25 m, as shown by the prepared isopach map in the previous section (Fig. 3.6). The vertical leakage crossing this aquitard is controlled by the head difference between the two aquifers and by the hydraulic resistance of the aquitard, which is a function of its vertical permeability and its thickness. If any fractures or joints are existing, it will speed up the leakage mechanism. The leakage factor values were rarely obtainable due to the deficiency in piezometer measurements from the conducted pumping tests, as mentioned earlier. The only available leakage factor values are reported by the MEW for 5 wells, as listed in Table 3.4.

| Well No. | Aquifer tested | Leakage factor, (m) |
|---|---|---|
| SW 2 PW | DM | 300 |
| SW 24 WL | DM | 1600 |
| SW 28 OW | KG | 760 |
| SW 80 WL | KG | 980 |
| SU 137 | DM | 150 |

Table 3.4: Reported leakage factor values obtained from pumping tests (Al-hajji,1978).

## 3.2.3 POTENTIOMETRIC WATER LEVELS OF THE AQUIFERS

**Initial water Levels**

Regional groundwater flow pattern of the KG and DM aquifers have the same general trend, flowing from the recharge areas in the south west, towards the discharge areas of the aquifers at the Arabian Gulf coastline (Fig. 3.10).

The initial water level maps for the KG and DM aquifers were prepared by the Ministry of Electricity and Water (MEW) for the year 1960. These two maps are the only source of data for the pre-development steady state conditions of the aquifers in Kuwait. Prior to 1960, the abstraction of groundwater in Kuwait was negligible, being limited to a few production wells completed in the DM aquifer in the Sulaibiya water well field. Figure 3.11

displays the regional initial water level map for the DM aquifer. This map was prepared using the kriging method, where the available initial potentiometric map was extrapolated to cover all of the modelled area. This was based on a number of water level measurements taken by (FAO, 1979) for the aquifer in Saudi Arabia at selected locations. However, no such regional extension was performed for the initial water level map of the KG aquifer, due to the lack of any water level measurements from Saudi Arabia (Fig. 3.12)

The two aquifers both had a relatively uniform pre-development gradient of 0.001 (dimensionless), except in the south eastern part, where the hydraulic gradient becomes steeper. The patterns of equipotentials show that the system is replenished by lateral groundwater flow (underflow) coming from Saudi Arabia, then flows in a south-west-north-east direction and discharges its water into the sea by seepage. The potentiometric levels in the DM aquifer, under steady state conditions, were higher than the KG levels by 5 to 10 m, within the region of Kuwait, indicating that the main direction of leakage was from the DM aquifer to the KG aquifer. However, in the Umm Gudair area, the water levels of the KG aquifer were higher than the DM potentiometric levels, causing the direction of the leakage to reverse towards the DM aquifer. Initial water level maps for the KG and DM aquifers indicate that the water levels were about 110 and 120 m amsl, respectively, at the south western corner of Kuwait, sloping toward the zero water level line, where it coincides with the Arabian Gulf coastline.

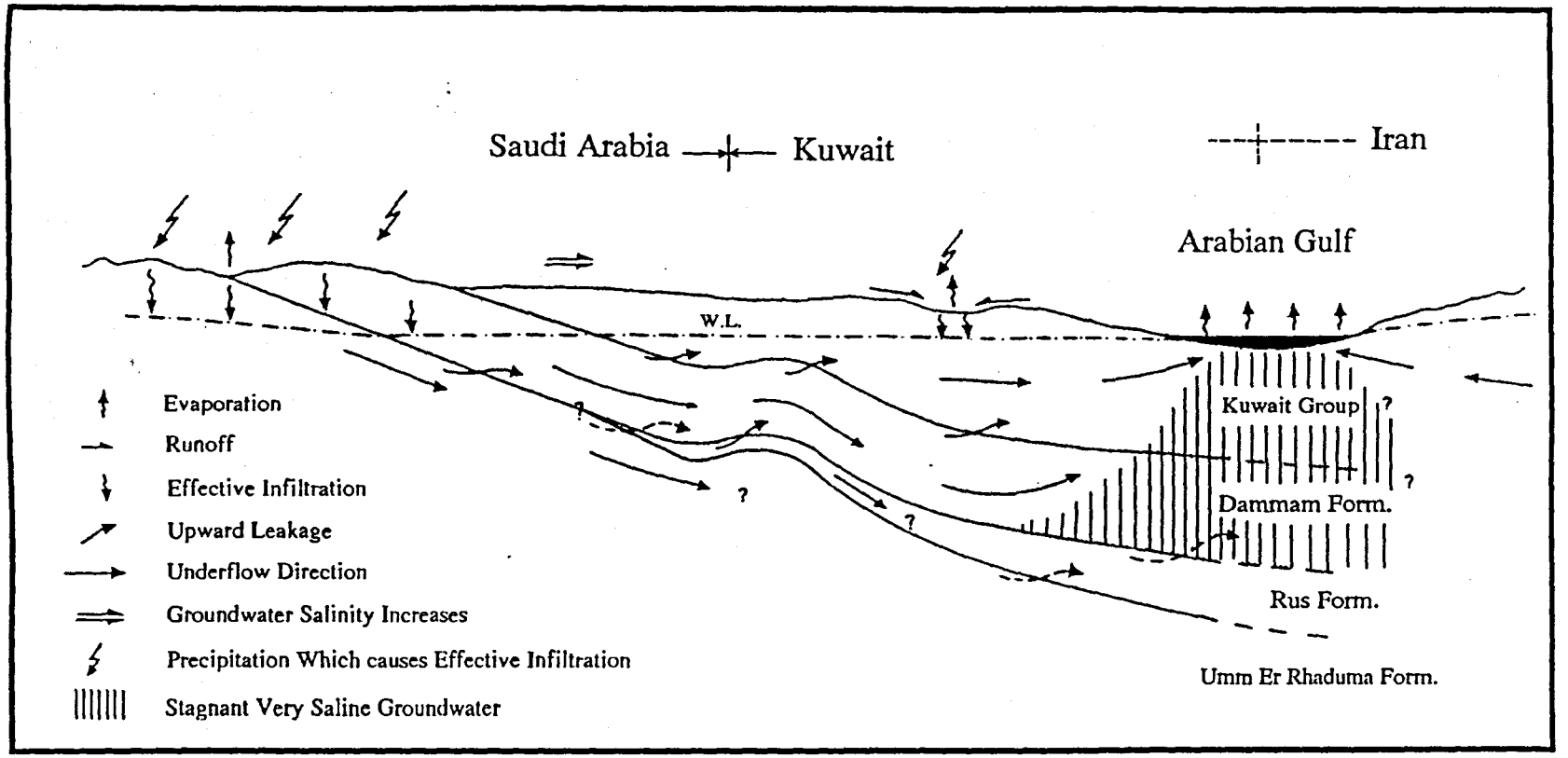


Figure 3.10: Schematic cross section showing the pattern of natural groundwater flow in Kuwait aquifer system (after Omer et al., 1981)

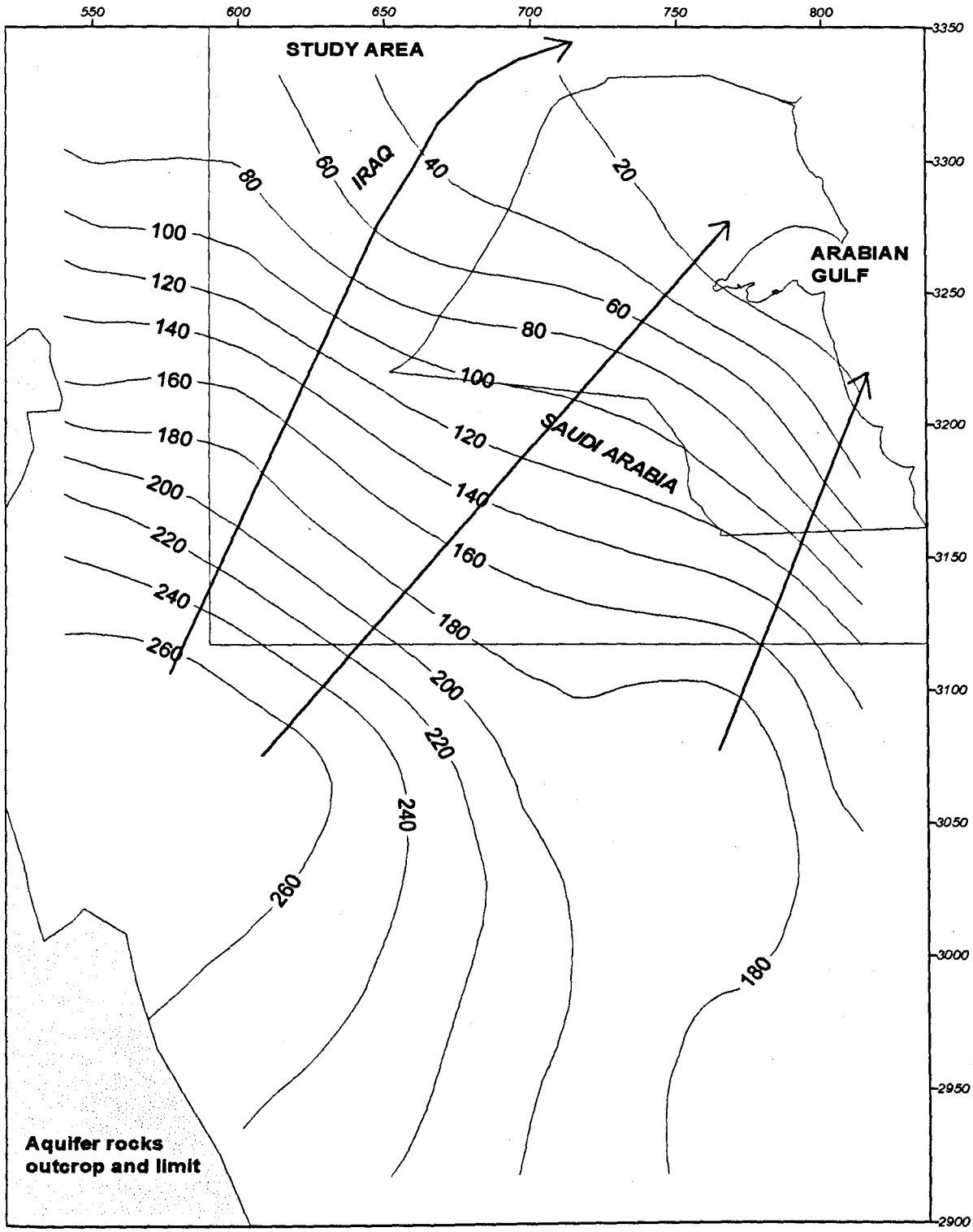


Figure 3.11: Regional initial potentiometric head of the Dammam aquifer, m amsl.

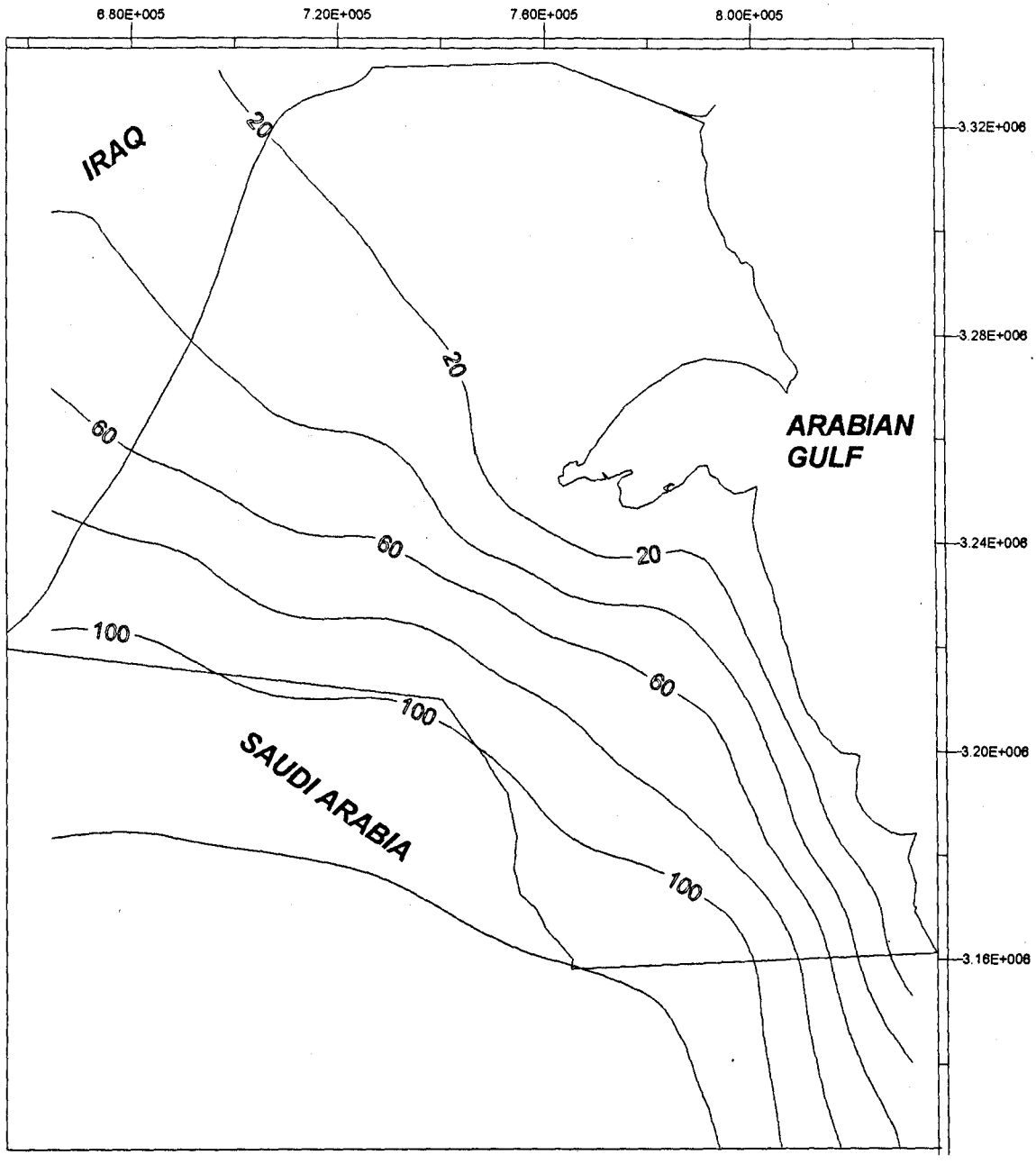


Figure 3.11: Observed initial water head of the Kuwait Group aquifer, m amsl (after Senay, 1994)

## Water Level Declines

The historical potentiometric water levels for the KG and DM aquifers have been recorded since the year of 1981, though the observation wells are limited to the locations of the wellfields and are not well distributed over. Generally, existing observation wells are largely restricted to the DM aquifer and an inadequate number are found in the KG aquifer. However, according to the availability of water level measurements in time and space, a number of potentiometric water level and total drawdown maps for both aquifers were prepared. These maps will be used as a target for the transient calibration of the numerical model in this study.

Figure 3.13 displays the water level contour map for the KG aquifer in 1988, that is the only water level map which could be prepared for KG aquifer, relying on enhanced measurements. For the DM aquifer it was much easier to produce a number of potentiometric contour and drawdown maps at successive intervals of time. Two potentiometric contour maps for the aquifer head in years 1990 and 1995 were prepared (Figures 3.14 and 3.15). In order to display the decline in the aquifer head more clearly, two maps showing the total drawdown in the aquifer potentiometric head to the same years (1990 and 1995) were prepared (Figures 3.16 and 3.17).

In response to pumping of groundwater from the KG and DM aquifers over about 36 years, cones of depression have developed progressively and partly interfere with each other between the wellfields.

Comparison between the two KG maps (the more recent aquifer map, and the initial one) indicates that, in addition to the general drop in the potentiometric levels between the two periods, three major areas of decline have developed: at Wafra farms area, Sulaibiya, and Shigaya-D wellfields, with an average of 15m decline in the water level at all three (in 1988). The decline in the potentiometric heads of the DM aquifer is more obvious than that which has occurred in the KG aquifer, reflecting the fact that the abstraction rate from the DM is higher.

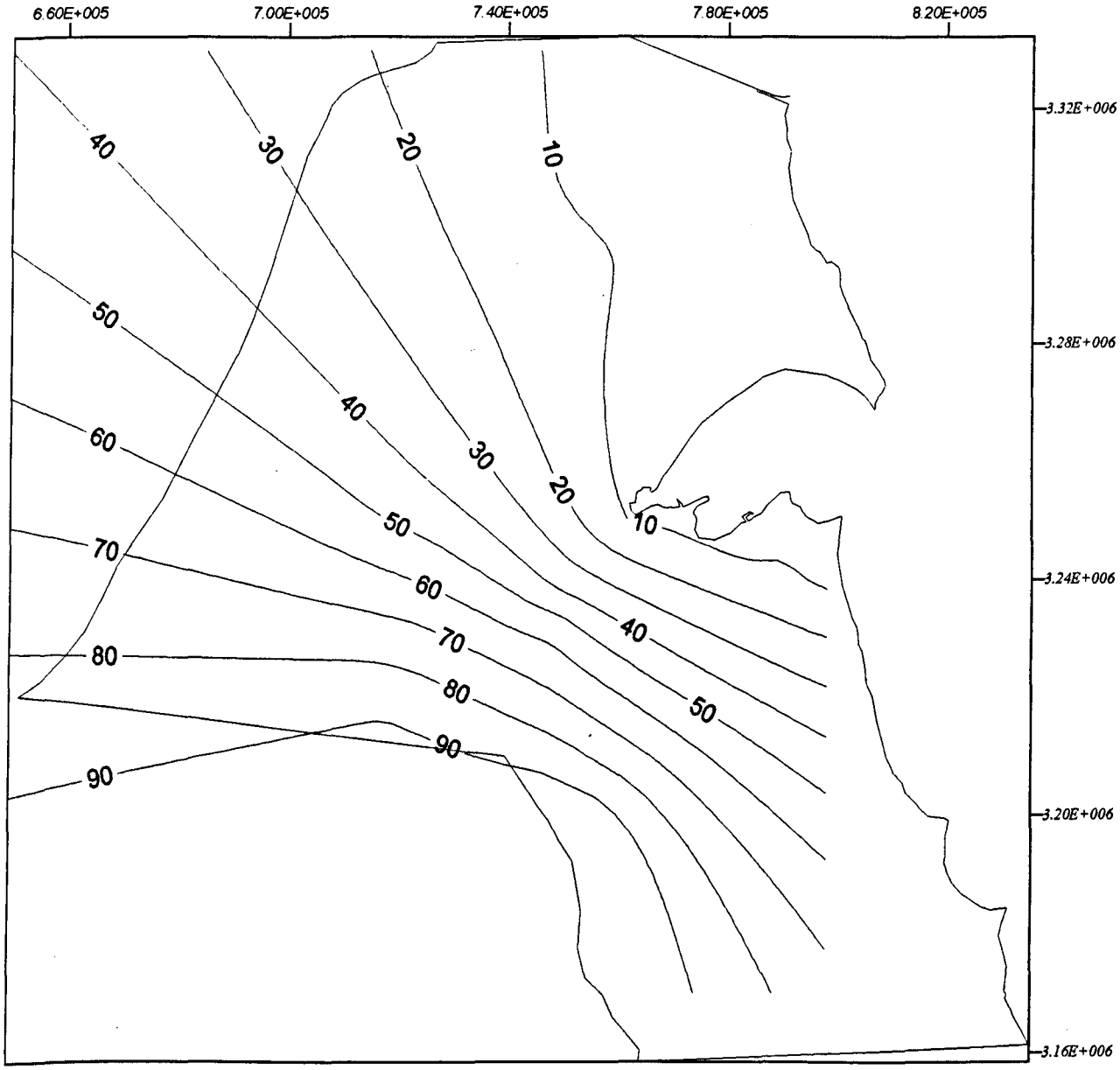


Figure 3.13: Observed water level for the Kuwait Group aquifer at 1988, m amsl.

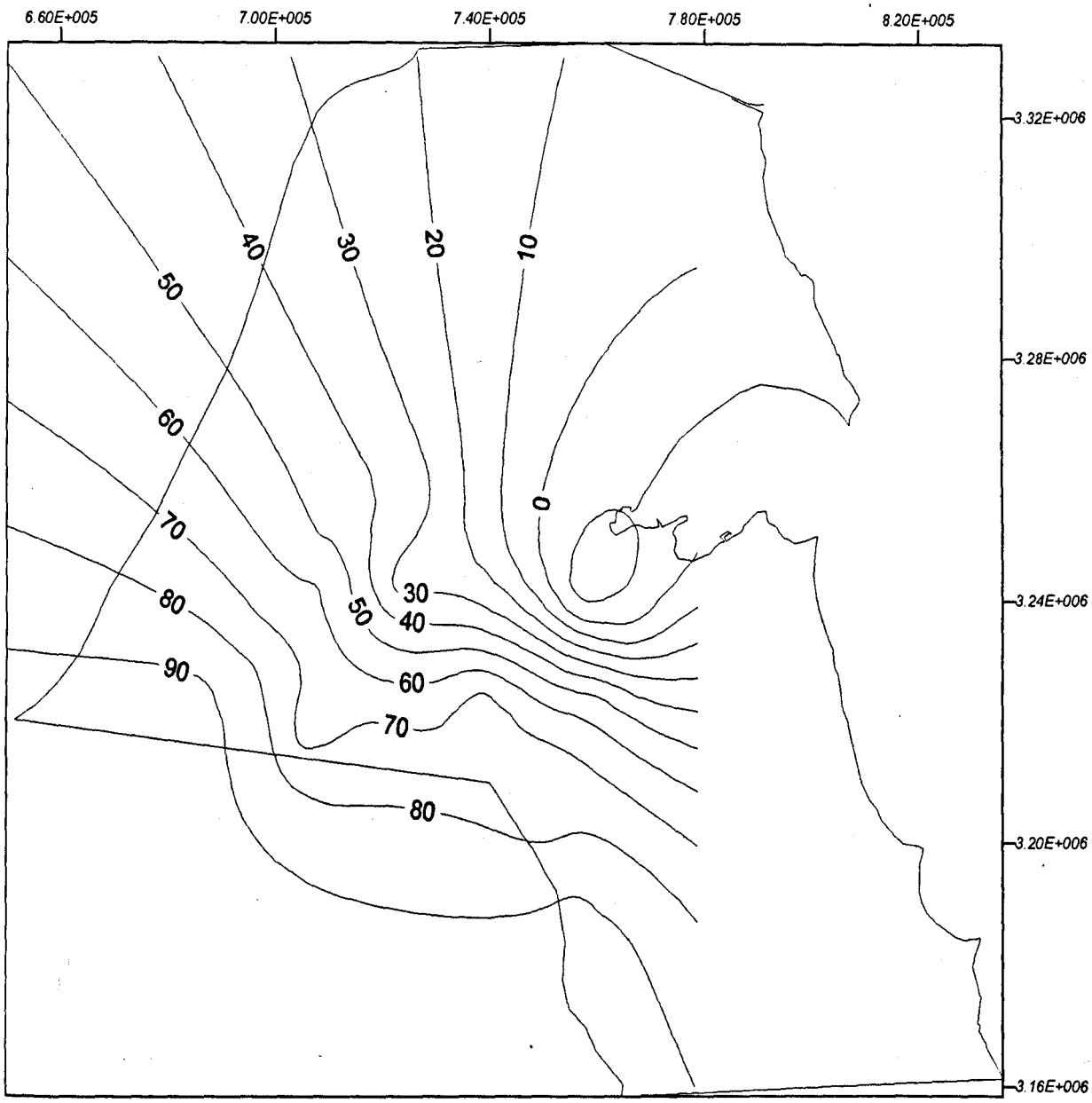


Figure 3.14: Observed potentiometric head of the Dammam aquifer at 1990, m amsl.

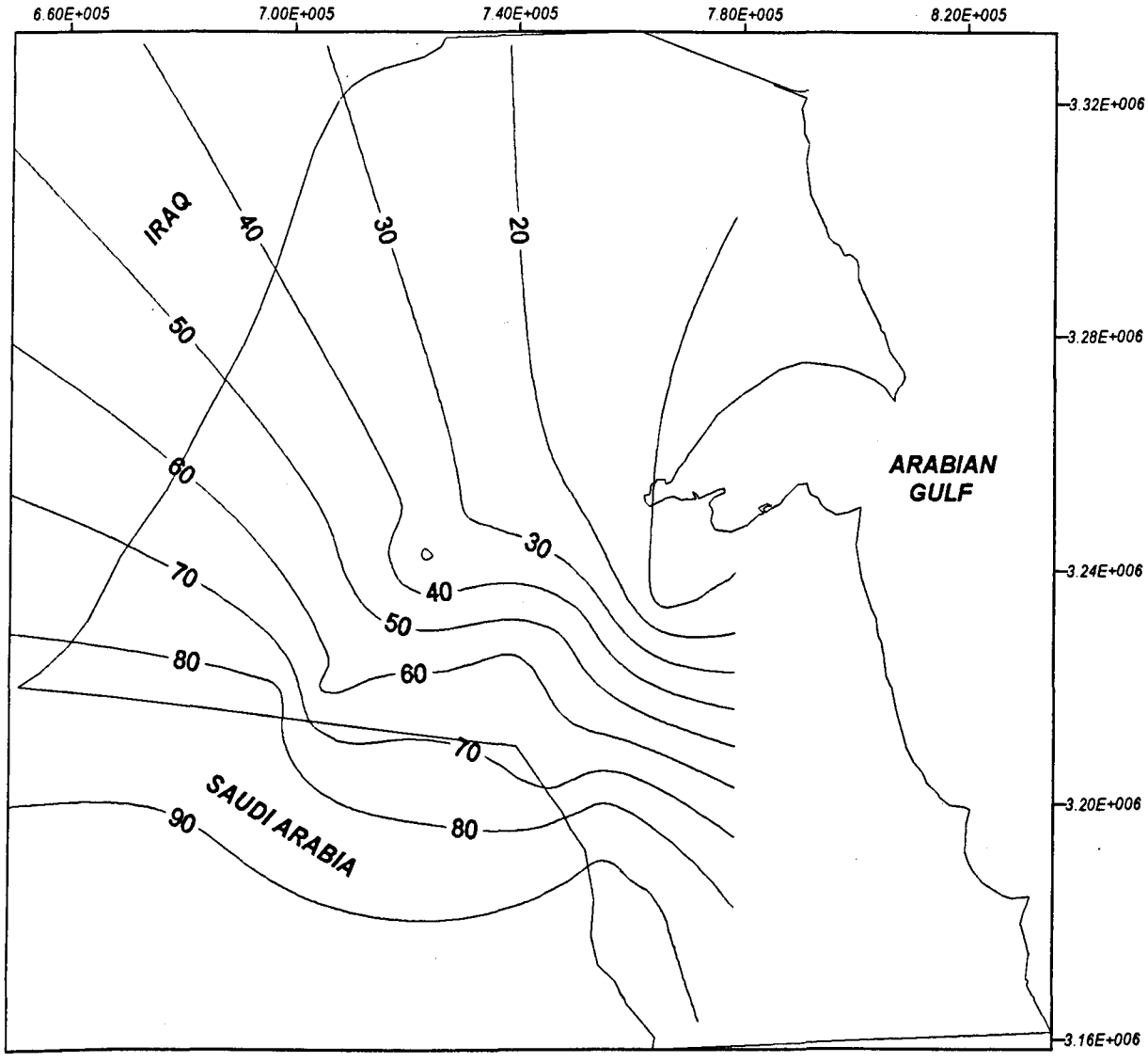


Figure 3.15: Observed potentiometric head of the Dammam aquifer at 1995, m amsl.

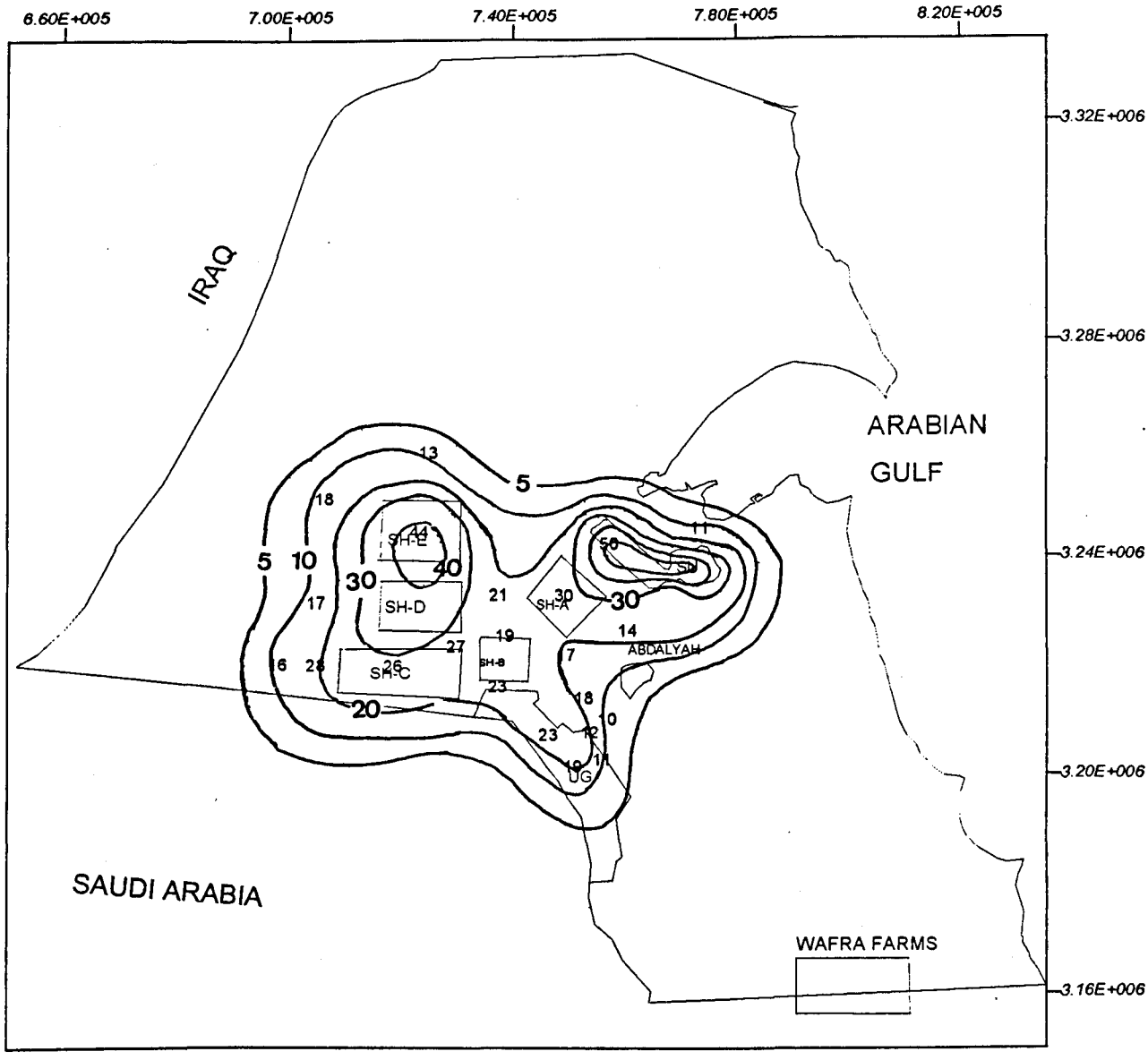


Figure 3.16 : Observed total drawdown in potentiometric head of the Dammam aquifer to 1990, m.

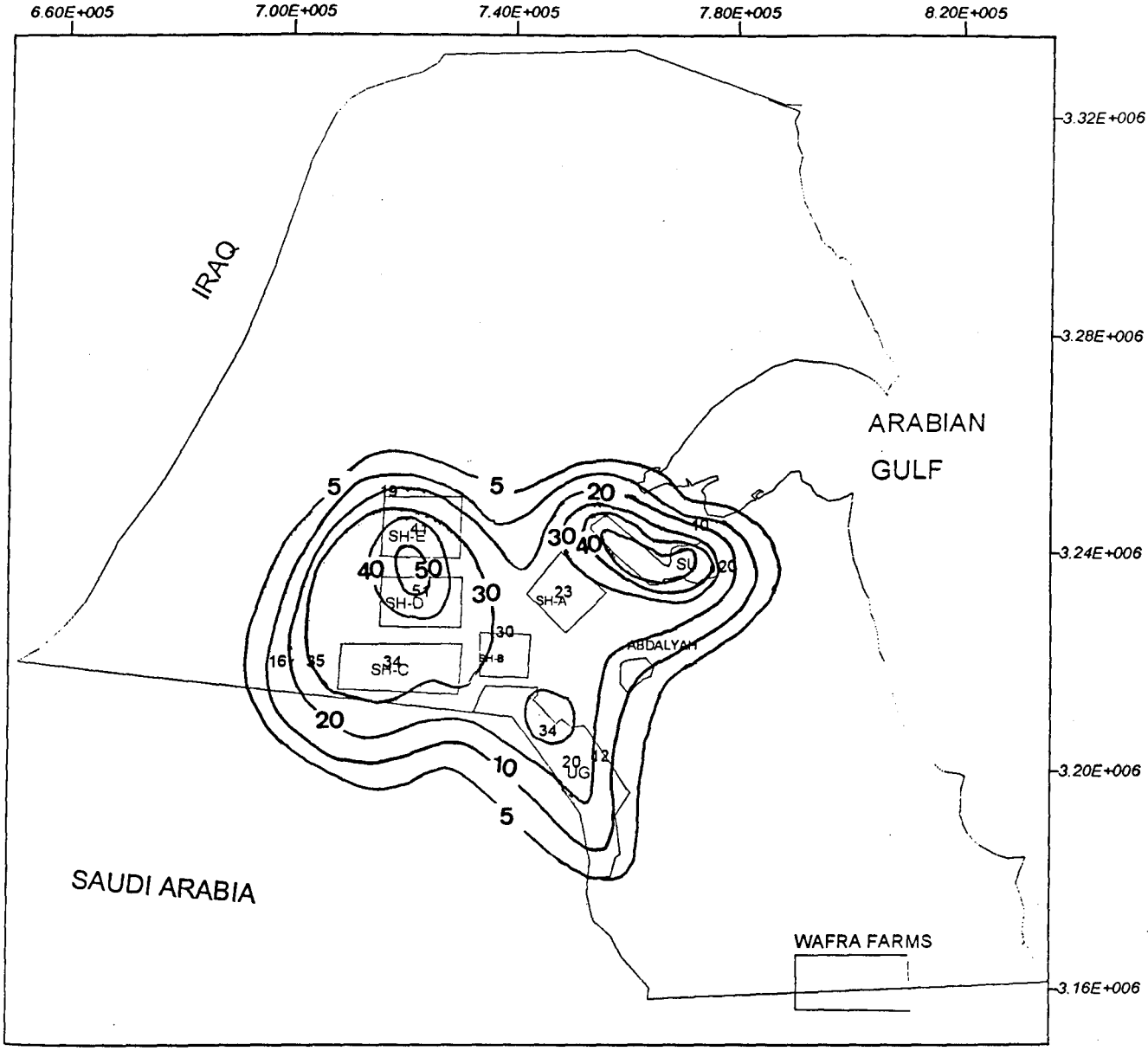


Figure 3.17 : Observed total drawdown in potentiometric head of the Dammam aquifer to 1995, m.

The total drawdown in potentiometric heads of the DM aquifer in 1986 was high. Two major cones of depression at the Sulaibiya wellfield, with about 60 to 70m drawdown, and at the Shigaya-D, with about 50m drawdown were produced by the groundwater abstraction from these two fields. Generally, these cones of depressions occurred at the same locations as the KG cones of depression (not including the Wafra area in which the KG is the only pumped aquifer). However, they have a wider extent in the vertical and horizontal directions in the DM aquifer than in the KG aquifer.

Later, the decline in the potentiometric heads of the DM aquifer decreased to 40 m at 1990 in the Shigaya-D, due to the reduction in the pumping from the Shigaya wellfields. This has been replaced by the newly established (in 1986) water wellfield at Umm Gudair area, and as a result a new cone of depression with a 20 m drop in potentiometric head was developed at the Umm Gudair location.

More recently, if the produced total drawdown in the potentiometric head of the DM aquifer in 1995 is compared with the produced drawdown in 1990, it indicates mostly the same tendency of decline at the majority of the wellfields, except at the Umm Gudair area where the total drawdown has increased to reach about 30 m.

The declining water levels in the KG and DM aquifer will give rise to a new hydrological situation resulting from the conceived hydraulic connection between the aquifers. As a result, the head difference between them will increase, causing a significant part of the pumped water from DM aquifer to be sourced from the KG aquifer by leakage.

### 3.2.4 GROUNDWATER UTILISATION IN KUWAIT

Figure 3.18 shows the location of existing water wellfields in Kuwait. Prior to the 1940's, groundwater withdrawal in Kuwait was limited to number of hand-dug wells drilled in the KG aquifer. In the early 1940's the Kuwait Oil Company (KOC) started exploiting the DM aquifer in different locations in Kuwait. In the mid-1940's, the company started operating the Abdaliya wellfield to supply water for Ahmadi city.

In the early 1950's the Ministry of Electricity and Water (MEW) constructed the first wellfield at Sulaibiya (1954) to supply water for Kuwait city. This wellfield was followed by the construction of other wellfields at different locations in Kuwait, tapping both DM and KG aquifers, to meet the increasing demands for water. The produced brackish groundwater from the water wellfields is used for blending with desalinated water, and for non-drinking and landscaping purposes. The brackish groundwater is supplied through a special distribution network.

Table 3.5 lists the existing wellfields in Kuwait, their first year of operation, the total number of wells, their designed production capacity, and the utilised aquifer.

| Wellfield | Starting year | Developed aquifer | Number of production wells | Designed operating capacity ($m^3/d$) |
|---|---|---|---|---|
| Abdaliya | 1945 | D M | 39 | 56,000 |
| Sulaibiya | 1951 | DM | 136 | 68,000 |
| Rawdhatain | 1960 | Upper KG | 26 | 16,000 |
| Umm Al-Aish | 1963 | Upper KG | 26 | 6,800 |
| Shigaya A | 1972 | KG+DM | 13 | 32,000 |
| Shigaya B | 1975 | DM | 16 | 39,000 |
| Shigaya C | 1975 | DM | 32 | 91,000 |
| Shigaya D | 1979 | DM | 24 | 55,000 |
| Shigaya E | 1979 | KG+DM | 30 | 77,000 |
| Umm Gudair | 1986 | KG+DM | 41 | 114,000 |
| U. G. expansion | 1989 | KG+DM | 26 | 68,000 |

Table 1.5: Existing groundwater wellfields in Kuwait.

The above table indicates that most of the produced water is mainly from the DM aquifer; Sulaibiya, Abdaliya, and Shigaya (B, C, and D) wellfields are producing from the DM aquifer only. However, Shigaya (A, and E), and Umm Gudair wellfields are producing from dual wells completed in the DM and KG aquifers.

Fresh groundwater lenses exist in the Upper Kuwait Group aquifer (TDS<500 mg/l), which has been discovered accidentally at the Rawdhatain and Umm Al-Aish areas in the 1960's. The discovery of these water lenses was followed by more exploration in the north eastern

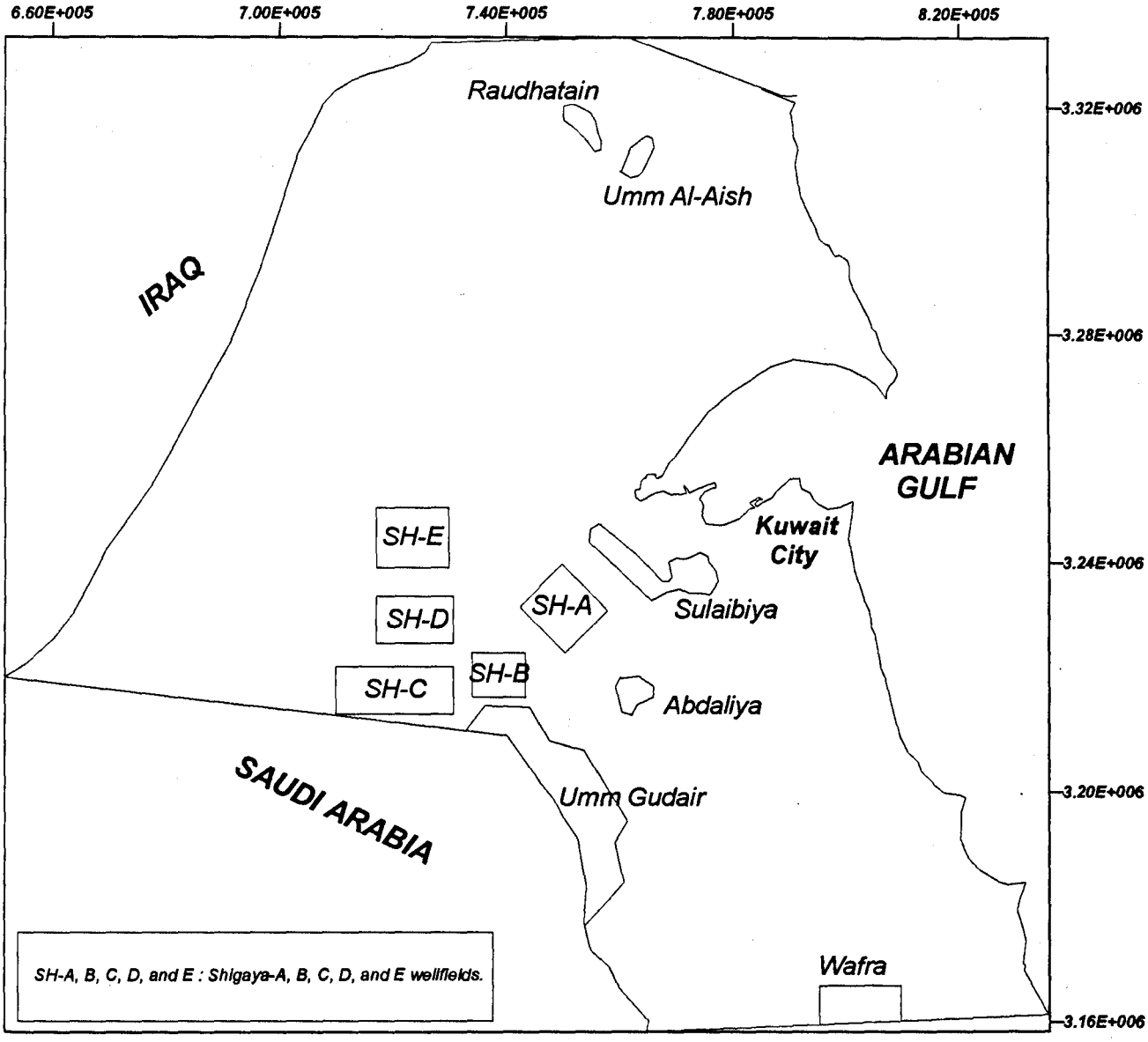


Figure 3.18: Location of the existing water wellfields in Kuwait.

area in an attempt to discover other locations containing a similar quality of water, but these exploration activities have failed to locate any additional fresh groundwater lenses.

In addition, many private agricultural farms were constructed and started abstracting brackish water from the KG aquifer, such as Wafra and Abdaly farms. The abstraction rates from these farms are uncontrolled and unmonitored by any authority, and hence the exact abstraction rates are unknown.

Table 3.6 shows the total groundwater abstraction rates of the individual wellfields during the period of 1960 to 1995.

| Year | Water Wellfields | | | | | | | |
|---|---|---|---|---|---|---|---|---|
| | Sulaibiya | Abdaliya | Shigaya A | Shigaya B | Shigaya C | Shigaya D | Shigaya E | Umm Gudair |
| 1960 | 5.9 | 4.7 | | | | | | |
| 1961 | 8.4 | 5.6 | | | | | | |
| 1962 | 13.3 | 6.7 | | | | | | |
| 1963 | 15.3 | 6.8 | | | | | | |
| 1964 | 16.2 | 7.7 | | | | | | |
| 1965 | 18.2 | 7.1 | | | | | | |
| 1966 | 20.8 | 7.6 | | | | | | |
| 1967 | 18.7 | 7.1 | | | | | | |
| 1968 | 20.1 | 7.7 | | | | | | |
| 1969 | 25.1 | 8.1 | | | | | | |
| 1970 | 25.8 | 9.1 | | | | | | |
| 1971 | 23.8 | 8.8 | | | | | | |
| 1972 | 24.1 | 8.3 | 3.9 | | | | | |
| 1973 | 25.5 | 9.4 | 4.0 | | | | | |
| 1974 | 26.1 | 9.4 | 7.0 | | | | | |
| 1975 | 23.4 | 9.4 | 5.2 | 3.6 | 5.6 | | | |
| 1976 | 26.3 | 9.2 | 7.2 | 4.3 | 3.4 | | | |
| 1977 | 25.4 | 8.6 | 5.3 | 4.6 | 7.1 | | | |
| 1978 | 19.0 | 9.3 | 6.2 | 5.4 | 17.0 | | | |
| 1979 | 21.9 | 8.1 | 4.7 | 4.7 | 18.0 | | | |
| 1980 | 22.7 | 8.4 | 4.1 | 4.3 | 9.7 | 9.0 | 2.7 | |
| 1981 | 21.9 | 8.7 | 4.8 | 6.3 | 8.8 | 8.0 | 5.3 | |
| 1982 | 25.4 | 8.9 | 4.4 | 6.8 | 8.5 | 9.8 | 9.8 | |
| 1983 | 27.2 | 11.0 | 3.0 | 7.7 | 15.0 | 10.0 | 10.0 | |
| 1984 | 21.6 | 11.0 | 3.6 | 8.6 | 14.0 | 15.0 | 12.0 | |
| 1985 | 21.2 | 12.0 | 3.3 | 7.2 | 15.0 | 11.0 | 12.0 | |
| 1986 | 21.8 | 11.0 | 4.5 | 7.8 | 15.0 | 12.0 | 12.0 | 2.6 |
| 1987 | 21.2 | | 5.1 | 9.6 | 19.0 | 14.0 | 16.0 | 23.0 |
| 1988 | 21.2 | | 6.2 | 8.8 | 18.0 | 11.0 | 14.0 | 29.0 |
| 1989 | 19.9 | | 3.7 | 7.2 | 15.0 | 7.3 | 15.0 | 28.0 |
| 1990 | 21.4 | | 4.8 | 6.3 | 16.0 | 6.5 | 12.0 | 16.0 |
| 1991 | 10.5 | | 0 | 0 | 0 | 0 | 0 | 0 |
| 1992 | 20.6 | | 0 | 0 | 0 | 6.7 | 3.1 | 11.2 |
| 1993 | 20.6 | | 2.5 | 3.1 | 0 | 9.5 | 1.6 | 27.0 |
| 1994 | 21.0 | | 4.3 | 3.5 | 13.5 | 8.6 | 1.8 | 36.1 |
| 1995 | 21.0 | | 4.3 | 3.6 | 14.0 | 9.6 | 3.5 | 40.2 |

Table 3.6: Total wellfields groundwater abstraction in Kuwait, in $Mm^3$.

Figure 3.19 displays the seasonal variation in groundwater production in Kuwait, where it increases in summer and decreases in winter.

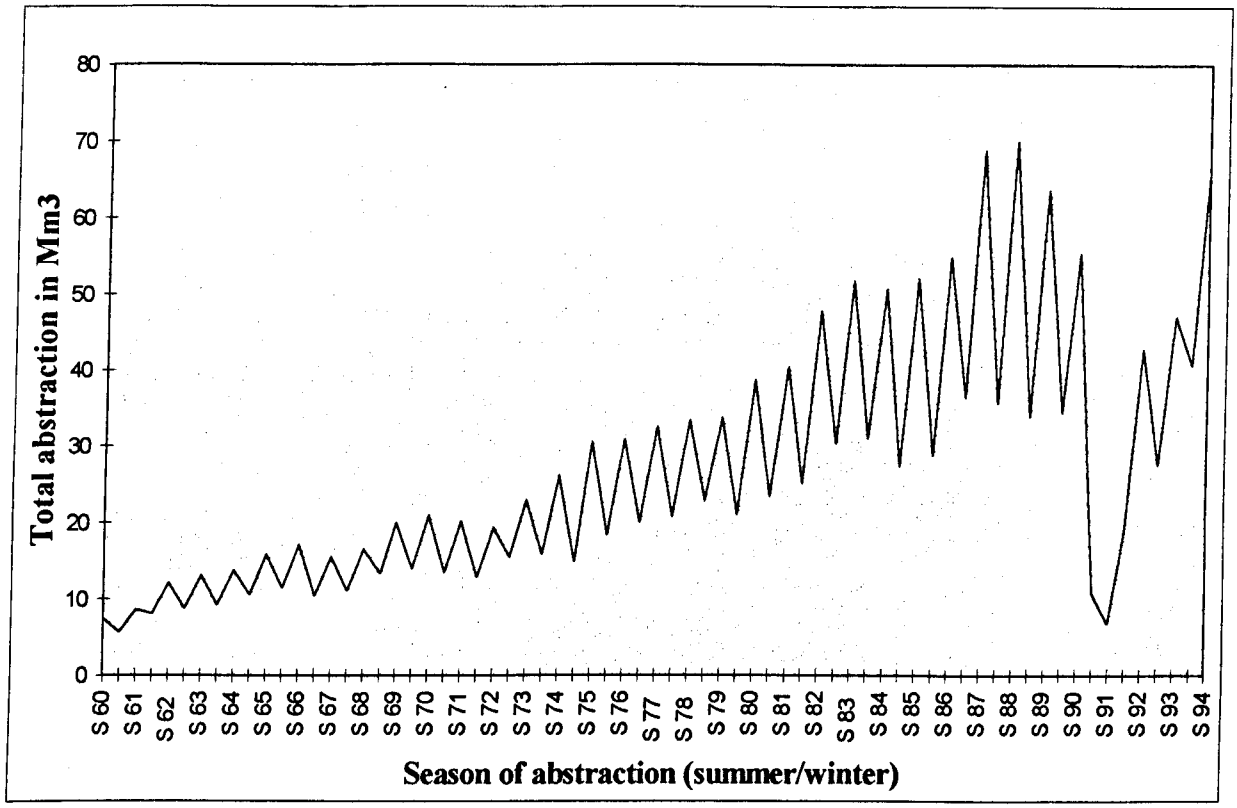


Figure 3.19: Seasonal fluctuation in groundwater abstraction from water wellfields in Kuwait.

The abstraction rate prior to the 1960's was relatively small and limited only to the eastern part of the Sulaibiya and Abdaliya wellfields. In the summer of 1960 the total abstraction rate was about 8 $Mm^3$. Moreover, the production rate was increased significantly, due to the increasing in demands for water in the country, (20 and 50 $Mm^3$ in the early 1970's and early 1980's respectively). In 1987 there was a significant increase in the production rate to reach 70 $Mm^3$, as a result of starting abstraction from the newly established Umm Gudair wellfield. The reduction in the abstraction rates in the early 1990's was due to the cessation of groundwater production because of the Iraqi invasion of Kuwait, and subsequently the gradual return of the wellfields to full operation.

### 3.2.5 WATER QUALITY

Figure 3..20 displays the earliest available isosalinity map for the DM aquifer in Kuwait prepared by Milton and Davies in 1961. This map shows that the TDS of the aquifer increases from about 2,000 mg/l in the south and south-west, where the aquifer naturally recharged through groundwater underflow, to about 40,000 mg/l near the Gulf coast, and to over 100,000 mg/l in northern Kuwait. The change in aquifer TDS from 10,000 mg/l to 40,000 occurs very rapidly in a relatively very small area in the central part of Kuwait. The zone to the north-east, where the TDS exceeded those of the sea water, could represent a non-flushed portion of the aquifer filled with connate water (Burdon and Al-Sharhan, 1986).

Figure 3.21 displays the latest DM aquifer salinity distribution map for 1990 (prepared by Al-Murad, 1994). By comparing this map with that for the aquifer pre-development conditions, it is clear that there is an increasing trend in the water salinity of the aquifer. The isosalinity contour line of 2,000 mg/l disappeared from the south-west of Kuwait and was displaced by inland movement of the higher salinity contour. This deterioration in the DM aquifer water quality is more evident and pronounced in the areas of the wellfields. At Shigaya, where the aquifer receives its best water, the aquifer salinity increased from about 2,000 mg/l to about 3,000 mg/l. This increase is attributed to the induced upward leakage from the deeper underlying saline zones. The reason for the increase in salinity in the area located between Umm Gudair and Wafra farms area, which reaches more than 15,000 mg/l, could be related to the upward leakage through a major fault which hydraulically connects the DM aquifer with the underlying saline zones. At Sulaibiya wellfield, where the water level decline in the DM aquifer reaches about 60 m from its initial pre-development level, the aquifer salinity increased from about 4,000 mg/l in 1961 to about 7000 mg/l in 1990 (with reported high $H_2S$ content). This may be related to the possible movement of the saline water (>1000 mg/l) from the north-east towards the wellfield because of changes in flow dynamics due to pumping.

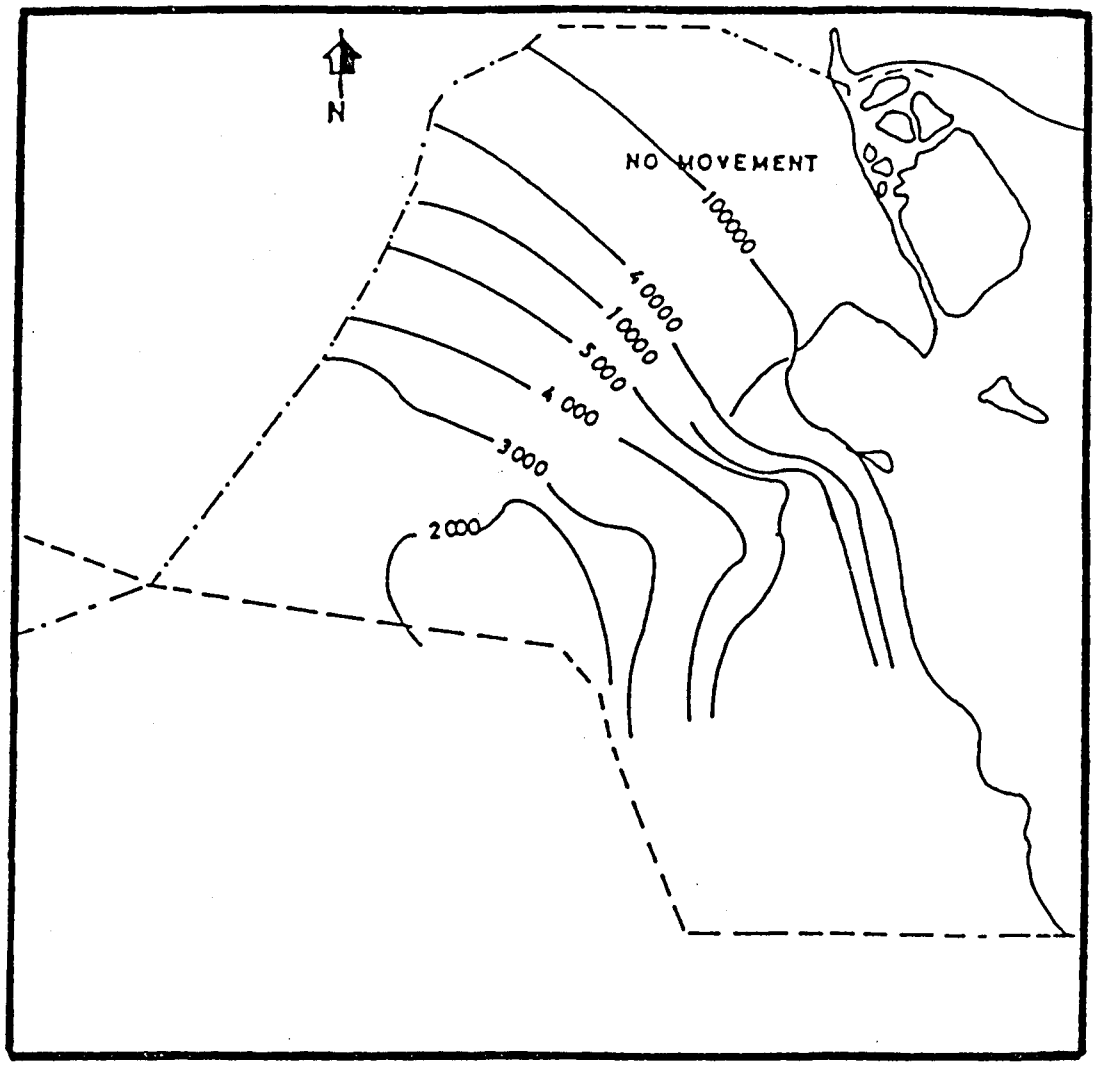


Figure 3.20: Observed pre-development salinity (mg/l) of the Dammam aquifer (Milton and Davies, 1961).

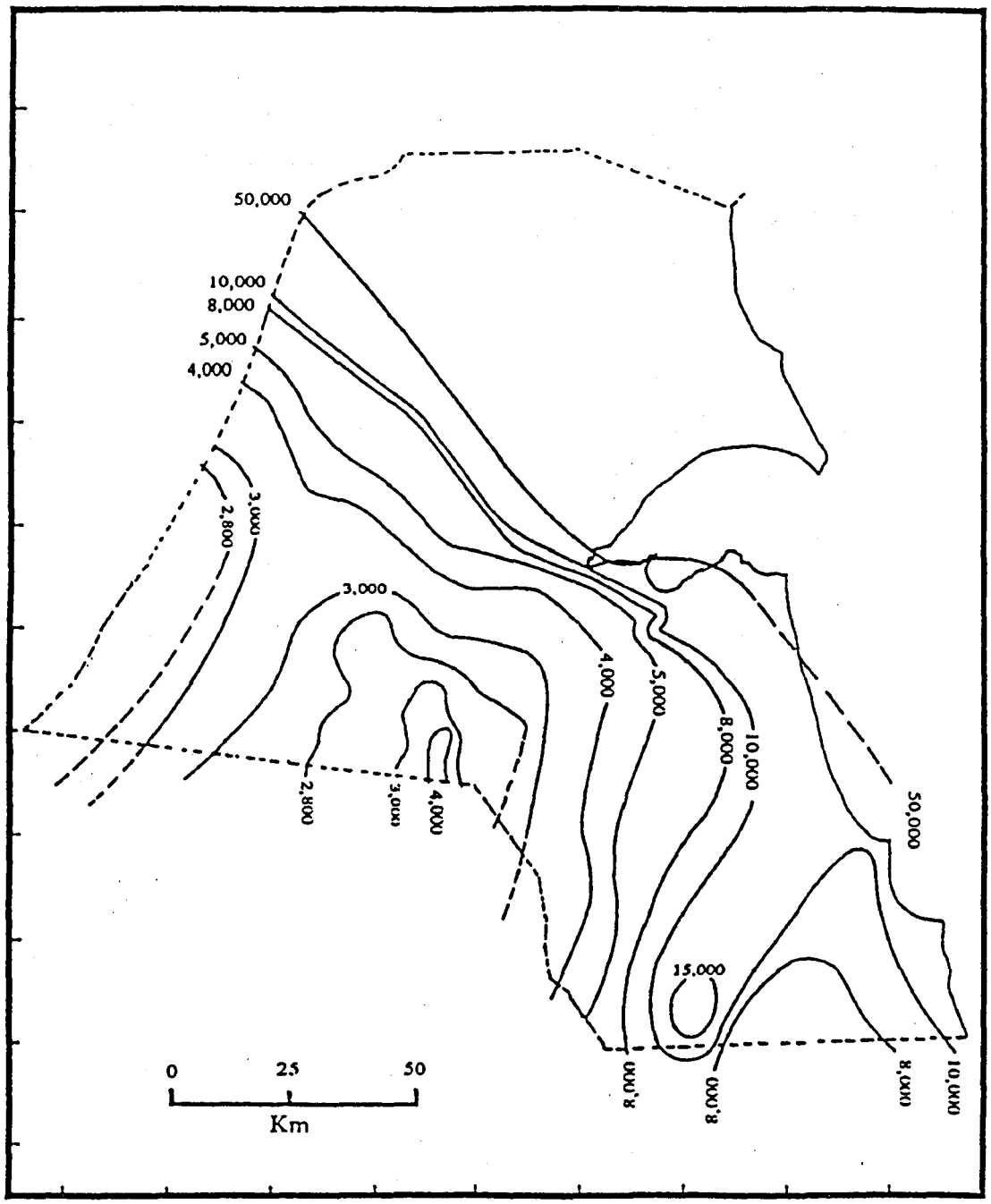


Figure 3.21: Observed salinity of the Dammam aquifer (mg/l) in 1990 (Al-Murad, 1994)

Available data on the KG aquifer salinity are very limited due to its lesser exploitation in Kuwait. However, it contains water similar in quality to that of the DM aquifer (Parsons, 1963). In general, the KG aquifer salinity ranges from about 3,000 mg/l in the south-west to over 100,000 mg/l in the north-east over a distance of about 150 Km (Amer et al. 1990).

In north-eastern Kuwait, the upper KG aquifer contains localised freshwater lenses (TDS < 500 mg/l) at Rawdhatain and Umm Al-Aish depression areas. These lenses are formed by the infiltration of runoff water in wadi and depressions (Parsons, 1963).

In conclusion, the increase in the observed salinity of the DM aquifer (and possibly the KG aquifer) might indicate that the groundwater system in Kuwait is subjected to lateral saline water intrusion from the east and north-east and an upward migration, or up-flow from the saline deep zones. These two processes are caused by the lowering of the aquifers potentiometric levels due to groundwater abstraction.

# 4. REGIONAL NUMERICAL GROUNDWATER MODEL

## *4.1 INTRODUCTION*

A numerical three-dimensional model was developed on a regional scale to simulate groundwater flow and solute transport for the two main aquifers in Kuwait; the Kuwait Group (KG) and the Dammam Formation (DM) aquifers. This model covers Kuwait and adjoining areas of Saudi Arabia.

The flow model can be used to:-

1. Achieve a representative set of aquifer and aquitard parameters that can be relied upon in the evaluation of the aquifer system. Also, calibrated aquitard and aquifers hydraulic parameters, and boundary conditions can be used to construct sub-regional models for particular areas for obtaining desired details at these locations (such as a construction of a single-well model to analyse an injection-recovery tracer test)
2. Determine the pre-development water budget of the aquifer system and use it to explain the present behaviour of the aquifer system.
3. Predict the hydraulic response of the aquifer system to future development plans in Kuwait; including groundwater abstraction from the existing and proposed water wellfields, and artificial groundwater recharge at selected sites. Thus, the optimum abstraction/recharge policy for the aquifers in Kuwait can be outlined.

The transport model can be used to :

1. Predict the change in water quality (in terms of TDS) of the aquifers during artificial groundwater recharge, and hence the efficiency of these aquifers for use to store freshwater.
2. Assist in selecting the optimal site to be used for storage of freshwater by artificial recharge.
3. Assist in selecting the optimal management options during artificial groundwater recharge at the recommended freshwater storage sites (such as injection/recovery rates, number and geometry of injection/recovery wells, duration of injection/recovery periods).

The finite-difference three-dimensional groundwater flow code "MODFLOW" was used to simulate the hydraulic system, and the three-dimensional transport model "MT3D" was used to simulate solute transport. The constructed model consists of a 73 x 70 cells (with variable grid spacing from 5 to 2km in the X and Y directions), calibrated and tested for steady and transient states. Transient simulations cover over a 36 year period starting in 1960, which is considered as the initial year prior to which no significant volume of groundwater was produced and ending in the current hydrological situation in 1996.

The hydrogeological setting of the study area (explained previously in Chapter Three) was used to formulate the conceptual model. This defines the hydrostratigraphic subdivisions, describes the flow system (including the model boundaries), and determines the relationships between the parameter values used in the numerical model and those used to formulate the conceptual model.

## *1.2 GROUNDWATER FLOW MODEL*

### 1.2.1 MODELLING APPLICATION PROCEDURES

A typical numerical groundwater flow modelling study involves four main stages.These steps should not be considered chronological; rather they should be regarded as a continuous feedback approach in the modelling procedures. In detail these stages are (Al-Murad, 1994):

**a) Data collection and conceptualisation of the aquifer system:** These data include the vertical and horizontal aquifer boundaries or geometry. The analyst may choose these boundaries as physical (no-flow, constant head, or a combination of both), or simply as convenient boundaries, e.g. to limit the modelling of a local aquifer of interest within a large regional aquifer (which is the case in this study). Once these boundaries are decided upon within a closed region, the following aquifer hydraulic data are collected:

1) aquifer transmissivity (T) or hydraulic conductivity ($K_h$) and saturated thickness (b), storage coefficient (S), aquitard leakage factor (L);
2) aquifer potentiometric head (h) both historical and present; and
3) estimated aquifer historical discharge and recharge rates in space and time (Q), for sources such as abstraction wells, rainfall and runoff infiltration, evapotranspiration rates, etc.

**b) Numerical model data preparation and parameter initialisation:** Once the aquifer boundaries are determined, the aquifer domain is divided into a rectangular grid (in the case of the finite-differences). Each block is assumed to have uniform aquifer parameters (T & S). Maps of the aquifer's transmissivity, storage coefficient and potentiometric head are prepared for the domain (often through the use of geostatistical mapping techniques), and based on these maps, aquifer parameters are specified at each node in the grid. These initial values are used for the primary stages in running the model and are updated during the course of the model construction procedures.

**c) Numerical model construction:** The objective of this phase is to construct a representative numerical model that will approximate the aquifer actual physical system. It is generally divided into two steps: 1) calibration by history matching and, 2) sensitivity analysis. The calibration procedures normally involve two steps; the first represents the steady state (equilibrium) condition of the aquifer modelled and the second represents its transient conditions. The different aquifer discharges are reconstructed in time and space, and applied to the aquifer system in the numerical model. The calculated potentiometric head distributions are compared to those observed in the field for the same time intervals. Depending on how close these comparisons are, the analyst may choose to refine the initial estimates of the aquifer input parameters (T, S and L), using a reasonable range of values, until a satisfactory comparison is obtained. Following the calibration procedures, a sensitivity analysis may be performed to measure the reliability of the used parameters. The importance of this phase depends on how much field data control is available for the aquifer parameters used in the simulation. These parameters may be changed, throughout the model or at a local zone of uncertainty in the grid, to learn what effect they may have on the overall process. Sensitivity analysis runs will indicate what parameters the computed potentiometric heads are sensitive to, and where additional field data are needed.

**d) Predictive simulation:** The main objective of predictive simulation is to estimate the aquifer performance under a variety of development scenarios. While in reality the aquifer can be developed only once at a considerable expense, a numerical model can be run many times at low expense over a short period of time. Prediction and observations of aquifer performance under different development options aids in selection of an optimum set of operating conditions to exploit the aquifer without endangering it. Examples of the use of these sets are the optimum design of wellfields and their locations, the prediction of water level declines resulting from proposed abstraction rates, the effects of proposed artificial

groundwater recharge, the effects of one abstraction area on another, calculating the aquifer water budget, and the relationship between water supply and salt water intrusion.

The following are detailed descriptions of the above procedures carried out during the construction of the numerical model for the Kuwait aquifer system.

### 4.2.2 CONCEPTUAL MODEL

The procedure for developing a mathematical flow model of a given aquifer system starts with the formulation of a conceptual model of the system. The conceptual model is a representation of the groundwater flow system (often pictorial) used to simplify the field problem and organise the associated field data to make the analysis of the system more tractable (Anderson & Woessner, 1992). Figure 4.1, describes and illustrates the conceptual model used in this study.

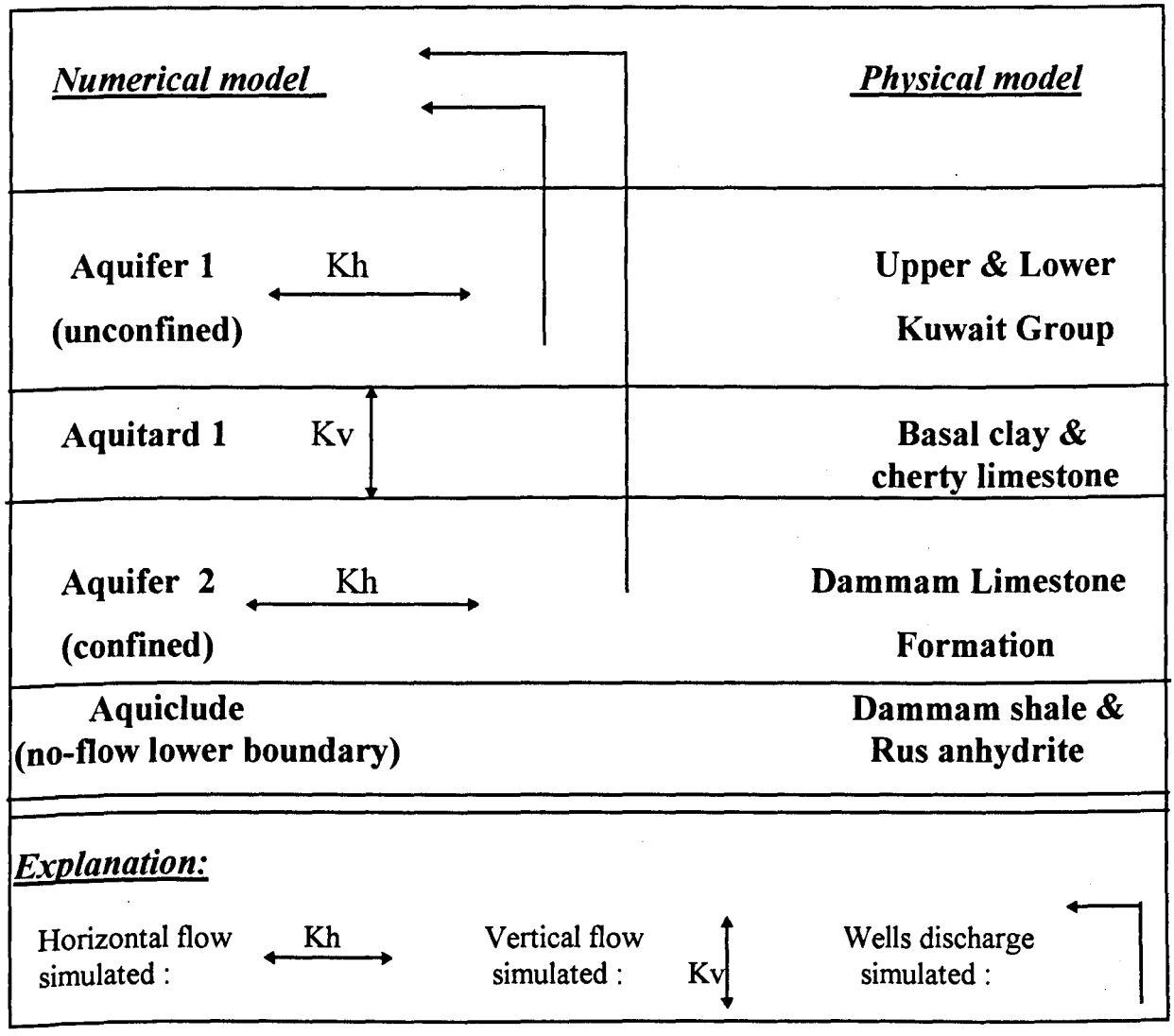


Figure 4.1: Conceptual model of Kuwait aquifer systems used in numerical simulation.

Based on the geological and hydrological setting of the modelled two aquifers (KG and DM), the conceptual model was formulated using the following assumptions:

1. The aquifer system is divided into three hydrostratigraphic units, the unconfined Kuwait Group (KG) aquifer, the leaky confined Dammam Formation (DM) aquifer, and the leaking aquitard which separates them.
2. The upper boundary of the model was taken as the phreatic water table of the Kuwait Group aquifer. The model domain was assumed to be isolated from lower layers by the low-permeability layers of limestones inter-bedded with shales (of the basal Dammam Formation) and anhydrites (of the Rus Formation).
3. The modelled area is bounded to the east by the Arabian Gulf coastline, represented as the sole physical boundary, which is considered to be a constant head boundary representing the approximate location of the contact between the aquifer water and the sea water. Otherwise, other boundaries of the model were assigned as hydraulic boundaries based on the regional flow pattern, deduced from the initial potentiometric water level maps for the two aquifers. To limit the modelled Kuwait area within the regional aquifer that extends to Saudi Arabia, a constant head boundary assigned to the south and the south-west of the modelled area at contour lines of 180 and 190m for the KG and the DM aquifers, respectively. For both aquifers, this boundary was modelled as a constant head boundary during the steady state calibration, and was converted to a general head boundary (mixed boundary conditions) during the transient calibration. On the other hand, no-flow boundaries were used to delineate the modelled area at the west, north-west, and south-east of Kuwait which are assigned to be perpendicular to the initial potentiometric lines of the two aquifers at those two locations. In addition, no-flow boundaries were used for the KG where the aquifer is dry in the south-west corner of Kuwait, and at the Ahmadi ridge where it is non-existent due to erosion.
4. There is no significant natural surface recharge to the model layers. This due to the extreme climatic conditions in Kuwait, since the average rainfall is only about five inches a year, and the evaporation rates (due to high ambient temperatures) extremely high and exceeding the rainfall rate (Bergstorm and Aten, 1964; Amer et al., 1992).
5. Vertical leakage between the aquifers occurs through the aquitard layer that separates them, the direction and magnitude of this leakage depending on the vertical resistance of the aquitard to vertical flow, and to the difference in water head between the two

aquifers. This vertical leakage is not well defined for aquifers in Kuwait and needed to be quantified through model calibration.

6. The aquifer system is conceptualised to receive its recharge through lateral inflow which comes from the Saudi Arabia side, where the discharge zone is the Arabian Gulf. The rate of this recharge was estimated for both aquifers under steady-state conditions, using a form of Darcy's Law. This quantifies the amount of groundwater percolating through a given cross-section (flow channel) of an aquifer which is delineated by two flow lines:

$$Q = T.i.W \qquad (4.1)$$

where **T** is the transmissivity, **i** is the hydraulic gradient, and **W** is the width of cross-section. The transmissivity values obtained by pumping tests, and the steady state water levels maps (Figures 3.11 and 3.12) for both aquifers were used in calculating the rate of recharge for each aquifer. A cross-section (A-B) was selected to pass through a zone with more reliable transmissivity data than what it is found on the actual boundary of the study area. The transmissivity for DM aquifer along this cross-section (Figure 3.9) ranges from about 100 to about 2000 $m^2/d$, whereas, the transmissivity for the KG aquifer (Figure 3.8) ranges from about 200 to about 500 $m^2/d$. The width of the selected flow channel is varied in both aquifers. It is taken as 150 km width in the DM aquifer and less wide (120 km) in the KG aquifer, because the aquifer becomes unsaturated at the western part of Kuwait. The hydraulic gradient for the steady-state (pre-development) case for both aquifers was taken as 0.001 (dimensionless). Hence, in this study a total of 121,000 (+ or - 10,000) $m^3/d$ of water was calculated to recharge the aquifer system by the lateral inflow, about 43,000 $m^3/d$ received by the KG aquifer, and about 78,000 $m^3/d$ by the DM aquifer. These rates will be used as a model calibration target during the steady-state conditions.

### 4.2.3 GRID DESIGN

Figure 4.2 displays the grid design of the numerical model. The domain is discretized using a square mesh consisting of 73 x 70 cells with irregular grid spacing. A finer grid spacing ($\Delta x = \Delta y$) of 2 km was assigned at the locations of wellfields to represent the expected steepness in the hydraulic gradient resulting from groundwater abstraction. This is because finer nodal spacing is required to define the highly curved surfaces (Anderson & Woessner,

Figure 4.2: Irregular finite-difference grids used in the regional model.

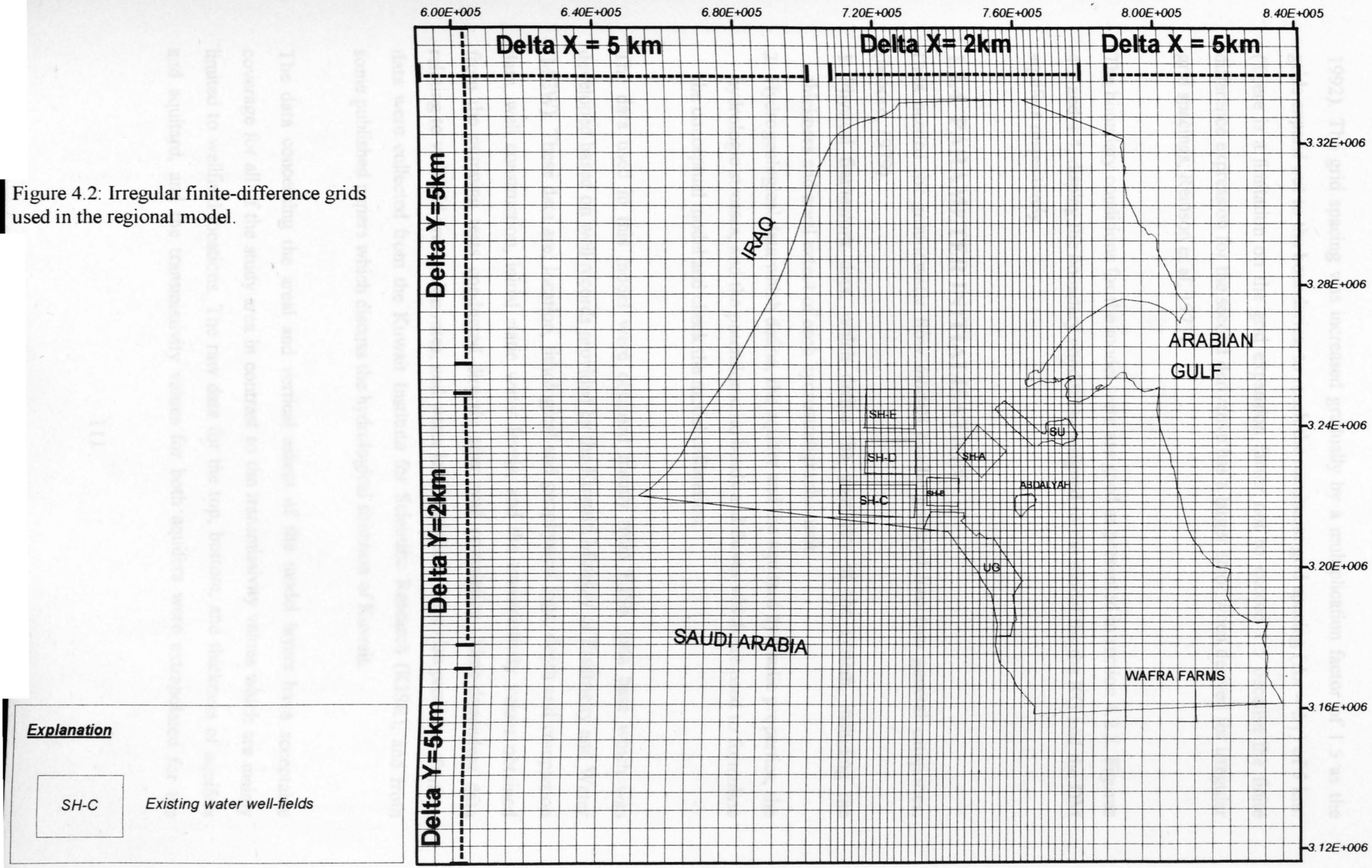

1992). The grid spacing was increased gradually by a multiplication factor of 1.5 as the grids expand out to the boundaries, to reach the maximum grid spacing ($\Delta x = \Delta y$) of 5 km. (There is a limitation on the grid expansion factor not to exceed 1.5 because the finite difference expression for the second derivative has a larger error when derived for irregular grid spacings; Remson et al, 1971).

The boundary conditions for the model were assigned as presented in section 4.2.2. Figures 4.3 and 4.4, display the boundary conditions assigned to the model for the KG and the DM aquifers respectively.

### 1.2.4 PARAMETER INITIALISATION

Data needed for groundwater flow models can be grouped into two general categories, (Moore, 1979) :

1. Physical framework data, which define the geometry of the system, including the thickness and areal extent of each hydrostratigraphic unit.
2. Hydrogeological data which define, the aquifer and the aquitard hydraulic properties, the hydrologic stresses, and the potentiometric heads and fluxes which are used to formulate the conceptual model and check the model calibration.

The data used in this model were obtained mainly from KISR data base which was developed based on well records provided by the Kuwaiti Ministry of Electricity and Water (MEW). These data are; location, lithological and geophysical logs, depth and completion date, well construction, initial static water levels, and the transmissivity values obtained from the pumping tests conducted directly after well completion. Time-dependent data relating to wellfield production rates, and water level variations were also provided. Further data were collected from the Kuwait Institute for Scientific Research (KISR), and from some published papers which discuss the hydrological situation of Kuwait.

The data concerning the areal and vertical extent of the model layers have acceptable coverage for all of the study area in contrast to the transmissivity values which are mainly limited to wellfield locations. The raw data for the top, bottom, and thickness of aquifers and aquitard, and the transmissivity values for both aquifers were extrapolated for the

Figure 4.3: Kuwait Group (KG) grid desgin and boundary conditions used in the regional model.

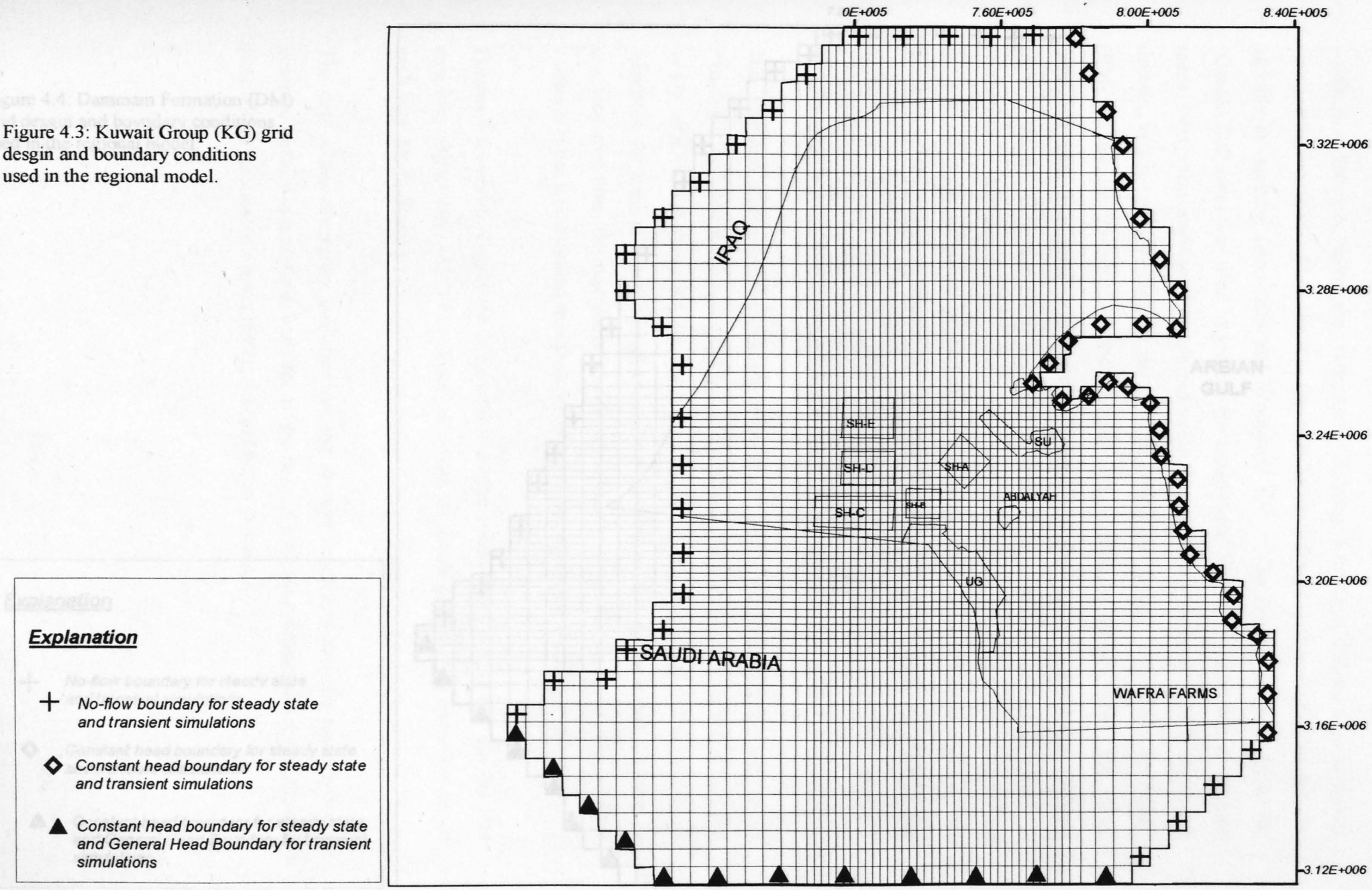

Figure 4.4: Dammam Formation (DM) grid desgin and boyndary conditions used in the regional model.

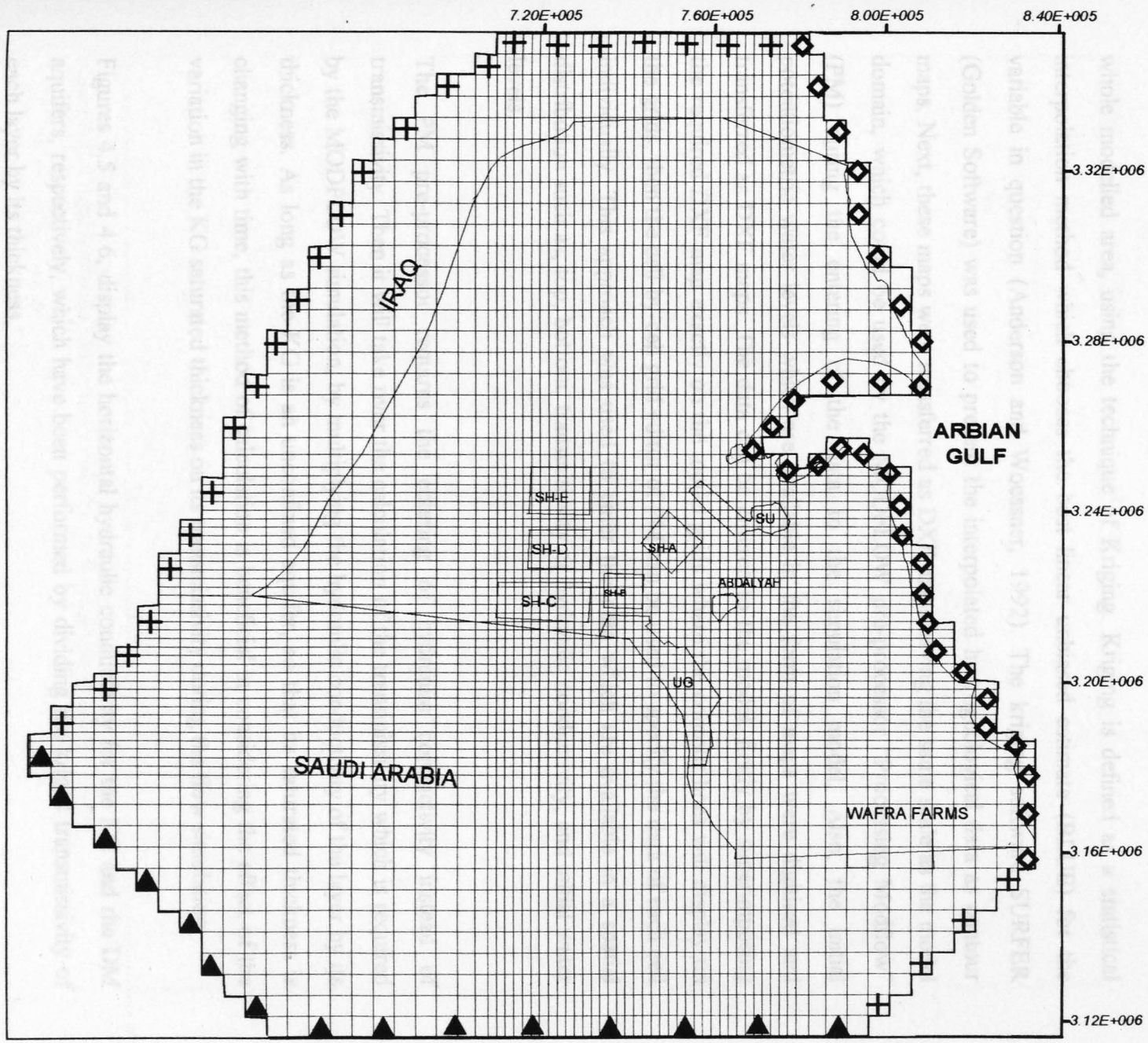


***Explanation***

+ *No-flow boundary for steady state and transient simulations*

◇ *Constant head boundary for steady state and transient simulations*

▲ *Constant head boundary for steady state and General Head Boundary for transient simulations*

whole modelled area, using the technique of Kriging. Kriging is defined as a statistical interpolation method which chooses the best linear unbiased estimate (BLUE) for the variable in question (Anderson and Woessner, 1992). The kriging software SURFER (Golden Software) was used to present the interpolated hydrogeological data as contour maps. Next, these maps were transferred as DXF maps having the same scale as the model domain, which could be used by the MODFLOW pre-processor "Processing Modflow" (PM) during the entering of the data to the simulation model. Also, the initial potentiometric water levels which are available in the form of maps were digitised and transferred as DXF maps. The data can be entered to the model, firstly by superimposing the required DXF map exactly on the model grids where the contour lines will display on the grids, then the cell-by-cell grid editor of PM can be used to specify the data of each cell individually. This approach was used to enter the data which are available in a spatial distribution such as; top, bottom, transmissivity or hydraulic conductivity, and initial water levels.

The PM pre-processor requires the entering of hydraulic conductivity instead of transmissivity. Then it will take over the calculation of the transmissivity which is required by the MODFLOW simulation, by multiplying the hydraulic conductivity of the layer by its thickness. As long as the KG is an unconfined aquifer, so that its saturated thickness is changing with time, this method of calculation is beneficial in considering the effect of the variation in the KG saturated thickness on its transmissivity during the flow simulation.

Figures 4.5 and 4.6, display the horizontal hydraulic conductivity for the KG and the DM aquifers, respectively, which have been performed by dividing the kriged transmissivity of each layer by its thickness.

The data which are rarely available like the storage coefficient and the porosity were assigned initially as a uniform value for all the cells of each layer separately, to be adjusted later within reasonable bounds during the calibration process.

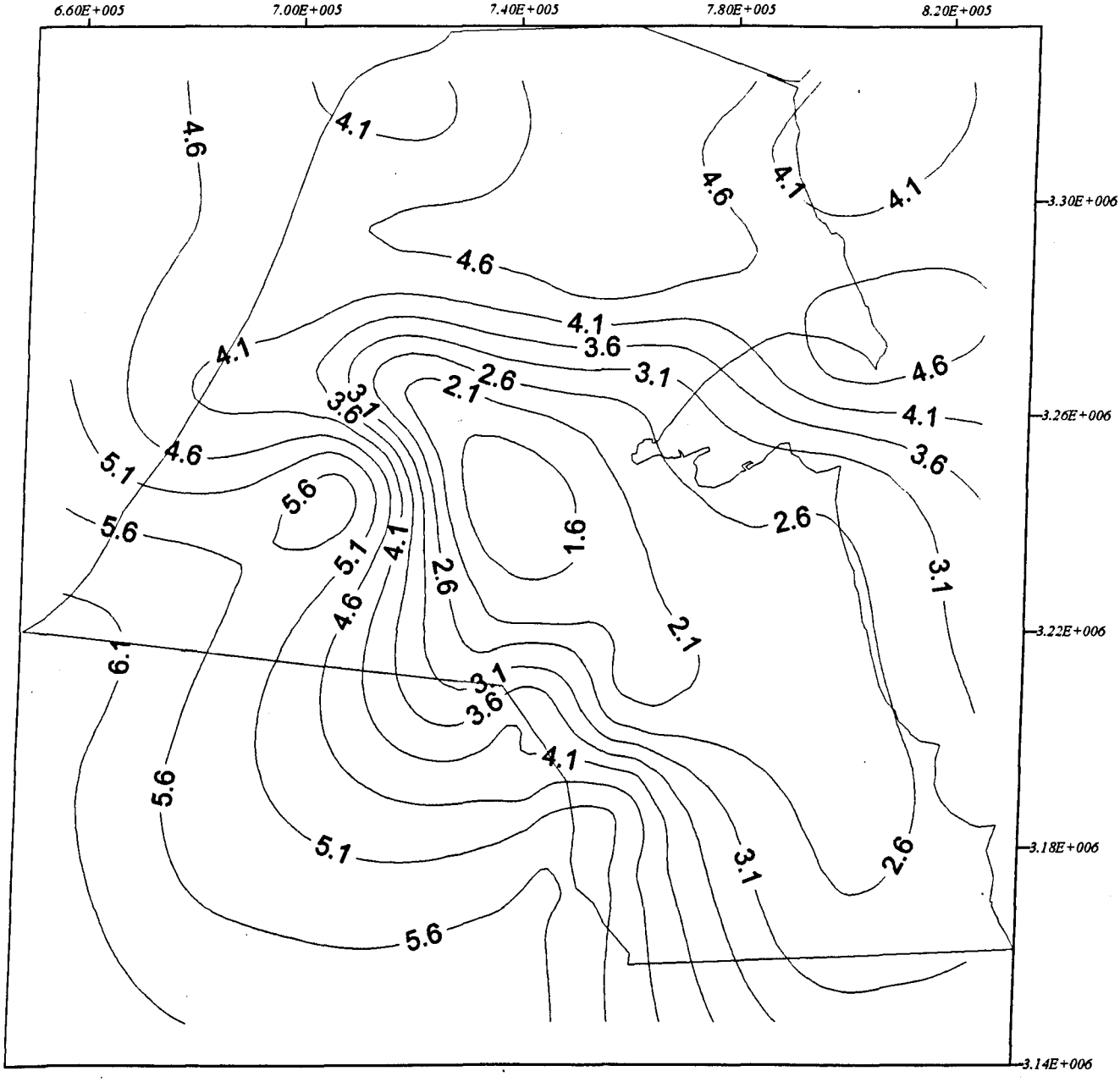


Figure 4.5: Kriged hydraulic conductivity map for the Kuwait Group aquifer (m/d).

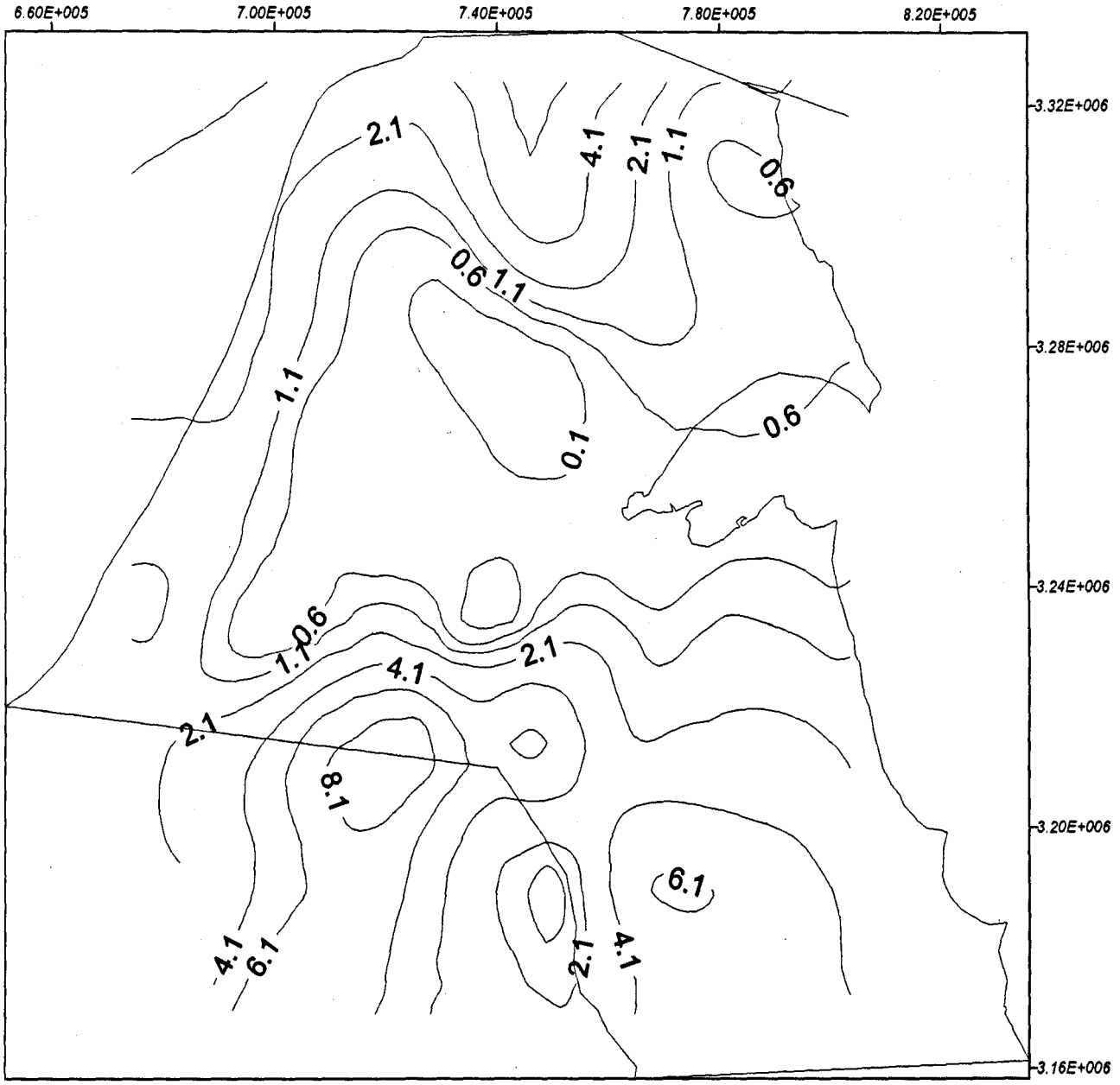


Figure 4.6: Kriged hydraulic conductivity map for the Dammam Formation aquifer (m/d).

### 4.2.5 NUMERICAL MODEL CALIBRATION

The numerical model calibration consisted of two stages, steady state and transient calibration or history matching. Usually, these two stages were run interactively; the computed aquifer parameters in one calibration were constantly evaluated and tested in the other calibration. When satisfactory results were achieved, then the model was considered calibrated and could be used for prediction using the calibrated hydraulic parameters computed in this stage. In the initial stages of calibrating the model under steady state conditions, it was found that in addition to the aquifer's hydraulic conductivity, the vertical leakage was a critical parameter affecting the simulated initial heads.

For MODFLOW simulations involving a multi-layer system, the vertical leakance term (known as VCONT) should be calculated for each nodal block in the grid (the blocks in the bottom has an exception of this, since the model assumes that the bottom layer is underlain by impermeable material and VCONT is thus zero). By using PM, there are two ways to specify the vertical leakance, either 1 or 2:

1. Specify the vertical leakance directly to the model as a function of the vertical hydraulic conductivity and the thickness of the semiconfining layer which separates between the two aquifers, as:

$$\text{VOCNT} = L = \frac{(K_v)_c}{b_c} \qquad (4.1)$$

where

$L$ vertical leakance, (1/T);

$(k_v)_c$ vertical hydraulic conductivity of the semiconfining layer, and

$b_c$ the thickness of the semiconfining layer.

2. Specify the vertical hydraulic conductivity for the upper and lower aquifers ,and by knowing their thickness , the PM will calculate the vertical leakance as :

$$\text{VCONT} = L = \frac{1}{2}\left(\frac{K_{v_1}}{b_1} + \frac{K_{v_2}}{b_2}\right) \qquad (4.2)$$

where

$b_1, b_2$ thickness of the upper and lower aquifers, respectively; (L), and

$k_{v_1}, k_{v_2}$ vertical hydraulic conductivity of the upper and lower aquifers, respectively;($L^2/T$).

In the case of Kuwait, insufficient vertical leakage data are available for the aquitard, since there are merely 5 leakage factor readings for only two locations (Table 3.4). As a result, it is not reasonable to rely on these readings to represent the vertical leakage between the two aquifers at all locations. Furthermore, the reported values displayed very wide limits, ranging from about 145 m to about 1,600 m with an unpredictable distribution.

The aquifers storage parameters also are not available in a reasonable areal distribution (as presented in Table 3.3), and only some porosity measurements are available as carried out on core samples in the laboratory in the course of study of Umm Gudair area (Khalaf et al, 1989). Thus, during the transient calibration, the aquifers storage parameters should be limited to a certain range of values and not exceed it for unrealistic numbers. The used ranges for storage parameters were assigned based on the existing values, and also to the recommended values from the literature for similar aquifers to the ones under consideration, (Younger, 1993; Domenico and Schwartz, 1990; Kruseman and de Ridder, 1990). However, these ranges may be exceeded and the matching between the observed and the simulated drawdowns is still unreachable. Because the vertical leakage between two aquifers depends on the head difference between them in addition to the aquitard resistance (de Marsily, 1986), the vertical leakage will vary according to the flow status (be is steady state or transient). Therefore, it was decided that the vertical leakage obtained by steady state calibration will be re-adjusted again during the transient calibration if the assumed ranges of aquifers storage parameters are exceeded without getting the desirable match. Hence, the model calibration in this study was done as one task, where an iterative procedure between the steady state and the transient calibrations was repeated until all the aquifer parameters were calibrated simultaneously and a match was achieved between the simulated and observed heads and fluxes in both stages of the calibration.

The approach used was as follows:

1. Initially, the vertical hydraulic conductivity for each layer was entered equal to its horizontal hydraulic conductivity.
2. Because normally the vertical hydraulic conductivity is less than the horizontal conductivity, the entered vertical hydraulic conductivity for each layer (as in 1) was multiplied by a factor ranging from 0.1 to 0.0002.
3. A different combination of multipliers for the vertical hydraulic conductivities of the two layers was used for each iteration.
4. The steady state calibration was started by simulating the initial potentiometric heads in both aquifers as dependent variables. The transmissivities of both aquifers were adjusted until the initial heads of both aquifers were simulated adequately.
5. The transient calibration was started by adjusting the storage coefficient and the effective porosity of the aquifers within allowable ranges which are assigned according to the available values obtained from pumping tests, and the recommended values in the literature for a similar aquifers to the ones under consideration. The transient calibration proceeded until a match was achieved between the measured and the simulated drawdown in potentiometric heads of the two aquifers during the simulated stress periods.
6. If the assigned ranges of storage parameters were exceeded during the previous step and a relatively small difference between the simulated and observed drawdown levels at some locations, then the steady state calibration in step 4 was restarted with small occasional modifications in the vertical hydraulic conductivity or the transmissivity if needed. After the model was calibrated under the steady state conditions with the new parameters, it was re-calibrated under the transient condition as in step 5. This alteration proceed alternatively between the steady state and transient calibrations proceeded until the model was calibrated under both conditions.
7. If the model calibration results in 6 were widely unacceptable, then the calibration process was started again from step 2 by changing the multiplication factor used to obtain the vertical hydraulic conductivity for the layers with relation to their horizontal hydraulic conductivity.

This loop procedure of calibration was undertaken until a good match was achieved between the measured and the simulated initial potentiometric heads for the KG and DM aquifers, and between the measured and the simulated drawdown in the water heads resulting from pumping the two aquifers during the simulated stress periods. A detailed explanation for the two stages of calibration presented as follows:

#### 4.2.5.1 STEADY STATE CALIBRATION

The aquifer system was in quasi-equilibrium conditions prior to the 1960's, since groundwater abstraction was minor (at less than 10 $Mm^3/y$). The available potentiometric levels under these quasi-equilibrium conditions were entered as initial heads and utilised in the steady state calibration.

Two major targets were used to check the validity of the steady state calibration. These were, the matching between measured and simulated initial water levels, and the attainment of a reasonable agreement between calculated and computed groundwater budget. Moreover, the water balance target should be achieved with a minimum discrepancy percent error, which can be calculated as (McDonald and Harbaugh, 1988):

$$D = \frac{100(IN - OUT)}{(IN + OUT)/2} \qquad (4.3)$$

where D is the discrepancy error, IN is the total inflow to the system, and OUT is the total outflow. This percent error taken as an indication of solution validity for the time step to which it applies. Ideally, the error should be less than 0.1% (Anderson and Woessner, 1992), but an error of around 1% is usually considered acceptable (Konikow, 1978).

By using constant head boundary conditions at the up-gradient and down-gradient boundaries of the aquifer system, hydraulic parameter calibrations were adjusted to reproduce the observed initial potentiometric heads for the aquifers (Figures 3.11 and 3.12). The hydraulic parameters which need to be adjusted during the steady state calibration are; the horizontal and vertical conductivities of both aquifers. The horizontal hydraulic

conductivity distribution obtained by kriging for both aquifers (Figures 4.5 and 4.6) were used as the initial horizontal hydraulic conductivity in the model.

The simulated potentiometric maps for the KG and DM aquifers at the end of the steady state calibration stage were compared to those observed for the pre-development conditions. It was difficult to obtain a good match between the observed initial water heads (Figures 3.11 and 3.12) and the simulated, unless the field-estimated aquifers horizontal hydraulic conductivity was largely changed. This problem was avoided taking in consideration that the initial observed water heads are less certain especially away from the measured points which are few and not well distributed. Thus, because the contouring process is subjective and it included errors, more concern during the calibration was put in matching the simulated heads with the actual field-measurement water heads. Whereas at other locations where the heads were extrapolated to draw the observed maps ( Figures 3.11 and 3.12), the heads were re-contoured to be matched with the simulated water heads based on more certain data.

Normally, calibration criteria are used expressing the average difference between the simulated and measured heads like mean error, mean absolute error, and root mean squared error (Anderson and Woessner, 1992). However, because the initial water heads were provided in the form of maps which are uncertain, the only way in evaluating the calibration results was with visual calibration. Figures 4.7 and 4.8 display the achieved matching between the re-contoured observed and simulated steady state potentiometric heads for the KG and DM aquifers, respectively.

The transmissivities values which have been obtained by the kriging method only without any basis of field measurements like pumping test, were subjected to more changes during the calibration. Whereas, the estimated transmissivity values depending on pumping tests have less modifications. Figures 4.9 and 4.10, display the hydraulic conductivity distribution in the KG and DM aquifers, respectively, obtained at the end of the calibration stage. Whereas, the vertical hydraulic conductivities of the KG and DM aquifers were found to be equal to 0.01 and 0.00015 of their horizontal conductivities, respectively.

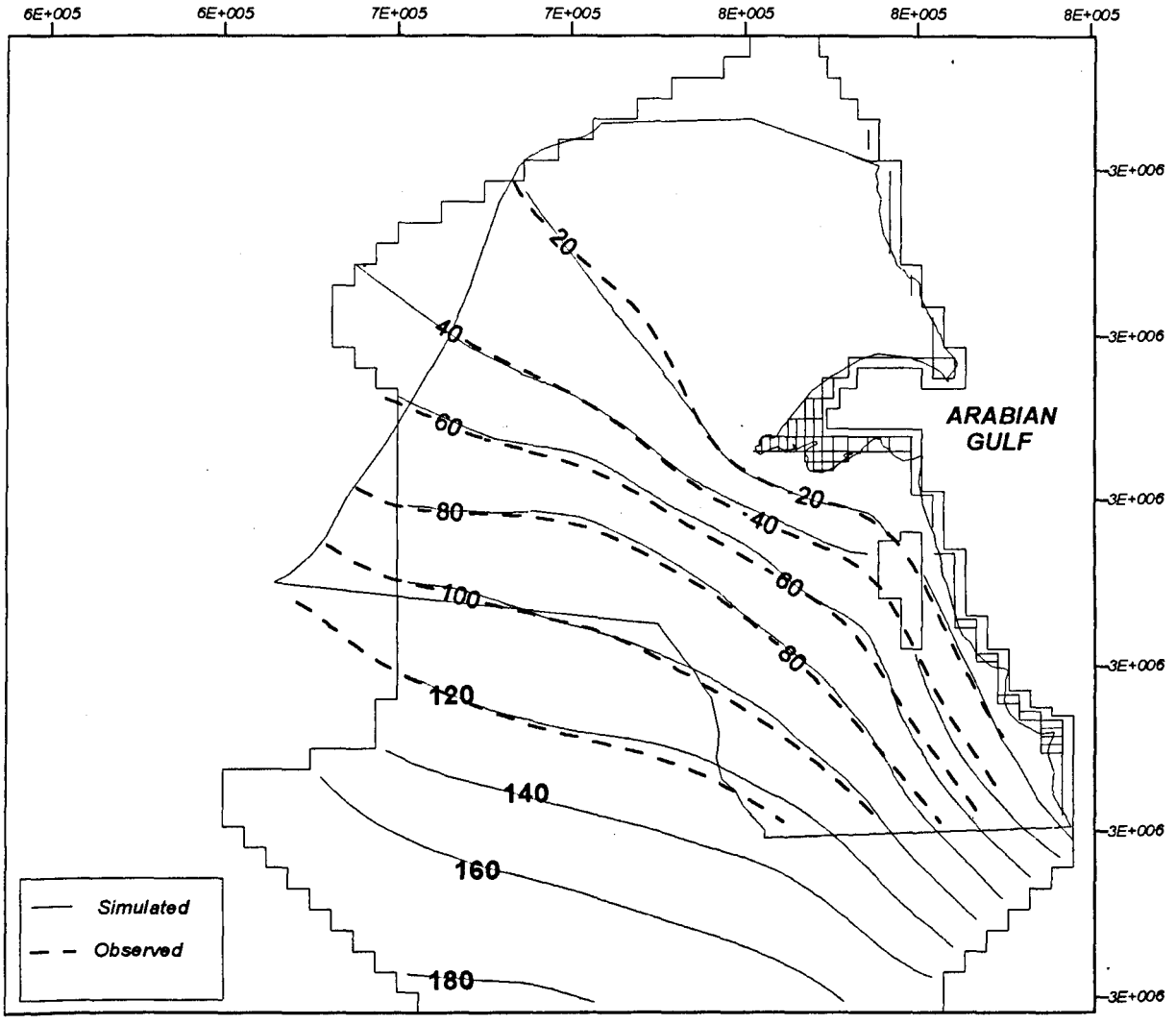


Figure 4.7: Matching between the simulated and observed water levels of the Kuwait Group aquifer obtained during the stead-state calibration of the regional model, m amsl.

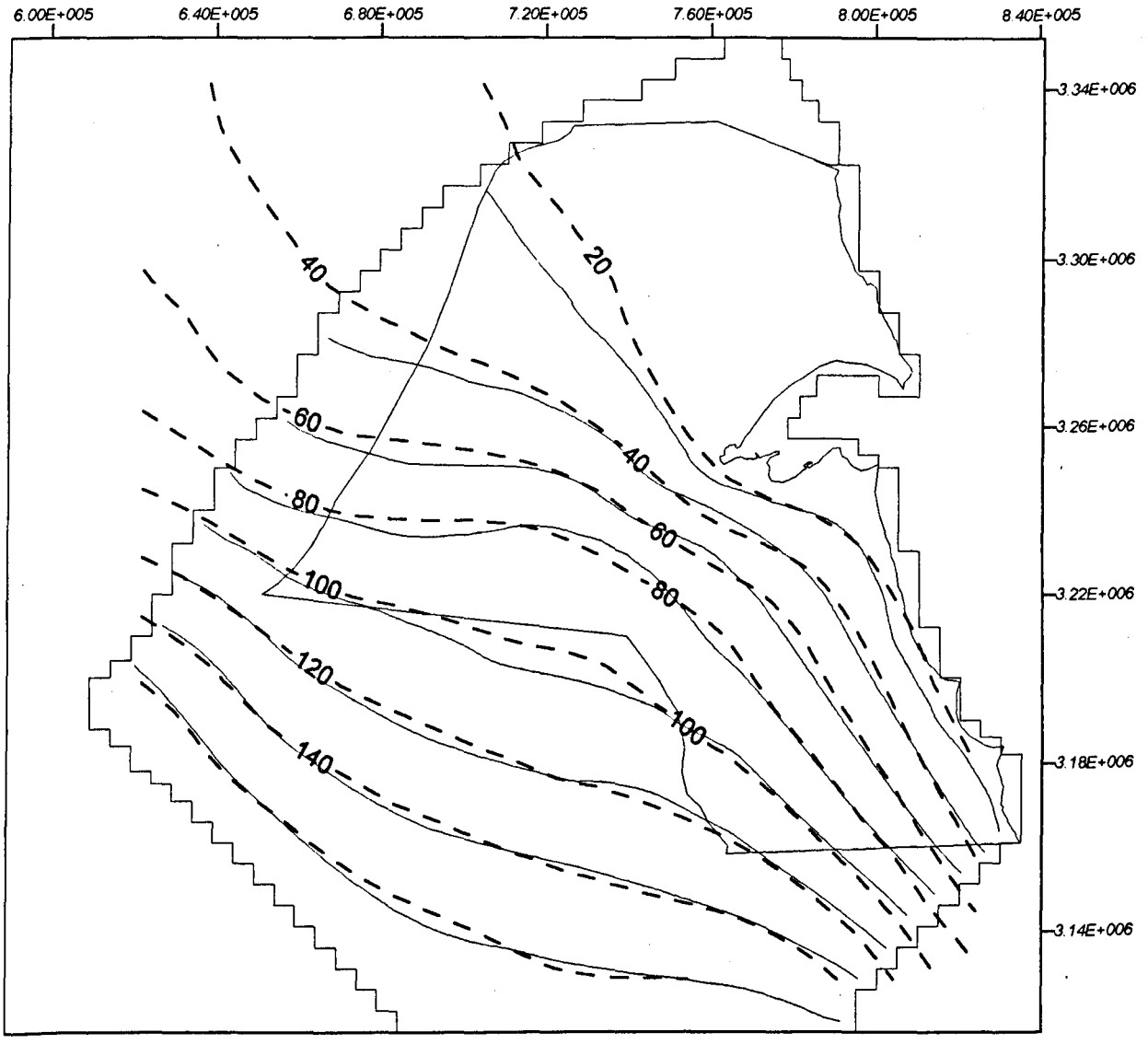


Figure 4.8: Matching between the simulated and observed potentiometric heads of the Dammam aquifer obtained during the steady-state calibration of the regional model, m amsl.

In addition to the match between the observed and simulated initial potentiometric heads of the aquifers during the steady state calibration, the computed water budget was agreed with the calculated one, with a minimum discrepancy error (0.01%) which is considered a highly acceptable result.

Table 4.1, illustrates the simulated steady state mass balance for the whole model domain. Also, it shows the simulated lateral inflow rates at a line crossing the modelled area from NW to SE directions (cross section A-B on Figures 3.8 and 3.9). These simulated inflow rates were compared with inflow rates calculated along the same line by this study (as a steady-state calibration target) and by Omar et al. (1981).

| **Flow Component** | **Simulated** | | **Calculated** | |
|---|---|---|---|---|
| | This study | | This study | Omar et al. 1981 |
| | whole model | at Kuwait boundary | at Kuwait boundary | at Kuwait boundary |
| **KG** | | | | |
| lateral flow in | 65,264 | 46,168 | 43,000 | 22,730 |
| lateral flow out | 77,285 | | | |
| leakage to DM | 19,089 | | | |
| leakage to KG | 31,115 | | | |
| Total KG flow in | 96,379 | | | |
| | | | | |
| **DM** | | | | |
| lateral flow in | 62,542 | 81,630 | 78,000 | 46,000-68,000 |
| lateral flow out | 50,516 | | | |
| Total DM in | 81,631 | | | |
| | | | | |
| **DOMAIN** | | | | |
| lateral flow in (= out) | 127,806 | | | |

Table 4.1: Simulated groundwater balance for the aquifer system under steady state conditions, and a comparison with groundwater inflow rates calculated by this study and by Omar et al. 1981 ($m^3$/day).

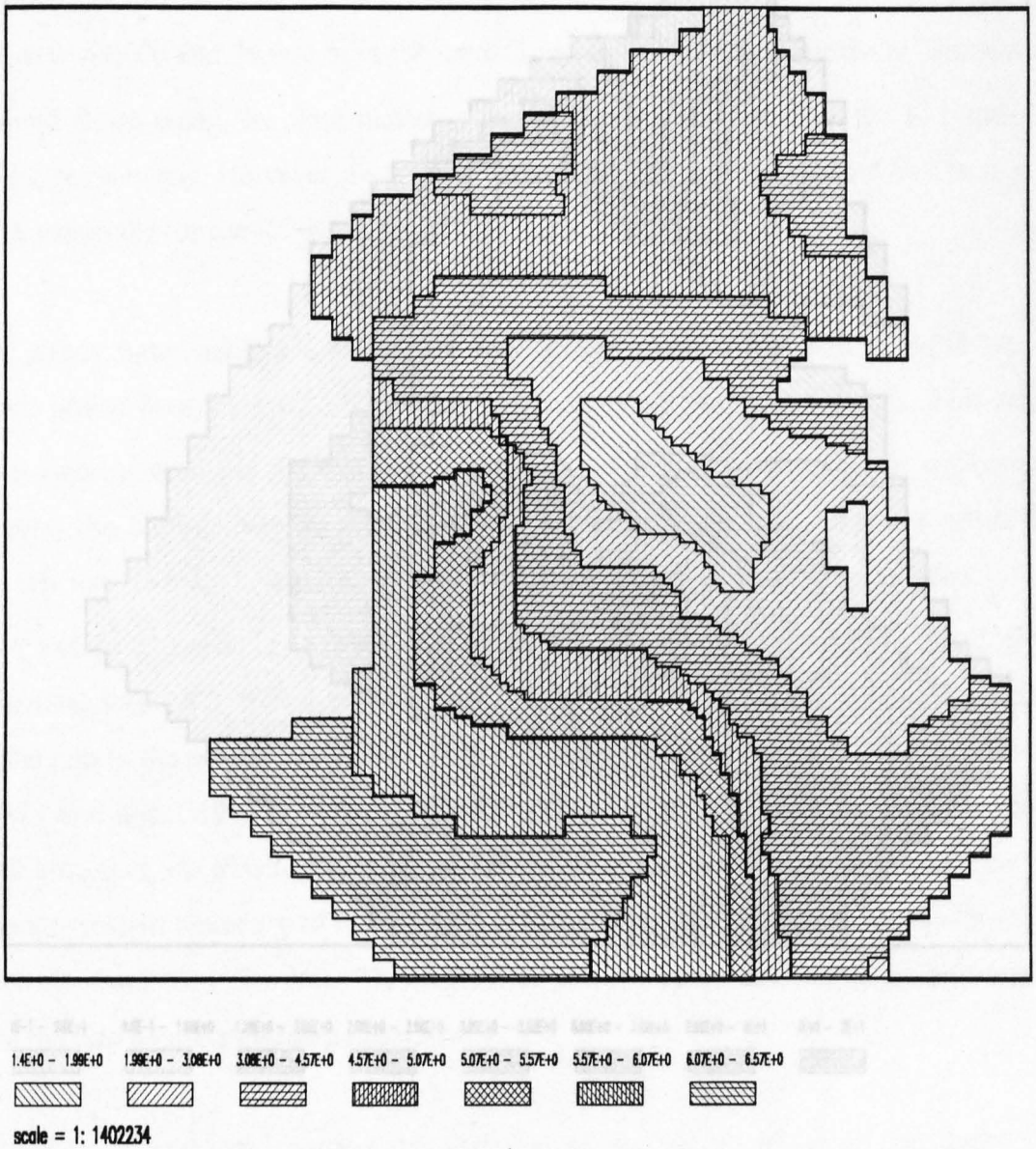


Figure 4.9: Calibrated hydraulic conductivity of the Kuwait Group (KG) aquifer, m/d.

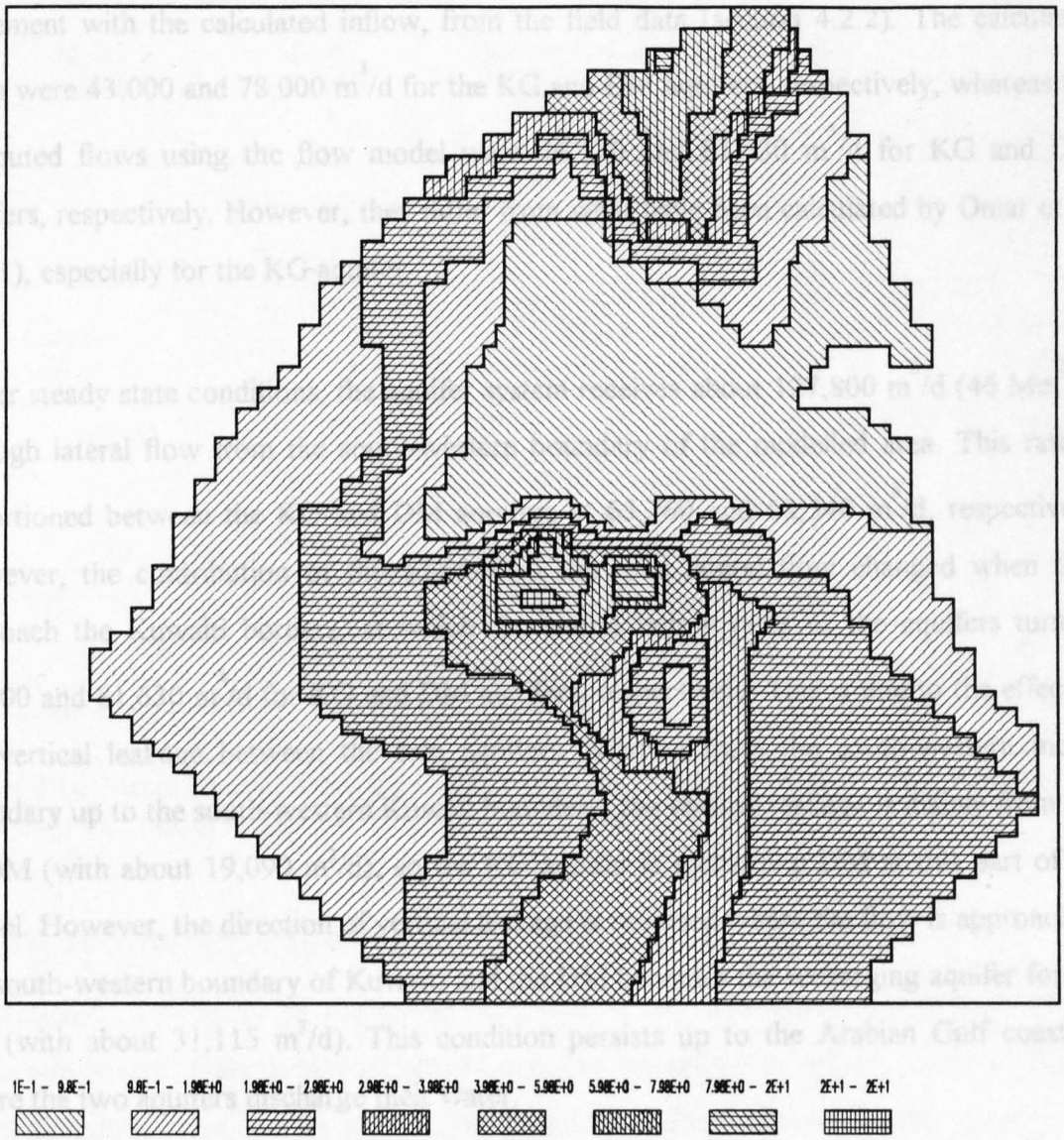


Figure 4.10: Calibrated hydraulic conductivity of the Dammam aquifer, m/d.

BRITISH LIBRARY

IMAGING SERVICES NORTH
Boston Spa, Wetherby
West Yorkshire, LS23 7BQ
www.bl.uk

# PAGE MISSING IN ORIGINAL

The computed steady state lateral inflow at the Kuwait boundary shows an acceptable agreement with the calculated inflow, from the field data (section 4.2.2). The calculated flows were 43,000 and 78,000 $m^3/d$ for the KG and DM aquifers, respectively, whereas the computed flows using the flow model were 46,170 and 81,630 $m^3/d$ for KG and DM aquifers, respectively. However, they differ from what have been calculated by Omar et al. (1981), especially for the KG aquifer.

Under steady state conditions, the aquifer system receives about 127,800 $m^3/d$ (46 $Mm^3/y$) through lateral flow from the south-western boundary of the modelled area. This rate is apportioned between the KG and DM aquifers at 65,260 and 62,540 $m^3/d$, respectively. However, the contribution of the aquifers to the total lateral flow changed when they approach the Kuwaiti borders, at which the lateral inflow rates of the aquifers turn to 46,000 and 81,630 $m^3/d$ for KG and DM aquifers, respectively. This is due to the effect of the vertical leakage between the two aquifers. Starting from the south-western model boundary up to the south-western Kuwait boundary, the vertical leakage is mainly from KG to DM (with about 19,090 $m^3/d$), so the KG aquifer is recharging DM at this part of the model. However, the direction of vertical leakage is reversed where the flow is approaching the south-western boundary of Kuwait, and the DM becomes the recharging aquifer for the KG (with about 31,115 $m^3/d$). This condition persists up to the Arabian Gulf coastline where the two aquifers discharge their water.

Figure 4.12, is a sketch showing the variation of the lateral inflow at the above three boundaries and the alteration in the vertical leakage direction between the two aquifers.

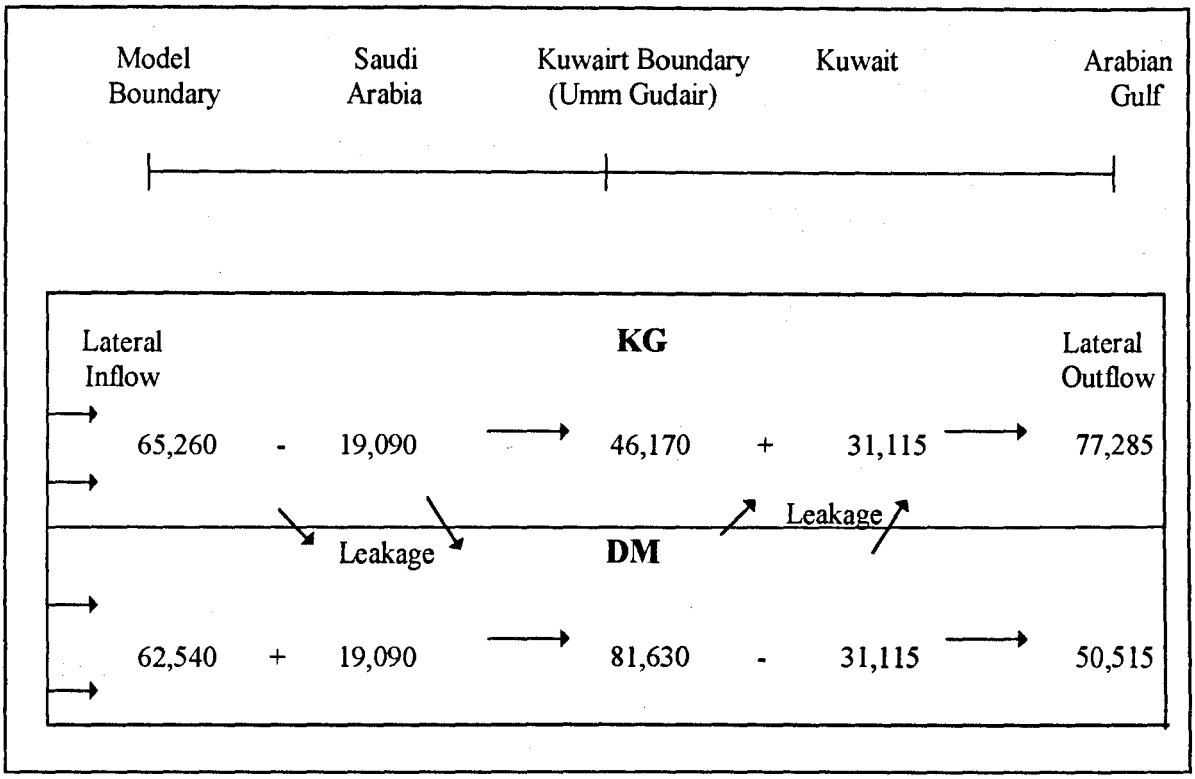


Figure 4.12: Sketch diagram showing simulated volume of the aquifer system mass balance at different points located in the direction of flow, in $m^3/d$.

### 4.2.5.2 TRANSIENT CALIBRATION

The transient calibration of the model consisted of the reconstruction of the abstraction history in Kuwait from 1960 to 1996, in order to reproduce the observed potentiometric head distribution during that period. The transient calibration was run for a total of 36 years, divided into 72 stress periods.

In water wellfields, a peak and trough can be recognised over a one-year period in the hydrographs of the observation wells, due to the seasonal fluctuations (summer/winter) in the production rates as shown in Figure 3.19. So stress periods of six months duration were accordingly chosen for model calibration. The seasonal groundwater abstraction rate from the aquifers at each wellfield (as presented in Table 3.6) were averaged separately over one stress period and distributed uniformly over the concerned grids. Summer period is taken from May to October and Winter period from November to April. Further discretization for the stress periods into smaller time units (time step) was done.

It is desirable to use small time steps, so that the numerical representation better approximates the partial differential equation (Anderson and Woessner, 1992). However, it is usually impractical to use extremely small time steps, a good order of magnitude for the initial time step size is the critical time step ($\Delta t_c$) allowed for an explicit formulation of the governing equation (De Marsily, 1986). This critical time step can be calculated as, (Anderson and Woessner, 1992) :

$$t_c = \frac{Sa^2}{4T} \qquad (4.4)$$

where, S is the storage coefficient, "a" the size of the grid ($a = \Delta x = \Delta y$), and T the transmissivity.

The minimum value for $\Delta t_c$ was calculated using the following:

| | |
|---|---|
| Storage coefficient: | S minimum = $10^{-4}$ |
| Size of a grid: | "a" minimum = 2000m |
| Transmissivity: | T maximum = 1000 $m^2/d$ |

The calculated initial time step (0.1 day) was used at the beginning of the simulation and was increased by a geometric progression of ratio 1.4 (which is suggested by De Marsily, 1986, to be a good choice). Also, the time step size was reduced again at all times during the simulation when a new withdrawal stress was imposed on the system. Table 4.2 shows the calculated time steps within one stress period.

| No. | Duration (day) | Elapsed Time (days) |
|---|---|---|
| 1 | 0.10 | 0.10 |
| 2 | 0.15 | 0.25 |
| 3 | 0.17 | 0.43 |
| 4 | 0.17 | 0.60 |
| 5 | 0.22 | 0.84 |
| 6 | 0.33 | 1.17 |
| 7 | 0.47 | 1.64 |
| 8 | 0.66 | 2.30 |
| 9 | 0.92 | 3.22 |
| 10 | 1.28 | 4.50 |
| 11 | 1.80 | 6.30 |
| 12 | 2.53 | 8.83 |
| 13 | 3.80 | 12.36 |
| 14 | 4.95 | 17.31 |
| 15 | 6.92 | 24.23 |
| 16 | 9.70 | 33.93 |
| 17 | 13.57 | 47.50 |
| 18 | 19.0 | 66.5 |
| 19 | 26.61 | 93.11 |
| 20 | 37.24 | 130.35 |
| 21 | 52.15 | 182.5 |

Table 4.2: Calculation time steps within one stress period.

The pumping from the wellfields can be from wells penetrating KG or DM aquifers separately, or from dual-wells which penetrate both aquifers. That is, the pumping rate from the multilayer well must be apportioned among the individual aquifers. The pumping rate for each aquifer can be approximately calculated as (McDonald and Harbaugh, 1988):

$$Q_{i,j,k} = T_{i,j,k}\left(\frac{Q_{WT}}{\Sigma T_{i,j,k}}\right) \qquad (4.5)$$

Where ;

$Q_{i,j,k}$ pumping rate from individual aquifer,

$Q_{WT}$ total pumping rate from the dual-well,

$T_{i,j,k}$ transmissivity for each aquifer individually, and

$\Sigma T_{i,j,k}$ total transmissivity for all the penetrated aquifers.

Actually, Equation 4.5 is an approximation, because it relates the pumping rate from each aquifer as a function of its transmissivity only, thereby ignoring the effect of the aquifer head on the pumping rate; however this is a necessary simplification since this head is initially unknown and needs to be calculated during the simulation (Anderson and Woessner, 1992). Generally, conventional finite difference codes do not recognise that a well that penetrates more than one aquifer layer or that it forms a pathway for water movement between layers. Consequently, the head in a multiaquifer well is a composite average of the heads in all the layers it penetrates (Papadopulos, 1966). The MODFLOW well package does not simulate the effects of multiaquifer wells, (which means the total pumping rates form dual-wells can be separated approximately between the two pumped aquifers (i.e. KG and DM) using equation 4.5, and place two separate wells in the same node, one in the KG aquifer and one in the DM aquifer). In Kuwait, the Shigaya -A, Shigaya E, and Umm Gudair water wellfields are the ones which have dual-wells penetrating the KG and the DM aquifers. Table 4.3, illustrates the average transmissivity for the wellfields and the contribution percentage of each aquifer if both aquifers are pumped from the same well.

| Water wellfield | **Shigaya A** | **Shigaya E** | **Umm Gudair** |
|---|---|---|---|
| Average transm. of KG ($m^2/d$) | 170 | 338 | 460 |
| Average transm. of DM ($m^2/d$) | 198 | 99 | 570 |
| Total transm. ($m^2/d$) | 368 | 437 | 1030 |
| Average % of pumping from KG | 46 | 77 | 44 |
| Average % of pumping from DM | 54 | 23 | 56 |

Table 4.3: The average transmissivities of the aquifers at the wellfields having dual-wells, and the percentage of groundwater contribution for each aquifer to the pumping of these wells.

Before starting the transient calibration, the constant head boundary at the up-gradient boundary (south-west and south of Kuwait) applied during the steady state simulation, was replaced by nodes that have a head-dependent flux to allow the fluctuation of the heads at the boundary under stressed conditions. This could be made by assuming that beyond each boundary node there exists a fixed point where the head in the aquifer does not change (Wilson and Gerhart, 1982). These conditions were simulated by using the General-Head Boundary (GHB) Package that has the similar concept to the Drain and River Packages (in

the MODFLOW model). Flow ($Q_b$) through the boundary is calculated as the product of the conductance of the boundary ($C_b$) and the difference between the head ($H_b$) at the fixed point and in the aquifer boundary ($H$), where flow into the model area is controlled by the following equation (Anderson and Woessner, 1992):

$$Q_b = C_b(H_b - H) \qquad (4.6)$$

where:

$Q_b$ : flow rate at which the water is supplied to the model boundary cell from the boundary b ($L^3/T$);

$C_b$ : conductance of the aquifer between the constant head at the fixed point and the model boundary cell ($L^2/T$);

$H_b$ : head at the fixed point source (L); and

$H$ : head at the model boundary cell.

In order to apply this option to the model, it is required to input both the head at the fixed point and the conductance between the model boundary cell and that point. The fixed point where the head in the aquifer does not change was selected at a distance corresponding to potentiometric elevations of about 250 m amsl for both aquifers. The conductance was calculated for each node inversely from equation 4.6 by using the constant head inflow rate ($Q_b$) as obtained from the steady state calibration, whereas the head at the model boundary cells ($H$) was taken equal to the aquifers initial heads (at the constant-head boundaries). The conductance ($C_b$) for GHB cells was found to range from 10 to 16 $m^2/d$ for the KG aquifer, and from 5 to 25 $m^2/d$ for the DM aquifer.

The simulated potentiometric heads at the end of the steady state simulation for KG and DM aquifers were taken as input for starting heads at the beginning of the transient calibration, and further adjustment in the computed aquifer storage parameters were made during the calibration process.

As mentioned earlier in this section, storage coefficient and effective porosity values for aquifers in Kuwait are very rarely available, so during the transient calibration, a trial and error adjustment for these two parameters was done using an assumed range of values. Based on the recorded values for the aquifers specific storage (presented in Table 3.3), the specific storage values for the model calibration use were assumed to range from $1x10^{-6}$ to $1x10^{-3}$ to for the KG aquifer, and from $1x10^{-7}$ to $1x10^{-4}$ $m^{-1}$ for the DM aquifer. The effective porosity was assumed to range from 0.05 to 0.2 as the possible upper and lower limits for both aquifers.

Figure 3.16, which displays a contour map of the observed total drawdown in potentiometric head in the DM aquifer to the year 1990, and the observed potentiometric head contour map at year 1988 for the KG aquifer (Fig. 3.13) were used as controlling factors in the evaluation of transient calibration results. The drawdown map was prepared with hand contouring because unrealistic patterns of drawdown were produced when SURFER kriging was utilised for contouring. In addition, a comparison between the head-time plots for the fluctuation in the observed and the simulated heads at the observation wells were used to assess the transient calibration results.

During the transient calibration, the simulation results were visually checked against these maps and water level hydrographs, and calibration was ended when satisfactory matching between the simulated and the observed post-development potentiometric levels (i.e. between the observed and simulated drawdowns) was obtained. After several runs with different specific storage and porosity values for both aquifers, an acceptable match was achieved.

For the KG aquifer, the calibrated specific storage was found to range from $1x10^{-5}$ $m^{-1}$, and $1x10^{-6}$ $m^{-1}$ for the DM aquifer. The calibrated porosity for the KG aquifer was found to be 0.07. The low porosity for the KG aquifer may refer to its poor sorting, resulting from the presence of silt and fine cementing materials, such as calcrete. The calibrated porosity for the DM aquifer was found to be 0.1.

Figure 4.13, shows the simulated drawdown in the DM potentiometric head to 1990, which reflects the degree of the achieved matching (if it is compared with the observed total drawdown for the same year presented previously in Figure 3.16). Moreover, Figure 4.14, shows the simulated potentiometric water levels for the KG aquifer at 1988 Vs the observed ones.

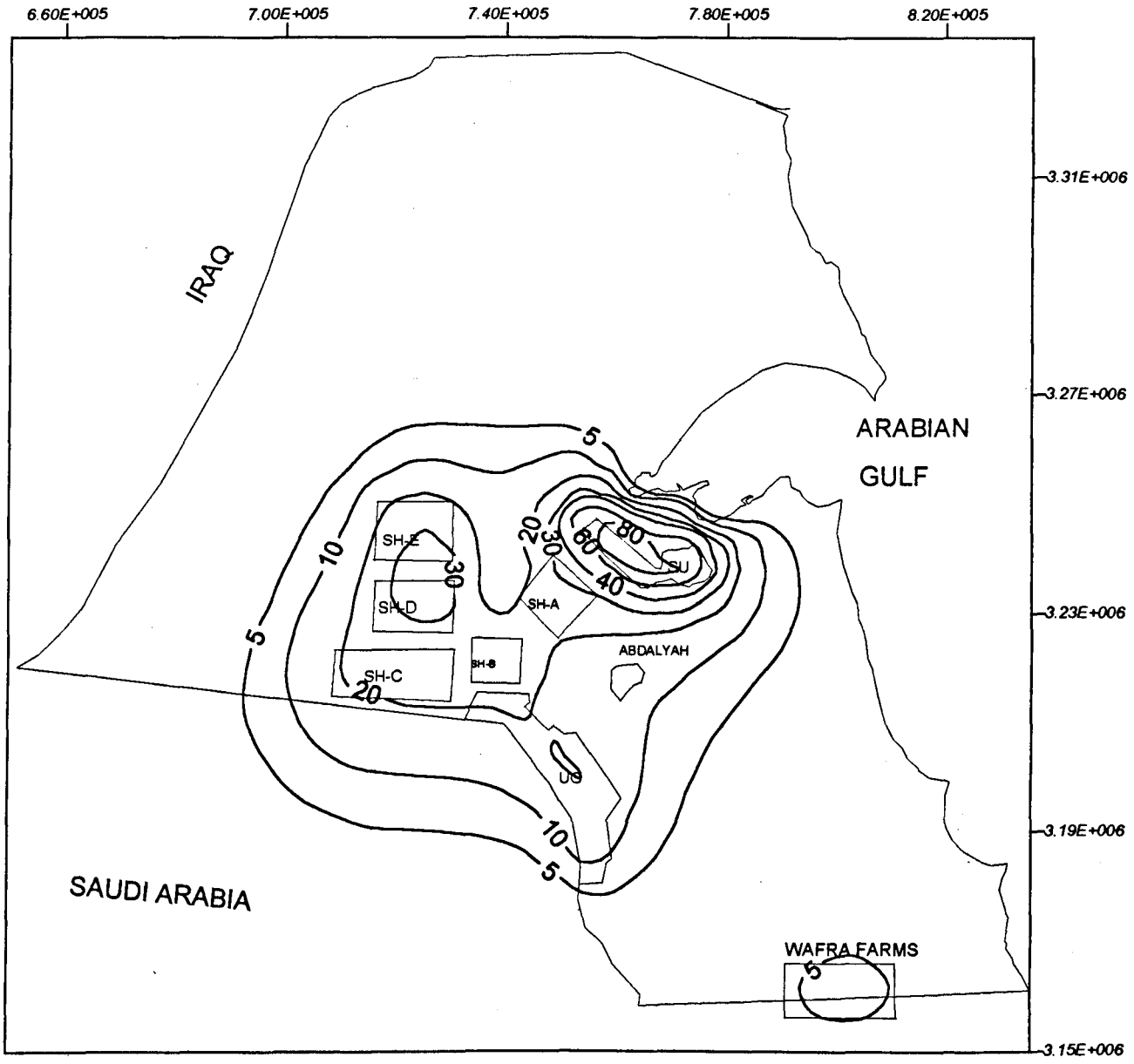


Figure 4.13: Simulated total drawdown in potentiometric head of the Dammam aquifer to 1990, m.

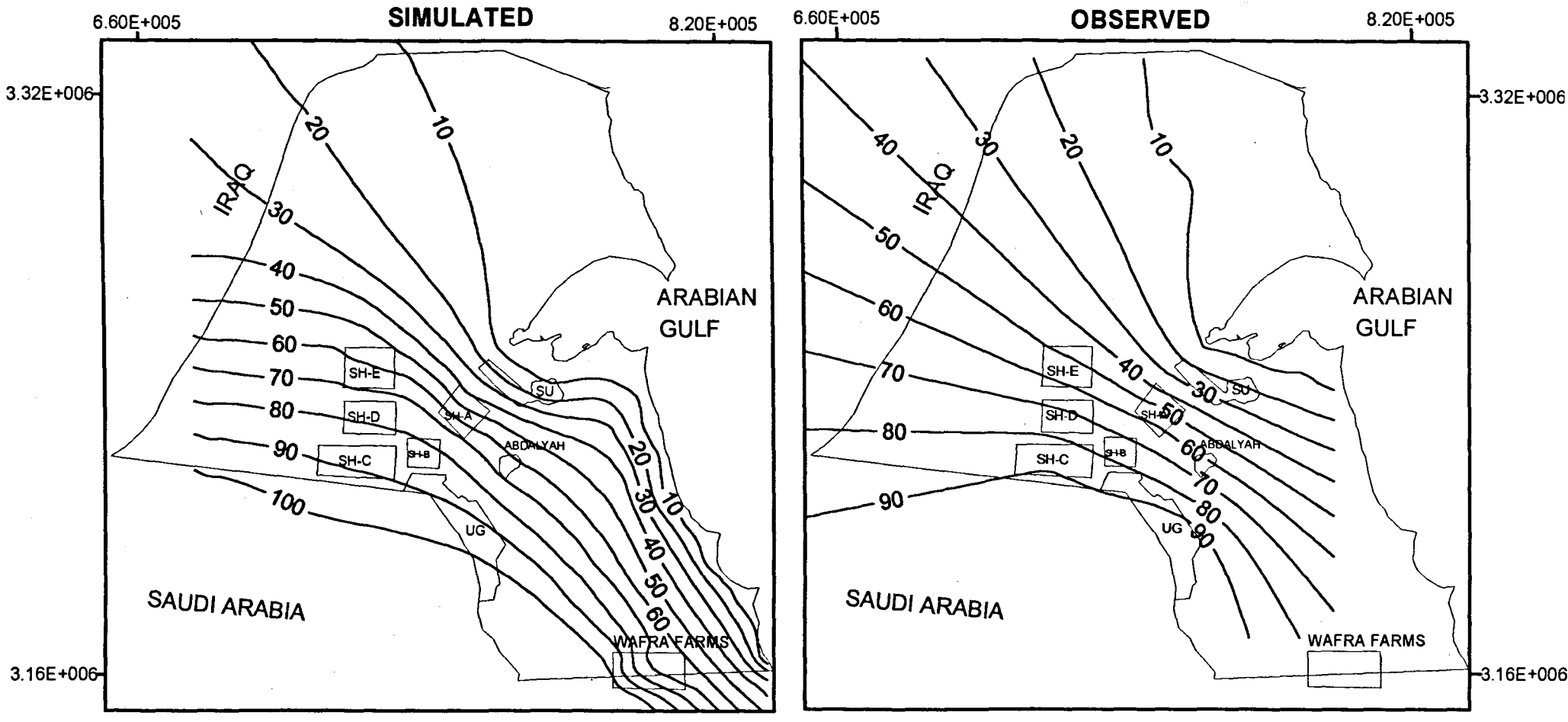


Figure 4.14: Simulated Vs observed water level maps for the Kuwait Group aquifer at 1988, m amsl.

The achieved matches between the observed and the simulated water levels at the end of transient calibration are presented in hydrograph plots showing the fluctuations in the simulated and observed water levels at selected observation wells tapping the DM aquifer (Figure 4.15).

Figures (4.16 a, b, c, d, and e), and Figures (4.17 a ,b ,c ,d, and e), are the simulated potentiometric level maps for the KG and the DM aquifers, respectively, for a number of stress periods selected at seven year intervals to show the historical development in the potentiometric heads of the aquifers resulting from the abstraction process.

Figures (4.16 a, b, c, d, and e) indicate a moderate general drop in the water level of the KG aquifer increasing with time at most of the areas. However, as shown in Figure 4.18, which displays the simulated KG potentiometric levels and the produced total drawdown at the last stress period (denoting the present situation of the aquifer), four cones of depression can be identified. The major decline (25m) resulting from pumping the KG aquifer only is observed at the Al-Wafra farms area. At the Sulaibiya wellfield another cone has been created with about 20 m drawdown, where the pumping is from the DM aquifer only. This indicates that the KG aquifer contributes to the water pumped from the DM aquifer by a vertical leakage due to the increase in the vertical hydraulic gradient between the two aquifers at this locality. Another two significant cones are developed at Shigaya-E and Umm Gudair with about 15 m decline, where both the KG and DM aquifers are pumped at these locations.

Figures (4.17 a, b, c, d, and e), and Figure 4.19, which exhibits the simulated total drawdown in the potentiometric head of the DM aquifer at the last stress period (1995), indicate the accelerated development in the decline of the aquifer potentiometric heads due to the increase in groundwater abstraction from year to year, and hence the establishment of new wellfields. A significant cone of depression reaching 80 m drawdown was developed early at the Sulaibiya wellfield in 1967, since it was the only existing wellfield at that time.

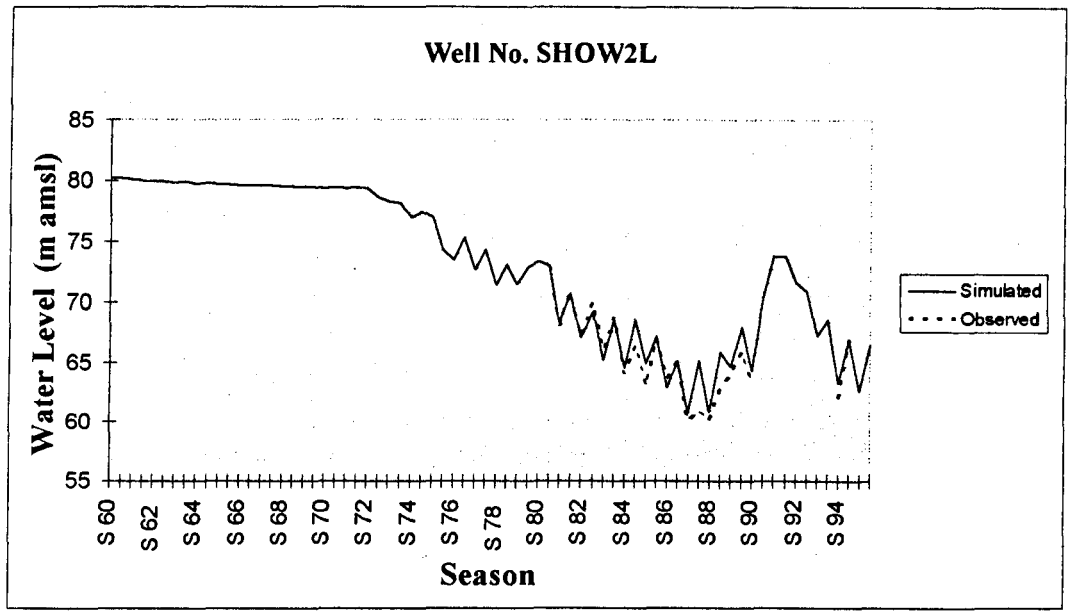


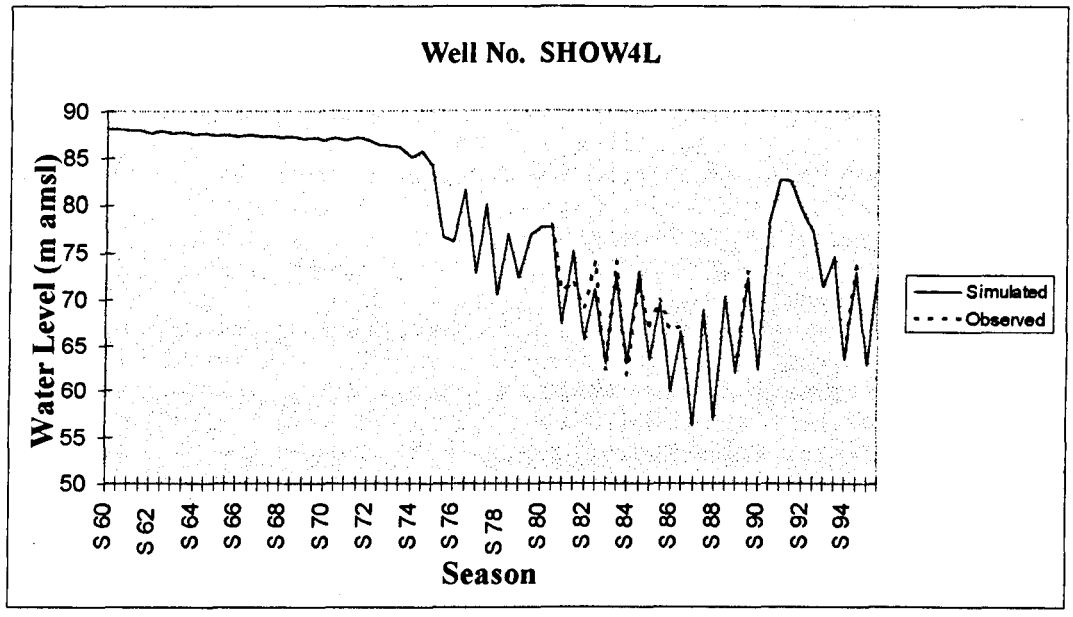


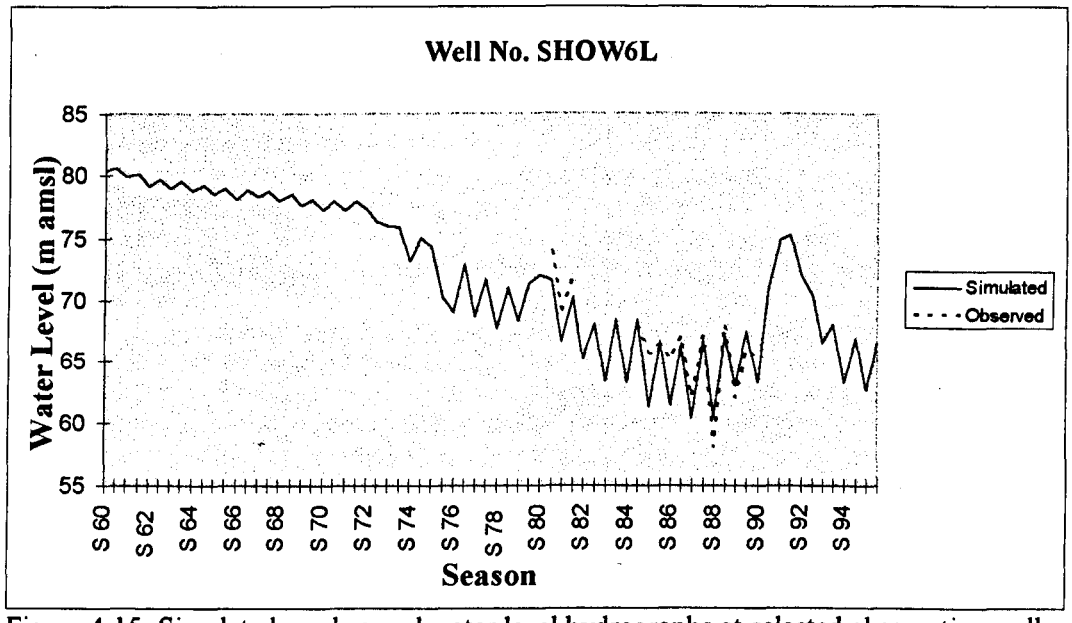


Figure 4.15: Simulated vs observed water level hydrographs at selected observation wells tapping the Dammam aquifer (DM), m amsl.

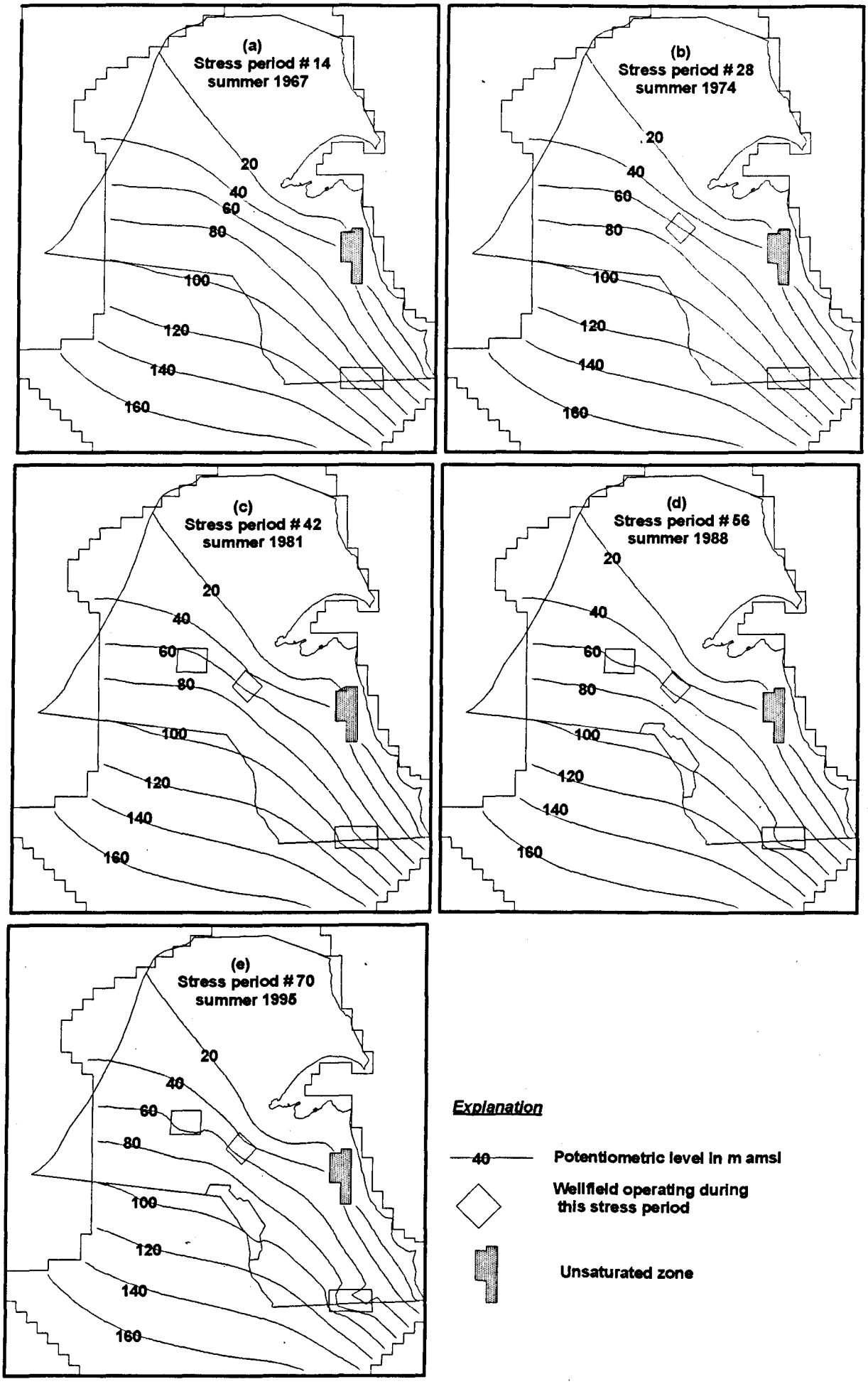


Figure 4.16: Simulated water level of the KG aquifer at the end of selected stress periods ( 7 years interval) of the transient condition.

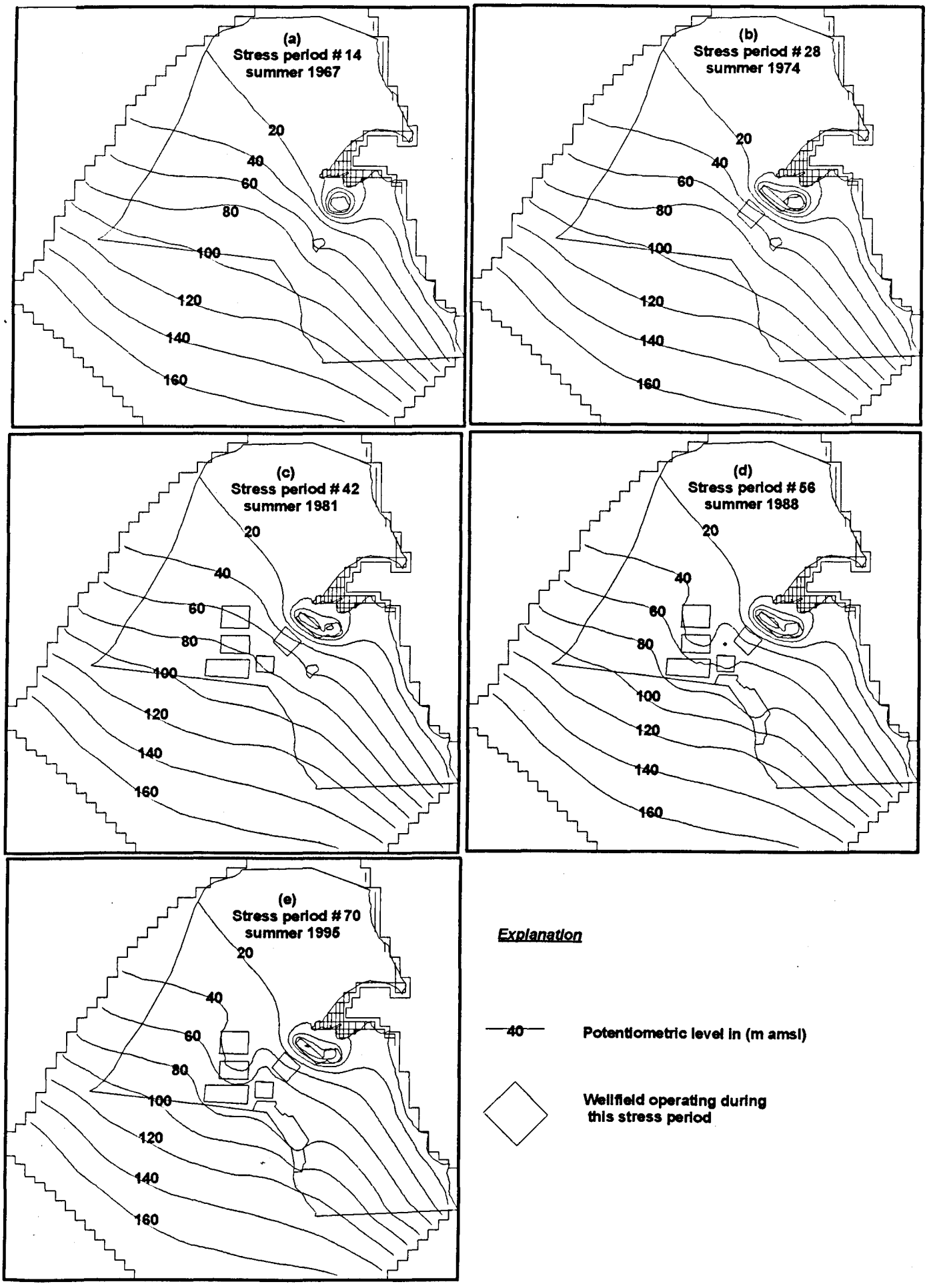


Figure 4.17: Simulated potentiometric heads of the DM aquifer at the end of selected stress periods (7 years interval) of the transient condition.

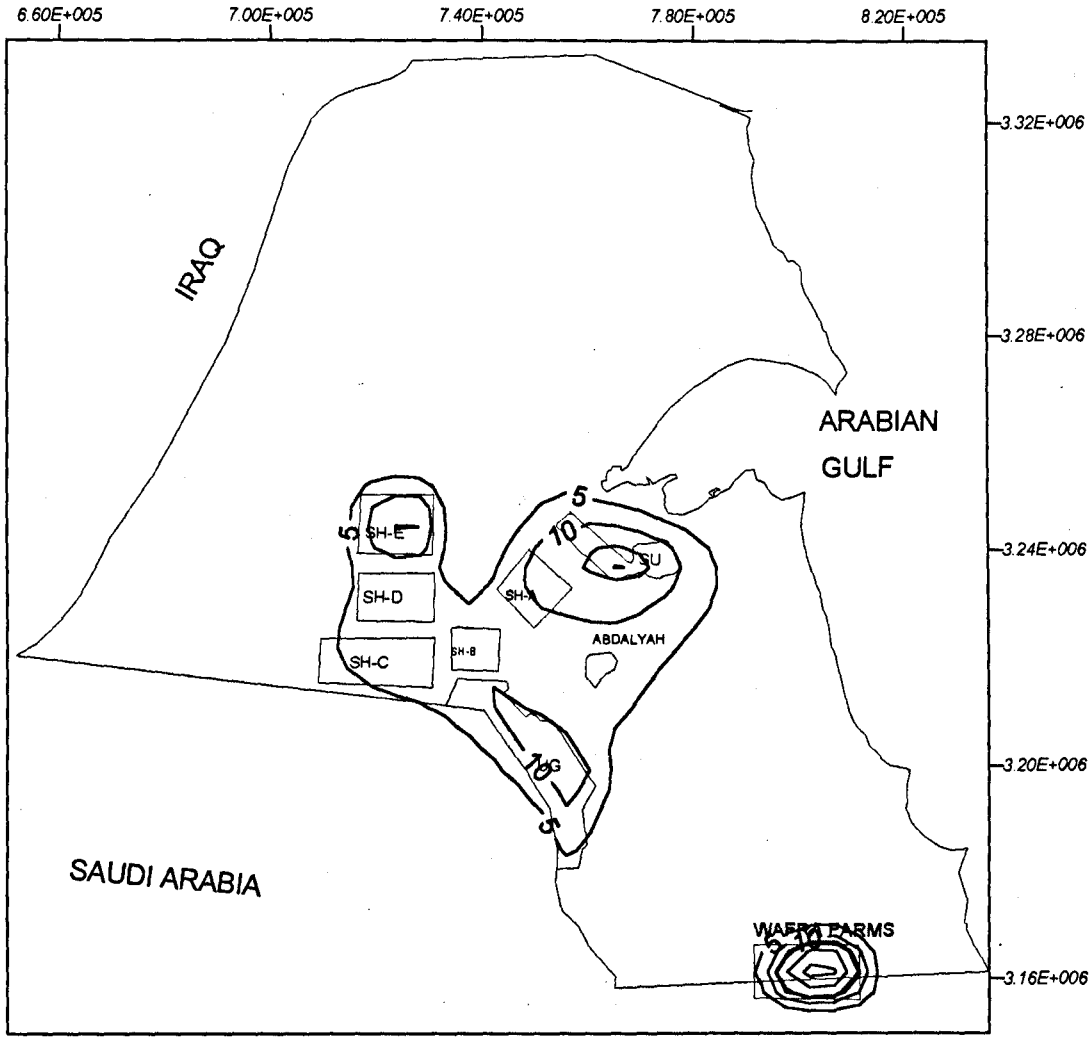


Figure 4.18: Simulated total drawdown in the Kuwait Group (KG) aquifer water level to 1995, m.

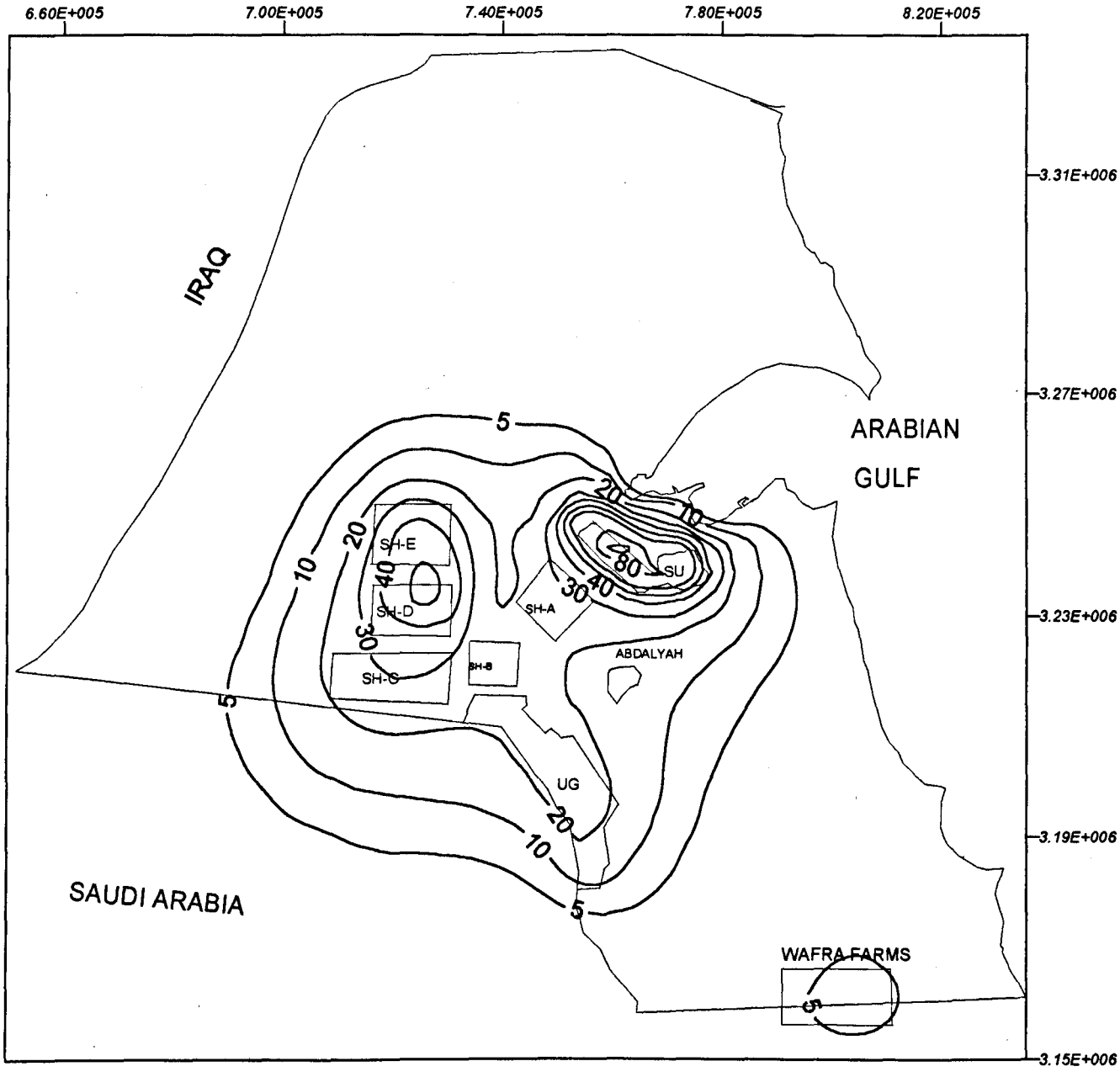


Figure 4.19: Simulated total drawdown in the Dammam aquifer potentiometric head to 1995, m.

However, the decline at this location is still approximately at the same level since that time even after the extension of the field at 1972, which suggests that the aquifer is probably attaining a pseudo-steady-state condition at this site. Another major cone of depression developed in the early eighties with about 20 m decline in the central part of Shigaya, and it has expanded with time to reach about 50 m drop by the last stress period. At Umm Gudair, which started production most recently (1986), the potentiometric levels were influenced by the pumping from the nearby wellfields even before the production from Umm Gudair started. The declining levels at Umm Gudair are developing rapidly, reaching about 30 m drop by the last stress period.

In general, water level drop in the aquifer system in Kuwait is caused by the disturbance of the natural steady state balance between the system inflow and its outflows by the abstraction wellfields, where the outflow exceeds the inflow, leading to the use of aquifer system storage. Table 4.4 lists the computed mass balance components for the aquifer system as a whole and for each aquifer separately at selected intervals.

| Flow Component | Steady State | Selected Transient stress Periods | | | | | |
|---|---|---|---|---|---|---|---|
| | | SP # 12 Sum. 66 | SP # 24 Sum. 72 | SP # 36 Sum. 78 | SP # 48 Sum. 84 | SP # 60 Sum. 90 | SP # 72 Sum. 96 |
| | | | | | | | |
| **KG** | | | | | | | |
| | | | | | | | |
| Storage in ** | 0 | 1.03 E+04 | 2.55 E+04 | 6.85 E+04 | 1.42 E+05 | 2.84 E+05 | 2.81 E+05 |
| Storage out ** | 0 | 0 | 0 | 0 | 0 | 0 | 0 |
| Leak. to DM | 1.9 E+04 | 6.45 E+04 | 7.44 E+04 | 8.59 E+05 | 1.05 E+05 | 1.31 E+05 | 1.34 E+05 |
| Wells ( - ) | 0 | 1.42 E+03 | 4.14 E+04 | 3.12 E+04 | 8.36 E+04 | 2.05 E+05 | 2.0 E+05 |
| Const. h. in* | 6.52 E+04 | 6.52 E+04 | 6.52 E+04 | 6.52 E+04 | 6.52 E+05 | 6.52 E+04 | 6.52 E+04 |
| Const. h. out | 7.73 E+04 | 7.58 E+04 | 7.40 E+04 | 7.24 E+04 | 7.09 E+04 | 6.89 E+04 | 6.67 E+04 |
| Total KG in | 9.63 E+04 | 1.48 E+05 | 1.60 E+05 | 1.98 E+05 | 2.69 E+05 | 4.15 E+05 | 4.13 E+05 |
| | | | | | | | |
| | | | | | | | |
| **DM** | | | | | | | |
| | | | | | | | |
| Storage in | 0 | 4.87 E+04 | 7.41 E+04 | 1.17 E+05 | 1.72 E+05 | 1.52 E+05 | 1.64 E+05 |
| Storage out | 0 | 0 | 0 | 0 | 0 | 0 | 0 |
| Leak. to KG | 3.11 E+04 | 6.76 E+04 | 6.47 E+04 | 5.96 E+04 | 5.67 E+04 | 6.00 E+04 | 6.18 E+04 |
| Wells ( - ) | 0 | 5.81 E+04 | 9.76 E+04 | 1.58 E+05 | 2.38 E+05 | 2.26 E+05 | 2.56 E+05 |
| Const. h. in* | 6.25 E+04 | 6.25 E+04 | 6.25 E+04 | 6.25 E+04 | 6.25 E+04 | 6.25 E+04 | 6.25 E+04 |
| Const. h. out | 5.05 E+04 | 4.92 E+04 | 4.76 E+04 | 4.54 E+04 | 4.32 E+04 | 4.18 E+04 | 4.07 E+04 |
| Total DM in | 8.15 E+04 | 1.76 E+05 | 2.12 E+05 | 2.68 E+05 | 3.41 E+05 | 3.48 E+05 | 3.64 E+05 |
| | | | | | | | |
| | | | | | | | |
| **DOMAIN** | | | | | | | |
| | | | | | | | |
| Storage in | 0 | 5.9 E+04 | 9.97 E+04 | 1.86 E+05 | 3.14 E+05 | 4.37 E+05 | 4.46 E+05 |
| Storage out | 0 | 0 | 0 | 0 | 0 | 0 | 0 |
| Wells (- ) | 0 | 5.93 E+04 | 1.02 E+05 | 1.91 E+05 | 3.21 E+05 | 4.30 E+05 | 4.56 E+05 |
| Const. h. in* | 1.27 E+05 | 1.27 E+05 | 1.27 E+05 | 1.27 E+05 | 1.27 E+05 | 1.27 E+05 | 1.27 E+05 |
| Const. h. out | 1.27 E+05 | 1.25 E+05 | 1.21 E+05 | 1.17 E+05 | 1.14 E+05 | 1.10 E+05 | 1.07 E+05 |
| Total IN | 1.77 E+05 | 3.25 E+05 | 3.72 E+05 | 4.66 E+05 | 6.10 E+05 | 7.63 E+05 | 7.77 E+05 |
| | | | | | | | |
| | | | | | | | |
| **Discrepancy %** | 0.01 | 0.00 | 0.00 | -0.01 | 0.00 | 0.00 | -0.01 |

Table 4.4: Mass balance results for Kuwait aquifer system, in $m^3$/day, (Sum. : Summer).

Note: * nodes converted to general head boundary (GHB) during transient calibration.
** (Storage in) means that water is taken out from the aquifer storage, and (Storage out) means that water is added to the aquifer storage.

The table indicates that the inflow rates to the system was constant at 127,000 $m^3/d$ during steady state condition and the transient condition. However, the outflow from the system to the down-gradient boundary has been slightly reduced from about 127,000 $m^3/d$ before abstraction to about 107,000 $m^3/d$ due to the diversion of flow from these boundaries by the abstracting wellfields.

In addition, the table shows that the water taken from aquifer storage was increased from about 59,000 $m^3/d$ at summer 1966 (stress period no. 12) to about 446,000 $m^3/d$ at the last stress period in Summer 1996. It has been found that this exploitation is proportional to the increase in pumping rate from the aquifer system which was increased constantly from about 59,000 $m^3/d$ at the first stress period (winter 1960) to reach 456,000 $m^3/d$ at the last stress period (summer 1996). The production rates from DM and KG aquifers are 134,000 and 256,000 $m^3/d$, respectively at the last stress period, which show that the DM aquifer is pumped at a higher rate than KG aquifer. Conversely, the volume of water taken from the aquifers storage during the transient condition, appears to be higher from the KG aquifer than what is taken from the DM aquifer. The extraction from the groundwater storage of the KG aquifer was extensively increased from about 10,000 $m^3/d$ at the year 1966 to about 281,000 $m^3/d$ at year 1996,while the extracted rate from the DM aquifer storage increased gradually from about 48,000 $m^3/d$ at 1966 to 164,000 $m^3/d$ at the year 1996.

This phenomenon can be understood if it is related to the influence of vertical leakage between the two aquifers. The simulated vertical leakage rate between the aquifers, indicates that part of the pumped water from DM aquifer is coming from KG aquifer; this leakage has been increased from 19,000 $m^3/d$ during steady state conditions, to about 134,000 $m^3/d$ in the final stress period. This indicate that the vertical flow was reversed from that during the steady state condition, to be from KG aquifer to DM aquifer. This is due to the building up of the vertical hydraulic gradient between the two aquifers created from the pumping of DM aquifer at a higher rate than KG aquifer, which confirms the above mentioned observation on its potentiometery at the abstraction locations.

However, at the locations which have not been influenced by any pumping, the vertical leakage remains the same as in the steady state condition, which is mainly from DM aquifer toward KG aquifer, where the potentiometric head in the DM aquifer still higher than the KG aquifer heads. Also, at the areas where the KG aquifer is the only pumped aquifer (such as Al-Wafra farms area), or at areas where dual-wells are used and the DM aquifer potentiometric head is higher (such as the Shigaya-E wellfield), the leakage is from the DM to the KG aquifer. Hence, the vertical leakage rate from the DM to the KG aquifer increased slightly due to the additional vertical leakage at these localities from about 31,000 $m^3/d$ at the steady state condition to about 61,000 $m^3/d$ at the last stress period.

### 4.2.6 MODEL VERIFICATION

The set of parameter values used during the calibration of the model may not accurately represent the actual field values due to the possible uncertainties which may be introduced in the course of calibration. Consequently, the model could be verified with another set of transient data different from what have been used during the calibration process. Verification of the model can be achieved when the verification targets are matched without changing the calibrated parameter values.

Unfortunately, as mentioned earlier, there is only one complete set of water level measurement data for the year 1988 for the KG aquifer which has been already used to calibrate the model. On the other hand, such transient data are available for the DM aquifer at serial intervals of time. As a result, the model was calibrated and verified for the DM layer, and calibrated only for the KG layer.

Figure 4.20, displays a satisfied matching between the simulated and the observed potentiometric head of the DM aquifer at 1995, which has been accomplished without changing the calibrated parameters of the model. In addition, this matching was exemplified in drawdown form in Figure 4.19 (which shows the simulated total drawdown in the potentiometric head of the DM to year 1995). This indicates reasonable verification if it is compared with Figure (3.17) which represents the total drawdown observed at the same year (1995).

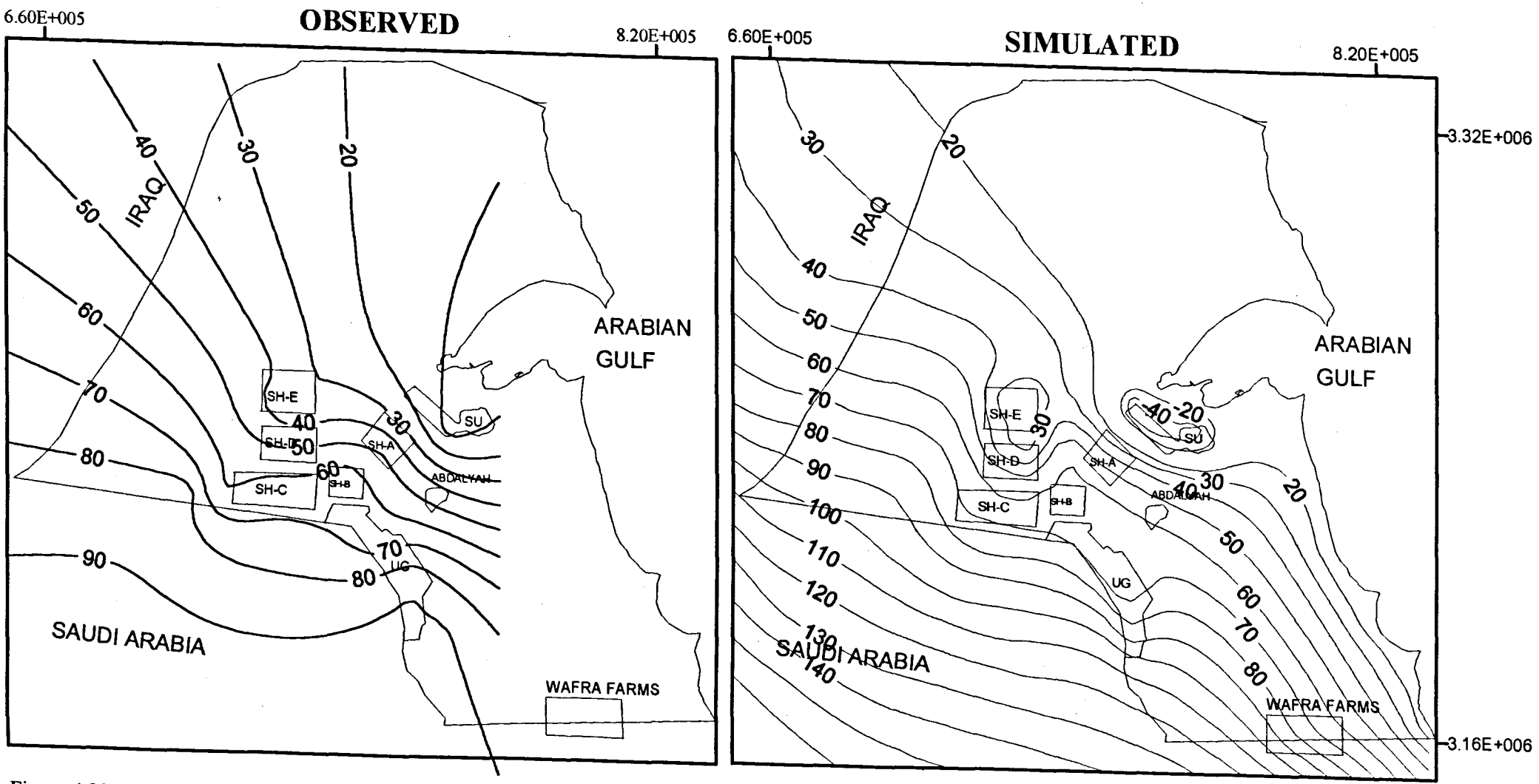


Figure 4.20: Simulated Vs observed potentiometric head of the DM Aquifer at 1995, m amsl.

### 4.2.7 PREDICTIVE SIMULATION

The Ministry of Electricity and Water (MEW) plans to increase groundwater production by expanding the existing wellfields, and by establishing new fields to meet the expected increase in groundwater demand.

The constructed regional flow model was used as a planning tool to predict and simulate the aquifer system behaviour in response to the possible future development of groundwater for the coming 15 years (1996-2010). Future development plans for the aquifer system in Kuwait consists of the construction and operation of new wellfields in addition to the existing ones. The simulated time was divided into 30 stress period, each for 6 months representing summer and winter seasons.

Three different scenarios were assigned, based on the feasibility of using the existing fields up to their maximum designed capacity. In addition to the possibility of constructing new water wellfields which have distinct priorities in the proposed development. Table 4.5, illustrates the possible wellfield operation schedule for different scenario runs, and their planned production capacity.

| Field | Scenario 1<br>Present development | Scenario 2<br>Controlled development | Scenario 3<br>Intensive development |
|---|---|---|---|
| **1- Existing fields** | Production from all fields increases with 5 % yearly up to their maximum capacity, reached in 2005.<br>Then production constant from 2005-2010 | As in Scenario 1 | As in Scenario 1 |
| **2- New fields** | | | |
| Umm Gudair (extension) | _ | Pumping rate = 60,000 $m^3/d$ (starting in 1995) | As in Scenario 2 |
| Shigaya-F | _ | Pumping rate = 40,000 $m^3/d$ (starting in 1995) | As in Scenario 2 |
| Atraf | _ | Pumping rate = 26,000 $m^3/d$ (starting in 1995) | As in Scenario 2 |
| Kabad | _ | Pumping rate = 60,000 $m^3/d$ (starting in 1995) | As in Scenario 2 |
| NW Shigaya | _ | Pumping rate = 70,000 $m^3/d$ (starting in 2005) | As in Scenario 2 |
| Area 3 | _ | _ | Pumping rate = 27,000 $m^3/d$ (starting in 2000) |
| Area 4 | _ | _ | Pumping rate = 22,000 $m^3/d$ (starting in 2001) |
| Area 5 | _ | _ | Pumping rate = 27,000 $m^3/d$ (starting in 2002) |
| Area 6 | _ | _ | Pumping rate = 27,000 $m^3/d$ (starting in 2003) |
| Area 7 | _ | _ | Pumping rate = 40,000 $m^3/d$ (starting in 2005) |

Table 4.5: Wellfield operation schedule for different development scenarios.

Figures 4.21, 4.22, and 4.23, display the simulated potentiometric heads by the year 2010 for the KG and DM aquifers, respectively, under the three scenarios. The results for Scenario 1 (present development) indicate that the current decline in the two aquifers heads will continue at the current cones of depression, to reach maximum declines of more than 35 m and 100 m for the KG and DM aquifers, respectively (Fig. 4.21).

The results for Scenario 2 (controlled development) indicate that in addition to the existing cones of depression, new ones will be created. At the newly introduced cones of depression, the decline in the potentiometric head is much higher in the DM aquifer than the KG aquifer, especially at the NW Shigaya wellfield, where the maximum declines of 20 m and 70 m at the KG and DM aquifers were simulated at this locality, respectively. The decline at the current cones of depression will spread out hugely for the DM aquifer heads

to reach 80 m, 70 m, and 140 m at the Shigaya-E, Umm Gudair, and Sulaibiya wellfields, respectively (Fig. 4.22).

Under intensive development (Scenario 3), conditions are similar to Scenario 2, but the declines are greater, reaching maximum drawdowns of 50 m and 160 m for the KG and DM aquifers, respectively. The potentiometric head of DM aquifer drops below the mean sea level in the central part of Kuwait (Fig. 4.23) and in the Jahra area, raising the possibility of upconing of more saline water in central Kuwait and invasion of sea water in the coastal areas. Also, the DM aquifer becomes unconfined at Shigaya-E, and Shigaya-D, where its potentiometric head drop below its top. Dewatering of the KG aquifer in the eastern part of Umm Gudair area was also indicated by the model for scenario 3.

In brief, the present and the expected future groundwater abstraction from aquifers in Kuwait is extensively exceeding the lateral recharge of the aquifer system which will lead to a continuation of the declining potentiometric heads. This will induce undesirable effects such as up-coning of deep saline waters and most probably the intrusion of sea water at the coastal areas that will deteriorate the groundwater quality. Also, some production wells in the KG aquifer may be abandoned as the water level will be lowered below their installed screens (such as the Shigaya-E, and the northern east part of Umm Gudair wellfields). From model simulation using different groundwater abstraction rates, the sustainable yield under which the existing drawdown in water head can be maintained at its present level is approximately 250,000 $m^3/d$ from both aquifers (KG and DM).

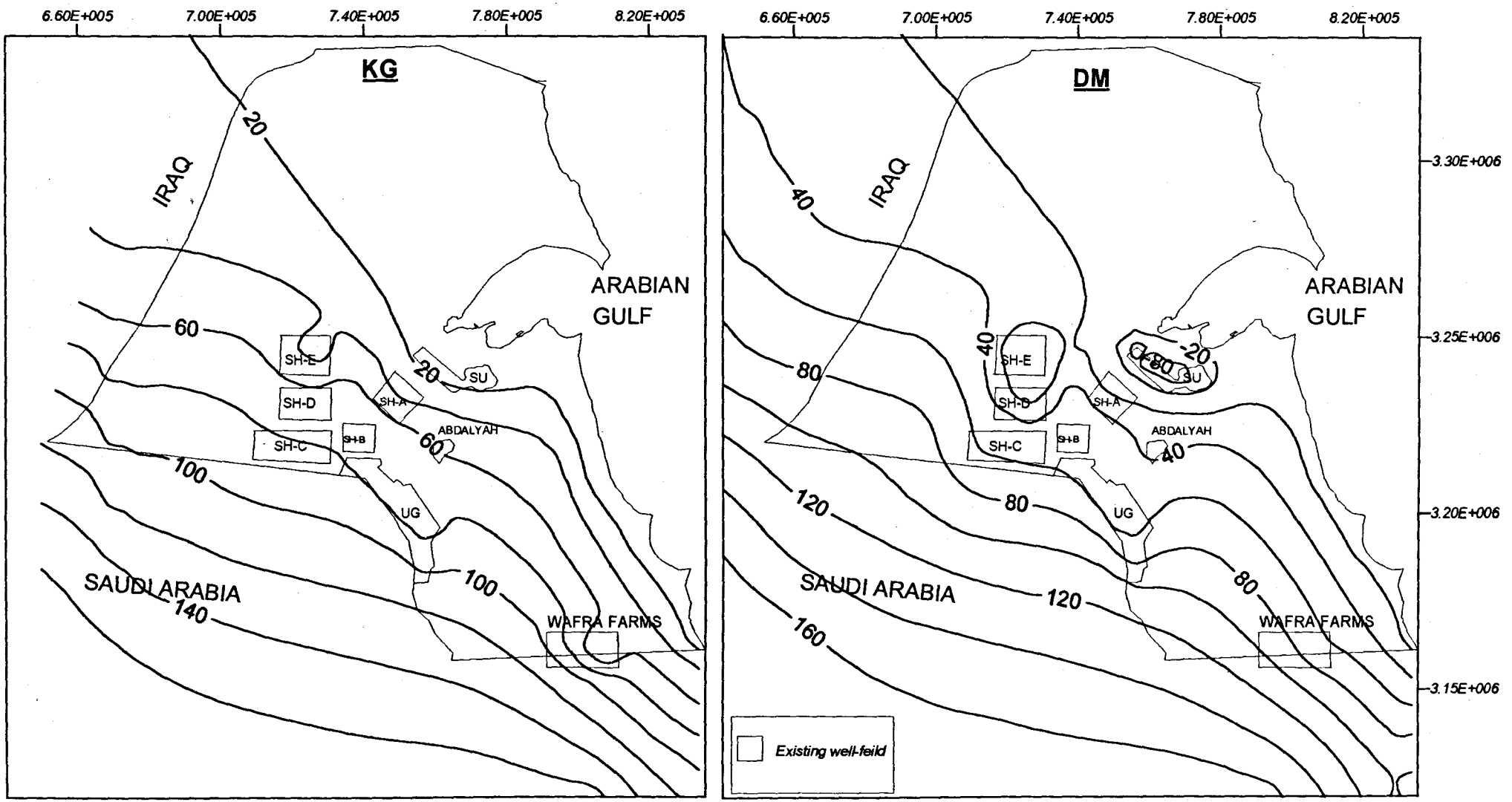


Figure 4.21: Simulated potentiometric head for the KG and DM aquifers by 2010 during Scenario 1 (present development)

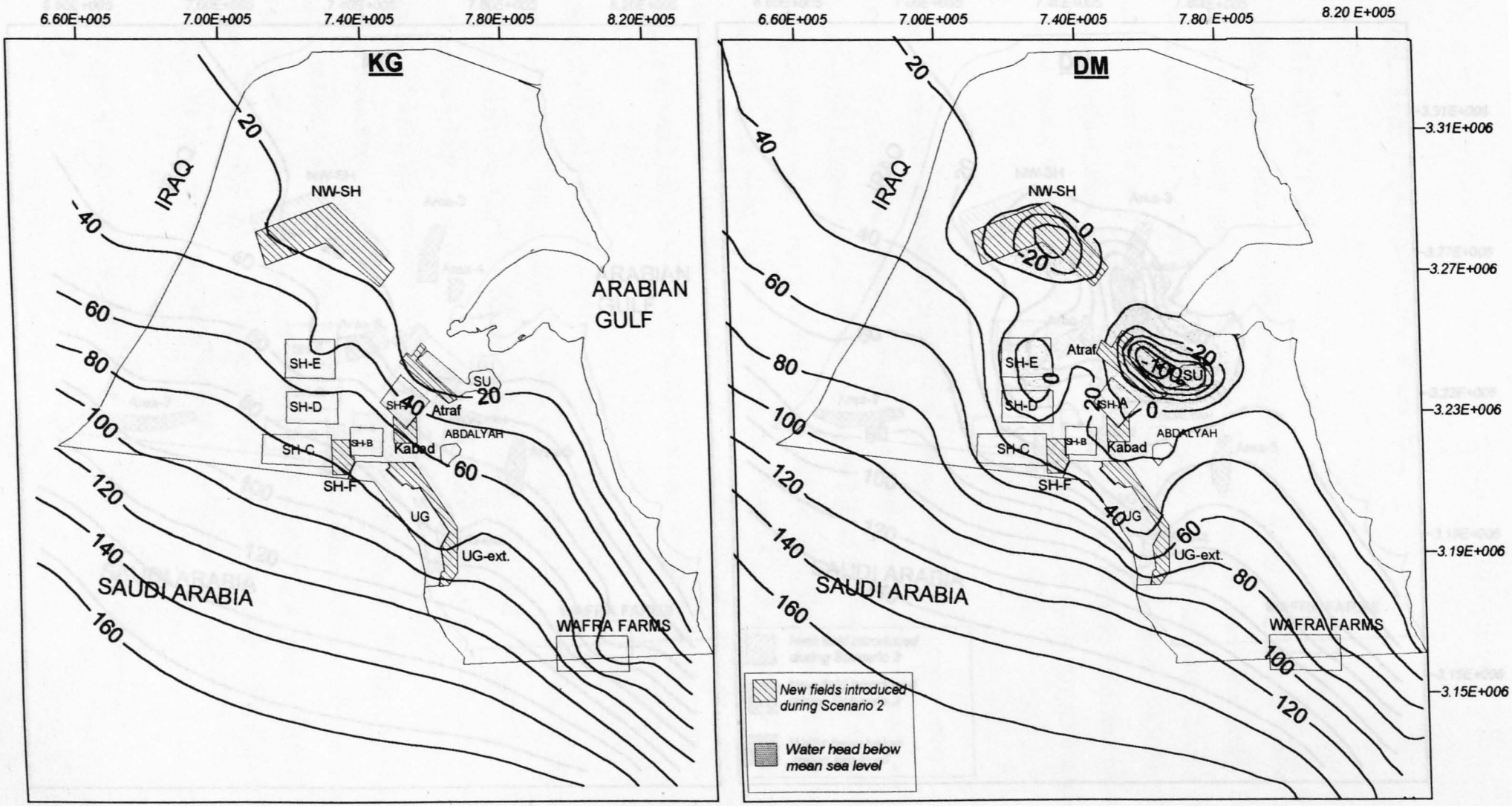


Figure 4.22: Simulated potentiometric head of the KG and DM aquifers by 2010 during Scenario 2 (controlled development), m amsl..

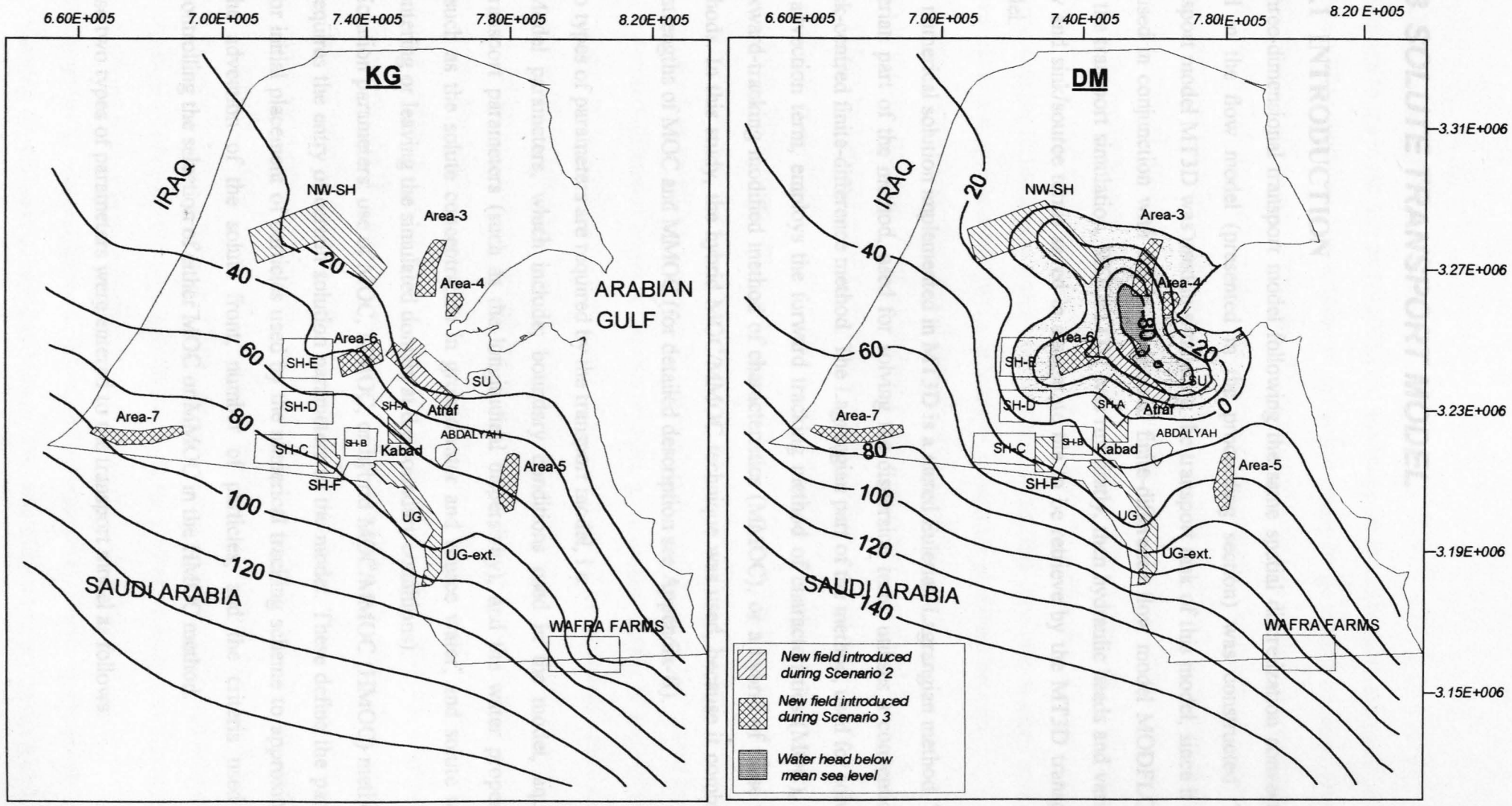


Figure 4.23: Simulated potentiometric head of the KG and DM aquifers by 2010 during Scenario 3 (intensive development), m amsl.

## 4.3 SOLUTE TRANSPORT MODEL

### 4.3.1 INTRODUCTION

A three-dimensional transport model following the same spatial discretization convection used in the flow model (presented in the proceeding section) was constructed. The transport model MT3D was used in simulating the transport task of this model, since it can be used in conjunction with the block-centred finite-difference flow model MODFLOW. For the transport simulation, MODFLOW was run firstly, then hydraulic heads and various flow and sink/source terms saved in a separate file to be retrieve by the MT3D transport model.

The numerical solution implemented in MT3D is a mixed Eulerian-Lagrangian method. The Eulerian part of the method, used for solving the dispersion term, utilises a conventional block-centred finite-difference method. The Lagrangian part of the method, used for solving the advection term, employs the forward tracking method of characteristics (MOC), and backward-tracking modified method of characteristics (MMOC), or a hybrid of these two methods. In this study, the hybrid MOC/MMOC technique was used, because it combines the strengths of MOC and MMOC (for detailed description see Appendix-II).

Two types of parameters are required by the transport model, i.e. :

1. Model parameters, which include; boundary conditions used in the model, aquifer transport parameters (such as the longitudinal dispersivity), and the water properties (such as the solute concentration in groundwater and source water, and solute mass entering or leaving the simulated domain at the boundary conditions).
2. Solution parameters: use of MOC, MMOC, or hybrid MOC/MMOC (HMOC) methods, requires the entry of certain solution parameters to the model. These define the pattern for initial placement of particles used by the numerical tracking scheme to approximate the advection of the solute front, number of particles, and the criteria used for controlling the selection of either MOC or MMOC in the HMOC method.

These two types of parameters were entered to the transport model as follows:

### 4.3.2 MODEL PARAMETERS

In addition to the saved files by MODFLOW, the transport model requires the input of:

1. Boundary conditions: The solution of the solute transport governing equation requires specification of boundary conditions. Three types of boundary conditions are considered in the MT3D transport model; (1) specified-concentration boundary, (2) specified concentration gradient, and (3) a combination of 1 and 2. The used boundary conditions in this regional transport model is the first type, that the concentration was specified along the model boundary and assumes to be unchanged throughout the simulation. This because the used model boundary is far enough from the well nodes that may introduce new changes to the groundwater concentration. Thus, this type of boundary condition will act as a source or sink of water entering or leaving the simulated domain.
2. Solutes concentration : That should be entered for the followings:
   a) Initial concentration of the groundwater. For this model, the Total Dissolved Solids (TDS) for the DM aquifer groundwater was assigned for the whole layer using the most recent isosalinity contour map for the aquifer (as in Figure 3.21). Whereas, such reliable TDS values are not available for the KG groundwater, where it is only available at some locations where the KG aquifer is utilised, otherwise its TDS was assumed to be higher than the DM groundwater TDS by 500 mg/l based on the observed difference between the two aquifers groundwater quality at the wellfields, where the two aquifers are operated. If water is pumped or artificially recharged to any wellfield, change in TDS of surrounding groundwater (at a distance > about 5000 m) will be very minor under the intended planning horizon (the maximum will be 10 years). Therefore, the uncertainty in assigning the TDS of KG aquifer groundwater at other areas in the model (excluding the simulated sites) will be insignificant. Moreover, the DM aquifer will be the only target aquifer for artificial groundwater recharge (reasons for selecting the aquifer will be explained later in Chapter 6), thus during the transport simulation, the changes in groundwater TDS will be mainly at this aquifer. Hence, if the DM aquifer is artificially recharged with freshwater, the influence of KG groundwater TDS in the simulated results will be through the vertical leakage which will be insignificant in changing the DM groundwater TDS, especially if the uncertainty in the KG groundwater will be + or - 500 mg/l.
   b) Groundwater concentration at the boundary conditions, which is the solute mass entering or leaving the simulated domain. This was assigned based on the initial TDS

of the DM aquifer, at the recharge (inflow) boundaries of the flow model, it is assigned as a source providing solute mass to the simulated domain, and at the discharge (outflow) boundaries of the flow model, it is assigned as a sink taking solute mass out of the simulated domain.

c) Water concentration at the source points, the concentration of the recharged water should be assigned at all the recharge wells during all the stress periods. In this study, where artificial groundwater recharge using injection wells need to be simulated, the TDS of the recharged water was assigned as 350 mg/l, that is the TDS of the potable water in Kuwait which could be available for artificial groundwater recharge practice. For sinks (abstraction wells), the concentration of sink water is generally equal to the concentration of groundwater in the aquifer and there is no need to specify it.

3. Dispersivity of the aquifers: The solute movement is strongly influenced by the heterogeneity of the aquifer that cause deviation from the average linear velocity, this deviation is defined by the hydrodynamic dispresion. A complete description for the solute transport in groundwater requires the consideration of hydrodynamic dispersion effects in addition to the advection. Hence, solving the solute transport governing equation (II-3, in Appendix-II) requires the determination of the hydrodynamic dispersion tensor which can be calculated using equation (II-7). The calculation of hydrodynamic dispersion tensor accordingly requires the input of the aquifers longitudinal dispersivity, and two transverse dispersivities (a horizontal and vertical transverse dispersivities). The value of longitudinal dispersivity needs to be entered directly to the model. whereas, the horizontal and vertical transverse dispersivities have to be assigned as ratios to the longitudinal dispersivity. Unfortunately, the dispersivity is not well identified for aquifers in Kuwait except the two dispersivity values which have been determined for the DM aquifer through a tracer injection/withdrawal field experiments at the Sulaibiya and Shigaya wellfields. Each of these tests was conducted for one month, yielding dispersivity values of 2.2 m (determined by this study, that will be explained in the next chapter) for the Sulaibiya wellfield, and 80 m (determined by Mukhopadhyay et al., 1994) for the Shigaya-C well field. Dispersivity values for other locations in the aquifer are not available. So, for the sake of comparing between the aquifer response for artificial groundwater recharge at selected locations, one dispersivity value was assigned for the aquifer at these sites, in order to eliminate the uncertainty due to variation of dispersivity between different sites. Dispersivity mainly

depends on the heterogeneity of the aquifer, and can be accurately estimated from tracers tests (Gelhar et al., 1985). Also, the accurate dispersivity estimation depends on the type, scale, and time of the tracer test (Gelhar et al., 1992). For the modelled aquifers, because there is a lack of such dispersivity field-estimated values, it was assumed that the dispersivity may follow the aquifer's transmissivity (because this is the only available relevant parameter for the aquifer). Since, Sulaibiya and Shigaya-C represent the lowest and the highest transmissivities of the DM aquifer, the DM dispersivity has also been assumed to be the lowest and the highest at these two fields. Hence, the dispersivity for the aquifer at other well fields was assumed to be equal to the average of the dispersivity at Sulaibiya and Shigaya-C, i.e. 41 m. The same ratios (0.1) and (0.05) which are suggested by the MT3D model were used in relating the horizontal and vertical transverse dispersivities ($\alpha_{TV}$ and $\alpha_{TH}$) to the longitudinal dispersivity ($\alpha_L$), respectively, which means that the standard isotropic dispersion model will be used in the solution.

### 4.3.3 SOLUTION PARAMETERS

In order to run the transport model, a number of solution parameters need to be entered to the model. The selection of these parameters will affecting the solution stability, and the maximum allowed step size required for the solution. The accuracy and stability of the applied solution should be assesses with the mass balance error. A mass budget is calculated by the model at the end of each transport step and accumulated to provide summarised information on the total mass into or out of the groundwater flow system, as:

$$\text{Error} = \frac{100\ (\text{IN} - \text{OUT})}{(\text{IN} + \text{OUT})/2} \qquad (4.7)$$

where IN is the total mass entering the groundwater flow system from external sources (such as injection wells), and OUT is the total mass leaving the groundwater flow system through sinks. Error is the percentage discrepancy between IN and OUT, which generally is an indication of the validity of a numerical solution and it should be small for the numerical solution to be acceptable (Zheng, 1990). In order to eliminate the discrepancy mass error, it

is desirable to use very small transport step. However, it is not practical because more computer space will be used, and the execution time will be longer.

The optimum selection of the solution parameters will help in using a larger transport step with a minimum mass balance discrepancy error. Following is the optimum combination of these parameters as determined for this model through a trail and error procedure :

1. PERCEL (courtant number), that is the number of cells a particle will be allowed to move in any direction in one transport step. It used to calculate the maximum allowed step size for particle tracking. This step size in then compared with other stability criteria (such as mass balance discrepancy), to determine an appropriate step size to be used in the simulation. Generally, it ranges from 0.5-1. In this model a value of 0.7 was used.
2. MXPART (maximum allowed number of total moving particles), a number of 10,000 was used in this model.
3. WD (concentration weighting factor), this has to be adjusted between 0 to 1 to achieve better mass balance, and it generally increased to toward 1 as advection becomes more dominant. For this model, a value of 0.62 was the optimum option.
4. DCEPS (negligible relative concentration gradient), chosen to be 0.0001
5. NPLANE (pattern for initial placement of particles), is a flag indicating whether the random or fixed pattern is selected for initial placement of moving particles. Because this model will be used in simulating the recharge/recovery process of freshwater into and from the aquifers, a random pattern was selected for initial placement of particles (i.e. NPLANE=0). This is as recommended by Zheng, (1990), who states that such an option generally leads to smaller mass balance discrepancy in nonuniform or diverging flow fields.
6. NPL (number of initial particles per cell to be placed at cells where DCCELL<DCEPS), where DCCELL is the relative cell concentration gradient (explained in Appendix-II). NPL=1 was assigned to this model.
7. NPH (number of initial particles per cell to be placed at cells where DCCELL>DCEPS). The selection of NPH depends on the nature of the flow field and also the computer memory limitation, generally it is preferred to use a smaller number in relatively uniform flow fields and larger number in relatively nonuniform flow fields (Zheng, 1990). Because the flow around the injection/recovery wells will be mainly

nonuniform, it was found that a large number of NPH (= 36) is necessary to be able of running this transport simulation. These particles will be randomly distributed within the cell block.

8. NPMIN (maximum number of particles allowed per cell). If the number of particles in a cell at the end of a transport step is fewer than NPMIN, new particles were inserted into that cell to maintain a sufficient number of particles. NPMIN=2 was selected for this model.
9. NPMAX (maximum number of particles allowed per cell). If the number of particles in a cell exceeds NPMAX, particles are removed from that cell until NPMAX is met. For this model, NPMAX was set to 72, which is twice the value of NPH (as recommended by Zheng, 1990).
10. SRMULT (multiplier for the particle number at source cells), SRMULT>1. Optimal results for this model was achieved with SRMULT= 1.2.
11. NPSINK (number of particles used to approximate sink cells in the MMOC scheme). The convention for this is the same as that for NPH. NPSINK=36 was assigned for this model.
12. DCHMOC (critical relative concentration gradient for controlling the selection use of either MOC or MMOC in the HMOC solution scheme). The MOC solution is selected at cells where DCCELL>DCHMOC, and MMOC solution is selected at cells where DCCEL<DCHMOC. DCHMOC=1 was used in this model.

Consequently, the optimum maximum allowed transport step size under which no significant mass balance discrepancy error is developed, was found to be 0.05 day, used for the initial stress period and increased gradually up to 0.15 day if the initial condition of the flow was proceeded, and reduced again at all times during the simulation when new withdrawal or injection stress were imposed on the system. The transport simulation was achieved with a mass balance error ranging from 0.0001 % to 0.2 %.

# 5. SINGLE-WELL INJECTION-RECOVERY TEST

## 5.1 INTRODUCTION

The Ministry of Electricity and Water (MEW) retained the Kuwait Institute for Scientific Research (KISR) to conduct artificial groundwater recharge experiments in three existing water wells. The author was one of the KISR team who carried out the field work. The main objective of the experiments was to assess the feasibility of recharging the aquifers of Kuwait through wells and to evaluate the operational problems that could be encountered during such operations. The results obtained were to be used in the design of a subsequent pilot project to evaluate the feasibility of artificial groundwater recharge at the large-scale.

The wells tested were wells SU-10 and SU-135 in the Sulaibiya wellfield, and Well C-105 in the Shigaya wellfield (Fig. 5.1). The Dammam limestone aquifer was the target of injection in Wells SU-10 and C-105, whereas the Kuwait Group clastic aquifer was the target in Well SU-135. At wells SU-135 and C-105, the recharge water was brackish groundwater mixed with tracers (such as, sodium fluoroscein, and tritium ). At Well SU-10, the recharge water was potable; hence the TDS and chloride were used as natural tracers since there was a contrast in their concentration between the recharge water and the brackish aquifer water.

Subsequent to injection, the injected water was withdrawn from each well until the quality of the pumped water reached the background level. Water level and tracer concentrations were measured at the test well during the injection and withdrawal periods.

The data obtained from the injection/withdrawal experiment at Well SU-10 were much more reliable than the data obtained in the other two experiments. Water injection was continued for one month in Wells SU-10 and C-105. However, in Well SU-135, where the Kuwait Group aquifer was the injected target, clogging became so severe that the injection

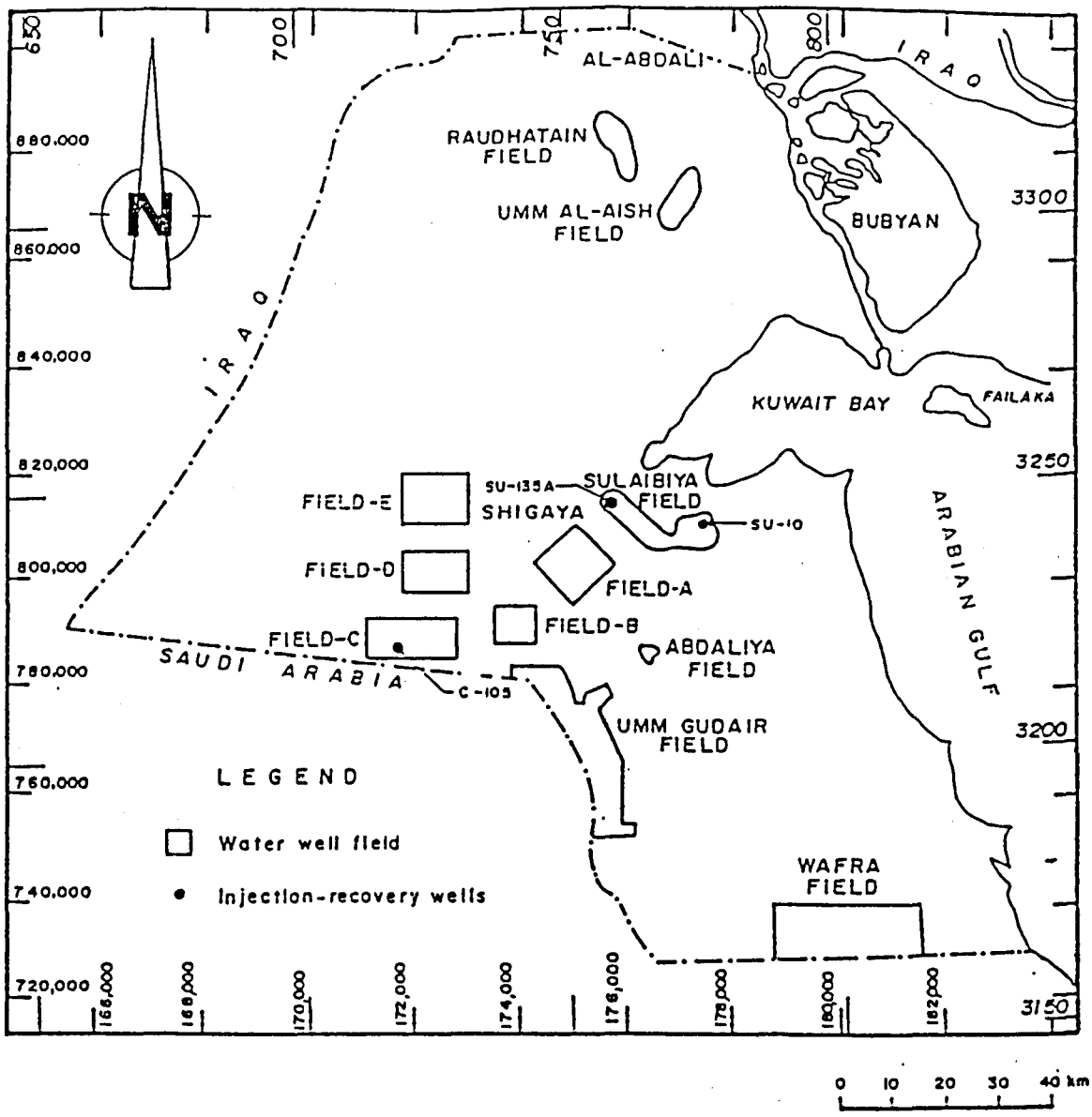


Figure 5.1: Location of injection-recovery test wells.

experiment could not be completed as planned, and was abandoned after only three days from the start of injection. In Well C-105, flowmeter data indicate that the groundwater flow in the vicinity of the well was restricted mainly to two major fractures (Mukhopadhyay et al., 1994). Under these circumstances, flow must have been turbulent, and Darcy's law will not be valid.

Because of those problems with the other two wells, analysis in this study, concentrates on the data from Well SU-10. These data were analysed with the help of a three- dimensional flow model (MODFLOW) and a solute transport model (MT3D) configured for a single well domain. The objectives of the study were:

1. To evaluate the development of well face clogging, and to differentiate between its possible causes.
2. To assess the quantity of water which could be injected successfully using a single well.
3. To estimate the dispersivity of the aquifer and its relation by other aquifer parameters.
4. To estimate the efficiency of the recharge-recovery process.

## 5.2 TEST SITE

The recharge borehole SU-10 is located in the eastern part of the Sulaibiya water wellfield, and is completed in the Dammam limestone aquifer. The well was drilled in 1956 for groundwater abstraction purposes. The construction details of the well, and a lithological log for the tapped aquifers, are shown in Figure 5.2. The total depth of the well is about 270 m. The Dammam Formation (DM) aquifer is penetrated at 115 m below the surface. The well casing is grouted through the Kuwait Group (KG) aquifer and open in the DM aquifer as an unscreened hole. Thus, the injection zone is in the DM limestone only. The KG aquifer is composed of interbedded layers of sandstone and silt, whereas the DM aquifer consists mainly of chalky limestone and dolomite. These two aquifers are separated by beds of basal clay and hard cherty limestone at the top of Dammam Formation, forming together an aquitard layer. Generally, the lithological sequence of the aquifers at this site is similar to that in the rest of Kuwait (see Chapter 3).

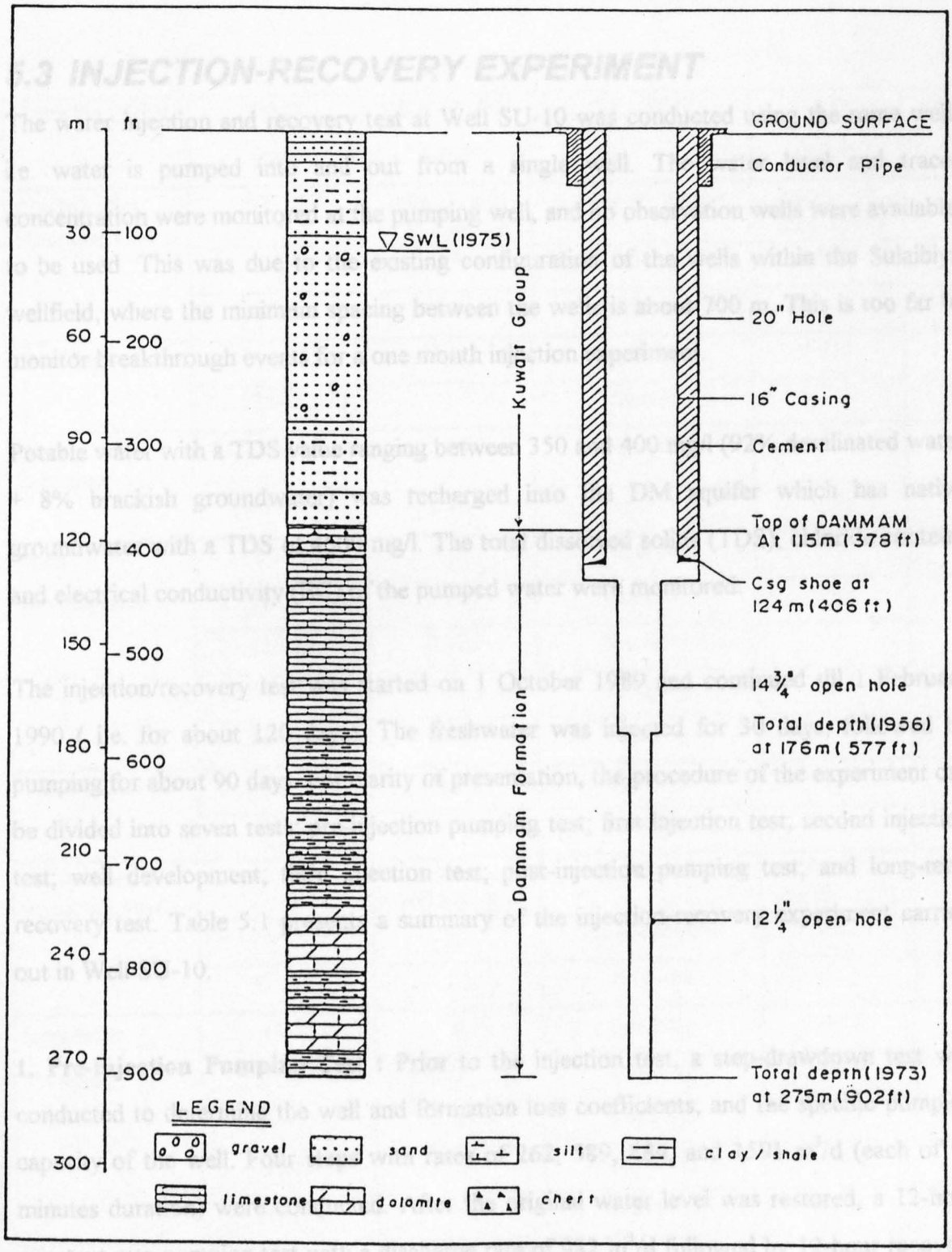


Figure 5.2: Lithological log and construction details for Well SU-10.

## 5.3 INJECTION-RECOVERY EXPERIMENT

The water injection and recovery test at Well SU-10 was conducted using the same well, i.e. water is pumped into and out from a single well. The water level and tracer concentration were monitored at the pumping well, and no observation wells were available to be used. This was due to the existing configuration of the wells within the Sulaibiya wellfield, where the minimum spacing between the wells is about 700 m. This is too far to monitor breakthrough events for a one month injection experiment.

Potable water with a TDS value ranging between 350 and 400 mg/l (92% desalinated water + 8% brackish groundwater) was recharged into the DM aquifer which has native groundwater with a TDS of 4500 mg/l. The total dissolved solids (TDS), chloride content, and electrical conductivity (EC) of the pumped water were monitored.

The injection/recovery test was started on 1 October 1989 and continued till 1 February 1990 ( i.e. for about 120 days). The freshwater was injected for 30 days, followed by pumping for about 90 days. For clarity of presentation, the procedure of the experiment can be divided into seven tests; pre-injection pumping test; first injection test; second injection test; well development; third injection test; post-injection pumping test; and long-term recovery test. Table 5.1 presents a summary of the injection-recovery experiment carried out in Well SU-10.

**1. Pre-injection Pumping Test :** Prior to the injection test, a step-drawdown test was conducted to determine the well and formation loss coefficients, and the specific pumping capacity of the well. Four steps with rates of 262, 589, 884, and 1591 $m^3/d$ (each of 90 minutes duration) were conducted. After the original water level was restored, a 12-hour constant-rate pumping test with a discharge rate of 982 $m^3/d$ followed by 12-hour recovery test was conducted to estimate the aquifer transmissivity.

**2. First Injection Test :** Before the injection test started, the wellhead was modified. The submersible pump was withdrawn from the borehole, the surface pipe layout was changed,

| OPERATION | TIME (day) | DURATION (day) | STATUS | RATE ($m^3/d$) | Number |
|---|---|---|---|---|---|
| **Pre-Injection Pumping Test** | 0-0.25 | 0.0625 each (90 minute) | 4 steps-drawdown | -262, -589, -884, -1591 | ST-1 |
| | 1-1.5 | 0.5 | constant-pumping | -982 | PT-1 |
| | 1.5-2 | 0.5 | recovery | | REC-1 |
| **First Injection** | 0-12.125 | 12.125 | injection | +655 | INJ-1 |
| | 12.125-13.125 | 1 | shut-in | | REC-2 |
| **Second Injection** | 13.125-18.165 | 5.04 | injection | +524 | INJ-2 |
| | 18.165-21 | 2.83 | injection | +393 | |
| **Well Development** | 21-23.29 | 2.29 | shut-in | | |
| | 23.29-23.415 | 0.125 | pumping | -982 | |
| | 23.415-23.54 | 0.125 | recovery | | |
| | 23.54-23.665 | 0.125 | pumping | -1571 | |
| | 23.665-24.29 | 0.625 | recovery | | |
| **Third Injection** | 24.29-34 | 9.71 | injection | +589 | INJ-3 |
| | 34-44.6 | 11 | shut-in | | |
| **Post-Injection Pumping Test** | 44.6-45 | 0.0625 each (90 minute) | 4 steps-drawdown | -393, -785 -1178, -1571 | ST-2 |
| | 45-45..5 | 0.5 | constant-rate | -982 | PT-2 |
| | 45.5-47 | 1.5 | recovery | | REC-3 |
| **long-term Pumping** | 47-53 | 6 | pumping | -982 | |
| | 53-54 | 1 | pumping | -524 | |
| | 54-55 | 1 | pumping | -982 | |
| | 55-56 | 1 | pumping | -1408 | |
| | 56-118 | 62 | pumping | -982 | |

Table 5.1: Injection-recovery experiment procedure at Well SU-10.

and the conductor pipe was lowered. Figures 5.3 and 5.4 are schematic diagrams showing the down-hole pipe assembly used for the injection and recovery tests respectively. The injection test was started with brackish water from the field pipe network at the a rate of 655 $m^3/d$. It was considered that this would give an easy start to the injection process because the recharge water in this case was more compatible with the aquifer water. After 24-hours, the injection was switched over to freshwater from the nearby freshwater pipeline. The water level inside the injection well rose with time, and it was possible to sustain the injection rate at 655 $m^3/d$ for about 12 day only before the water level rose to about 2 m below the land surface. The injection operation was suspended for 1 day to observe the well behaviour.

**3. Second Injection Test :** Subsequently, in order to maintain the water level 2-3 m below the land surface, the injection rate was lowered to 524 $m^3/d$ (for 5 days), followed by 393 $m^3/d$ (for 3 days), before once more suspending injection temporarily.

**4. Well Development :** It was decide to develop the injection well in order to improve the injection capacity of the well, which had been reduced because of clogging. Before the development activity was started, the well was shutdown for 2 days. The injection pipe was withdrawn and a submersible pump was installed. The well was back-pumped in two steps at rates of 982 $m^3/d$, and 1571 $m^3/d$, each for 3 hours. Turbid yellowish brown water was recovered for the first half-hour during the first step of backpumping.

**5. Third Injection Test :** The injection test started again after well development. The water level inside the injection well was maintained 2-3 m below the land surface. It was possible to sustain an average injection rate of around 589 $m^3/d$ for 9.7 day, when the injection was stopped. At this time, the injection test during all three phases was completed for about 30 days. A total of 16416 $m^3$ of water was injected, of which 15504 $m^3$ was potable water.

**6. Post-injection Pumping Test :** After the injection test was completed, the injection pipe was withdrawn and the submersible pump installed. During a period of 11 days (when the well was shut down), the recovery of water level inside the injection well was recorded. To assess the change in well condition after the injection experiment, a step-drawdown test with rates of 393, 785, 1178, and 1571 $m^3/d$ was conducted, each sustained for 90 minutes duration. This was followed by a 12- hour constant-rate (982 $m^3/d$) pumping test, and a 12-hour recovery test.

**7. Long-term Recovery Test :** First, the injected water was pumped back from the same injection well at a rate of 982 $m^3/d$ for 6 days. In order to observe the dependence of recovery efficiency on the pumping rate, the well was also pumped at three different rates (524, 982, and 1408 $m^3/d$ ), each for 1 day, and the tracer concentrations were monitored. The well was subsequently pumped at an average rate of 982 $m^3/d$, and monitored for variation in water level and tracer concentration continuously for 62 days. The pumping was stopped at the end of this period, as the tracer concentration in the recovered water reached the level existing in the native water. A total of 70400 $m^3$ of water was pumped from the well by this date. Figure 5.5 displays the water level changes during the entire injection/recovery experiment as measured in the test well.

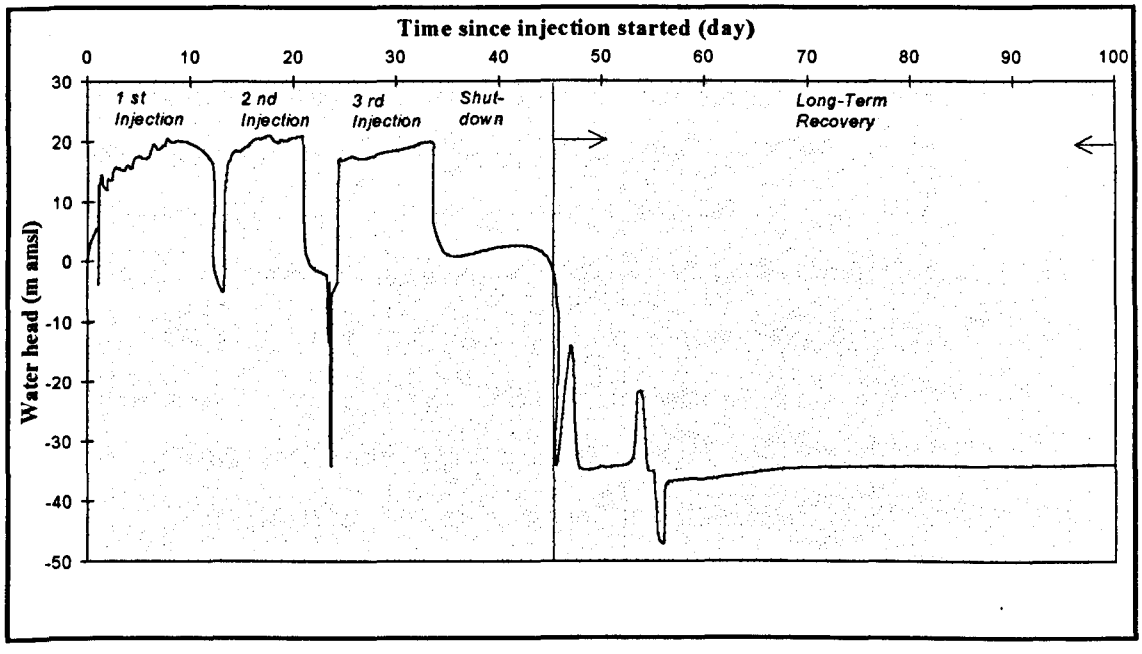


Figure 5.3: Observed water level changes during the injection/recovery experiment.

The absence of water level and tracer concentration data from observation wells is a limiting condition for this study. Calculation methods for some aquifer parameters (such as storativity, vertical hydraulic conductivity, and effective porosity) require such observation well readings. In addition, flowmetering was not used during the test. Thus it will be impossible to identify the vertical variation in the aquifer response to injection and pumping. Also, no geophysical logging (such as temperature or conductivity) was undertaken in the borehole after the freshwater injection was completed to monitor recharge water movement in the radial and vertical directions.

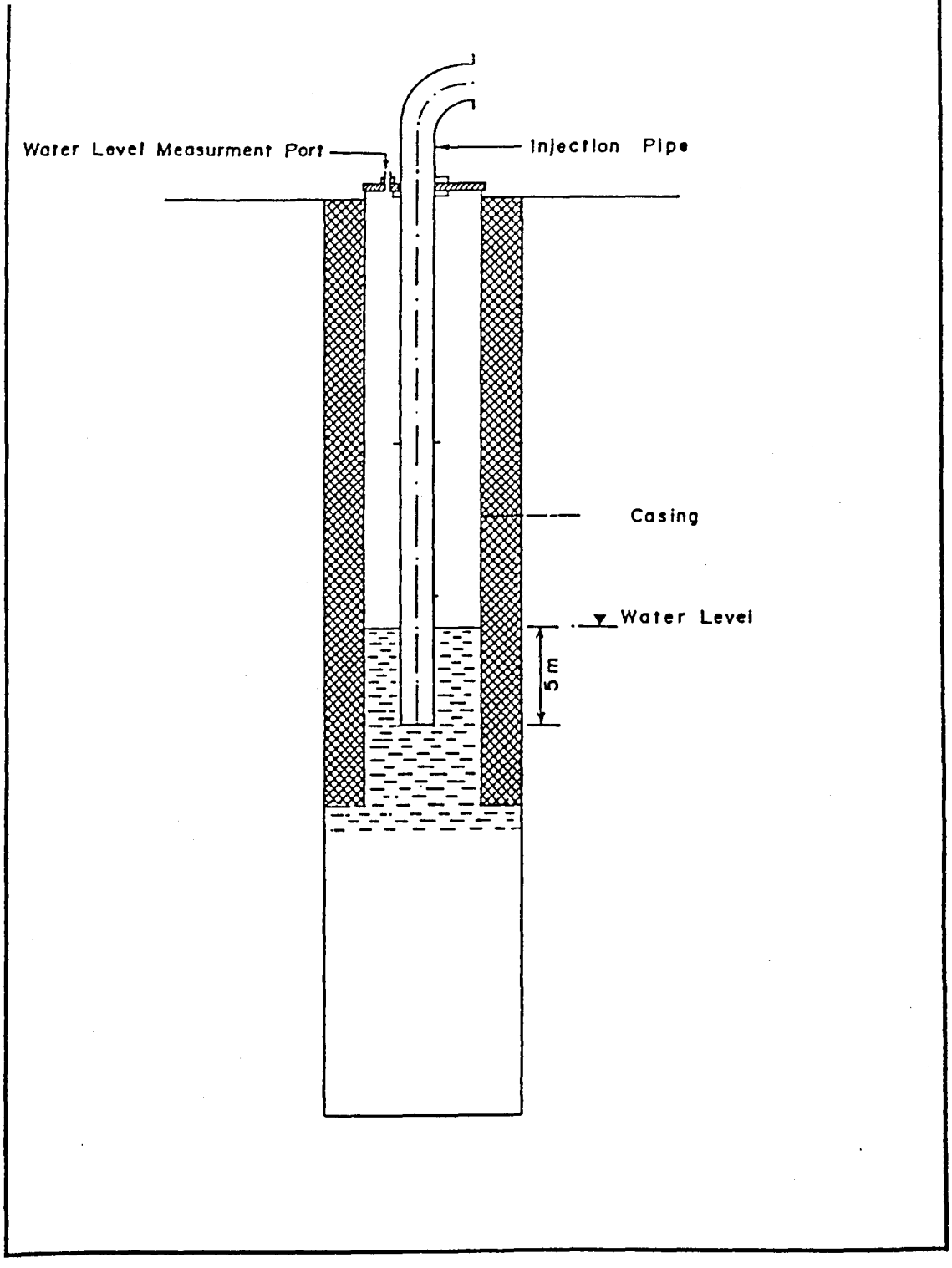


Figure 5.4: Schematic diagram showing the down-hole pipe assembly used for injection test (after Mukhopadhyay, 1994).

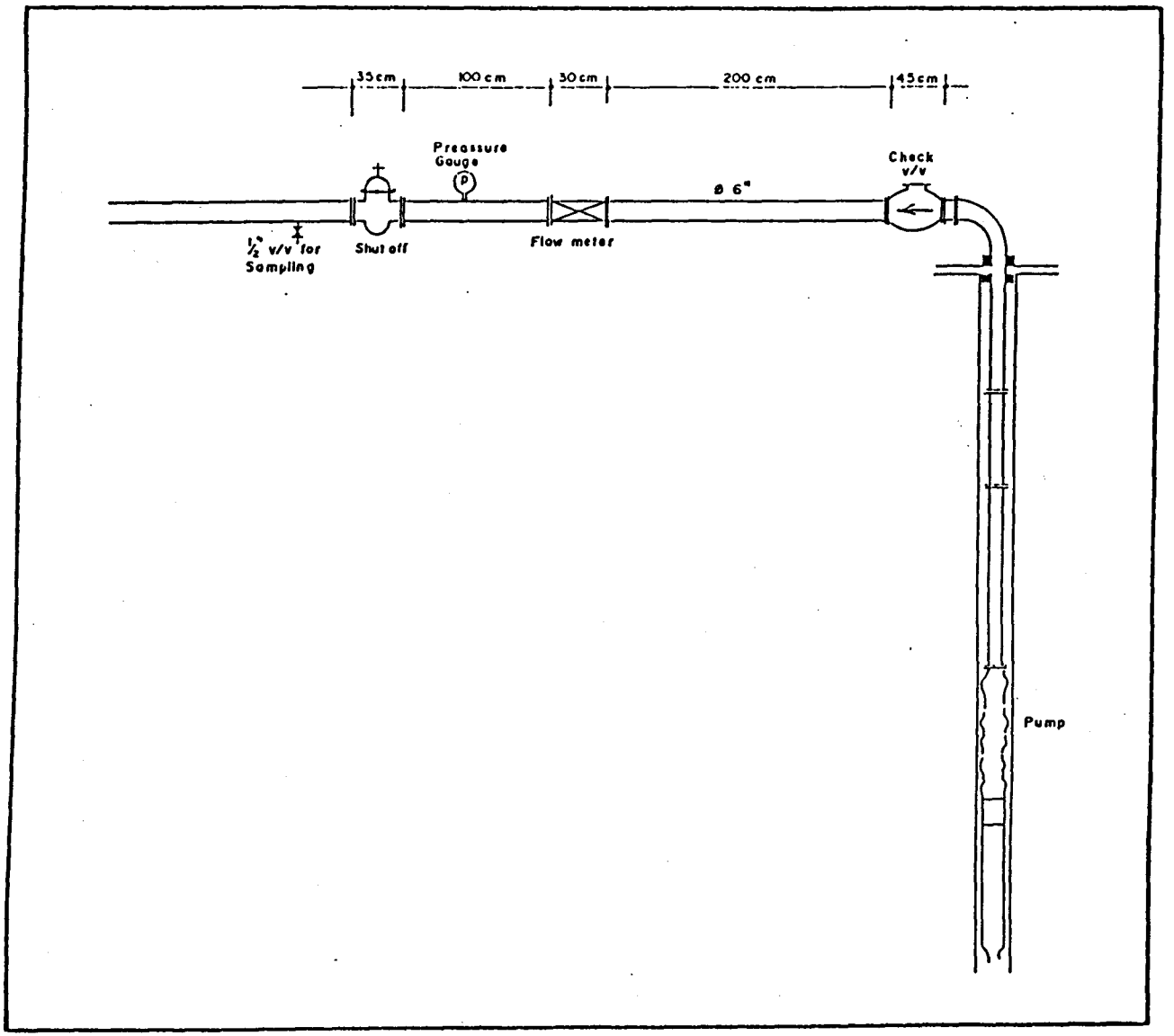


Figure 5.5: Schematic diagram showing the down-hole pipe assembly used for recovery test (after Mukhopadhyay, 1994).

## 5.4 METHODS OF INTERPRETING THE EXPERIMENTAL DATA

### 5.4.1 NUMERICAL MODEL

A three-dimensional block-centred finite difference numerical model was constructed for a single-well domain to analyse the injection-withdrawal test. The groundwater flow was solved by MODFLOW$^{EM}$ (McDonald and Harbaugh, 1988). The transport of dissolved constituents in the groundwater was simulated by the three-dimensional transport model MT3D (Zheng, 1993).

The groundwater flow pattern around the test well (SU-10) is asymmetrical, as this well is located at the edge of a cone of depression which is produced by the pumping of the Sulaibiya wellfield within which the well is located. The DM potentiometric surface in the vicinity of the well (within a radius of 500 m) was declining from about (-14 m amsl) at the north eastern corner to about (-20 m amsl ) toward the centre of the cone of depression at the south western corner. There was, thus a transient pre-existing flow with a hydraulic gradient of 0.006, which was steeper than the initial steady regional hydraulic gradient (which is 0.001). A three-dimensional model instead of a radial model was thus preferred to represent the pre-test groundwater flow pattern around the well more accurately.

In the absence of any physical limit in the test site, the assignment of appropriate boundary conditions for the numerical model is somewhat difficult. It was also impossible to calibrate the single-well model (which was limited to a small area of the wellfield) over a long stress period. Thus, the pre-test flow pattern resulted from operating the water wellfields for about 30 years, was difficult to define properly.

Consequently, the technique of Telescopic Mesh Refinement (Ward et al., 1987) was used to construct the single-well model to represent the injection-withdrawals experiment in reasonable detail and to define the modelled area within meaningful boundaries. This was achieved through defining sub-regional boundaries within the regional flow model, which then define a new smaller problem domain. For more accuracy in defining the boundary

conditions (which were selected to be constant-head), the telescopic refinement was done in two steps, until the model grids became small enough to obtain the desired detail. First, an intermediate model was created based on the regional model, then this intermediate model was utilised in constructing the intended single-well model.

#### 5.4.1.1 INTERMEDIATE MODEL

A nested sub-regional area, representing 5x5 cells of the coarsely-spaced (2000m x 2000m) regional model (presented in Chapter 4) was selected. This area was chosen so that the test well (Well SU-10) occupies the mid node. Subsequently, the area was remodelled with a finer grid spacing using a three-dimensional intermediate numerical model consisting of 2 layers (KG and DM aquifers), with 50x50 cells of regular spacing (200x200m). Figure 5.6 displays the embedded cells of the intermediate model within the regional model. The calibrated aquifer parameters obtained from the regional model were transferred and entered to the redefined intermediate model. The regional model was run under transient flow conditions, starting from the pre-development steady state water level (in 1960) until the start of the experiment (summer 1989). The resulting simulated hydraulic heads (summer 1989) of the aquifers were transferred to the intermediate model as initial heads. This model was calibrated only under steady-state conditions, and a slight adjustment was made for the aquifer parameters and hydraulic heads at the boundaries in order to match the simulated and observed aquifer potentiometric heads.

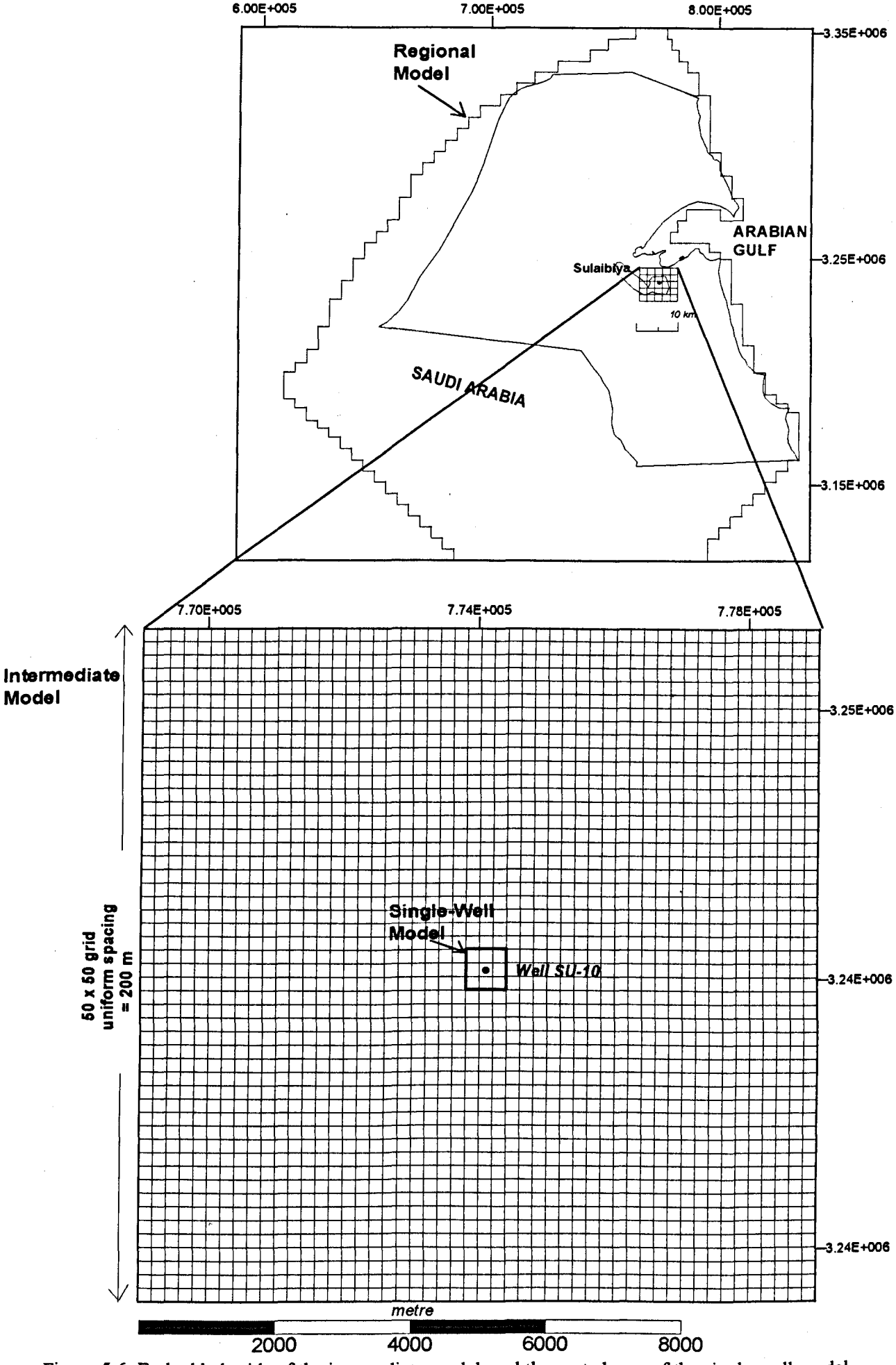


Figure 5.6: Embedded grids of the inermediate model, and the nested area of the single-well model.

#### 5.4.1.2 SINGLE-WELL MODEL

For the single-well model, an area around the injection well was chosen for the intermediate model. In order to produce a symmetrical spatial discretization around the well, the grid was selected to locate the well in the central node.

Based on the data availability and the capability of the used modules in representing some hydraulic and transport features, the model was constructed using the following assumptions :

1. The model consisted of two layers representing the unconfined KG, and the leaky confined DM aquifers, which are separated by an aquitard layer. No further subdivisions of the KG and the DM aquifers were attempted due to the lack of available aquifer parameters data for individual zones within these aquifers.
2. The upper limit of the model is the water table in the KG aquifer, and the lower limit of the model is low permeability zone at the bottom of DM aquifer.
3. The layers had uniform thickness of 110, 150, and 10 m for the KG and DM aquifers, and the intervening aquitard, respectively.
4. Aquifers are homogeneous within the modelled area with uniform aquifer properties over the extent of the model. Initially, the calibrated values from the intermediate model were used for assigning the aquifer parameters for the layers, as presented in Table 5.2.
5. The test well fully penetrates the recharged DM aquifer.
6. Vertical leakage between the layers occurred through the aquitard layer.
7. Well face clogging which could not be handled by the model, was taken into account by reducing the hydraulic conductivity of the well node and the adjacent four nodes.

| Layer | Thickness (m) | Hydraulic conductivity (m/d) | Effective porosity | Specific Storage ($m^{-1}$) | Vertical leakance ($d^{-1}$) |
|---|---|---|---|---|---|
| Kuwait Group | 110 | 2.5 | 0.07 | $1 \times 10^{-5}$ | |
| Dammam Formation | 150 | 0.70 | 0.05 | $1 \times 10^{-6}$ | |
| Aquitard | 10 | | | | $1 \times 10^{-5}$ |

Table 5.2: Initial aquifers parameters as entered to the single-well model using the steady- state calibrated parameters of the intermediate model.

The construction of a numerical model for a single-well domain requires the use of very fine nodal spacing to represent adequately the steep hydraulic gradient existing around the well,

and also for better reproduction of the water level and tracer concentration during the calibration stage. Hence, comparable results with the observed ones can be obtained. Otherwise, enormous differences will be detected which make the calibration process unreliable.

The boundary conditions of the model which were assigned as constant-heads during the transient calibration have to be placed at a safe distance from the test well node. This is to ensure that the radius of influence during the injection or pumping will not reach these boundaries which may effect the simulated results. This can be achieved either through large nodal spacing or by using a large number of nodes. However, a model with a large number of nodes is not preferred when it is necessary to minimise data handling, computer storage, and computation time. Therefore, a trade-off was obtained between the need for using the minimum number of nodes with fine nodal spacing to get the desired detail from the modelled system, and between placing the constant-head boundary nodes at a sufficient distance from the test well.

First, a preliminary model with uniform nodal spacing was constructed, using the aquifers parameters obtained from the intermediate model. The maximum pumping rate recorded during the long-term recovery test was introduced in this model, and the maximum possible radius of influence was simulated. This distance was subsequently used to decide on the position of the single-well model boundary.

Later, the final design for the single-well three dimensional model was selected. The domain was discretized using a square mesh consisting of 55x55 cells with irregular grid spacing. A very fine cell (0.5 x 0.5 m) was used at the centre of the model, to represent the location of the well. Away from this node, the grid spacing was gradually increased in all directions using an expansion factor of 1.2. A distance of 409 m between the well node and the boundary node in the x and y directions was modelled, where $\Delta x = \Delta y$ was considered. The boundary nodes had the largest nodal spacing of 68.7 m (Figure 5.7 displays the grid discretization of the single-well model). The calibrated steady-state aquifer heads obtained by the intermediate model were entered to the single-well model as initial water heads.

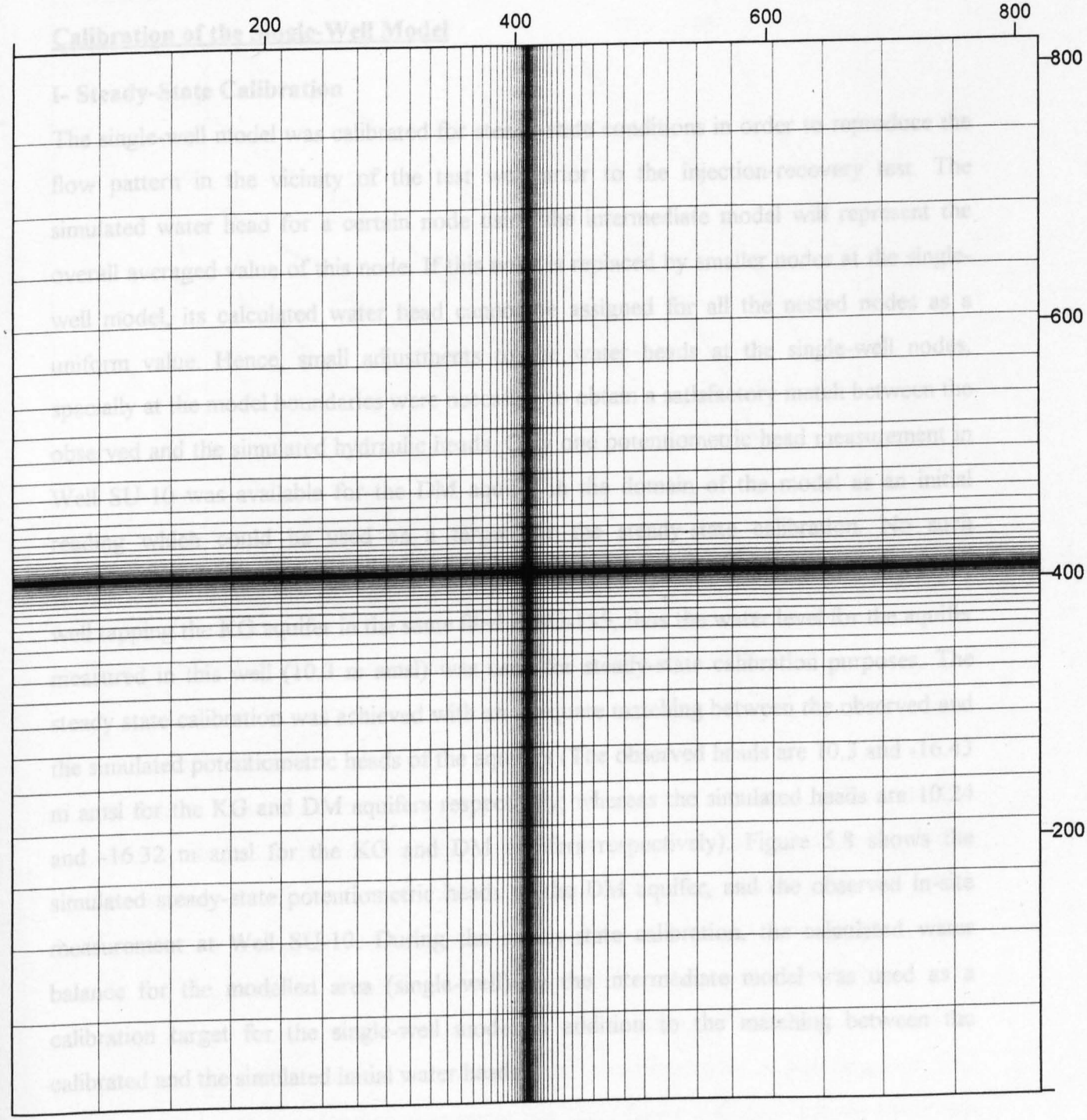


Figure 5.7: Grid discretization of the single-well model (in metres).

## Calibration of the Single-Well Model

### I- Steady-State Calibration

The single-well model was calibrated for steady-state conditions in order to reproduce the flow pattern in the vicinity of the test well prior to the injection-recovery test. The simulated water head for a certain node using the intermediate model will represent the overall averaged value of this node. If this node is replaced by smaller nodes at the single-well model, its calculated water head cannot be assigned for all the nested nodes as a uniform value. Hence, small adjustments to the water heads at the single-well nodes, specially at the model boundaries were necessary to obtain a satisfactory match between the observed and the simulated hydraulic heads. Only one potentiometric head measurement in Well SU-10 was available for the DM aquifer in the domain of the model as an initial reading which could be used as a target for the steady-state calibration. No such measurements were available for the KG aquifer as it was cased in the test well. The only well tapping the KG aquifer in the same filed is SU-135, thus the water level for the aquifer measured in this well (10.3 m amsl) was used for steady-state calibration purposes. The steady state calibration was achieved with an adequate matching between the observed and the simulated potentiometric heads of the aquifers (The observed heads are 10.3 and -16.43 m amsl for the KG and DM aquifers respectively; whereas the simulated heads are 10.24 and -16.32 m amsl for the KG and DM aquifers respectively). Figure 5.8 shows the simulated steady-state potentiometric heads of the DM aquifer, and the observed in-site measurement at Well SU-10. During the steady-state calibration, the calculated water balance for the modelled area (single-well) by the intermediate model was used as a calibration target for the single-well model in addition to the matching between the calibrated and the simulated initial water heads.

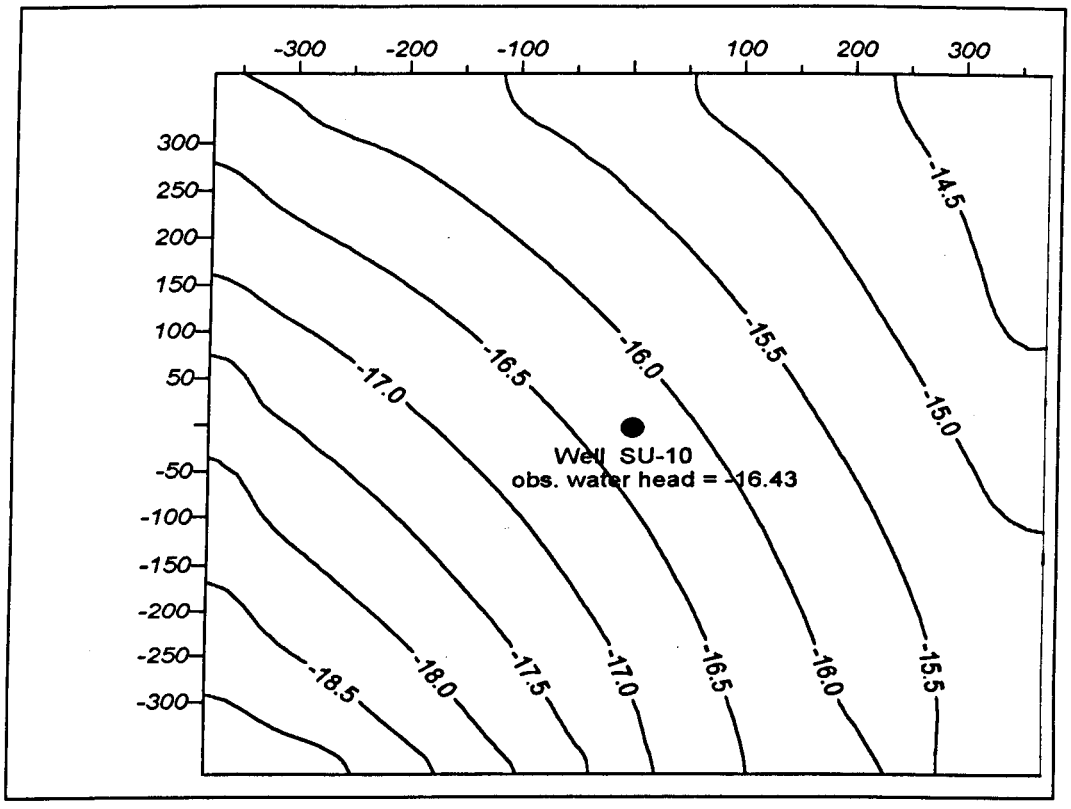


Figure 5.8 : Simulated pre-test DM potentiometric heads versus the observed water head measurement at the test well, (m amsl). The x, and y model dimensions are in metres.

**II- Transient Calibration**

Constant head boundary conditions were used during the transient calibration. The hydraulic heads at the boundaries were assumed to represent the regional groundwater conditions, since those were not affected by the operation of the surrounding wells which were shut down during the test. Moreover, the test was conducted for a relatively short period, and the boundary heads were not expected to change significantly due to the pumping of more remote wells. Figure 5.9 shows the radius of influence, simulated by pumping the test well for about 70-days using the possible maximum pumping rate (982 $m^3/d$) recorded during the long-term recovery test. This figure indicates that the maximum radius of influence during the whole test will not reach the model boundary.

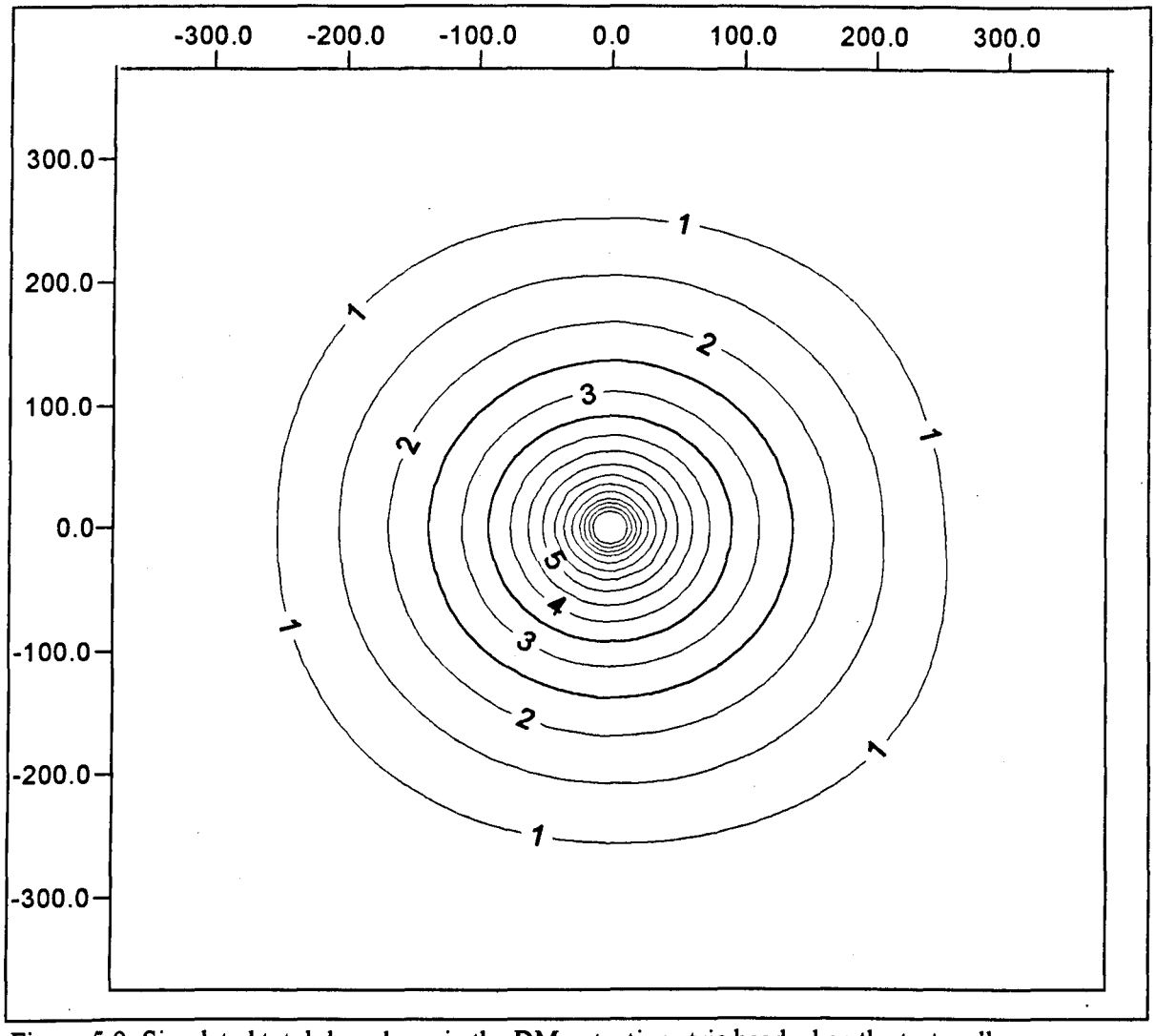


Figure 5.9: Simulated total drawdown in the DM potentiometric head when the test well was pumped during the long-term recovery test showing the maximum radius of influence, (m).

Note: The maximum drawdown in the pumped well is 21.2 m.

The results of the model simulation will be effected by the time step used. In order to simulate the rapid change in water levels during the initial stages of injection or pumping, small time steps are recommended to be used at the beginning, and the duration of the time step may be increased in a geometric progression as the hydraulic head tends to stabilise with time. In the present case, an initial time step of 0.01 day and a multiplication factor of 1.2 were used during each stress period. It was found that no significant improvement in the simulated heads occurred at an initial time step duration of less than 0.01 day. Each stress period was taken to represent a constant rate of injection or recovery.

The use of water level measured in the pumping well itself as a calibration target was not a straight forward procedure. The drawdown in a pumped well consists of two components; the aquifer loss and the well loss. Aquifer loss is the head loss that occurs in the aquifer where the flow is laminar. It is time-dependent and varies linearly with the well discharge. Well loss is divided into linear and non-linear components. Linear well loss is caused by damage to the aquifer during drilling and completion of the well. Non-linear well loss is the loss that occurs inside the bore hole and the suction pipe when the flow is turbulent. All of these well losses are responsible for the drawdown inside the well being greater than its theoretical value, which consists of aquifer loss only (Kruseman and de Ridder, 1990). The aquifer and well losses can be determined by a step-drawdown test. For the drawdown in a pumped well, Jacob (1947) gave the following equation:

$$S_w = BQ + CQ^2 \qquad (5.1)$$

Where B, C, Q are the aquifer loss coefficient, well loss coefficient, and discharge rate, respectively.

The simulated drawdown using the numerical model is the drawdown resulting from the aquifer loss only, where the additional drawdown due to well loss was not taken into consideration by the model. Therefore, in order to use the measured drawdown inside the pumping well for calibration purposes, it should be corrected by subtracting the drawdown due to well loss from the total drawdown. In this study, before comparing the simulated with the observed water level measurements, the measured levels were corrected by subtracting from drawdowns due to well loss. The aquifer and well loss coefficients (B and C) were obtained from the pre-injection step-drawdown test (see section 5.4.2). These coefficients and the discharge or recharge rates (Q) at each injection and pumping phase were used in calculating the additional drawdown or build-up inside the well due to well loss.

Additionally, the expected influence of the wellfield operation was estimated for the changes in water levels in the nearby well SU-11 which was shut down during the test. This was used to correct the water level measurements at the test well SU-10 (as presented in Table 5.6).

Accordingly, the corrected water level readings obtained from the pre-injection constant-rate pumping and recovery tests were used in calibrating the model for the transient conditions. Any numerical model can be calibrated using various combination of aquifers parameters, which may or may not represent the "true" values (Anderson and Woessner, 1992). Inadequacy of available data for the vertical leakage factor significantly influenced the calibrated results. Thus, in the transient calibration, the vertical leakance obtained during the steady-state calibration was readjusted in addition to the storage parameters in order to match the simulated and the observed drawdown resulting from the constant-rate pumping test. The subsequent recovery data proved very beneficial in obtaining the most reliable value for vertical leakage. The steady-state and transient calibrations were linked together and re-done using an iterative approach until the aquifer parameters determined for the steady-state and transient conditions agreed simultaneously. The calibrated parameters in this case are likely to be more accurate than calibrating the model separately for each condition. Figure 5.10 displays the matching achieved during the transient calibration between the simulated and the observed potentiometric head of the DM aquifer as obtained from the pre-injection constant-rate and recovery tests.

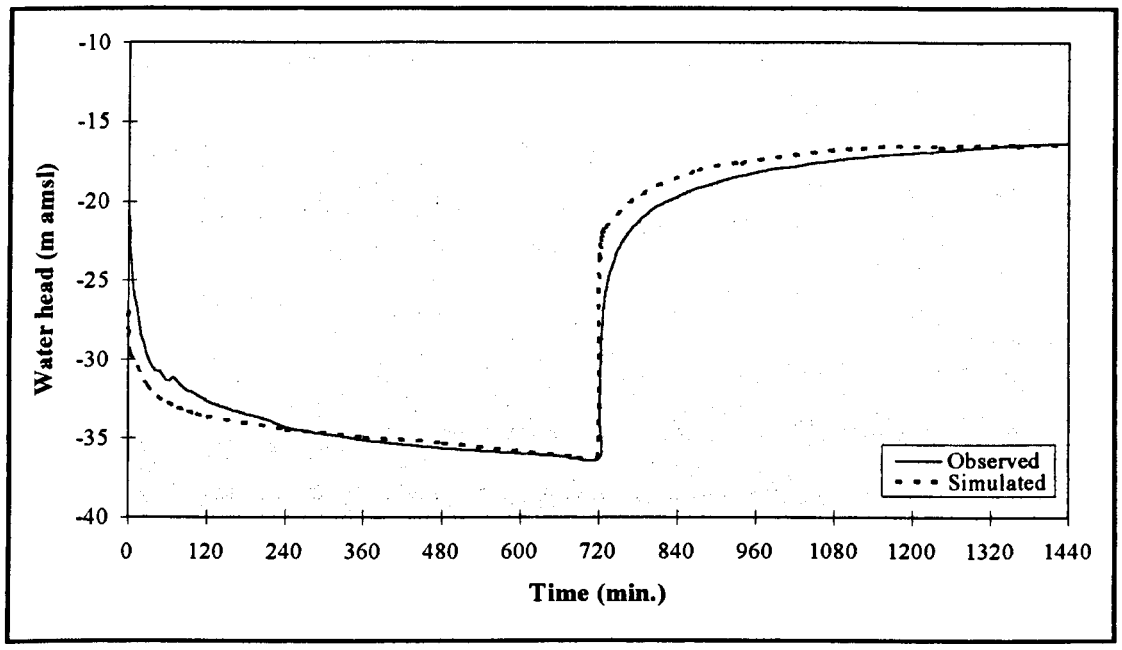


Figure 5.10: Obtained match between the observed and the simulated aquifer potentiometric head during the pre-injection constant-rate and recovery tests, which were used for the transient calibration.

The DM aquifer's parameters were obtained during the steady-state and transient calibrations, whereas, the KG aquifer's parameters were left untouched and kept as they had been entered to the model. Table 5.3 presents the calibrated DM aquifer's parameters.

| Layer | Thickness (m) | Hydraulic conductivity (m/d) | Effective porosity | Specific Storage (1/m) | Vertical leakance (1/day) |
|---|---|---|---|---|---|
| Dammam Formation (DM) | 150 | 0.34 | 0.05 | $1 \times 10^{-6}$ | |
| Aquitard | 10 | | | | $5 \times 10^{-5}$ |

Table 5.3: More reliable DM aquifer parameters for the single-well model, as calibrated through iterative procedure between the steady-state and transient calibration.

The steady-state and transient calibrations were achieved with a low water balance discrepancy error. It was about (0.01 %) for the steady-state calibration, and ranged from 0.04 % to about 0.07 % for transient calibration, which can be considered as negligible.

**Verification of the Single-Well Model**

The model was verified using the measured drawdown during the pumping stages specially during the long-term recovery test. The verification was completed successfully where the intended match was achieved without any modifications to the aquifers parameters or to the boundary conditions. Figure 5.11 shows the observed and the simulated water heads of the DM aquifer during the long-term recovery (starting from 45th to 118th day from the start of the experiment).

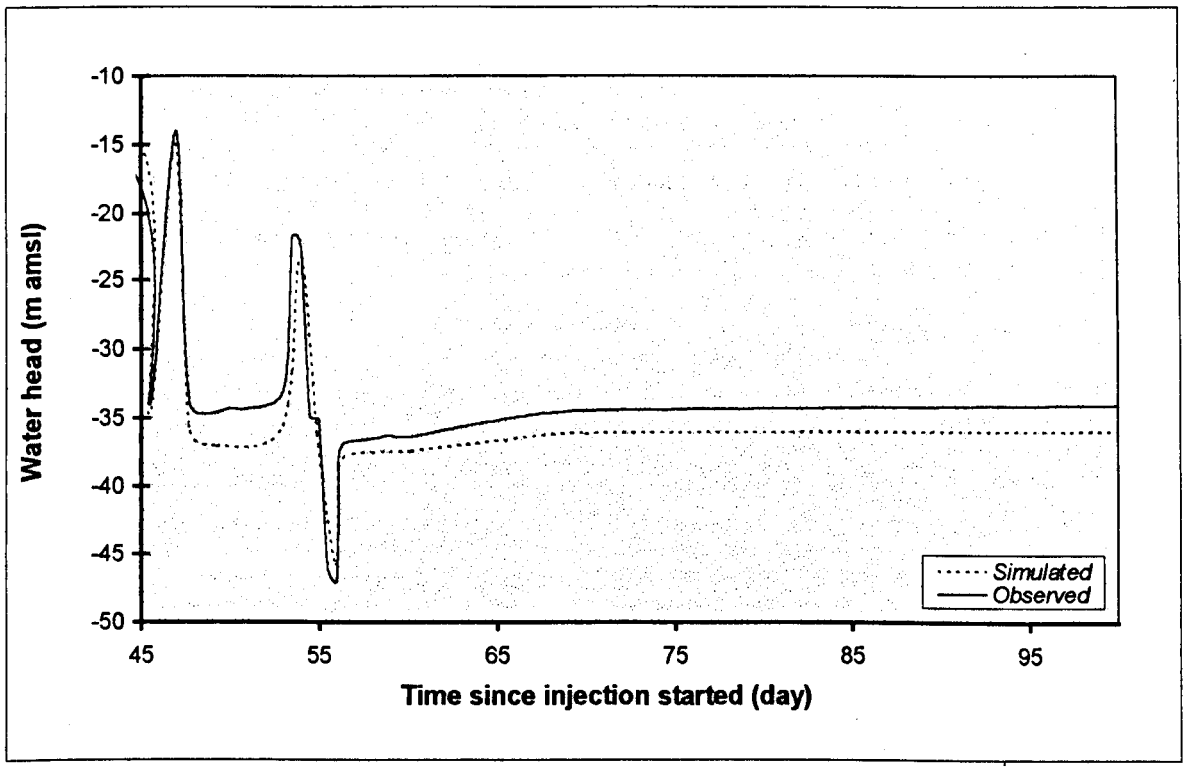


Figure 5.11: Simulated and observed change in the DM potentiometric head during the long-term recovery test.

## 5.4.2 PUMPING TEST DATA INTERPRETATION

Prior the construction of the single-well model (presented in the previous section), the conducted constant-rate pumping tests and the subsequent recoveries were analysed to determine the aquifer's transmissivity (or the hydraulic conductivity) to be used as input data for the model. However, the model could not be calibrated precisely with such data. This may relate to the difference in the scale of representation, where the pumping test data are representing a small area of the aquifer, and the numerical model is averaging the

aquifer properties for a larger domain. Therefore, two values of the aquifer hydraulic conductivity were determined. These are 0.34 and 0.2 m/d, as obtained by the numerical model calibration and by the pumping test data interpretation respectively. These values will be used later as reference points to quantify the reduction in aquifer hydraulic conductivity which resulted from clogging of the well face during water injection. Usually, the step-drawdown tests are used to determine the well and aquifer head losses and hence the well efficiency. Thus, the pre-injection and post-injection step-drawdown tests conducted during this experiment will be used to determine the changes in the injection well conditions which could result from water injection (i.e. by comparing the well loss before and after the injection, additional well loss due to clogging can be quantified). Accordingly, the results of the constant-rate pumping, recovery, and step-drawdown tests will be used in addition to the numerical model to quantify and differentiate between the possible causes of well face clogging.

The Aquifer Test Solver AQTESOLV™ (Glenn Duffield, 1995) was used to interpret the constant-rate pumping test and recovery data. This software is based on the best known analytical solutions used for determining aquifer parameters using the time-drawdown data measured during an aquifer test. To analyse the data, this software provides an automatic and visual curve matching features. Virtual curve matching is analogous to traditional methods of aquifer test analysis with graph paper and type curves. The automatic curve matching features uses a nonlinear weighted least-squares parameter estimation algorithm to match type curves or straight lines to time-displacement data measured during an aquifer test. The automatic curve matching feature minimises the errors between the position of the type curve (simulated displacement) and the observed measurements (Glenn Duffield, 1995).

Solution are available for various options; for confined, unconfined, and leaky aquifers as follows:

1. Confined aquifer solutions:
    - Theis (1935) for constant-rate test
    - Theis (1935) for variable rate test.
    - Cooper-Jacob (1946) for constant-rate test

- Cooper-Jacob (1946) for variable rate test.
- Theis Recovery (1935)
- Papadopulos-Cooper (1967) for constant rate test in large-diameter well.

2- Unconfined aquifer solutions:

- Neuman (1974) for constant-rate test, solution with delayed gravity response.
- Streltsova (1974), solution for piezometers.

3- Leaky aquifer solutions:

- Hantush-Jacob (1955), no storage in aquitard.
- Hantush (1960), with storage in aquitard.
- Moench (1985), large-diameter well, solution with storage in aquitard.

Furthermore, this software includes solutions for fractured aquifer pumping and slug tests.

For the tested DM aquifer, it was found that the most appropriate solution for the constant-rate pumping test data was the Hantush-Jacob (1955) method for the leaky aquifer which does not include storage in aquitard. The Theis recovery (1935) method is valid in interpreting the recovery data.

**Hantush-Jacob (1955) leaky aquifer solution**

This solution can be used under the following assumptions:

1. Aquifer has infinite areal extent
2. Aquifer is homogeneous, isotropic and of uniform thickness
3. Aquifer potentiometric surface is initially horizontal
4. Pumping well is fully penetrating
5. Flow to pumping well is horizontal
6. Flow is unsteady
7. Water is released instantaneously from storage with decline of hydraulic head
8. Diameter of pumping well is very small so that storage in the well can be neglected
9. Aquifer is leaky
10. Confining bed has infinite areal extent, uniform vertical hydraulic conductivity and uniform thickness
11. Confining bed is overlain by an infinite constant-head plane source
12. Flow in the aquitard is vertical.

The drawdown during the constant-rate pumping test can be approximated based on Hantush-Jacob (1955) as;

$$s = \frac{Q}{4\pi T} w(u, r/B) \qquad (5.2)$$

where:

Q = discharge rate ($L^3/T$)

T = aquifer's transmissivity ($L^2/T$)

$w(u, r/B)$ = Hantush well function = $\int_u^\infty \frac{e^{-y-r^2/4B^2y}}{y} dy$

$$u = \frac{r^2 S}{4Tt}$$

$$B = \sqrt{\frac{Tb'}{K'}}$$

S = aquifer storativity (dimensionless)

t = time since the start of pumping (T)

r = distance from well to piezometer (L)

$b'$ = thickness of aquitard (L)

$K'$ = vertical hydraulic conductivity of aquitard (L/T)

The calculated aquifer hydraulic conductivity by this method using the pre-injection and post-injection constant-rate pumping tests data are 0.2 and 0.26 m/d, respectively (Figures 5.12 and 5.13). The calibrated value of aquifer hydraulic conductivity from the numerical model (0.34 m/d) is little different from these values, further bolstering confidence in the numerical model results.

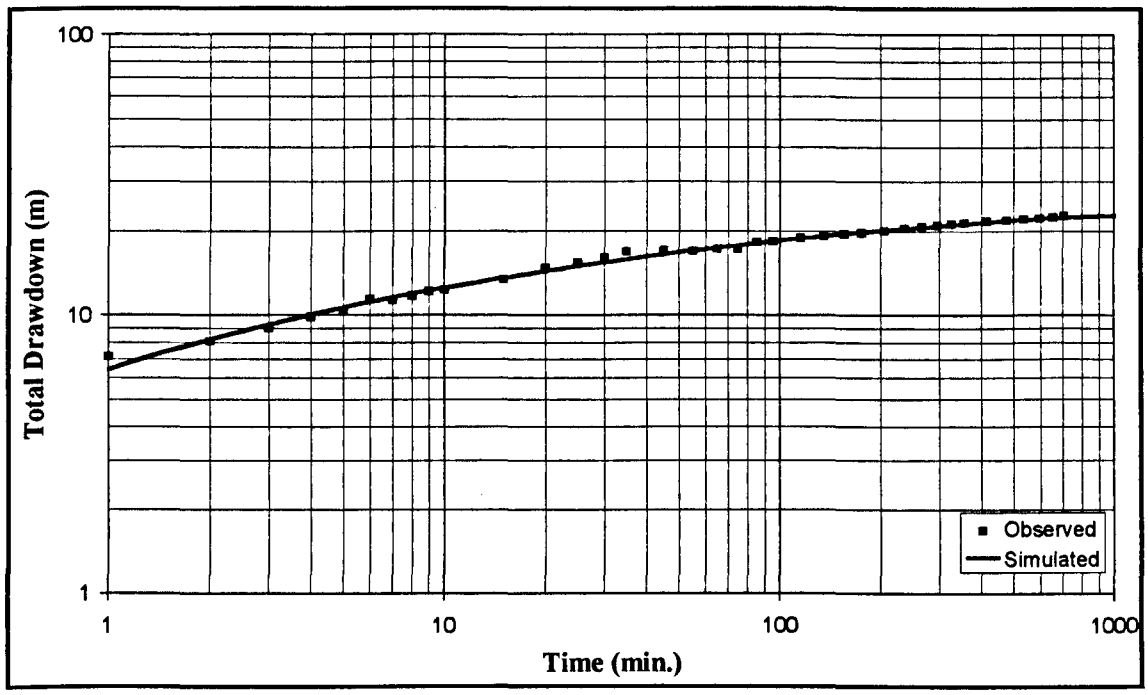


Figure 5.12 : Curve matching between the observed drawdown in aquifer head during the pre-injection constant-rate pumping test with type curve obtained using the Hantush-Jacob (1955) method

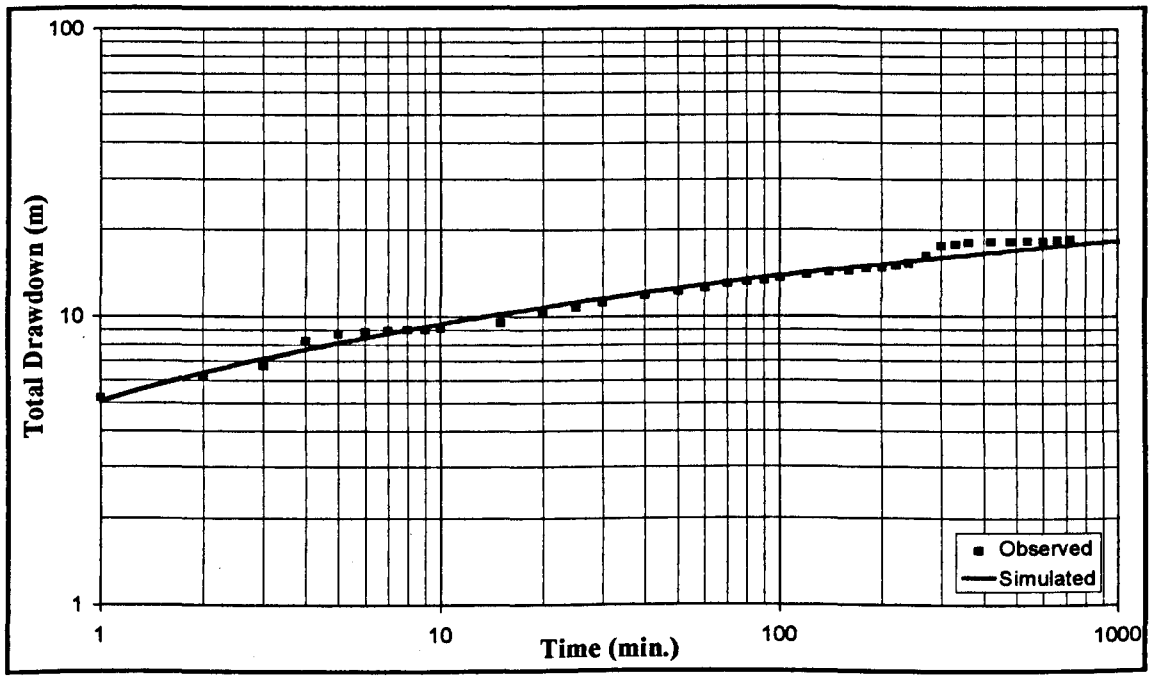


Figure 5.13: Curve matching between the observed drawdown in aquifer head during the post-injection constant-rate pumping test with type curve obtained using the Hantush-Jacob (1955) method

**Theis's (1935) Recovery Method**

In addition to the assumptions (1-8) at the above Hantush's (1955) method, another two assumptions are considered when using Theis's recovery method, these are;

1. Aquifer is confined
2. Values of (u) are small (i.e., r is small and t is large).

The residual drawdown after a pumping test with a constant discharge is

$$s'' = \frac{Q}{4\pi T}\left[\ln\left(\frac{4Tt}{r^2S}\right) - \ln\left(\frac{4Tt''}{r^2S''}\right)\right] \qquad (5.3)$$

where:

$s''$ = residual drawdown (L)

$S''$ = aquifer's storativity during recovery (dimensionless)

$t''$ = time since pumping stopped (T)

The calculated aquifer hydraulic conductivity by this method using the recovery data after the pre-injection and post-injection constant-rate pumping tests are 0.2 and 0.24 m/d , respectively (Figures 5.14 and 5.15). These are consistent with the previously obtained values.

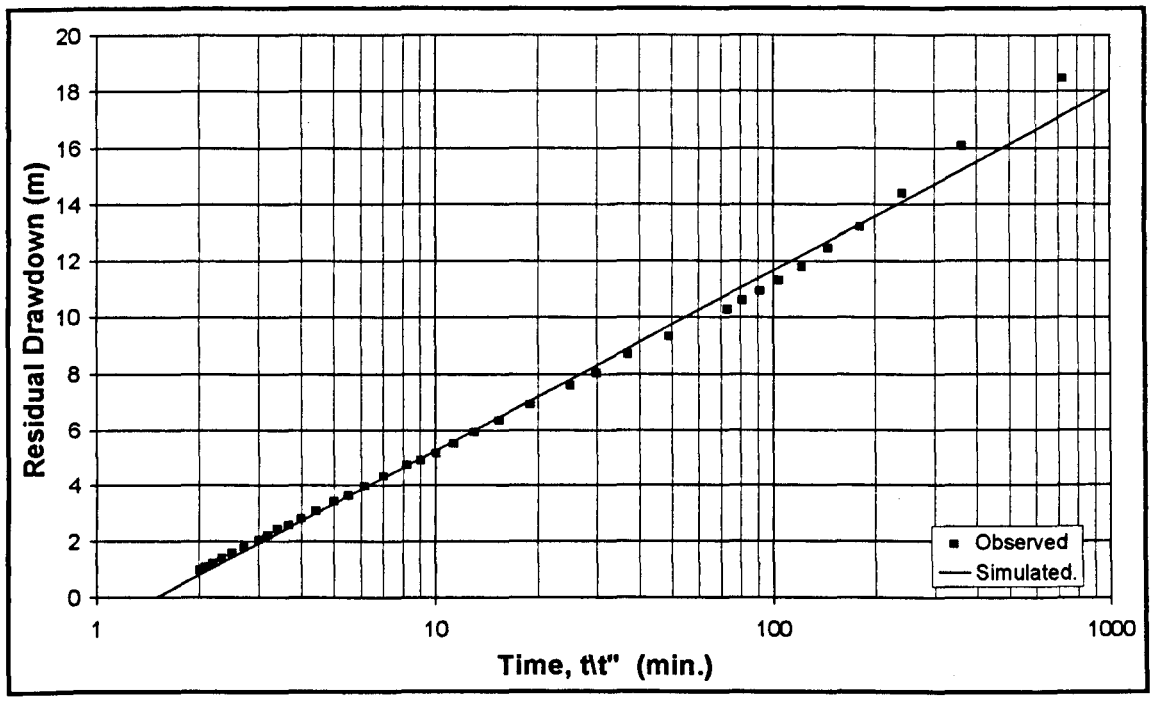


Figure 5.14: Fitted straight line through the observed residuals drawdown recorded after the pre-injection constant-rate pumping test using Theis Recovery (1935) method.

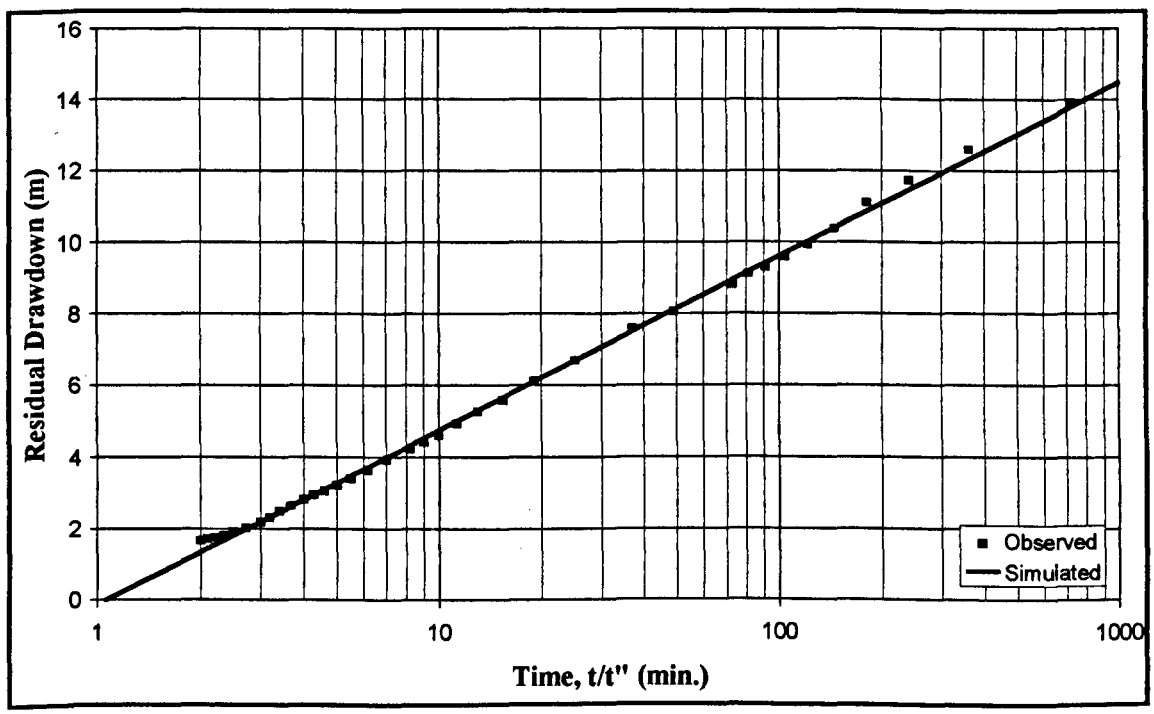


Figure 5.15: Fitted straight line through the observed residuals drawdown recorded after the post-injection constant-rate pumping test using Theis Recovery (1935) method.

In the same way of analysing recovery data after constant-rate pumping test, recovery data after water injection was analysed to determine the aquifer hydraulic conductivity. Thus, at various stages of the experiment, especially before and after water injection, the changes in the aquifer's hydraulic conductivity can be identified. Figure 5.16 shows the residual drawdown versus time as recorded after the first injection phase.

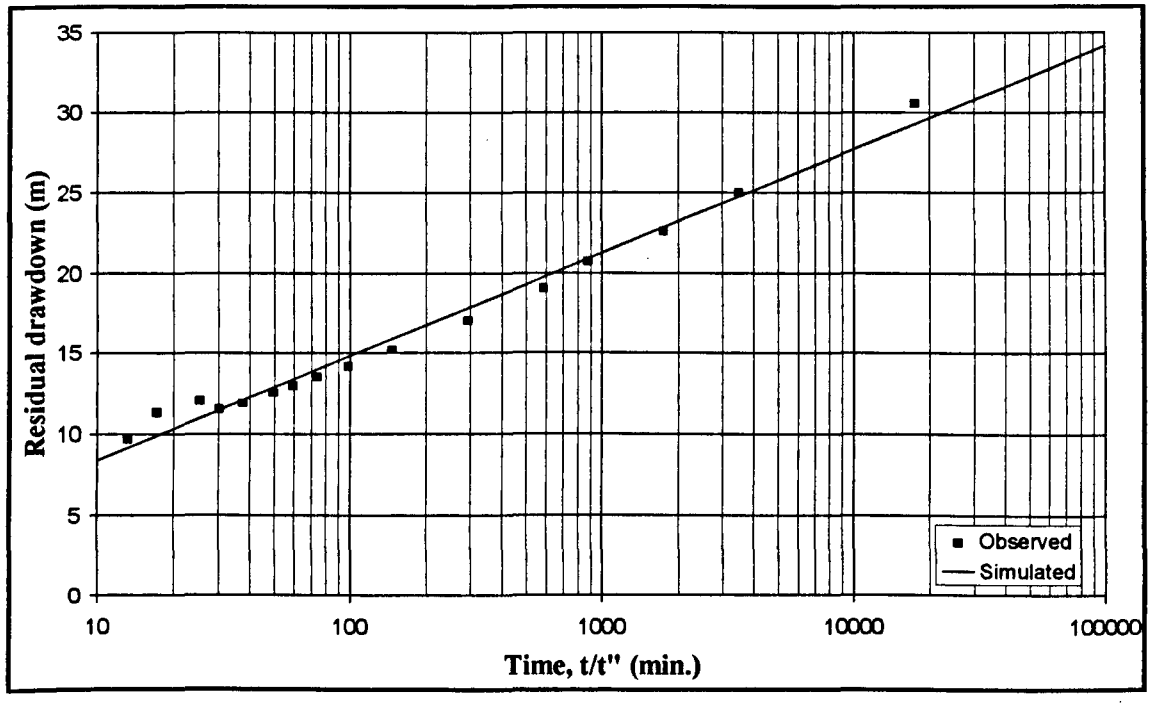


Figure 5.16: Fitted straight line through the observed residuals drawdown recorded after the first injection phase using Theis Recovery (1935) method.

The option of analysing the step-drawdown tests is not included in AQTESOLV; thus these tests were analysed manually using the Hantush-Bierschenk method.

**Hantush-Bierschenk method**

Hantush (1964) expresses the drawdown in a well during the n-th step of a step-drawdown test as:

$$s_{w(n)} \sum_{i=1}^{n} \Delta Q_i B(r_{ew}, t - t_i) + CQ_n^2 \qquad (5.4)$$

$s_{w(n)}$ = total drawdown in the well during the n-th step at time t

$r_{ew}$ = effective radius of the well

$t_i$ = time at which the i-th step begins ($t_1 = 0$)

$Q_n$ = constant discharge during the n-th step

$Q_i$ = constant discharge during the i-th step of that preceding the n-th step

$\Delta Q_i = Q_i - Q_{i-1}$ = discharge increment beginning at time $t_i$

The aquifer and well loss coefficients were determined by this method for the pre-injection and post-injection step-drawdown tests as follow;

1. Plot the observed drawdown in the well against the corresponding time on a semi-log paper,(t on the logarithmic scale)
2. Determine the increments of drawdown $\Delta s_{w(i)}$ for each step (Fig. 3.17).
3. Determine the values of $s_{w(n)}$ corresponding to the discharge $Q_n$ for each step, using $s_{w(n)} = \Delta s_{w(1)} + \Delta s_{w(2)} + \ldots + \Delta s_{w(n)}$
4. Plot the values of $s_{w(n)}/Q_n$, for each step against the corresponding values of $Q_n$ on arithmetic paper, and fit a straight line through the plotted points.
5. Determine the slop of the line, that will be the value of well loss coefficient (C), whereas, the interception point on the $s_{w(n)}/Q_n$, where Q = 0 is the aquifer loss coefficient (B).

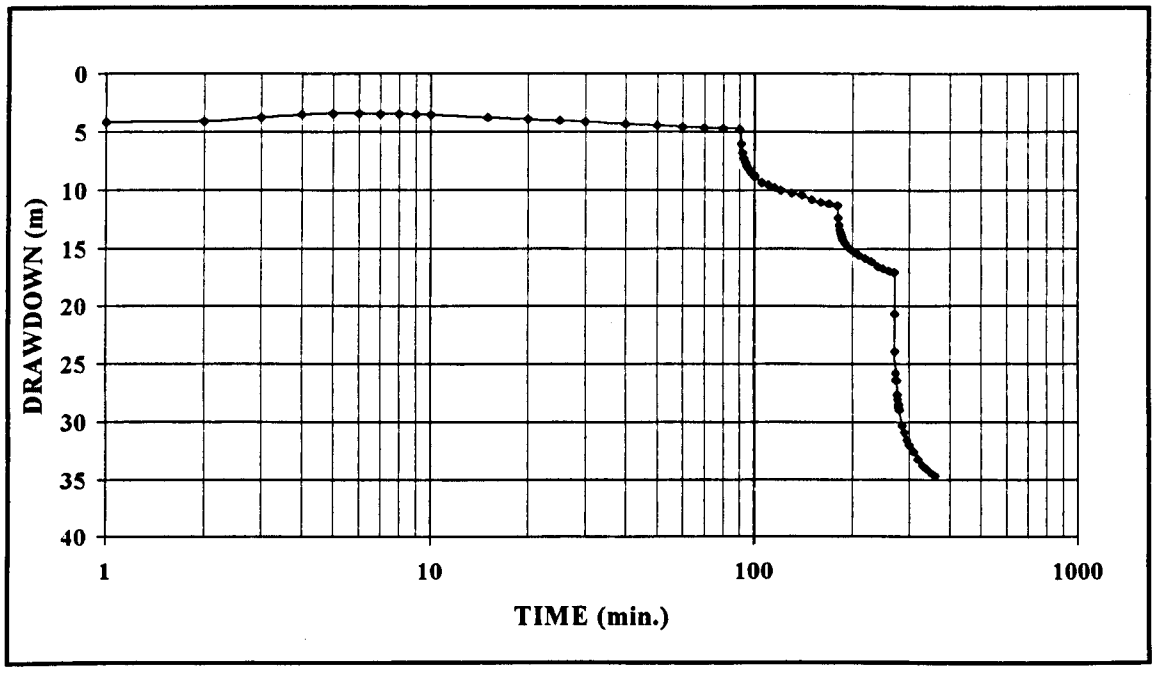


Figure 5.17: Plotted drawdown observed at the four steps during the pre-injection step-drawdown test.

Table 5.4 presents the pre-injection and post-injection step-drawdown tests data as determined using Hantush-Bierschenk method.

| | Pre-injection Test | | | | Post-injection | | | |
|---|---|---|---|---|---|---|---|---|
| | Step 1 | Step 2 | Step 3 | Step 4 | Step 1 | Step 2 | Step 3 | Step 4 |
| Discharge Rate $Q_n$ ($m^3/d$) | 262 | 587 | 883 | 1592 | 393 | 785 | 1178 | 1570 |
| Drawdown increment $\Delta s_{w(i)}$ (m) | 4.69 | 6.56 | 5.78 | 17.63 | 4.90 | 7.95 | 3.94 | 13.31 |
| $s_{w(n)}$, (m) | 4.69 | 11.25 | 17.03 | 34.66 | 4.92 | 12.85 | 16.79 | 30.1 |
| Specific Drawdown $s_{w(n)}/Q_n$ ($d/m^2$) | 0.018 | 0.019 | 0.0193 | 0.022 | 0.0125 | 0.0164 | 0.0142 | 0.019 |
| Aquifer loss coeff.(B) ($d/m^2$) | 0.017 | | | | 0.012 | | | |
| Well loss coeff. (C) ($d^2/m^5$) | 2.81 E-6 | | | | 5.46 E-6 | | | |

Table 5.4: Determined specific drawdown, and the estimated head loss coefficients with the Hantush-Bierschenk method for the pre-injection and post-injection step-drawdown tests.

Utilising the Hantush-Bierschenk's method in determining the head loss coefficients (B and C) using the pre-injection step-drawdown test was possible, where a straight line passing through all the plotted points of $s_{w(n)}/Q_n$ against $Q_n$ was drawn (Fig. 5.18). Whereas, the plotted points for the post-injection step-drawdown test are scattered. Thus, a straight line can be drawn only between the points of the first and the fourth steps, while other points were ignored (Fig. 5.18). The calculated aquifer (B) and well (C) losses coefficients are 0.017 $d/m^2$ and $2.81 \times 10^{-6}$ $d^2/m^5$, respectively for the pre-injection test, and 0.012 $d/m^2$ and $5.46 \times 10^{-6}$ $d^2/m^5$, respectively for the post-injection test.

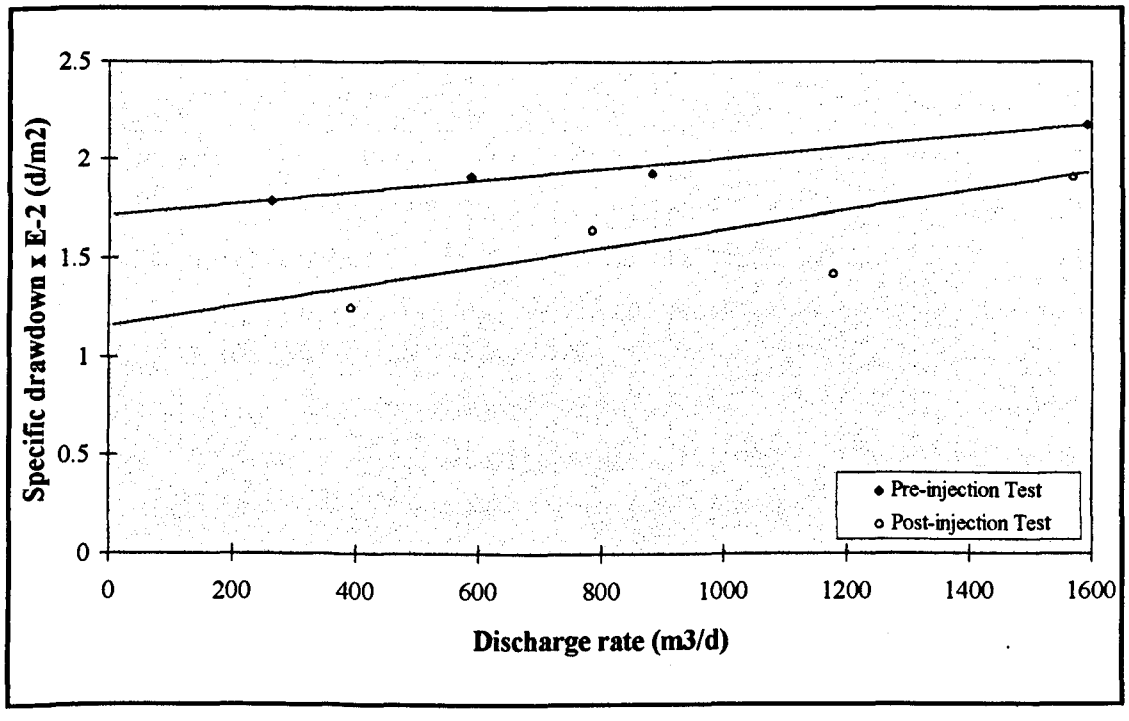


Figure 5.18: Determination of head loss coefficients (B and C) for the pre-injection and post-injection step-drawdown tests using Hantush-Bierschenk's method.

Table 5.5 summarises the obtained results from analysing the data of constant-rates, recovery, and step-drawdown tests carried out during this experiment.

| Number | Test | Duration (min.) | ΔH (m) | K (m/d) | Q ($m^3/d$) | B ($d/m^2$) | C ($d^2/m^5$) | S x $10^{-3}$ | Method of Analysis |
|---|---|---|---|---|---|---|---|---|---|
| ST-1 | Step-Drawdown Test Before Injection; | | | | | 0.017 | $2.81 \times 10^{-6}$ | | C |
| | Step 1 | 90 | - 4.69 | 0.32 | - 262 | | | | |
| | Step 2 | 90 | - 11.25 | 0.28 | - 587 | | | | |
| | Step 3 | 90 | - 17.03 | 0.18 | - 883 | | | | |
| | Step 4 | 90 | - 34.66 | 0.19 | - 1592 | | | | |
| PT-1 | Constant-Pumping Before Injection Started | 720 | - 22.54 | 0.21 | - 982 | | | 3 | A |
| REC-1 | Recovery after PT-1 | 720 | - 0.56 | 0.20 | | | | | B |
| INJ-1 | First Injection Period | 17460 | + 34.97 | | + 655 | | | | |
| REC-2 | Recovery after INJ-1 | 1440 | | 0.123 | | | | | B |
| ST-2 | Step-Drawdown Test after Injection Completed | | | | | 0.012 | $5.46 \times 10^{-6}$ | | C |
| | Step 1 | 90 | - 4.92 | | - 393 | | | | |
| | Step 2 | 90 | - 12.85 | | - 785 | | | | |
| | Step 3 | 90 | - 16.79 | | - 1178 | | | | |
| | Step 4 | 90 | - 30.1 | | - 1570 | | | | |
| PT-2 | Constant-Pumping after Injection Completed | 720 | - 18.49 | 0.24 | - 982 | | | 6 | A |
| REC-3 | Recovery after PT-2 | 720 | - 1.66 | 0.24 | | | | | B |

Table 5.5: Obtained Dammam aquifer parameters by pumping and recovery tests for Well SU-10.

A : Hantush-Jacob (1955), Leaky aquifer
B : Theis Recovery (1935), Confined aquifer
C : Hantush-Bierschenk

## 5.5 EVALUATION OF INJECTION-WITHDRAWAL EXPERIMENTAL DATA

### 5.5.1 HYDRAULIC RESULTS

The observed water levels in the injection well during periods of injection cannot be matched straight forwardly with the water levels obtained using the numerical model. The observed levels are much higher than the simulated ones. Figure 5.19 illustrates the build-up inside the recharge well, as observed and simulated during the injection test.

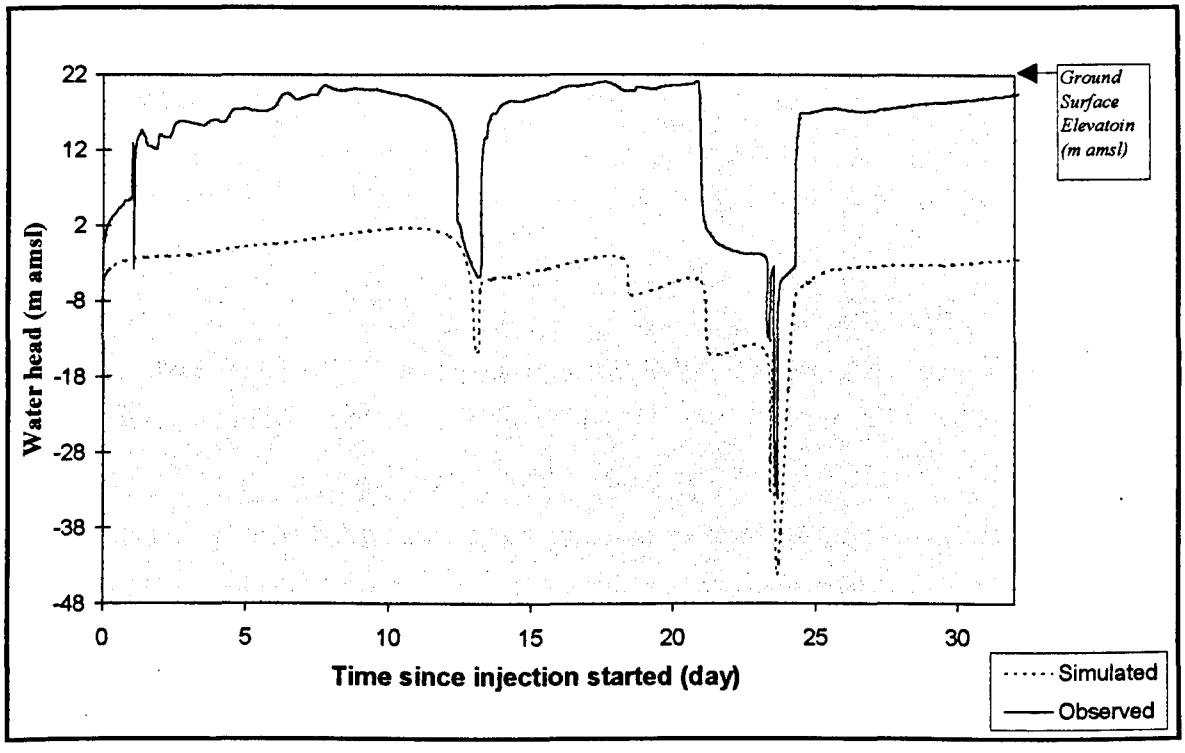


Figure 5.19: Difference between the simulated and the observed build-up inside the recharge well as obtained during the injection test, which is related to the effect of well face clogging.

It appears from Figure 5.19 that there is an additional well loss affecting the well under injection conditions. The injection head increased rapidly during the first hour to reach about 14 m, then it increased gradually at the end of the first day to reach 20 m. When the recharge water was changed to freshwater instead of brackish groundwater on the second day, the head increased again in the same manner as in the first day and reached about 26.7 m at the first half an hour of the second day. Then the increase in the head was gradual until

it reached about 27.5 m at the end of the first injection phase. The rise in the water level at the other two injection phases occurred in the same way as in first injection phase, increased very rapidly at the beginning and with moderate increase for the rest of the test. The additional rise in the observed head above that expected from the aquifer, is controlled by the injection rate and injection period. This difference increased as injection rate increased, with an average of about 0.7 of the simulated head. It was necessary to reduce the injection rate during the experiment as the recharge proceeded in order to maintain the water level inside the well below the land surface. This to avoid the technical problem which will hinder the completion of the injection process. As a result, the well injection capacity was reduced due to this rise in water head. A better indicator of well's injection capacity is its specific injection rate (SIR), which is defined as the injection rate divided by the rise of water table inside the well (Harpaz 1970).

### 5.5.2 WELL FACE CLOGGING

The difference between the simulated and the observed heads inside the injection well is due to the clogging of the well face. This problem is considered to be significant in limiting the use of injection wells for artificial groundwater recharge. In order to analyse the injection test data and to get a match between the simulated and the observed water head, the clogging factor should be quantified. The growth rate of clogging as a function of several factors should be identified. The clogging of the well face is due to many factors such as, inorganic precipitation of dissolved solids, bacterially-mediated deposition, and pore-blocking by suspended solids in the injected water. In addition, the presence of entrained air in the injected water, and ionic reactions that may result in dispersion of clay particles and swelling of colloids in a clastic aquifer, could also contribute significantly to clogging (Kimrey, 1989).

The recharged water in the present study was potable, which means it was chlorinated and contained a chlorine residual at sufficient levels to prevent bacterial growth; consequently bacterial processes are not likely to be a significant factor during the injection test. Also, the performed continuous injection time is less than 12 days, and hence it is not long enough for bacteria to grow, which takes at least 2 weeks for a colony to grow and seal the well face (Huisman, 1983).

If the injected water is incompatible with the aquifer's native water and minerology, then clogging due to chemical reactions may result, due to precipitation and ion-exchange. Mukhopadhyay et al. (1992), based on a thermodynamic computer model EQ3NR (Wolery, 1983), concluded that the mixture of potable recharge water with groundwater in the DM aquifer of the Sulaibiya wellfield is compatible. It is not expected to cause major problems in the formation of precipitates that may clog the pore spaces in the aquifer resulting in the reduction of its hydraulic conductivity. Also, their study suggests that the compatibility of the desalinated potable water with the DM limestone may not be significant in the clogging process.

The most critical cause of clogging the well face and formation pores close to the well is the particulate matter consisting dominantly of suspended solids carried by the recharge water. These suspended solids may deposit on the well face, and due to the high entrance velocity of recharge water into the aquifer, result in the clogging of the well face and aquifer pores close to the well, hence reducing injection rates. Because of the relatively small area in the well bore, particulate matter may clog the aquifer pores resulting in the reduction of the permeability of the aquifer near the well. The recharge water during this study contained very low suspended solids (about 0.2 mg/l). However, during the backpumping of the well after 20 days of injection, turbid yellowish brown water was recovered for the first half-an-hour of pumping, suggesting the deposition of suspended material like iron oxides derived from the water distribution network.

Entrapment of air bubbles in recharge water also could be another factor in causing well clogging. Gas binding in the aquifer may result from gas coming out of solution when the temperature of the injected water is less than the temperature of the native water (Baffa et al. 1965). Also, air mixed with the recharged water at the surface pipes entering the injection pipe can cause clogging. These pipes for this experiment have a large diameter (6 inch) which cannot be filled completely by the recharged water due to the low injection rate, thus the empty part of these pipes will be occupied by air.

#### 5.5.2.1 CLOGGING EVALUATION

The mathematical model (MODFLOW) does not include the effects of clogging during well injection. In order to reproduce the observed aquifer response during water injection and to evaluate the effect of clogging on the well injection capacity, the hydraulic conductivity of the aquifer in the vicinity of the well and the surrounding four nodes was reduced until a match between the observed and the simulated heads was achieved.

It was difficult to get a reasonable fit between the observed and the simulated water head for the all readings. This is due to the development of clogging which cannot be quantified precisely, because it is a function of time, and the hydraulic conductivity cannot be treated as a time dependent parameter. So, for each injection phase, the clogging which is very severe at the beginning of the injection was determined by reducing the hydraulic conductivity at the well node and the surrounding four nodes until the a match between the observed and the simulated head was achieved for the initial periods only. Later, the hydraulic conductivity was changed again to get a match between the simulated and observed level for subsequent periods. For matching the later periods, the last water head reading (at the end of the injection phase) was considered representative of the final degree of clogging. Thus, two values of the aquifer's hydraulic conductivity in the vicinity of the test well were obtained, at the beginning and at the end for each injection phase (the other nodes of the model still used the original calibrated value).

By relating the reduced hydraulic conductivity of the aquifer at a given time with the calibrated initial hydraulic conductivity of the aquifer (0.34 m/d), the percentage of reduction in aquifer hydraulic conductivity can be determined at this time. This percentage can be used to represent the clogging factor at a given time (dimensionless), which can be defined as;

$$\text{Clogging factor (t)} = 1 - (k_t / k_{init.}) \qquad (5.5)$$

where;

$k_t$ : Hydraulic conductivity of the aquifer at the vicinity of the test well at time (t), (L/T).

$k_{init.}$: Initial value of the aquifer hydraulic conductivity,

$k_{init.}$ = 0.34 m/d if the method of finding $k_t$ is numerical model.

$k_{init.}$ = 0.2 m/d if the method of finding $k_t$ is recovery test data analysis.

Table 5.6 presents the hydraulic conductivity of the DM aquifer at the well node and adjacent four nodes obtained using the numerical model through matching the simulated head inside the test well with the observed. The clogging factor calculated based on the new values of hydraulic conductivity and the initial values were also presented.

| Time (day) | $\Delta H$ (m) | $\Delta H_0$ (m) | $S_{CORR}$ (m) | Q ($m^3/d$) | S.I.R. $m^2/d$ | $K_t$ m/d | Clogging factor | Method of Analysis |
|---|---|---|---|---|---|---|---|---|
| 0.041 | 14.07 | 0 | 14.07 | 655 | 46.5 | 0.180 | 0.47 | First Injection 1* |
| 1 | 20.08 | -0.5 | 19.58 | 655 | 33.45 | 0.142 | 0.58 | |
| 1.02 | 27.2 | -0.5 | 26.7 | 655 | 24.53 | 0.092 | 0.73 | |
| 2 | 28.94 | -1.2 | 27.74 | 655 | 23.6 | 0.088 | 0.74 | |
| 3 | 30.73 | -2.11 | 28.62 | 655 | 22.8 | 0.085 | 0.75 | |
| 5 | 31.95 | -5.49 | 26.46 | 655 | 24.7 | 0.081 | 0.76 | |
| 7 | 33.27 | -6.26 | 27.01 | 655 | 24.2 | 0.078 | 0.77 | |
| 9 | 34.29 | -7.2 | 27.09 | 655 | 24.1 | 0.075 | 0.78 | |
| 12.125 | 35.97 | -8.48 | 27.49 | 655 | 23.8 | 0.068 | 0.80 | |
| 13.125 | 8.62 | -7.38 | 1.24 | 0 | 0 | 0.120 | 0.40 | Recovery data after 1st injection (2*) |
| 13.29 | 22.78 | -7.38 | 15.4 | 524 | 34 | 0.132 | 0.61 | Second Injection 1* |
| 15 | 33.59 | -9.37 | 24.22 | 524 | 21.64 | 0.075 | 0.78 | |
| 18 | 35.46 | -10.93 | 24.53 | 524 | 21.33 | 0.075 | 0.78 | |
| 19 | 35.04 | -11.26 | 23.78 | 393 | 16.53 | 0.061 | 0.82 | |
| 21 | 34.09 | -12.01 | 22.08 | 393 | 17.8 | 0.061 | 0.82 | |
| 24.3 | 28.5 | -11.74 | 16.76 | 589 | 35.6 | 0.170 | 0.50 | Third injection 1* |
| 26 | 31.44 | -13 | 18.44 | 589 | 31.94 | 0.153 | 0.55 | |
| 28 | 31.64 | -13.4 | 18.24 | 589 | 32.29 | 0.153 | 0.55 | |
| 30.97 | 33.09 | -14.56 | 18.53 | 589 | 31.79 | 0.153 | 0.55 | |
| 32.97 | 33.69 | -15.16 | 18.53 | 589 | 31.79 | 0.153 | 0.55 | |

Table 5.6: Measured and recovered water level rise during injection and the equivalent clogging factor for Well SU-10.

Figure 5.20 shows the development of clogging factor with time and its influence on the specific injection rate (SIR) of the test well during the injection test.

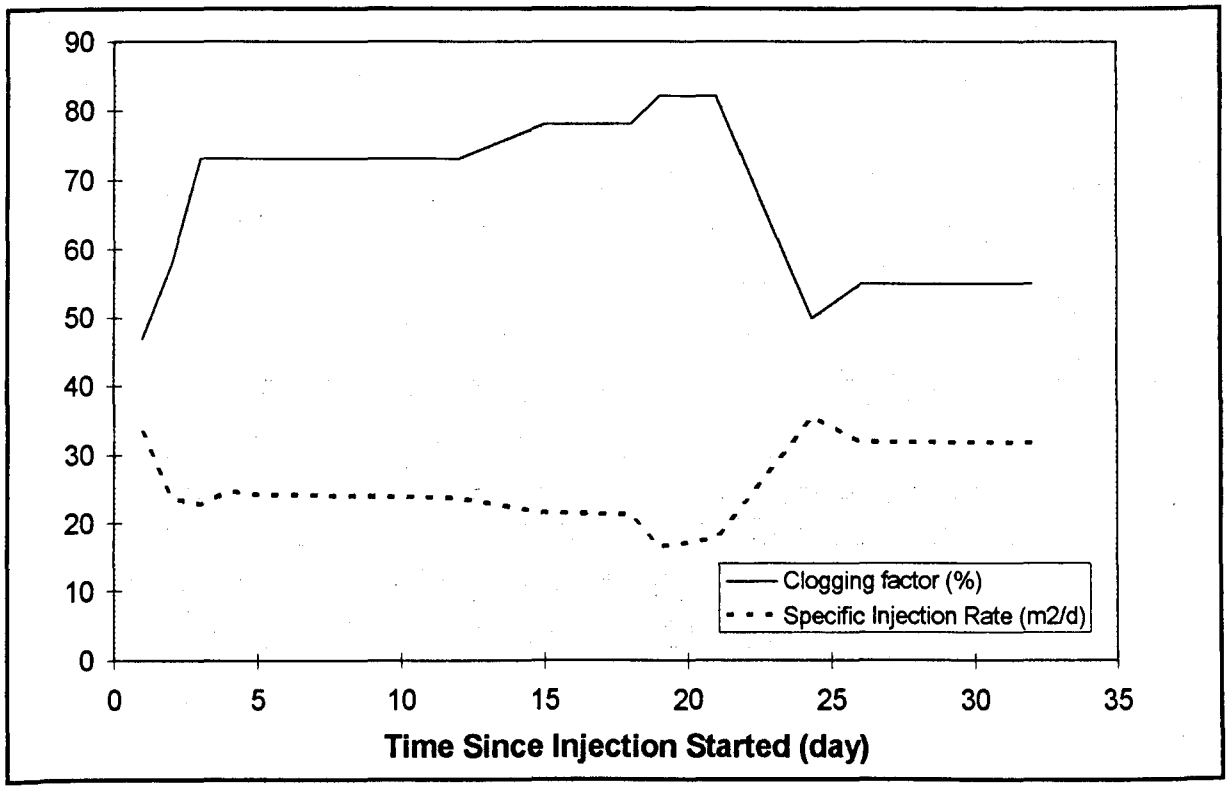


Figure 5.20: Development of well face clogging during the injection test, and the variation in SIR of the injection well as a result of this clogging.

From Figure 5.20, the effect of well face clogging in reducing the SIR of the well is clear. At the first two days of injection, the clogging factor was developed sharply to reach about 0.73, then it increased gradually to reach a maximum limit of 0.82 making further injection of water difficult. Later, after the well was developed, the clogging was reduced to about 0.4. During the third injection phase, the clogging factor was increased again to 0.5 at the first day of this phase, and increased gradually to reach 0.55 at the end of the injection test.

The SIR varied inversely with the increase of clogging factor, and vice versa. The SIR of the test well declined along with the cumulative injected amounts and with the duration of recharge. The initial SIR of the well was 46.5 $m^2/d$, however, it declined to 23.8 and 17.8 $m^2/d$ at the end of the first and second injection phases, respectively. After the well was developed through backpumping, the SIR was restored temporarily to reach 35.6 $m^2/d$, then it lowered again to 31.8 $m^2/d$ at the end of the injection test (Table 5.6).

Table 5.7 shows the observed drawdown during the long-term recovery, plus the corrected drawdown and the calculated specific well capacity.

| Time (day) | $\Delta H$ (m) | $\Delta H_0$ (m) | $S_{corr}$ (m) | Q ($m^3/d$) | Q/s ($m^2/d$) |
|---|---|---|---|---|---|
| 49 | -8.38 | -8.66 | 16.99 | -982 | -57.8 |
| 51 | -13.71 | -6.24 | -19.95 | -982 | -49.22 |
| 53 | -13 | -4.61 | -18.6 | -982 | -52 |
| 53.5 | -3.14 | -4.29 | -7.43 | -471 | -63.39 |
| 53.8 | -3.12 | -4.18 | -7.3 | -471 | -64.52 |
| 54 | -4.26 | -4.04 | -8.3 | -471 | -56.75 |
| 54.5 | -17.12 | -3.4 | -20.52 | -982 | -47.86 |
| 55 | -17.88 | -2.96 | -20.84 | -982 | -47.86 |
| 55.5 | -29.78 | -2.05 | -31.83 | -1408 | -44.24 |
| 56 | -31.65 | 1.01 | -32.66 | -1408 | -43.11 |
| 60.5 | -20.73 | -0.83 | -21.56 | -982 | -45.55 |
| 65 | -18.05 | -3.76 | -21.81 | -982 | -45.03 |
| 70 | -20.25 | -0.92 | -21.17 | -982 | -46.39 |
| 75 | -18.34 | -2.76 | -21.1 | -982 | -46.54 |
| 85 | -15.41 | -5.23 | -20.64 | -982 | -47.58 |
| 90 | -13.79 | -7.01 | -20.80 | -982 | -47.21 |
| 99.13 | -18.04 | -2.52 | -20.56 | -982 | -47.76 |

Table 5.7: Measured and corrected drawdown during the long-term recovery test.

### 5.5.2.2 DIFFERENTIATION BETWEEN CLOGGING CAUSES

The clogging factor determined above was under injection conditions. The residual clogging on the well face after the injection was terminated and the well was in a static situation is determined here. This is done by assuming that the resulting build-up during the injection test can be treated as equivalent to a drawdown measurement which occurred due to a constant-rate pumping test having the same duration and rate as the injection test. Thus, the following recovery of water heads can be analysed using the traditional analytical solutions for recovery tests to find the hydraulic conductivity of the aquifer. Hence, by

relating the calculated hydraulic conductivity using these data with the initial value (0.2 m/d) as determined previously by analysing the pre-injection recovery test data (which followed the pre-injection constant-rate pumping test), the clogging factor for the well at a static conditions can be quantified (using Equation 5.5). The recovery data following the first injection stage were analysed earlier (in section 5.4.2) using the Theis (1935) Recovery solution with AQTESOLV, where the aquifer hydraulic conductivity was found to be 0.123 m/d. Thus, the clogging factor was determined for the well in a static condition as being 0.35.

Because the injection test was not continuous and was interrupted by well development and injection with variable rates, the first injection phase was the only phase used in the differentiation between the two clogging processes. The first injection phase was completed in about 12 days with an approximately constant injection rate (655 $m^3/d$). On the other hand, the second injection phase was conducted with a variable injection rate, and hence the assumptions of Theis (1935) recovery solution cannot be met. The third injection phase was conducted after the well was developed which may change the status of the well and the nearby formation pores. Thus the known initial hydraulic conductivity of the aquifer (0.2 m/d) may have increased and becomes unreliable for comparison with the calculated hydraulic conductivity for the post-injection recovery test.

It was found that the clogging factor during the injection process is much higher than the calculated clogging under shut down conditions. This means that part of clogging occurred temporarily during the injection and disappeared when the injection was stopped. In order to differentiate between the possible causes of clogging based on this phenomenon, the following assumptions were applied:

1. Total clogging of the well face is caused by air entrapment, and deposition of suspended solids.
2. Clogging developed during the first hour of injection is completely caused by air entrapment. This was proved by the sudden and abrupt build-up in the water level in the injection well. This occurred at the first hour during the second day of injection when the recharge source was switched from groundwater to freshwater, with lower suspended solids. This means that the additional rise in water head cannot be related to deposition

of suspended solids and is more likely caused by the entrance of air in the injection pipe as a result of opening of the freshwater network.

3. Temporary clogging could be caused by the air entrapment during the injection which disappears when the injection stops.
4. The remaining clogging which was determined under static conditions by the recovery test data is entirely due to the suspended solids.
5. The total clogging which was determined at the end of the injection period and immediately before the injection was stopped is composed of the suspended matter which is calculated by the recovery test, and from the clogging caused by air entrapment.
6. The clogging due to suspended solids is developed in a linear relationship (Huisman, 1983).

In order to differentiate between the two clogging causes (deposition of suspended solids, and air entrapment), the following steps were followed;

1. Determine the total clogging factor for the first day of the injection test using the numerical model, and ascribe this degree of clogging entirely to air entrapment ("air entrapment cause").
2. Determine the clogging factor at the end of injection period (immediately before the injection is stopped) using the numerical model, and assume this is due to a combination of both air entrapment and suspended solids ("mixed causes").
3. Determine the clogging factor during the recovery after the injection was completed, and attribute this to the accumulated suspended solids ("suspended solids cause").
4. Now back-calculate using the "mixed causes" value determined at the last period of injection to separate the two causes. Clogging due to suspended solids will be assigned as being equal to the "suspended solids cause" (determined at 3), and the rest will be referred to the air "entrapment cause".
5. Draw a straight line between the two values of clogging as caused by air entrapment, the first value (determined at 1) and the last value (determined at 4).

From this analysis, it is possible to find the causes of well face clogging limiting the water injection. Figure 5.21 shows the development of clogging factor during the first injection period, and its possible causes.

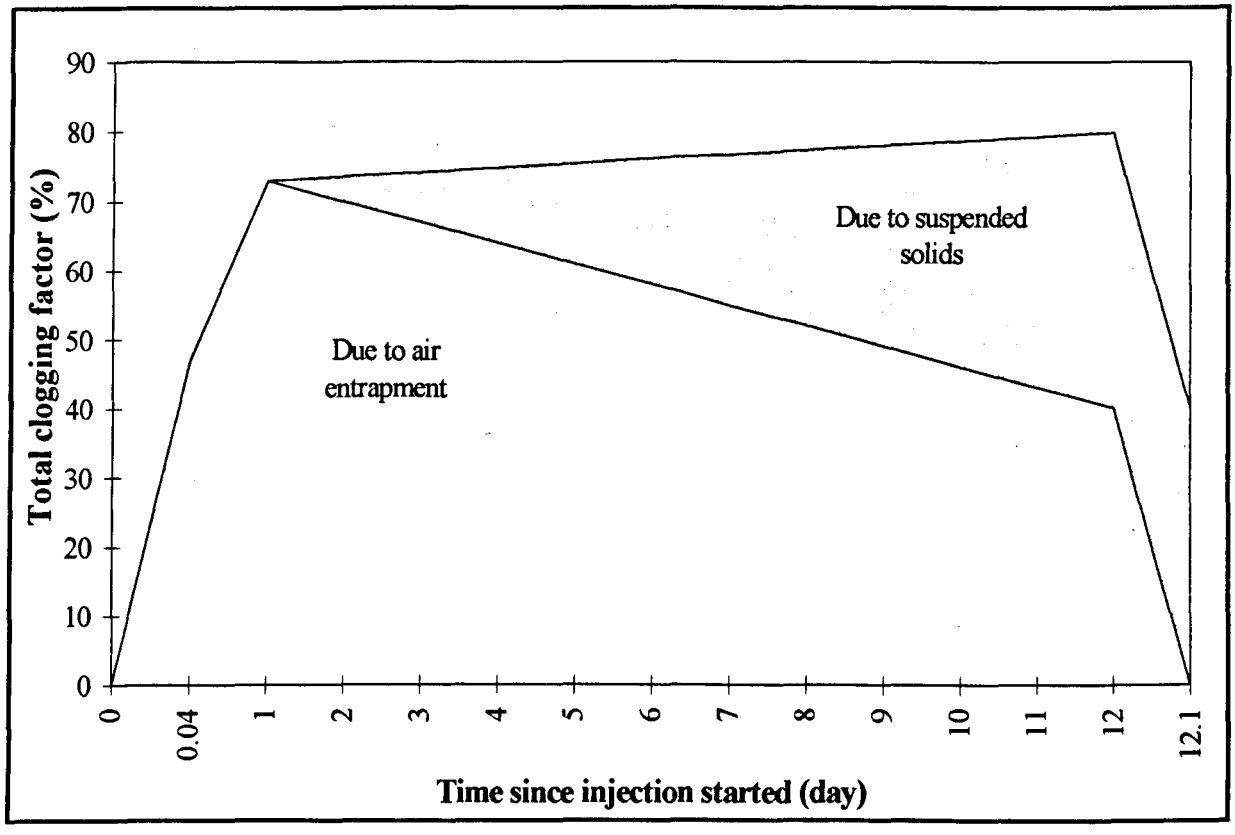


Figure 5.21: Development of well face clogging during the water injection resulting from the possible two causes, suspended solids and air entrapment.

It was clear that most of the clogging occurred due to air entrapment, and not due to the formation or recharge water properties. This means that the clogging during this experiment is probably due to the injection system, introducing air bubbles in the recharge water. Therefore, if this can be avoided in the future, the injection capacity of the well can be increased.

The step-drawdown tests can be used to determine the change in aquifer and well conditions as a result of water injection. The use of the Hantush-Bierschenk method (as explained in section 5.4.2) for determining the head loss coefficients (B and C) using the pre-injection step-drawdown test was successful. However, applying the same method to determine the head loss coefficients using the post-injection step-drawdown test data was less reliable. This was shown by the distribution of scatter points of specific drawdown (Fig.

5.18), which means that the well may become unstable after completing the well injection experiment.

The calculated aquifer (B) and well (C) loss coefficients using the pre-injection step-drawdown test are 0.017 $d/m^2$, and $2.81 \times 10^{-6}$ $d^2/m^5$, whereas these coefficients after the injection was completed are 0.012 $d/m^2$, and $5.46 \times 10^{-6}$ $d^2/m^5$, respectively. The comparison between the estimated head loss coefficients before and after the injection, indicates that the well loss increased after the injection to twice its value before the injection. Hence, this may be related to the effect of well face clogging. However, aquifer loss after the injection is less than its value before the injection, which may indicate the possibility of improvement in the aquifer hydraulic conductivity around the well.

The improvement in the aquifer hydraulic conductivity which occurred after the completion of injection was also verified by the calculated values using the post-injection constant-rate and recovery tests which is approximately 0.25 m/d. This value is higher than the calculated hydraulic conductivity using the pre-injection pumping test, which was found to be 0.2 m/d.

The increase in the aquifer hydraulic conductivity around the well may be due to the development of the well which was carried out before the injection finished with about 9 days. Also, it could be related to the dissolution of some formation minerals such as calcite during the injection process, especially given the highly corrosive nature of the recharge water. Unfortunately, the chemical analysis of the recovered water samples did not consider a specific determination for the dissolved substances independently, (the total dissolved solids was provided only). Thus, the possibility of calcite dissolution cannot be assessed using the available sampling data about the recovered water composition.

It is more likely that clogging of the well occurred at its inner wall and did not penetrate the aquifer for a long distance to clog its pores, and it is mainly due to air entrapment. This conclusion was confirmed by the ease of developing the well. After the well was developed after 20 day of injection, the well capacity was restored with simple backwashing for a few hours. Also, during the long-term recovery the well reached its initial specific pumping capacity (47 $m^2/d$) during the normal production rate of the well, which means that no serious damage has occurred to the well.

### 5.5.3 TRANSPORT SIMULATION

The storage of freshwater in brackish aquifers is a miscible displacement process. Thus, if the objective of artificial groundwater recharge is to store freshwater for subsequent use, the quality of the recovered water will be a critical issue. The success of artificial recharge practice will be evaluated according to the expected recovery efficiency, which is defined as the volume of usable water which can be recovered relative to the total injected volume. The most significant factors affecting recovery efficiency are; mechanical dispersion, molecular diffusion, gravity segregation, and background hydraulic down-gradients (Kumar and Kimbler, 1970; Merritt, 1985). For any mathematical description of freshwater storage in saline aquifers, these factors should be considered.

If freshwater is injected through a well into a brackish aquifer, it will displace the native water away from the injection well. As the interface between the freshwater and brackish water moves in the aquifer, the mixing between the two fluids will generate a transition or mixed zone in which the composition of either fluid will vary from 100 % to 0 %. The mixing of the two fluids takes place as a result of diffusion and dispersion. The diffusion arises from the random motion of the molecules of the two fluids. The mechanical dispersion is the process whereby some of the injected fluid spreads beyond the spatial limits of its displacement volume while some of the resident fluid remains within these spatial limits. Well-defined bulk displacement does not occur because movement of fluid outward from the well is through a number of discrete pathways which vary in size and tortuosity, and flow varies within the cross section of each one (Merritt, 1985). Thus, at the transition zone, the aquifer pores are filled with a mixture of freshwater and native water. When the injected water is pumped back, the size of this transition zone will determine the recovery efficiency of the injected water. As thickness of the transition zone gets narrower, the mixing is smaller and hence the recovery efficiency will be higher.

Groundwater flow modelling is based on the concept of the equivalent homogeneous porous medium by which it is assumed that the real heterogeneous aquifer can be simulated as a homogeneous porous medium at the scale of cells or elements. Then, the average linear velocity is defined using a bulk average hydraulic conductivity for each cell. The aquifer response is however, strongly influenced by the presence of local heterogeneities that cause

deviations from the average linear velocity. These deviations are assumed to be represented by dispersion (Anderson and Woessner, 1992). When dispersion acts primarily in the direction of gross fluid movement, it is called "longitudinal dispersion", and if it acts in a direction perpendicular to gross fluid movement, it is called "transverse dispersion".

The mechanical dispersion and molecular diffusion can be represented together by the hydrodynamic dispersion coefficient. The molecular diffusion effect is generally secondary and negligible compared to the mechanical dispersion effect (Diffusion becomes significant when groundwater velocity is very low; Zheng, 1990).

Gravity segregation occurs when two miscible fluids of different densities are in contact. With the passing of time, the fluid with the higher density will sink and spread along the bottom, whereas, the lighter fluid will rise (Esmail and Kimbler, 1967).

In this experiment, the contrast between the densities of the recharged water and the native water is insignificant. The initial TDS of the groundwater at the test well is 4500 mg/l. Whereas, the TDS of the recharged water ranged between 350-400 mg/l. Thus, the most important factor which is affecting the recovery efficiency at the study area is the mechanical dispersion.

The constructed single-well model was used to estimate the aquifer dispersivity, and hence to simulate the behaviour of the injected water and the produced transition zone between the two fluids. Accordingly, the recovery efficiency was determined. The recorded TDS of the recovered water at the test well during the long-term recovery was used as a target in calibrating the transport model.

The three-dimensional transport model MT3D ( Zheng, 1990) was used in this simulation. The numerical solution which is implemented in this software is a mixed Eulerian-Lagrangian method. The Lagrangian part of the method provides three options for solving the advection term. The Method Of Characteristics (MOC) employs forward-tracking, the Modified Method Of Characteristics (MMOC) applies backward-tracking modified, and a third method is a hybrid of these two.

The Eulerian part of the method (used for solving the dispersion and chemical reactions term in Equation II-3, Appendix-II), utilises a conventional block-centred finite-difference method. The MOC technique solves the advection term with a set of moving particles, and eliminates numerical dispersion for sharp front problems. However, it needs to track a large number of moving particles especially for three-dimensional simulations, which consumes a large amount of computer memory and execution time. The (MMOC) approximates the advection term by directly tracking the model points of a fixed grid backward in time, and by using interpolation techniques. The MMOC technique eliminates the need to track and maintain a large number of moving particles. Therefore, it requires much less computer memory and is generally more efficient computationally than MOC, but it has the disadvantage of introducing some numerical dispersion at the sharp concentration fronts. The hybrid MOC/MMOC technique combines the strengths of MOC and MMOC based on automatic adaptation (DCHMOC) of the solution process to the nature of concentration field. When sharp concentration fronts are present, the advection term is solved by forward-tracking MOC through the use of moving particles dynamically distributed around each front. Away from such fronts, the advection term is solved by the MMOC technique with nodal points directly tracked backward in time. When a front dissipates due to dispersion, the forward tracking stops automatically and the corresponding particles are removed (Zheng, 1990).

In this simulation, the hybrid MOC/MMOC technique was used because close to the well, a sharp concentration front will exist during the injection and recovery cycles. Whereas, far away from the wells, concentration fronts will be smoother.

Since any particle tracking scheme requires the evaluation of velocity at an arbitrary point in a flow domain, the first step in particle tracking calculation is to construct a velocity interpolation scheme based on the hydraulic heads calculated by the flow model at the nodes of the finite-difference cells. For particles located in areas of relatively uniform velocity, the first-order Eulerian algorithm is sufficient accurate. However, for particles located in areas of strongly converging or diverging flow (for example, near sources or sinks), the first order algorithm may not be sufficiently accurate, unless $\Delta t$ is very small. In this case a higher order fourth-order Runge-Kutta method can be used. The basic idea of

this method is to evaluate the velocity four times for each step; once at the initial point, twice at two trail midpoints, and one at a trail end point. A weighted velocity based on values evaluated at these four points is then used to move the particle to the new position. The fourth-order Runge-Kutta algorithm is normally more accurate and permits the use of larger time steps. However, it requires more computational effort than is required by the first-order Eulerian algorithm, making it far less efficient than the latter for three-dimensional simulations (Zheng, 1993).

MT3D has these two options of interpolation algorithms, in addition to a mixed option combining them together in which the Runge-Kutta algorithm is used in sink/sources, otherwise the Eulerian algorithm is used. In this simulation the particle tracking algorithm used is the mixed option to ensure sufficient accuracy throughout the finite-difference grid without the need to use such small time steps.

The MT3D transport model uses an explicit version of the block-centred finite-difference method to solve the dispersion terms.

The following model parameters were determined through trial-and-error for the successful running of the model :

- Concentration weighting factor (WD) = 0.5
- Negligible relative concentration gradient (DCEPS) = 0.0001
- Pattern for initial placement of particles (NPLANE) = 0
- Number of particles per cell (in case of DCCELL <= DCEPS) = 1
- Number of particles per cell (in case of DCCELL > DCEPS) = 16
- Minimum number of particles allowed per cell (NPMIN) = 4
- Maximum number of particles allowed per cell (NPMAX) = 32
- Multiplier for particles number at source cells (SRMULT) = 1
- Pattern of displacement of particles for sink cells (NLSINK) = 1
- Number of particles used to approximate sinks cells (NPSINK) = 9
- Criteria for controlling the selective use of either MOC or MMOC in the HMOC solution scheme (DCHMOC) = 0.001

The transport model boundaries were assigned as a constant-mass located at constant-head boundaries as in the flow model. Due to the small grid spacing used, a small transport time step was essential to avoid the numerical instability in the solution which can be measured by the large mass balance discrepancies. A small transport time step requires a large amount of computer memory and execution time. Thus, the largest initial optimum transport step size under which the mass discrepancy error did not occur, was 0.001 day. During execution, it was increased proportionally to 0.05 day. Though, it was decreased again whenever there was a change in the status of the test, like changing the operation from recharge to discharge, or increasing, or lowering the recharge or discharge rates. The transport simulation was achieved with very minimum mass discrepancy error, ranged from 0.001% to 0.2 %, which is a satisfactory result.

The freshwater injection-recovery simulation scenario was as follows: Freshwater with a TDS of 350 mg/l was injected into the DM aquifer having a TDS of 4500 mg/l for about 30 days (injection rate was varied during this period; as shown in Table 5.1), and after a delay of about 13 days, it was recovered back from the same injection well at a rate of 982 $m^3/d$ for about 70 days. The initial injection of brackish water was neglected during the simulation because it was for a very short period (1 day). The flow was simulated using MODFLOW, and the heads, fluxes across cell interfaces in all directions, and location and flow rate of the test well were saved in unformatted head and flow files. Then MT3D was run for the transport solution using the outputs generated by MODFLOW.

In order to use a mass fraction during the transport simulation instead of the actual TDS, the concentration of the injected water was assigned as ($C_0$= 1), whereas the TDS of the native water is (C = 0). Thus, the mass fraction of injectant (which is the mass of injected water in a water sample to total mass of the water sample) was simulated as a function of time producing a breakthrough curve. The observed TDS of the recovered water was converted to mass fraction consisting of different proportions of native groundwater (which has a TDS of 4500 mg/l) and injected freshwater (with a TDS of 350 mg/l). The sampled TDS during the recovery stage only was considered. The TDS of injected water during the injection stage was ignored, because during water injection, the water was sampled at the

injected well, and hence it will not be accurately representing the change in aquifer water quality.

The effective porosity of the aquifer is a very sensitive parameter in changing the transport simulation results. This parameter is not accurately determined for the aquifers in Kuwait. Hence, two values (0.05 and 0.1 representing lower and higher limits) were used in the model to determine the dispersivity of the aquifer.

To estimate the aquifer dispersivity, one porosity value was used first, while the other aquifer parameters were held constant. Through trial-and-error, the dispersivity under which the observed and the simulated mass fractions (breakthrough curves) of recovered water can be matched, was selected. Then, the other limit of aquifer porosity was used to find a new value of dispersivity. The match between the observed and the simulated breakthrough curves of water TDS was achieved with two different values of porosity and dispersivity. Under the low porosity (0.05), the estimated longitudinal dispersivity was found to be 4 m; with a porosity of (0.1), the dispersivity was 2.2 m. Thus, the same match between the observed and simulated breakthrough curves can be achieved either with high aquifer porosity and low dispersivity, or vice versa. This means that there is an inverse relationship between the porosity and the dispersivity to get the same recovery efficiency. Due to absence of any data about the ratio of the transverse dispersivity to the longitudinal dispersivity, it was assumed to be constant at 0.1.

Figure 5.22 shows the achieved match between the time distribution of the simulated and the observed breakthrough curve of recovered water relative concentration.

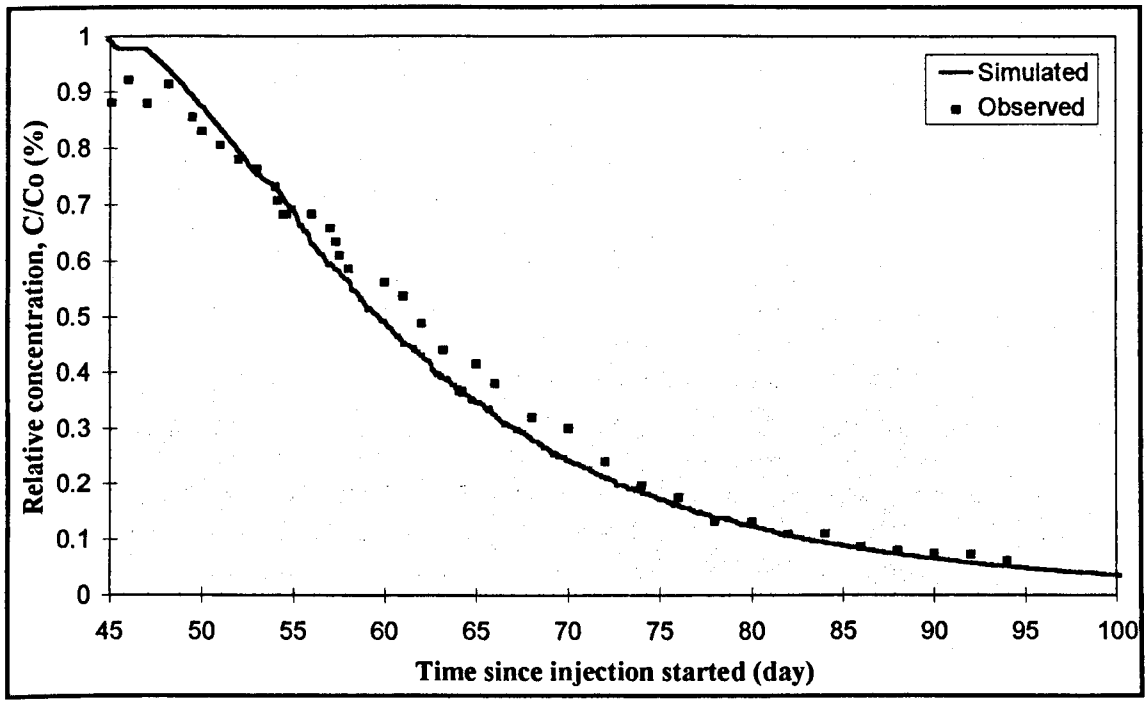


Figure 5.22: Simulated versus observed breakthrough curve of recovered water relative concentration.

The injected water was pumped after a delay of 13 days, which lowered the relative concentration around the well from 1 (representing freshwater), found directly after the injection was stopped, to about 0.97 at the beginning of the recovery stage. The water was recovered for about three days with this relative concentration. Later, its relative concentration was decreased gradually to reach the zero level after about 60 days of pumping. The 0.5 relative concentration was approached after 15 days of pumping.

During initial stages of recovery, there is a slight shift for the observed concentration measurements from the simulated breakthrough curve, whereas the last readings were matched closely. The early deviation could be related to the vertical variation in the clogging development. The clogging of the well face will not be a uniform mechanism in the vertical section due to the variation in aquifer properties at this scale. The heavily-clogged ones will respond to the pumping very slowly, whereas the less clogged zones will respond rapidly. As the pumping proceeds and clogging starts clearing with the pumped water, more zones open and contribute to better water quality compared to water that comes from the zones with less clogging which have already drained their good water earlier. This was clear from the fluctuation in TDS with time; it lowered and then improved again. After about 16

days (which may be the time where the clogging was completely removed from the well face), the whole aquifer starts to respond equally. The fluctuation in water TDS disappeared and the match between the observed and simulated TDS was more reasonable.

Figure 5.23 shows the simulated relative concentration around the injection well after the freshwater injection was completed. It indicates that pure injected freshwater does not move far from the injection well (about 8 m), because of the short period of injection, and low transmissivity of the aquifer. The length of the mixing zone is about 30 m, where the zone representing the equal mixing (50 %) between the two fluids is located at (25 m) from the well. The native water is at 40 m distance from the well, where the injected water does not reach.

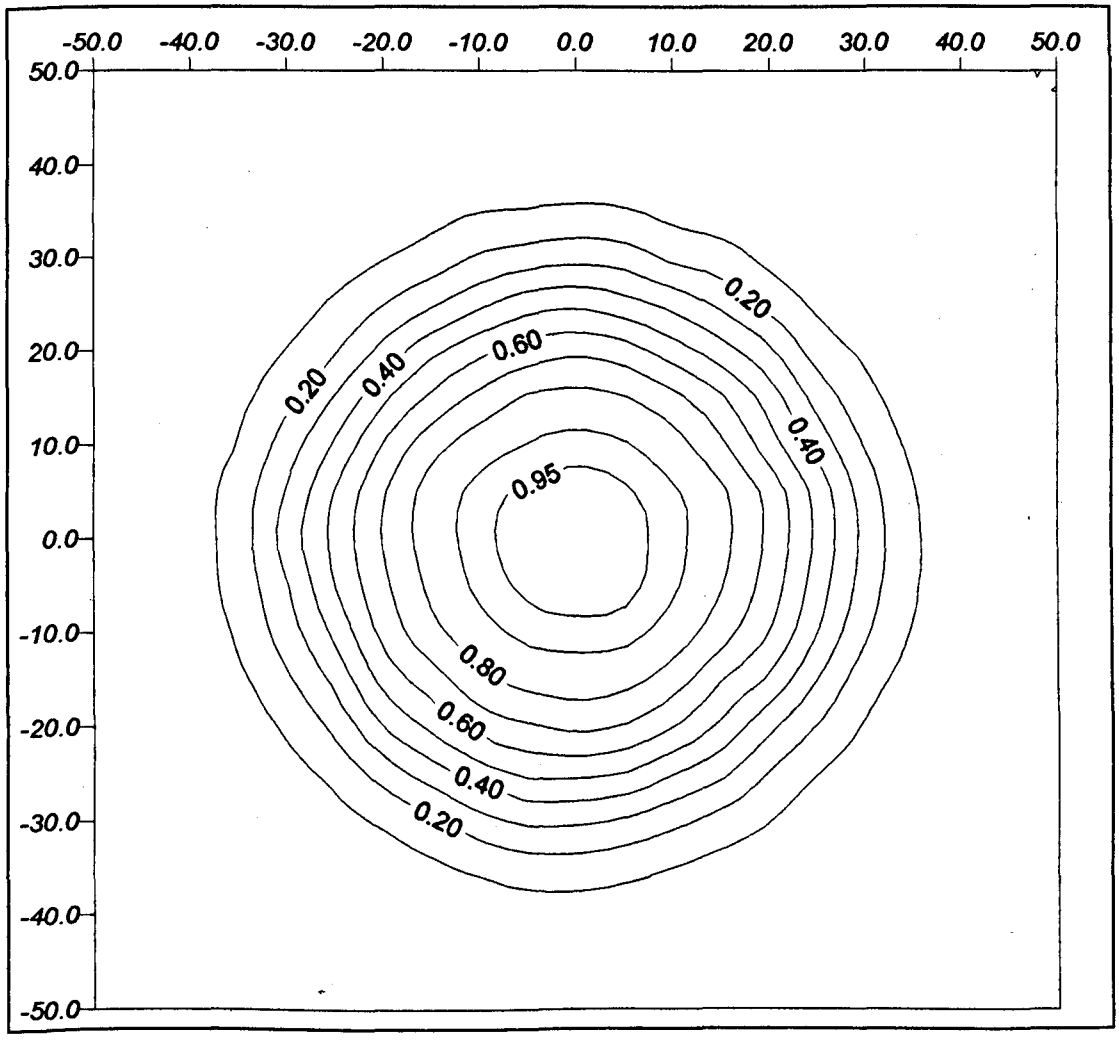


Figure 5.23: Simulated relative concentration ($C/C_0$) around the test well after the freshwater injection was completed.

The model was also run using the actual TDS of the injected freshwater and native water instead of using the relative concentration to find the recovery efficiency of the injection process.

The objective of artificial recharge in Kuwait is to store freshwater and recover it back with a TDS of 1500 mg/l or less, which is the maximum allowable TDS for drinking use (WHO, 1969). Hence during this experiment, the recovery efficiency at this TDS was observed to be 20 % (Table 5.8).

From sensitivity analysis, it was found that the recovery efficiency increases as the porosity and dispersivity of the aquifer decrease. Both porosity and dispersivity could be manipulated to produce approximately the same recovery efficiency. This was also indicated during the calibration of the transport model to find the dispersivity of the aquifer, where the reduction of dispersivity to half requires increasing the dispersivity by 1.8 to obtain the same recovery efficiency. If either the effective porosity or dispersivity of the aquifer are reduced to the half, then the recovery will be increased (Table 5.8).

| TDS of recovered water (mg/l) | Recovery efficiency using original aquifer parameters | Recovery efficiency with reduction in porosity by 0.5 | Recovery efficiency with reduction in dispersivity by 0.5 |
|---|---|---|---|
| < 500 | 0.6 | 1.3 | 1.4 |
| < 1000 | 8.5 | 17 | 17.5 |
| < 1500 | 20 | 32.5 | 33 |
| < 2000 | 37.5 | 49 | 50 |
| < 2500 | 58.5 | 70 | 71 |
| < 3000 | 88 | 97 | 98 |
| < 3250 | 100 | > 100 | > 100 |

Table 5.8: Simulated recovery efficiency using the calibrated aquifer parameters, and increase in the recovery efficiency which can result if the effective porosity or dispersivity of the aquifer are reduced to half of their original values.

Figure 5.24 displays the simulated recovery efficiency using the original calibrated aquifer parameters, and the recovery efficiency produced by reducing the aquifer effective porosity to half while keeping the other aquifer parameters unchanged. Because the obtained recovery efficiencies through reducing the porosity or the dispersivity of the aquifer are

relatively similar (Table 5.8), thus for clarity in presenting the recovery efficiency curves, this figure includes the recovery efficiency resulting from reducing the aquifer porosity only.

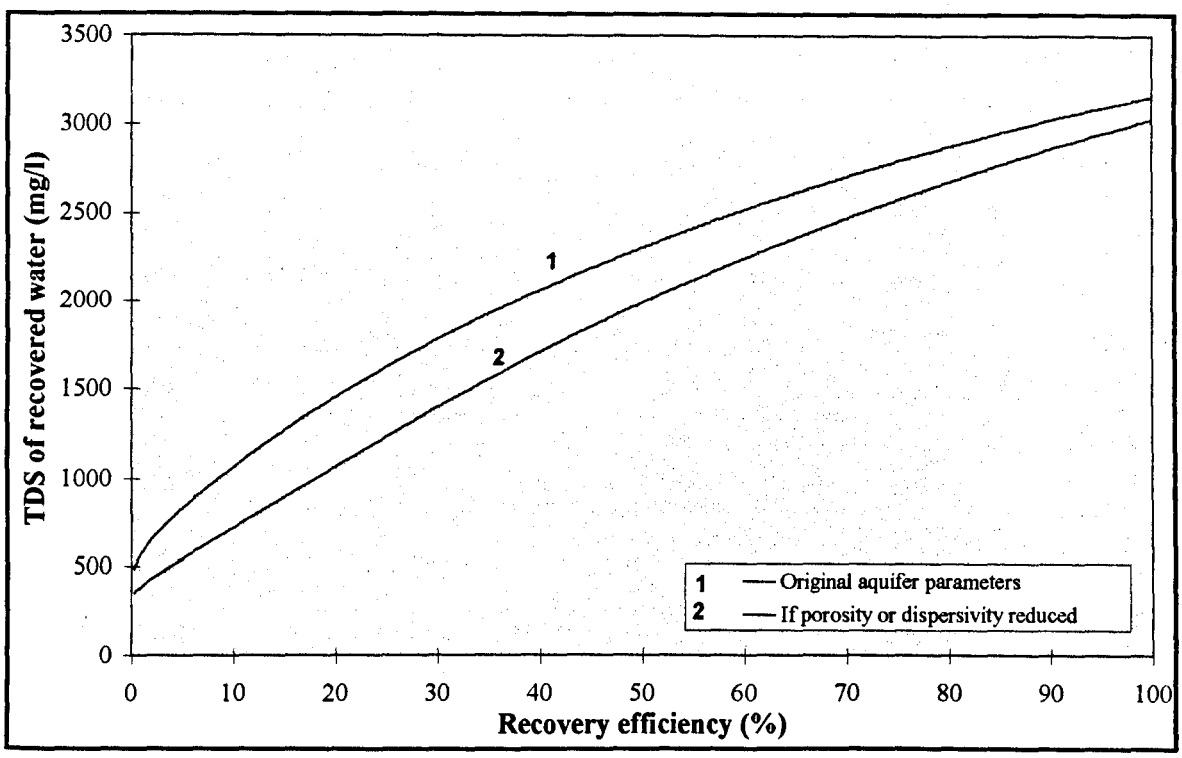


Figure 5.24: Simulated recovery efficiency using the calibrated aquifer parameters, and recovery efficiency resulting from reducing the aquifer porosity to half of its original calibrated value.

It was noticed from Table (5.8), that the improvement in the recovery efficiency is high at low values of TDS, and is lowered as the TDS increases (Table 5.9).

| TDS of recovered water (mg/l) | Percentage of improvement in recovery efficiency, if porosity or dispersivity reduced to 0.5 of their original values |
|---|---|
| < 500 | > 100 |
| < 1000 | 100 |
| < 1500 | 65 |
| < 2000 | 33 |
| < 2500 | 19 |
| < 3000 | 11 |

Table 5.9: Percentage of improvement in recovery efficiency with the TDS of recovered water TDS.

# 6. OPTIONS FOR AQUIFER STORAGE AND RECOVERY

## *6.1 INTRODUCTION*

Artificial groundwater recharge could be a viable management option for Kuwait based on the current and the expected overdraft of the aquifers, the availability of freshwater for artificial groundwater recharge, and anticipated water demand during emergencies.

In this study, three major motivations for aquifer storage and recovery are identified. These are:

1. To improve the water system operation efficiency.
2. To develop a long-term underground strategic reserve.
3. To improve the aquifer yield from the existing brackish wellfields.

Most of the urban potable water comes from sea water desalination plants. These plants have fixed optimal operational capacities. Operation of desalination plants at other outputs results in sub-optimal efficiencies. Water demand, however, varies significantly between summer and winter seasons. Hence, for most of the year, desalination plants are operating at poor or low efficiency. Short-term storage could help even out the seasonal demand fluctuations which would result in better operational efficiencies of the desalination plants. The first objective of aquifer storage and recovery is to provide such seasonal storage.

Kuwait, being an arid country, has no rivers, canals or lakes. Hence an emergency reserve of water would be essential in the event of emergency conditions such as :

1- Sea water pollution

2- Mechanical failure of desalination plants

3- Vandalism or terrorist activities resulting in partial or total loss of desalination plant capacity.

Underground artificial storage of potable water, safe from the above dangers, could be developed by injecting the excess desalinated water in an appropriate aquifer over a period of time, resulting in the development of a large storage capacity.

The third motivation concerns replenishment and restoration of the existing, depleted brackish aquifers. Artificial recharge and storage in such aquifers will result in the rise of the depleted potentiometric heads. This will lead to the following:

1- Decreasing the possibility of salt water upconing.
2- Reduce the lateral movement of saline water.
3- Continued use of wells which would otherwise be abandoned due to declining water levels
4- Reduced pumping costs.

In this chapter the suitable target aquifer is identified. Then all the available sites for storage and recovery are ranked according to the transmissivity of the aquifer, specific injection rates of the recharge wells in the site, and the recovery efficiency. General criteria, as well as specific criteria, are used to select the most appropriate sites (one for seasonal storage, and one for long-term storage). The regional model (in Chapter 4) is used to predict the hydraulic and transport responses of the selected aquifer to water injection and recovery at the ranked sites.

## 6.2 SELECTION OF THE TARGET AQUIFER FOR ARTIFICIAL RECHARGE

The Kuwait Group and the Dammam limestone are the two aquifers that produce usable water in Kuwait and are available potentially for artificial recharge.

As indicated by the injection-withdrawal experiment conducted for the KG aquifer at well SU-135, the Kuwait Group aquifer may be less viable for the artificial groundwater recharge. During this experiment the well was injected for three days only and the injection had to be stopped because of severe clogging of injection well screens. Therefore, this will reduce the injection capacity of the well with time resulting in the extensive well

development including surging and pumping to improve the well injection capacity, which is a costly and time-consuming process.

In addition, the hydraulic conductivity of the KG aquifer may deteriorate during injection because of the swelling of montmorillonitic clay present in the aquifer especially in the southern part of Kuwait (Khalaf et al., 1989).

The water injection-recovery experiment at well SU-135 gave a bad indication about the liability of the Kuwait Group aquifer to clogging, which of course will reduce its capability in accepting recharge water. However, the general description that this aquifer is not a suitable for artificial recharge based on clogging results obtained locally at Well SU-135, may be an unwise judgement. Thus, the aquifer could be appropriate at other locations, but in general because its clastic nature, it will be more subjected to clogging more than the fractured Dammam limestone aquifer.

On the other hand, the KG aquifer seems to have low dispersivity, suggesting a potentially high recovery efficiency for the aquifer. Hence, if remedial measures could be developed to prevent or reduce the clogging of the well screen, the aquifer could be appropriate for artificial recharge, especially for storing freshwater for long periods. Measures to improve the specific injection capacity of the KG aquifer wells could include the pretreatment of injected water before recharge to make it more compatible with the native water and aquifer materials, particularly to avoid the swelling of clay colloids in the aquifer. More attention should be paid to remove suspended solids from the source water.

On the other hand, the Dammam limestone aquifer could be more viable for artificial groundwater recharge as indicated by the injection-withdrawal experiments conducted for wells SU-10, and C-105, at the Sulaibiya and Shigaya-C wellfields, respectively. These experiments were completed as planned with comparatively few problems. Clogging from air and suspended solids that developed during injection were removed by simple backwashing, and with no permanent damage to the aquifer.

Worldwide experience also indicates that problems associated with recharge are much less in the case of limestone aquifers than is the case with clastic aquifers (Pyne, 1989). Kimrey (1989) suggested that desalinated water would be an ideal fluid for injection into carbonate aquifers of the Arabian Gulf region, whereas its injection to clastic aquifers could encounter clogging problems that may require more extensive preliminary evaluation. In addition, even if the potentiometric head in this confined aquifer rises above the ground surface due to injection, it will have very limited impact on the water table close to the ground surface.

The DM aquifer in Kuwait exhibits a wide range of transmissivity values, ranging from 25 to 9000 $m^2/d$. This makes the selection of a suitable site for artificial recharge on the basis of aquifer transmissivity (or expected recovery efficiency) very flexible.

The majority of groundwater abstraction is from the DM aquifer, which leads to the existence of sufficient storage space at the cone of depressions (where the decline in aquifer head ranges from 50-100 m). This in contrast to the KG aquifer (where the maximum decline in aquifer head is about 30 m). At the same time due to the high abstraction rate, the aquifer is more vulnerable to water quality deterioration due to upward leakage of saline water from deep horizons, or due to saltwater encroachment. Thus, such undesirable effects can halted by artificial recharge.

Consequently, the Dammam aquifer could be a better aquifer for artificial groundwater recharge than the KG aquifer. Hence, in this study, it has been selected to be the target aquifer for artificial groundwater recharge in Kuwait.

## 6.3 CLASSIFICATION OF AVAILABLE SITES FOR ARTIFICIAL RECHARGE

The evaluation of suitability of any site for artificial recharge should be based on reliable hydraulic and transport aquifers parameters. In Kuwait, aquifer parameters estimated under field conditions are limited to wellfields only, and at other locations, the data availability is very limited.

However, model-derived calibrated hydraulic parameters are available from the regional flow model which was presented in Chapter Four. These parameters have a greater degree of uncertainty than do field-derived parameters. Therefore, all the existing water wellfields were initially assumed to be promising sites for artificial groundwater recharge on the grounds that the aquifer parameters at these sites are more reliable than those for the other areas.

These wellfields were classified according to the recharged (DM) aquifer transmissivity, wells specific injection rates (SIR) and recovery efficiency. Later, the sites will be ranked according to this classification in order to select the optimum site (one for short-term and one for long-term storage/recovery of freshwater) that exhibit a high specific injection rate and high recovery efficiency.

### 6.3.1 TRANSMISSIVITY

The wellfields were classified according to their transmissivity, and grouped in five different classes of transmissivity; low, low-moderate, moderate- high, high, and very high, as shown in Table 6.1.

| Site | DM aquifer transmissivity ($m^2/d$) | Transmissivity Class |
|---|---|---|
| Sulaibiya | 30-100 | Low |
| Shigaya-E<br>Shigaya-A | 80-120<br>120-360 | Low-Medium |
| Umm Gudair<br>Shigaya-D | 270-800<br>250-1200 | Medium-High |
| Shigaya-B | 600-1600 | High |
| Shigaya-C | 2000-9000 | Very high |

Table 6.1: Classification of the sites available for artificial groundwater recharge according to the transmissivity of DM aquifer.

### 6.3.2 SPECIFIC INJECTION RATE (SIR)

The storage capacity of an aquifer to store water is dependent mainly on the aquifer parameters and the available space in the aquifer. However, the capacity of wells to accept the injected water is another control factor. The capacity of the wells to absorb the quantities of injected water depends on:

1. Well construction details.
2. Formation capacity.

The available injection sites for artificial groundwater recharge can be classified according to the specific injection rates of their wells. This is defined as the well injection rate divided by the rise of water table inside the well.

All the existing wells in Kuwait were designed for production purposes only, and as such they have a specified operating capacity based on their depth, diameter, and pump capacity. In the DM aquifer the wells are not screened. It has been observed from the injection-recovery experiment at well C-105, that the achieved injection rate was greater than the installed capacity of the well. However, it is not practical to inject water into a well at a rate

greater than its installed pumping capacity, because the removal of solids from the clogged well face by backpumping will be less effective than in the wells with higher pumping rates (Harpaz, 1970).

Another factor which could limit the injection capacity of the wells is the method of injection. The most practicable method of injection, includes the development of the well within a short period and at a low cost is the reversing of flow in the well and letting the recharging water in through the pressure column with the pump already installed in the well. This method has the advantage of developing the well during the recharging stage, since a frequent backwashing and redevelopment of injection wells is needed to restore their injection capacity. However, it will limit the injection rate due to the resistance to flow of the impellers inside the pump (Harpaz, 1971).

Accordingly, in this study, the initial injection rate at the proposed artificial recharge sites was assumed to be equivalent to the designed pumping capacity of the wells.

**Accounting For Clogging Effect**

Usually, the injection capacity of the wells will decline as the cumulative injected amounts grows and the duration of recharge lengthens. Hence, clogging of the well face and the surrounding aquifer pores will cause:

1. Resistance to inflow, i.e. reduction in injection rate; and
2. Technical difficulties resulting from head loss causing excessive rise of the water level inside the well until it lies above ground level.

The reduction in initial injection rate and the developed head loss resulting from clogging can be identified if an actual injection test is conducted, but these effects cannot be reliably predicted. Nevertheless, any assessment of artificial groundwater recharge should include a consideration of clogging.

Clogging mainly depends on aquifer properties, injection well design, and on the injection process itself (such as the injection method, quality of injected water, the compatibility of

the injected water with the native water, and the degree of remedial measures which could be considered to prevent clogging). The injection procedures are not perfect at every well or site. So, the only way by which the clogging effects can be predicted is by relating clogging potential to the aquifer parameters alone.

During the injection-withdrawal experiment at well SU-10 which is located in the Sulaibiya wellfield, a total of 16,416 $m^3$ of water was injected within 30 days, thus the average injection rate is found to be 547 $m^3/d$. Comparing this rate with the initial one which is about 655 $m^3/d$, the reduction in the initial injection rate was found to be 16.5 %. The additional build-up of head inside the well (SU-10) which resulted from the clogging was found to be about 0.7 of the simulated build-up. On the other hand, during the experiment at well C-105 (which is located in the Shigaya-C wellfield), the additional head was found to be about 0.2 of the simulated head. However, the initial injection rate was sustained without any reduction due to the sufficient space available for water to rise inside the injection well.

In order to predict the development of clogging, it was assumed that for a given water quality and injection condition, the transmissivity of the aquifer will be the only significant factor in determining the clogging rate: Low aquifer transmissivity will cause high clogging, and vice versa.

According to the classification of the prospective sites for artificial recharge, the Sulaibiya and Shigaya-C belong to the low and the very high groups, respectively. Therefore, the percentage reduction in the injection rate and the developed head loss observed were assumed to be highest at SU-10, and lowest at C-105, based on their transmissivities. Subsequently, the percentage of reduction in injection rate and additional head loss due to injection at other wellfields were assumed to be within these two limits, assigned to each field according to the aquifer transmissivity (Table 6.2).

| Injection Site | Transmissivity Class | Assumed initial injection rate ($m^3/d$) | Assumed % of reduction in initial injection rate, due to clogging | Completed injection rate ($m^3/d$) | Assumed ratio of additional build up inside the wells due to clogging, relative to the simulated build up |
|---|---|---|---|---|---|
| Sulaibiya | Low | 500 | 16.5 * | 417 | 0.7 * |
| Shigaya-E<br>Shigaya-A | Low-Medium | 580<br>1340 | 14 | 499<br>1152 | 0.5 |
| Umm Gudair<br>Shigaya-D | Medium-High | 1600<br>2300 | 12 | 1408<br>2024 | 0.4 |
| Shigaya-B | High | 2450 | 8 | 2254 | 0.3 |
| Shigaya-C | Very High | 2850 | 0 * | 2850 | 0.2 * |

Table 6.2: Quantification of the clogging effects on injection rate and water level rise inside the injection wells at the available sites for artificial recharge.

Note: * Observed values from actual injection/withdrawal tests at Wells SU-10 and C-105.

Presumably, the percentage reduction in initial injection rate of the wells as well as the head loss resulting from clogging will not exceed the assumed limits if more care is taken to prevent clogging in the future. This is because, during the conducted tests at wells SU-10 and C-105, no remedial measures were considered to prevent clogging, except the chlorine concentration that exists normally in the potable water (which is the recharge water). Moreover, if the well could be developed very easily through back-pumping at short intervals during the injection period, this would minimise clogging effects, and the injection capacity of the wells could be restored at frequent intervals. This could be achieved by placing the pump at the bottom of the rising main, and using a non-return valve and recharge valve above the pump to allow the use of the rising main for dual-purposes (O'Shea, 1984).

To obtain the assumed well injection rate (completed injection rate; in Table 6.2), it was assumed that the injection wells will be developed through back-pumping frequently every month for three days duration to restore the injection capacity of the wells. This is based on the completed well development during the actual injection/production experiment at the Sulaibiya site.

The regional flow model (in Chapter 4) was used to simulate aquifer response to water injection at the selected sites. The simulated aquifer heads for the present situation (1995)

(as in Figures 4.16 and 4.17) were used as initial heads during simulation. Water injection was introduced at each injection site separately, while other fields were operating. The simulation time was for one stress period (6 months) divided into 15 time steps with a multiplication factor of 1.4. All the wells in the tested field were injected simultaneously with uniform injection rate that is the assumed completed injection rate (as presented in Table 6.2).

Figures 6.1 (A, B, and C) and 6.2 (A, B, C, and D) show the simulated change in the DM aquifer potentiometric head as a result of water injection in a particular field, and pumping in the other fields.

To verify the feasibility of injection rates without causing rising water table inside the wells to rise above ground level, the simulated build up in the aquifer potentiometric head at each site was multiplied by the equivalent assumed ratio of additional build up inside the well resulted from clogging. This build-up in head was added to the simulated head to obtain the total build-up inside the injection wells. It was found that the assumed injection rates are adequate and can be completed within the allowable limit of water level rise.

Table 6.3 exhibits the simulated range of water level rise in the DM aquifer at the sites available for water injection, the assumed additional head rise inside the injection wells due to clogging, and the total water level rise inside the wells.

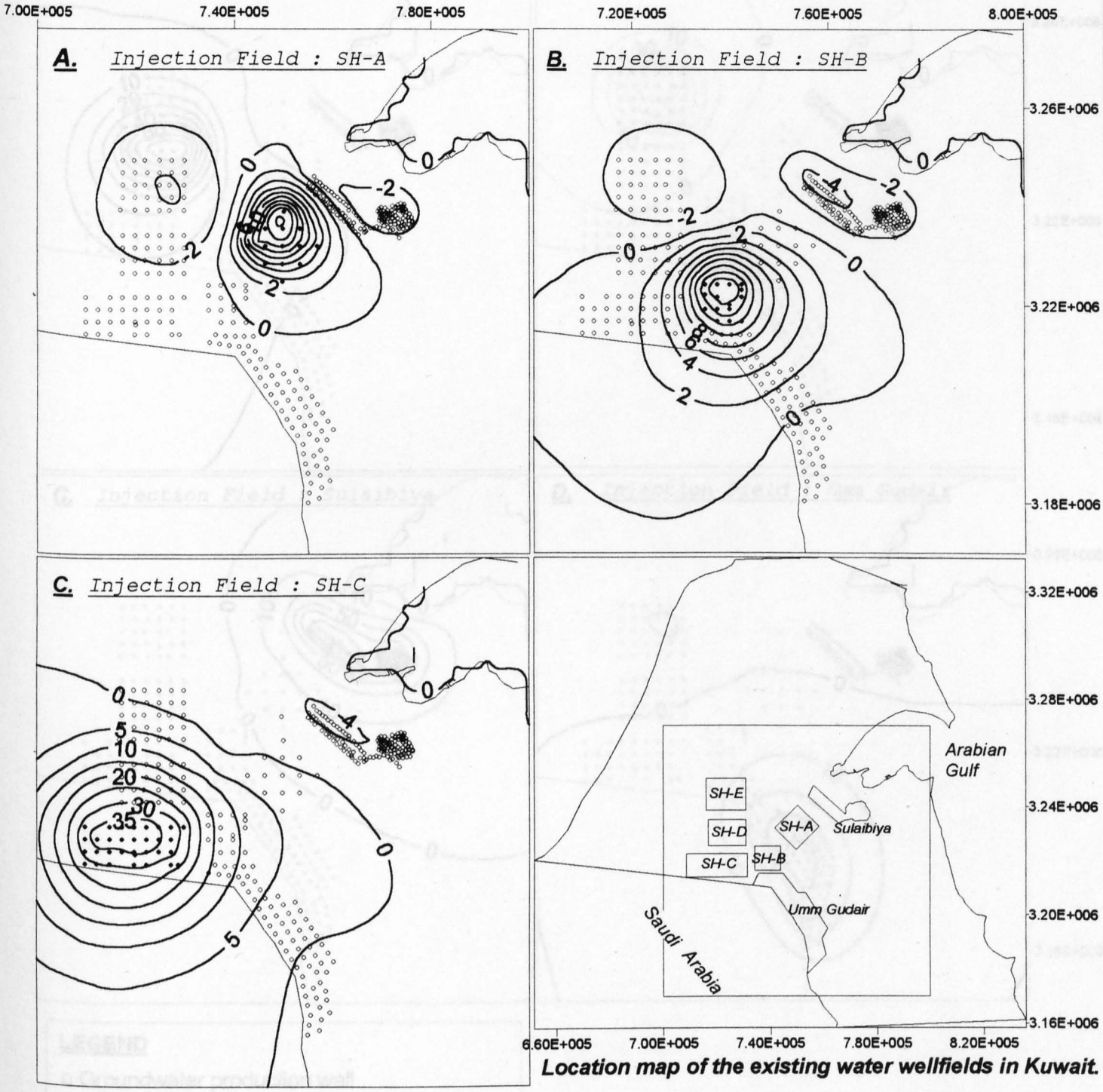


***Location map of the existing water wellfields in Kuwait.***

**LEGEND**

o Groundwater production well

● Injection well

__ 5 ____ build-up (m) __ -5 ____ Drawdown (m)

SH-A,B, and C : Shigaya-A,B, and C wellfields

Figure 6.1 (A,B, and C): Simulated change in the DM potentiometric head after six months of water injection at the injection fields Shigaya-A, B, and C, whilst groundwater is produced from other fields at the same time.

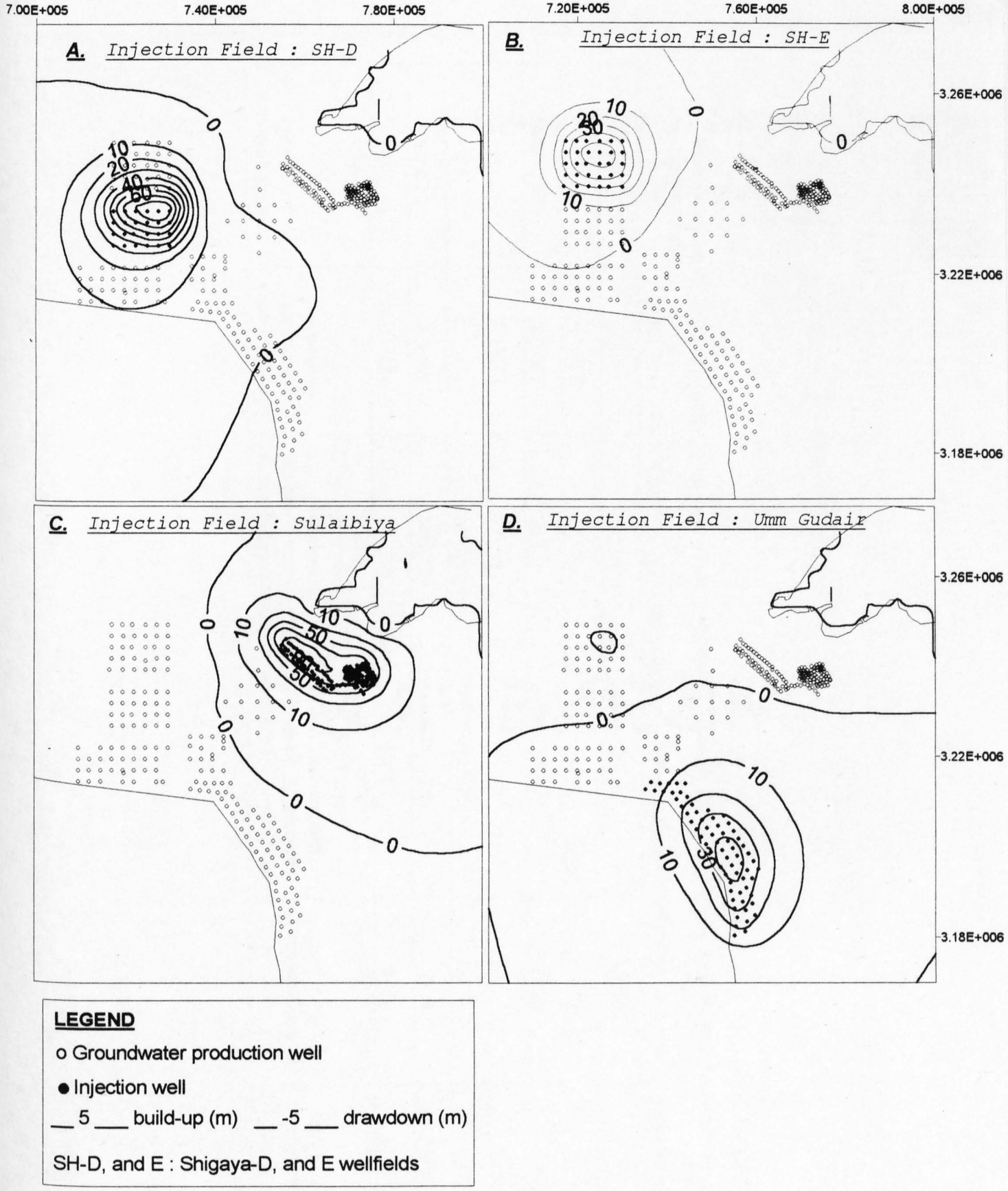


Figure 6.2 (A, B, C, and D): Simulated change in the DM potentiometric head after six months of freshwater injection at the injection fields Shigaya-D and E, Sulaibiya, and Umm Gudair, whilst goundwater is produced from all the other fields at the same time.

| Injection Site | Assumed completed injection rate ($m^3/d$) | Average of simulated build-up in the aquifer (m) | Average of the assumed additional build-up inside injection well due to clogging (m) * | Total build-up inside the injection well due to injection (m) | Allowable build-up inside the injection well (m) | Specific Injection Rate (SIR) ($m^2/d$) |
|---|---|---|---|---|---|---|
| Shigaya-B | 2080 | 16-18 | 7.2-8.1 | 23.2-26.1 | 125-140 | 79-90 |
| Shigaya-A | 1005 | 8-18 | 4.8-10.8 | 12.8-28.8 | 90-110 | 34.8-78.5 |
| Shigaya-C | 2565 | 30-35 | 12-14 | 42-49 | 150-170 | 52-61 |
| Umm Gudair | 1280 | 20-40 | 10-20 | 30-60 | 110-120 | 21.3-42.6 |
| Shigaya-D | 1840 | 40-50 | 20-25 | 60-75 | 150-165 | 24.5-30.6 |
| Shigaya-E | 435 | 20-30 | 12-18 | 32-48 | 150-160 | 9-13.6 |
| Sulaibiya | 350 | 50-60 | 35-42 | 85-102 | 90-110 | 3.4-4.1 |

Table 6.3: Classification of the available sites for artificial groundwater recharge according to their wells Specific Injection Rate (SIR).

Note: * Assumed additional build-up inside the injection well = Simulated build-up in the aquifer X assumed ratio of additional build-up inside the injection well due to clogging (presented in Table, 6.2).

The above table, indicates that the specific injection rates (SIR) for wells are not entirely controlled by transmissivity of the aquifer at the injected site. The use of multiple-wells in artificial groundwater recharge has another influence in increasing the build-up inside the injected wells located in the same field. The geometry of the field and spacing between the wells will determine the degree of this influence. For example, in the Shigaya-A (which has a lower transmissivity than Shigaya-C) the wells seem to have higher specific injection rates. This may be related to the large spacing and configuration of the wells in Shigaya-A (about 3500 m) compared to that in Shigaya-C (about 2000 m).

For the same reason, the very low specific injection rate estimated for Sulaibiya is related to the close spacing between the wells in this site, which is about 700 m. Certainly, if a single-well is used for injection, the specific injection rate will be higher than that obtained using a multiple wells. This is clear from the analysis of specific injection rate for the actual injection-withdrawal test conducted for SU-10 at Sulaibiya field (presented in Chapter 5). The estimated SIR at that test ranged from 20-30 $m^2/d$, which is much higher than the simulated value (3-4 $m^2/d$) in this chapter where all the wells in the field are injected. However, the difference between the simulated and actual values are not related only to the number of injection wells, but also to the duration of injection which is varied between the SU-10 test which was for one month, and between the conducted simulation in this section which is for six months.

### 6.3.3 RECOVERY EFFICIENCY

If freshwater is injected into an aquifer containing brackish groundwater, and stored until needed, it is not possible to recover all the stored volume of freshwater. The physical processes which influence the recoverability of the injected freshwater are the hydrodynamic dispersion, buoyancy stratification, and down-gradient displacement by the local background flow system (Merritt, 1985).

Hence, the percentage of usable water which could be recovered relative to the total volume of injected freshwater (recovery efficiency) should be assessed, because it is considered as the prime indicator of the success of the artificial groundwater recharge practice.

Recovery Efficiency = Volume of usable water / volume of water injected

In the definition of recovery efficiency, the quality of usable water can vary according to the intended use of the recovered water. In this study, because the recovered water will be used for drinking purposes, the maximum allowable TDS of water for drinking as recommended by World Health Organisation (WHO) (i.e. 1500 mg/l) will be used as a target for recovery.

The solute-transport regional model (presented in Chapter 4) was used in simulating the expected recovery efficiency at the existing wellfields. The recovery efficiency for each field was estimated separately by injecting freshwater (TDS=300 mg/l) at all the wells of the concerned field, while the other fields are pumped to meet the forecasted groundwater demand. To avoid the effect of injection volume varying from site to site, the freshwater was injected at the same rate and for the same duration at all the injection sites.

The grid spacing used in the regional model was large (2000x2000 m). The simulated changes in TDS as a result of injecting freshwater into the DM aquifer will vary slightly under the given simulation time. Hence, a longer simulation period was required for greater variation in TDS. During the solute transport simulation a very small transport step (equal to 0.05 day) was essential to get reasonable results with respect to minimising the numerical oscillation resulting from the larger transport step. Thus, as long simulation period was difficult to obtain because of computer storage limitations.

The transport equation (No. II-3, presented in Appendix II) is linked to the flow equation through the relationship :

$$v_i = -\frac{K_{ii}}{\omega}\frac{\partial h}{\partial x_i} \qquad (6.1)$$

where;

$v_i$ : Linear pore water velocity, (L/T)

$K_{ii}$ : principal component of hydraulic conductivity tensor, (L/T)

$h$ : hydraulic head

$\partial x_i$ : distance along the respective Cartesian coordinate axis, (L)

$\omega$ : aquifer porosity, dimensionless.

Therefore, the limitation of the regional model to simulate the variation in water TDS during the injection process, was solved based on Equation 6.1, by reducing the effective porosity of the aquifers to accelerate the flow velocity of the recharged water at the injected node. Hence, it will reach the adjacent nodes within a manageable simulation period, where the change in native water TDS can be produced, and thus the recovery efficiency later can be identify. This way may be acceptable only for comparison purposes to differentiate between the available sites for injection, since the long simulation periods are difficult. It was found that if the original effective porosity of the aquifers is reduced by a factor of 0.1, then it will cause the same effect as increasing the simulation time by the order of 2.5.

However, the reduction of aquifer porosity will also cause an overestimation of the recovery efficiency. This was concluded from the analysis of the single-well injection-recovery experiment conducted at SU-10. Because no accurate value of porosity is available for the aquifers in Kuwait, a sensitivity analysis was done for that test. The simulated recovery efficiency was matched with the observed using two options, either with high porosity and low dispersivity, or vice versa. It has been found that if porosity is reduced by half, the dispersivity should be increased by factor of 1.8 to get the same recovery efficiency. Hence, if the effective porosity of the aquifers in the regional model was to be reduced, the dispersivity had to be increased correspondingly to cancel the effect of porosity reduction in recovery efficiency.

In this study, the transport model was run using porosity equal to 0.1 of the calibrated ones for a simulation time of 10 years, and accordingly the aquifers dispersivities were increased proportionally based on the ratio obtained at SU-10, to be 7.9, 288, and 147 m at Sulaibiya, Shigaya-C, and the remaining fields, respectively. Reducing the porosity by this factor will produce a change in the water TDS as the effect of 25 years of transport simulation if the original porosity of the aquifers was used. This simulation period was divided equally between injection of freshwater and recovery.

The available sites for storing freshwater were classified according to the percentage of usable water which could be recovered (assumed to have a TDS content of 1500 mg/l). The TDS of the injected water was taken to be 350 mg/l, whereas, the TDS of the native water

in the DM aquifer was assigned for the whole layer using the most recent isosalinity contour map for the DM aquifer (as in Fig. 3.21). Unfortunately, reliable TDS values for the KG groundwater are not available. Hence, it was assumed to be higher than the DM groundwater quality by 500 mg/l at the locations where these values are unreliable. This variance in TDS values between the DM and KG groundwater was based on the actual levels between the two aquifers groundwater quality at the wellfields where the two aquifers are utilised (see section 4.3).

The available sites for artificial groundwater recharge were tested separately using the transport model (MT3D) to estimate the possible recovery efficiency which could be obtained at each site. The used solution was Method Of Characteristic (MOC), because it is more suitable than MMOC (Modified Method Of Characteristics) for problems with large mesh (Zheng, 1990). All the existing wells separately in each site were injected with freshwater (TDS= 350 mg/l) simultaneously using the assumed injection rate for 5 years, then the same injection wells were pumped using the same injection rate for the next 5 years. If the concerned site is injected with freshwater, the others were simulated as pumping fields. The transport model was used to simulate the TDS of the recovered water as a function of time until the same volume of injected water is recovered. For each site the recovery efficiency was estimated at a selected node having relatively the average aquifer transmissivity.

Table 6.4 displays the recovery efficiency for different ranges of recovered water TDS simulated for each injection site separately.

| Injection site | TDS of native water mg/l | Recovery efficiency percent, if recovered water has a TDS of : (TDS in mg/l) | | | | | | | |
|---|---|---|---|---|---|---|---|---|---|
| | | <500 | <1000 | <1500 | <2000 | <2500 | <3000 | <3500 | <4000 |
| Shigaya-A | 2800 | 0.1 | 8 | 24.3 | 53.4 | 100 | | | |
| Shigaya-E | 3800 | 0 | 7.5 | 22 | 42 | 76 | 100 | | |
| Shigaya-D | 3500 | 0 | 4.2 | 15 | 29 | 51 | 100 | | |
| Shigaya-B | 3200 | 0 | 3.4 | 14 | 23 | 41 | 79 | 100 | |
| Sulaibiya | 4700 | 0 | 0.6 | 13.6 | 23 | 35 | 50.7 | 74 | 100 |
| Umm Gudair | 3700 | 0 | 0.2 | 13 | 29 | 55 | 82 | 100 | |
| Shigaya-C | 3100 | 0 | 0 | 3 | 12 | 29 | 100 | | |

Table 6.4: Classification of the available sites for artificial groundwater recharge according to the estimated percentage of recovery efficiency using the regional transport model.

## 6.4 SITE SELECTION CRITERIA

The objectives of artificial groundwater recharge will determine the method used for storing and recovering the freshwater.

Hence, if the objective is to store fresh water for subsequent use during emergencies, the injection process should be carried out for long time until a sufficient volume of freshwater is created. Also, the selection of site and design of injection and recovery systems will be undertaken to recover most of the injected water.

On the other hand, where recharged water is used merely to raise the potentiometric heads, the objective is to use the existing well system and minimise the injection cost. Nevertheless, according to the availability of water and the need of the aquifer for such augmentation by injection, the freshwater can be stored for the short-term.

Potable water demand, and consequently the groundwater abstraction and desalinated freshwater production have a seasonal variation in Kuwait. The demand is high in summer and low in winter. Therefore, surplus freshwater which becomes available during winter, when the freshwater consumption is lower than the installed capacity of the distillation plants, could be injected into the aquifer. In summer, when water demand increases, the

stored water could be pumped to help meet this demand. This could be done through seasonal cycles of freshwater storage and recovery.

The available sites for artificial groundwater recharge which have been classified previously will be ranked using several criteria, in order to select the most appropriate site for short and long-term storage and recovery. First, general criteria will be used to determine the suitability of each site for the storage of freshwater. Subsequently, two sets of criteria will be used to select two optimum sites, one for short-term cyclic storing and recovery, and the other for developing a long-term strategic reserve.

The criteria used were derived mostly from the results of the injection-withdrawal experiments discussed in Chapter 5, in addition to the results and recommendations of Mukhopadhyay et al. (1992).

### 6.4.1 GENERAL CRITERIA

The areas where aquifer parameters are not available were not considered for artificial recharge. Aquifer parameters are known for the existing wellfields, but at other locations they are not determined. For other locations, aquifer parameters were estimated from the mathematical model (discussed in Chapter 4). These parameters have a degree of uncertainty compared to the field estimated parameters. If the aquifer parameters for other locations could be obtained using field data at a later date, then these sites can be considered for ranking purposes. The majority of the appropriate locations with good water quality and reasonable aquifer transmissivity were already in use, and other locations are unsuitable, because of proximity to oil fields, or areas of urban development.

1. The salinity of the native groundwater should be as low as possible. The mixing between the recharged and the native water is unavoidable, leading to the deterioration of the injected water volume. The recovery efficiency decreases with increasing native water salinity. In addition, if the difference between the native and the injected water salinity is high, buoyancy effects resulting from density variation will be predominant as this will also reduce the recovery efficiency (Merritt, 1985). Further, it was observed in Kuwait that $H_2S$ (hydrogen sulphide) is associated with higher salinity water (>10,000 mg/l TDS) (Abu-Sada, 1988). Since the presence of $H_2S$ in the recovered water, even in trace

amounts, will make it non-potable, the high salinity areas are to be avoided. Hence, to obtain recovered water of reasonable water quality, it was decided that the salinity of the target aquifer at the proposed site should not exceed 5,000 mg/l TDS.

2. The sites located close to the borders should be avoided. There is a possibility of losing the injected freshwater at these locations, which could move outside Kuwait region making the recovery of this water at later stages difficult. In addition, the injection process at these locations will reduce the rate of groundwater lateral inflow coming from the Saudi Arabia side which represents the only source of recharge to the aquifer system in Kuwait.
3. The available potentiometric head should be sufficient to accommodate the rise in water level due to the normal aquifer loss and, in addition to well loss resulting from clogging and turbulent flow. Also, the depth of the potentiometric surface of the target aquifer at the proposed site should not be too deep, as this would increase the cost of pumping during the withdrawal stage.
4. The site should be located as close as possible to the source of injection water and to the consumption centres, to minimise water transportation costs. Also, it is preferable to place the selected site close to service facilities like roads, and electric power supply, to minimise the project construction costs.
5. The proposed site should be surrounded by other wellfields in the direction of regional flow, to prevent the movement of injected water towards the discharge point at the Gulf. Thus, the moved water can be trapped by the down-head gradient pumping wells.

### 6.4.2 CRITERIA FOR SELECTING THE LONG-TERM STORAGE SITE

1- Select a site which has high recovery efficiency, so it will be more efficient in storing the freshwater for long time.

2- Avoid the extremely high transmissivity zones of the aquifer. High transmissivity causes large-scale mixing between the injected and the native groundwater, which will reduce the recovery efficiency of the recovered water. This was observed from the results of the injection-withdrawal experiment in well C-105, located in the Shigaya-C wellfield, where the transmissivity of DM aquifer is very high (reaching about 4,000 $m^2/d$).

3- The vertical hydraulic gradient between the aquifer system units (which controls the recovery efficiency) should be as low as possible.

### 6.4.3 CRITERIA FOR SELECTING THE SHORT-TERM (SEASONAL) STORAGE SITE

1. Specific injection rate (SIR) should be high, so more volume of water can be stored within a short time. Hence, the sites with extremely low transmissivity should be avoided.
2. Select sites with high cones of depression (which are mostly in water-depleted areas). These areas require restoration of potentiometric heads. In addition, more water could be injected and stored at these locations because they had sufficient storage space. The injection of freshwater at cones of depressions may speed up the mixing between the injected and the native water due to the presence of steep hydraulic gradient, and that could reduce the recovery efficiency. However, the quality of the recovered water is not so important as long as the quality of the injected water is better than the native water.
3. Vertical leakage between the aquifers is acceptable. The upper KG aquifer could be replenished indirectly through the injection of the DM aquifer. For example, it has been found within the Shigaya-C wellfield that the simulated vertical leakage from the KG toward the DM aquifer, which was about 19,000 $m^3/d$ at the time, was reversed after the injection was undertaken into the DM aquifer to be from the DM aquifer towards the KG aquifer at about 4,000 $m^3/d$.

## *6.5 SITE SELECTION*

First, all the existing wellfields were considered as possible sites for artificial groundwater recharge because they are the only areas in Kuwait where reliable aquifer parameter values are available.

The fields where the groundwater abstraction induces lateral groundwater inflow which recharge the aquifer system with a relatively good water quality (<3000 mg/l) was excluded. These are Umm Gudair, and Shigaya-C wellfields. The injection of water at these two locations is not recommended, because it will reverse the existing hydraulic gradient reducing the lateral groundwater inflow. Therefore, these two sites should be used for groundwater production only, to induce the natural recharge.

Table 6.5 presents a comparison between the simulated lateral groundwater inflow before the injection started under transient condition in 1996, where all the fields are operating for pumping purposes only, and between the simulated lateral inflow during injection of the DM aquifer at Umm Gudair and Shigaya-C fields.

| Lateral Inflow ($m^3/d$) | Before injection | During injection at Umm Gudair | During injection at Shigaya-C |
|---|---|---|---|
| To KG | 70,173 | 58,739 | 69,468 |
| To DM | 108,168 | 99,783 | 94,825 |
| Total | 178,341 | 158,522 | 164,293 |
| **Deficit in lateral inflow due to injection** | 0 | -19,819 | -14,048 |

Table 6.5: Simulated deficit in the rate of lateral groundwater inflow when the DM aquifer was injected with water at Shigaya-C, and Umm Gudair fields.

There is another reason for not using Umm Gudair field for artificial groundwater recharge. The productivity of this field, is about 40 % of the total groundwater production in Kuwait. Thus, if it is used for artificial recharge, then it will be very difficult to replace its production rate with another wellfield.

### 6.5.1 LONG-TERM STRATEGIC RESERVE SITE

Based on the above criteria, Shigaya-A wellfield seems to be the optimal site, where the DM aquifer can be used to store freshwater for a long time, for subsequent use during emergency conditions. In particular, Shigaya-A is selected because of the following reasons:

1. It has the highest recovery efficiency (24 % for TDS < 1500 mg/l), as presented in Table 6.4.
2. The wells at this site have a relatively high specific injection rate ranging from about 35 to 78 $m^2/d$.
3. The aquifer potentiometric head at this site has a sufficient depth (90-100 m), so there is enough space for the water to rise inside the injection wells when the well face is clogged during injection due to the relatively low aquifer transmissivity. Table 6.3, indicates that the total build-up in the head of injected DM aquifer will be about (50-54 m) at this site if the wells are recharged with water at a rate equal to their existing installed capacity.

4. Shigaya-A is located at a relatively short distance from the source of recharged water and from demand centres. Therefore, the conveyance costs will be relatively low.

### 6.5.2 SHORT-TERM STORAGE SITE

Shigaya-B wellfield could be the optimum injection site for the seasonal storage and recovery of freshwater. The reasons of selecting this site for such purpose, are;

1. The wells at this site have the highest specific injection rates (SIR) ranging from 79 to 90 $m^2/d$ (Table 6.3). Thus, large volumes of water can be stored and retrieved within a limited period using injection and recovery cycles of 6 months each.
2. It is located in the centre of the existing wellfields. Hence the recharged water will raise the potentiometric head of the aquifer and enhance water quality over an extended region.
3. It has a relatively good recovery efficiency (14 % for TDS< 1500 mg/l), as shown in Table 6.4.

# 7. MANAGEMENT OPTIONS FOR AQUIFER STORAGE AND RECOVERY

## *7.1 INTRODUCTION*

Most of the desalinated water for urban demand in Kuwait is produced by multi-stage flash desalination, coupled with electricity generation (Al-Rgobah, 1989). Operational efficiency of these plants is at a maximum for certain constant production rates of desalinated water. However, the urban demand for water varies considerably between summer and winter months. Hence, because of the fluctuations in desalinated water demand, the desalination plants are operating under sub-optimal conditions for most of the time. Operational efficiencies of desalination plants could be improved by coping with varying demands through the cyclic injection and recovery of desalinated water in a selected aquifer. The selected aquifer could be injected with excess desalinated water during winter months and the water recovered during summer months, when demand is high. Such a scheme will result in the operation of desalination plants at an optimum rate irrespective of the demands for freshwater. In the present chapter, the optimum procedures for storing and recovering freshwater at the recommended site for seasonal storage (Shigaya-B wellfield) are identified, taking into consideration the various management decisions, such as recharge water availability, injection/pumping rates, storage periods, and target quality of the recovered water.

The present chapter also examines the options available for the storage of freshwater in the aquifer for long-term periods at the recommended site (Shigaya-A wellfield). The long-term storage is vital for Kuwait, to establish security against the partial or total loss of desalination plants in case of mechanical failures or major terrorist activities. The various management variables which must be satisfied to establish such storage include, the number of injection wells, injection/recovery rates, duration of injection and quality of recovered water. Possible scenarios of freshwater shortage have been identified. The operational procedures for long-term storage are different to those for seasonal cyclic storage and recovery.

The storage and recovery of water at the selected sites were simulated using a new numerical model constructed with a finer grid spacing than the regional model to cover these sites in more detail. With small grid spacing, the variation in TDS values can be modelled properly.

## 7.2 AVAILABILITY OF WATER FOR RECHARGE

### 7.2.1 SOURCES OF WATER FOR RECHARGE

The aim to create a sufficiently large freshwater lens which can act as a strategic reserve for subsequent use, need a sustainable source of freshwater with reasonable quantity and has to be identified prior to any feasibility study. Also, the seasonal availability of recharge water for the cyclic storage-recovery purpose has to be determined.

Based on the climatic and hydrologic conditions and the water use pattern in Kuwait, the following sources of freshwater are available for artificial groundwater recharge:

1. Desalinated water
2. Treated wastewater
3. Surface run-off

These can be ranked according to their quantity, quality, suitability and feasibility of recharge (Mukhopadhyay et al. 1992):

**1. Desalinated Water**

The source of freshwater for urban consumption in Kuwait is a mixture of desalinated water and brackish groundwater. Desalinated water is the main source, and is a by-product of electric power generation. The power plants in Kuwait are designed to fulfill the dual functions of generating electricity and producing freshwater by sea water desalination. The multi-stage flash evaporation (MSF) system is mainly used in Kuwait for sea water desalination. The demand of freshwater during winter is lower than the demand in summer. This makes the difference between the installed capacity of the MSF plants and the actual desalinated water production high in winter, but low during summer. Figure 7.1 shows seasonal fluctuation in the urban freshwater demand.

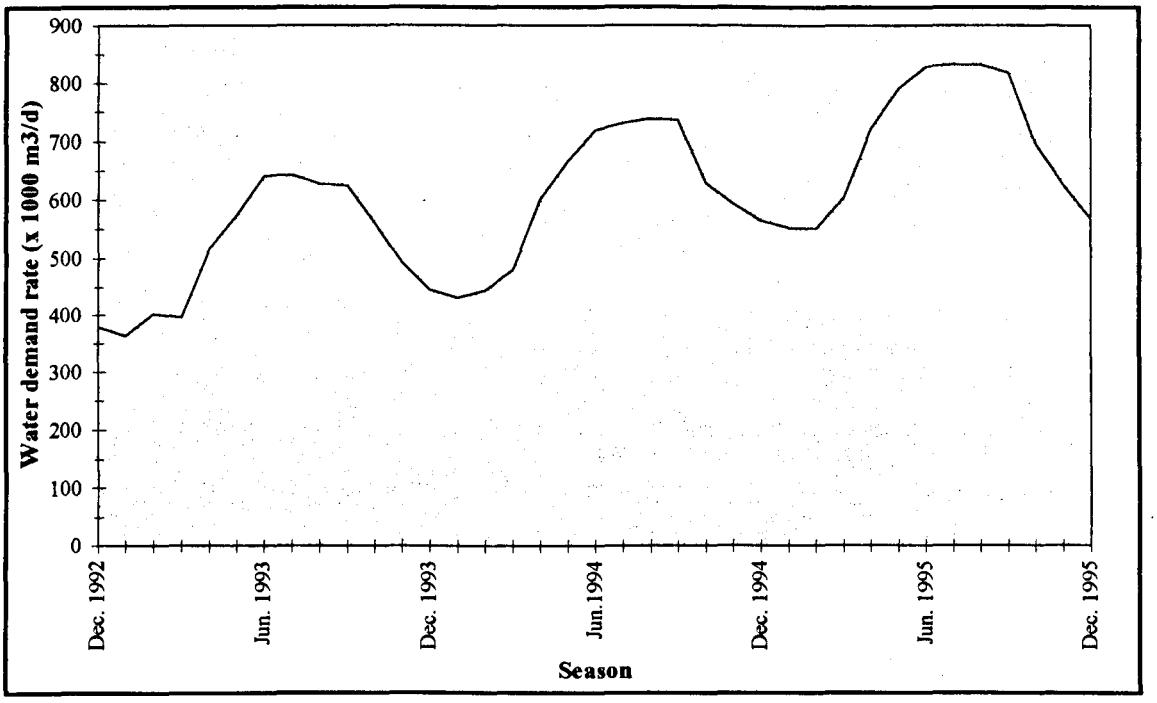


Figure 7.1: Seasonal fluctuation in the urban freshwater demand.

Therefore, it will be possible to run the MSF units at optimum capacities throughout the year which will provide a surplus of desalinated water for artificial recharge during winter.

The suitability of desalinated water for artificial recharge should be evaluated according to the following considerations:

- Solution of solid salts may take place when the fresh water is injected into the Kuwait Group clastic aquifers, leading to deteriorating quality of the recovered water, and thus decreasing the recovery efficiency. The swelling of clay minerals as a result of changing their geochemical state is a possibility, which will reduce the pore space and permeability of the aquifer (Kimrey, 1985)
- If the Dammam Limestone aquifer is injected with desalinated water which is highly corrosive, the carbonate minerals may dissolve.
- Delivery of the desalinated water to remote recharge sites would require a large capital expenditure which could be prohibitively expensive.
- The availability of desalinated water for artificial recharge has seasonal fluctuations because of variations in freshwater demand.

One of the advantages of using desalinated water are the very low or non-existent pretreatment requirements. Hence, if desalinated water is sufficient quantities, it will be an ideal potential source for artificial recharge in Kuwait.

**2. Treated Wastewater**

Treated wastewater is widely used for artificial recharge in many parts of the world. This practice can improve the quality of the treated wastewater if long infiltration paths and percolation times through the unsaturated zone are assured, which can be achieved by using spreading basins to recharge the aquifer. This would only be possible for KG aquifer in this case.

Treated wastewater is available in very large quantities. The quantity exceeds 250,000 $m^3/d$ at present, and certainly will increase in the future as the population increases.

The volume of available treated water suggests that the use of this water for artificial recharge is feasible. This source is dependable having moderate seasonal and gradual long-term variations. However, long-term monitoring of the quality of the recharged water is essential to assure that the recovered water has an acceptable quality for the intended use.

**3. Surface Run-off**

Rainfall is infrequent in Kuwait, being limited mainly to four months out of the whole year, but a considerable amount of water can originate which could be used for artificial recharge. The quality of surface run-off water is usually good if not affected by polluted land and air.

A number of topographical depressions such as Raudhatain, Umm Ar-Rimmam, and Al-Aujah are located in the desert far away from the industrialised and urbanised areas of Kuwait. These depressions contain freshwater (<500 mg/l) as groundwater lenses (Senay, 1977; Omar, 1982), and were identified as appropriate locations for recharging the upper KG aquifer with surface run-off water using spreading basins.

Parsons Corporation (1963) estimated that an average of 608,000 $m^3$ of water could be made available annually for artificial recharge in the Raudhatain depression. Hamdan (1986) estimated that the annual harvestable surface run-off reaching the Umm Ar-Rimmam and Al-Aujah basins is about 386,000 $m^3$ for each location. The difference between these estimates suggests low and uncertain volumes of this source. However, due to its high quality, and the low-cost of construction for harvesting facilities, it could be used for artificial recharge on a small scale.

Surface run-off in the urban areas of Kuwait may also be a significant source for recharge water. About 18 million $m^3$ water harvested every year from the storm drainage network and this may be utilised for artificial recharge (Hamdan, 1986).

### 7.2.2 RANKING OF WATER SOURCES FOR RECHARGE

The various sources of the available water for artificial recharge can be ranked according to the above criteria. The desalinated water could be considered as the principal source for artificial recharge in Kuwait, because it has the best quality, and also the most viable source especially during winter.

The second in ranking is the treated wastewater, because of its poor quality. This could be improved by reverse osmosis, or by increasing the flow path between the injection and the recovery points. Also, its quality could be improved by increasing the residence time of the water in the aquifer, because the aquifer materials (especially the clastics) can operate as a good filtering media.

The last source in importance is the surface run-off water even with its high quality, because its availability is not assured for long-term planning.

Therefore, the planning for artificial groundwater recharge in Kuwait should be based primarily on the availability of desalinated water, and consider the treated water as an alternative, especially for surface recharge through spreading basins to improve its quality to meet the specifications for water use.

## 7.3 NUMERICAL MODEL (SUB-REGIONAL)

A large grid spacing was necessary to model the aquifer system in Kuwait on a regional scale (presented in Chapter 4). Though, the temporal variations in TDS during freshwater injection using the regional model were not significant within the simulation period. So, it was necessary to run model for longer period to get significant changes in water quality for assessing the feasibility of artificial groundwater recharge (section 6.3.3). Also, because the minimum grid spacing is 2000 m, it was impossible to locate wells at a closer distance for evaluating the aquifer response at local areas.

Hence, in order to obtain more reliable results and simulate the freshwater injection at the recommended sites for storage and recovery in greater detail, it was necessary to construct a model with smaller grid spacing. This model was designed to cover most of the existing wellfields and particularly the two recommended sites. The selected area to be modelled was nested on the regional model coarse grids. Then this sub-regional model was modelled separately.

The sub-regional model domain was discretized using a rectangular mesh consisting of 80 x 176 cells with a uniform grid spacing, where ($\Delta x = \Delta y = 500$ m). In order to minimise the number of inactive cells, the model was rotated to be parallel to the direction of regional flow. Figure 7.2 displays the grid design of the sub-regional model, and the boundary conditions

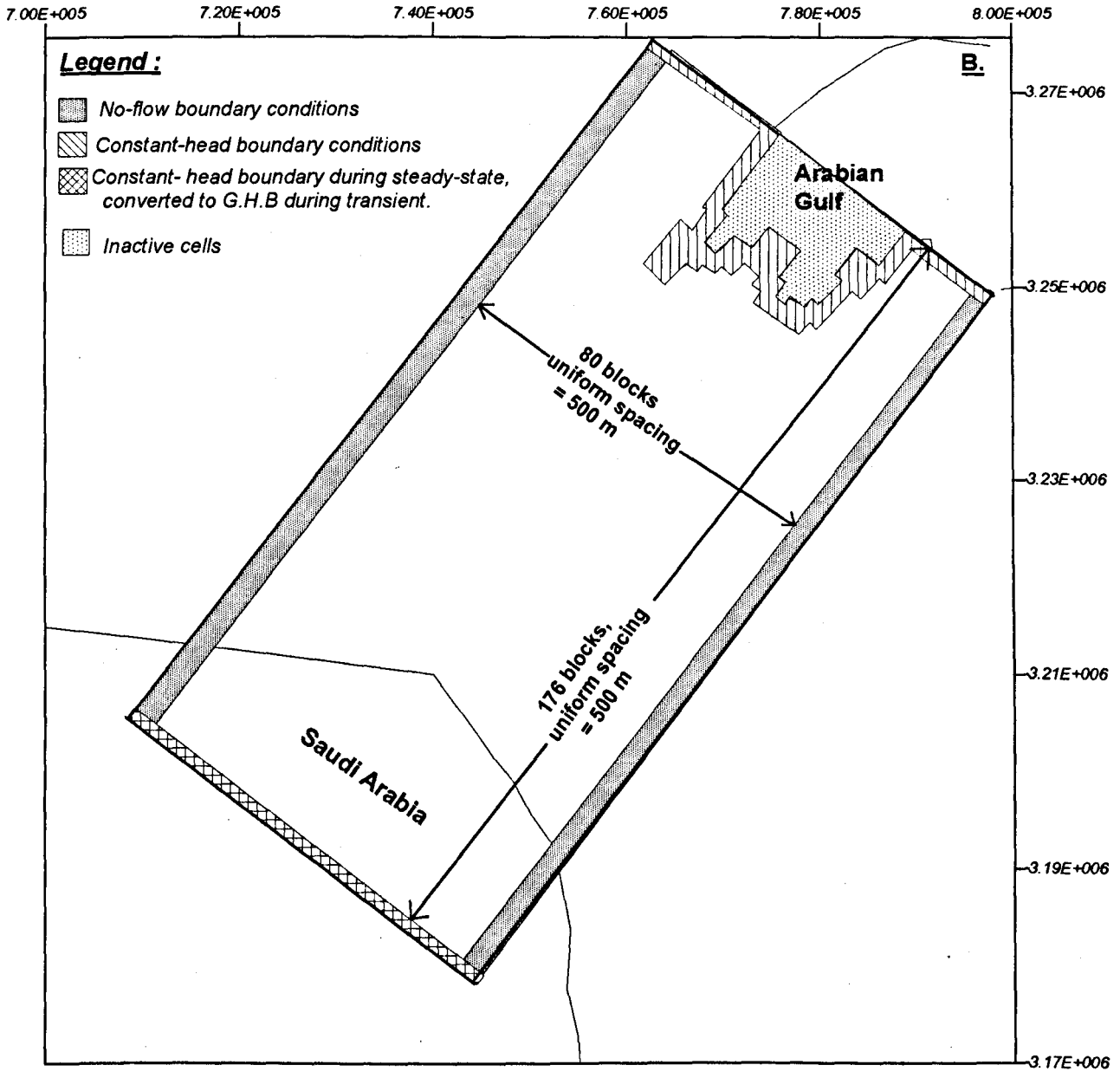


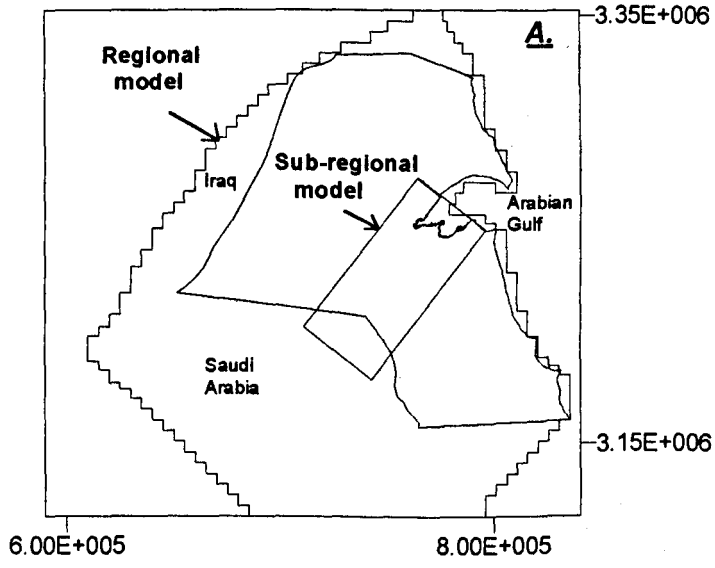


Figures 7.2 (A and B) : (A) Location of the sub-regional model relative to the regional model. (B) Domain discretization and boundary condtions of the sub-regional model.

The model is bounded by the Arabian Gulf coastline in the east direction as a physical boundary, which is considered as a constant head boundary. The boundaries which are perpendicular to the initial flow lines of the aquifers were assigned as no-flow boundaries. In the south west where the initial potentiometric contours are 110 and 115 m amsl for the KG and DM aquifers respectively, the model boundary was selected as a constant head during the steady-state calibration. Then during the transient calibration this boundary was converted to general head boundary (mixed boundary conditions). Whereas, the other boundary conditions were unchanged.

The computer model MODFLOW was used in simulating the groundwater flow. The calibrated aquifers parameters from the regional model were used in the sub-regional model. The sub-regional model was calibrated under steady-state and transient conditions, where the aquifers parameters were adjusted slightly to obtain a match between the simulated and the observed potentiometric heads. The transient calibration of the model consisted of the abstraction history from 1960 to 1996, in order to reproduce the observed potentiometric head distribution during that period. The transient calibration was undertaken for a period of 36 years, divided into 72 stress periods.

The calibration was done in the same manner as in the regional model calibration (section 4.2.5). However, due to the use of finer grid spacing, the initial time step was smaller in order to eliminate the numerical solution instability. The calculated initial time step (0.05 day) was used at the beginning of the simulation and was increased in a geometric progression of ratio 1.4 . Also, the time step size was reduced whenever a new withdrawal stress was imposed on the system. The calibration of the model was completed with a minimum percent of discrepancy error that is (0.02 %) for the steady-state calibration and ranging from 0.00 to 0.03 % for the transient calibration (varying from one stress period to another).

Table 7.1 presents the computed water balance for the aquifer system under steady-state conditions.

| Flow component | Rate ($m^3/d$) |
|---|---|
| **KG** | |
| lateral flow in | 19,961 |
| lateral flow out | 34,483 |
| leakage to DM | 3,050 |
| leakage to KG | 17,572 |
| Total KG flow in | 37,533 |
| | |
| **DM** | |
| lateral flow in | 20,696 |
| lateral flow out | 6,186 |
| Total DM in | 23,746 |
| | |
| **DOMAIN** | |
| lateral flow in (= out) | 40,657 |

Table 7.1: Computed water budget by the sub-regional model for the aquifer system under steady state conditions.

Figures 7.3 and 7.4 show the simulated versus observed steady-state potentiometric heads of the KG and DM aquifers, respectively. Figure 7.5 displays the simulated total drawdown of the DM aquifer to the year 1995. The simulated drawdowns are in reasonable agreement with measured drawdown (presented earlier in Fig. 3.17).

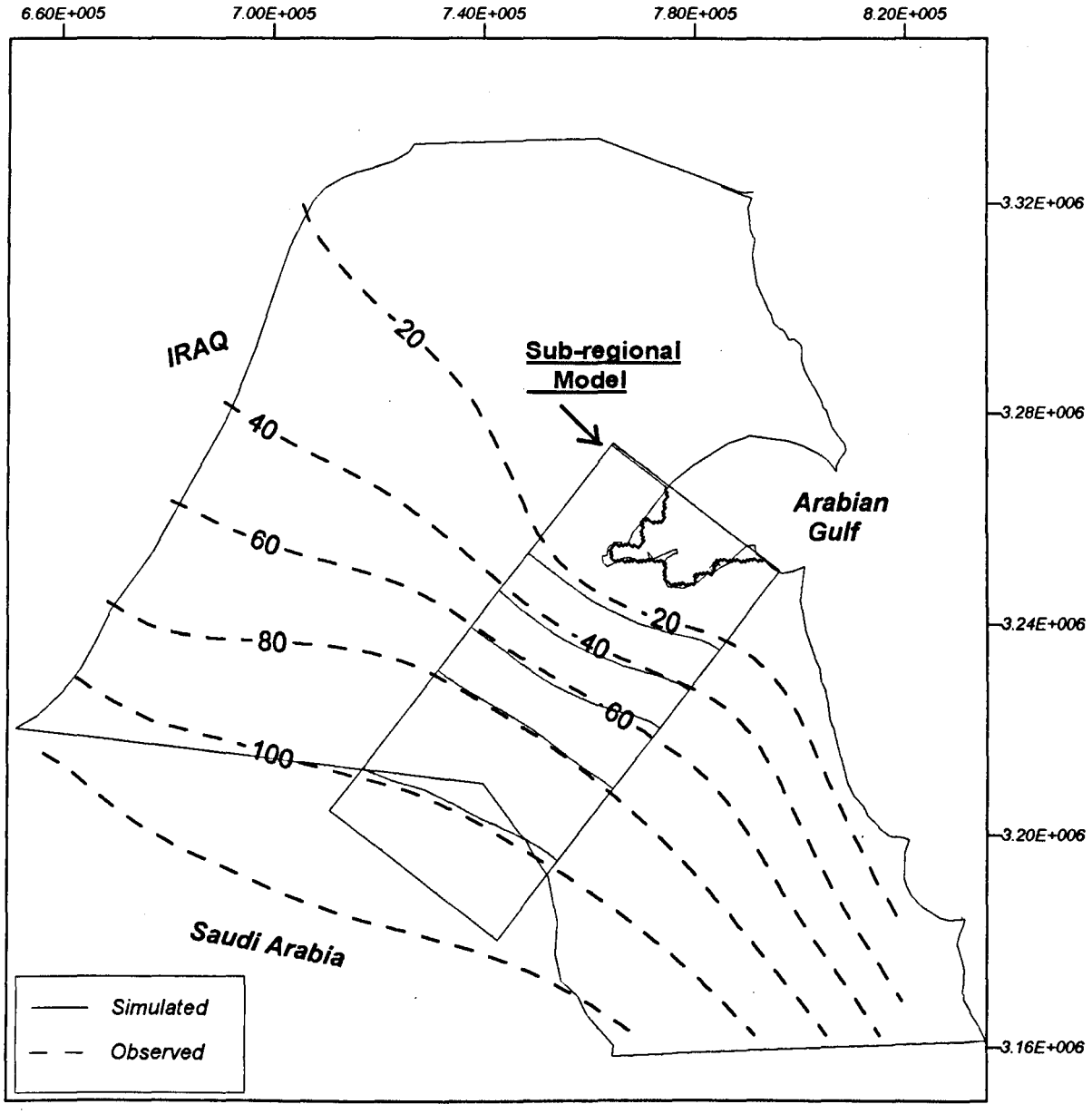


Figure 7.3: Matching between the simulated and observed water level of the Kuwait Group aquifer obtained during the steady-state calibration of the sub-regional model, m amsl.

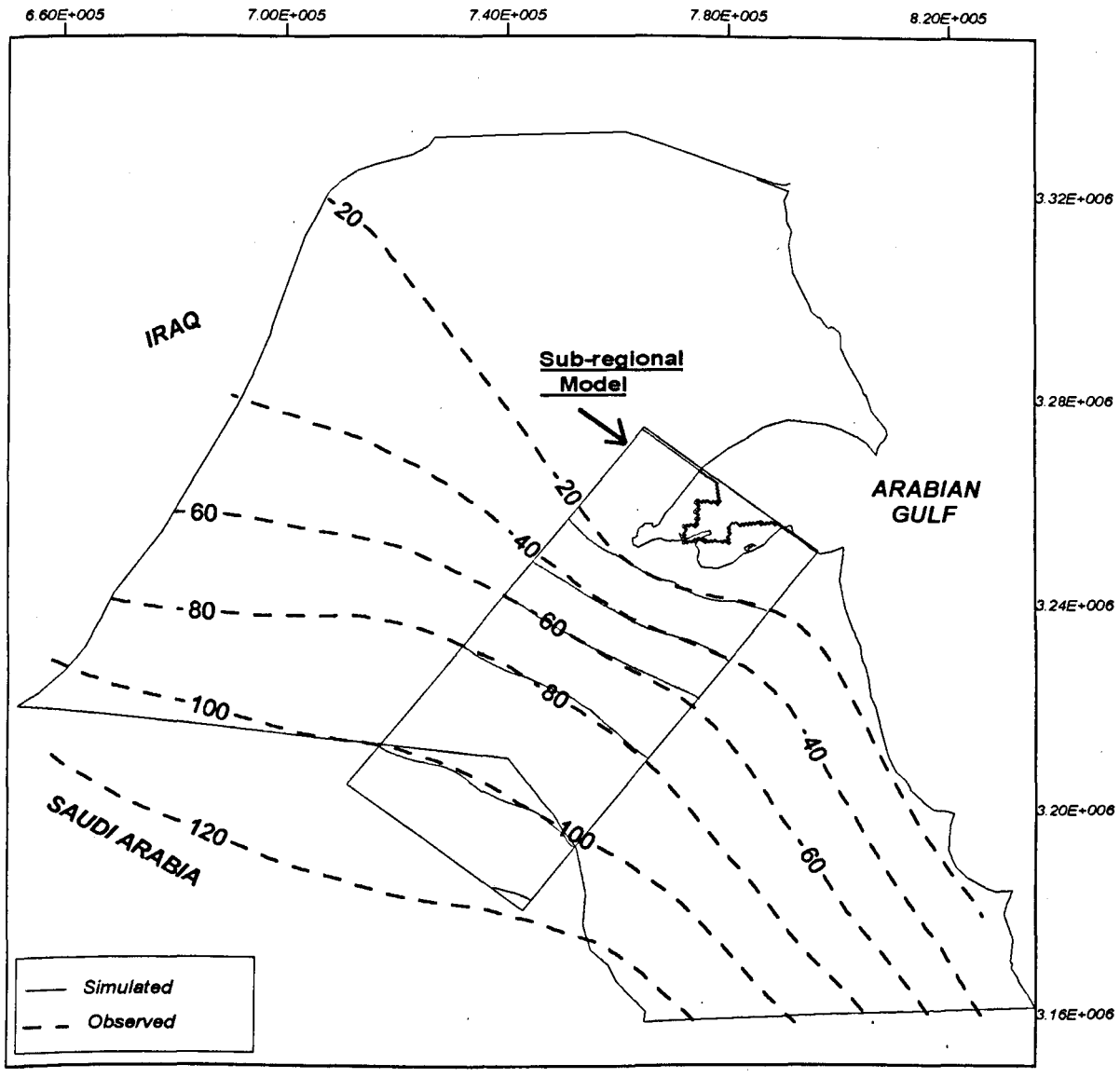


Figure 7.4: Matching between the simulated and observed initial potentiometric head of the Dammam aquifer during the steady-state calibration of the sub-regional model, m amsl.

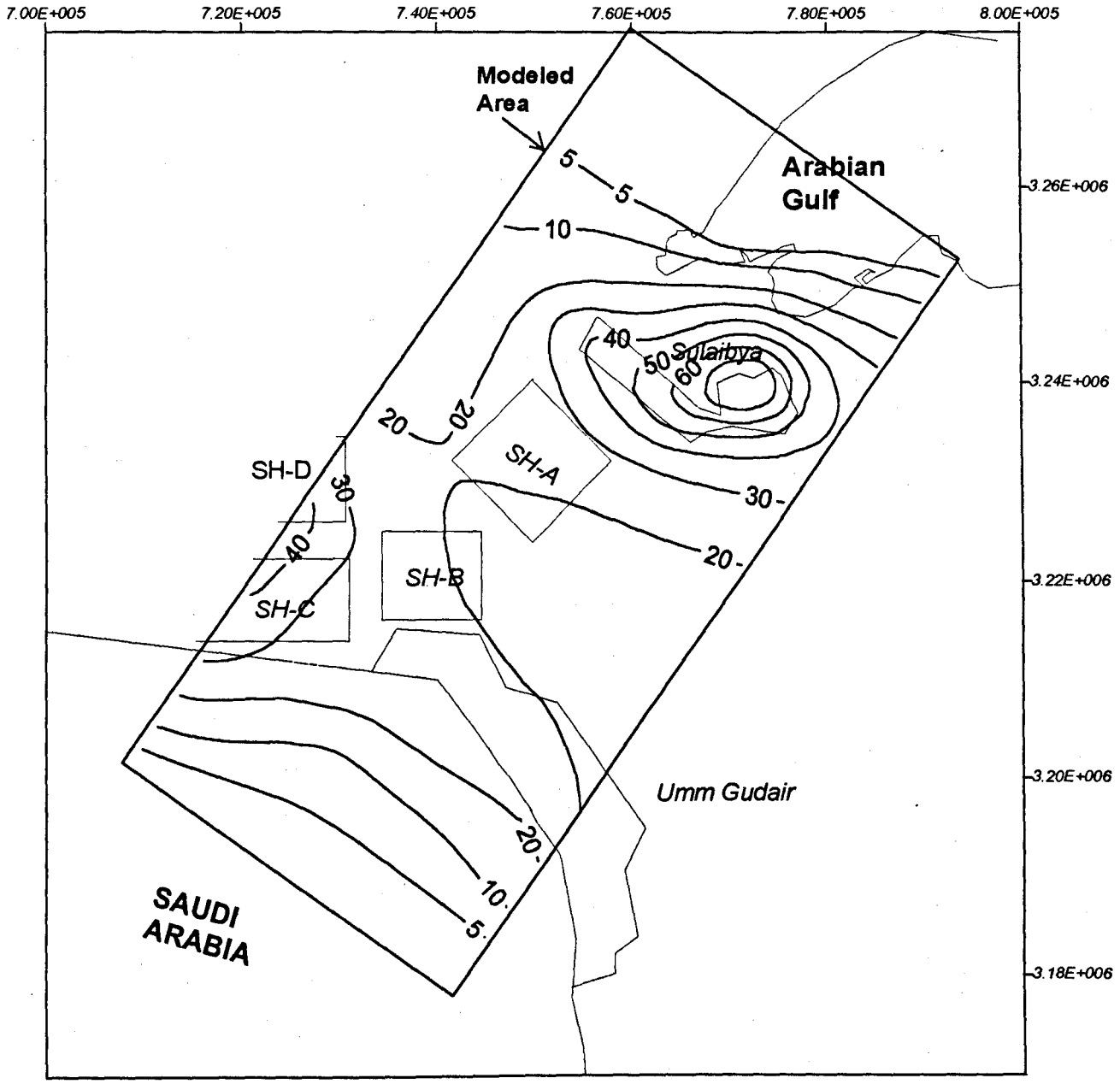


Figure 7.5: Simulated total drawdown in potentiomeric head of the Dammam aquifer to year 1995 using the sub-regional model, (m).

The solute transport part of the model was solved using the software MT3D, following the same procedures of constructing the regional transport model as explained previously in Chapter Four. Also, the transport aquifer's parameters were assigned to this model similar to the regional model transport parameters.

The following model parameters were found to be the most efficient in running the model with minimum error in mass balance, and with a reasonable size of transport time steps. The time step size should be not too large as to cause solution instability, and yet not so small as to require long computation time or excessive use of disc space. The optimum transport time step size was found to be 0.02 day increasing to 0.1 day, but it was necessary to keep it at the lower level at the beginning of pumping or injection stress periods. The resulting percent of mass balance discrepancy error during the transport simulation ranged from 0.01 to 1.05 %.

- Concentration weighting factor (WD) = 0.5
- Negligible relative concentration gradient (DCEPS) = 0.01
- Pattern for initial placement of particles (NPLANE) = 0
- Number of particles per cell in case of DCCELL <= DCEPS) = 1
- Number of particles per cell in case of DCCELL > DCEPS) = 20
- Minimum number of particles allowed per cell (NPMIN) = 2
- Maximum number of particles allowed per cell (NPMIN) = 40
- Multiplier for particles number at source cells (SRMULT) = 1
- Pattern of displacement of particles for sink cells (NLSINK) = 1
- Number of particles used to approximate sinks cells (NPSINK) = 20
- Criteria for controlling the selective use of either MOC or MMOC in the HMOC solution scheme (DCHMOC) = 1

## 7.4 SEASONAL CYCLES OF STORAGE AND RECOVERY

Groundwater is considered as a major component of the water system in Kuwait. A certain percentage of groundwater is blended with desalinated water to distribute this mixture as freshwater for consumers. Also, groundwater is used for irrigation and industrial uses. The abstraction of brackish groundwater will continue to increase following the expected expansion in the urban and irrigation demand.

The two utilised aquifers in Kuwait (KG and DM aquifers) are already subjected to overpumping creating a massive decline in the potentiometric head of the aquifers. The potentiometric head of the DM aquifer presently (1995) has three major cones of depression (Fig. 4.19), where the drop in head reaches 90, 50, and 30 m at Sulaibiya, Shigaya-D, and Umm Gudair wellfields, respectively. The decline in DM aquifers head drops below the main sea level by about 60 m, especially at the coastal areas, such as Sulaibiya field.

Also, the KG aquifer has cones of depression coincident with those in the DM aquifer, although the maximum decline is less at 30 m (Fig. 4.18).

The salinity of pumped groundwater has increased significantly during the last two decades (as shown in Figure 3.21). This could be related to the lowering of aquifer heads, inducing the upconing of the deep saline waters, and probably the lateral intrusion of sea water.

The Ministry of Electricity and Water (MEW) has plans to establish new wellfields to meet the increasing demands for groundwater. This will result in further decline of potentiometric heads and deterioration of groundwater quality.

The aquifers response for future pumping schemes was simulated under possible likely scenarios of groundwater production in Kuwait (discussed previously in Chapter 4). It was observed from the simulation that expanded decline in the aquifers potentiometric heads will be increased in the next 15 years.

The decline in the existing cones of depression at the DM aquifer heads under the expected intensive development will increase by year 2010 to about 160, 85, 70 m at Sulaibiya, Shigaya-D, and Umm Gudair wellfields, respectively. In addition a new cone of depression will be created at NW Shigaya with about 60m drop in head (as shown in Fig. 4.23). At that time, the flow condition in the DM aquifer will change from confined to unconfined in the western part of Kuwait, especially at Shigaya-D, and Shigaya-E wellfields.

The predictive simulation, also indicates that the water table level of KG aquifer may drop below the top of some well screens. At the Umm Gudair wellfield, the decline in the KG water table may be below the installed well screens resulting in the dewatering of the aquifer, especially in the eastern part of the field (where the present saturated thickness of the aquifer is about 30 m).

As a result, the effects which may produced by the current and the future declining in the water heads of the aquifers in Kuwait, can be summarised as follow:

1. Deterioration of groundwater quality by increasing the vertical upconing of the deep saline water, or by sea water intrusion, especially in the coastal areas (Sulaibiya field and Shigaya-E wellfields).
2. Increased cost of pumping
3. Some wells in the future may have to be abandoned in the KG aquifer, and new wells installed with deeper screens.

Consequently, the aquifers in Kuwait require artificial replenishment since the outflow of the system exceeds the natural inflow. Therefore, if artificial groundwater recharge is implemented, it can increase the aquifers yield by raising their depleted water heads to prevent the invasion of saline water through upconing or sea water invasion. Also, if the yield of the existing wellfields is increased, the need for constructing new wellfields can be postponed.

On the other hand, the desalination plants are not operating at their optimum capacity. The optimum capacity is about 75 % of the maximum installed capacity (personal communication, Abdel-Jawad, Research Scientist in Desalination Department, KISR). The

sub-optimum use of desalination plants is due to the seasonal variation in freshwater demand, where it increases in summer and decreases in winter. Thus, in winter the plants are working at a lower capacity than the optimum, while during summer they are working with a capacity exceeding their optimum capacity.

In Kuwait there are no natural storages, such as dams, lakes, or surface reservoirs. Hence, the desalination plants are constructed with a maximum capacity equal to the expected peak in water demand.

Therefore, through a type of conjunctive use, the aquifers could be used as underground storage to store the surplus of desalinated water during winter for later use during summer. Hence, the plants can operate with their optimum capacity all over the year without any seasonal fluctuation. In addition, this storage can be used as a stand-by storage to meet the difference between the maximum plants capacity and the freshwater peak demand which should result in the postponement of new desalination plants. At the same time, the depleted aquifers will be restored through raising their water heads and combating saline water encroachment.

To assess the feasibility of applying this cyclic storage and recovery scheme into the DM aquifer at Shigaya-B wellfield, which is the recommended site for this purpose (as explained in section 6.5.2), the quantity and quality of water which could be stored and recovered should be determined.

### 7.4.1 INJECTION VOLUME

As described previously (in section 6.3.2), the Shigaya-B wellfield has a very high specific injection rate (SIR) which ranges from 79 to 90 $m^2/d$. It was shown in Table 6.3 that the injection rate which could be completed during one season (six months) at this site is 2080 $m^3/d$ per well. The site includes 16 wells, but if this number is assumed to be 20 wells in order to increase the field capacity, hence a rate of 46,600 $m^3/d$ of water can be injected and recovered. The volume of freshwater which could be stored using this rate (which is equivalent to the present designed wells pumping capacity) is small compared to the required volume. For a seasonal storage, sufficient volumes of water equal to the difference between the optimum capacity of the desalination plants and the high or low

freshwater demands need to be stored or recovered within a 6 months period. This means all the surplus of desalinated water during the summer has to be stored, and the deficit in freshwater demand (if desalination plants operate to their optimum capacity) should be met by underground storage.

Thus, because the excess space in the aquifer (unsaturated thickness) is still available if the wells are injected at that rate, it was assumed that the injection rate could be increased to optimise all the available space in storing more freshwater. The sub-regional flow model (in section 7.3) was used to determine the maximum injection rate under which the build-up in aquifer head will not exceed the ground level (taking into account the effect of clogging as presented in Table 6.3). This injection rate was found to be 7000 $m^3/d$ per well.

Therefore, the maximum rate of water which could be injected successfully using all the wells in Shigaya-B field with a maximum utilisation of the available space of the aquifer is 140,000 $m^3/d$. Also, the same rate of water can be recovered.

### 7.4.2 RECOVERY EFFICIENCY

For the objective of increasing the aquifer yield, the quality of the recovered water is not a major issue since the quality of the recharged water is better than the aquifer water. However, the quality of the recovered water is very important in balancing the operation of desalination plants. This quality will decide the actual volume of the recovered water needed to replace the difference between the optimum capacity of desalination plants and the freshwater peak demand during summer.

The sub-regional transport model was used to simulate the variation in the TDS of the aquifer water during the injection half-cycles, and the TDS of the recovered water during the recovery half-cycles.

The simulated period is 10 years (1996-2005), and it is divided into 20 stress periods. Each represents one half-cycle (season) which is either injection or recovery. The whole simulation time is alternating between injection and recovery. Further, each stress period was divided into time steps, and the time steps divided into smaller units which are

transport steps. To overcome problems of instability may be introduced by the numerical solution, the size of the transport time steps was kept as small as possible (0.02-0.1 day).

The recovery efficiency will be affected by the injected and the recovered volumes of water. In order to eliminate this effect, recovery efficiency was estimated first regardless of the actual need for desalinated water during summer and winter, where a constant rate (7000 $m^3/d$) was used for the injection and recovery cycles. Later, the actual rates required to operate the desalination plants with their optimum capacity will be considered.

During the simulation, all the wells in the Shigaya-B field were injected during summer and pumped during winter simultaneously. Whereas, the other fields are pumped through the whole simulation period based on the predicted groundwater abstraction rates. The TDS of the DM native water ranges from 2800 and 3000 mg/l at the injected site, whereas, the TDS of the recharged water is constant at 350 mg/l.

Figure 7.6 displays the simulated water concentration profile as a result of the cyclic injection/recovery scheme at Shigaya-B site.

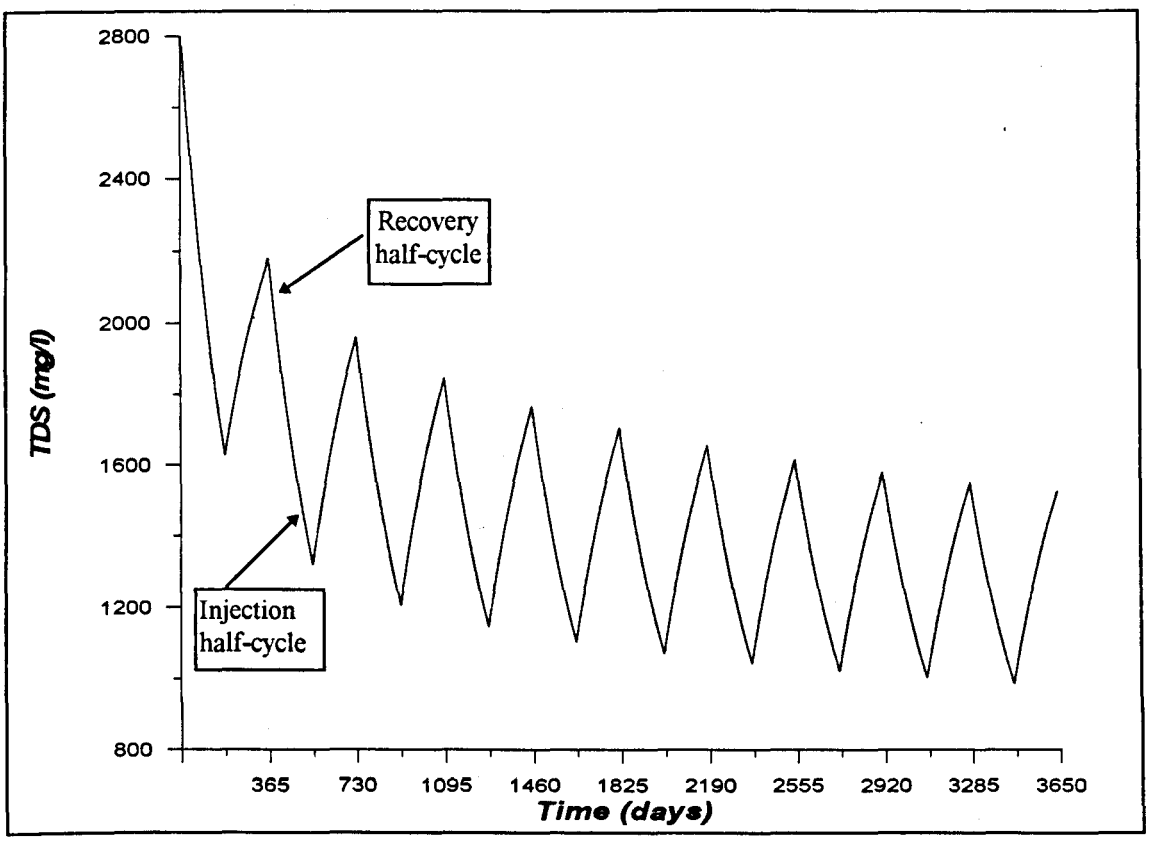


Figure 7.6: Concentration profile of the aquifer water during injection half-cycles, and for the recovered water during recovery half-cycles, simulated during the seasonal cyclic injection/recovery in the Shigaya-B wellfield.

The mean percentage of recovery efficiency during the recovery half-cycles was presented in Table 7.2.

| **Recovery half-cycle Period** | **% of Recovery efficiency if TDS of recovered water is:** | | |
|---|---|---|---|
| | **< 1000** | **< 1500** | **< 2000** |
| Sum. 1996 | 0 | 0 | 58 |
| Sum. 1997 | 0 | 12 | 100 |
| Sum. 1998 | 0 | 20 | 100 |
| Sum. 1999 | 0 | 25 | 100 |
| Sum. 2000 | 0 | 30 | 100 |
| Sum. 2001 | 0 | 34.5 | 100 |
| Sum. 2002 | 0 | 38 | 100 |
| Sum. 2003 | 0 | 41.5 | 100 |
| Sum. 2004 | 0 | 45 | 100 |
| Sum. 2005 | 2 | 48 | 100 |

Table 7.2: Recovery efficiency for the recovered water simulated during recovery half-cycles at the Shigaya-B field, (TDS in mg/l).

Table 7.2 indicates that the recovery efficiency is improving with the increasing number of injection/recovery cycles. Table 7.3 shows the percentage of improvement in the recovery efficiency as function of injection/recovery cycles.

| Recovery half-cycle period | % of improvement in the recovery efficiency at TDS <1500 mg/l * |
|---|---|
| Sum. 1996 | 0 |
| Sum. 1997 | > 100 |
| Sum. 1998 | 72 |
| Sum. 1999 | 26 |
| Sum. 2000 | 20 |
| Sum. 2001 | 15 |
| Sum. 2002 | 10 |
| Sum. 2003 | 9 |
| Sum. 2004 | 8 |
| Sum. 2005 | 7 |

Table 7.3: Percentage of improvement in recovery efficiency from cycle to cycle.
Note: * % of improvement in recovery efficiency = (recovery efficiency at the concerned cycle - recovery efficiency at former cycle)/ recovery efficiency at former cycle.

The recovery efficiency was improved significantly during the first few cycles, then improved at a slow rate until it became nearly constant. The improvement in recovery efficiency as the cycles proceed is attributed to the gradual outward movement of the transition zone between the injected freshwater and original brackish groundwater at the end of each cycle. Thus, the quality of native water before any cycle starts is better than the quality at the previous one, and so on. Generally, the quality of the native water was improved from about 2800 mg/l at the beginning to reach 1550 mg/l after the end of the last cycle with a complete recovery of injected water.

### 7.4.3 ROLE OF CYCLIC INJECTION/RECOVERY IN THE OPTIMUM OPERATION OF DESALINATION PLANTS

The future urban freshwater demand and thus the groundwater and desalinated water production were assumed to increase annually at a rate of about 3 % based on the present rate of population growth. The present installed capacity of desalination plants is 1,054,000 $m^3/d$, and it is proposed to increase it up to 1,162,000 $m^3/d$ by year 2000 by establishing new units. Also, it is assumed that a new units will be added in 2005 to increase the capacity of desalination plants to 1,270,000 $m^3/d$. This is based on the previous trend in the desalination plants development.

Table 7.4 displays the predicted desalinated water production rate, the optimum operating capacity of the desalination plants, and the difference between them. Figure 7.7 shows these rates in a graphically form.

| Year | Freshwater consumption x 1000 $m^3/d$ | Desalinated water consumption x 1000 $m^3/d$ | Optimum capacity of desalination plants x 1000 $m^3/d$ | Difference between desalinated water optimum production and consumption x 1000 $m^3/d$ |
|---|---|---|---|---|
| Sum. 1996 | 619 | 574 | 792 | +218 |
| Win. 1996 | 874 | 810 | 792 | -18 |
| Win. 1997 | 638 | 591 | 792 | +201 |
| Sum. 1997 | 900 | 834 | 792 | -42 |
| Win. 1998 | 565 | 608 | 792 | -184 |
| Sum. 1998 | 927 | 859 | 792 | -65 |
| Win. 1999 | 677 | 627 | 792 | +165 |
| Sum. 1999 | 955 | 885 | 792 | -93 |
| Win. 2000 | 696 | 645 | 792 | +147 |
| Sum. 2000 | 983 | 911 | 873 | -38 |
| Win. 2001 | 718 | 665 | 873 | +209 |
| Sum. 2001 | 1014 | 939 | 873 | -66 |
| Win. 2002 | 739 | 685 | 873 | +189 |
| Sum. 2002 | 1044 | 967 | 873 | -94 |
| Win. 2003 | 761 | 705 | 873 | +168 |
| Sum. 2003 | 1075 | 996 | 873 | -123 |
| Win. 2004 | 784 | 726 | 873 | +147 |
| Sum. 2004 | 1107 | 1025 | 873 | -152 |
| Win. 2005 | 807 | 748 | 873 | 125 |
| Sum. 2005 | 1140 | 1056 | 952 | -184 |

Table 7.4: Difference between the optimum capacity of desalination plants and the desalinated water consumption, where (+) surplus, and (-) shortage.

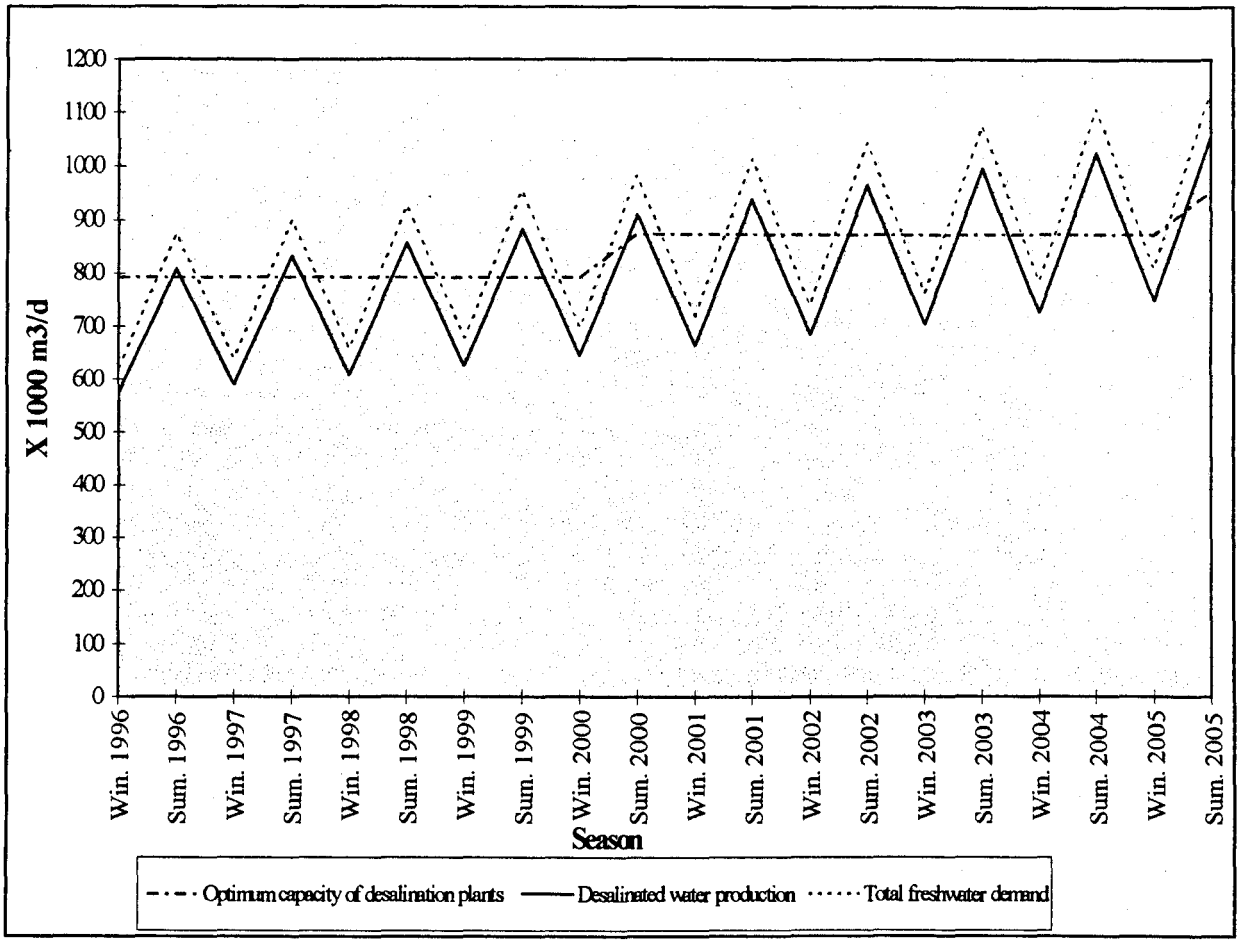


Figure 7.7: Forecasted urban freshwater demand and the desalination plants production rate.

During the injection half-cycles, the desalinated water is injected into the aquifer when there is a surplus of water available, as presented in Table 7.4. This rate should not exceed the maximum injection capacity of the field which was determined to be 140,000 $m^3/d$. The availability of desalinated water during winter exceeds the aquifer capacity for injection. Thus, at all the injection half-cycles, the total injection rate at the site was taken to be equal to the maximum injection capacity of the site.

The pumping rate during recovery half-cycles (summer) is controlled by the need of the stored water to meet the difference between the optimum capacity of desalination plants and the peak in urban freshwater demand.

Currently, the components of the freshwater which are supplied to consumers are desalinated water and groundwater. The difference between the freshwater demand and desalinated water production (given in Table 7.4 and Figure 7.7) represents the volume of

the groundwater which is added to the desalinated water. About 92 % of freshwater is desalinated water and the rest is brackish groundwater.

The balance between these sources is:

$$C_c V_c = C_d V_d + C_g V_g \qquad (7.1)$$

where;

$C_c$ and $V_c$: TDS, and volume of consumed freshwater, respectively.

$C_d$ and $V_d$: TDS, and volume of desalinated water, respectively.

$C_g$ and $V_g$: TDS, and volume of groundwater, respectively.

According to the simulated recovery efficiency (as presented in Table 7.2) the quality of the stored water when it is recovered back (as recovered water) will not be suitable for direct potable purposes. However, its quality is much better than the original brackish groundwater. Therefore, if the recovered water is blended with desalinated water, the percent of this water in forming the consumed freshwater will be higher than using the existing groundwater. In this case the difference between the peak freshwater demand during summer and the optimum capacity of desalination plants will be substitute by the recovered water.

Hence, the freshwater for consumers use can be represented by the following expression:

$$C_c V_c = C_d V_d + C_g V_g + C_r V_r \qquad (7.2)$$

where:

$C_r$ and $V_r$: TDS, and volume of recovered water, respectively.

Brackish groundwater and recovered water can form together the blend water, as

$$C_b V_b = C_g V_g + C_r V_r \qquad (7.3)$$

where:

$C_b$, and $V_b$ : TDS, and volume of blend water, respectively.

The volumes of recovered water and groundwater needed for blending purpose to substitute the difference between the urban freshwater demand and the optimum production is determined by using the following steps:

1- Determine the difference between the optimum production capacity of the plants

and the freshwater demand. This difference represents the required volume of blend water to replace the deficit in desalination plants production.

$$V_b = V_c - V_o \qquad (7.4)$$

Where:

$V_o$: Optimum capacity of the desalination plants.

2- Determine the required quality of $V_b$ to balance the volumes and qualities in Equation 7.2. Where the TDS for different sources are: $C_c$ is 350 mg/l, $C_d$ is 30 mg/l, and $C_g$ is 4000 mg/l.

If $V_d$ is replaced by $V_o$, and $(C_g V_g + C_r V_r)$ by $V_b$ in Equation 7.3, then :

$$C_c V_c = C_d V_o + C_b V_b \qquad (7.5)$$

using the known TDS values of freshwater and desalinated water,

$$V_c = 30 V_o + C_b V_b \qquad (7.6)$$

because $V_o = V_c - V_b$ as in Equation 7.4, then

$$V_c = 30 V_c - 30 V_b + C_b V_b$$

Solving this Equation

$$C_b = (320 V_c / V_b) + 30 \qquad (7.7)$$

3- Determine $V_g$ and $V_r$, which are the volumes of recovered and groundwater within the blend water volume $V_b$.

From Equation 7.3, $C_g$ can be replaced with its value, and $V_g$ with $(V_b - V_r)$, then

$$C_b V_b = 4000 (V_b - V_r) + C_r V_r$$

Solving this Equation

$$V_r = (C_b - 4000 / C_r - 4000) V_b \qquad (7.8)$$

From Equation 7.8, the volume of recovered water which is required for blending purposes to replace the difference between the optimum production capacity of desalination plants and urban freshwater demand during the recovery half-cycles cannot be determined unless its quality is known in advance. At the same time the exact TDS of this water cannot be simulated without knowing the pumping rate. Therefore, an iterative procedure was used to solve this interaction as follows;

- First, the mean TDS values for each recovery half-cycle as simulated during the assessment of the recovery efficiency (Fig. 7.6) were used as a prospective TDS for the recovered water.
- Use Equation 7.8 to calculate the required volume of stored water $V_r$ based on these TDS.
- Use the calculated $V_r$ in the transport sub-regional model, and simulate the TDS.
- Return to Equation 7.8 and calculate $V_r$ with the new simulated TDS. This $V_r$ will be closer to the required one.
- Use the new calculated $V_r$ in the transport model again and simulate TDS which will be more accurate than the previous estimations.

The above procedure was repeated until the required volume and quality of recovered water was determined. The sub-regional model was used to simulate the water TDS during injection-recovery cycles. As the recovered water is pumped, its TDS is decreased with time and this change take place at very small intervals and it is unrealistic to consider these changes. Hence, the mean value of TDS for each recovery half-cycle was used in calculating the volume of stored water which needs to be recovered. Table 7.5 shows the TDS of the recovered water required to replace the difference between the water peak demand during summer and the optimum capacity of the desalination plants. The recovery rates of this water during summer seasons are presented in Table (7.6)

| **Recovery half-cycle no.** | **Year** | **Simulated TDS of the recovered water ($C_r$) (mg/l)** | | |
|---|---|---|---|---|
| | | **Minimum** | **Maximum** | **Mean** |
| 1 | 1996 | 1628 | 1738 | 1683 |
| 2 | 1997 | 1106 | 1466 | 1294 |
| 3 | 1998 | 966 | 1496 | 1250 |
| 4 | 1999 | 974 | 1600 | 1318 |
| 5 | 2000 | 1020 | 1262 | 1145 |
| 6 | 2001 | 851 | 1289 | 1084 |
| 7 | 2002 | 860 | 1410 | 1160 |
| 8 | 2003 | 917 | 1442 | 1204 |
| 9 | 2004 | 933 | 1443 | 1212 |
| 10 | 2005 | 932 | 1437 | 1208 |

Table 7.5: Simulated TDS of the recovered water during the recovery half-cycles (summer).

Note: Minimum and maximum TDS were simulated at the beginning and end of each recovery half-cycle, respectively.

At some recovery half-cycles (e.g. 8 and 9), the required volume of recovered water exceeds the installed capacity of the pumping wells. Thus, the desalination plants need to be operated with rates higher than their optimum capacities. The blend water in this situation is:

$$C_b V_b = C_g V_g + C_r V_r + C_b A \qquad (7.9)$$

where ;

$A = V_b$ - available $(C_g V_g + C_r V_r)$, which is the additional volume of water needed for blending due to the lack in recovered water. The available sources are the desalinated water and groundwater only. Thus,

$$C_b A = C_d V_{d1} + C_g V_{g1} \qquad (7.10)$$

where:

$V_{d1}$ : additional volume of desalinated water

$V_{g1}$ : additional volume of groundwater.

From Equation 7.10, replace $V_{g1}$ with $(A - V_{d1})$, $C_d$, and $C_g$ with their actual values, the Equation 7.10 can be solved to find $V_{d1}$

$$V_{d1} = A\,(C_b - 4000/-3970) \qquad (7.11)$$

Finally, the volume of $V_{d1}$ is the additional volume of desalinated water which has to be produced above the optimum production capacity of the desalination plants to meet the peak in urban freshwater demand.

Table 7.6 presents the freshwater demand during summer period, and the required rates of desalinated water, groundwater, and recovered water to replace the shortage in freshwater supply resulting from operating the desalination plants with their optimum capacity during summer.

| Recovery half-cycle No. | Year | Urban freshwater consumption ($V_c$) x 1000 $m^3/d$ | Optimum capacity of desalination plants ($V_o$) x 1000 $m^3/d$ | Blend water ($V_b$) x 1000 m3/d | | | |
|---|---|---|---|---|---|---|---|
| | | | | Total ($V_b$) | Brackish groundwater ($V_g$) | Recovered water ($V_r$) | Additional desalinated water ($V_{d1}$) |
| 1 | 1996 | 874 | 792 | 82 | 62 | 20 | 0 |
| 2 | 1997 | 900 | 792 | 108 | 56 | 52 | 0 |
| 3 | 1998 | 927 | 792 | 135 | 48 | 87 | 0 |
| 4 | 1999 | 955 | 792 | 163 | 37 | 126 | 0 |
| 5 | 2000 | 983 | 873 | 110 | 66 | 44 | 0 |
| 6 | 2001 | 1014 | 873 | 141 | 59 | 82 | 0 |
| 7 | 2002 | 1044 | 873 | 171 | 47 | 124 | 0 |
| 8 | 2003 | 1075 | 873 | 202 | 49 | 140 | 13 |
| 9 | 2004 | 1107 | 873 | 234 | 51 | 140 | 43 |
| 10 | 2005 | 1140 | 952 | 188 | 52 | 136 | 0 |

Table 7.6: Contribution of different sources in supplying the urban freshwater demand during summer seasons.

As shown in the Table 7.6, that the surplus of desalinated water which is available during winter, could be stored and recovered back to meet the difference between the optimum capacity of desalination plants and the peak in freshwater demand during summer. The zero values of additional desalinated water ($V_{dl}$) needed to meet the freshwater demand, indicates that the objective of operating the desalination plants with their optimum capacity was achieved.

Figure 7.8 shows the degree to which the injection/recovery seasonal cycles of desalinated water can help to keep the desalination plants working at their optimum capacity all through the year. It shows the optimum desalination plants production capacity, and the volume of water that the cyclic injection/recovery system can obtain or provide during the operation of desalination plants at their optimum capacity. During winter the surplus of desalinated water that could not be injected (because it exceeds the injection capacity of the aquifer at this site (i.e. >140,000 $m^3/d$) was subtracted from the optimum capacity of the plants. While, during summer the additional volume of desalinated water ($V_{dl}$) produced above the optimum capacity of the plants (as presented in Table 7.6) was added.

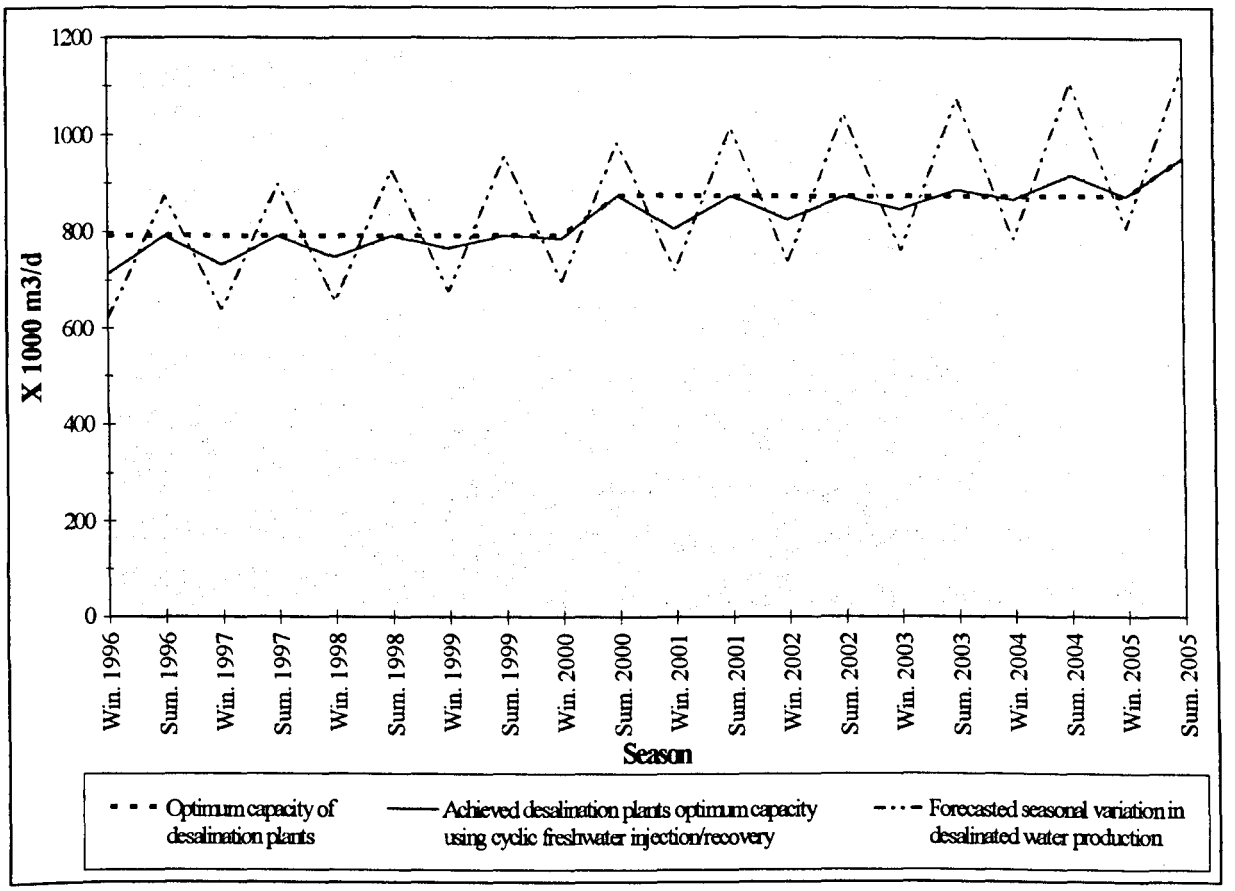


Figure 7.8: Achieved operational rate of desalination plants if cyclic injection-recovery of freshwater is applied, with a comparison to the optimum capacity of the plants and the actual seasonal fluctuation in desalination plants operation.

These results indicate the beneficial role of the injection/recovery cycles play in reducing the seasonal fluctuations of the desalination plants production below or above their optimum capacity. However, the exact optimum operation capacity cannot be attained because of the limited storage capacity at the selected site (Shigaya-B wellfield), since not all the surplus desalinated water available during winter can be injected. Therefore, if additional wells are drilled at this site which prove to have high specific injection capacities, then all the available water could be injected and consequently a greater volume could be recovered. Around ten wells would need to be constructed each with an installed pumping capacity of 7000 $m^3/d$. This expansion of the field capacity in storing and recovering the desalinated water would postpone the need for establishing new desalination plants in the future for about three years.

Figure 7.9 displays the simulated head of the DM aquifer at a selected node using the sub-regional model during the seasonal cycle of injection/recovery. The injection rate all over the injection half-cycles is constant at 7000 $m^3/d$ per well (if engineering specification of the wells permits for this rate), whereas the recovery rate is based on volume of water required to replace the shortage in desalination plants production during summer period if they are working with their optimum capacities (as presented in Table 7.6).

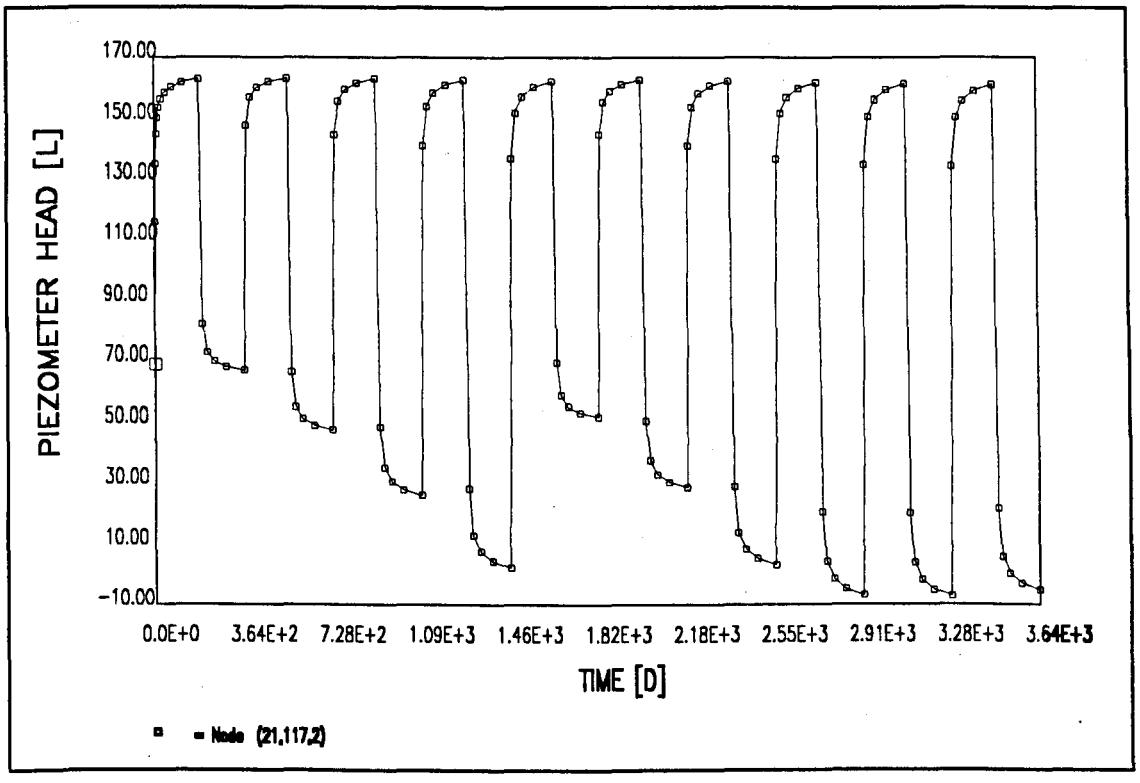


Figure 7.9: Simulated head of DM aquifer during the cyclic injection/recovery option at a selected well node in the injected site Shigaya-B. (piezometer head is shown in m amsl)

### 7.4.4 ROLE OF CYCLIC INJECTION/RECOVERY IN INCREASING THE AQUIFER YIELD

The role of seasonal cyclic injection/recovery in keeping the desalination plants working all the year at their optimum capacity was outlined earlier. The quality of the recovered water is the most critical controlling factor in this regard. The influence of such a seasonal storage and recovery scheme on increasing the aquifer yield needs to be evaluated. The quality of the recovered water in this case will not be a critical issue. The objective of increasing the aquifer yield by raising its depleted water head requires a regional hydraulic evaluation of the aquifer response to such an artificial groundwater recharge scheme. Therefore, the regional flow model (described in Chapter 4) was used to simulate this response.

A comparison between two scenarios was made:

- One considered the continuation of brackish groundwater abstraction to meet the forecasted demand for the next 10 years (1996-2005). Only the existing wellfields were considered in this scenario. It was assumed that the wellfields abstraction rate will increase annually by 3 % until 90 % of the designed pumping capacity of each field is reached.
- Scenario two is same as the first scenario, except that includes the seasonal injection/recovery of desalinated water at Shigaya-B using the maximum capacity of the aquifer to store and recover the water. This rate was identified (in section 7.4.1) as 140,000 $m^3/d$ for the entire site. The water was injected at this rate during the injection half-cycles (winter), and recovered during the recovery half-cycles (summer).

Figure 7.10 shows the simulated drawdown in the DM aquifer potentiometric head at the last pumping period (summer 2005) under the conditions of Scenario One.

Figure 7.11 (A and B) displays the simulated changes in the DM aquifer potentiometric head when the cycles of injection/recovery at Shigaya-B wellfield were included in addition to the groundwater abstraction from the other wellfields, at the last injection half-cycle (winter 2005), and the last recovery half-cycle (summer 2005), respectively.

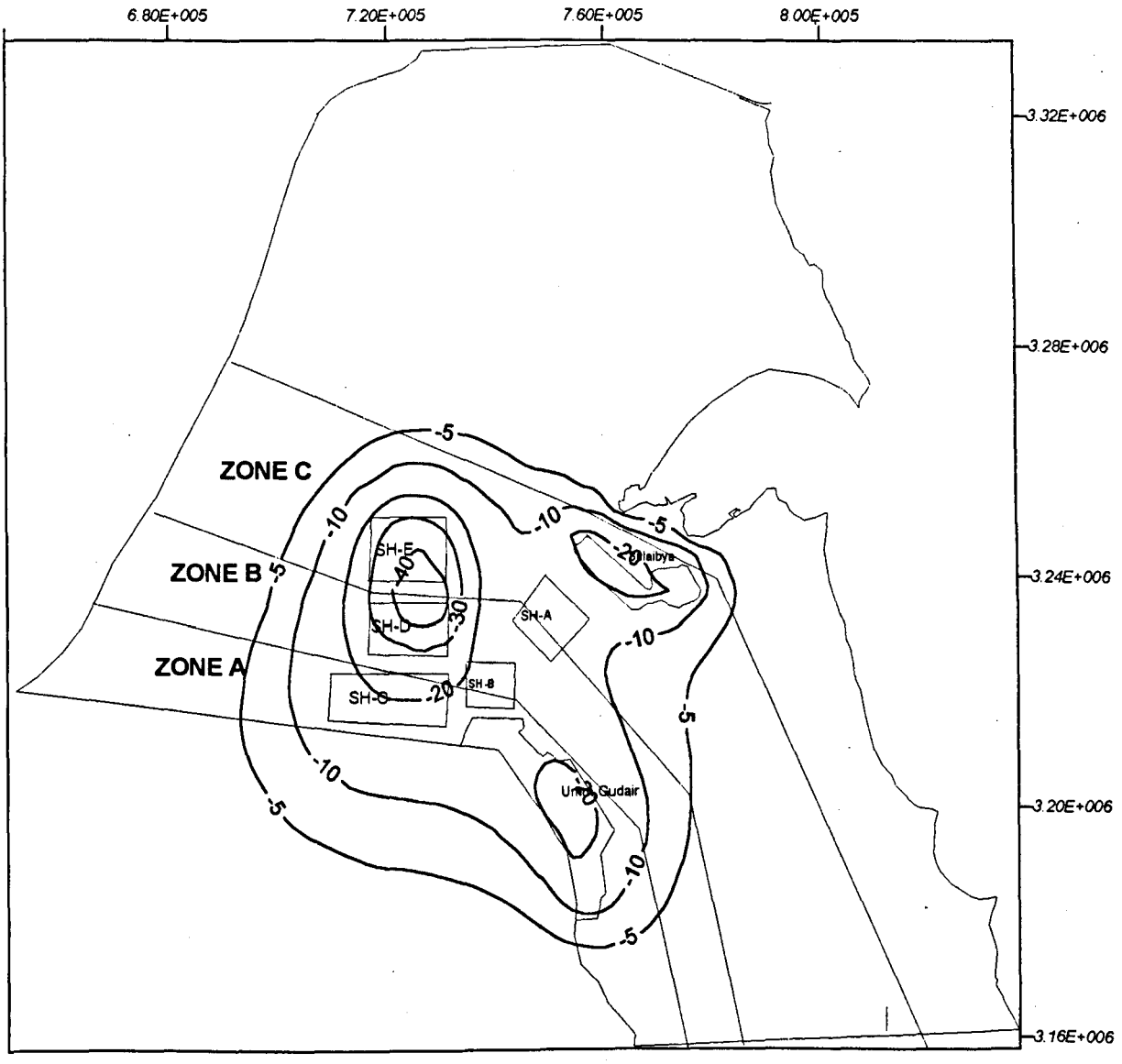


Figure 7.10: Simulated drawdown in the Dammam aquifer potentiometric head from 1995-2005 under Scenario 1 due to the groundwater abstraction from the existing wellfields using the regional model, (-) is drawdown, (in metre).

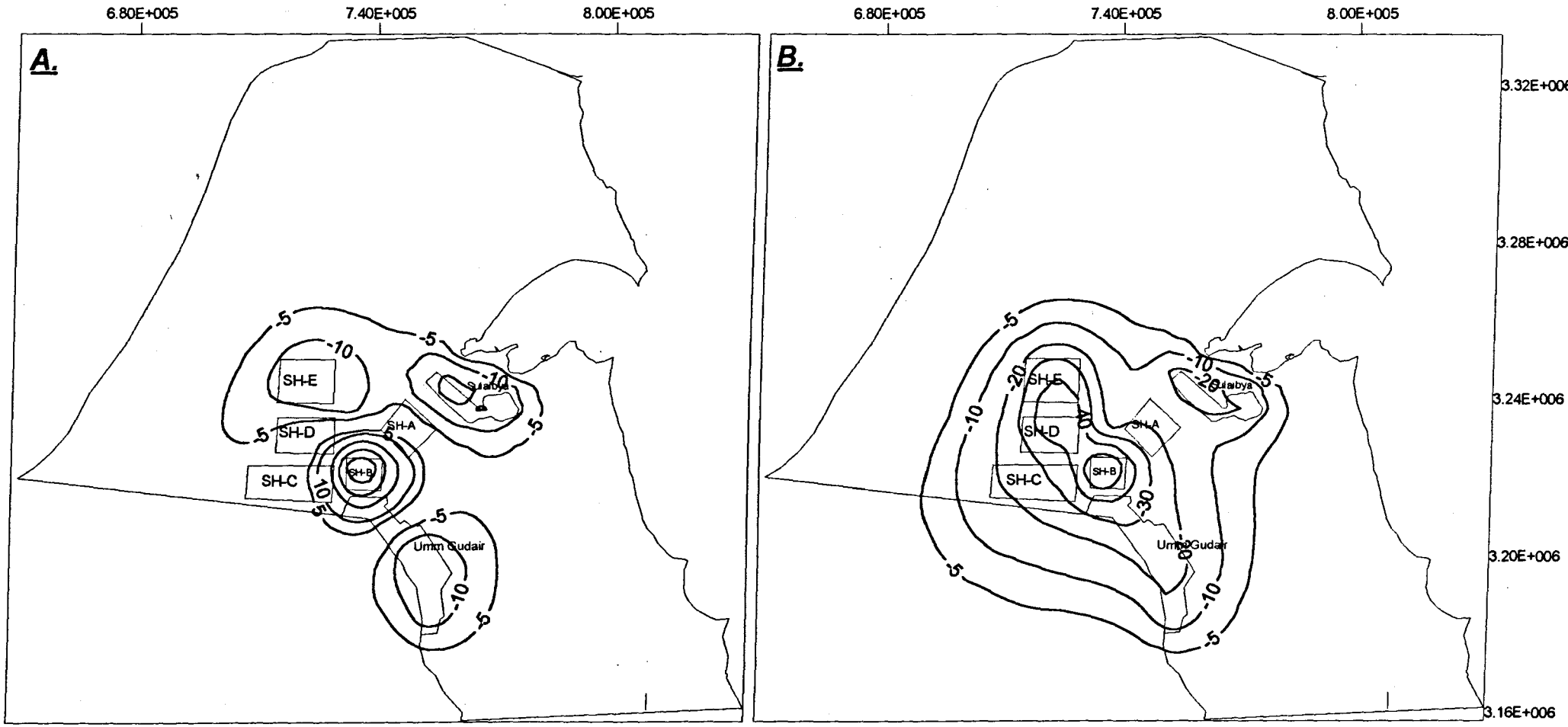


Figure 7.11 (A and B): Simulated changes in the Dammam aquifer potentiometric head during the seasonal freshwater injection/recovery at the Shigaya-B wellfield using the regional model, (+) build-up, and (-) drawdown (in metre) . A: at the last injection half-cycle (winter 2005). B: at the last recovery half-cycle (2005).

By comparing Figure 7.10 with Figure 7.11, it is clear that the potentiometric head of the injected aquifer was raised significantly during the injection half-cycles. Whereas, the increase in the aquifer head during the recovery half-cycles was minor. Table 7.7 presents the simulated decline in the aquifer head from (1996-2005) at the major cones of depression under Scenario One (i.e. before the seasonal injection/recovery was practiced). Also, it shows the resulted change in aquifer head at the same locations and for the same period during the injection/recovery scheme. The difference between these two values is the increase in water head due to the seasonal artificial groundwater recharge at the Shigaya-B site.

| **Wellfield (cone of depression)** | **Drawdown before seasonal injection/recovery (m)** | **Change in W. L. during seasonal injection/recovery (m)** | | **Difference in W. L. before and after injection (= expected water level rise) (m)** | |
|---|---|---|---|---|---|
| | | **Injection season (winter)** | **Recovery season (summer)** | **Winter** | **summer** |
| Shigaya-D | -50 | -15 | -45 | +35 | +5 |
| Sulaibiya | -30 | -20 | -20 | +10 | +10 |
| Umm Gudair | -22 | -15 | -25 | +7 | -3 |
| Shigaya-B (injected site) | -17 | +45 | -55 | +62 | -38 |

Table 7.7: Expected rise in the DM aquifer head if the seasonal cycles of injection/recovery are implemented at the Shigaya-B wellfield.

The above table shows that the aquifer head at the main cones of depression increased during the injection period to about 35m at Shigaya-D with the second main cone of depression in the DM aquifer head. However, during the recovery season this increase was reduced to 5 m. The increase in the aquifer head during the injection period could be for a short- term like the increase in the aquifer storage, which increases during the injection half-cycles and returns back to the original situation when the stored water is recovered during the recovery half-cycles.

Therefore, the increase in the water head which could be achieved during the recovery half-cycles is more representative in judging the actual rise in the water head as result of the

seasonal cycles of injection/recovery. The total rise in water head in the final recovery half-cycle is 10 and 5 m at the Sulaibiya and Shigaya-D wellfields, respectively.

At the Umm Gudair and Shigaya-B wellfields the water head dropped by 3 and 38 m respectively at the last recovery season with respect to its level before the seasonal injection/recovery began. This is because the Shigaya-B is the injected/recovered site, where it was pumped during the recovery half cycles with a rate higher than its normal production (which has been used during Scenario one). Also, the Umm Gudair field is located nearby this field and was effected by the high recovery rate.

To maximize the benifit from cyclic freshwater injection/recovery practice in increasing the aquifer yield among the objective of operating the desalination plants with their optimum capacity, another location rather than Shigaya-B could be selected. It was found that the Shigaya-D wellfield could be this alternative site. This is because it is located in a highly depleted area where the decline in the aquifer head has created the second largest cone of depression in the whole of Kuwait. Therefore, the aquifer response to the seasonal injection/recovery of freshwater at this site was also simulated. The injection rate during the injection half-cycles was set equal to the existing installed pumping capacity of the wells (1840 $m^3/d$ each). While the production rate during the recovery half-cycles was similar to the predicted abstraction rate for this field. The other wellfields were assumed to operate at the normal abstraction rate as in Scenario one.

Figure 7.12 (A and B) shows the simulated changes in the DM aquifer potentiometric head at the last injection and recovery half-cycles (winter and summer 2005) if seasonal cyclic of injection/recovery was introduces at Shigaya-D wellfield (i.e. under Scenario Two). The total increase in the aquifer head is 17, 5, 2, 1 m in summer; and 80, 10, 7, 20 m in winter, at the injected site, Sulaibiya, Umm Gudair, and Shigaya-B wellfields, respectively.

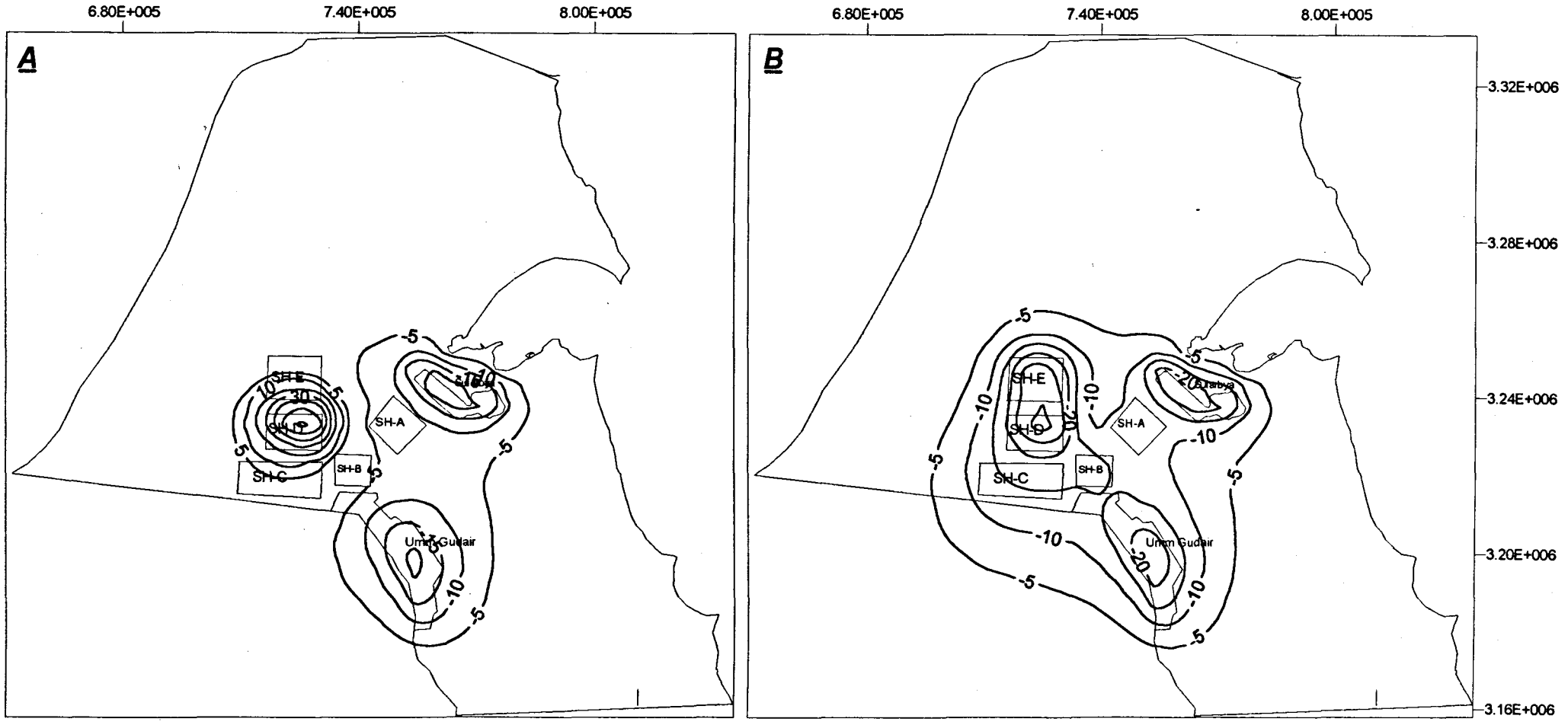


Figure 7.12 (A and B): Simulated changes in the DM aquifer potentiometric head during the seasonal injection/recovery at Shigaya-D field using the regional model. (A) at the last injection half-cycle (winter 2005), and (B) at the last recovery half-cycle (summer 2005). (+) build-up, and (-) drawdown, (in metre).

To maximise the benefits from the artificial groundwater recharge in increasing the aquifer yield, the groundwater abstraction pattern in addition to the artificial groundwater recharge should be managed in a more efficient way.

The optimum injection/abstraction alternative is the one which can achieve the followings objectives :

1. Optimally utilise the freshwater injection into the aquifer in increasing the yield of the aquifer system.
2. Minimise the decline in the aquifer potentiometric head due to the groundwater abstraction.
3. Protect the groundwater quality from deterioration effects, and (if possible) improve it.

After several runs with different scenarios the optimum option was determined to achieve the above objectives. The Kuwait region was divided into three zones (A, B, and C) as shown in Fig. (7.10). These zones were arranged laterally in the direction of regional groundwater flow.

Zone A includes Umm Gudair and Shigaya-C wellfields. This zone is recommended to be the zone of production, in which the pumping should be maximised to reach the installed pumping capacity of the wells. Also, the pumping should be sustained at a constant rate all the year at the same rate without any seasonal fluctuation trying to reach the steady state drawdown in the aquifer potentiometric head.

Zone B includes Shigaya-A, Shigaya-B, and Shigaya-D wellfields. As this is located in the midst of the other existing wellfields, it is considered as the best injection zone. At this zone, the injection of freshwater will be carried out during winter time when freshwater is available. Later, this zone will be pumped to utilise the freshwater stored during summer time, when the water demand is high.

Zone C includes the Sulaibiya, NW-Shigaya, Atraf, and Shigaya-E wellfields. It is located close to the Arabian Gulf shoreline which is the natural discharge zone of the aquifer system, and where the sea water effect becomes more dominant. This zone is the control zone, which can be pumped if the water demand during summer exceeds the production

rate from zones A and B, or if zone B is already used for freshwater injection. But the pumping from this zone should be minimised as far as possible.

By applying this pumping/injection policy, the following advantages can be obtained:

1. Induced lateral inflow to recharge the whole aquifer system.
2. Artificial recharge of the KG aquifer (indirectly through vertical leakage) because it is mostly pumped at zone B (injection zone).
3. The replenishment of the aquifer will be more effective.
4. Saline water intrusion will be halted.
5. Injected freshwater will be recovered by the down-gradient wells in Zone C before it escapes to the Gulf.

## 7.5 LONG-TERM STRATEGIC RESERVE

Kuwait depends mainly on desalination plants as its major source of freshwater. Partial or total loss of desalination plant capacity due to any reason will cause a freshwater crisis. The nature and scale of such a crisis cannot be predicted, but (if it does occur) it is very likely to occur to different degrees of severity. It could be due to limited mechanical failure or terrorist activities to one desalination plant, or could be the result of a complete destruction of all desalination plants and available freshwater surface storages.

Therefore, different scenarios of the crisis should be assessed with relation to the expected freshwater demand and the available sources of freshwater at that time. Then, the optimum solution for each scenario can be determined.

### 7.5.1 FORECASTED FRESHWATER DEMAND

The average domestic water demand is usually controlled by the weather, seasonal factors, and social structure. In Kuwait the current domestic water demand is about 330 l/d per capita which is a very high rate when compared to other countries. For example, average per capita domestic demands of 230, 125, and 106 l/d are quoted for the USA, Australia, and the Netherlands respectively (Viswanathan, 1989). The total domestic water demand is made up of several components; Kitchen, bathroom, toilet, and laundry.

Under emergency conditions in Kuwait, it is assumed that the domestic water demand could be reduced to about 50 l/d per capita used for drinking and cooking purposes only. The rest of water demand for toilets, bathrooms, and laundry could be met by brackish groundwater supply. Assuming a population level of 2 million people, thus the freshwater demand will be 100,000 $m^3$/d. Assuming a duration of the emergency is nine months (270 day) which is the required to establish a new reverse osmosis (RO) plant (personal communication, Abdel-Jawad M. , Research Scientist in the desalination department, KISR). Hence, the total required storage of freshwater is 27 $Mm^3$. Under emergency conditions, the quality of the freshwater for drinking and cooking could be relaxed to 1500 mg/l which is the maximum allowable TDS for such purposes (WHO, 1969).

## 7.5.2 SOURCES OF FRESHWATER DURING EMERGENCY

At the present time, if any emergency takes place, the freshwater demand will be met by two sources:

1. Surface reservoirs and elevated towers where desalinated water is stored.
2. Fresh groundwater lenses existing in the northern part of Kuwait.

The total storage capacity of these sources is not adequate to meet the freshwater demand under the kinds of critical conditions outlined above. Moreover, the surface reservoirs are vulnerable to sabotage. Thus, in this study, the feasibility of storing freshwater in the aquifers as a third source which is safe from vandalism will be assessed.

**1-Fresh Groundwater Lenses**

Underground freshwater lenses exist in the Raudhatain and Umm Al-Aish areas (Fig. 3.18). The safe yield of these two fields is about 10,000 $m^3$/d which is insufficient to meet the predicted freshwater demand during emergency conditions. The TDS of this water is about 500 mg/l. If it could be blended with brackish groundwater having a TDS of 4000 mg/l to get a mixed water with a TDS of 1500 mg/l (using Equation 7.3), the available volume would be increased to 14,000 $m^3$/d.

**2- Surface Reservoirs**

Presently, the desalinated water is stored in man-made surface reservoirs and elevated towers which are part of the water distribution network. The storage capacity of these reservoirs is 8 $Mm^3$. If the TDS of the stored desalinated water is relaxed to 1500 mg/l by blending it with brackish groundwater, the available volume can be increased to 12.7 $Mm^3$ (as calculated by Equation 7.3).

**3-Underground Strategic Reserve**

Through a long-term practice, surplus desalinated water if the desalination plants work with their maximum installed capacity, could be injected into the aquifer, stored, and recovered back when it is needed. The feasibility of creating such storage from a hydrological and management point of view has to be evaluated. The Shigaya-A wellfield was recommended earlier (as discussed in 6.5.1) to be the optimum site for such a purpose based on the hydrological characteristics of the injected DM aquifer. The most important factor in selecting this site is its good recovery efficiency compared to other sites.

An implementation of water injection on a large scale requires more than one well if the volume to be injected and the required injection rate exceeds the capacity of a single well. Thus, the recovery efficiency could be changed due to the design and management parameters. The recovery efficiency of a group of wells, as well as the possible injection rate, depend on the extent of their interaction. The recovery efficiency can be increased if the wells are closely spaced. This will make the injected freshwater bodies form a common transition zone with adjoining saline water. Also when the freshwater is withdrawn from the wells, the mixing of the trapped saline water and the injected freshwater will be small (Merritt, 1985). However, if the wells are closely spaced, this will limit the injection rate for each because of the hydraulic gradients at nearby wells. So, the optimum geometric arrangement of the wells, and the schedule of injection and withdrawal has to be identified.

The existing spacing of the wells in Shigaya-A wellfield is about 3500 m. Using the current geometry of these wells, freshwater can be injected at high rates (about 3200 $m^3/d$). The contact between the created freshwater bodies will be minimal, they will essentially form small cylinders of freshwater surrounding the injection wells. Also, the using of the wells

with their existing geometry, will extended the utilised land area by the artificial groundwater recharge process which is not economically feasible. Therefore, it is assumed that new wells with different geometry from the existing ones will be constructed. The objective of the new design is to reduce the utilised area of the aquifer, maximise the recovery efficiency, and maximise the injection rate.

After several runs using the sub-regional transport model with various design alternatives, the optimum option was selected. It was found that the minimum well spacing under which a reasonable volume of water can be injected ranges from 1000 -1500 m. With lesser spacing the injection rate will drop significantly. The maximum well-injection rate which can be undertaken without raising the water head inside the injection-wells (calculated as described in section 6.3.2) was found to range from 1500 to 1750 $m^3/d$ depending on the number of the injection wells and their configuration. The arrangements of the wells in triangular or square pattern are the only possible simulated options because grid nodes did not correspond exactly to other arrangements such as circular patterns. To be able to use part of the existing wells, a square or triangular pattern placed in the middle of the field could be the optimum well configuration.

The same injection wells could be used to recover the stored freshwater. The recovery efficiency increases proportionally with the volume of injected water. But, the rate at which a given volume of freshwater is injected or recovered does not affect recovery efficiency. However, for a better recovery efficiency, withdrawal schedules should resemble the inverse of the injection schedules (Merritt, 1985).

If the injection and withdrawal rates are known, then there are two other factors which determine the number of wells needed to create an sufficient underground strategic reserve of freshwater;

- The freshwater demand during emergency conditions for which the number of wells should be enough to supply the freshwater within the given time.
- The maximum duration required to store the necessary volume of freshwater, where the usable freshwater which can be recovered should be equal to the freshwater demand. The number of wells has to be at least enough to recover the needed freshwater during

the emergency. But determining the number of wells which are required to reduce the duration of freshwater injection should be related to the cost. A trade-off between the cost of constructing more injection wells, and a longer time of injection with less wells has to be achieved.

### 7.5.3 SCENARIOS OF FRESHWATER CRISIS

The possible shortage in freshwater supply could occur at different scales ranging from limited loss of supply to a complete loss of freshwater. Three scenarios (A, B, and C) were considered here.

Scenario A considers a limited shortage in freshwater, assumed to occur due to mechanical failure or terrorist action against one or two desalination plants. Under this emergency, the existing storage of freshwater (surface reservoirs and fresh groundwater lenses) will be adequate to replace the lost portion of freshwater, and there is no need for artificial underground freshwater storage in this case.

Scenario B assumes that all the desalination plants were destroyed, but the surface reservoirs are unaffected and are at full capacity.

Scenario C is the most critical option, in which all the desalination plants and the surface reservoirs were subject to hostile action, and were completely destroyed.

With Scenarios B and C, the underground strategic reserve for freshwater is essential to overcome the freshwater crisis. Based on the earlier analysis, the Shigaya-A wellfield, where the target aquifer is DM, will be evaluated. In addition, the contribution of the available freshwater storages in meeting the freshwater demand for Scenarios B and C will be evaluated.

**Scenario B**

The available freshwater storage capacity of the surface reservoirs and the safe yield of the freshwater wellfields (Raudhatain and Umm Al-Aish) will be enough for about 150 days, but because this time is not enough to rebuild the damaged desalination plants, the strategic reserve of freshwater is needed to overcome the emergency condition (which is assumed to last 270 days). The expected daily freshwater demand for drinking and cooking use only is 100,000 $m^3/d$. The following available storages can contribute to this daily rate for 270 days;

- Freshwater lenses will supply 14,000 $m^3/d$
- Surface storages will supply 47,000 $m^3/d$

Therefore, the remaining 39,000 $m^3/d$ should be provided from the underground strategic reserve. If the withdrawal rate of freshwater from this reserve during the emergency condition is assumed to be 2000 $m^3/d$, then 20 wells are required.

The wells were designed in a triangular configuration pattern located at the centre of the Shigaya-A wellfield in 5 rows and 4 columns (Fig. 7.14). The spacing between the wells is 1500 m, except between the central three rows where the spacing is reduced to 1000 m trying to increase the recovery efficiency. The maximum well-injection rate which could be completed, is 1750 $m^3/d$ for each of wells. The maximum simulated rise in water head is 60 m at the centre of the field (Fig. 7.13). Then the additional rise in water head which could developed inside the injection wells due to well face clogging was estimated to be 36 m (estimated as explained in 6.3.2). Thus, the total rise inside the injection wells is about 96 m which is still below the land surface (the maximum allowable water head rise is 90-100 m).

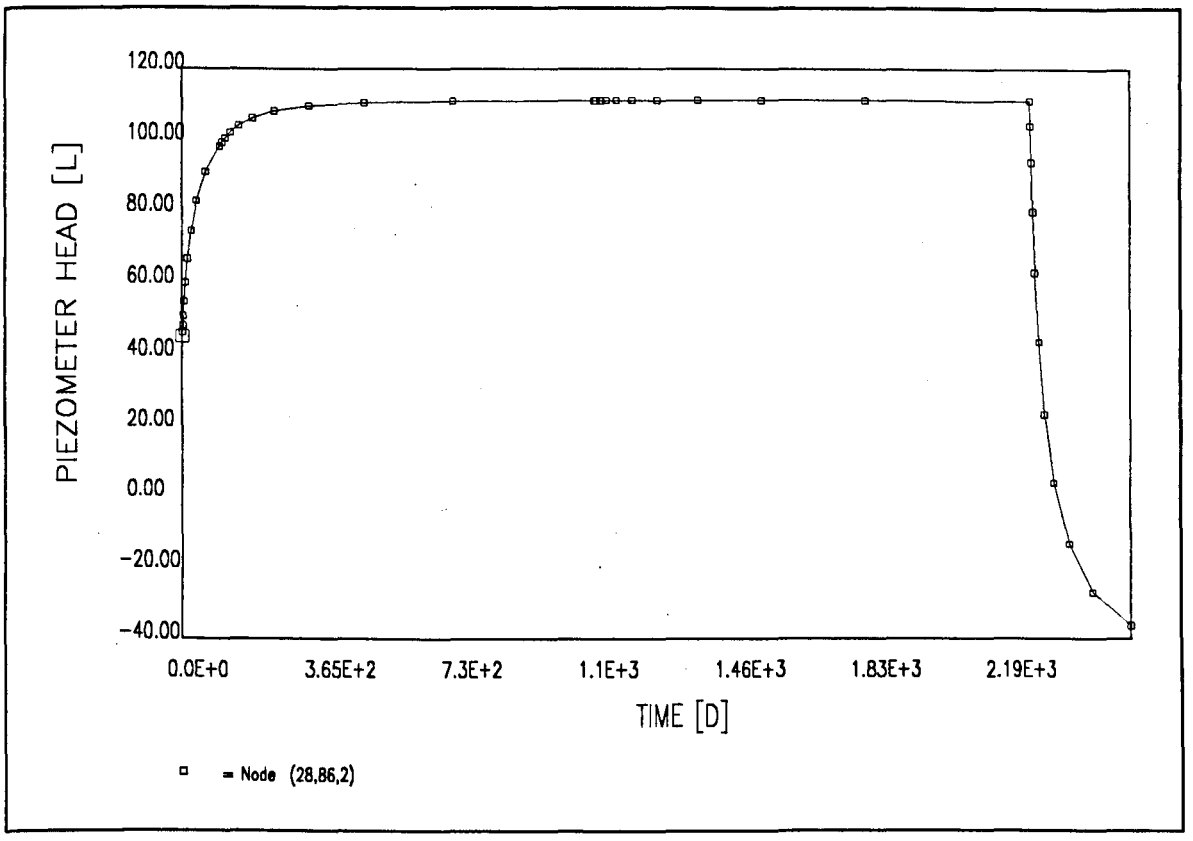


Figure 7.13: Time-head plot at a selected node showing the simulated changes in the DM aquifer potentiometric head (using the sub-regional model) during the freshwater injection and recovery stages at the strategic reserve (Shigaya-A wellfield) under scenario B.

Note: Piezometer head in m amsl.

The recovery efficiency for water having a TDS <1500 mg/l, was estimated, using the solute transport sub-regional model, where all the wells were injected and pumped with an equal-rates (1750 $m^3/d$) simultaneously. At the central wells of the configuration pattern, the recovery efficiency is 19.5 % which is marginally higher than the recovery efficiency at the outer wells which is about 15.5 %, thus, a mean value of this recovery efficiency (17.5 %) was used. Based on this recovery efficiency, the volume of freshwater which should be recharged into the aquifer to be able of recovering the required volume of water (<1500 mg/l) for emergency use is 53.2 $Mm^3$. Using the maximum recharge rate estimated by the flow model, the period which is essential to create such storage of freshwater using the 20 wells with a rate of 1750 $m^3/d$ is 4.16 year. Figure 7.14 displays the simulated isosalinity contours lines of the created water lens after the freshwater injection was completed using the 20 injection wells.

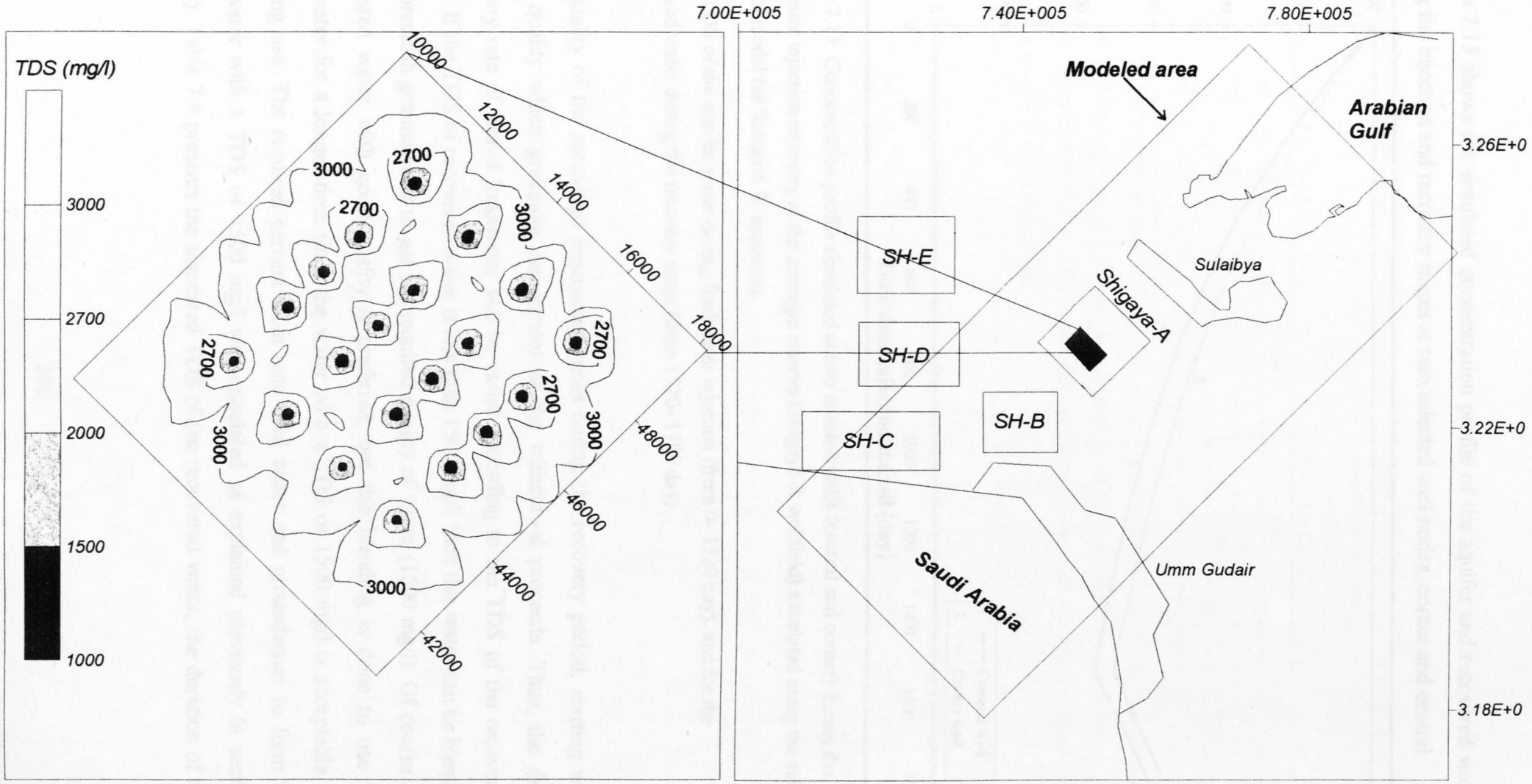


Figure 7.14: Simulated isosalinity map (in mg/l) for the recommended strategic reserve fater the freshwater injection was completed in 4.16 year (as Scenario B of the emergency conditions assumes) using 20 injection wells.

Figure 7.15 shows the simulated concentration profile of the aquifer and recovered water during the injection and recovery stages at two selected well nodes, corner and central.

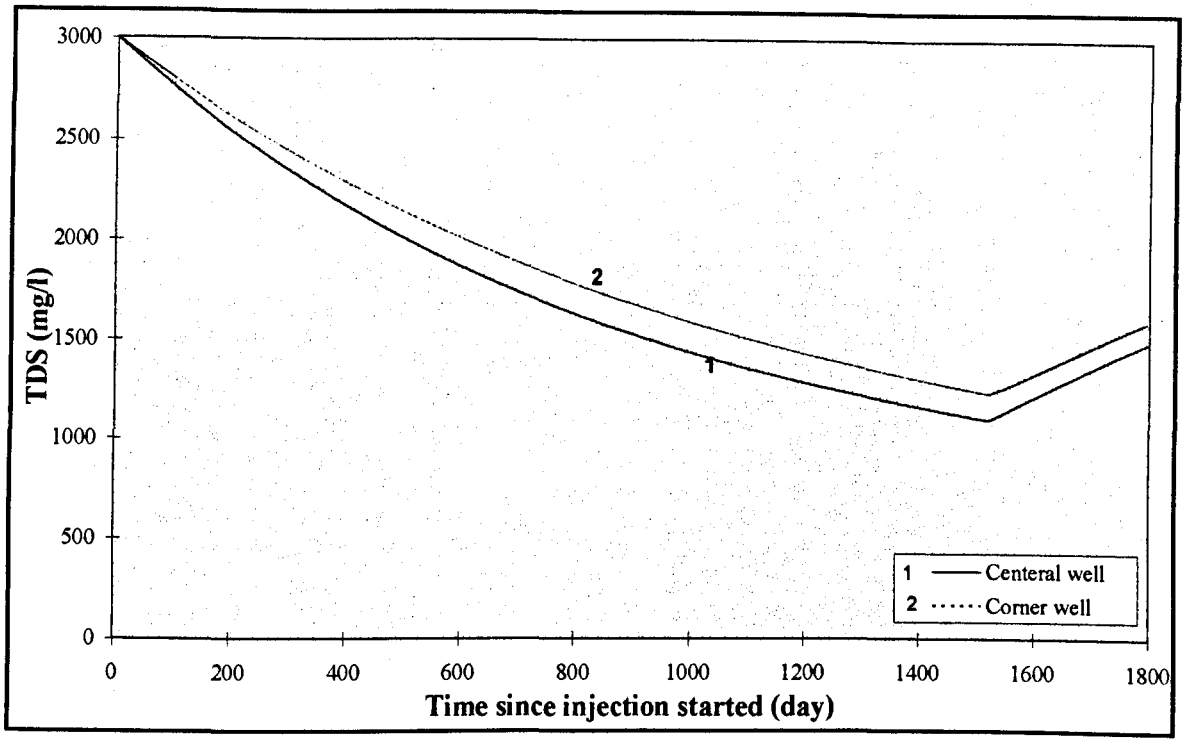


Figure 7.15: Concentration profile simulated at two selected wells (central and corner) during the freshwater injection-recovery at the strategic reserve (Shigaya-A wellfield) simulated using the sub-regional model (as Scenario B assumes).

Note: TDS of the aquifer water during freshwater injection (from 0- 1520 day), and for the recovered water during the recovery stage (from 1520- 1790 day).

The quality of the recovered freshwater varies during the recovery period, starting with good quality which gradually deteriorates as the withdrawal proceeds. Thus, the daily recovery rate of stored freshwater will be varied according to the TDS of the recovered water. If the TDS of recovered water is less than 1500 mg/l, then this water can be blended with brackish groundwater to get the required quality of water (1500 mg/l). Of course the recovered water with good quality is preferred, but this blending is done to use the freshwater for a longer time since the water with a TDS of 1500 mg/l is acceptable for drinking use. The required percent from recovered water and groundwater to form the freshwater with a TDS of 1500 mg/l was calculated as explained previously in section (7.4.3). Table 7.8 presents the simulated TDS of the recovered water, the duration of this

recovery, the required rate of pumping of this water to be blended with brackish groundwater, and the contribution rate of groundwater in constituting the freshwater.

| TDS of recovered water (mg/l) | Duration (day) | Total recovery rate of the stored water ($m^3/d$) | Additional rate of groundwater for blending ($m^3/d$) | Total freshwater demand ($m^3/d$) |
|---|---|---|---|---|
| 1100 | 27 | 34000 | 6000 | 40000 |
| 1200 | 58 | 35080 | 4920 | 40000 |
| 1300 | 58 | 36360 | 3640 | 40000 |
| 1400 | 61 | 37740 | 2260 | 40000 |
| 1500 | 65 | 40000 | 0 | 40000 |

Table 7.8: The required withdrawal rate of the stored water to meet the freshwater demand during the emergency conditions (as scenario B assumes) based on its TDS, and the portion that the groundwater can add when it is mixed with the recovered water. Total recovery rate is representing the withdrawal rate from all the 20 well.

Table 7.9 presents a summary of the optimum procedure for freshwater storage and recovery at the recommended underground strategic reserve (Shigaya-A wellfield) which could be used in supplying freshwater during the emergency conditions as Scenario B assumes.

| | |
|---|---|
| Total number of wells | 20 |
| Well-injection rate | 1750 $m^3/d$ |
| Duration of recharge stage | 1520 day (4.16 year) |
| Total recharged freshwater | 53.2 $Mm^3$ |
| Duration of emergency | 270 day |
| Total freshwater demand during the emergency | 27 $Mm^3$ |
| Total usable freshwater (TDS <1500 mg/l) recovered from the underground strategic reserve for emergency use. (daily recovery rate as in Table, 7.8) | 9.7 $Mm^3$ |
| Total blended groundwater (TDS = 4000 mg/l) for emergency use. (daily pumping rate as in Table, 7.8) | 0.8 $Mm^3$ |
| Total production from freshwater lenses at Raudhatain and Umm Al-Aish wellfields | 3.8 $Mm^3$ |
| Total stored freshwater in surface reservoirs for emergency use. | 12.7 $Mm^3$ |

Table 7.9: Summary of the optimum injection and withdrawal schedules during the creation of the strategic freshwater reserve to face the freshwater emergency as Scenario B assumes.

**Scenario C**

If the freshwater crisis occurred where all the desalination plants and surface reservoirs are destroyed, then the shortage in freshwater should be met completely by the underground strategic reserve in addition to the abstracted freshwater from Raudhatain and Umm Al-Aish wellfields. These two fields can supply freshwater with 14,000 $m^3/d$, and hence 86,000 $m^3/d$ should be supplied by the strategic reserve.

If the withdrawal rate is assumed to be similar to the injection rate, then a larger number of wells will be needed to create the underground storage for such a scenario. Hence, the withdrawal rate was assumed to be higher than the injection rate (maximum 2150 $m^3/d$ per well). Therefore, the essential number of wells required to recover the needed freshwater is 40 wells.

The required number of wells in this scenario is larger than the required number for scenario B, that will increase the sum of the resulted build-up caused by the greater number of injection wells, thus the spacing between these wells has to be greater. The wells were located in a uniform space (1500 m), designed in a triangular pattern with 5 rows and 8 columns placed at the western south of the Shigaya-A wellfield (as in Fig. 7.17), where the quality of aquifer water with minimum TDS is found (3000 mg/l).

The sub-regional flow model was used to find the possible maximum well-injection rate which could be completed within the allowable limit of water level rise (90- 100 m). The rate was found to be 1500 $m^3/d$ which is lower than the completed rate under scenario B. This is due to the increase in the sum of the resulted build-up caused by the greater number of injection wells. The maximum total rise in water head was estimated to be 97 m, where 61m is the simulated build-up (as in Fig. 7.16), and 36 m represents the additional rise inside the injection wells which may be caused by well face clogging, (calculated as explained in 6.3.2).

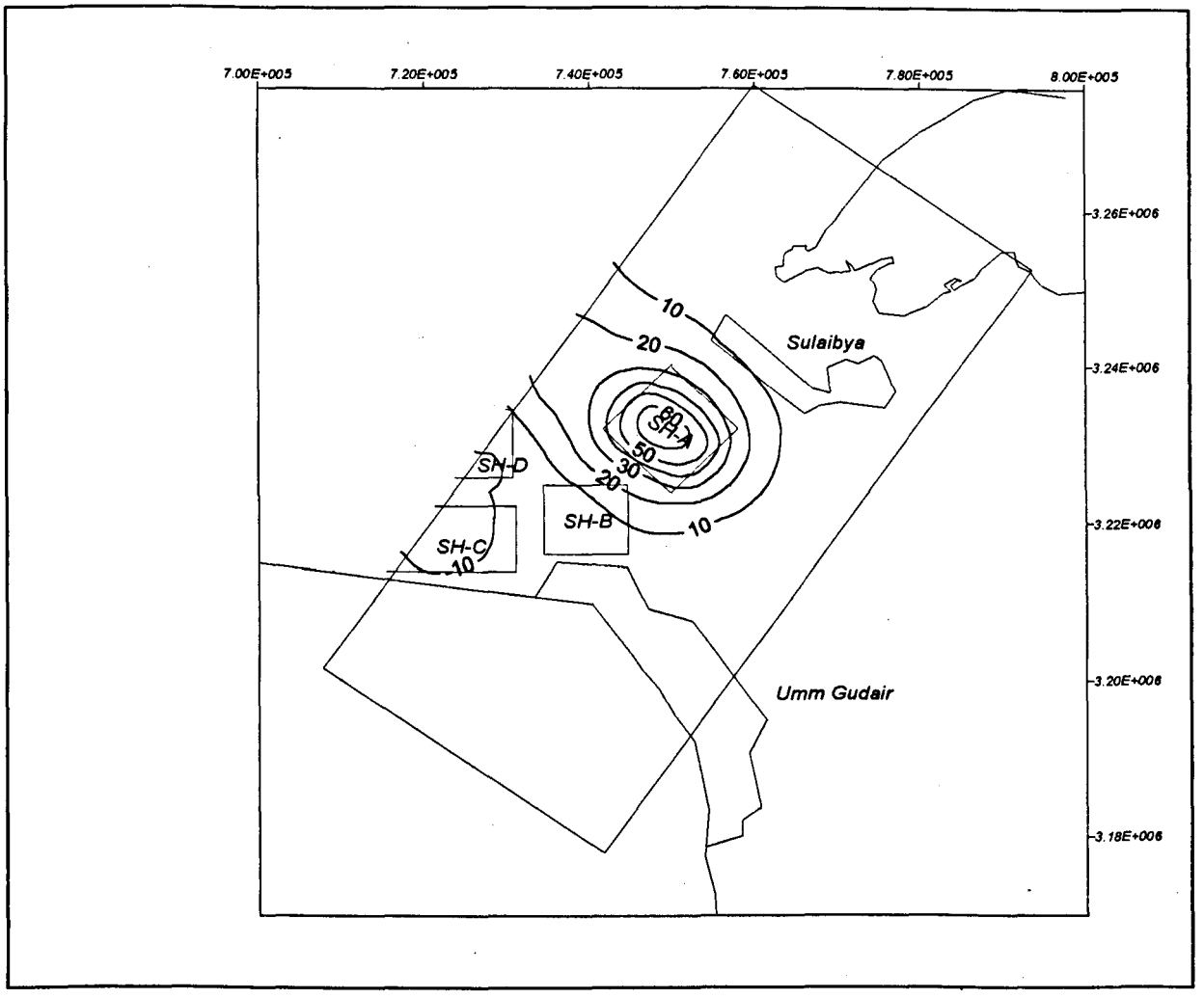


Figure 7.16: Simulated changes in the Dammam aquifer potentiometric head a after water injection (Q= 1500 $m^3/d$ per well) was completed in 5.26 years (as Scenario C of emergency conditions assumes). (+) build-up, and (-) drawdown (in metre).

All the 40 wells were injected simultaneously with freshwater at an equal-rate (1500 $m^3/d$), where the TDS of the injected freshwater is 350 mg/l, and the TDS of the aquifer water is 3000 mg/l. The transport sub-regional model was used to simulate the change in the aquifer water TDS during the injection stage, and the TDS of the recovered water during the recovery stage. Figure 7.17 shows the simulated isosalinity contour lines of the created body of freshwater after the injection was completed and before any withdrawal process takes place.

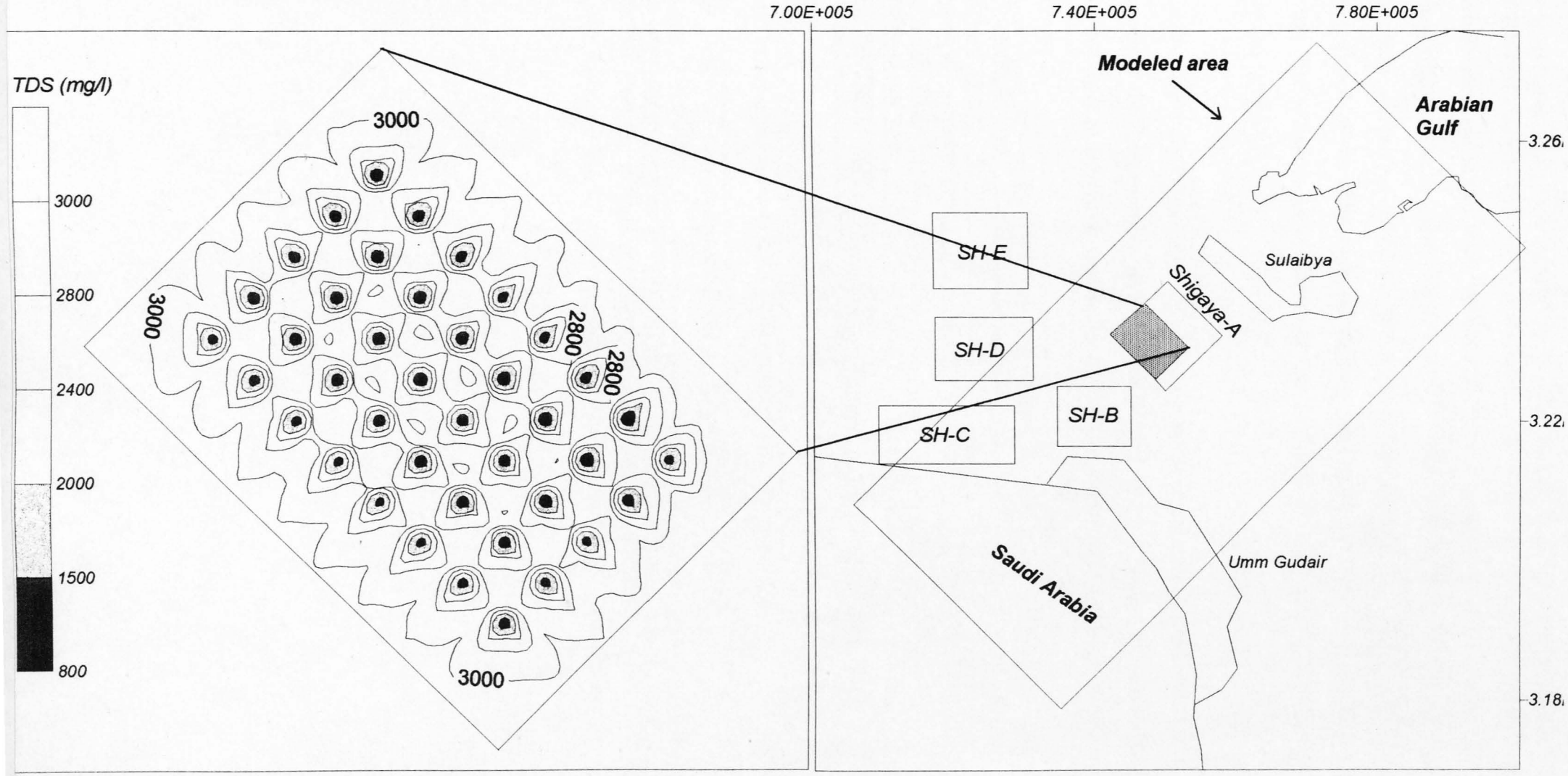


Figure 7.17 : Simulated isosalinity map (in mg/l) for the recommended strategic reserve after freshwater injection was completed in 5.26 years (as Scenario C for the emergency conditions assumes) using 40 injection wells.

The mean recovery efficiency of water with a TDS <1500 mg/l was estimated to be 14 %. This is lower than the estimated recovery efficiency in scenario B which may be related to the larger distance between the injection wells. In the same manner as calculated in scenario B, the required recovery rate of the stored water was estimated based on its quality (which ranges from 1000 to 1500 mg/l). In addition the required percent of groundwater to be blended with the recovered water to increase its TDS to 1500 mg/l was determined (as explained in section 7.4.3).

Table 7.10: presents a summary of the optimum procedure for freshwater storage and recovery at the recommended underground strategic reserve (Shigaya-A wellfield) which could be used in supplying freshwater during the emergency conditions as Scenario C assumes.

| | |
|---|---|
| Total number of wells | 40 |
| Well-injection rate | 1500 $m^3/d$ |
| Duration of recharge stage | 1922 day (5.26 year) |
| Total recharged freshwater | 115.32 $Mm^3$ |
| Duration of emergency | 270 day |
| Total freshwater demand during the emergency | 27 $Mm^3$ |
| Total usable freshwater (TDS <1500 mg/l) recovered from the underground strategic reserve for emergency use. (average withdrawal rate per well is 2030 $m^3/d$) | 21.9 $Mm^3$ |
| Total blended groundwater (TDS = 4000 mg/l) for emergency use. | 1.3 $Mm^3$ |
| Total production from freshwater lenses at Raudhatain and Umm Al-Aish wellfields. | 3.8 $Mm^3$ |
| Total stored freshwater in surface reservoirs for emergency use. | 0 |

Table 7.10: Summary of the optimum injection and withdrawal schedules during the creation of the strategic freshwater reserve to face the freshwater emergency as Scenario C assumes.

To summarise, the storage of freshwater in the aquifer to be used during any possible accidental loss of regular sources of domestic supply seems to be feasible. This can be achieved at the recommended site, where the aquifer parameters allow the injection and recovery of sufficient volumes of water. In addition, the various management options which are required to accomplish such objective are reasonable and could be implemented.

Table 7.11: Summarises the portion that the different sources of freshwater can supply during the two assumed scenarios of freshwater emergency.

| **Freshwater emergency scenario** | **Freshwater demand (%)** | **Available freshwater (%)** | | |
|---|---|---|---|---|
| | | **Natural freshwater lenses** | **Surface storages** | **Underground artificial storage** |
| **B** | 100 | 14 | 47 | 39 |
| **C** | 100 | 14 | 0 | 86 |

# 8. OPTIMAL OPERATION TO MAINTAIN FRESHWATER STORAGE

## 8.1 INTRODUCTION

The delay in recovering artificially-recharged, stored freshwater from aquifers which is aimed to be used as strategic reserve will lead sometimes to a displacement of this water by regional groundwater flow. In order to overcome such an effect and maintain the stored freshwater for a longer time a certain technique is proposed in this study. This involves installation of "gradient-control" pumping wells outside the storage area, which would be used to create a zero hydraulic gradient around the area. Thus, the influence of groundwater flow on shifting the stored freshwater mound away from its position and deteriorating the quality of stored water will be reduced.

A management model based on linear systems theory was used to find the optimal pumping schedules of these gradient-control wells. Also, the optimal abstraction rates from the groundwater supply wells which surround the freshwater storage could be determined. The hydraulic response of the aquifer system was represented by the simulation model that is linked to a linear programming optimisation model using response functions. In the linear programming, the objective was to minimise the total pumping rate of the gradient-control wells while maintaining the desirable hydraulic gradient around the freshwater storage area and meeting the groundwater demand by the supply wellfields.

The continuity of the groundwater system defined by response coefficients, maximum drawdown allowable at pumping wells, and the maximum and minimum pumping rates of wells were included as constraints to the solution.

The results illustrate that the stored water can be maintained within its location using minimum pumping rates of the hydraulic gradient-control wells while the groundwater demand is met by production from the surrounding supply wellfields. The transport model was also used to verify the obtained optimal results; the improvement in the recovery efficiency after using the hydraulic gradient wells was clearly demonstrated.

## 8.2 PROBLEM DESCRIPTION

The injection of freshwater into a suitable brackish aquifer seems to be a feasible management option to store a surplus of freshwater for subsequent use. The stored water might will not be used directly after the completion of water injection, and may thus need to be stored for long a time until it is needed. However, the existing flow pattern resulting from pumping the nearby domestic supply wells will cause the stored water to move away from the intended storage area. Moreover, the surrounding cones of depression will speed groundwater velocity due to from the steep hydraulic gradient around the storage area; this will further accelerate the mixing mechanism between the stored freshwater and the native water, and hence will reduce the recovery efficiency.

In this study, where the use of the Shigaya-A wellfield as a long-term strategic reserve for storing freshwater for emergency use was simulated (as explained in section 7.5.3, for the assumption of Scenario B emergency conditions), the influence of such factors was critical. The solute transport simulation indicates that the freshwater lens will be displaced from its initial location after 6 years of storage by about 800 m down-gradient from the storage area in the direction of regional groundwater flow (Figure 8.1). Also, after about four years of storage, the intended usable stored water which has a TDS < 1500 mg/l will be completely irrecoverable.

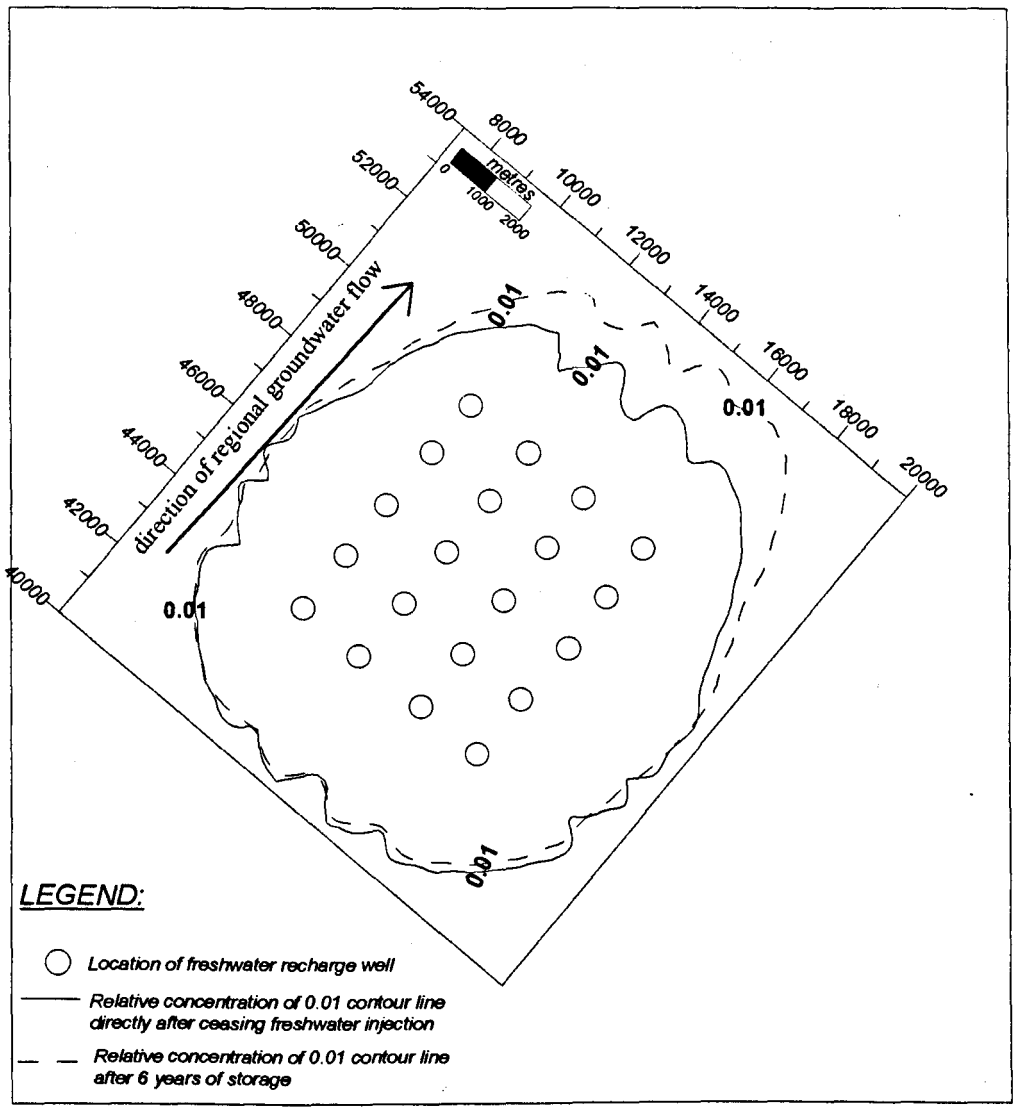


Figure 8.1: Displacement of the stored freshwater lens at the Shigaya-A wellfield (for the location see Fig. 8.2) resulting from the existing regional groundwater flow after a residence time of 6 years.

## 8.3 SOLUTION BASIS

It was found in this study that there was a solution which could be adopted in approaching problems of this nature. This can be implemented by installing an array of wells outside the storage area and using them to create a very low hydraulic gradient ("hydraulic barrier" or stagnation zone) around the area so that negligible movement of stored water occurs. The approach is based on using a management model to find the optimum pumping rates of the hydraulic gradient-control wells which can produce such a stagnation zone. At the same time, the groundwater demand should be met by the groundwater wellfields while maintaining the stored freshwater lens. Thus, the optimal pumping rate of the hydraulic gradient-control wells as well as the optimal development of the DM limestone aquifer within the modelled area and during the planning period can be determined.

The freshwater lens which has been already created at Shigaya-A wellfield (section 7.5.3) was used to demonstrate this approach. It was assumed that this freshwater lens needed to be maintained for six years. In order to reduce the computer storage space and computation time, water wellfields were divided into sub-fields (each consisting of a number of wells) instead of applying the solution for each individual well. Thus, the problem domain which needed to be solved by the management model to achieve the planned objective was divided into three components (as shown in Figure 8.2);

SW: groundwater sub-fields which should be pumped to meet the groundwater demand (= 37 sub-fields). Subsequently they will be termed "groundwater supply wells".

CW: hydraulic gradient-control wells located around the freshwater storage area which will operate to create the desirable hydraulic gradient at GC nodes,
(= 19 wells).

GC: hydraulic gradient-control nodes, where the minimum hydraulic gradient needs to be maintained to create a stagnation zone around the freshwater lens, (= 42 nodes). Each two adjacent nodes (A and B), as shown in Figure 8.2, together comprise one hydraulic gradient-control pair ( i.e., 21 pairs ).

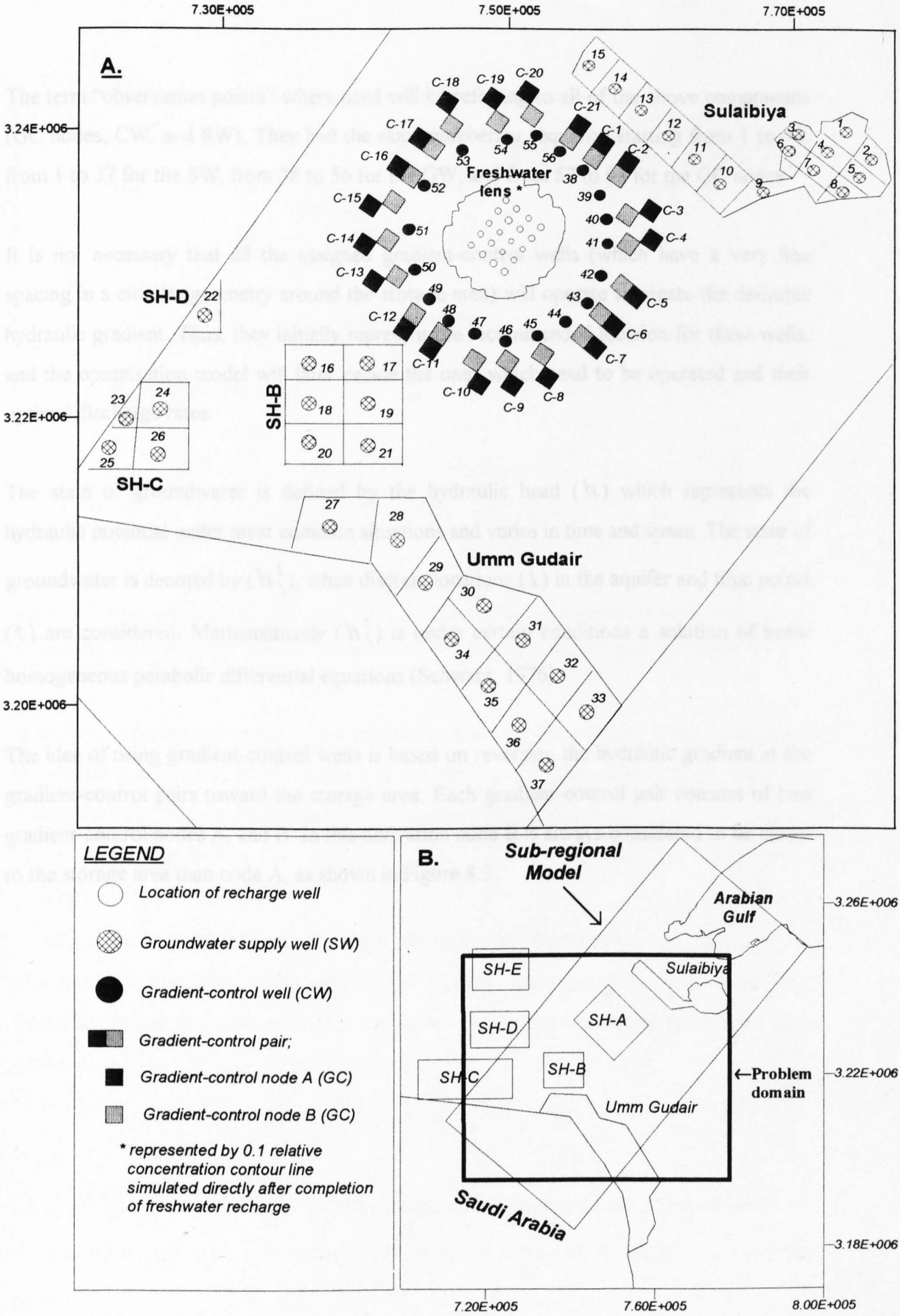


Figure 8.2 (A, and B): (A) Components and (B) location of the problem domain to be solved using the management model.

The term "observation points" where used will be referring to all of the above components (GC nodes, CW, and SW). They had the same numbering sequence starting from 1 to 98; from 1 to 37 for the SW, from 38 to 56 for the GW, and from 57 to 98 for the GC nodes.

It is not necessary that all the assigned gradient-control wells (which have a very fine spacing in a circular geometry around the storage area) will operate to create the desirable hydraulic gradient. Thus, they initially represent the recommended location for these wells, and the optimisation model will later decide the ones which need to be operated and their optimal discharge rates.

The state of groundwater is defined by the hydraulic head ($h$) which represents the hydraulic potential under most common situations and varies in time and space. The state of groundwater is denoted by ($h_i^t$), when discrete locations ($i$) in the aquifer and time points ($t$) are considered. Mathematically ($h_i^t$) is under certain conditions a solution of linear homogeneous parabolic differential equations (Schwarz, 1976).

The idea of using gradient-control wells is based on reversing the hydraulic gradient at the gradient-control pairs toward the storage area. Each gradient-control pair consists of two gradient-control nodes A, and B. In this derivation node B is always considered to be closer to the storage area than node A, as shown in Figure 8.3.

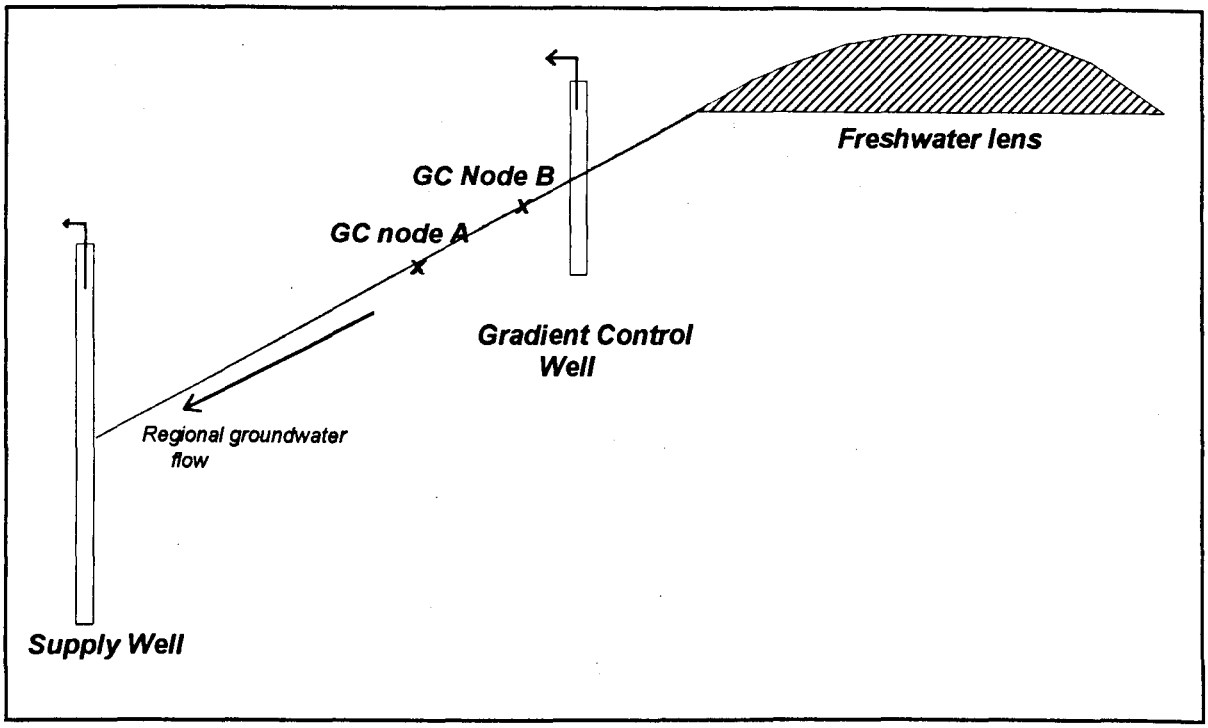


Figure 8.3: Conceptual diagram for the present groundwater flow pattern which needs to be changed by creating a zero hydraulic gradient between the nodes A and B using the gradient-control wells.

In order to stop the movement of the stored water toward the pumping areas developed by the nearby groundwater supply wells, it is necessary to create an inward slope toward the freshwater lens, thus the following relation should be produced :

$$H_A \geq H_B \tag{8.1}$$

where

$H_A, H_B$ : are the hydraulic head at nodes A, and B, respectively.

The hydraulic head at a given node, and at a given stress period is equal to the initial hydraulic head at this node minus the drawdown resulted at the end of the current stress period, thus ;

$$H_A = H_A^{-n} - S_A(k,n), \text{ and } H_B = H_B^{-n} - S_B(k,n) \tag{8.2}$$

where

$H_A^{-n}, H_B^{-n}$ : are the initial hydraulic heads at nodes A, and B, respectively.

$S_A(k,n), S_B(k,n)$ : are the drawdown at nodes A, and B, respectively, up to stress period $n$.

Substituting Equation. 8.2 in Equation. 8.1, and solving it, the following is the gradient-control constraint which should be met;

$$S_B(k,n) - S_A(k,n) \geq H_B^{-n} - H_A^{-n} \quad \forall n \text{ pair}, \forall n \tag{8.3}$$

The optimal minimum pumping rates of the hydraulic gradient-control wells required to produce such drawdown in aquifer water head at gradient-control nodes can be determined using the management model.

The management model used consists of several steps. First, the hydraulic aquifer response will be represented by response coefficients generated by the simulation flow model. Then, these coefficients will be used with another set of formulated constraints to define a linear programming problem. The optimisation model will be used later to solve the linear programming problem in order to obtain the optimal pumping rates of the hydraulic gradient wells and the supply wells. Equation 8.3 will be one of the constraints imposed on the linear programming problem. Finally, the optimisation outputs need to be verified using the simulation flow model. Figure 8.4 presents a flow chart of the management model steps.

The gradient-control wells may pump some of the stored water during the maintaining process. Therefore, the appropriate location for gradient-control wells where such an effect will not exist can be determined using the transport model (through sensitivity analysis). The optimal pumping rates for gradient-control wells will be entered into the transport model, and the water quality of the water pumped by these wells can be simulated. If it is found that there is a portion of stored water pumped by these wells, then they have to be located further away from their previous locations. In order to minimise such effects, the objective of the management model was chosen to be the creation of a zero hydraulic gradient at the gradient-control pairs with a minimum pumping rates by the gradient-control wells. Furthermore, the used management model provides an option of stopping the gradient-control wells completely, and use the supply wells only to create the desired gradient at the gradient-control pairs.

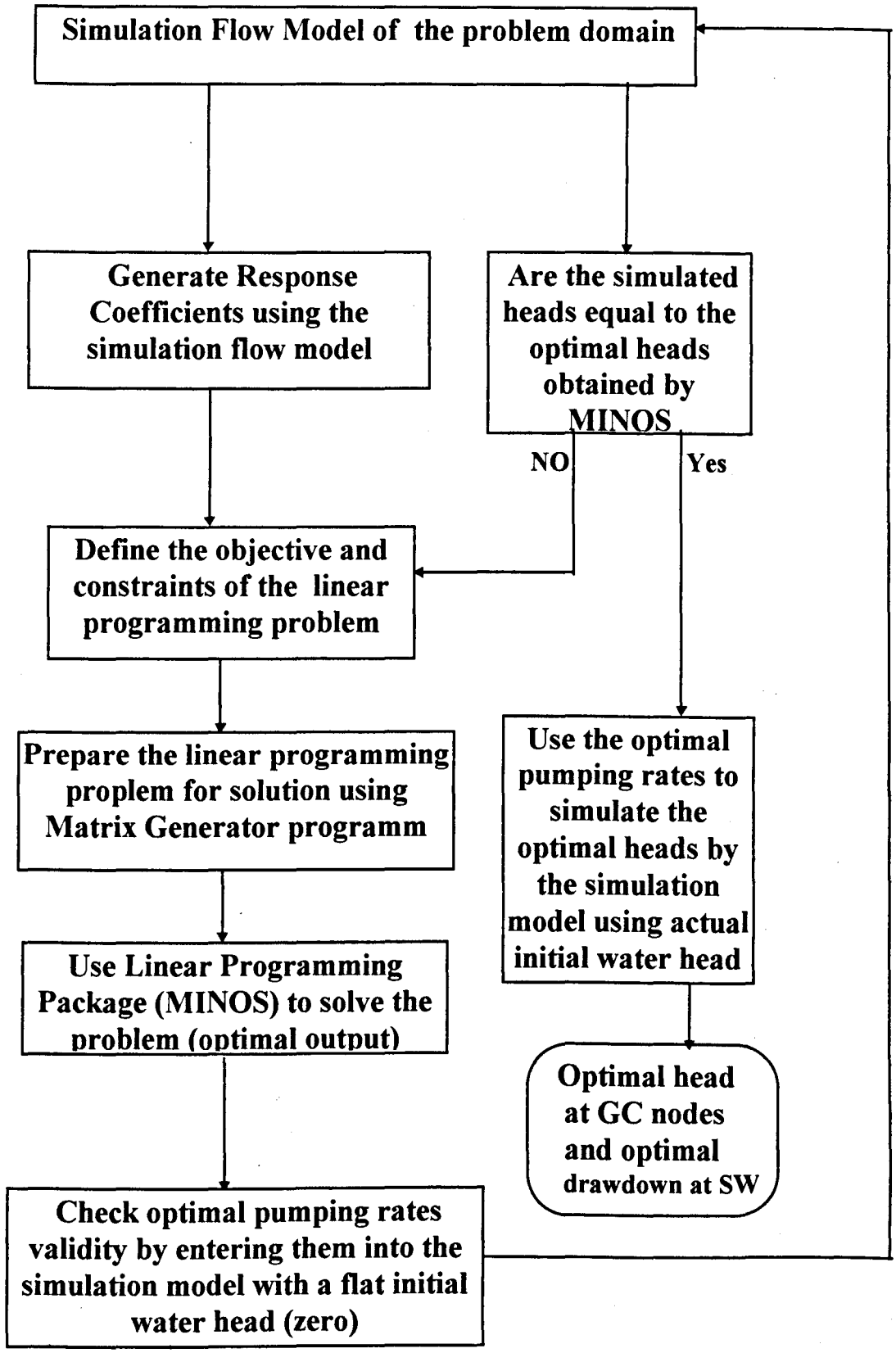


Figure 8.4: Flow chart for the steps of the used management model.

## 8.4 SIMULATION MODEL

The three-dimensional sub-regional model (presented in section 7.3) was used as a simulation hydraulic model. The model was already calibrated under steady-state and transient conditions, where the regional distribution of the two main aquifers parameters (KG and DM) were determined.

## 8.5 RESPONSE FUNCTIONS

The simulation component of groundwater hydraulic management model was linked to a linear programming algorithm by means of a response function approach that served to express the state variables of the system (e.g., drawdowns) as linear functions of decision variables (e.g. pumpage). The idea in this approach is that each unit pulse of pumping in a system causes a particular influence on drawdown over space and time. These quantitative influences on drawdown can be obtained by subjecting the calibrated simulation model of the flow domain to unit discharges at each of the pumping wells. The resulting set of coefficients may then be included in an optimisation model as part of the constraints.

Using linear systems theory and Green's functions, Maddock (1972) has shown that the discrete form of drawdown response functions is given by :

$$s(k,n) = \sum_{j=1}^{M} \sum_{i=1}^{n} \beta(k,j,n-i+1) Q(j,i) \qquad (8.4)$$

where;

$s(k,n)$ : drawdown at point $k$ at the end of the pumping period $n$ due to the pumping of $M$ wells, averaged over the finite-difference cell, [L];

$\beta(k,j,n-i+1)$ : drawdown at point $k$ at the end of the pumping period n due to a unit pulse of pumping at well $j$ applied throughout the pumping period $i$ L/T2];

$Q(j,i)$ : average volumetric rate of discharge at the well $j$ during pumping period $i$ [l3/T];

$M$ : total number of observation points.

The drawdown was generated at each of the 98 observation points $M$ using the hydraulic simulation model after successively subjecting each of the 56 wells (GC + SW) to a unit discharge (-1 $m^3$/sec ) for the first period and zero for the remaining periods. Drawdowns calculated in this manner represent the $\beta's$ in Equation 8.4. A planning period of 7 years was considered in the management problem, divided into 7 stress periods. The resulting set of response functions [a total of 38,416 = No. of wells (i.e. no. of variables) (56) x No. of observation points (98) x No. of planning periods (7)] was then assembled to form the response matrix, the consistency of which was confirmed by computing drawdowns for the applied problem with both the response matrix and the original groundwater simulation model.

In order to eliminate the influence of the existing flow pattern in obtaining aquifer response coefficients, and to relate the aquifer response during pumping only to its properties, the initial water heads of both layers in the simulation model were assigned to zero (i.e. flat potentiometric surface), only during the generating of response functions.

## *8.6 OPTIMISATION MODEL*

### 8.6.1 LINEAR PROGRAMMING FORMULATION

There was a possibility that some portion of the stored freshwater will be pumped by the hydraulic gradient-control wells which were located close to the storage area. Hence, the assigned goal was to minimise the pumping rates of mound gradient-control wells. That should be achieved while the hydraulic gradient around the storage area is maintained at a minimum level, and groundwater demand is met over the planning horizon, subject to the physical capability of the aquifer and the installed capacity of the pumping wells. The groundwater produced by the gradient-control wells can also make a contribution to meet groundwater demand. The objective function of the optimisation model was formulated as follows:

$$\text{Min } Z = \sum_{k=1}^{C} \sum_{n=1}^{N} Q(k,n) \qquad (8.5)$$

where

$Q(k,n)$: pumpage of the gradient-control well $k$ during the period $n$,

$C$ : total number of gradient-control wells (GC), and

$N$ : total number of planning periods.

Seven constraint sets were assigned (Yazicigil, 1996) to be imposed on the management model, as follows:

1. The equation of the state variable (i.e., Equation 8.4 ) must be maintained to ensure the continuity of the system.
2. Hydraulic gradient at gradient-control pairs around the freshwater lens has to be maintained as in Equation 8.3.

The values of $S_A(k,n)$, and $S_B(k,n)$ (in Equation 8.3) were to be obtained using the flow model during the matrix generation as defined by Equation 8.1. Whereas, the aquifer water heads $H_A^{-n}$, and $H_B^{-n}$ (in Equation 8.3) for the gradient-control points will be obtained directly with the simulation flow model using the actual pumping or injection rates.

The obtaining of water heads $H_A^{-n}$, and $H_B^{-n}$ for this constraint using the simulation model was given flexibility in using different scenarios which would give different optimal solutions. Within the area bounded by the gradient-control wells, many scenarios with different management options (such as injection or pumping with different rates, or even shut-down conditions) could be assumed. Also, the number and geometry of wells could be changed easily without any modification to the formula of the applied management model. The only difference was replacing the simulated values of water heads $H_A^{-n}$, and $H_B^{-n}$ with the ones of the new scenario.

In this study, the hydraulic simulation will start as initial conditions with the flow pattern as produced after the completion of water injection at Shigaya-A site (completed in 4.16

years, using 20 injection wells with 0.02 $m^3/s$ per well, while other wellfields are pumped) as presented in Figure 8.5. Then water injection was stopped at the recharge site and the freshwater lens needed to be maintained for six years, and at the seventh year the stored water had to be recovered back from the same injection wells. At all the 7 planning periods, groundwater demand should be met by the groundwater supply wells. Also, the water produced by the gradient-control wells will be contributed in meeting the groundwater demand. The simulated aquifer water heads were extracted for the gradient-control nodes at all the 7 planning periods and saved in a separate file to be included later in the optimisation model as right-hand side values for Equation 8.3.

3. Yearly water demand should be met from all wells.

$$\sum_{k=1}^{W} Q(k,n) \geq D(n) \quad \forall n = 1,2,\ldots\ldots,7 \tag{8.6}$$

$W$ : total number of wells ( CW and SW),

$D(n)$: groundwater demand at $n$ planning period.

4. Maximum allowable drawdowns should not be exceeded:

$$S(k,n) \leq S_{max}(k) \quad \forall k, \forall n \tag{8.7}$$

This was to ensure that no undesirable effect could be created by the optimum solution, and to find the optimum abstraction rates for the supply wells which will not produce a decline in aquifer water head below certain limits. This could be used to specify certain limit of drawdown to prevent undesirable effects which may result from over-pumping, like saline water intrusion at the coastal areas (for example at Sulaibiya wellfield). This constraint is very beneficial in finding the optimal aerial distribution for groundwater abstraction from the aquifer which can be achieved with the maximum drawdown in the aquifer water head.

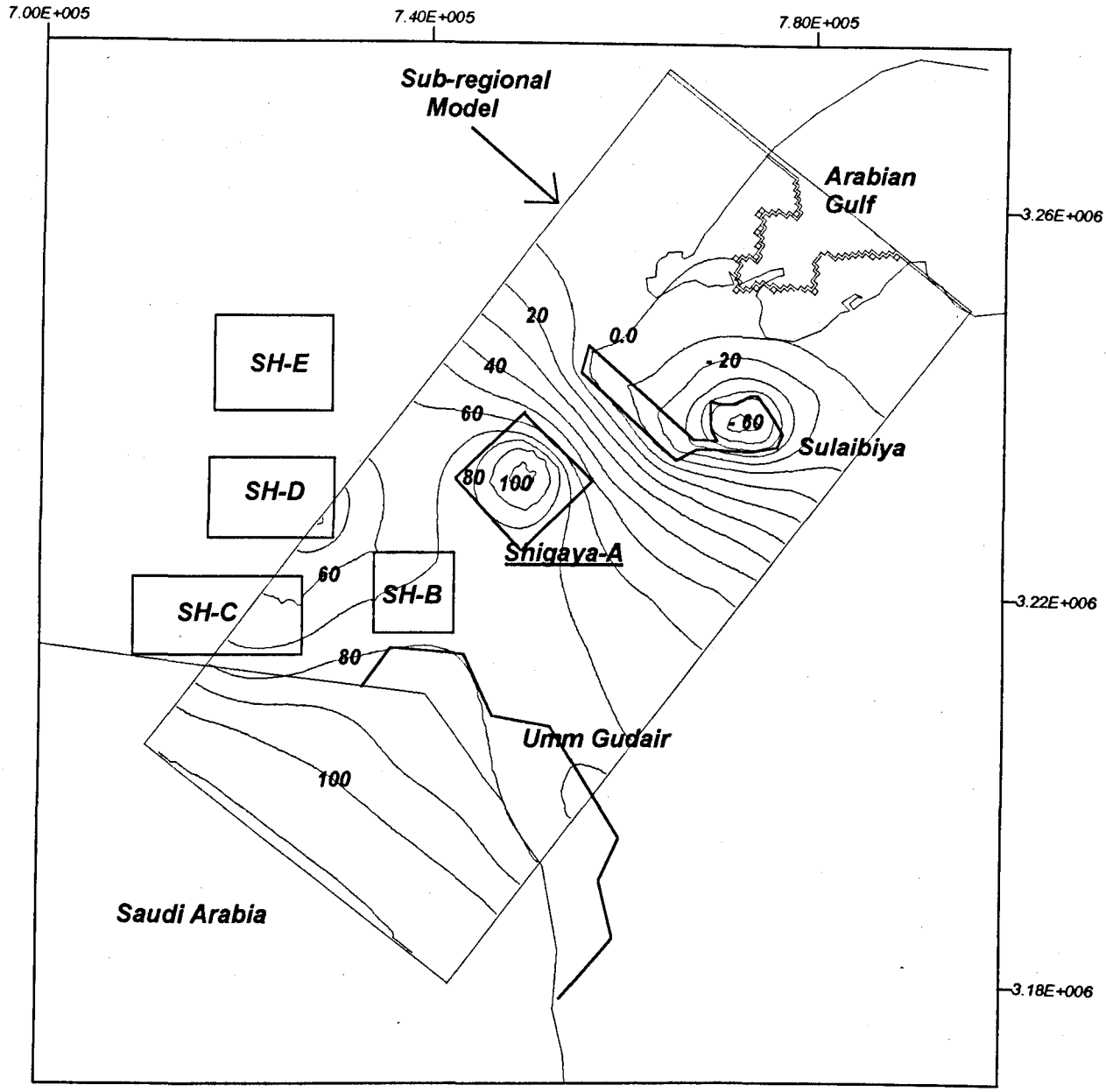


Figure 8.5: Simulated potentiometric head of the DM aquifer at year 2000 used as initial heads for the management model. It respresents water heads after a completion of freshwater injection at Shigaya-A field using 20 wells with injection rate of 1750 m3/d per well for 4.16 years (as Scenario B assumed, in section 7.5.3). (m amsl)

5. Installed pumpage capacity of the wells should not be exceeded :

$$Q(k,n) \leq Q_{max}(k) \quad \forall k, \forall n \tag{8.8}$$

This to make sure that the installed pumping capacity of wells is not exceeded. Also, this constraint can be used as a shut-down option, where any well during any time period can be switched off for any reason (such as for maintenance ). This can be achieved by assigning this constraint (upper pumpage limit) to zero. Also, it can be used to shut-down all or part of the gradient-control wells, and allow the supply wells to be operated with an optimal rates, under which the intended hydraulic gradient around the storage area can be created.

6. Pumpage lower limits by supply wells should be met :

$$Q(k,n) \geq Q_{min}(k,n) \quad \forall k, \forall n \tag{8.9}$$

This is to force some wells to meet at least a specified water demand, the lower bounds may be set to that specified value. Otherwise it can be set to zero giving the optimisation model the freedom in specifying this value.

7. Non-negativity limitations

$$Q(k,n) \geq 0, \text{ and } S(k,n) \geq 0 \quad \forall k, \forall n \tag{8.10}$$

The objective function (Equation 8.5) and the set of constraints given by Equations 8.3, 8.4, 8.6, 8.7, 8.8, 8.9, and 8.10 constitute a linear programming problem that can be solved using the regular simplex algorithm to obtain the optimum solution. The resulting linear optimisation problem had 842 constraints and 1078 decision variables (not including the upper and the lower bounds on pumping rates, and maximum drawdown). The MINOS optimisation algorithm (Murtagh and Saunders, 1983) was used to solve the linear programming problem.

## 8.6.2 OPTIMISATION ALGORITHM (MINOS)

### 8.6.2.1 INTRODUCTION

MINOS is a Fortran-based computer system designed to solve large-scale linear and nonlinear optimisation problems. It can solve the linear problems in the following form :

$$\mathrm{Min}_{x,s}\ C^T x \text{ subject to } Ax + Is = 0\ ,\ l \le \begin{pmatrix} x \\ s \end{pmatrix} \le u \qquad (8.11)$$

where the elements of $x$ are called structural variables (or column variables) and $s$ is a set of slack variables, $l$ and $u$ are the lower and upper bounds, respectively, that can be re-defined.

MINOS solves linear programs using an implementation of the primal simplex method (Dantzig, 1963). The simplex method partitions the constraints $Ax + Is = 0$ into the form

$$Bx_B + Nx_n = 0 \qquad (8.12)$$

where the basis matrix $B$ is square and nonsingular. The elements of $x_B$ and $x_N$ are called the basic and nonbasic variables, respectively; they are a permutation of the elements of $x$ and $s$. At any given stage, each nonbasic variable is equal to its upper or lower bound, and the basic variables take on whatever values are needed to satisfy the general constraints. If an optimal solution to a linear program exists, then it will have the form of ; $Bx_B = -Nx_n$. The simplex method reaches such a solution by performing a sequence of iterations, in which one column of $B$ is replaced by one column of $N$ (and vice versa), until no such interchange can be found that will reduce the values of $C^T x$.

If the components of $x_B$ do not satisfy their upper and lower bounds, then the current point is infeasible, and the optimal solution cannot be founded.

### 8.6.2.2 DATA INPUT FORMAT

The input of objective function and constraints into MINOS require a certain format, where two files are required SPEC and MPS.

**I. SPECS File**

The SPECS file sets various run-time parameters that describe the nature of the problem being solved and the manner in which a solution is to be obtained. The file consists of sequence of card images in free format, each of which contains a keyword and certain associated values. It includes type of the objective function (maximise or minimise), and number of constraints (rows) and variables (columns).

**II. MPS File**

The MPS file is required for the problem to specify names and values for variables and constraints, where a very fixed format must be used for this file. Various " header cards" divided the MPS file into several sections as follows:

NAME
ROWS
COLUMNS
RHS
BOUNDS
ENDATA

**1. The NAME card**

This card contains the word NAME in columns 1-4, and the name of the problem in columns 15-22.

## 2. The ROWS section

The general constraints are commonly referred to as rows. This section contains one constraint for each row, where type and name of the constraints are included. The row-types are E, G, and L which represent either the constraint type is equal to, greater than, or lower than right-hand side of the constraint equation, respectively. The row- type N stands for "Not binding" is used to define the objective function, that always must occupies the last row.

In this section the total number of constraints are 842, entered to the MPS file in the following sequence:

- Row 1, is the constraint on total groundwater demand for all the 7 planning periods which has G type.
- Rows 2-8, constraints of groundwater demand for each planning period, from 1 to 7 planning periods, all have G type (Equation. 8.7)
- Rows 9-694, represent the drawdown constraints at each observation point during all the planning periods. Each 7 rows will include drawdown constraints for a single point at the 7 planning periods successively. All these rows has E type (Equation. 8.4).
- Rows 695- 841, represent the drawdown constraints at the gradient-control pairs, where the difference in drawdown between nodes A and B at each gradient-control pair should be greater than (G type) the difference in initial head between these two nodes at any time (Equation. 8.6). They had the similar sequence of the previous rows.
- Row 842 (last row), is the objective function constraint and it has the type (N).

## 3. COLUMNS section

For each variable $Q_i$ (in Equation. 8.1), the COLUMNS section defines the name for $Q_i$ and lists the nonzero coefficients $\beta_{ij}$ (generated as response coefficient using Equation. 8.1) in the corresponding column of the constrain matrix. For example, the variable $Q_{0101}$ that is the pumping rate at the first well at the first planning period, which already generates number of response coefficients ($\beta$) at all the observation points at all the planning periods. Thus, at each row of this section, the following format should be used:

- Name of the variable (for example $Q_{0101}$)

- Name of response coefficient $\beta$ which is generated by the concerned variable (for example $\beta_{9807}$, that is the name of response coefficient $\beta$ at the observation point No. 98 at the seventh planning period).
- Value of $\beta_{9807}$ coefficient as produced by $Q_{0101}$.

Using the above format, all the variables starting from $Q_{0101}$ to $Q_{5607}$ and the generated response coefficients by each variable individually will be defined successively from $\beta_{0101}$ to $\beta_{9807}$. Starting with defining the first variable and its generated response coefficients $\beta$ at each observation point from the first to the last planning period one by one. Then define the second variable and its response coefficients $\beta$ as defined for the first variable, and so on for all variables. Number of rows in this section are 38,416, which are equal to the generated coefficients ($\beta$) of the response matrix.

**4. RHS section**

This section specifies the values of the right-hand side of the constraint equations 8.3, 8.4, and 8.6. The format is as in the COLUMNS section.

**5. BOUNDS section**

This section specifies the upper ($\lambda$) and lower bounds ($\mu$) used for constraints of the form of $\lambda \leq \begin{pmatrix} x \\ s \end{pmatrix} \leq \mu$, which is used for the constraint equations 8.7, 8.8, 8.9, and 8.10. The format is as in the COLUMNS section.

**6. ENDATA** The MPS file should be ended with the word ENDATA.

The objective function (Equation 8.5) and the set of constraints given by equations 8.3, 8.4, 8.6, 8.7, 8.8, 8.9, and 8.10, which constitute the linear programming problem were converted into SPECS and MPS formatted files using a "matrix generator program" (Yazicigil, 1996) The objective function, response coefficients, and other

constraints were prepared in a certain format to be read by the matrix generator which accordingly will create the required two files (SPECS and MPS). Then these two files were used by MINOS, where the problem was solved and the optimal solution was found.

## 8.7 OPTIMAL SOLUTION VALIDITY

The outputs from MINOS are the optimal discharge rates from the gradient-control wells and from the groundwater supply wells that are essential to create the minimum hydraulic gradient around the storage area and to meet the groundwater demand. Also, optimal hydraulic gradient and optimal drawdown at all the observation points were included.

Before applying the optimal outputs, they had to be verified by finding if the simulation model would give the same results as calculated by MINOS or not. This was done by entering the optimal discharge rates calculated by MINOS into the hydraulic simulation model using the initial flat head (zero) that was utilised during the generating of response coefficients. It was found that the produced drawdowns by the simulation and the optimisation models were exactly the same. This means that the solution is verified and the optimal pumping rates are valid to be used in simulating the actual response of the aquifer system using the real aquifer water heads.

## 8.8 MANAGEMENT MODEL RESULTS

Using the management model, the intended minimum hydraulic gradient around the freshwater storage area was obtained with a minimum pumping rate by the gradient-control wells. From the 19 gradient-control wells which were suggested initially to maintain the hydraulic-gradient around the freshwater storage, only eight wells were selected by the management model to operate. The achieved objective value (total pumping rate from all the gradient-control wells over the 7 years planning horizon) is 0.3 $m^3$ /s, which is very close to the target objective value (zero). On the other hand, the optimal pumping rates from the supply wells were obtained which are controlled by groundwater demand at each year and by the maximum drawdown at the pumping wells. Table 8.1 illustrates the optimal discharge rates of the gradient-control wells and the groundwater supply wells as obtained by the optimisation model.

| Well No. | Well Type | Optimal discharge rates at the following planning periods : (x 0.01 $m^3/s$) | | | | | | |
|---|---|---|---|---|---|---|---|---|
| | | 1 | 2 | 3 | 4 | 5 | 6 | 7 |
| 2 | SW | 0 | 0 | 0 | 0 | 0 | 0 | 7.894 |
| 3 | SW | 0 | 0 | 0 | 0 | 0 | 0 | 9.652 |
| 14 | SW | 0 | 0 | 0 | 0 | 0 | 0 | 3.878 |
| 15 | SW | 0 | 0 | 0 | 0 | 0 | 0 | 6.710 |
| 16 | SW | 0 | 1.738 | 2.418 | 2.767 | 3.445 | 3.299 | 0 |
| 17 | SW | 0 | 0 | 3.120 | 5.472 | 4.987 | 4.756 | 6.851 |
| 18 | SW | 8.044 | 4.758 | 3.762 | 3.224 | 2.899 | 2.802 | 0 |
| 19 | SW | 3.124 | 11.061 | 10.009 | 8.367 | 7.759 | 7.432 | 11.007 |
| 20 | SW | 15.00 | 11.584 | 8.928 | 9.051 | 8.548 | 8.295 | 0 |
| 21 | SW | 15.00 | 13.570 | 11.107 | 9.927 | 9.327 | 8.984 | 13.382 |
| 22 | SW | 1.590 | 5.636 | 4.686 | 3.893 | 3.763 | 3.605 | 0 |
| 23 | SW | 13.478 | 10.156 | 9.189 | 8.747 | 8.462 | 8.310 | 0 |
| 24 | SW | 7.838 | 5.320 | 4.687 | 4.390 | 4.166 | 4.065 | 0 |
| 26 | SW | 15.00 | 15.00 | 14.245 | 13.621 | 13.232 | 13.021 | 0 |
| 31 | SW | 15.00 | 14.149 | 11.956 | 10.699 | 9.955 | 9.495 | 0 |
| 32 | SW | 12.118 | 8.662 | 7.508 | 6.858 | 6.470 | 6.230 | 0 |
| 33 | SW | 11.341 | 8.623 | 7.590 | 7.009 | 6.661 | 6.446 | 0 |
| 35 | SW | 15.00 | 11.766 | 10.547 | 9.885 | 9.54 | 9.275 | 14.834 |
| 36 | SW | 8.399 | 6.781 | 6.230 | 5.933 | 5.762 | 5.659 | 0 |
| 37 | SW | 11.89 | 10.038 | 9.365 | 9.007 | 8.802 | 8.679 | 15.00 |
| 38 | CW | 1.428 | 0.903 | 0.805 | 0.774 | 0.767 | 0.768 | 0 |
| 39 | CW | 1.07 | 0.729 | 0.663 | 0.644 | 0.642 | 0.646 | 0 |
| 40 | CW | 0.485 | 0.148 | 0.083 | 0.062 | 0.058 | 0.058 | 0 |
| 41 | CW | 1.094 | 0.564 | 0.456 | 0.0426 | 0.425 | 0.431 | 0 |
| 44 | CW | 0.018 | 0 | 0 | 0 | 0 | 0 | 0 |
| 48 | CW | 0.036 | 0 | 0 | 0 | 0 | 0 | 0 |
| 53 | CW | 1.044 | 0.711 | 0.656 | 0.644 | 0.654 | 0.668 | 0 |
| 54 | CW | 0.889 | 0.61 | 0.572 | 0.563 | 0.568 | 0.576 | 0 |
| 55 | CW | 0.32 | 0.29 | 0.302 | 0.307 | 0.312 | 0.316 | 0 |
| 56 | CW | 1.526 | 0.974 | 0.862 | 0.825 | 0.815 | 0.817 | 0 |

Table 8.1: Optimal discharge rates for the supply and gradient-control wells during the 7 planning periods as obtained by the optimisation algorithm (MINOS).

Note: The wells which are not included in the table, either they had the maximum or minimum pumpage rate. From 1 to 15, and from 38 to 56 any well not included, has 0 pumping rate. Whereas, from 16 to 37 any well not included, has the maximum pumping rate ( 0.15 m3/s).

**SW** : groundwater supply wells (from 1 to 37), from 1-15 locate down-gradient, and from 16-37 locate up-gradient from the storage area. **CW** : gradient control wells (from 38 to 56).

### 8.8.1 HYDRAULIC RESULTS

The hydraulic gradient around the storage area was reduced significantly using the gradient-control wells. Also, the optimal drawdowns at the pumping wells (SW and CW) were obtained.

Appendix III, includes a comparison between the hydraulic head at the gradient-control pairs with and without using the gradient-control wells.

Appendix III, shows that using the gradient-control wells to create a stagnation zone around the storage area is possible. The simulated water heads at the gradient-control nodes (A and B) for each gradient-control pair has almost the same value, which was the objective for using the gradient-control wells. For example, under the normal conditions of groundwater abstraction before using gradient-control wells, the average hydraulic gradient at the down-gradient-control nodes C-1 to C-4, and from C-18 to C-21 (Figure 8.2) is about 0.004. Whereas, this value was reduced significantly when the gradient-control wells were simulated to be about $4.5 \times 10^{-5}$ .

Figure 8.6 shows the simulated potentiometric head of the DM aquifer after 6 years of storing freshwater at the Shigaya-A wellfield (at 2007), where no controls was used and all wellfields are operated with their predicted uncontrolled rates to meet the future groundwater demand. In contrast, Figure 8.7 displays the potentiometric heads of the aquifer for the same residence time if the optimum pumping rates for the gradient-control wells and the groundwater supply wells are used.

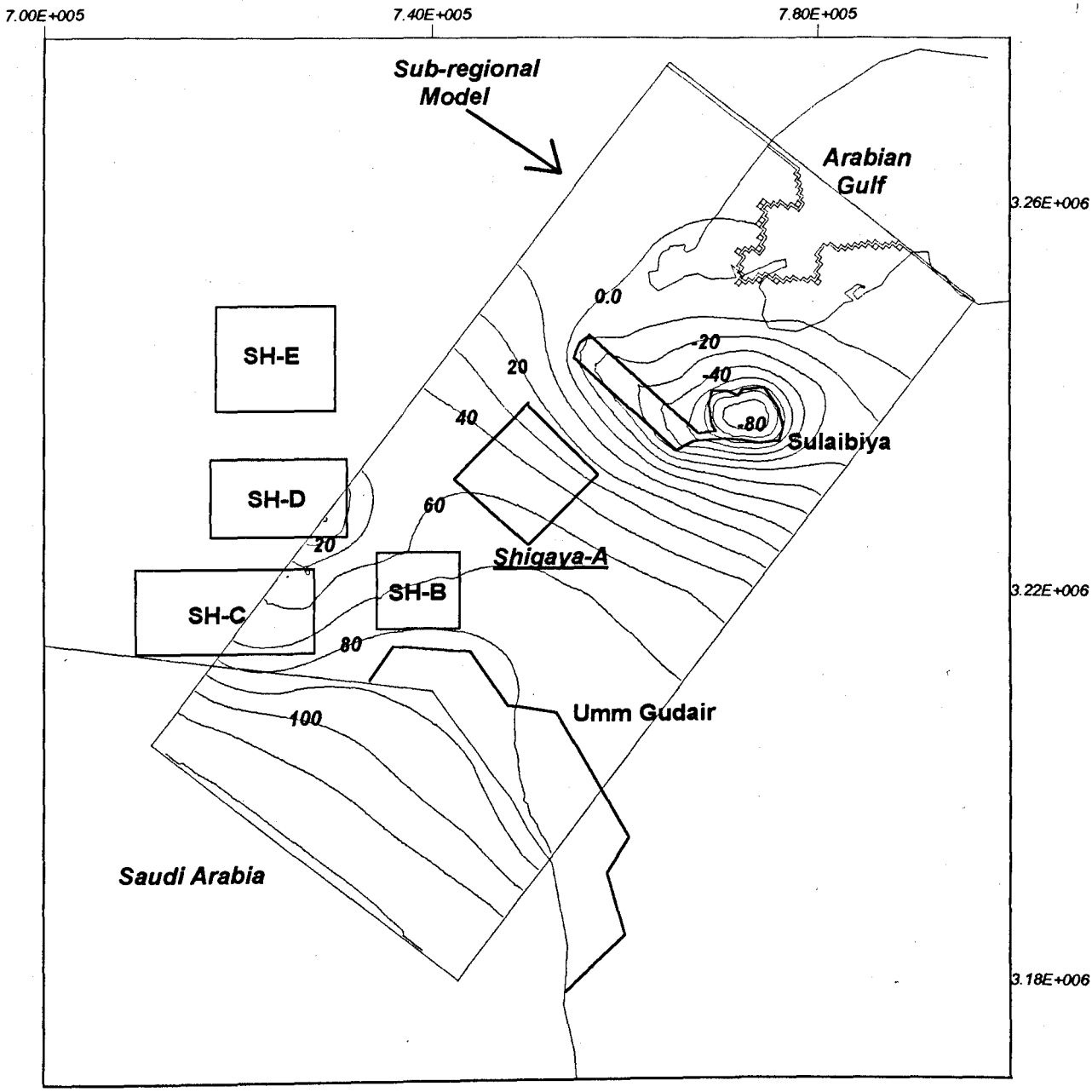


Figure 8.6: Simulated potentiometric head of the DM aquifer after 6 years of storing freshwater at Shigaya-A wellfield if groundwater abstraction proceeds without any control to maintain the freshwater mound.

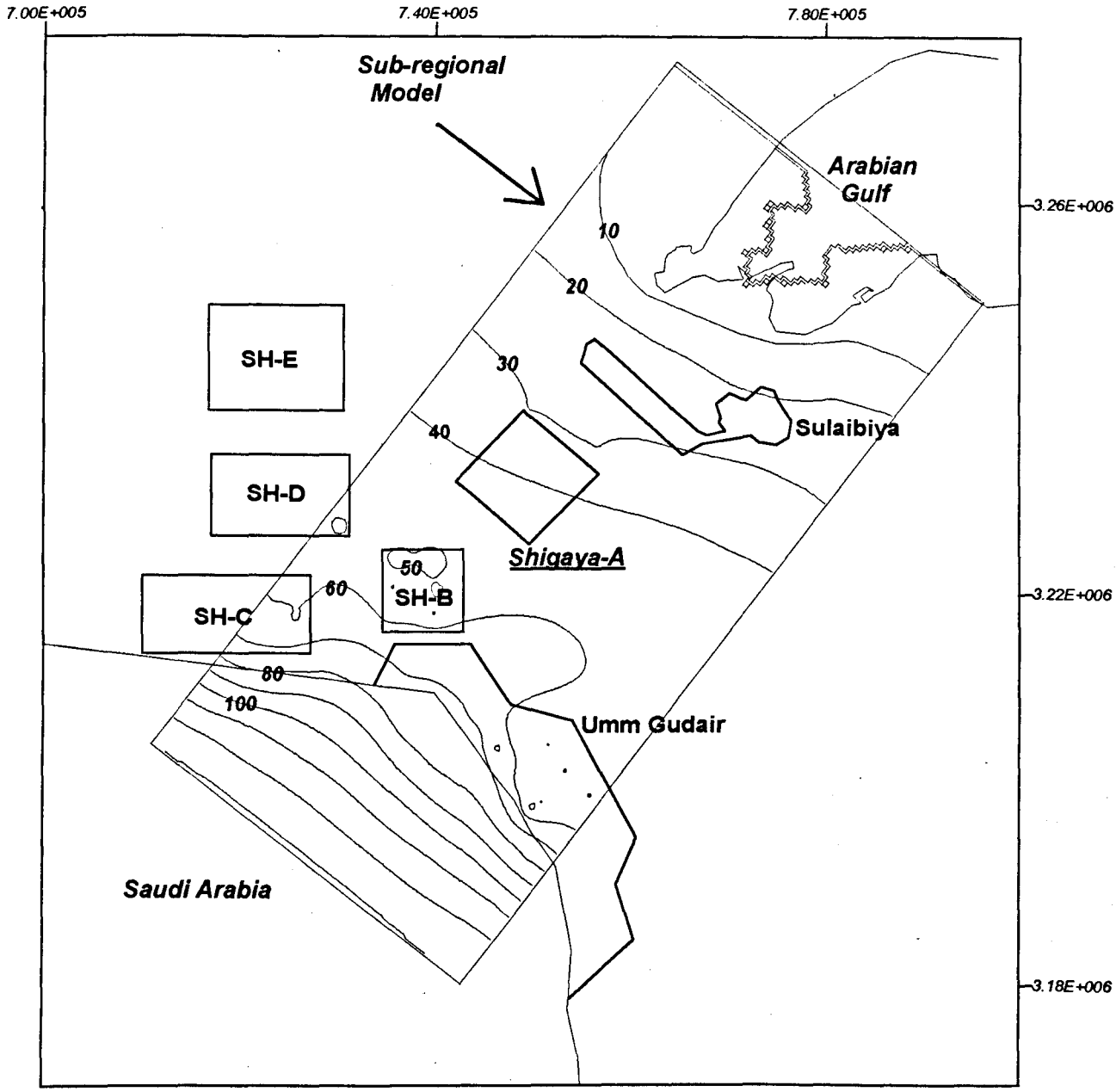


Figure 8.7: Simulated potentiometric head of the DM aquifer after 6 years of storing freshwater at Shigaya-A wellfield if optimum pumping rates of the gradient-control and supply wells are used as determined by the management model. (pumping rates are presented in Table 8.1).

There was a difference in aquifer potentiometric surface between the two maps (Figure 8.6 and 8.7) which were produced by pumping the same volume of groundwater from the aquifer. The steep hydraulic head at the Sulaibiya wellfield created by the non-optimal abstraction from the supply wells was flattened when the optimal solution was applied. The optimal solution indicates that the groundwater abstraction should be met by the up-gradient wellfields including, Shigaya-B, C, D, and Umm Gudair. The most productive field as suggested by the management model is Umm Gudair, where about 130,000 $m^3/d$ of groundwater can be produced by this field with a drawdown ranging from about 30-40 m. Whereas, the less productive field as selected by the management model is the Sulaibiya. This was selected to operate only during the recovery period at about 16,000 $m^3/d$. Drawdown at this field was maintained at a range of 20 to 30 m. The optimal pumping rates from the DM aquifer may preferred to the present abstraction development since they produced the same volume of groundwater. The optimal solution moves the steep hydraulic gradient from the coastal areas which may vulnerable to saline water intrusion to the up-gradient boundary of the modelled area that is near the recharge zone. Thus, more groundwater which has good water quality (about 2500 mg/l) will be induced to enter the aquifer system by such a flow pattern, and the undesirable flow from the Gulf will be eliminated. This confirms the possible optimal outlines for groundwater abstraction in Kuwait as recommended earlier by this study (presented in section 7.4.4).

### 8.8.2 TRANSPORT RESULTS

The optimal discharges rates were used to simulate the change in stored water TDS using the sub-regional transport model (section 7.3). The simulated results indicate that the freshwater lens under dynamic flow conditions can be maintained in its location and will not move away with the regional groundwater flow if gradient-control wells are used.

Figure 8.8, shows the position of the freshwater lens directly after the stopping of freshwater injection, and its position after 6 years of storage if the gradient-control wells are used to maintain it.

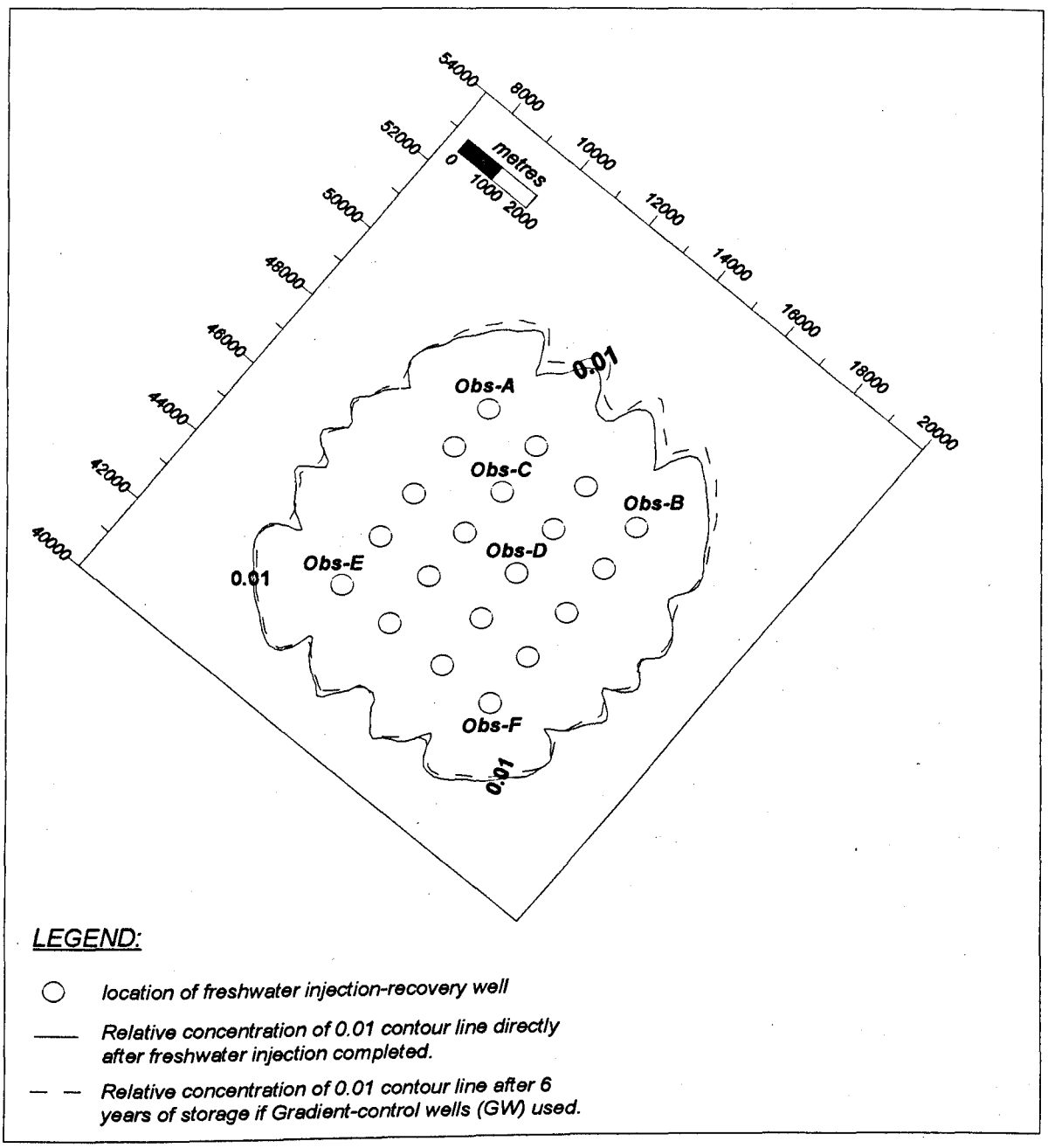


Figure 8.8: Displacement of the stored freshwater lens after 6 years of residence time if gradient-control wells are used to maintain it.

By comparing Figure 8.8 with Figure 8.1, it is clear the significant role that the gradient-control wells can play in protecting the stored freshwater from moving away with the regional groundwater flow.

The recovery efficiency of the stored water was also maintained using the gradient-control wells. Generally, the recovery efficiency was degraded with time whether the gradient-control wells were used or not. However, if gradient-control wells were used, the percent of reduction was much less.

The stored water with a TDS < 1500 mg/l, that is the intended usable water needed to be recovered at any time during the storage period, was found to have vanished after about 4 years of storage if gradient-control wells were not used. By the same time, water with this quality can be recovered with an average efficiency of about 10 % (about 5.2 $Mm^3$) if gradient-control wells were used (recall that the original recovery efficiency of this water is about 18 % if it is recovered back without any delay between the recharge and recovery stages). This indicates that at the time where all the usable stored water is completely irrecoverable, about 55 % of it can be recovered if gradient-control wells are utilised to maintain it. Furthermore, after six years about 30% of this water can be recovered.

Table 8.2, presents a comparison between the recovery efficiency of stored water with a TDS < 1500 mg/l with and without using the gradient-control wells at selected wells within the storage area (4 at the border of the storage site, and 2 at the centre ), as shown in Figure 8.8.

| Obs. Well No. | * Original Recovery Efficiency ( % ) | Recovery efficiency (%) , if gradient control wells (CW) are used or not | | | | | | | | | | | |
|---|---|---|---|---|---|---|---|---|---|---|---|---|---|
| | | After 1 year | | After 2 years | | After 3 years | | After 4 years | | After 5 years | | After 6 years | |
| | | Without CW | With CW | Without CW | With CW | Without CW | With CW | Without CW | With CW | Without CW | With CW | Without CW | With CW |
| A (BW) | 18.5 | 13.15 | 16.6 | 8.3 | 13.92 | 3.1 | 11.32 | 0 | 8.71 | 0 | 6 | 0 | 3.22 |
| B (BW) | 18.1 | 11.8 | 16.5 | 6.2 | 13.8 | 0 | 11.3 | 0 | 8.7 | 0 | 6 | 0 | 3.3 |
| C (IW) | 18.4 | 13.35 | 15.85 | 9.3 | 13.15 | 5 | 11.73 | 1.4 | 9.74 | 0 | 7.61 | 0 | 5.55 |
| D (IW) | 18.7 | 14.6 | 17.5 | 10.4 | 15.5 | 5.9 | 13.6 | 2.1 | 11.66 | 0 | 9.7 | 0 | 7.68 |
| E (BW) | 13.3 | 9.65 | 12.4 | 6.1 | 10.84 | 2.4 | 9.3 | 0 | 7.7 | 0 | 5.96 | 0 | 4.25 |
| F (BW) | 13.2 | 9.7 | 12.4 | 5.9 | 10.7 | 1.8 | 8.9 | 0 | 7.13 | 0 | 5.3 | 0 | 3.36 |

Table 8.2: Comparison between the simulated recovery efficiency of the stored water with a TDS < 1500 mg/l after a successive years of storage with and without applying the gradient-control wells (CW) to maintain the freshwater mound.

Note : BW is a border well , and IW is an internal well at the storage site, as in Figure 8.8.

* Recovery efficiency simulated directly after recovering the stored water without any delay in time.

From Table 8.2, it was noticed that the border wells were more subjected to quality deterioration during the storage period than the internal wells due to the high mixing rate at the outer transition zone between the stored water and the native groundwater. Thus, the role of gradient-control wells in improving the recovery efficiency was much clearer at the border wells than at the central wells, especially at the down-gradient border wells (Obs-A, and Obs-B) which were more affected by the regional flow. At the border wells , if no gradient-control wells were used, the usable stored water will be completely irrecoverable after 4 years. However, using the gradient-control wells, about 80 % of this water can be recovered by these wells. Figure 8.9, shows the degree of improvement in the stored water TDS during the storage and the recovery stages at a border and an internal wells after the gradient-control wells were used.

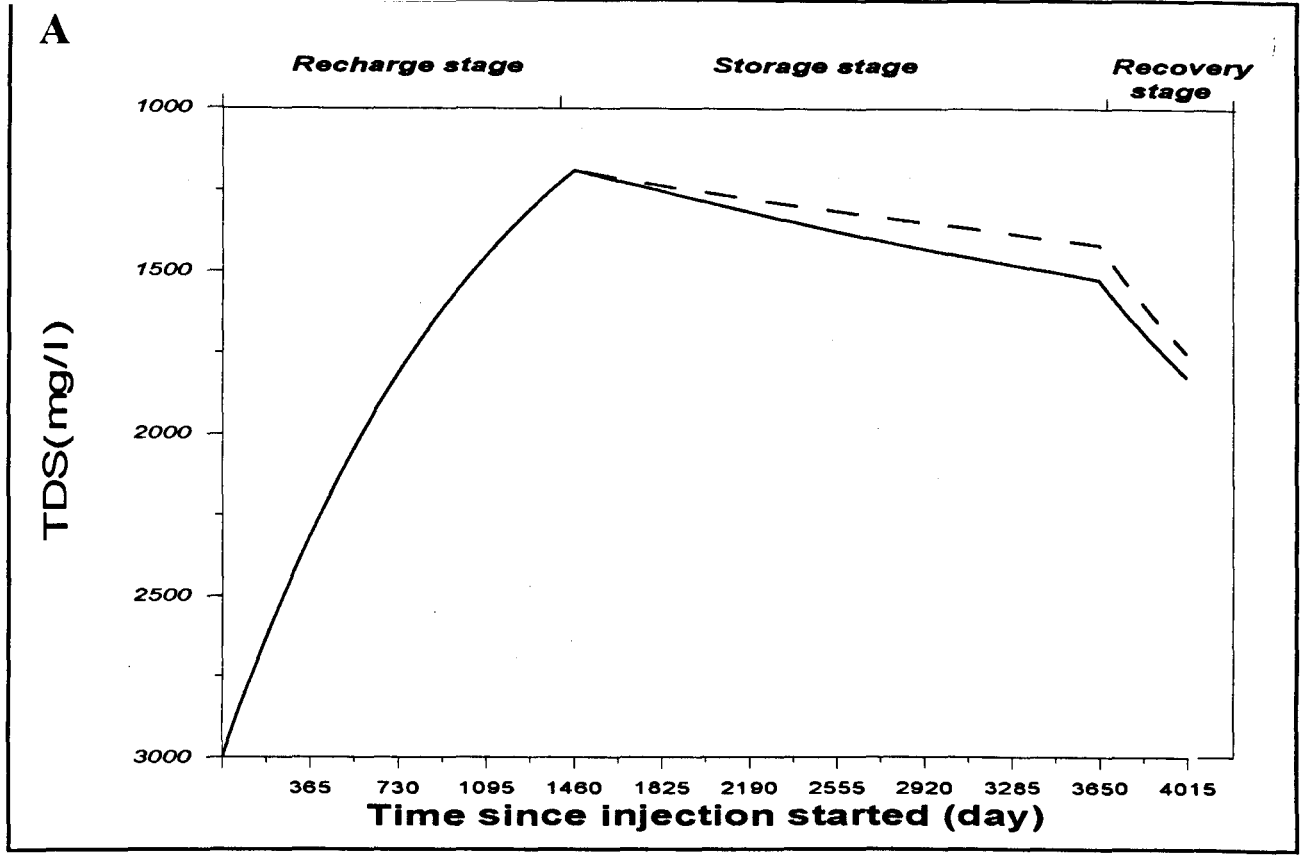


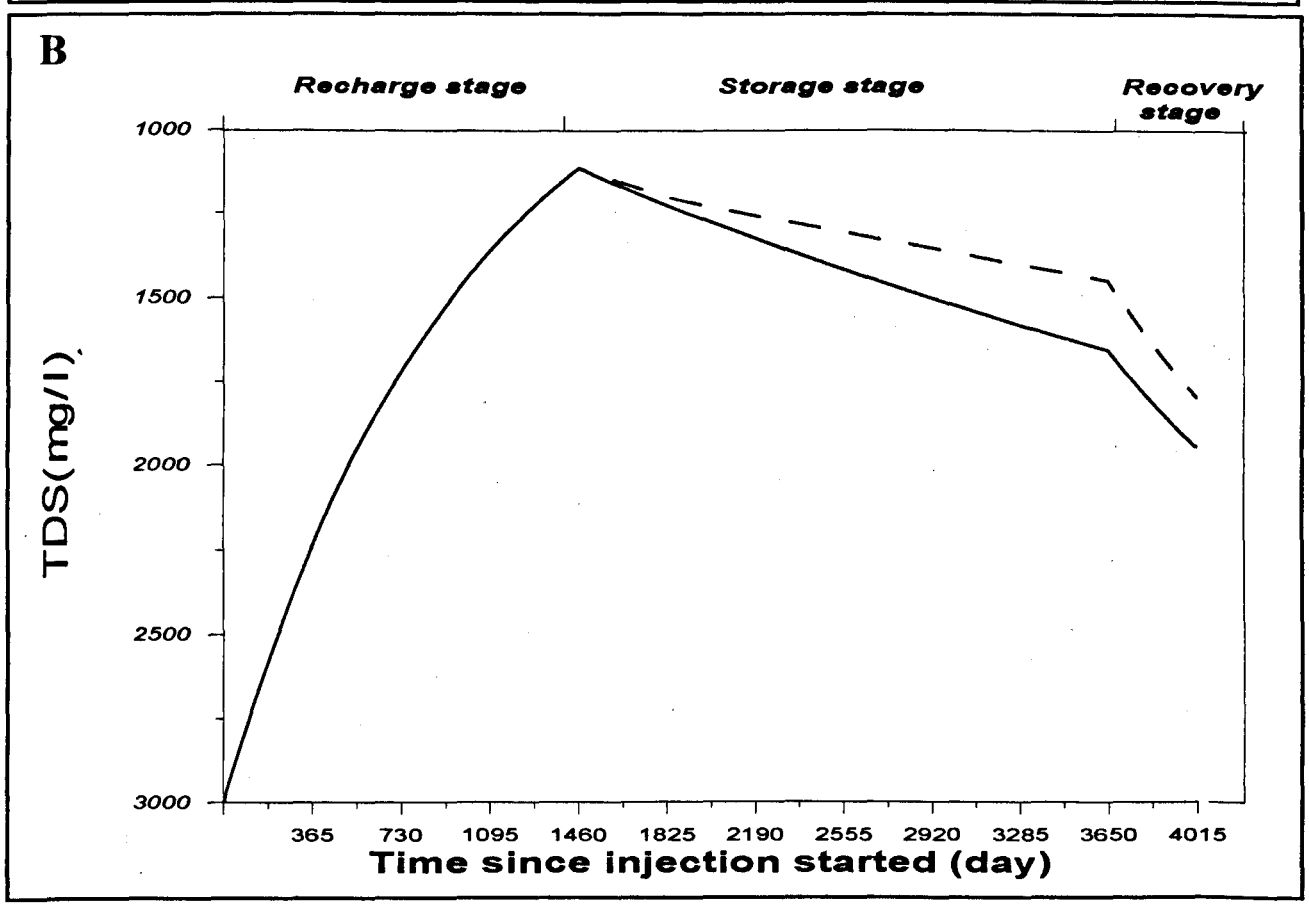


Figures 8.9 (**A** and **B**): Comparsion between the change in simulated TDS for the stored water (after freshwater recharge completed) during 6 years of storage, and a one year recovery with (- - - - ), and without ( ——— ) using gradient control wells, **A** at an internal well No. Obs-C, and **B** at a border well No. Obs-F (as shown in Figure 8.8).

If the minimum pumpage constraints at all supply wells were set to zero, the optimisation model would not include the abstraction from the down-gradient supply wells within the optimal solution (Sulaibiya wellfield). Thus, the down-gradient-control wells are operated with minimum pumping rates. However, if the down-gradient supply wells forced to operate to meet a specified volume of groundwater demand, the down-gradient-control wells will be selected by the optimisation solution to operate with a higher pumping rate to reverse the hydraulic gradient toward the storage area which is increased by pumping the down-gradient supply wells. Thus, another scenario was used, where the down-gradient wellfield (Sulaibiya) was pushed to produce 25,920 $m^3/d$ of groundwater. As a result, the objective value as calculated by the optimisation model using this scenario was raised from 0.3 $m^3/s$ to 0.61 $m^3/s$. Hence, it is obvious that as the abstraction from the supply wells increased, as the pumping of the gradient-control wells located between the supply wells and the storage area will be increased. This to overcome the speeding of stored water movement toward the pumping supply wells.

This was during the 6 years of storage, but at the seventh planning period (which is the recovery stage where wells at the storage site were operated to recover the stored water back), all the gradient-control wells were shut-down as chosen by the management model. In this case, the hydraulic gradient starts to be maintained by the optimal pumping rates by the supply wells themselves. Thus, in addition to the up-gradient supply wells the down-gradient supply wells began to operate during the recovery stage without any enforcement for them to work.

# 9. MAIN FINDINGS, CONCLUSION, AND RECOMMENDATIONS

## 9.1 INTRODUCTION

This study indicates that the artificial groundwater recharge is a feasible management option for Kuwait to improve its water system efficiency, increase the aquifer yield, and develop a long-term underground strategic reserve to be used during emergency conditions. This is the first study to investigate the possible benefits that artificial recharge can bring to the overall water system situation in Kuwait, rather than simply to consider artificial recharge to store freshwater in the aquifers for emergency use.

Conclusions, results, and recommendations drawn from this study can be divided into five different sections discussing the following topics:

1. Groundwater modelling (flow and solute transport);
2. Groundwater abstraction;
3. Water injection-withdrawal experiment;
4. Artificial groundwater recharge; and
5. Hydraulic gradient-control to maintain the stored freshwater lens using management models.

## 9.2 GROUNDWATER MODELING

This study was carried out using three three-dimensional numerical groundwater flow and transport models; firstly a regional model covers all of Kuwait and the surroundings areas of Saudi Arabia; the sub-regional model covers the wellfields region, and a single-well model was used to simulate a freshwater injection-withdrawal experiment conducted in the Sulaibiya wellfield.

### 9.2.1 FLOW MODELS

The major factor limiting the use of groundwater models with high accuracy is the inadequacy of reliable aquifer parameters. Existing pumping test data for aquifers in Kuwait are not sufficiently reliable to estimate aquifer storativities, and the vertical leakage factor for the aquitard separating the two main aquifers (KG and DM). This is because in all the available pumping tests, water level was measured in the pumped well and no piezometers were used, which are required to estimate the aquifers storativities and the aquitard vertical leakance. Moreover, the aquifers in Kuwait are considered to be multi-aquifers, with each aquifer divided into different hydrological sub-units. This was not considered during the pumping tests, where the pumped well was completed in the whole aquifer without any distinction between the various vertical zones. Also, the historical measurements for water levels and water quality are very rare (especially for the KG aquifer) because very few observation wells were used to monitor the aquifers.

Thus, in order to overcome this lack of aquifer parameters, model calibration in this study was done through an iterative loop procedure trying to obtain more reliable parameters. The steady state and transient calibrations were combined and done as one task. This was carried out iteratively until the match between the simulated and observed steady-state aquifers heads was achieved, as well as between the simulated and the observed total drawdown in the aquifer heads. The model was robustly calibrated and verified under steady-state and transient conditions. This rigorous approach to calibration was very beneficial in obtaining more reliable calibrated aquifer parameters. The aquifer parameters and the aquitard vertical leakance were determined throughout the modelled region (which is a very extensive area).

### 9.2.2 TRANSPORT MODEL

Using the regional transport model (which has a coarse nodal spacing) has a limitation resulting from the need to run the model for a long time in order to observe changes in groundwater quality during freshwater injection. The long simulation time is impractical because of the computer storage limitation, and it is also a very time-consuming process, especially if very small time steps are needed to avoid any numerical instability in the solution. In this study, such a limitation was solved by reducing the aquifer porosity to

accelerate the flow velocity of the recharged water at the injected node. This approach is acceptable only for comparison purposes to differentiate between the recovery efficiency for a number of injection sites. It was found that if the original porosity of the aquifer is reduced by a factor of 0.1, then it will cause the same effect as increasing the simulation time by an order of 2.5. Based on the results from the injection-withdrawal test in Well SU-10, it was found that the reduction of aquifer porosity will also cause an overestimation of the recovery efficiency. Thus, according to the ratio obtained at that test, if the aquifer porosity is reduced by half, the dispersivity should be increased correspondingly by a factor of 1.8 to eliminate the effect of porosity reduction. In conclusion, small nodal spacings are essential in transport simulations in order to obtain more reasonable results. In this study, the use of a model with coarse nodal spacing was initially required to model the area on a regional scale (especially from the hydraulic point of view). However, later when the transport simulation becomes an essential task to simulate the aquifer response to freshwater injection and recovery, a model (sub-regional model) with a finer nodal spacing covering the wellfields area only, was constructed.

### 9.2.3 RECOMMENDATIONS

For a better representation of the aquifer system using groundwater models, the following are recommended based on the deficiencies in the field-estimated data:

1. More accurate aquifer parameters should be obtained through pumping tests using observation wells with multi-elevations.
2. Test drilling is needed in many areas of Kuwait, where little or no drilling and sampling has been done.
3. Continuous monitoring of the aquifer system is necessary in terms of potentiometry and salinity. This should be undertaken from observation wells completed in different horizons within each aquifer, so that the vertical variation in potentiometric head and water quality are fully monitored.
4. In order to facilitate the evaluation and management of the Kuwait aquifer system, a hydrological data base for Kuwait is essential.

## 9.3 GROUNDWATER ABSTRACTION

Using the regional model to simulate the aquifer system response to the present and future groundwater abstraction, it was clear that the outflow from the system is exceeding the inflow to it.

### 9.3.1 PRESENT DEVELOPMENT

From simulating the present-day groundwater abstraction, the following conclusions were made:

1. A mass balance calculation for the aquifer system suggests that at present (1996) the aquifer system is under large stress, with a negative balance between its inflow and outflow rates. This deficit is met by exploitation of aquifer storage.
2. As a result of the disturbance to the natural steady state balance by the abstraction from wellfields, a major drop in the aquifers potentiometric surface has occurred all over Kuwait. Steep and wide cones of depression have been developed (more extensively in the DM aquifer than in the KG aquifer). Three major cones of depression in the DM aquifer potentiometric head were developed with a decline of 100, 50, and 30 m at the Sulaibiya Shigaya-D, and Umm Gudair wellfields.
3. Under pre-development steady-state conditions, the vertical leakage west of the NW Kuwait border was from the KG aquifer toward the DM aquifer. However, from the NW border up to the Arabian Gulf (discharge zone), the direction of vertical leakage changed to be from the DM aquifer to the KG aquifer.
4. Under transient conditions (developed due to pumping), a reversal of vertical leakage from the KG aquifer towards the DM aquifer occurs at all the DM abstraction wellfields.

### 9.3.2 FUTURE DEVELOPMENT

The regional flow model was also used to predict the future behaviour of the Kuwait aquifer system for the next 15 years (1996-2010) in response to the planned abstraction wellfields. The predictive simulation indicates that the current decline in the two aquifers head will continue at the current cones of depression. In addition, new cones of depression will be created at the newly introduced fields. For example, the DM aquifer head was predicted to decline below the mean sea level by about 60 m after 5 years from pumping the NW-Shigaya wellfield. The creation of relatively large and steep cones of depression with

heads below the mean sea level at areas close to the saline front (e.g., Sulaibiya NW-Shigaya, and Shigaya-E) will inevitably cause the front to invade these areas. This is expected to lead to a deterioration in the groundwater quality as the abstraction continues. By the year 2010 large coastal areas of the aquifers (especially the DM aquifer) might be lost due to their salinization by sea water intrusion.

### 9.3.3 RECOMMENDATIONS

The existing development of groundwater should be managed in a more effective manner to reduce the decline in aquifers heads and the deterioration in water quality. The following are some issues to be considered:

1. Some wellfields should be abandoned (such as the Sulaibiya wellfield) because the DM aquifer potentiometric head at this field has already declined below the mean sea level by about 80 m. This is inducing sea water intrusion, which is indicated be the deterioration of the groundwater quality at this field from 4000 mg/l TDS (in 1960) to about 7000 mg/l TDS (in 1990).
2. The planned development for new wellfields should be re-evaluated using groundwater management models depending on field-estimated aquifers parameters. Abstraction from wellfields close to the saline water front should be managed very sensitively.
3. Groundwater should be restricted in use for blending with desalinated water to meet drinking water demand. Other demands like agricultural and gardening uses should be met with treated wastewater to relax stresses imposed on the limited groundwater resource.

## *9.4 WATER INJECTION-WITHDRAWAL EXPERIMENT*

An interpretation of a pilot water injection-withdrawal experimental data (conducted at Well SU-10 which is located in the Sulaibiya wellfield, where the DM limestone was the injected aquifer) was very beneficial in; (1) understanding the practical difficulties caused by clogging which will limit water injection, (2) estimating the aquifer dispersivity, and (3) determining the recovery efficiency of freshwater injection and recovery. The test data were analysed using a single-well numerical groundwater flow and transport model.

### 9.4.1 WELL FACE CLOGGING

It was clear that the injection of the DM aquifer is technically feasible, if open hole completion is practiced. Even if clogging occurs from air entrapment and suspended solids, the effect can be removed by backpumping the well. The rapid clogging during injection and equally rapid clearing during pumping suggest that the clogging might be due to entrapped air rather than suspended solids. It was possible by analysing the water injection-withdrawal experimental data using the single-well flow model (presented in Chapter 5) to quantify the well face clogging factor. It also was possible to identify the various causes of clogging and differentiate between their effects.

- Air Entrapment : It was clear that most of the clogging occurred due to air entrapment, and not due to the formation or recharge water properties. This means that the clogging during this experiment has probably been due to the injection system, introducing air bubbles in the recharge water. Therefore, if this cause can be avoided in the future during water injection in Kuwait, the injection capacity of wells will be increased. The clogging factor was found to range from 0.73, developed in the first hours of the test, to about 0.80, observed directly before stopping the water injection. Causes of the clogging was found to be 100% due to air entrapment in the first two days. Then the air seemed to seep out over the remaining days, while a deposition of suspended solids built up as the injection test proceeds. By the last hour of the experiment it was found that the air entrapment represented about 55% of the total clogging, and suspended solids accounted for the remaining percentage. It is more likely that clogging of well occurred at its inner wall and did not penetrate the aquifer for a long distance to clog its pores. This was concluded from the increase in the aquifer hydraulic conductivity around the well obtained from analysing the post-injection pumping tests data. No serious damage had occurred to the well, since its capacity was restored easily after about 20 days of water injection with a simple backwashing for a few hours. This also was confirmed by the long-term recovery, the well reached its initial specific pumping capacity during the normal production rate.
- Suspended solids : During backwashing of the well, turbid yellowish brown water was recovered for the first half-hour of pumping, suggesting the physically deposition of suspended material like iron oxides derived from the water distribution network.

No other causes, such as chemical reactions or biological actions, seemed to be causing any clogging to the well face and the surrounding formation pores.

### 9.4.2 AQUIFER DISPERSIVITY

Because the aquifer porosity is not well known, two values representing the maximum and minimum limits were assigned. Using these values, it was possible using the single-well model to estimate the DM aquifer dispersivity through matching the simulated and the observed breakthrough curves. The matching was achieved with two different values of aquifer porosity and dispersivity. Under the low porosity (0.05), the estimated longitudinal dispersivity was found to be 4m; with a porosity of (0.1), the dispersivity was 2.5m. This means that the same match can be obtained either with high aquifer porosity and low dispersivity, or vice versa.

### 9.4.3 RECOVERY EFFICIENCY

The objective of artificial groundwater recharge in Kuwait is to store freshwater and recover it back with a TDS of 1500 mg/l or less. During this experiment, the recovery efficiency at this TDS was observed to be 20%. From sensitivity analysis, it was found that the recovery efficiency increases as the porosity and dispersivity of the aquifer decrease. If either the porosity or dispersivity are reduced by half, then the recovery efficiency will be increased by a factor of 1.65.

### 9.4.4 RECOMMENDATIONS

The interpretation of the single-well injection-withdrawal experimental data has been constrained by the limitation of sufficient data describing the radial and vertical aquifer response precisely to the water injection and pumping. In order to model the test and interpret the experimental data more accurately, the following is recommended:

Observation Wells : In order to monitor the movement pattern of the injected water and the concentration distribution of tracers used, observation wells completed in different aquifer zones are necessary within the close proximity of the well (10-100 m) for both water level measurement and sampling. The data collected will help in:

- Visualising the time and distance dependent behaviour of the displacement front between the injected and native water;
- Indicating the vertical movement of the injected water; and
- Modelling the injection-recovery process on a site specific basis, including the estimation of aquifer porosity.

Flow-metering : This is required to identify the various intake capacities of the vertical units of the aquifer to water injection, and their contribution rates during pumping.

Water quality sampling : During the injection and recovery tests, water quality should be analysed to determine changes in water composition. This will facilitate determination of the chemical processes (such as dissolution and precipitation) which may be caused by the incompatibility between the recharged water and formation materials and water.

Future studies should be conducted to evaluate the compatibility of injected water with formation water and materials.

## 9.5 ARTIFICIAL GROUNDWATER RECHARGE

Artificial groundwater recharge was found to be potentially a very beneficial management alternative for Kuwait; to improve its water system efficiency, increase the aquifer yield, and to create a strategic reserve for emergency use. Two alternatives for injecting, storing, and recovering freshwater were investigated, seasonal and long-term storages. Through seasonal cyclic injection and recovery of water, it will be possible to operate the desalination plants all over the year irrespective of the seasonal fluctuation in water demand, and of the same time increase the aquifer yield. Through long-term storage, a sufficient volume of freshwater could be stored in the aquifer for subsequent use during emergency conditions. The regional numerical groundwater flow and transport model (presented in Chapter 4) was used to identify the optimum locations to store freshwater, and the sub-regional model (presented in Chapter 7) was used to find out the optimum management variables to inject and recover freshwater at the selected sites. These variables include; number and geometry of injection/recovery wells, injection/recovery rates, duration of injection required to create the intended quantity and quality of freshwater. Also, the

recovery efficiency of the freshwater storing and recovery practice was identified. The DM Limestone was preferred to the KG as the most appropriate aquifer for water injection. This is mainly due to less practical difficulties caused by well face clogging that will arise from recharging this fissured aquifer comparing with the clogging developed after recharging the granular KG aquifer. The various sources of recharge water (desalinated water, treated wastewater, and runoff water) were ranked based on their dependability of supply, quality, compatibility with native groundwater and aquifer material, and expected conveyance cost. It has been found that planning for artificial groundwater recharge in Kuwait should be based primarily on the availability of the desalinated water, and consider the treated wastewater as an alternative, especially for surface recharge through spreading basins to improve its quality to meet the specification for water use.

### 9.5.1 SEASONAL CYCLE OF WATER INJECTION AND RECOVERY

The current and proposed groundwater abstraction from the aquifers in Kuwait as indicated by the simulation flow model are seriously exposed to a mis-managed development, where the groundwater is abstracted (or may be mined) regardless of the aquifers safe yield. Because the TDS of the groundwater in the utilised aquifers is already high (ranges from 3000 to 7000 mg/l), any further deterioration will make these aquifers less usable in the future. By that time, any remedy will be impossible. On the other hand, the urban demand for freshwater varies considerably between summer and winter months resulting in operating the desalination plants under sub-optimal conditions. It has been found that if the artificial groundwater recharge is practised by integrating the aquifers and the desalinated water production together, the desalination plants can operate with their optimum capacity irrespective of demands for freshwater, and in the same time the aquifer yield can be restored. Two benefits follow from this practice:

1. Operating Desalination Plants at Optimum Capacity: This can be done through a seasonal cyclic storage and recovery of desalinated water. It is possible to store the excess desalinated water during winter months, and recover the stored water later during the summer to meet peak water demand. In addition, using the aquifers as a stand-by storage to meet the peak water demand, the establishment of new desalination plants can be postponed depending on the aquifer storage capacity and the number and capacity of

injection/recovery wells. The optimum site to be used as a seasonal storage was found to the Shigaya-B wellfield. The main reasons for selecting this site are; (1) its capacity to store and recover large volumes of water within a short period of time; and (2) its location in a highly depleted area, thus the aquifer head can be restored and the undesirable effects effecting groundwater quality can be reduced. The number of wells required to make the desalination plants operate with their optimum capacity all over the year are 20 wells, where their theoretical optimum injection (during the injection cycles) and pumping (during the recovery cycles) rates are 7000 $m^3/d$ per well. The initial recovery efficiency was found to be improved with the increasing number of injection/recovery cycles from 12% to about 48% obtained after 10 cycles.

2. Increasing the Aquifer Yield: At the same time, the depleted aquifers heads were restored to a certain degree using the cycle of water injection/recovery. For example, recharging the Shigaya-D wellfield at a rate of 1840 $m^3/d$ per well using 24 wells on a seasonal basis was found to raise the DM aquifer heads at the major cones of depression by 80, 20, 10, and 7 m at the recharged site, Shigaya-B, Umm Gudair, and the Sulaibiya wellfields, respectively. Thus, the aquifer yield at the water wellfields was increased, and the possibility of groundwater quality deterioration due to sea water intrusion or upward leakage of saline water from underlying layers is reduced.

In general, it has been found that in order to maximise the benefits from artificial groundwater recharge in increasing the aquifer yield, it should be practised in conjunction with groundwater abstraction. In order to achieve this objective, in this study the Kuwait region was divided into three zones, each showing a different degree of response to groundwater abstraction and/or artificial groundwater recharge. These zones were arranged laterally in the direction of the regional groundwater flow; up-gradient zone (Zone A), down-gradient zone (Zone C), and Zone B in between these two zones.

Zone A: The water injection at this zone was found to cause a reduction in the natural groundwater inflow recharging the whole system. Thus, the wellfields at this zone (Umm Gudair and Shigaya-C) were excluded from use for artificial groundwater recharge. However, this zone is the most suitable location to produce groundwater because it is recharged with a relatively good quality water (TDS ranges from 2500 to 3000 mg/l). Hence, the abstraction from this zone will induce the lateral groundwater inflow to the

aquifer system. Also, with optimum constant pumping rates, a pseudo-steady state drawdown in the aquifers heads could be reached at this zone.

Zone B : This zone was found to be the optimum location for cyclic injection/recovery of water, because the aquifers heads at this zone are very depleted. Thus, during the injection cycles the resulted increase in aquifers heads and the improvement in water quality will be maximised over an extensive area.

Zone C : This locates close to the Arabian Gulf coastline which is the discharge zone of the aquifer system. This means that the recharged water will flow toward the Gulf. Also, the implementation of artificial recharge in this zone will not increase the aquifers heads on a regional scale. However, the specific benefits for the zone itself will be valuable in halting sea water intrusion. Groundwater abstraction from this zone should be minimised to avoid such undesirable effects.

### 9.5.2 LONG-TERM STRATEGIC RESERVE FOR EMERGENCY CONDITIONS

It has been found that the injection, storage and recovery of a sufficient volume of freshwater is a feasible option to meet the shortage in freshwater supply which may occur during emergency conditions. The Shigaya-A wellfield was found to be the optimum site to be used as a long-term underground strategic reserve. This is mainly due to its high recovery efficiency, and the sufficient depth of the aquifer potentiometric head at this site which allows the build-up in water head inside the injection well if it is clogged. Emergency conditions were assumed to persist for 270 days. Three different scenarios for the emergency to occur were assumed in this study. They are classified according to the degree of severity, ranging from a limited deficit in freshwater resulting from a limited failure of one or two desalination plants, to a total loss of the desalination plants capacity and of the surface reservoir capacity. The optimum management variables required to store a sufficient volume of freshwater in order to fulfil the shortage in freshwater supply during each scenario were separately identified as follows:

- Scenario A : very limited mechanical failure or terrorist action against one or two desalination plants was assumed. Under this scenario the available storages and the capacity of desalination plants would be adequate to replace the lost portion of freshwater, and there was no need for artificial underground freshwater storage in this case. However, under the other two scenarios, underground artificial storage was necessary.
- Scenario B : total loss of desalination plants assumed to occur, but the surface reservoirs were still available. Under this scenario, a volume of 53.2 $Mm^3$ of freshwater had to be injected into the aquifer to be able to recover 9.7 $Mm^3$ (which is the freshwater demand during emergency conditions). Meaning that the recovery efficiency is 18.2%. This was done using 20 wells with an injection rate of 1750 $m^3/d$ per well for about 4.16 years. The optimum spacing of the wells, under which the maximum injection rate and maximum recovery efficiency can be obtained, was found to be 1000 m.
- Scenario C : total loss of the desalination plants capacity and of the surface reservoir capacity assumed to occur. Under this scenario, where freshwater supply was completely lost, more water had to be stored (about 115.32 $Mm^3$) in order to recover 21.9 $Mm^3$ of freshwater to meet freshwater demand during the period of the emergency. This involves the use of 40 injection wells with a rate of 1500 $m^3/d$ per well over 5.26 years. The optimum spacing for these wells was found to be 1500 m.

### 9.5.3 RECOMMENDATIONS

Three main aspects are addressed below to maximise the benefits of artificial groundwater recharge practice:

1. In order to predict the size of the expected shortage in freshwater, the daily domestic consumption per capita has to be known. Also, the portion for drinking and cocking use has to be identified for a better planning in creating such a storage.
2. For the purpose of creating a long-term freshwater strategic reserve for the emergency use, the proposed site for this purpose is recommended to be used initially as a seasonal cyclic storage (for about 3-5 years). This will help in improving the recovery efficiency at this site with the successive cycles of water injection/recovery. Consequently, the

volume of freshwater which needs to be injected in order to create the required freshwater storage for the emergency use will be less.

3. The recharge wells should be constructed as Aquifer Storage Recovery (ASR) wells to permit them to be used for dual purpose (i.e. for abstraction as well as recharge). This design also will help in developing the injection wells (if they became clogged) from time to time without much effort and loss of time.
4. For the purpose of increasing aquifer yield through artificial recharge, future modelling studies should allow for water density variation, to fully identify the saline water front movement and its effect on groundwater quality in the coastal wellfields. Hence, the optimum locations for water injection to halt the sea water intrusion can be identified.
5. In this study, the only source which was considered for recharge was desalinated water. However, for future studies, the treated wastewater could be considered based on its availability and its compatibility for recharge. Thus, the artificial groundwater recharge may be practiced in a continuous manner to provide a sustained recharge source in order to increase the aquifer yield in the long run regardless of the fluctuation in operational schedules of the desalination plants. This also requires the identification of the areas which are suffering from water quality deterioration due to the upward leakage of the deep saline water. This will in turn require more representative water quality samples taken at different depths in the aquifers, and a quantification for the upward leakage coming from the underlying saline aquifers. These data were not available the present study. Therefore, it is recommended to take these into consideration in future studies concerned with increasing the aquifer yield through artificial groundwater recharge.

## 9.6 HYDRAULIC-GRADIENT CONTROL TO MAINTAIN STORED FRESHWATER LENS

The freshwater mound artificially created in aquifers, may be displaced from its location by the regional groundwater flow after ceasing the injection process, and its quality may deteriorate as the residence time lengthens. In this study a new technique was introduced to solve such a problem which may exist at any aquifer having a strong down-gradient displacement effect. This was achieved through proposing hydraulic gradient-control pumping wells outside the storage area to create a zero hydraulic gradient (i.e. a stagnation

zone) around the freshwater mound. The optimum pumping rates for these wells required to create such conditions, as well as the optimum pumping rates for the supply wells located on the modelled area (which is the maximum pumping rates with a minimum drawdown) were determined using the management models.

It was possible using this technique to stop the displacement of the stored freshwater mound from its location (comparing with the down-gradient displacement for about 800 m in its position after 6 years of residence, if no such control wells were used). Also, at the time where all the total usable water (with a TDS<1500 mg/l) was completely irrecoverable (which was found to be after 4 years of storage), by using the gradient-control wells it was possible to recover about 55% of this water. This recovery efficiency varied between the border and the internal wells. If the gradient-control wells were not used, the deterioration in water quality at the stored mound was much higher at the border wells than the internal wells. This because the mixing rate between the recharged water and the native groundwater is much higher at the margins. This furthermore was induced by the groundwater abstraction from the surrounding supply wells. Thus, the role of gradient-control wells in improving the recovery efficiency was much clearer at the border wells than at the internal wells. At the border wells, if no gradient-control wells were used, the usable stored water will be completely irrecoverable after 4 years. However, using the gradient-control wells, about 80 % of this water can be recovered by these wells.

# References


Abu-Sada, S. M. (1988). The Essentials of Groundwater Resources of Kuwait. KISR Report No. 2665, Kuwait Institute for Scentific Research, Kuwait.

Aguado, E. and Remson.I. (1974). Ground-Water Hydraulics In Aquifer Management. *Journal of the Hydraulic Division,* 100 (HY1), p 103-118.

Ahlfeld, D.P., Mulvey, J.M. and Pinder, G.F. (1988). Contaminated Groundwater Remediation Design Using Simulation Optimization, and Sensitivity Theory: 2. Analysis of a Field Site. *Water Resources Research,* 24 (3), p 443-452.

Aiken, A., and Pyne, D. (1992). Aquifer Storage Recovery catches on as water cache recedes. Water Environment and Technology, 4 (11), p. 12-16.

Al-Awadi, E.A. (1988). Stratigraphic Study of the Dammam Formation in Umm Gudair Area. M. Sc. Thesis, Kuwait University.

Al-Murad, M.A. (1994). Evaluation of The Kuwait Aquifer System and Assessment of Future Wellfields Abstraction Using A Numerical 3D Flow Model. M. Sc. Thesis, Arabian Gulf University, Bahrain.

Al-Otaibi, M.M. (1993). Evaluation and Interpretation of Pumping Test Data For Selected Wells in Kuwait Group Aquifer, Kuwait. M Sc. Thesis, Department of Civil Engineering, University of Newcastle upon Tyne.

Al-Rqobah, H. and Al-Munayyis, A. (1989). A Recarbonation Process For Treatment of Distilled Water Produced by MSF Plants in Kuwait. Ministry of Electricity and Water, Kuwait.

Al-Sarawi, M. (1980). Tertiary Faulting Beneath Wadi Al-Batin (Kuwait). *Geological Society of American Bulletin,* Part I (91), p 610-618.

Amans, L., and Jones, E. (1989). Beating the peak in summer demand. *Southwest and Texas Water Works Journal,* 77 (4), July 1989.

Amer, A. (1990). Assessment of Groundwater in Kuwait Using Remote Sensing Technology. Kuwait Institute For Scientific Research, Kuwait. KISR Report 4038.

Anderson, M.P. and Woessner, W.W. , (1992). *Applied groundwater Modelling: Simulation of flow and advective transport.* Academic Press: London, 381p.

Anderson, M.P. (1979). Using Models to Simulate the Movement of Contaminants Through Groundwater Flow Systems. *Environmental control,* 9 (1), p 97-156.

Atwood, D.F. and Gorelick, S.M. (1985). Hydraulic Gradient Control For Groundwater Contaminant Removal. *Journal of Hydrology,* 76 (1), p 85-106.

Bachmat, Y., Mandel, S. and Bugayevski, M. (1988). A Single-Well Tracer Technique For Evaluating aquifer Parameters, I. Theoretical work. *Journal of Hydrology,* 99 (1), p 143-163.

Baffa, J., Barksdale, C., Bechert, M. and Brashears, M. (1965). Experience With Injection Wells For Artificial Ground Water Recharge. *AWWA,* p 629-639.

Basagaoglu, H. and Yazicigil, H. (1995). Optimal Capacity-Expansion Planning In Multiaquifer Systems. *Journal of Water Resources Planning and Management,* 120 (6), p 836-855.

Bear, J. and Verrujit, A. , (1987). *Modelling Groundwater Flow and Pollution.* D. Reidel Publishing Company: USA, 414p.

Bergstrom, R.E. and Aten, E. (1964). National Recharge and Localization of Fresh Groundwater in Kuwait. *Journal of Hydrology,* 2 (1), p 213-231.

Bichara, A. (1988). Redevelopment of Clogged Recharge Wells. *Journal of Irrigation and Drainage Engineering,* 114 (2), p 343-350.

Bichara, A. (1974). An Experimental Study of Long-term Artificial Recharge of Groundwater into Confined Aquifers Using Wells. Ph. D. Thesis, University of Strathclyde.

Bouwer, H. (1996). Issues of Artificial Recharge. *Water Science and Technology,* 33 (10-11), p 381-390.

Bouwer, H., Pyne, R. and Coodrich, J. (1990). Recharging Ground water. *Civil Engineering,* p 63-67.

Brothers, K. and Katzer, T. (1990). Water Banking Through Artificial Recharge, Las Vegas Valley, Clark County, Nevada. *Journal of Hydrology,* 115 p 77-103.

Brown, D.L. and Silvey, W.D. (1985). Artificial Recharge to a Freshwater-Sensitive Brackish-Water Sand Aquifer, Norfolk, Virginia. U.S. Geological Survey, Professional Paper 939.

Brown, R.F. and Keys, W.S. (1985). Effects of Artificial Recharge on the Ogallala Aquifer, Texas. U.S. Geological Survey, Water-Supply Paper 2251.

Brown, R.F. and Signor, D.C. (1972). Groundwater Recharge. *Water Resources Bulletin,* 8 (1), p 132-149.

Burdon, D.J. and Al-Sharhan, A. (1968). The Problem of Paleokarstic Dammam Limestone Aquifer in Kuwait. *Journal of Hydrology,* 6 (1), p 385-404.

Castro, J.E. (1994). Aquifer Storage Recovery, Myrtle Beach, South Carolina. Proceedings of the Second International Conference on Ground Water Ecology, American Water Resources Association, p 105 -114.

Chen, C. (1985). Analytical and Approximation Solutions to Radial Dispersion from an Injection Well to a Geological Unit with Simultaneous Diffusion into Adjacent Strata. *Water Resources Research,* 21 (8), p 1068-1076.

Colarullo, S.J., Heidari, M. and Maddock, T., III, (1984). Identification of an Optimal Groundwater Management Strategy in a Contaminated Aquifer. *Water Resources Bulletin,* 20 (5), p 747-760.

Compagnie General de Geophysique. (1968). Shigaya Geophysical Survey. Report to Government of Kuwait.

Danskin, W.R. (1985). A Policy Evaluation Tool: Management of a Multiaquifer System Using Controlled Stream Recharge. *Water Resources Research,* 21 (11), p 1731-1747.

deMarsily, G. , (1986). *Quantitative Hydrogeology: Hydrology for Engineers.* Academic Press: London, 440p.

Domenico, P.A. and Schwartz, F.W. , (1990). *Physical and Chemical Hydrogeology.* John Wiley and Sons: New York, 824 pp.

Duffield, G.M. (1995). AQTESOLV, Aquifer Test Solver: User's Guide and Documentation. Geraghty & Miller, Inc. Modelling Group, Virginia, USA.

Dwarkanath, A., and Ibison, M. (1991). Aquifer Storage and Recovery solves city's water crisis. Public Works, 122 (9), p. 88-91.

Edworthy, K. and Downing, R. (1979). Artificial Groundwater Recharge and Its Relevance in Britain. *Journal of the Institution of Water Engineers and Scientists,* 33 (2), p 151-172.

Esmail, O.J. and Kimbler, O.K. (1967). Investigation of the Technical Feasibility of Storing Fresh Water in Saline Aquifers. *Water Resources Research,* 3 (3), p 363-695.

FAO. (1979). Survey and Evaluation of Available Data On Shared Water Resources in the Gulf State and the Arabian Peninsula. Report Prepared for the Secretariat of the Congress of Ministers of Agriculture in the Gulf State and Arabian Peninsula. Vol.3, map 2, sheet 1, Rome.

Fetter, C.W. (1994). *Applied Hydrogrology.* Macmillian College Publ. Co.: New York, 691 p.

Flavin, R.J. and Hawnt, R.J. (1979). Artificial Recharge for Storage by the Thames Water Authority in the Lee Valley, London, England. International Symposium Artificial Ground Water Recharge Research Results and Practical Applications, Dortmund, German Assoc. for Water Resources and Land Improvement, Bull.11, Vol.1, p 101 -136.

Freeze, R.A. and Cherry, J.A. , (1979). *Groundwater.* Prentice Hall: N.J, 604p.

Fried, J.J. and Combarnous, M.A. (1971). Dispersion in Porous Media. *Advance Hydroscience,* 7 (1), p 169-282.

Gelhar, L., Mantaglou, A., Wetly, C. and Rehfeldt, K. (1985). A Review of Field-Scale Physical Solute Transport Processes in Saturated and Unsaturated Porous Media. *Water Resources Research,* 15 (6), p 1387-1397.

Gelhar, L.W., Welty, C. and Rehfeldt, K. (1992). A Critical Review of Data on Field-Scale Dispersion in Aquifers. *Water Resources Research,* 28 (7), p 1955-1974.

Gerges, N.Z., Howles, S.R. and Sibenaler, X.P. (1996). South Australian Experience in Aquifer Storage and Recovery. Proceedings of an International Symposium on Artificial recharge of Groundwater, Finland, , p 75 -83.

Gorelick, S.M. (1983). A Review Of Distributed Parameter Groundwater Management Modeling Methods. *Water Resources Research,* 19 (2), p 305-319.

Guven, R.W., Falta, W., Molz, F.J. and Melville, J.G. (1985). Analysis and Interpretation of Single-Well Tracer Tests in Stratified Aquifers. *Water Resources Research,* 21 (5), p 676-684.

Hamdan, L. and El-sayed, M. (1986). In Criteria for Development of Kuwait's First National Natural Reserve. Kuwait Institute For Scientific Research (Unpublished), Kuwait.

Hamlin, S. (1987). Hydraulic/Chemical Changes During groundwater Recharge by Injection. *Ground Water,* 25 (3), p 267-274.

Haney, J., Leach, M. and Sobchak, L. (1988). Dry Wells - Solution or Pollution: An Arizona Status Report. Proceedings of the FOCUS Conference on Southwestern Ground Water Issues, National Water Well Association, Dublin OH.

Harpaz, Y. (1971). Artificial Ground-Water Recharge by Means of Wells in Israel. *Journal of the Hydraulic Division,* 12 p 1947-1964.

Harpaz, Y. (1970). Practical Experiences of Well Recharge. Artificial Groundwater Recharge Conference Proceedings, University of Reading, England, Paper 12.

Heidari, M. (1982). Application of Linear System's theory and Linear Programming to Ground Water Management in Kansas. *Water Resources Bulletin,* 18 (6), p 1003-1012.

Hoehn, E. and Roberts, P.V. (1982). Advection-Dispersion Interpretation of Tracer Observations in an Aquifer. *Ground Water,* 20 (4), p 457-465.

Hoopes, J. and Harleman, D. (1967). Dispersion in Radial Flow from a Recharge Well. *Journal of Geophysical Research,* 72 (14), p 3595-3607.

Huang, H. (1991). On a One Dimensional Tracer Test Model. *Ground Water,* 29 (1), p 18-20.

Huisman, O. , (1983). *Artificial Groundwater Recharge.* Pitman Advanced Publishing Program: London, 320p.

Huyakorn, P.S., Anderson, P.F., Molz, F., Guven, O. and Melville, J. (1986). Simulation of Two-Well Tracer Tests in Stratified Aquifer at the Chalk River and Mobile Sites. *Water Resources Research,* 22 (7), p 1016-1030.

Jones, G.P. (1976). Feasibility of Artificial Recharge in Kuwait. Ministry of Electricity and water, Kuwait.

Joseph, J.B. (1981). Artificial Groundwater Recharge. *Water Services,* 85 (1024), p 303-304.

Kasslar, P. (1973). The Structural and Geomorphic Evaluation of the Persian Gulf, in the Persian Gulf: Holocene Carbonate Sedimentation and Diagenesis in a Shallow Epicontinental Sea. Springer-Verlag, Berlin, West Germany, pp. 11-32.

Katzer, T. and Brothers, K. (1989). Artificial Recharge in Las Vegas Valley, Clark County, Nevada. *Ground Water,* 27 (1), p 50-56.

Khalaf, F., Mukhopadhyay, A., Naji, M., Al-Otaibi, M., Saleh, N., Al-Sayed, M. et al.. (1989).Geological Assessment of the Eocene and Post-Eocene Aquifers of Umm Gudair. Kuwait Institute for Scientific Research. Report No. KISR 3176.

Kimbler, O.K. (1975). Cyclic Storage of Fresh Water in Saline Aquifers. Louisiana Water Resources Research Institute. Bulletin 10.

Kimrey, J.O. (1989). Artificial Recharge Of Groundwater and Its Role In Water Management. *Desalination,* 72 p 135-147.

Kimrey, J.O. (1985). Proposed Artificial Recharge Studies in Northern Qatar. U.S Geological Survey, Open-File Report 85-343.

Kinniburgh, D., Gale, I., Smedly, P., Darling, W., West, J., Kimblin, R., Parker, A., Rae, J., Aldous, P., and O'Shea, M. (1994). The effects of historic abstraction of groundwater from the London basin aquifers on groundwater quality. *Appl. Geochem,* 9 (2), pp. 175-195.

Krizek, R., Castillo, E. and Karadi, G. (1973). Theoretical Study of Dispersion in Fractured Rock Aquifer. *Journal of Geophysical Research,* 78 (3), p 558-573.

Krone, R.B. (1970). Borehole Recharge: The Compatibility of Recharge water With The Aquifer. Artificial Groundwater Recharge Conference Proceedings, University of Reading, England, Paper 10.

Kruseman, G.P. and de Ridder, N.A., (1990). *Analysis and Evaluation of Pumping Test Data.* International Institute for Land Reclamation and Improvement: Netherlands, 377p.

Kumar, A. and Kimbler, O. (1970). Effect of Dispersion, Gravitational Segregation, and Formation Stratification of the Recovery of Freshwater Stored in saline Aquifers. *Water Resources Research,* 6 (6), p 1689-1700.

Kwiatkowski, P.J., Skehan, S. and Muniz, A. (1990). Application of Groundwater Artificial Recharge in a Brackish/Saltwater Environment. Proceedings of the International Symposium on Tropical Hydrology and Fourth Caribbean Islands Water Resources Congress, American Water Resources Association, Maryland, , p 377 -386.

Li Cijun, Bahr, J.M., Reichard, E.G., Butler, J.J. and Remson, L. (1987). Optimal Sitting of artificial Recharge: An Analysis of Objective Functions. *Ground Water,* 25 (2), p 141-150.

Maddock, T., III. (1972). Algebraic Technological Function From a Simulation Model. *Water Resources Research,* 8 (1), p 129-134.

Masciopinto, C., Palmisano, V., Tangorra, F. and Vurro, M. (1991). A Decision Support System For Artificial Recharge Plant. *Water Science and Technology,* 24 (9), p 331-342.

May, J.E. (1985). Feasibility of Artificial Recharge in the Coastal Plain near Atlantic City. U.S. Geological Water -Resources Investigations Report 85-4063.

McDonald, M.G. and Harbaugh, A.W. , (1988). *A Modular Three-Dimensional Finite-Difference Groundwater Flow Model.* U.S. Geological Survey, Technique of Water - Resources Investigation Book 6, Chapter A1:

Merritt, M. (1985). Subsurface Storage of Freshwater in South Florida: A digital Model Analysis of Recoverability. U.S. Geological Survey Water Supply. Paper 2261.

Merritt, M., Meyer, F., Sonntage, W. and Fitzpatrick, D. (1983). Subsurface Storage of Freshwater in South Florida: A Prospectus. U.S. Geological Survey, Water Resources Investigations Report 83-4214.

M.E.W. , (1996). *Statistical Year Book (Water).* Ministry of Electricity and Water, Kuwait.

Milton, D.I. (1967). Geology of Arabian Peninsula, Kuwait. U.S. Geological Survey; Prof. Paper 560-E.

Milton, D.I. and Davies, C.S. (1961). The Water Resources of Kuwait and Their Utilization. Mimeographed Report, Kuwait Oil Company, Kuwait.

Missimer, T., Walker,C., and Boletscher, F. (1992). Use of Aquifer Storage and Recovery technology to improve membrance water treatment plant efficiency, Collier County, Florida. *Desalination,* 87 (1-3), p. 269-280.

Molz, F., Guven, O., Melville, J., Grocker, R. and Matteson, K. (1986). Performance, Analysis and Simulation by Two-well Tracer Test at the Mobile Site. *Water Resources Research,* 22 (7), p 1031-1037.

Molz, F., Melville, J., Guven, O., Grocker, R. and Matteson, K. (1985). Design and Performance of Single-well Tracer Tests at the Mobile Site. *Water Resources Research,* 21 (10), p 1497-1502.

Molz, F., and Bell, L.C. (1977). Hydraulic Gradient Control in Aquifers Used for Fluid Storage. *Water Resources Research,* 13 (4), p 795-798.

Montgomery, H. (1988). UK experience in the groundwater recharge of partially treated sewage: Potential for irrigation purposes. Treatment and Use of Sewage Effluent for Irrigation, Butterworths London, p 129-135.

Moore, J.E. (1979). Contribution of Groundwater Modeling to Planning. *Journal of Hydrology,* 43 (1), p 121-128.

Moranville, M., Kessler, D. and Greenkown, K. (1976). Dispersion in Non-uniform and Anisotropic Porous Media. American Water Resources Association, Advances in Groundwater Hydrology.

Moulder, E.A. (1970). Freshwater Bubbles: A Possibility For Using Saline Aquifers to Store Water. *Water Resources Research,* 6 (3), p 1528-1531.

Mualem, Y. and Bear, J. (1974). The Shape of the Interface in Steady Flow in a Stratified aquifer. *Water Resources Research,* 10 (6), p 1207-1215.

Mukhopadhyay, A., Szekely, F. and Senay, Y. (1994). Artificial Ground Water Recharge Experiments in Carbonate and Clastic Aquifers of Kuwait. *Water Resources Bulletin,* 30 (6), p 1091-1105.

O'Shea, M.J. (1984). Borehole Recharge of the Folkestone Beds at Hardham, Sussex, 1980-81. *Journal of the Instituation of Water Engineers and Scientists,* 38 (1), p 9-24.

Ogata, A. and Banks, R. (1961). A Solution of the Differential Equation of Longitudinal Dispersion in Porous Media. U. S. Geological Survey Prof. Paper. 411-B.

Omar, S.A., Al-Yacoubi, A. and Senay, Y. (1981). Geology and Groundwater Hydrology of the State of Kuwait. *Journal of the Arabian Gulf and Arabian Peninsula Studies,* 1 p 5-67.

Omer, S.S. (1982). Artificial Recharge into the Kuwait Group at Ar-Raudhatain. M. Sc. Thesis, Department of Civil Engineering, Technical University, Loughbrough, U.K.

Papadopulos, I.S. (1966). Nonsteady Flow to Multiaquifer Wells. *Journal of Geophysical Research,* 71 (20), p 4791-4797.

Pavelic, P. and Dillion, P. (1996). The Impact Of Two Seasons Of Stormwater Injection On Groundwater Quality in South Australia. Proceedings of An International Symposium on Artificial Recharge of Groundwater, Finland, , p 105 -126.

Pickens, J.F. and Grisak, G.E. (1995). Scale-Dependent Dispersion in a Stratified Grannular Aquifer. *Water Resources Research,* 17 (4), p 1191-1211.

Pickens, J.F. and Grisal, G.E. (1981). Scale-Dependent Dispersion in a Stratified Grannular Aquifer. *Water Resources Research,* 17 (4), p 1191-1211.

Pickens, J.F., Jackson, R.E., Inch, K.J. and Merritt, W.F. (1981). Measurement of Distribution Coefficients Using Radial Injection Dual-Tracer Test. *Water Resources Research,* 17 (2), p 529-543.

Pyne, D. (1989) Aquifer Storage Recovery: A new water supply alternative. Water: Laws and Management. American Water Resources Association, Bethesda, Maryland, USA. p. 12B-27-- 12B-31.

Pyne, D. (1989). Aquifer Storage Recovery in Kuwait. Report submitted to United Nations Educational, Scientific and Cultural Organization (UNESCO).

Rae, J. and Parker, A. (1992). Groundwater quality in the recharged London Basin, England. I: phase associations of iron, manganese, and sulfur in Tertiary sands. *Environmental Geology and Water Sciences,* 19 (2), p. 127-135.

Rebhun, M. and Schwarz, J. (1995). Clogging and Contamination Processes in Recharge wells. *Water Resources Research,* 4 (6), p 1207-1217.

Rehman, A., Smerdon, E. and Hiller, E. (1969). Effect of Sediment Concentration on Well Recharge in a Fine Sand Aquifer. *Water Resources Research,* 5 (3), p 641-646.

Rosenwald, G.W. and Green, D.W. (1974). A Method For Determining The Optimum Location of Wells In a Reservoir Using Mixed-integer Programming. *Society Petroleum Engineering Journal,* 14 (1), p 44-54.

Saunders, M. and Murtagh, B.A. (1995). MINOS 5.4 User's Guide. Systems Optimization Laboratory, Stanford University, Technical Report SOL 83-20R.

Sauty, J. (1980). An Analysis of Hydrodispersive Transfer in Aquifers. *Water Resources Research,* 16 (1), p 145-158.

Schwarz, J. (1976). Linear Models for Groundwater Management. *Journal of Hydrology,* 28 (1), p 372-392.

Senay, Y. (1977). Groundwater Resources and Artificial Recharge in Rawdatain Water Field, Kuwait. Groundwater Administration, Ministry of Electricity and Water, Kuwait.

Singh, S. and Murty, V. (1980). Storages of Freshwater in Saline Aquifers. *Journal of the Irrigation and Drainage Division,* Paper No. (IR2),

Sniegocki, R.T. and Brown, R.F. (1970). Clogging in Recharge Wells Causes and Cures. Artificial Groundwater Recharge Conference Proceedings, University of Reading, England. Paper 13.

Sniegocki, R.T. (1963). Problems in Artificial Recharge Through Wells in the Grand Prairie Region, Arkansas. U.S. Geological Survey; Water Supply Report No. 1615-F.

Suryanarayana, S. and Akan, A.O. (1996). Optimization of wastewater Recharge. Proceedings of an International Symposium on Artificial Recahrge of Groundwater, Finland, , p 303 -308.

Tibbals, C.H. and Frazee, J.M. (1976). Groundwater Hydrology of the Cocoa Well-field Area, Orange County, Florida. U.S. Geological Survey, Open File Report 75-676.

Todd, D.K. (1970). The Future Prospects of Artificial Groundwater Recharge. Artificial Groundwater Recharge Conference Proceedings, University of Reading, England, Paper 15.

Vecchioli, J. (1972). Experimental Injection Of Tertiary-Treated Sewage In A Deep Well At Bay Park, Long Island, N. Y.- A summary Of Early Results. *New England Water Works Assoc Journal,* 86 (2), p 87-103.

Viswanathan, M.N. (1989). Measures for Water Conservation in Arid Zones. Report Submitted to Kuwait Institute for Scientific Research, Kuwait.

W.H.O. (1969). Operation and Control of Water Treatment Processes. World Health Organization, Monograph Series No. 49, Geneva.

Warner, D. and Doty, L.F. (1967). Chemical Reaction between Recharge Water and aquifer water. IASH-UNESCO Symposium on Artificial Recharge and Management of Aquifers, Haifa, Israel,

Warner, D. and Doty, L.F. (1967). Chemical Reaction between Recharge Water and aquifer water. IASH-UNESCO Symposium on Artificial Recharge and Management of Aquifers, Haifa, Israel, p 278 -288.

Water Resources Board. (1972). Artificial Recharge of the London Basin. Reading, Water Resources Board.

Willis, R. and Yeh, W.W. , (1987). *Groundwater System Planning and Management.* Prentice-Hall, Inc. New Jersey, 416p.

Willis, R. and Liu, P. (1984). Optimization Model for Ground-Water Planning. *Journal of Water Resources Planning and Management,* 110 (3), p 333-347.

Willis, R.A. (1983). A Unified Approach To Regional Groundwater Management In Groundwater Hydraulics. *Water Resources Research,* 15 (6), p 1305-1312.

Wilson, W.E. and Gerhart, J.M. (1982). Simulated Effects of Groundwater Development on the Piezometric Surface of the Floridan Aquifer, West Central Florida. U.S. Geological Survey Prof. Paper 1217.

Wolery, T.J. (1983). EQ6. A Computer Program for Reaction-Path Modeling of Aqueous Geochemical Systems: User's Guide and Documentation. Lawrence Livermore National Laboratory, University of California. No. UC-70.

Wood, W.W. (1980). Development of Technical Site Selection Criteria For Artificial Recharge. Proceedings of the symposium on Wastewater Reuse for Groundwater Recharge, Held on Sep. 1979 at California State Polytechnic University. California State Water Resources Central Board, p 73-79.

Yazicigil, H. (1990). Optimal Planning and Operation of Multiaquifer System. *Journal of Water Resources Planning and Management,* 116 (4), p 435-454.

Yazicigil, H. (1996), University of Middle East (Personal communication).

Yazicigil, H., Al-Layla, R.I. and de Jong, R.L. (1987). Optimal Management of a Regional Aquifer in Eastern Saudi Arabia. *Water Resources Bulletin,* 23 (3), p 423-434.

Younger, P.L. (1993). Simple Generalized Method for Estimating Aquifer Storage Parameters. *Journal of Engineering Geology,* 26 (1), p 127-135.

Zheng, C. (1993). Extension of the Method Of Characteristics For Simulation of Solute Transport in Three Dimensions. *Ground Water,* 31 (3), p 456-465.

Zheng, C. (1990). MT3D, A Modular Three-Dimensional Transport Model: Documentation and User's Guide. S.S. Papadpulos & Associates Inc., Maryland, USA.

Zuber, A. (1986). Interpretation of Tracer Data in Variable Flow Systems. *Journal of Hydrology,* 86 (1/2), p 45-57.

*Appendix I*

# GROUNDWATER FLOW MODEL (MODFLOW)

## I.1 Groundwater Flow Equation

The three-dimensional non-equilibrium movement of groundwater of constant density through a heterogeneous and anisotropic porous medium can be described by the partial differential equation:

$$\frac{\partial}{\partial x}\left(K_{xx}\frac{\partial}{\partial x}\right)+\frac{\partial}{\partial y}\left(K_{yy}\frac{\partial}{\partial y}\right)+\frac{\partial}{\partial z}\left(K_{zz}\frac{\partial}{\partial z}\right)=S_s\frac{\partial h}{\partial t}+W(x,y,z,t) \qquad \text{(I-1)}$$

where

| | |
|---|---|
| $x, y, z$ | Cartesian, co-ordinates aligned along the major axes of hydraulic conductivities $K_{xx}$, $K_{yy}$ and $K_{zz}$; ($LT^{-1}$) |
| $h$ | potentiometric head (L); |
| $S_s$ | specific storage of the porous material ($L^{-1}$); |
| $t$ | time (T); and |
| $W$ | volumetric flux per unit volume and represents sources and/or sinks of water ($T^{-1}$) |

The transmissivity tensor may be generated by multiplying equation (I-1) by the thickness of the aquifer (b), resulting in the nonlinear Boussinesq equation:

$$\frac{\partial}{\partial x}\left(T_{xx}\frac{\partial}{\partial x}\right)+\frac{\partial}{\partial y}\left(T_{yy}\frac{\partial}{\partial y}\right)+b\frac{\partial}{\partial z}\left(T_{zz}\frac{\partial}{\partial z}\right)=S\frac{\partial h}{\partial t}+bW(x,y,z,t) \qquad \text{(I-2)}$$

where

| | |
|---|---|
| $T_{xx}, T_{yy}$ | components of the transmissivity tensor ($L^2/T$); and |
| $S$ | storage coefficient (dimensionless) |

## I.2 The Finite Difference Method (FDM)

The finite difference method involves establishing a grid system by dividing the aquifer system into **n** number of blocks in the **x**, **y** and **z** directions. Each block is assumed to have uniform properties. Then the continuous partial derivatives in equation (I-2) are replaced by finite difference approximations, which result in **n** linear algebraic difference equations with **n** unknowns. These equations, using matrix solution algorithms, yield values of head at the center of different blocks at various time horizons. MODLFOW$^{EM}$ model is based on a block-centered finite difference grid system. The nodal points representing the position at which the solution is obtained, are centered between the grid lines. The finite difference equation for the general partial differential equation (I-2) was derived by Pinder and Bredehoeft (1968) in a somewhat rigorous mathematical treatment. Using Darcy's Law, an alternative simpler approach was presented by McDonald & Harbaugh (1988), the authors of MODFLOW$^{EM}$, and is printed below:

The flow equation for a given block (i,j,k) may be expressed in words as: the sum of outflow minus the sum of inflow equals the change in storage and a source/sink terms (continuity equation). In more concise form, it is:

$$Q(out) - Q(in) = S_{s_{i,j,k}} \frac{\Delta h_{i,j,k}}{\Delta t}(\Delta v) + W_{i,j,k}(\Delta v) \qquad \text{(I-3)}$$

where

$Q_{i,j,k}$ : flow rate out or into the cell ($L^3/T$);

$S_{s_{i,j,k}}$ : specific storage defined as the ratio of the volume of water which can be injected per unit volume of aquifer material per unit change in head (I/L);

$\Delta v = \Delta x . \Delta y . \Delta z$ : volume of the cell ($L^3$); and

$\Delta h_{i,j,k}$ : head change over a time interval of length in cell i,j,k

From Darcy's Law:

$$Q = K.A.i \qquad \text{(I-4)}$$

where

Q : flow rate ($L^3/T$);

k : hydraulic conductivity (L/T);

A : cross sectional area ($L^2$); and

i : hydraulic gradient (L/L)

Therefore, differences in flow in the **x** direction are:

$$Q_x(out)-Q_x(in)=K_{xx_{i,j+1/2,k}}(DZDY)\frac{Dh_{j+1/2}}{DX_{j+1/2}}-K_{xx_{i,j-1/2,k}}(DZDY)\frac{Dh_{j-1/2}}{DX_{j-1/2}} \qquad \text{(I-5)}$$

where

$K_{xx_{i,j+1/2,k}}$ hydraulic conductivity in the **x** direction at face **j+1/2;**

$K_{xx_{i,j-1/2,k}}$ hydraulic conductivity in the **x** direction at face **j-1/2;**

$\Delta h_{j+1/2} / \Delta x_{j+1/2}$ hydraulic gradient in the **x-** direction at face **j+1/2;**

$\Delta h_{j-1/2} / \Delta x_{j-1/2}$ hydraulic gradient in the **x-** direction at face **j-1/2;**

$\Delta h_{j+1/2} = h_{i,j+1,k} - h_{i,j,k}$

$\Delta h_{j-1/2} = h_{i,j,k} - h_{i,j-1,k}$

Similarly, in the **y** and **z** direction,

$$Q_y(out)-Q_y(in)=K_{yy_{i+1,j,k}}(\Delta X\Delta Z)\frac{\Delta h_{i+1/2}}{\Delta y_{i+1/2}}-K_{yy_{i-1/2,j,k}}(\Delta X\Delta Z)\frac{\Delta h_{i-1/2}}{\Delta y_{i-1/2}} \qquad \text{(I-6)}$$

and

$$Q_z(out)-Q_z(in)=K_{zz_{i,j,k+1/2}}(\Delta X\Delta Y)\frac{\Delta h_{k+1/2}}{\Delta Z_{k+1/2}}-K_{zz_{i,j,k-1/2}}(\Delta X\Delta Y)\frac{\Delta h_{k-1/2}}{\Delta Z_{k-1/2}} \qquad \text{(I-7)}$$

McDonald & Harbaugh (1988) used in their model, the term "hydraulic conductance", which is defined as:

$$C=\frac{K.A}{L} \qquad \text{(I-8)}$$

where

C is the conductance ($L^2/t$); and

L is the length of the flow path (L)

Substituting equation (I-8) into equation (I-5) yields

$$Q_x(\text{out}) - Q_x(\text{in}) = C_{R_{i,j+1/2,k}}(\Delta h_{j+1/2}) - C_{R_{i,j-1/2,k}}(\Delta h_{j-1/2}) \tag{I-9}$$

where

$C_{R_{i,j-1/2,k}}$ is the conductance in row **i** and layer **k** between nodes **i,j-l,k**

$C_{R_{i,j+1/2,k}}$ is the conductance in row **i** and layer **k** between nodes **i,j+l,k**

Similarly, in equations (4.6) and (4.7)

$$Q_y(\text{out}) - Q_y(\text{in}) = C_{C_{i+1/2,j,k}}(\Delta h_{i+1/2}) - C_{C_{i-1/2,j,k}}(\Delta h_{i-1/2}) \tag{I-10}$$

$$Q_z(\text{out}) - Q_z(\text{in}) = C_{V_{i,j,k+1/2}}(\Delta h_{k+1/2}) - C_{V_{i,j,k-1/2}}(\Delta h_{k-1/2}) \tag{I-11}$$

where conductances are defined analogously to in equation (I-9).

By substituting equations (I-9), (I-10) and (I-11) into equation (I-3).

$$\begin{aligned} & C_{R_{i,j+1/2,k}}(\Delta h_{j+1/2}) - C_{R_{i,j-1/2,k}}(\Delta h_{j-1/2}) + \\ & C_{C_{i+1/2,j,k}}(\Delta h_{i+1/2}) - C_{C_{i-1/2,j,,k}}(\Delta h_{i-1/2}) + \\ & C_{V_{i,j,k+1/2}}(\Delta h_{k+1/2}) - C_{V_{i,j,k-1/2}}(\Delta h_{k+1/2}) = \\ & S_{S_{i,j,k}} \frac{\Delta h_{i,j,k}}{\Delta t}(\Delta v) + W_{i,j,k}(\Delta v) \end{aligned} \tag{I-12}$$

The left hand side of equation (I-12) accounts for flow into cell **i,j,k** from the six adjacent cells. Flows entering or leaving the cell from outside the aquifer, such as drains, areal recharge, evapotranspiration, and wells are expressed by the source/sink term in the right hand side of the equation.

Finally, the time derivative term (the cell hydrograph) in equation (I-12) is approximated using the backward differences as follows:

$$\frac{\Delta h^{m}_{i,j,k}}{\Delta t_{m}} = \frac{h^{m}_{i,j,k} - h^{m-1}_{i,j,k}}{t_{m} - t_{m-1}} \tag{I-13}$$

where

$h^{m}_{i,j,k}$ & $t_{m}$ head and time at the end of the time step evaluated; and

$h^{m-1}_{i,j,k}$ & $t_{m-1}$ head and time at the end of the preceding time step.

Writing equation (I-12) in backward difference form (implicit formulation) yields:

$$\begin{aligned}
&C_{R_{i,j+1/2,k}}(\Delta h^{m}_{j+1/2}) - C_{R_{i,j-1/2,k}}(\Delta h^{m}_{j-1/2}) + \\
&C_{C_{i+1/2,j,k}}(\Delta h^{m}_{i+1/2}) - C_{C_{i-1/2,j,,k}}(\Delta h^{m}_{i-1/2}) + \\
&C_{V_{i,j,k+1/2}}(\Delta h^{m}_{k+1/2}) - C_{V_{i,j,k-1/2}}(\Delta h^{m}_{k-1/2}) = \\
&S_{S_{i,j,k}} \frac{h^{m}_{i,j,k} - h^{m-1}_{i,j,k}}{t_{m} - t_{m-1}}(\Delta v) + W_{i,j,k}(\Delta v)
\end{aligned} \tag{I-14}$$

In equation (I-14) , heads at the beginning of the time step ($h^{m-1}_{i,j,k}$) all conductances, and all coefficients related to the node **i,j,k** are known. The seven heads at time $t_m$, the end of the time step, are unknown. By writing this equation for the **n** number of cells in the system, **n** equations with **n** unknowns will be obtained, which can be solved simultaneously. However, the resulting number of equations in most of the cases will be less than the number of model cells, as these equations are written only for the variable head cells or active cells. That is, the head in the cell is allowed to vary with time. There are four other types of cells that can be simulated in the MODFLOW$^{EM}$ model. These are: constant-head, no-flow, constant flux and head dependent flux cells, which can be used to reflect and depict the different types of boundaries encountered in the groundwater flow problems.

*APPENDIX II*

# SOLUTE TRANSPORT MODEL

# MT3D (Zheng, 1990)

## II.1 Introduction

MT3D is a transport model for simulation of advection, dispersion and chemical reactions of solutes in groundwater flow systems in either two or three-dimensions. It can be used in conjunction with the block-centered finite-difference flow model MODFLOW.

The numerical solution implemented in MT3D is a mixed Eulerian-Largangian method. The Lagrangian part of the method, used for solving the advection term, employs the forward-tracking method of characteristics (MOC), the backward-tracking modivied method of characteristics (MMOC), or hybird of these two methods. The Eulerian part of the method, used for solving the dispersion and chemical reaction terms, utilizes conventional block-centered finite-difference method.

## II.2 Governing SoluteTransport Equation

The partial differential equation describimg three-dimensional transport of solutes in groundwater can be written as follows (e.g., Javandel, et al., 1984):

$$\frac{\partial C}{\partial t} = \frac{\partial}{\partial x_i}\left(D_{ij}\frac{\partial C}{\partial x_i}\right) - \frac{\partial}{\partial x_i}(v_i C) + \frac{q_s}{\varnothing}C_s + \sum_{k=1}^{N} R_k \qquad \text{(II-1)}$$

where

$C$ : concentration of solutes dissolved in groundwater, $M/L^3$ ;

$t$ : time, T ;

$x_i$ : distance along the respective Cartesian coordinates axis, L;

$D_{ij}$ : hydrodynamic dispersion coefficient, $L^2/T$;

$v_i$ : seepage or linear pore water velocity, L/T

$q_s$ : volumetric flux of water per unit volume of aquifer, representing sources (+), and sinks (-), $T^{-1}$ ;

$C_s$ : concentration of the sources or sinks, $M/L^3$

$\varnothing$ : porosity of porous medium, dimensionless;

$\sum_{k=1}^{N} R_k$ : a chemical reaction term, $ML^{-3}\,T^{-1}$

Assuming that only equilibrium-controlled linear or non-linear sorption and first-order irreversible are reactions are involved in the chemical reactions, the chemical reaction term in equation 4. can be expressed as (Grove and Stollenwerk, 1984):

$$\sum_{k=1}^{N} R_k = -\frac{\rho_b}{\varnothing}\frac{\partial \bar{C}}{\partial t} - \lambda\left(C + \frac{\rho_b}{\varnothing}\bar{C}\right) \qquad \text{(II-2)}$$

where

$\rho_b$ : bulk density of the porous medium, $M/l^3$

$\bar{C}$ : concentration of solutes sorbed on the porous medium, $MM^{-1}$

$\lambda$ : rate of constant of the first-order rate reactions, $T^{-1}$

Subsittuting equation II-2 into equation II-1, and rearranging equation terms, equation II-1 becomes:

$$R\frac{\partial C}{\partial t} = \frac{\partial}{\partial x_i}\left(D_{ij}\frac{\partial C}{\partial x_j}\right) - \frac{\partial}{\partial x_i}(v_i C) + \frac{q_s}{\varnothing}C_s - \lambda\left(C + \frac{\rho_b}{\varnothing}\bar{C}\right) \qquad \text{(II-3)}$$

where $R$ is the retardation factor, defined as

$$R = 1 + \frac{\rho_b}{\varnothing}\frac{\partial \bar{C}}{\partial x_i} \qquad \text{(II-4)}$$

Equation (II-3) is the governing equation underlying in the transport model. The transport equation is linked to the flow model equation through the relationship:

$$v_i = -\frac{k_{ii}}{\varnothing}\frac{\partial h}{\partial x_i} \qquad \text{(II-5)}$$

where

$k_{ii}$ : principal component of the hydraulic conductivity tensor, L/T;

$h$ : hydraulic head, L.

The hydraulic head is obtained from the solution of the three-dimensional groundwater flow equation (I-1).

In this study, the transport model will be used to simulate the change in water TDS during the freshwater injection into brackish groundwater, where no cheamical reactions will take place. Thus, the only dominant factors that will effect such process are dispersion, advection, and sinks or sources, that are represented by the first, second, and third terms on the right-hand side of equation II-3, respectively.

## II.2.1 Advection

The term $\frac{\partial}{\partial x_i}(v_i C)$ in equation II-3 is referred to as the advection term, that describes the transport of miscible solutes at the same velocity as the groundwater. To ensure the degree of advection domination, a dimensionless Peclet number (Pc) is usually used. The Peclet number is defined as:

$$P_c = \frac{|v| L}{D} \qquad \text{(II-6)}$$

where

$|v|$ : magnitude of the seepage velocity vector, L/T;

$L$ : characteristic length, commonly taken as the grid cell width, L;

$D$ : dispersion coefficient, $L^2/T$

In advection-dominant (sharp front) problems, the Peclet number has a large value. For advection-dominated problems, the solution of the transport equation by standard numerical procedures (like finite-difference method) is plagued to some degree by two types of numerical problems. The first type is numerical dispersion, which has an effect similar to that of physical dispersion, but is caused by truncation errors. When physical dispersion is small, numerical dispersion becomes a serious problem, leading to the smearing of concentration fronts which should have a sharp appearance. The second type of numerical problem is artificial oscillation which is typical of many higher-order schemes desgined to eliminate numerical dispersion, and tends to become more severe as the concentration front becomes sharper.

## II.2.2 Dispersion

Dispersion in porous media refers to the spreading of solutes over a greater region than would be predicted solely from groundwater velocity vectors. The dispersion term in equation II-3, $\frac{\partial}{\partial x_i}\left(D_{ij}\frac{\partial C}{\partial x_j}\right)$, represents a pragmatic approach through which realistic transpoert calculation can be made without fully describing the heterogeneous velocity field which is impossible to do in practice.

The hydrodynamic dispersion tensor is used by MT3D in the following component forms as proposed by Burnett and Frind (1987):

$$D_{xx} = \alpha_L \frac{v_x^2}{|v|} + \alpha_{TH} \frac{v_y^2}{|v|} + \alpha_{TV} \frac{v_z^2}{|v|} + D^*$$

$$D_{yy} = \alpha_L \frac{v_y^2}{|v|} + \alpha_{TH} \frac{v_x^2}{|v|} + \alpha_{TV} \frac{v_z^2}{|v|} + D^*$$

$$D_{zz} = \alpha_L \frac{v_z^2}{|v|} + \alpha_{TV} \frac{v_x^2}{|v|} + \alpha_{TV} \frac{v_y^2}{|v|} + D^*$$

$$D_{xy} = D_{yx} = (\alpha_L - \alpha_{TH})\frac{v_x v_y}{|v|}$$

$$D_{xz} = D_{zx} = (\alpha_L - \alpha_{TV})\frac{v_x v_z}{|v|}$$

$$D_{yz} = D_{zy} = (\alpha_L - \alpha_{TV})\frac{v_y v_z}{|v|} \qquad \text{(II-7)}$$

where

$\alpha_L$ : longitudinal dispersivity, L;

$\alpha_{TH}$ : horizontal transverse dispersivity, L;

$\alpha_{TV}$ : vertical transverse dispersivity, L;

$D^*$ : effective molcular coefficient, $L^2/T$ ;

$v_x, v_y, v_z$ : components of the velocity vector along the x, y, and z axes, L/T;

$|v| = \left(v_x^2 + v_y^2 + v_z^2\right)^{1/2}$ : magnitude of velocity vector, L/T.

### II.2.3 Sinks and sources

The third term in the governing equation, $\frac{q_s}{\varnothing} C_s$ , is the sink/source term, which represents solute mass dissolved in water entering the simulated domain through sources, or solute mass dissolved in water leaving the simulated domain through sinks. Sinks or sources may be classified as areally distributed or point sinks or sources. the areally distributed sinks or sources include recharge and evapotranspiration. The point sinks or sources include wells, drains, and rivers. For sources, it is necessary to specify the concentration of source water. For sinks, the concentration of water in the sink generally is equal to the concentration of groundwater in the aquifer and need be not specified.

## II.3 Eulerian-Lagrangian Solution

The governing solute transport equation (II-3), can be expressed in the Lagrangian form as:

$$\frac{DC}{Dt} = \frac{1}{R}\frac{\partial}{\partial x_i}\left(D_{ij}\frac{\partial C}{\partial x_j}\right) - \frac{q_s}{R\varnothing}(C - C_s) - \frac{\lambda}{R}\left(C + \frac{\rho_b}{\varnothing}\bar{C}\right) \qquad \text{(II-8)}$$

where $\frac{DC}{Dt}$ , indicates the rate of change in solute concentration ($C$) along the pathline of a contaminant particle. By introducing the finite-difference algorithm, this substantial derivative can be expressed as :

$$\frac{DC}{Dt} = \frac{C_m^{n+1} - C_m^{n^*}}{\Delta t} \qquad \text{(II-9)}$$

so that equation (II-8) becomes

$$C_m^{n+1} = C_m^{n^*} + \Delta t \, X \, RHS \qquad \text{(II-10)}$$

where

$C_m^{n+1}$ : average solute concentration for cell $m$ at the new time level $(n+1)$;

$C_m^{n^*}$ : average solute concentration for cell $m$ at the new time level $(n+1)$ due to advection alone, also referred to as the intermediate time level $(n^*)$;

$\Delta t$ : time increment between the old time level $(n)$ and the new time level $(n+1)$;

RHS : represents the finite-difference approximation to the terms on the right-hand side of equation (II-8). The finite-difference approximation is explicit if the concentration at the old time $(C^n)$ is used in the calculation of RHS ; it is implicit if the concentration at the new time level $(C^{n+1})$ is used.

Equation (II-10) constitutes the basic algorithm of mixed Eulerian-Lagrangian method used in the MT3D transport model. In this method, the term $C_m^{n^*}$ in equation II-10, which accounts for effect of advection, is solved with a Lagrangian method, while the second term in equation (II-10), which accounts for the effects of dispersion, sink/source mixing, and chemical reactions, is solved with a finite-difference method.

Depending on the use of different Lagrangian techniques to approximate the advection term, the mixed Eulerian-Lagrangian method may be classified as : the method of characteristics; the modified method of characterstics; and a combination of the two. Each of these three solution schemes is utilized in the MT3D transport model.

## II.3.1 Method Of Characteristics (MOC)

This method was implemented in the U. S. Geological Survey two-dimensional transport model (Konikow and Bredehoeft, 1978). It uses a conventional particle tracking technique for solving the advection term. At the begining of the simulation, a set of particles is distributed in the flow field either randomly or with fixed pattern. A concentration and a position in the Cartesian coordinate system are associated with each of these particles. Particles are tracked forward through the flow field using a small time increment. At the end of each increment, the average concentration at cell ($m$) due to advection alone over the time increment, or $C_m^{n^*}$, is evaluated from the concentrations of moving particles which happen to be located within cell ($m$). This is expressed in the following equation:

$$C_m^{n^*} = \frac{1}{NP} \sum_{L=1}^{NP} C_L^n \qquad \text{(II-11)}$$

where

NP : number of particles within cell $m$;

$C_L^n$ : concentration of the $L^{th}$ particle at time level $n$;

After completing the evaluation of $C_m^{n^*}$ for all cells, the weighted concentration, $C_m^{n\hat{}}$ is calculated based on $C_m^{n^*}$ and the concentration at the old time level $C_m^n$:

$$C_m^{n\hat{}} = \omega\, C_m^{n^*} + (1-\omega)\, C_m^n \qquad \text{(II-12)}$$

where $\omega$ is a weighting factor between 0 and 1. $C_m^{n\hat{}}$ is then used to calculate the second term in equation (II-10), or the changes in concentration due to dispersion, sinks/source mixing, and chemical reactions with an explicit finite difference method, i.e.,

$$\Delta C_m^{n+1} = \Delta t \times \mathrm{RHS}\,(C_m^{n\hat{}}) \qquad \text{(II-13)}$$

The concentration for cell ($m$) at the new time level ($n+1$) is then the sum of the

$C_m^{n^*}$ and $\Delta C_m^{n+1}$ terms (II-14)

The first step in MOC is to generate representative particles in the finite-difference grid. Instead of placing a uniform number of particles in every cell of the grid, a dynamic approach is used in MT3D to control the distribuation of moving particles. The number of particles placed at each cell is normally set either to a higher level (NPH), or at a lower level (NPL), according to the so-called " relative cell concentration gradient (DCCELL) ", defined as:

$$DCCELL_{i,j,k} = \frac{CMAX_{i,j,k} - CMIN_{i,j,k}}{CMAX - CMIN} \qquad \text{(II-15)}$$

where

$CMAX_{i,j,k}$ , $CMIN_{i,j,k}$ : are the maximum and minimum concentration in the immediate vicinity of the cell $(i,j,k)$, respectively.

CMAX , CMIN : are the maximum and minimum concentration in the entire grid, respectively.

with a dynamic approach, a criterion of DCEPS (negligible relative concentration gradient) can be defined, which is a small integer number near zero. Then the higher number of particles (NPH), is placed in cells where the relative concentration gradient is greater than DCEPS, and the lower number of particles (NPL), in cells where the relative concentration gradient is less than DCEPS.

As particles leave source cells or accumulate at sink cells, it becomes necessary to insert new particles at sources, or remaove particles at sinks. At non-source or non-sink cells, it also becomes necessary to insert or remaove particles as the cell concentration gradient changes with time. This is done in the dynamic insertion-deletion procedure by specifying the minimum and maximum numbers of particles allowed per cell, called NPMIN and NPMAX, respectively.

## II.3.2 Modified Method Of Characterstics (MMOC)

This method is similar to the MOC technique except in the treatmwnt of advection term. Unlike the MOC which tracks a large number of moving particles forward in time and keeps track of the concentration and position of each particle, the MMOC places one fictitious particle at the nodal point at each new time level $(n+1)$ The particle is tracked backward to find its position at the old time $(n)$. The concentration associated with that position is used to approximate the $C_m^{n^*}$ term in equation II-11:

$$C_m^{n^*} = C^n(x_p) = C^n(x_m - d) \qquad \text{(II-16)}$$

where

$x_p$ : position which particle starting from nodal point $(m)$ reachs when it is tracked backward along the reverse pathline over the time increment $\Delta t$;

$x_m$ : position vector of nodal point $(m)$;

$d$ : characteristic nodal displacement, or the distance along a particle path from $x_m$ to $x_p$;

$C^n(x_p)$ : concentration at position $x_p$ at the old time level $(n)$.

### II.3.3 Hybrid Method Of Characteristics (HMOC)

The preceding methods (MOC and MMOC) have some strengths and some drawbacks. One of the most desirable features of the MOC technique is that it is free of numerical dispersion. The major drawback of the MOC is that it can be slow and requires a large amount of computer memory espacially for three dimensions models. On the other hand, MMOC techniqe is faster than the MOC, requires much less computer memory. However, it introduces some numerical dispersion, espacially for sharp front problems.

Thus, a third option of using a hybrid of the two methods (MOC and MMOC) referred as hybrid method of characterstics (HMOC) is provided by MT3D. The HMOC technique combines the strengths of the MOC and the MMOC techniques by using an automatic adaptive scheme. This scheme involves automatic adaption of the solution process to the nature of the concentration field. When sharp concentration fronts are present, the advection term is solved by the MOC, and away from such fronts, the advection term is solved by the MMOC. By selecting an appropariate criterion for controlling the switch between the MOC and MMOC schemes, the adaptive procedure can provide accurate solution to the transport problem. Under certain circumstances, the manual selection of either the MOC or MMOC scheme may be more efficient.

In this study, the HMOC technique was used because through artificial freshwater recharge using injection wells, relatively sharp concentration fronts will exist around the injection wells during the injection and recovery stages, where MOC is essential to solve the advection term at these fronts. Whereas, far away from the wells, concentration fronts will be smoother, and hence MMOC can be used to reduce the required computer memeory and computation time for the simulation espacially for the used models which are three-dimensional.

*Appendix-III*

## *HYDRAULIC GRADIENT AT THE HYDRAULIC GRADIENT-CONTROL PAIRS WITH AND WITHOUT USING THE GRADIENT-CONTROL WELLS IN MAINTAINING THE STORED WATER LENS*

| | With gradient | control wells | | Without | gradientl | control wells |
|---|---|---|---|---|---|---|
| Gradient Control Pair No. | Water head at node A | Water head at node B | Hydraulic gradient between A and B | Water head at node A | Water head at node B | Hydraulic gradient between A and B |
| | 1 st period | | | | | |
| C-1 | 19.6922 | 19.715 | 4.56E-05 | 9.69378 | 12.6743 | 0.005961 |
| C-2 | 20.9503 | 20.972 | 4.34E-05 | 12.8806 | 15.8955 | 0.00603 |
| C-3 | 24.022 | 24.0427 | 4.14E-05 | 17.4268 | 20.5005 | 0.006147 |
| C-4 | 27.6892 | 27.7094 | 4.04E-05 | 25.0989 | 27.917 | 0.005636 |
| C-5 | 36.3301 | 36.2158 | 2.29E-04 | 41.8782 | 41.9399 | 0.000123 |
| C-6 | 39.7355 | 39.7225 | 2.60E-05 | 48.4077 | 48.4284 | 0.0000414 |
| C-7 | 42.5128 | 42.5213 | 1.70E-05 | 54.0686 | 54.0567 | -0.000024 |
| C-8 | 45.1344 | 44.7754 | 7.18E-04 | 59.9561 | 58.9778 | -0.00196 |
| C-9 | 45.9313 | 45.6919 | 4.79E-04 | 62.2244 | 61.4323 | -0.00158 |
| C-10 | 45.7833 | 45.6406 | 2.85E-04 | 62.0366 | 61.4448 | -0.00118 |
| C-11 | 45.1927 | 45.2058 | 2.62E-05 | 60.3303 | 60.1536 | -0.00035 |
| C-12 | 44.8528 | 44.8634 | 2.12E-05 | 58.7408 | 58.4589 | -0.00056 |
| C-13 | 44.1946 | 44.2126 | 3.60E-05 | 54.7218 | 54.9681 | 0.000493 |
| C-14 | 43.3378 | 43.1901 | 2.95E-04 | 52.1704 | 52.2189 | 0.000097 |
| C-15 | 42.0621 | 41.7202 | 6.84E-04 | 50.3173 | 50.0706 | -0.00049 |
| C-16 | 40.2053 | 40.2114 | 1.22E-05 | 47.7569 | 47.926 | 0.000338 |
| C-17 | 36.8921 | 36.677 | 4.30E-04 | 44.1192 | 44.1573 | 0.0000762 |
| C-18 | 30.9455 | 30.9632 | 3.54E-05 | 36.4863 | 37.8786 | 0.002785 |
| C-19 | 26.1489 | 26.1727 | 4.76E-05 | 28.0698 | 29.3558 | 0.002572 |
| C-20 | 23.2706 | 23.2966 | 5.20E-05 | 20.7775 | 22.0629 | 0.002571 |
| C-21 | 20.2638 | 20.2866 | 4.56E-05 | 13.1663 | 15.8533 | 0.005374 |
| | 2 nd period | | | | | |
| C-1 | 19.6452 | 19.6549 | 1.94E-05 | 5.12491 | 7.99541 | 0.005741 |
| C-2 | 20.9951 | 21.004 | 1.78E-05 | 8.19457 | 11.1244 | 0.00586 |
| C-3 | 23.7431 | 23.749 | 1.18E-05 | 12.8186 | 15.7678 | 0.005898 |
| C-4 | 26.5866 | 26.5905 | 7.80E-06 | 20.6605 | 23.3611 | 0.005401 |
| C-5 | 32.5706 | 32.3727 | 3.96E-04 | 37.8435 | 37.7808 | -0.00013 |

| | | | | | | |
|---|---|---|---|---|---|---|
| C-6 | 35.0358 | 34.8935 | 2.85E-04 | 44.6964 | 44.5914 | -0.00021 |
| C-7 | 36.9428 | 36.8216 | 2.42E-04 | 50.5579 | 50.4341 | -0.00025 |
| C-8 | 38.8356 | 38.4013 | 8.69E-04 | 56.9025 | 55.7236 | -0.00236 |
| C-9 | 39.2905 | 38.9534 | 6.74E-04 | 59.4462 | 58.484 | -0.00192 |
| C-10 | 38.8417 | 38.6036 | 4.76E-04 | 59.2751 | 58.561 | -0.00143 |
| C-11 | 37.8553 | 37.8606 | 1.06E-05 | 57.4954 | 57.2169 | -0.00056 |
| C-12 | 37.306 | 37.2752 | 6.16E-05 | 55.7941 | 55.3588 | -0.00087 |
| C-13 | 36.3369 | 36.3428 | 1.18E-05 | 51.1605 | 51.2356 | 0.00015 |
| C-14 | 35.5047 | 35.3597 | 2.90E-04 | 48.1538 | 48.0207 | -0.00027 |
| C-15 | 34.445 | 34.1423 | 6.05E-04 | 45.8837 | 45.4679 | -0.00083 |
| C-16 | 33.0449 | 33.0171 | 5.56E-05 | 43.1798 | 43.2643 | 0.000169 |
| C-17 | 30.5406 | 30.3504 | 3.80E-04 | 39.3094 | 39.2455 | -0.00013 |
| C-18 | 26.2417 | 26.2476 | 1.18E-05 | 31.7507 | 32.9911 | 0.002481 |
| C-19 | 22.9066 | 22.9157 | 1.82E-05 | 23.4958 | 24.5917 | 0.002192 |
| C-20 | 21.049 | 21.0594 | 2.08E-05 | 16.3784 | 17.4827 | 0.002209 |
| C-21 | 19.5396 | 19.5499 | 2.06E-05 | 8.64589 | 11.2069 | 0.005122 |
| | 3 rd period | | | | | |
| C-1 | 18.8464 | 18.8501 | 7.40E-06 | 3.98436 | 6.83742 | 0.005706 |
| C-2 | 20.2232 | 20.2253 | 4.20E-06 | 7.0235 | 9.94148 | 0.005836 |
| C-3 | 22.8862 | 22.8869 | 1.40E-06 | 11.6395 | 14.578 | 0.005877 |
| C-4 | 25.5144 | 25.5131 | 2.60E-06 | 19.4928 | 22.1855 | 0.005385 |
| C-5 | 30.8144 | 30.6084 | 4.12E-04 | 36.7499 | 36.6757 | -0.00015 |
| C-6 | 33.0217 | 32.8602 | 3.23E-04 | 43.6632 | 43.5466 | -0.00023 |
| C-7 | 34.7151 | 34.5712 | 2.88E-04 | 49.5762 | 49.4427 | -0.00027 |
| C-8 | 36.4702 | 36.0158 | 9.09E-04 | 56.0135 | 54.809 | -0.00241 |
| C-9 | 36.8877 | 36.5138 | 7.48E-04 | 58.6161 | 57.6317 | -0.00197 |
| C-10 | 36.3587 | 36.0734 | 5.71E-04 | 58.4589 | 57.7296 | -0.00146 |
| C-11 | 35.148 | 35.154 | 1.20E-05 | 56.6782 | 56.3851 | -0.00059 |
| C-12 | 34.4427 | 34.4234 | 3.86E-05 | 54.9621 | 54.5041 | -0.00092 |
| C-13 | 33.4625 | 33.4653 | 5.60E-06 | 50.2267 | 50.2777 | 0.000102 |
| C-14 | 32.6766 | 32.5225 | 3.08E-04 | 47.1226 | 46.9643 | -0.00032 |
| C-15 | 31.6407 | 31.3525 | 5.76E-04 | 44.764 | 44.3265 | -0.00088 |

| | | | | | | |
|---|---|---|---|---|---|---|
| C-16 | 30.3114 | 30.2885 | 4.58E-05 | 42.0021 | 42.0821 | 0.00016 |
| C-17 | 28.0086 | 27.8422 | 3.33E-04 | 38.0793 | 38.01 | -0.00014 |
| C-18 | 24.1414 | 24.1409 | 9.99E-07 | 30.5177 | 31.7472 | 0.002459 |
| C-19 | 21.2383 | 21.2406 | 4.60E-06 | 22.3172 | 23.3913 | 0.002148 |
| C-20 | 19.6701 | 19.6736 | 7.00E-06 | 15.2464 | 16.3263 | 0.00216 |
| C-21 | 18.567 | 18.5712 | 8.40E-06 | 7.5145 | 10.0554 | 0.005082 |
| | 4 th period | | | | | |
| C-1 | 18.143 | 18.1453 | 4.60E-06 | 3.56151 | 6.40994 | 0.005697 |
| C-2 | 19.5369 | 19.5385 | 3.20E-06 | 6.58553 | 9.50011 | 0.005829 |
| C-3 | 22.1918 | 22.1929 | 2.20E-06 | 11.1898 | 14.1273 | 0.005875 |
| C-4 | 24.782 | 24.782 | 0 | 19.0358 | 21.7278 | 0.005384 |
| C-5 | 29.9641 | 29.7508 | 4.27E-04 | 36.2933 | 36.2185 | -0.00015 |
| C-6 | 32.1558 | 31.9821 | 3.47E-04 | 43.2105 | 43.0932 | -0.00023 |
| C-7 | 33.8514 | 33.6923 | 3.18E-04 | 49.1256 | 48.9917 | -0.00027 |
| C-8 | 35.668 | 35.1744 | 9.87E-04 | 55.5656 | 54.3607 | -0.00241 |
| C-9 | 36.1136 | 35.6961 | 8.35E-04 | 58.1702 | 57.1855 | -0.00197 |
| C-10 | 35.5261 | 35.1963 | 6.60E-04 | 58.0144 | 57.2854 | -0.00146 |
| C-11 | 34.1336 | 34.1359 | 4.60E-06 | 56.2365 | 55.9429 | -0.00059 |
| C-12 | 33.2957 | 33.2795 | 3.24E-05 | 54.5219 | 54.063 | -0.00092 |
| C-13 | 32.2495 | 32.2509 | 2.80E-06 | 49.7867 | 49.835 | 0.0000966 |
| C-14 | 31.4565 | 31.2902 | 3.33E-04 | 46.6771 | 46.5161 | -0.00032 |
| C-15 | 30.3897 | 30.0983 | 5.83E-04 | 44.3113 | 43.8718 | -0.00088 |
| C-16 | 29.0452 | 29.0253 | 3.98E-05 | 41.5458 | 41.6252 | 0.000159 |
| C-17 | 26.7705 | 26.6131 | 3.15E-04 | 37.6217 | 37.5518 | -0.00014 |
| C-18 | 23.0021 | 23.0026 | 9.99E-07 | 30.0724 | 31.2979 | 0.002451 |
| C-19 | 20.2325 | 20.2343 | 3.60E-06 | 21.8925 | 22.9603 | 0.002136 |
| C-20 | 18.763 | 18.7652 | 4.40E-06 | 14.8349 | 15.9078 | 0.002146 |
| C-21 | 17.8021 | 17.8047 | 5.20E-06 | 7.0994 | 9.63479 | 0.005071 |
| | 5 th period | | | | | |
| C-1 | 17.89 | 17.9018 | 2.36E-05 | 5.57336 | 8.27053 | 0.005394 |
| C-2 | 19.3257 | 19.3373 | 2.32E-05 | 8.50915 | 11.276 | 0.005534 |
| C-3 | 22.0341 | 22.0397 | 1.12E-05 | 12.9378 | 15.723 | 0.00557 |

| | | | | | | |
|---|---|---|---|---|---|---|
| C-4 | 24.6987 | 24.71 | 2.26E-05 | 20.4487 | 23.0209 | 0.005144 |
| C-5 | 30.0814 | 29.8593 | 4.44E-04 | 37.0597 | 36.9898 | -0.00014 |
| C-6 | 32.4095 | 32.225 | 3.69E-04 | 43.7848 | 43.6757 | -0.00022 |
| C-7 | 34.2589 | 34.0886 | 3.41E-04 | 49.5904 | 49.4674 | -0.00025 |
| C-8 | 36.3333 | 35.7775 | 1.11E-03 | 55.9927 | 54.8072 | -0.00237 |
| C-9 | 36.9316 | 36.4573 | 9.49E-04 | 58.654 | 57.6848 | -0.00194 |
| C-10 | 36.3727 | 35.9989 | 7.48E-04 | 58.5948 | 57.8829 | -0.00142 |
| C-11 | 34.9601 | 34.9215 | 7.72E-05 | 56.9984 | 56.6835 | -0.00063 |
| C-12 | 34.0462 | 33.9679 | 1.57E-04 | 55.3979 | 54.9112 | -0.00097 |
| C-13 | 32.6001 | 32.5877 | 2.48E-05 | 50.7494 | 50.7287 | -0.000041 |
| C-14 | 31.5574 | 31.3779 | 3.59E-04 | 47.5753 | 47.3561 | -0.00044 |
| C-15 | 30.3448 | 30.0415 | 6.07E-04 | 45.0841 | 44.6076 | -0.00095 |
| C-16 | 28.877 | 28.8692 | 1.56E-05 | 42.2385 | 42.3141 | 0.000151 |
| C-17 | 26.5227 | 26.3763 | 2.93E-04 | 38.2567 | 38.1915 | -0.00013 |
| C-18 | 22.6645 | 22.6892 | 4.94E-05 | 30.7261 | 31.9597 | 0.002467 |
| C-19 | 19.8813 | 19.9003 | 3.80E-05 | 22.7616 | 23.8334 | 0.002144 |
| C-20 | 18.422 | 18.4394 | 3.48E-05 | 16.0244 | 17.0926 | 0.002136 |
| C-21 | 17.5159 | 17.5286 | 2.54E-05 | 8.83137 | 11.2415 | 0.00482 |
| | 6 th period | | | | | |
| C-1 | 17.5598 | 17.5652 | 1.08E-05 | 4.74872 | 7.50576 | 0.005514 |
| C-2 | 18.9908 | 18.9957 | 9.80E-06 | 7.73234 | 10.5539 | 0.005643 |
| C-3 | 21.6922 | 21.6944 | 4.40E-06 | 12.234 | 15.0698 | 0.005672 |
| C-4 | 24.3321 | 24.3341 | 4.00E-06 | 19.8589 | 22.4658 | 0.005214 |
| C-5 | 29.6513 | 29.4324 | 4.38E-04 | 36.6356 | 36.563 | -0.00015 |
| C-6 | 31.9343 | 31.756 | 3.57E-04 | 43.3837 | 43.2709 | -0.00023 |
| C-7 | 33.7375 | 33.5763 | 3.22E-04 | 49.1744 | 49.0465 | -0.00026 |
| C-8 | 35.7423 | 35.2167 | 1.05E-03 | 55.5048 | 54.3257 | -0.00236 |
| C-9 | 36.3291 | 35.8851 | 8.88E-04 | 58.0872 | 57.1246 | -0.00193 |
| C-10 | 35.8249 | 35.4764 | 6.97E-04 | 57.9678 | 57.2576 | -0.00142 |
| C-11 | 34.5211 | 34.4826 | 7.70E-05 | 56.284 | 55.9886 | -0.00059 |
| C-12 | 33.6747 | 33.5972 | 1.55E-04 | 54.6405 | 54.1807 | -0.00092 |
| C-13 | 32.3128 | 32.284 | 5.76E-05 | 50.0195 | 50.0416 | 0.0000442 |

| | | | | | | |
|---|---|---|---|---|---|---|
| C-14 | 31.2742 | 31.0822 | 3.84E-04 | 46.932 | 46.7502 | -0.00036 |
| C-15 | 30.0402 | 29.7266 | 6.27E-04 | 44.5447 | 44.0947 | -0.0009 |
| C-16 | 28.5559 | 28.5445 | 2.28E-05 | 41.7727 | 41.8502 | 0.000155 |
| C-17 | 26.1676 | 26.0146 | 3.06E-04 | 37.8567 | 37.7905 | -0.00013 |
| C-18 | 22.2784 | 22.2829 | 9.00E-06 | 30.3708 | 31.5941 | 0.002447 |
| C-19 | 19.5037 | 19.5096 | 1.18E-05 | 22.3518 | 23.4192 | 0.002135 |
| C-20 | 18.0615 | 18.0678 | 1.26E-05 | 15.5005 | 16.5703 | 0.00214 |
| C-21 | 17.175 | 17.1806 | 1.12E-05 | 8.10407 | 10.5642 | 0.00492 |
| | 7 period | | | | | |
| C-1 | 6.99107 | 6.47488 | 1.03E-03 | -9.72353 | -8.03245 | 0.003382 |
| C-2 | 7.61334 | 7.15313 | 9.20E-04 | -7.35422 | -5.59305 | 0.003522 |
| C-3 | 9.88904 | 8.7581 | 2.26E-03 | -2.08502 | -0.90225 | 0.002366 |
| C-4 | 12.6919 | 11.6683 | 2.05E-03 | 6.23035 | 7.24121 | 0.002022 |
| C-5 | 17.2559 | 15.9671 | 2.58E-03 | 22.7875 | 21.5008 | -0.00257 |
| C-6 | 20.4155 | 19.1013 | 2.63E-03 | 30.4602 | 29.1272 | -0.00267 |
| C-7 | 22.3436 | 21.0513 | 2.58E-03 | 36.1489 | 34.836 | -0.00263 |
| C-8 | 26.3647 | 24.1759 | 4.38E-03 | 44.1153 | 41.2969 | -0.00564 |
| C-9 | 28.0572 | 26.2444 | 3.63E-03 | 47.5333 | 45.2226 | -0.00462 |
| C-10 | 27.2075 | 25.8662 | 2.68E-03 | 46.9093 | 45.1936 | -0.00343 |
| C-11 | 25.3502 | 24.5597 | 1.58E-03 | 44.3433 | 43.322 | -0.00204 |
| C-12 | 24.409 | 23.3321 | 2.15E-03 | 42.201 | 40.7574 | -0.00289 |
| C-13 | 21.4494 | 19.6393 | 3.62E-03 | 35.0837 | 33.6227 | -0.00292 |
| C-14 | 19.5033 | 17.474 | 4.06E-03 | 31.1352 | 29.3543 | -0.00356 |
| C-15 | 16.4036 | 14.3009 | 4.21E-03 | 27.2909 | 25.173 | -0.00424 |
| C-16 | 15.7502 | 14.6305 | 2.24E-03 | 25.569 | 24.5271 | -0.00208 |
| C-17 | 12.6958 | 11.3743 | 0.002643 | 20.8779 | 19.4952 | -0.00277 |
| C-18 | 10.4555 | 9.43224 | 2.05E-03 | 14.8266 | 14.3396 | -0.00097 |
| C-19 | 8.09906 | 6.90777 | 2.38E-03 | 7.22035 | 6.479 | -0.00148 |
| C-20 | 7.70875 | 6.79566 | 1.83E-03 | 1.5251 | 1.09842 | -0.00085 |
| C-21 | 6.68556 | 6.10122 | 1.17E-03 | -6.55787 | -5.22996 | 0.002656 |